P O R E S T R U C T U R E A N D C R U D E O I L
P E R M E A B I L I T Y O F H A R D E N E D C E M E N T P A S T E
A N D C O N C R E T E

by

CHIKE CHRISTIAN OYEKA

B.Sc. (Eng.) Hons. (Nigeria); M.Eng. (Sheffield)

Thesis submitted to the
University of Sheffield for the
Degree of Doctor of Philosophy
in the Faculty of Engineering

Department of Civil and Structural Engineering

August, 1978

PAGE

NUMBERING

AS ORIGINAL

DEDICATED TO THE MEMORY OF MY LATE FATHER

MR. ONYEKA WILFRED OYEKA

(1908 - 1973)

SUMMARY

Large concrete structures are being built for oil production, storage and transportation. The effects of crude oil on the properties of concrete are not well known and little data is available in the published literature.

This investigation, covering hardened cement pastes (HCPs) and concrete is divided into three parts: the first studies their porosity, the second their permeability to crude oil and ways of reducing permeability, and the third, changes in their properties when oil saturated. Two types of superplasticisers were used as water reducing additives.

Test results show that the porosity of D-dried pastes at 28 days were between 0.1435 and 0.4181 cc/gm of paste for OPC with W/C = 0.3 to 0.7; and 0.1925 to 0.3457 cc/gm of paste for SRPC with W/C = 0.4 to 0.6. The wide-pore volume, corresponding to Powers' capillary porosity occupy 77.5 to 90% of the pore volume in OPC and 72 to 83% in SRPC pastes. Adding 1 and 2% superplasticiser reduced the wide-pore volume and hydraulic radius. Concrete porosity was from 16.0 to 23.4% in OPC and 16.8 to 22.3% in SRPC for effective W/C ratios from about 0.3 to about 0.9.

The permeability of HCP and Concrete decreases with time and with low admixture concentration and increases with applied oil pressure. SRPC samples were more permeable than OPC. The permeability of concrete is influenced by workability, aggregate grading, fine aggregate concentration and cement content. Optimum values were obtained. Superplasticisers significantly reduce the permeability.

The mechanical properties of HCPs and concrete studied here were adversely affected by oil saturation. Cube strength and elastic modulus were reduced by amounts depending on the porosity of the concrete, but HCP properties were nearly constant after 4 months in oil. It appears that the oil mainly affects the paste-aggregate bond strength. Concrete deterioration with time (after initial saturation) was very small.

ACKNOWLEDGEMENTS

The author wishes to thank the Department of Civil and Structural Engineering of the University of Sheffield for providing the facilities for conducting this research.

His greatest gratitude goes to Dr. A. J. Watson, for his constant encouragement, criticisms and supervision throughout the period of the research. My thanks go also the Prof. T. H. Hanna for his concern and encouragement, and to Dr. B. Rand of the Department of Ceramics, Glasses and Polymers for his assistance in the construction of the adsorption apparatus.

The author also acknowledges the assistance of both the clerical and technical staffs on this department, in particular, Messrs. R. Newman, A. R. Hook and D. Derek. Acknowledgements are due to Mr. Wright in the Department of Chemistry for analysing the crude oil samples, and Mr. A. Sanby in the Department of Chemical Engineering for assistance in the glass works.

My thanks go also to the University of Nigeria, Nsukka, for their financial support.

CONTENTS

LIST OF FIGURES

LIST OF TABLES

LIST OF PLATES

NOTATIONS

A	Crude Oil Absorption (gm/cc)
Å	Angstrom Unit = 10^{-10} meter
A_o	Air Content (%)
A_i	Admixture Residue on drying to 1000°C (gm/gm)
C	Cement Weight (Kg)
E	Elastic Modulus (KN/mm^2)
f_c	Compressive Strength (Cube) of Concrete (N/mm^2)
I_o	Loss on ingnition (gm/gm)
K	Coefficient of Permeability (cm/sec)
k	Admixture Concentration (% of Cement Weight)
m	Degree of Hydration (%)
P	Porosity (% or cc/cc or cc/gm)
P/P_s	Relative humidity
P_c	Capillary Porosity (cc/cc)
r	Regression Coefficeint
r_h	Hydraulic radius
S_c	Compressive Strength of HCP
V	Volume of a Cement Paste (cm^3)
V_s	Porosity of HCP at 100% relative humidity
W_e	Porosity of HCP obtained as Evaporable Water at 105°C (gm/cc)
W_n	Non-evaporable Water content (gm)
W_n^o	Non-evaporable Water of fully hydrated HCP
W_a	Weight of HCP (SSD) in air (gm)
W_d	Weight of HCP dried to 105°C (in air) (gm)
W_w	Weight of HCP immersed in distilled water (gm)
p	Pressure head
γ	Surface tension of a liquid
d	Pore diameter

Note: Other notations used in this thesis are described at appropriate places.

ABBREVIATIONS

OPC	Ordinary Portland Cement
SRPC	Sulphate Resisting Portland Cement
W/C	Water/Cement
CTR	Samples dried (to 55°C or 105°) and stored sealed in Constant temperature room 16 ± 0.5°C
SSD	Samples stored in Water and Tested in Saturated Surface Dry Condition
exp	Exponent
C-S-H	Calcium Silicate Hydrate

CHAPTER 1

INTRODUCTION

1.1 General Introduction

For the storage or transportation of liquids in concrete containers, a designer must ensure that there is no significant leakage or contamination of the liquid and that the concrete itself is not attacked by the liquid. If the concrete does react with the liquid, then the designer needs to know by how much and at what rate the material properties change with time.

Steel and concrete are presently used for either the storage or transportation of many liquids and steel structures are mainly used for mineral oil tanks. Storage requirements for mineral oil are increasing rapidly and tank sizes now exceed 160,000 m^3. Such sizes are determined by safety and economy. A survey of tanks presently in service by Hampe[1] shows that although steel tanks presently have lower initial costs than concrete, ultimately through their service life, concrete tanks offer better economy. For many particular storage purposes concrete tanks have clear advantages of durability and safety eg; underground tanks, sea tanks and floating drilling platforms with under-water storage facilities, tanks in or near residential areas.

The history of petroleum oils in concrete tanks dates back to 1914[2] but the early use of concrete tanks was unsucessful because of seepage of oil through the concrete and leaks at the joints. During the second world war the use of concrete greatly increased due to shortage of steel, but it was only recently[3] that more successful attempts were made at storing crude oil in concrete tanks. Today, many concrete tanks for crude oil storage are in use[1]. Some of the most famous are the Ekofisk - field[4] and the Shell - Esso Brent offshore oil field[5]. In the former a rich mix of 1:2:2 was used. This gave a 28 daycompressive strength of 43 N/mm^2; water-reducing admixture was used and the water-cement (W/C) ratio was 0.40. In the latter a grade 50 concrete, with mix proportion of 1:1.6:2.8 and a W/C of 0.43 and ½% by cement weight of a plasticiser was used. Marion and Mahfonz[6] reported that the Ekofisk concrete mix was adequately durable to both sea-water and the crude oil. Though no details were given, they claim that there was no deterioration of the concrete in the crude oil and no significant oil

penetration into a concrete test-specimen.

There are results, however, which show that concrete deteriorates when in contact with crude oil especially if saturated by the oil. Meissner[7] reported some small reduction in compressive strength of specimens soaked for 180 days in aviation gasoline; Biczok[8] reported a 40% reduction in compressive strength of concrete containing 100 litres of oil per m^3 of concrete but a full regain of the strength after removal of the oil; Lea[9] reported that petroleum distillates, having low sulphur contents, have no general effect on mature concrete but that both reinforcement and steel joists were heavily corroded and on heating burnt fiercely; Hansen[10] found that the creep rate of concrete saturated with paraffin oil after 5 years increased much faster than that of concrete in air or water and also observed lower strength for oil saturated specimens.

1.2 Purpose of the Present Research

This research investigates the porosity of hardened cement pastes (HCPs) and concrete; permeability and absorption of HCPs and concrete to crude oil and on changes in some mechanical properties of HCPs and concrete when saturated with crude oil The investigation studies:

1. The pore structure of HCPs and the porosity of concrete with and without admixture
2. The permeation of crude oil into the pore system of the HCPs and concrete
3. The effects of different mix design parameters on the permeability of concrete to crude oil in order to make recommendation for suitable mix designs.
4. The deterioration of concrete in crude oil - this involves the measurements of compressive strengths, static modulus of elasticity and volumetric strains under compressive loads, for oil saturated, water saturated and oven-dried concrete specimens.

1.3 Scope of the Investigation

The approach adopted in this investigation is to study separately the behaviour of cement pastes and concrete as stated in section 1.2. Matti[11,12] and Faiyadh[13] have carried out intensive investigations into the effects of crude oil on some material and mechanical properties of

concrete. This present investigation is a continuation of on-going studies in this department on the behaviour of oil soaked or saturated concrete with a view to making a more efficient use of concrete for crude oil storage.

A study of the pore structure of HCPs is given in chapter 4. Ordinary portland cement (OPC) and sulphate resisting portland cement (SRPC) were used and at various W/C ratios and superplasticising admixture concentrations. A method of calculating the porosity of concrete is presented.

An extensive study of the permeability of HCPs and concrete to crude oil is made in chapter 5. Both ordinary portland cement (OPC) and sulphate resisting portland cement (SRPC) was investigated with various mix designs and admixture concentrations.

In chapter 6 are the results of investigations into some mechanical properties of HCPs and concrete. Results from chapters 4, 5 and 6 are further discussed in chapter 7. Predictions of the permeability of crude oil to concrete and of the behaviour of crude oil saturated HCPs and concrete are presented.

The conclusions are presented in chapter 8, together with recommendations for further work.

CHAPTER 2

LITERATURE REVIEW

This chapter is divided into 3 main sections. Section 2.1 describes the pore structure of hardened cement pastes (HCPs) and concrete. It includes a discussion on the nature of portland cement hydration products and its microstructure and on methods for measuring the pore structure of cement pastes and concrete. Section 2.2 discusses the permeability of both HCPs and concrete and methods for measuring the permeability. Section 2.3 discusses the theories on strength and elastic modulus of HCPs and concrete, relationship between strength and elastic modulus and porosity, and finally a brief discussion on concrete corrosion and methods employed in detecting and assessing corrosion problems in concrete.

2.1 Pore Structure of Hardened Cement Pastes (HCPs) and Concrete

2.1.1 Importance of Pore Structure

Surface area and porosity play a very important role in determining the physical and engineering properties of portland cement pastes and consequently of concrete. It has been established that the strength of concrete descreases exponentially with increasing porosity of the HCP because strength is in the solid not in the pores[14,15,16]. It is also known that relative humidity influences dimensional stability of concrete. As relative humidity increases more water vapour enters the pores of the paste, and the paste or concrete expands. As the relative humidity decreases the concrete shrinks[17,18]. Such volume changes set up stresses which may damage the concrete. Helmuth and Turk[19] have shown a linear relationship between porosity and shrinkage - both reversible and irreversible. Pores of different sizes have different effects on both strength and volume changes.

Helmuth and Turk[20] and Fagerlund[21] have demonstrated an almost linear relationship between porosity and elastic modulus. Similarly, Parrott and Illston[22] provided evidence that basic creep of HCPs of various moisture contents is proportional to a function of the porosity. Porosity also influences the course of hydration in cement pastes. In the small pores, hydration reaction stops because the nuclei of the hydration products have not enough room to grow into crystals[23,24]. This is a disadvantage from the

point of strength. However in very small pores water does not freeze, consequently, only the larger pores are responsible for the damage that may be caused by freezing and thawing of water in concrete[25]. Permeability of concrete depends on the size, volume, orientation and interconnectivity of the pore system[23,26].

Recently, interest in the porous nature of HCPs has grown due to the need to produce concrete of very low porosities. Very low porosity pastes have been obtained by hot-pressing techniques[16,27]; by physico-chemical methods developed by Brunauer and co-workers[28]; and by the use of additives to reduce mixing water[29,30].

2.1.2 Nature of Portland Cement Hydration Products

When cement is mixed with water, the unhydrated cement particles are dispersed in an aqueous solution as shown in fig. (2.1) taken from ref. 31. In the first few minutes of mixing, the reaction rate is rapid and calcium silicate hydrate-cement gel (C-S-H) forms a coating around the cement grains. As hydration progresses,hydration products gradually fill the capillary pores formed. Early hydration is confined to the narrow pores producing tobermorite crystallites which is a stronger material and acts as a solid link between the coated cement particles, so producing a continuous solid matrix within the cement paste.

Powers[23] found that the products of a completely hydrated portland cement occupy twice the volume of the anhydrous material. Once set, the total volume of the pastes changes by less than 0.3% during the entire hydration period. For pastes with $W/C > 0.38$, the volume of the hydrate produced is insufficient to fill the space available and the remaining void space is called capillary pores. For W/C less than 0.38 hydration stops before completion because of insufficient space for the hydration to continue.

2.1.3 Models for the Microstructure of HCPs

Despite intensive study, many aspects of the structure of HCP remain imperfectly understood. Powers and Brownyard[23] were the first to carry out on extensive investigation into the nature of HCP and their work has formed the basis upon which all subsequent ideas on the subject have been based. Their experiments were based on water vapour adsorption of partially and fully hydrated cement pastes. Using the BET theory[32], they obtained surface

areas of about 180-200 m^2/gm of paste for mature pastes; and the surface areas are proportional to the non-evaporable water content of the paste. At vapour pressure in the range 45-100% saturation, the amount of water absorbed was directly proportional to the initial w/c ratio. On this basis, Powers classified the cement paste pores in to two groups: those occupied by water at vapour pressure < 0.45 - the gel pores, and the remainder - capillary pores. Gel pores are now thought to be below about 16-20Å[33] diameter.

With the developments of electron optical and X-ray diffraction techniques, much more has become known about the basic structure of HCPs. The most important work was by Brunauer[34] who investigated the nature of calcium silicate hydrate (C-S-H) prepared by reacting lime (CaO) and silica (SiO_2) in water, and found that the structure depended on the CaO/SiO_2 ratio. The X-ray diffraction patterns of C-S-H showed a layered structure, similar to that found in HCPs; which are characteristic of the natural mineral tobermorite and so Brunauer termed the C-S-H gelcomponent of the HCP 'tobermorite gel'. On the basis of his results and further water vapour sorption studies, Brunauer postulated that the basic structure of cement hydrate consisted of about 70% C-S-H gel, 20% Calcium hydroxide, 7% ettringite and calcium aluminate monosulphate hydrate, and 3% unhydrated clinker residue and other minor constituents.

A typical structure of C-S-H envisaged by Brunauer is shown in fig. (2.2)[31] which also shows the average dimensions of the various phases together with the states in which water is held in the system (apart from the chemically combined water - W_n). The type 1 water is considered to be outside the influence of any surface forces. Type 2 is one or two molecular layers thick and adsorbed onto the outside surface of the C-S-H sheets. Type 3 is confined between adjoining crystal surfaces hence more strongly held than types 1 and 2. Type 4 is held between the layers of the C-S-H and is commonly called the 'interlayer water'. The classifications, though artificial serve as a convenient method of reference when discussing the model structures, and also demonstrates the need to carefully specify the drying procedure before any porosity test.

Similar models have been proposed by Ishai[31] and Powers[35] who modified his original ideas to incoporate new evidence. In fact, this model is normally refered to as 'Powers' model' or sometimes 'Powers/Brunauer model'. Summarily the model states that [36]: 1, C-S-H gel is a layer

structured material consisting ultimately of tobermorite like units in groups of 2 or 3 layers with each layer about 9 Å thick; 2, On D-drying[37] the layers collapse on each other and remove any interlayer space; 3, the closure is irreversible and soaking in water does not separate the layers (Brunauer later retracted from this view[38]); 4, adsorption of water vapour yields the true surface area of the paste and this value does not include interlayer surfaces. Areas measured by Nitrogen are inappropriate because of limited penetration of nitrogen molecules into the paste.

With this model, the above authors and many more have explained many physical and mechanical properties of cement pastes such as strength, shrinkage, creep, permeability and freeze-thaw mechanism.

In a large number of papers[39,40,41,42], Feldman and co-workers put forward a new model for the structure of the C-S-H gel in HCP based on nitrogen adsorption and later on helium flow pycnometry. These authors reject the 'Powers/Brunauer model' on the basis that the surface area and porosity of D-dried pastes, as measured by water vapour adsorption, is wrong because 80% of the uptake of water is interlayer water (ie that between the tobermorite sheets) and is therefore part of the hydrate structure. Summarily, their model states that: 1. C-S-H gel is a layer-structured material, with layers that are somewhat irregular in thickness but approximately parallel, and relatively large numbers of layers are grouped in 'packets'; 2. On drying, the layers collapse on each other and remove the interlayer space; 3. the layers are not permanently sealed and exposure to increasing relative humidity after drying permits gradual re-entry of water into the interlayer spaces; 4. Due to this re-entry of water, water-vapour adsorption isotherms yield surface areas that are too high. Evidences obtained in several ways are interpreted as suggesting that the N_2 surface areas are at least approximately correct. Their model is schematically represented in fig. (2.3)[39]. With this model the authors and some others have explained the mechanisms of creep, shrinkage, modulus of elasticity and density changes in HCPs[43,44,45,46].

During the last few years there has been a lively controversy on the validity of the different models [38,42,47,48,49]. So far no generally acceptable agreement has been reached. The Feldman model lacks quantitative details and recent pore structure measurements using methods independent of sorption[36] adds more credibility to the Powers/Brunauer model. Thus amongst many technologists[50] and to the present writer the 'Power/Brunauer model' gives

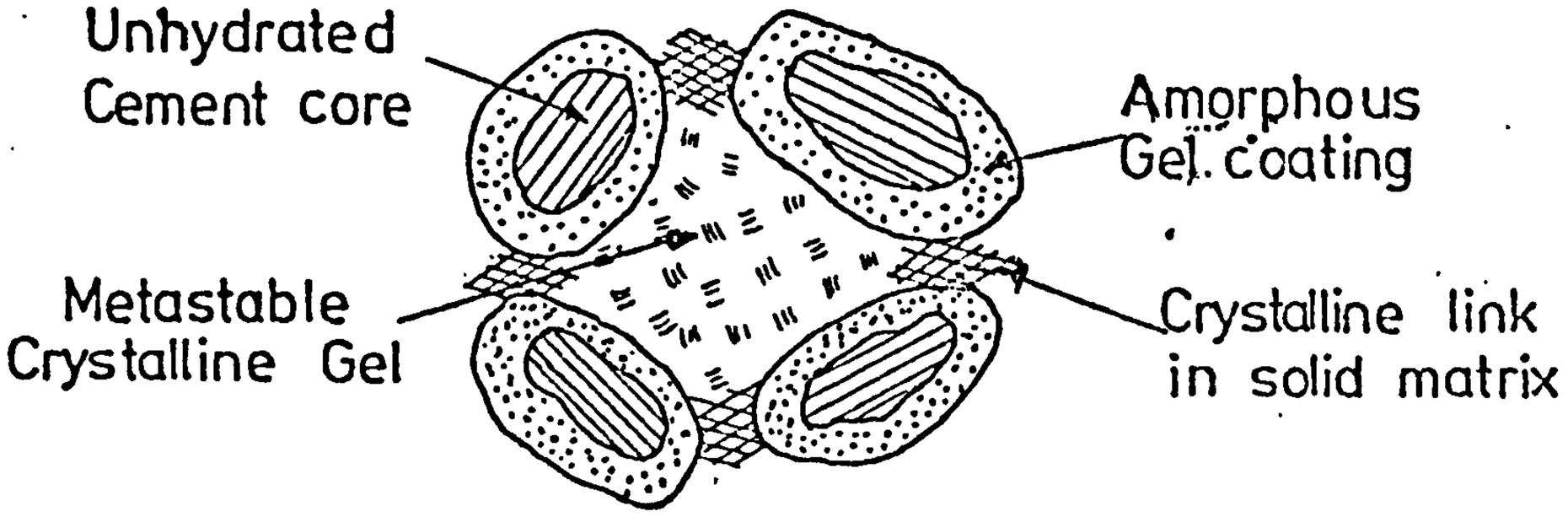

FIG(2.1) MICROSCOPIC MODEL REPRESETATION OF THE STRUCTURE OF HCP. (ref. 31)

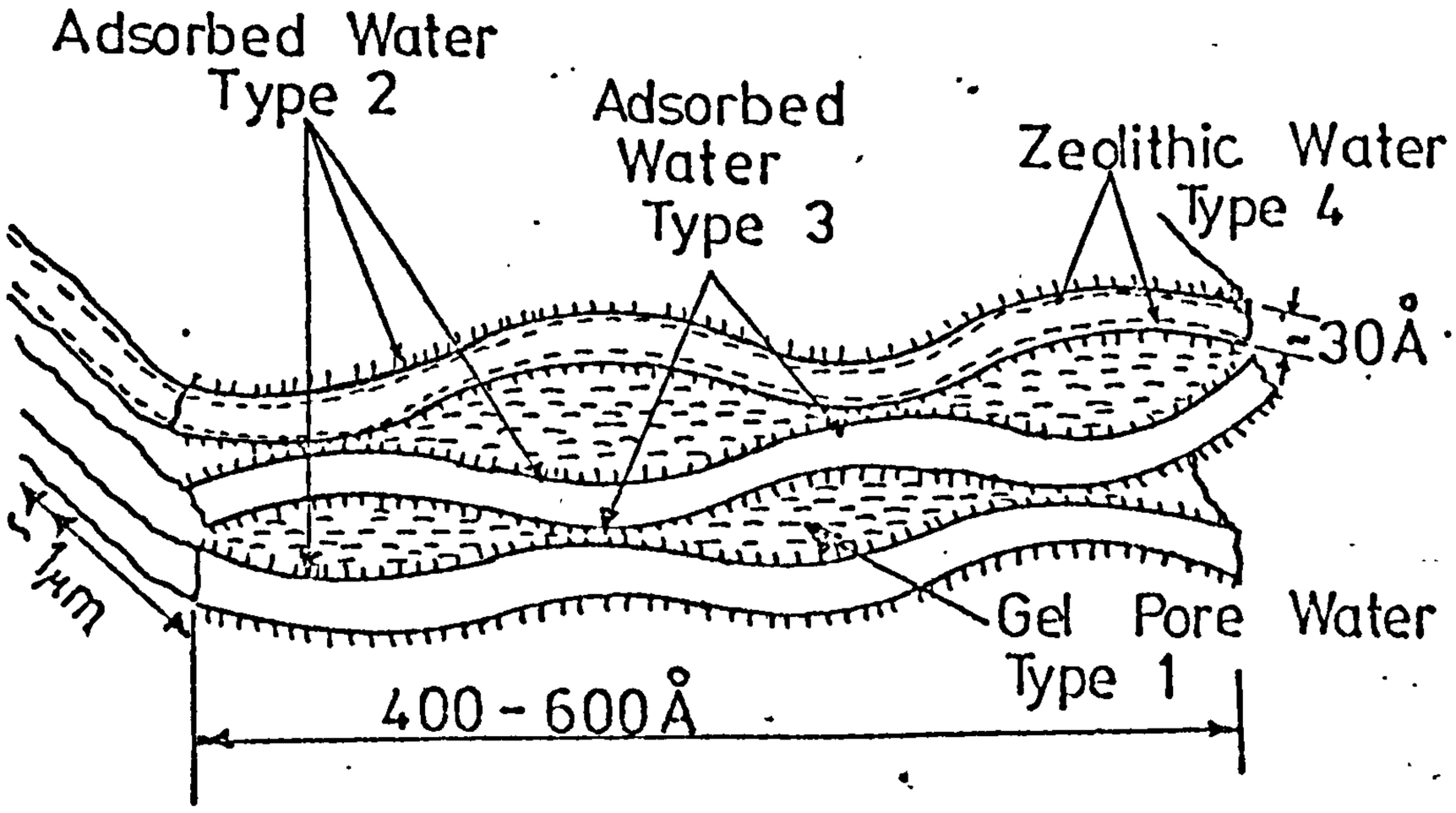

FIG (2.2) SCHEMATIC MODEL REPR. OF THE CEMENT GEL BY POWERS' MODEL (ref. 31)

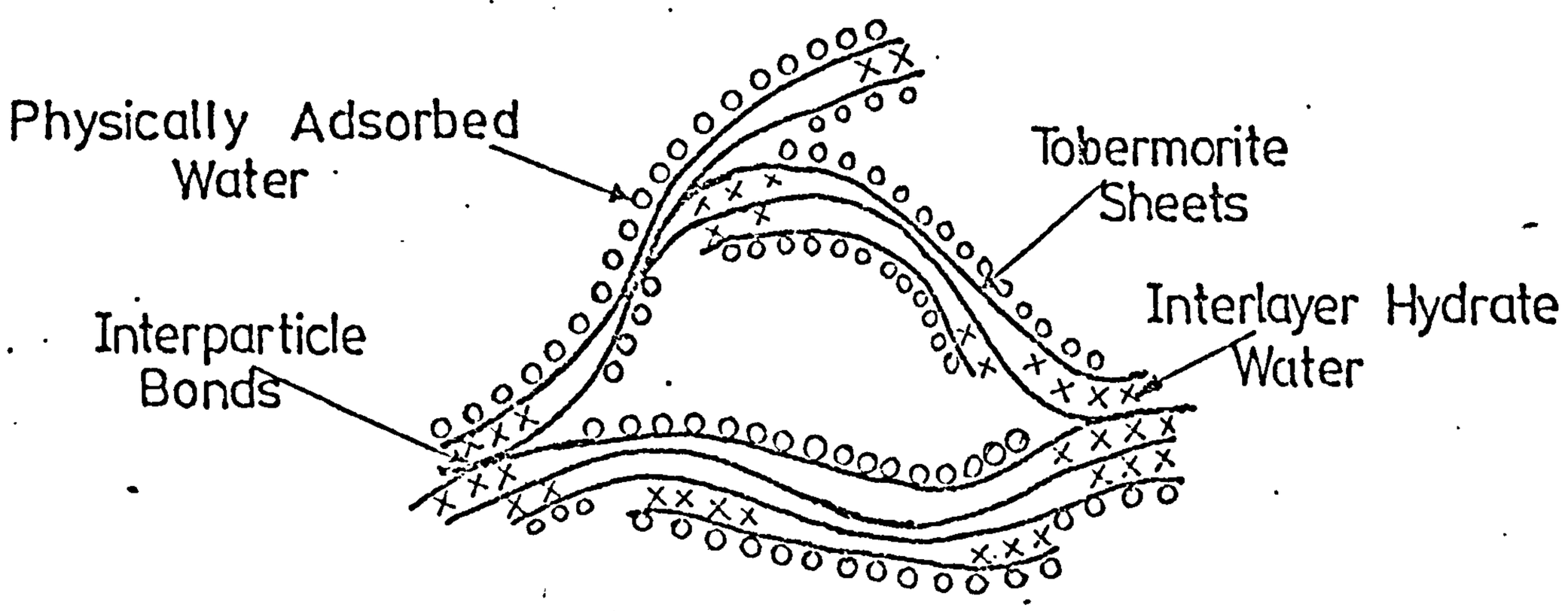

FIG(2.3) SCHEMATIC MODEL REPR. OF THE CEMENT PASTE BY FELDMAN-SEREDA MODEL (ref. 39)

the clearest quantitative explanation of the structure of HCP.

2.1.4 Methods Employed in Pore Structure Measurement

2.1.4.1 Introduction

The purpose of pore structure analysis is to determine the total pore volume and surface; distributions of the pores and surfaces; and the shape of the pores. The first two methods of pore structure analysis were introduced in 1945 - the mercury intrusion porosimetry by Ritter and Drake[51] and the adsorption method by Wheller[52]. The former method cannot furnish information about the pore surfaces. Neither method is able to determine pore shape but usually assumptions are made in order to facilitate analysis. The pore shapes usually assumed are cylindrical and parallel-plate shapes[53]. Both the mercury porosimetry and the gas adsorption methods, with modifications, are used in industry and research to date.

2.1.4.2 The Mercury Porosimetry

This applies the principle that a nonwetting liquid (ie one forming a contact angle greater than 90^{o}) will intrude the open pores of a solid only under pressure. This pressure, p, is given by[54]

$$p = \frac{4\gamma\cos\theta}{d} \qquad (2.1)$$

where p = pressure required to intrude a pore

γ = surface tension of the liquid

d = diameter of the intruded pore

θ = contact angle between liquid and pore wall

Equation (2.1) shows that the pore diameter intruded is a direct function of the applied pressure. It has been found that under the right conditions a pressure of 700 atmospheres (709 N/m^2) is needed to intrude pores of 100 Å and greater; Although some workers report using pressures large enough for 20Å, the method is conidered practical only for the analysis of pores of about 100Å diameter and greater[38,55].

There are several disadvantages of this method: 1) At high pressures

the pores may be deformed or even destroyed by the intruding mercury. 2) The pore diameter measured represents the entry pore diameter which has the same capillary pressure as a straight cylindrical pore. 3) The measurement of the contact angle is uncertain expecially at high pressures. 4) Only pore volume distribution can be measured with no information on pore surface. However, despite its short comings some workers[56] prefer it to sorption methods and it is in extensive use at the present time.

2.1.4.3 Sorption Methods

Various theories have been advanced to explain the adsorption of gases and vapours by solid materials. The most widely used is the multi-molecular adsorption theory or the BET for brevity[32]. A summary and discussion of the applications of this theory has been made by Gregg and Sing[57]. The theory rests on the concept that the adsorption of a gas or vapour by a material is a result of a physical attraction between the molecules of the gas and the surface molecules of the material. Any material surrounded by and in equilibrium with a certain gas or vapour at a temperature, T and relative vapour pressure, P/Ps, adsorbs physically a certain amount of gas which depends on P/Ps and is proportional to the total external and internal surface of the material. The relationship between the amount of adsorbed gas at a constant temperature and P/Ps is called an adsorption isotherm.

Braunauer divided physical adsorption isotherms into 5 groups - fig. (2.4)[57]. The majority of building materials tend to have isotherm II using water vapour as adsorbate[58], although isotherm II and III are theoretically valid only for non-porous materials. Isotherms IV and V are valid only for porous materials while isotherm I is only for materials with extremely narrow pores, like gels. In the low P/Ps range, isotherms of building materials, like HCPs, show a type II isotherm but in the higher P/Ps range capillary condensation occurs and their graphs differ from type II .

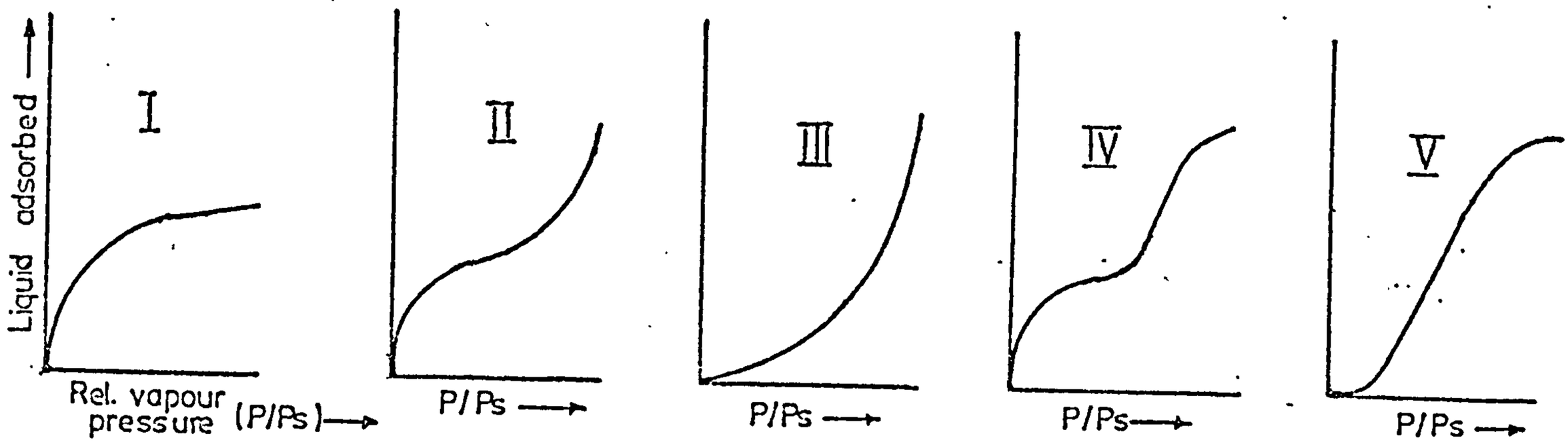

FIG(2.4) THE 5 ADSORPTION ISOTHERMS AS CLASSIFIED BY BRUNAUER (ref. 58)

Powers and Brownyard[23] were the first investigators to apply the BET theory in the study of the pore structure of cement pastes. Their mathematical solution - for which reference should be made to their original papers for the complete solution-is given by:

$$\frac{1}{w} \cdot \frac{x}{1-x} = \frac{1}{V_m C} + \frac{C-1}{V_m C} \qquad (2.2)$$

where x = P/Ps is the relative vapour pressure

w = quantity of vapour adsorbed at P/Ps (gm/gm of paste)

C = Constant, related to the heat of adsorption

V_m = Quantity of vapour adsorbed when the material surface is covered by a monomolecular layer.

A plot of experimental values of $\frac{1}{w} \cdot \frac{x}{1-x}$ against x gives a straight line, the slope of which gives $(C-1)/V_m C$ and the intercept gives $1/V_m C$. Hence C and V_m can be determined. The pore volume and surface area are then given by:

$$V_p = wV_m \quad (cc/gm) \qquad (2.3)$$

$$S = V_m \times 6.102 \times 10^{23} \cdot A_m \quad (m^2/gm) \qquad (2.4)$$

where A_m = area which each adsorbed molecule covers = 11.4 Å for water vapour[59].

This method of analysis gives only the total pore volume and total surface area and not their distributions. Brunauer and co-workers developed two methods for complete pore structure analysis. The first they called the 'Modelless method'[60] for the analysis of the wide-pores (mesopores, 16-500Å) hydraulic radius). This is based on the part of the adsorption - desorption isotherms in which capillary condensation takes place (P/Ps > 0.45). The second, they called the 'MP - method'[61] for the analysis of micropores (16Å and under - hydraulic radius). These two methods, which will be treated in greater detail in chapter 4, form the principal methods of analysis of pore structure of HCP in this thesis.

The BET method for pore structure analysis does not specify the adsorbate, consequently both nitrogen at liquid nitrogen temperatures and water vapour have been used. It has long been found that pore structure values obtained with nitrogen as the adsorbate are always smaller than those obtained with water vapour. Typical values are shown in table (2.1)[33]. Many arguments have been put forward to explain these differences but none is universally accepted[33,39,40,41,47]. Although the physical behaviour of HCP has been shown to depend on pore structure, no clear definition of porosity has yet been found. In this investigation water-vapour is used to measure the pore structure of HCP because the investigation is concerned with the movement of liquid in the pore system.

W/C ratio	Age (yrs)	Total pore Vol. (ml/gm)		Total Pore Surface (m^2/gm)	
		H_2O	N_2	H_2O	N_2
0.35	12	0.1264	0.0748	208.0	56.7
0.40	12	0.1776	0.1059	202.6	79.4
0.50	12	0.2615	0.1792	194.6	97.3
0.60	$2\frac{1}{2}$	0.3110	0.2493	193.8	132.3
0.70	$2\frac{1}{2}$	0.4008	0.2758	199.6	139.5

Table (2.1) Pore volumes and surface areas of HCPs determined by water vapour and Nitrogen adsorptions[33]

2.1.4.4 Other Methods

Several other methods have been proposed for measuring pore structure and are presently in use. Notably amongst these is the 't-method' of DeBoer and workers[62,63]. In a series of 7 papers they put forward a method suitable for the analysis of micropores. The surface area obtained by this method are not always equal to those obtained by the BET method. Brunauer, et al incorporated the basic 't-method' theory in their 'MP-method' and later[64] suggested ways of making the two values match exactly. Some other methods include: electron microscopy, low angle X-ray scattering and X-ray diffraction analysis[36]. Feldman and Sereda[65] introduced the helium flow pycnometer and claimed much success in its use for both porosity and density measurements, but the results obtained are still liable to interpretations in differing ways[48,49]. A good review of many other minor methods has been given by Haynes[66].

2.1.5 Calculation of Concrete Porosity

There is not yet a widely accepted method of determining concrete porosity. A common method is by finding the weight loss on drying a concrete specimen to a constant weight at 105°C. This method often gives unreliable results because of variations in the method of drying, the shape and thickness of the specimens and the difficulty of determining just when a sample is saturated surface dry (SSD).

The most reliable method is by summing the separate porosities of the individual constituents of the concrete and the air content in the specimen. Fagerlund[21,67] gave a generalized formula for calculating concrete porosity, (P_c) :

$$P_c = P_p \cdot V_p + P_A(1 - V_p) \qquad (2.5)$$

where P_p = cement paste porosity

V_p = volume fraction of cement paste

P_A = aggregate porosity

The cement paste porosity is given by

$$P_p = \left[(W_o - 0.75W_n)\frac{1}{\rho_w} + A_o\right] \times 10^{-3} \qquad (2.6)$$

where W_o = mixing water (Kg/m^3)

W_n = non-evaporable water (Kg/m^3)

ρ_w = density of water

A_o = air content

Equation (2.6) given decreasing porosity with hydration (age). The difficulty is in an accurately determining W_n, since this has quantitative significance according to Powers' model. The equation also neglects the fact that as concrete matures added porosity might be introduced due to microcracks[68].

2.2 Permeability of HCPs and Concrete

2.2.1 Introduction

Any solid composed of particles randomly aggregated is both porous and permeable[24]. The permeability of HCP has an important bearing on the vulnerability of concrete to frost action[69]. Permeability determines the liquid-retaining ability of materials. The problem is not necessarily the loss of the liquid, which in most cases is negligible, but the leaching of lime compounds - in the case of water - which may lead to efflorescence[70]. In the case of liquids, like crude oil, it could lead to dirty tank walls and high risks of fire accidents. In reinforced and prestressed concrete, the ingress of moisture or other stored liquids could result in the corrosion of the reinforcing steel. The corrosion of steel may lead to its expansion resulting in concrete cracking and spalling; or loss of bond between the steel and concrete.

2.2.2 Permeability Theories

2.2.2.1 Introduction

The permeability of a material is linked to the pore structure of the material. The correlation between porosity and permeability is largely empirical[23,24,71] due to the complexity of the pore structure of many materials, like HCPs and concrete. The methods for calculating the permeability of HCPs and concrete will now be examined.

2.2.2.2 Darcy's Law

This is the basic theory for laminar flow through a homogeneous porous

medium. In its fundamental form it is given by:

$$Q = KA \frac{\Delta h}{l} \qquad (2.7)$$

And in the differential form by:

$$\frac{dq}{dt} = KA \frac{\partial h}{\partial l}$$

where Q = fluid flow rate (cm^3)

$\frac{dq}{dt}$ = quantity of fluid flowing per unit time

A = x-sectional area

$\frac{\partial h}{\partial l}$ = hydraulic gradient across the specimen

l = thickness of the specimen

K = a constant (cm/sec) called the coefficient of permeability; its value is a function of the properties of the porous medium and of the liquid. It represents the permeability of a certain medium to a particular liquid at a specified condition eg. temperature.

Muskat[72] modified equation (2.7) into:

$$\frac{dq}{dt} = \frac{K_i}{\mu} \cdot A \cdot \frac{\partial h}{\partial l} \qquad (2.8)$$

μ = viscosity of the fluid at the specified temperature - dynes/cm^2

K_i = Coefficient of permeability (cm^2). This coefficient is a property of the medium alone and is therefore, independent of the passing fluid. Schiedegger[73] called it the 'specific' permeability.

The coefficient, K_i, in equation (2.8) is however, of limited use since when fluids flow through channels as small as say cement pastes, the viscosity appears to be a function of the size of the channel[71] and hence is highly variable and indeterminate.

2.2.2.3 Model theories

These theories represent attempts at relating flow to the microstructure of the medium by visualizing the pore system as composed of various forms of capillaries. The simplest capillaric model is that of a bundle of straight parallel capillaries of uniform diameter - δ[23,73]. The flow, Q, through a

capillary is given by the Hagen - Poiseulle equation:

$$Q = \frac{\pi\delta^4}{128}\frac{dp}{dl} \qquad (2.9)$$

for n such capillaries per unit x-section of the model the flow:

$$q = \frac{n\,\delta^4}{128}\cdot\frac{dp}{dl} \qquad (2.10)$$

compared with Darcy's law - equation (2.7)

$$K = \frac{n\pi\delta^4}{128} \qquad (2.11)$$

Pore volume, P, per unit x-sectional area is given by

$$P = \tfrac{1}{4}xn\pi\delta^2 \qquad x = \text{length of the pore}$$

$$\therefore \quad P = \tfrac{1}{4}n\pi\delta^4 \qquad (2.12)$$

$$\text{hence} \quad K = \frac{P\delta^2}{32} \qquad (2.13)$$

The factor 32 is usually replaced by some arbitrary factor - T^2 - the tortuosity which indicates that the actual flow path is T times longer than the apparent flow path which is considered straight across the porous medium. The specific internal surface area, S, of the model is given by:

$$S = n\pi d = \frac{4p}{\delta}$$

$$\therefore \quad K = \frac{p^3}{T^2S^2} \qquad (2.14)$$

A serious set-back in the use of this model is that all the pores are considered unidirectional and to pass from one face of the medium right through to the other face. This evidently is far remote from the fact[26]. A more realistic approach was put forward by Schiedegger[74], known as the "series model" it assumes that the capillaries are of different pore diameter put together in series one after another. Equation (2.13) is then modified by varying the diameter of each capillary along its length according to the pore size distribution.

2.2.2.4 The Kozeny Theorem

This is one of the most widely accepted explanations of permeability considering the geometrical properties of a porous medium. The basic expression assumes that:

$$K = C \cdot \frac{M^2}{F(P)} \qquad (2.15)$$

where M = hydraulic radius
C = a dimensionless constant
F(P) = some function of the porosity

The theory assumes that: (1) no pores are sealed; (2) pores are distributed at random; (3) pores are "reasonably" uniform in size; (4) porosity is not too high; (5) diffusion phenomena are absent - section 2.2.2.6; (6) fluid motion through a batch of capillaries. The detailed solution of the Kozeny theory can be found in some books of fluid dynamics[72,73] and is not reproduced here. Kozeny obtained:

$$q = \frac{CP^3}{\mu S^2} \frac{\delta h}{\delta l} \qquad (2.16)$$

compared with Darcy's law:

$$K = \frac{CP^3}{S^2} \qquad (2.17)$$

C is called the Kozeny constant. Introducing the tortuosity factor - T them:

$$K = \frac{CP^3}{TS^2} \qquad (2.18)$$

Carman[75] found C = 0.2 for a variety of media, and for a media with very small pores, the equation gave very high permeabilities. He then modified the theory by assuming that only part of the porosity, (called the effective porosity) is effective in liquid transmission.

The Kozeny's equation (2.18) has been modified, eg. the Kozeny-Carman equation:

$$K = \frac{P^3}{5S^2(1 - P)^2} \qquad (2.19)$$

Powers[76] adopted Kozeny's equation (2.17) for the bleeding rate of cement pastes and found that the effective porosity - P_c - should be used instead of the total porosity P. From experiments, he obtained:

$$P_c = P - \sigma(1 - P) \qquad (2.20)$$

where σ = A constant, defined as the amount of immobile fluid per unit volume of solids in the medium.

2.2.2.5 The Drag Theories

There are two approaches to permeability based on drag theory as follows: (A) The walls of the pores are treated as obstacles to an otherwise straight flow of the viscous fluid. The drag of the fluid on the pore walls is estimated from the Navier - Stokes equations and the sum of all drags is then equated to the resistance of the porous medium to the flow (ie. equal to μ/K in Darcy's law). The theory[73] assumes a random distribution of circular cylindrical fibres of the same diameter and accounts for the permeability on the basis of the drag on individual element. This aspect of the drag theory gives good results in cases of highly porous media like fibres. In a highly colloidal media like cement pastes its application is limited. (B) The viscous drag of a moving fluid on a particle is developed when a particle falls through a fluid, or when fluid flows through a granular bed where the particles are in fixed positions. This concept of viscous drag is approached by considering the drag on a single particle moving under gravitation through a large body of fluid. Schiedegger[73] gave a general solution of the above concept.

Powers et al[71] considered the drag as a function of size and shape of the particles and of thevelocity and viscosity of the fluid - ie. Stoke's law. They further visualised HCPs as an aggregation of discrete particles, and due to the extreme smallness of the interparticle spaces, any fluid in them may be treated as adsorbed and the viscosity of this fluid a function of the dimensions of the interparticle spaces and the kinds and amounts of the dissolved materials. The authors produced an extensive solution of the problem and much of the earlier concepts of Powers' model were based on the results of this solution.

2.2.2.6 Diffusion Phenomena

Permeability under a fluid pressure difference may be described as a diffusion phenomena. Fluid adsorbed at the internal walls of the pores diffuses along a concentration gradient brought about by a pressure gradient. This process is normally described by the diffusivity equation, and it is characteristic of relatively high density materials with micropores such as HCPs and concrete[77].

Fick's law of diffusion is given by[78]

$$\frac{\partial C}{\partial t} = D \cdot \frac{\partial^2 C}{\partial x^2} \qquad (2.21)$$

where D = diffusion coefficient (cm^2/sec)

C = fluid concentration at a point x, and at a time t

This form of Fick's law has been applied to the drying process of concrete and a review of the applications has been given by Hughes et al[79]. Murata[77] was the first to apply it in analysing the permeation of a liquid (water) into concrete. He calculated the diffusion coefficient and related it to the permeability coefficient. Matti[12] utilized Murata's solution in calculating the coefficient of permeability of concrete to crude oil.

Equation (2.21) has been used whenever there is a concentration gradient ie. flow is unsteady. When the flow becomes steady ie. as much fluid leaves a given volume element as enters it per unit time, then:

$$\frac{\partial C}{\partial t} = 0 \qquad (2.22)$$

and the solution reduces to Darcy's law. Since the work done in this thesis is of the steady state type, solutions by diffusion theories do not apply and is therefore not further discussed.

2.2.3 Permeability of HCPs

The permeability of HCPs is not a simple function of its porosity, but depends on the size, distribution and continuity of the pores. Thus although cement gel generally has a porosity of 28%, its permeability is

very low, about 7×10^{-14} cm/sec[24]. The permeability of cement pastes as a whole depends mainly on its capillary porosity. The relationship between the two is shown in fig. (2.5).

For pastes with the same degree of hydration, the permeability decreases with decreasing W/C ratio - fig. (2.6). A reduction in W/C ratio from 0.7 to 0.3 lowers the permeability a thousand fold. Permeability decreases rapidly with progress of hydration. This is because the gel gradually fills up some of the original capillary spaces. Table (2.2) shows that for a paste of 0.7 W/C ratio the permeability reduces a thousand fold between 7 days and 1 year.

Age (Days)	Coeft. of Permeability K - (cm/sec)
Fresh	2×10^{-4}
5	4×10^{-8}
6	1×10^{-8}
8	4×10^{-9}
13	5×10^{-10}
24	1×10^{-10}
ultimate	6×10^{-11} (Calculated)

Table (2.2) Variation in Permeability of cement pastes of W/C = 0.7, with progress of hydration[69]

Certain other factors influence the permeability of HCPs eg: for the same W/C ratio coarse cements tend to produce more permeable pastes than fine ones[69]; chemical composition of the cement also affects permeability, however, Powers[69] stated that the ultimate values of permeability are unaffected by these 2 factors. Drying HCPs increase permeability probably because some of the gel between the capillaries are raptured by shrinkage thus opening new passages. It is also known that oven-drying of HCPs at high temperatures is destructive to the cement paste structure[15].

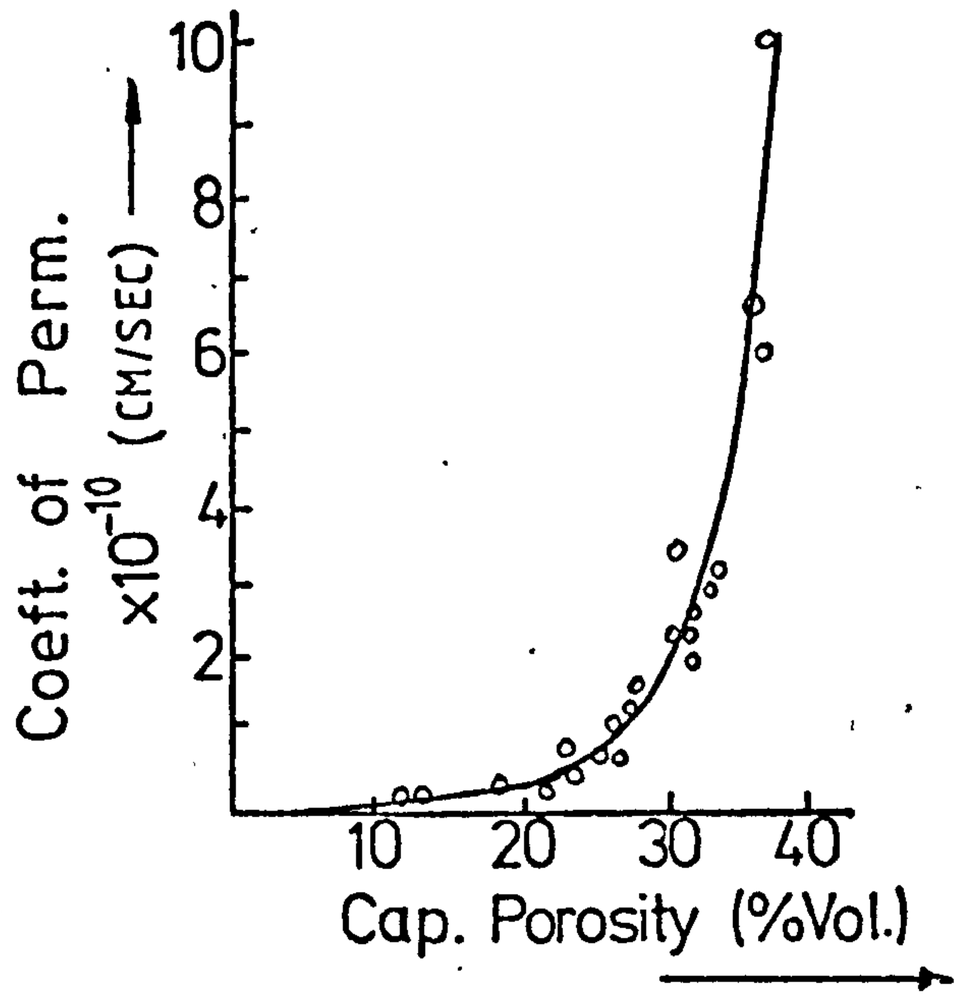

FIG(2.5) RELATIONSHIP BETWEEN PERMEABILITY & CAPILLARY POROSITY OF HCPS. (ref. 24)

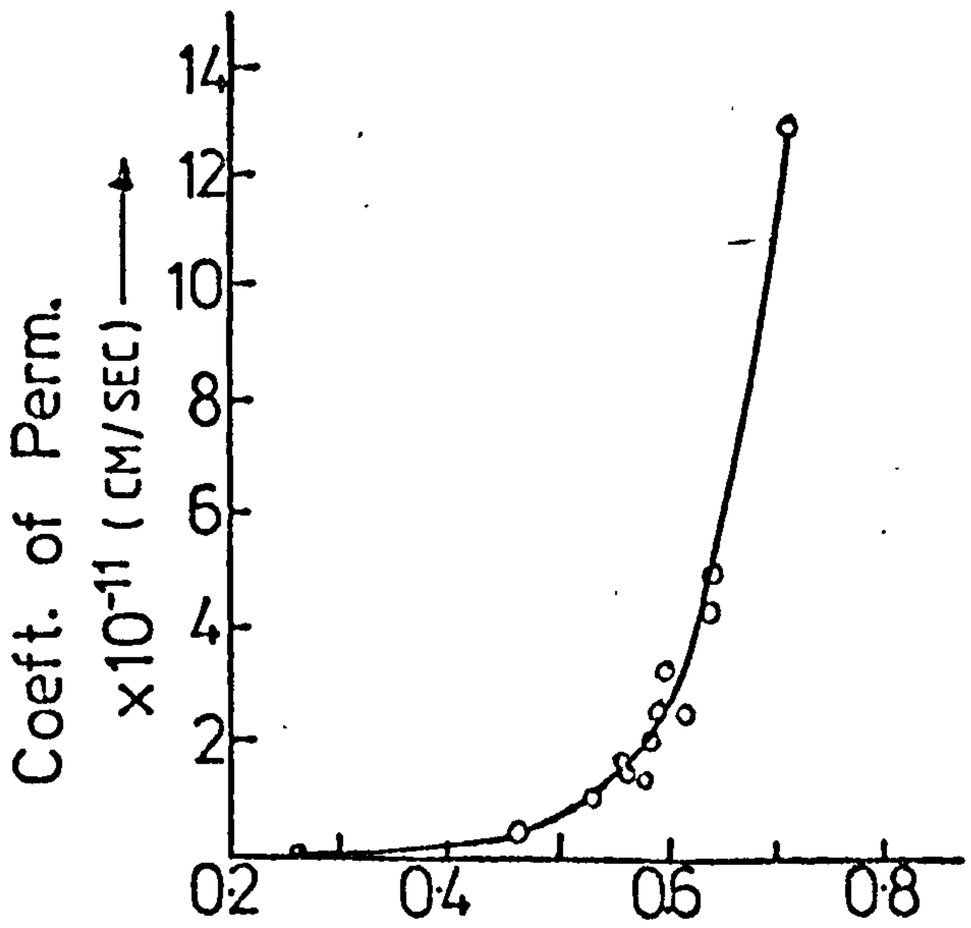

FIG(2.6) RELATIONSHIP BETWEEN PERMEABILITY & W/C RATIO FOR MATURE HCPS. 93% HYDRATION. (ref. 69)

2.2.4 Permeability of Concrete

Compressive strength has been used as a convenient measure for assessing concrete quality[78,80]. However, it has long been recognised that strength can only be an indirect measure of durability and that other parameters governing the case of movements of liquids and gases would provide a better assessment. The British standard for testing concrete provides the simple 30 min. water-absorption test[81]. More elaborate methods have been devised for assessing air[82,83] and water[84] permeabilities of concrete cores or test specimens. An improvement on the above 30 min. water-absorption test is the initial surface absorption test (ISAT)[81,82,83] developed by Levitt. In this test, water absorption of a concrete surface is determined at an applied hydrostatic head.

The absorption methods have many disadvantages eg: (1) fluid is applied under pressure at the lower surface of the specimen but very often the absorption of the outer surface is different from that of the concrete bulk due to orientation of the coarse aggregates and the formation of a rich layer of concrete close to the surfaces. (2) The values obtained are largely affected by some other phenomena like diffusion and in the case of different liquids by molecular effects[73]. Figg[87] developed a simple method for the measurement of air and water permeabilities of in-situ concrete. He avoided some of the surface effects by boring a hole into the concrete and measuring the rate of flow of air or water applied in the hole through a hypodermic needle.

The study of the permeability of concrete has intensified in recent years because of the greater need to store many liquids. To produce more efficient and economical concrete hydraulic structures, the following information is needed:

(1) Volume of pores accessible to the liquid under a defined pressure head.

(2) Capillary character of the pores or permeability of the pore system.

(3) The kinetics of liquid penetration eg. depth and rate of penetration[68,88].

The methods being used in the study of permeability are steady and unsteady state permeability tests, and absorption tests. A review of unsteady permeability tests has been given by Matti[12]. Steady state

permeability tests are difficult to accomplish due to the difficulty of obtaining equal inflows and outflows. Investigators in this area have, therefore, used high pressures upto 35 N/mm^2[89,90,91]. The use of such high pressures could lead to the destruction of the concrete pore structure.

Very few authors have attempted to correlate the permeability of concrete with other concrete properties, and the few available results are inconclusive[87,92]; figs. (2.7) and (2.8).

Matti[12] made an extensive study of the rate of penetration of crude oil into concrete. He found that the depth of oil penetration, D, increased with time, t and oil pressure, following the relationship

$$D = At^B \qquad (2.23)$$

where $B = 1/3.4$

A = function of oil pressure

For concrete of W/C = 0.6, partially dried before test he obtained coefficient of permeability of between $1.09 - 1.90 \times 10^{-10}$ cm/sec under 65.5 m head of crude oil. Apart from Matti's work, very little has been done on the permeability of concrete to liquids other than water[11].

2.3 Compressive Strength and Elastic Modulus of HCPs and Concrete

2.3.1. Introduction

The mode of failure of concrete is illustrated in fig. (2.9) which shows a typical stress-strain behaviour. Up to a certain proportion of the ultimate stress, the strain is linearly proportional to the stress. When the critical stress - σ_c - is exceeded, both the longitudinal and lateral strain increase at a faster rate than the stress and the volumetric strain decreases. X-ray and ultrasonic measurements indicate that at this point of deviation from linear elastic behaviour considerable microcracking of the specimen occurs in a direction parallel to that of the compressive load. Failure usually occurs when the specimen splits along the compressive axis. In most cube tests failure occurs at 45° to the axis because of the constraints on the specimen ends during the test[93]

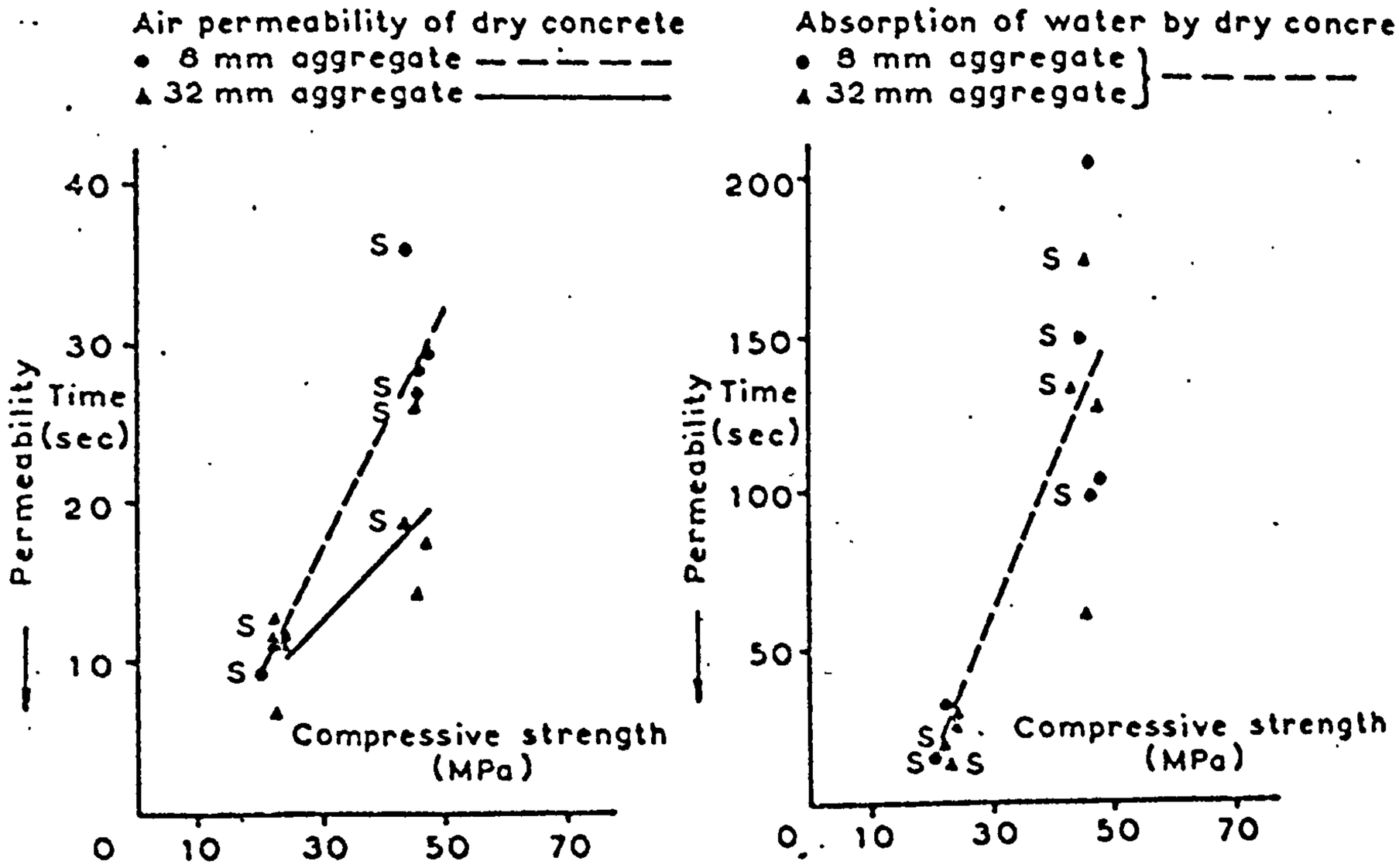

FIG(2.7) RELATIONSHIP BETWEEN COMPR. STRENGTH & PERMEABILITY OF CONCRETE DRIED TO 105°C PRIOR TO TESTING. S=Sealed storing (ref. 92)

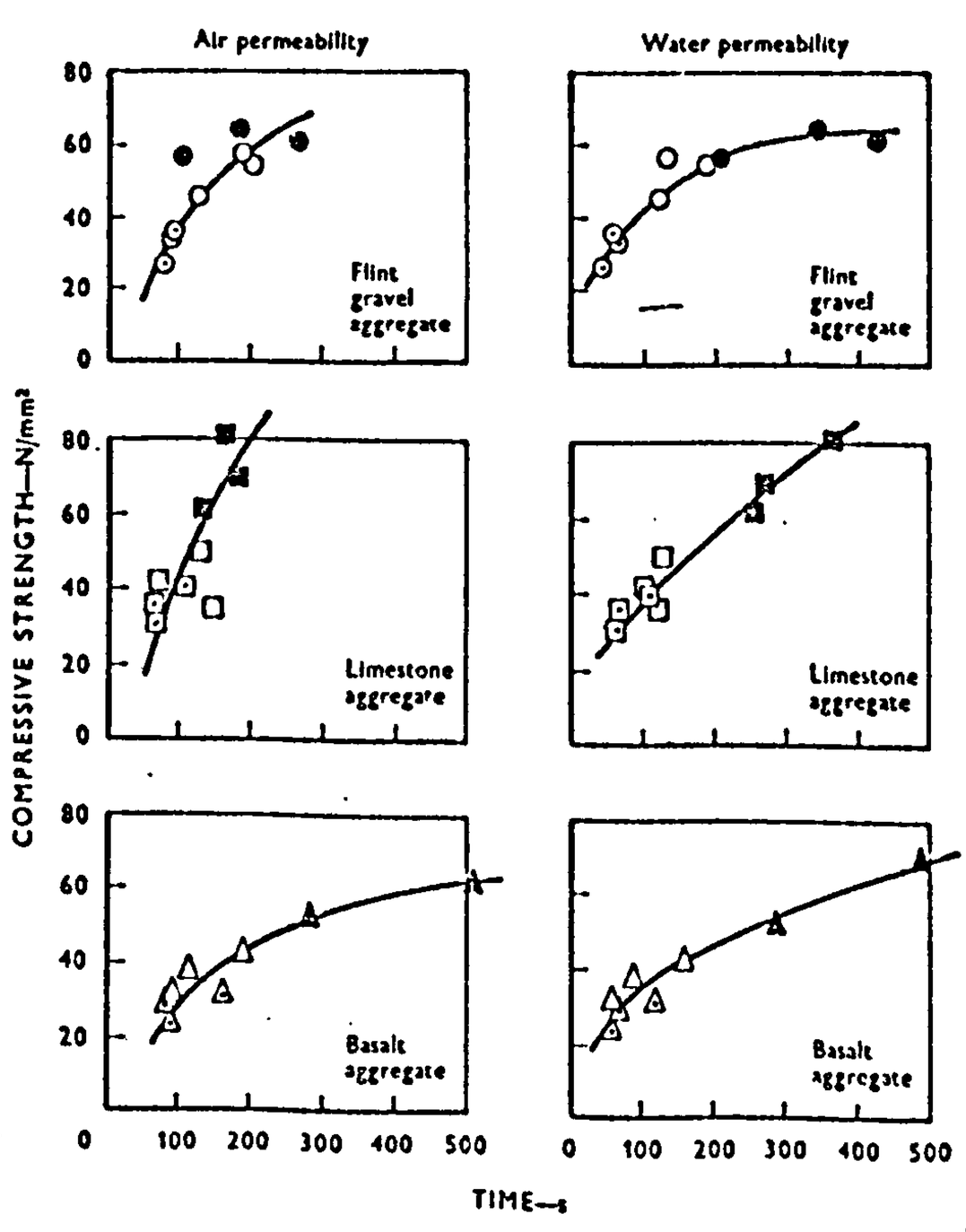

FIG(2.8) RELATIONSHIP BETWEEN COMPR. STRENGTH & AIR- & WATER-PERMEABILITY OF CONCRETE (ref. 87)

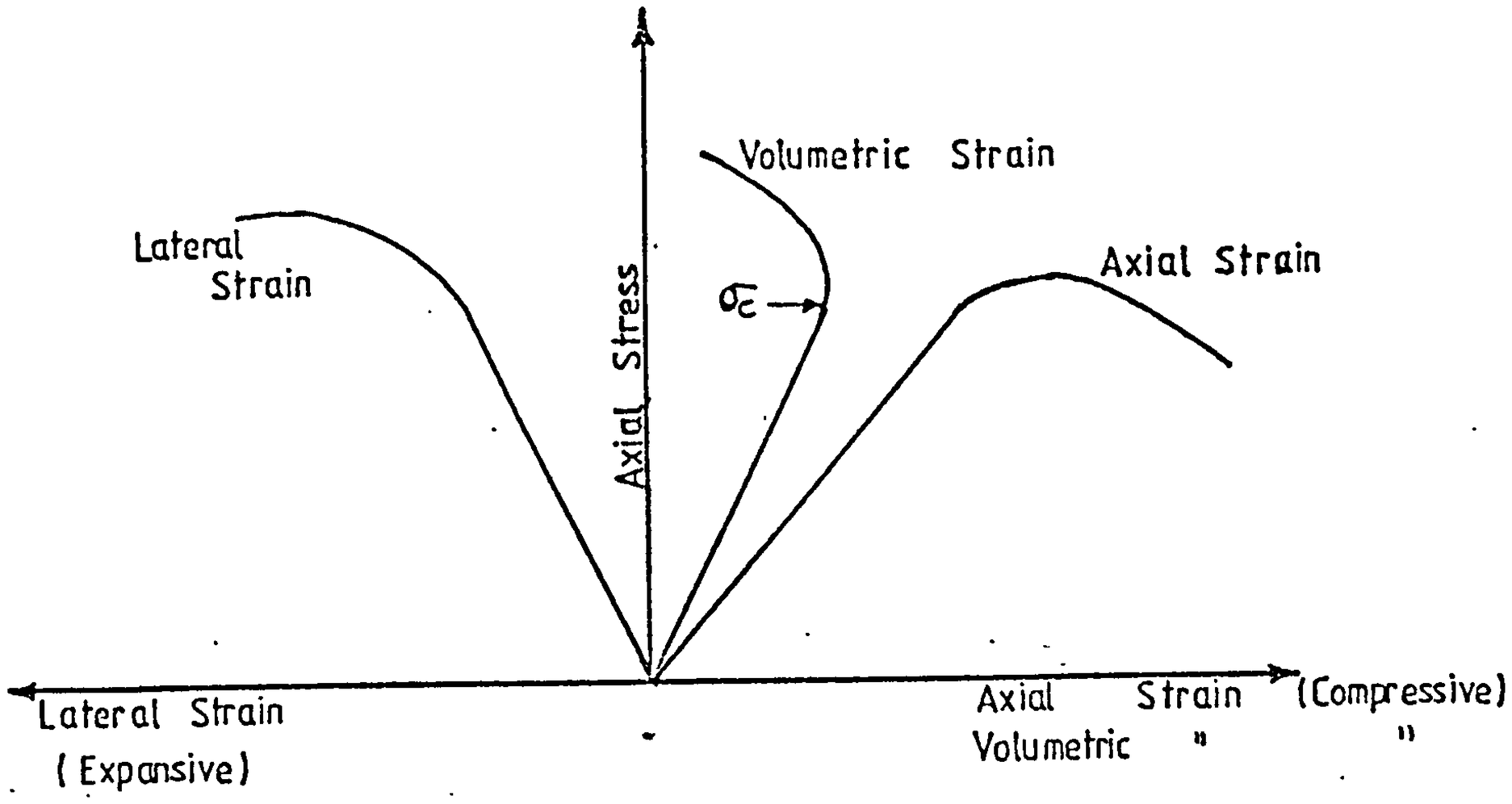

FIG(2.9) TYPICAL STRESS–STRAIN BEHAVIOUR OF CONCRETE OR MORTAR UNDER COMPRESSION

2.3.2 Theories on the Origin of Strength in HCPs

Powers[23,24,94] and others believe that two kinds of cohesive bonds - physical attraction between solid surfaces, and chemical bonds – determine the strength of cement pastes. The physical attraction of Van der Waals forces holds the particles in positions of least potential energy and are considered to be the most important.

Williamson[95] considers calcium hydroxide as one of the principal bonding agents between C-S-H layers and notes that no calcium hydroxide is seen on fracture surfaces until a paste is 3 days old. Later results, however, show that cements with high calcium hydroxide are not necessarily stronger than ones of lower calcium hydroxide[34].

Philleo[96] considers the strength as being a result of secondary bonding (Van der Waals) and explains the increase in strength with hydration as being caused by the increased surface area over which the bonds act. Feldman and Sereda[39] consider the bonding force as 'interparticle bond' and consider chemical bond as very insignificant. The nature of the interparticle bonds is not certain but is not Van der Waals forces since it is independent of surface area but is influenced by interlayer water.

Some investigators explain strength from a porosity basis by applying Griffith's theory[97]. The pores are considered as points of stress concentration that act as crack initiators. This theory has been used to explain the disparity.

between compressive and tensile strengths.

2.3.3 Porosity/Strength Relationship for HCPs and Concrete

It has been found that porosity, which produces stress concentrations, is by far the most important single variable determining strength.

Powers and Brownyard[23] related the strength of HCPs and mortar to the gel-space ratio - X. This they defined as the ratio of the volume of cement hydrate to the volume of space available for the hydrate; and is given by:

$$X = \frac{2.06U_c a}{U_c a + \frac{V_w}{C}} \qquad (2.24)$$

where C = weight of cement

U_c = specific volume of cement

a = fraction of cement that has hydrated

V_w = volume of water in the original mix

They found that their strength values followed the relationship:

$$S = S_o X^n \qquad (2.25)$$

Where S_o = strength at zero porosity and n is a constant. The nature of their model and of equ. (2.4) and (2.25) indicated that maximum strength is reached when the products of hydration fills all available capillary space, regardless of the degree of hydration. Their model neglected the volume of unhydrated cement and could not, therefore, account for the high strength of very low porosity pastes (ie. low W/C ratios) obtained by some special processes such as pressure compaction[98]. More recent workers have, therefore, redefined porosity as the ratio of volume of pores (determined from content of evaporable water of an SSD specimen) to the total volume of the specimen.

It is found that an inverse exponential relationship fits most published data on the strength and porosity of HCPs and concrete. Thus the compressive strength data of Kaplan[99] on poorly compacted concrete, of Te,'eni[100], Mills[101] and Lawrence[15] on HCPs; Powers[23] on mortar and Manning and Hope[29] on polymer impregnated concrete all fit an equation of the type:

$$S = S_o \exp(-b)P \qquad (2.26)$$

where b = a constant

P = porosity

S_o = strength of imaginary paste of zero porosity

It is important to note that either capillary porosity or total porosity values can be used in equation (2.26) with of course different values obtained for b and S_o. Similarily, porosity values obtained by either the Powers' model or the Feldman-Sereda model fit the equation. Kaplan's data on the flexural strength of concrete were also found to fit the equation[99].

2.3.4 Porosity/Elastic Modulus relationship for HCPs and Concrete

The influence of porosity on elastic modulus of HCPs and concrete has been extensively studied[20,21,23,29,102,103]. Hansen[103], considered concrete, cement mortar and cement paste as two-phase materials consisting of aggregate and mortar, aggregate and cement paste, and cement paste and void respectively. He presented the equation for the elastic modulus of concrete and HCPs:

$$E = E_o \frac{1 - P}{1 + 2P} \qquad (2.27)$$

where E_o = modulus of material without pores

Lawrence et al[104], by applying the MacKenzie model for cement paste arrived at the general equation:

$$E = E_o \frac{1 - P}{1 + CP} \qquad (2.28)$$

which is identical to Hansen's if C (a constant) = 2

Powers[23] proposed an equation of the type:

$$E = E_o (1 - P)^n \qquad (2.29)$$

He found that n = 3 for cement pastes. Fagerlund[21] found that n varies between 3.5 and 4.5 for concrete. Helmuth and Turk[20] found Powers' equation with n = 3 fitted their data on dynamic modulus of elasticity irrespective of whether the capillary or total porosity was used. Hansen[103] found that n = 4

fitted Kaplan's data[99] on elastic modulus of concrete containing large voids.

Some investigators have also proposed an inverse exponential relationship similar to that used in compressive strength, of the form:

$$E = E_o \exp(-b) P \qquad (2.30)$$

Te'eni[100] analysed his data for HCPs using this equation and found b = 4.5. Ryskewitsch[105] found b = 4 to 7 fitted his data on plaster of Paris.

2.3.5 Corrosion of Concrete

The corrosion (or deterioration) of concrete can produce the following changes[106,107]:

1. visual deterioration
2. chemical changes
3. changes in concrete strength - tensile or compressive
4. changes in the elastic modulus
5. changes in length or volume

A lot of work has been done on the durability of HCPs and concrete and the possible mechanisms of their deterioration in aggressive environments, eg., sea-water. It is known that some mineral oils attack concrete[9] but little information is available on it. The present thesis will deal with concrete corrosion in crude oil.

CHAPTER 3

EXPERIMENTAL PROGRAMME, MATERIALS AND PREPARATION OF SPECIMENS.

3.1 Introduction

The pore structure, permeability and most physical properties of hardened cement pastes (HCPs) and concrete are considerably affected by the casting and curing conditions. In the case of HCPs, the problem is mainly that of prevention of segregation (Bleeding) and for concrete ensuring that each test specimen contains the designed mix parameters and is also free from segregation. In this research, a lot of effort was exercised in maintaining uniformity in casting and curing.

3.2 Experimental Programme

The various experimental programmes are detailed in the relevant chapters but the main areas of study are:

(i) Pore structure analysis of HCPs with 20 cement pastes (OPC and SRPC) using different W/C ratios, superplasticiser admixture concentrations and test conditions. All pastes were initially cured in water at 16 ± 0.5°C for 27 days. All but four of the pastes were D - dried[37] before testing. A sorption apparatus has been developed and used for these tests.

(ii) Permeability of HCPs and concrete using 24 HCP specimens (OPC and SRPC) with 5 W/C ratios and 4 different admixture concentrations and 137 concrete mixes of various mix designs and admixture concentrations. A permeability apparatus already developed in this department[12] was modified to allow for the smaller samples of HCPs.

(iii) Compressive strength and elastic modulus of HCPs and concrete specimens and also volumetric changes under load for concrete using 12 different mixes with OPC, SRPC and OPC containing 4% superplasticiser admixture. For some specimens the test covered periods of upto 15 months.

3.3 Materials

3.3.1 Cements

COMPOUND COMPOSITION	ABBREVIATION	% BY WEIGHT	
		OPC	SRPC
Tricalcium Silicate	C_3S	63.1	64.0
Dicalcium Silicate	C_2S	8.9	96.0
Tricalcium aluminate	C_3A	11.0	2.4
Tetracalcium aluminoferite	C_4AF	6.4	14.3
Silica	SiO_2	19.7	
Insoluble residue		1.5	
Alumina	Al_2O_3	5.5	
Ferric oxide	Fe_2O_3	2.1	
Lime	CaO	65.5	
Magnesium oxide	MgO	1.1	
Sulphur trioxide	SO_3	2.5	
Alkalis	Na_2O	0.2	
	K_2O	0.6	
Loss on Ignition	I_o	1.4	1.5
Specific surface		333 m^2/Kg	378 m^2Kg
Specific gravity	S.G.	3.12	3.13

Table (3.1) Chemical Composition of the cements used in the investigations[31]

Ordinary Portland cement (OPC) and sulphate - resisting Portland cement (SRPC) manufactured and marketed by the Blue Circle group, Hope cement Works, near Sheffield, were used. These types of cement were chosen for the investigations because they are the two types most commonly used at present for sea structures or for the means of storage and transportation of crude oil[5]. Their approximate chemical compositions are given in table (3.1).

3.3.2. Aggregate

Natural river aggregates were used.

The coarse aggregates were continuously graded irregular shaped gravel of 10 mm maximum size down to 5 mm. They were obtained from Bradsford river, Derbyshire. This maximum size was chosen primarily because of the need to make the permeability test specimens as small as possible in order to obtain quick steady state flow, and secondly because in many precast structural members, like pipes, the thicknesses are relatively small and as Neville[109] pointed out the maximum size of aggregate should be between 1/5 to $\frac{1}{4}$ of the structural concrete section, thereby necessitating the use of small aggregate sizes. The coarse aggregate grading is given in table (3.2).

The fine aggregate was a dried river quartzite sand graded to zone 2 of B.S. 882:1201:1965 and sizes shown in table (3.3). They were obtained from Bradsford river, Derbyshire. Values from tables (3.2) and (3.3) are plotted in fig. (3.1)

Coarse Aggregate Properties:

Natural and irregular river gravel
10 mm ($\frac{3}{8}$") maximum size
water absorption 1.9%
Grading:

Sieve Sizes		% passing	B.S. requirements
in	mm		
$\frac{3}{4}$	19.0 mm	100	100
$\frac{1}{2}$	12.7	100	100
$\frac{3}{8}$	9.52	96	85 - 100
3/16	4.72	6	0 - 20
No. 7	2.40	0.8	0 - 5

Table (3.2) Coarse Aggregate Grading

Fine Aggregate Properties:

Washed and dried river sand

Zone 2 grading

Water absorption 0.86%

Grading:

Sieve Sizes		% Passing	B.S. Requirement
in.	mm		
$\frac{3}{8}$	9.52	100	100
3/16	4.72	98.9	90 - 100
No. 7	2.40	87.3	75 - 100
14	1.20	76.5	55 - 90
25	0.60	52.1	35 - 90
52	0.30	16.6	8 - 30
100	0.15	4.0	0 - 10
200	0.075	0	0

Table (3.3) Fine Aggregate Grading

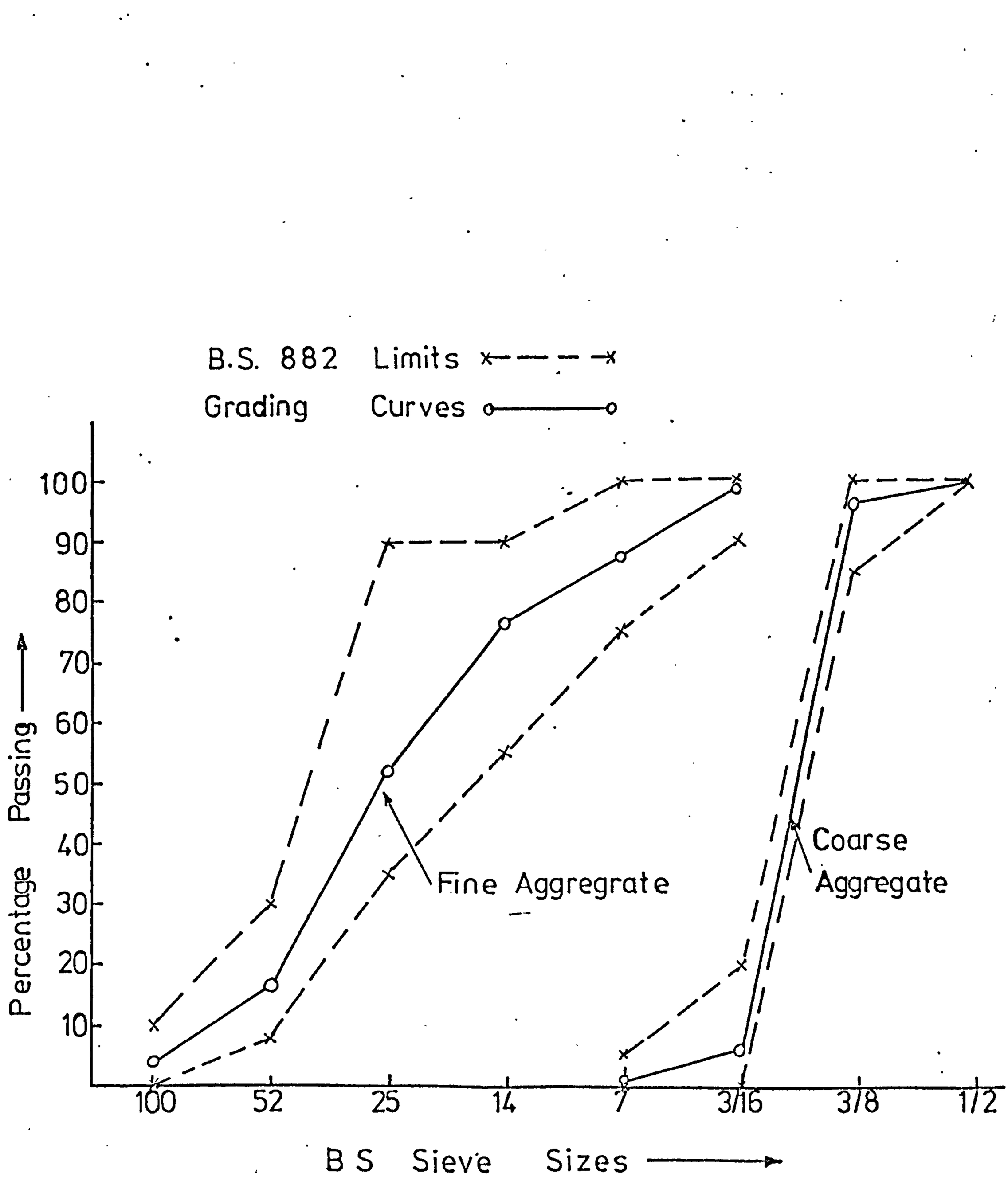

FIG(3.1) GRADING CURVES FOR FINE & 10mm COARSE AGGREGATES

For the permeability tests, four gradings, corresponding to Zones 1, 2, 3 and 4 of B.S. 882:1965 were used. They were obtained by sieving the fine aggregate and proportioning the various sizes to correspond exactly to the desired grading. The actual gradings of the fine aggregate are shown in table (3.4) and plotted in fig. (3.2)

SIEVE SIZES		% PASSING			
(in)	(mm)	ZONE 1	ZONE 2	ZONE 3	ZONE 4
$\frac{3}{8}$	9.52	100	100	100	100
3/16	4.72	98	98	98	98
No. 7	2.40	77	86	92	97
No. 14	1.20	55	70	87	95
25	0.60	24	44	64	90
52	0.30	12	16	26	32
100	0.15	5	5	5	8
200	0.075	0	0	0	0

Table (3.4) Grading of fine Aggregate used for Permeability tests

3.3.3 Admixtures

Two types of admixtures were used. These were: the Melment L10 manufactured by Hoechst (U.K.) Ltd. which chemically is a sulphonated melamine formaldehyde condensate; and the Cormix SP1 manufactured by the Cormix division of Joseph Crosfield & Sons, Warrington which is a Napthalene sulphonate formaldehyde condensate. These are in categories A and B respectively of the C and C.A. superplasticiser admixture classfications[110]. These two types were chosen because they are easily available and commonly used in the construction industry[111].

Superplasticisers are commonly used either to improve workability or to allow a water reduction in the concrete mix and improve concrete quality without loss of workability[110,112,113,114]. They were administered in both cement pastes and concrete in 5 doses of 1, 2, 3, 4 and 6% by weight of the cement content.

3.3.4 Crude Oil

Kuwait crude oil was used throughout the tests. A chemical analysis was carried out by the chemistry department of this university to identify its chemical composition, table (3.5). Earlier tests[12] had establish that the main properties of the crude oil do not change significantly after contact with concrete.

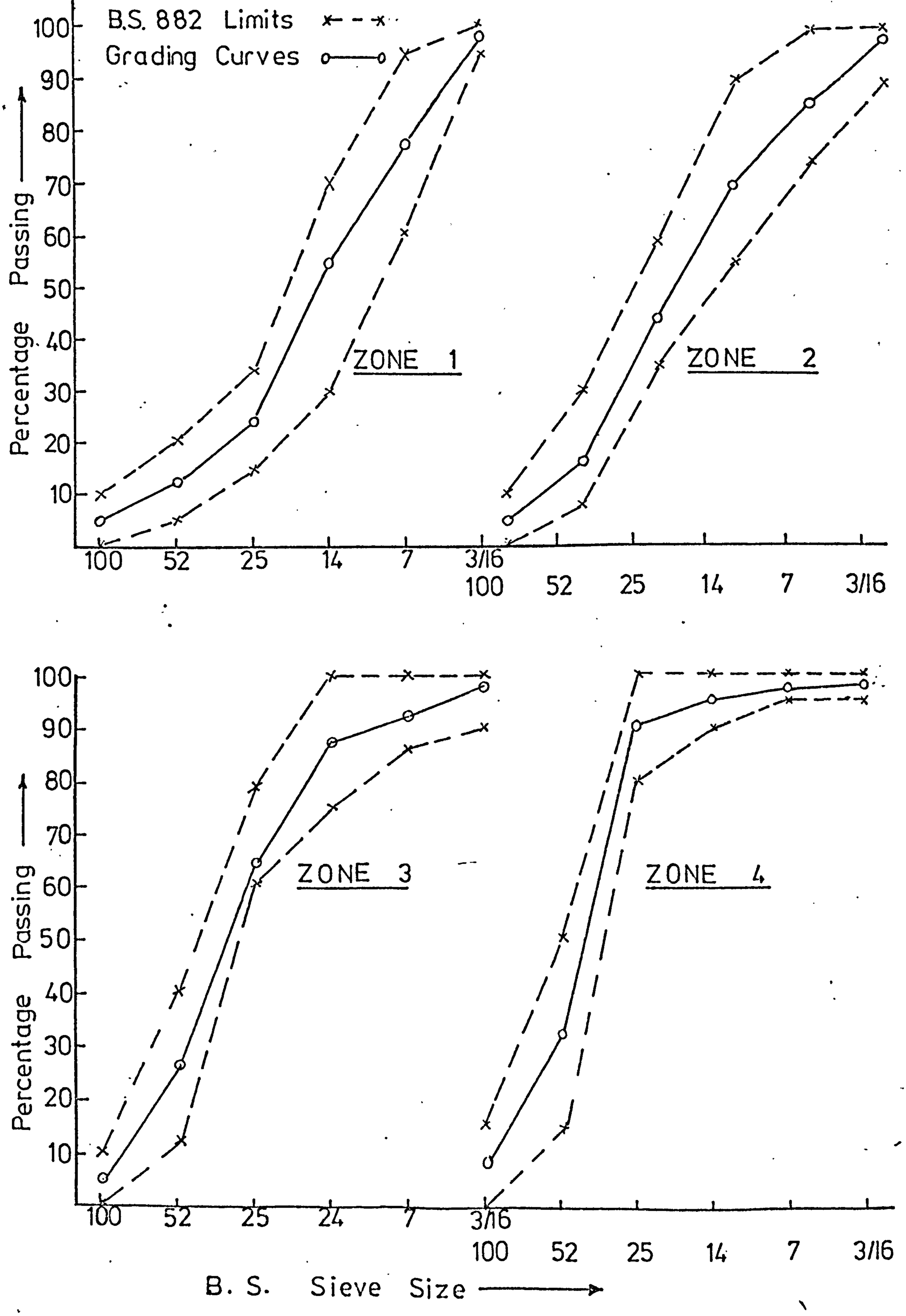

FIG(3.2) GRADING CURVES FOR FINE AGGREGATE USED FOR PERMEABILITY TESTS

1. Distillation upto 300°C (Cumulative % of total volume)

Temperature °C	% Volume (Cumul.)
40 - 80	4.70
80 - 90	9.12
90 - 110	10.22
110 - 120	11.88
120 - 145	14.64
145 - 159	18.51
159 - 165	20.72
165 - 181	34.26
181 - 190	43.10
190 - 200	47.24
200 - 218	59.12
218 - 235	66.03
235 - 255	75.70
255 - 280	85.37
280 - 290	88.96
290 - 295	92.27
295 - 300	100.00

2.	Sulphur Content	2.07 - 2.09%
3.	Moisture content (as H_2O)	1.15%
4.	Calcium content	none detected
5.	Specific gravity (at 16°C)	0.890 - 0.891
6.	Viscosity at 15°C	0.2243 centistokes
	30°C	0.2045 centistokes
	60°C	0.1847 centistokes
7.	Wax content	5.7% by wt.
8.	Surface tension at 16°C	32.17 dynes /cm
9.	Molecular sizes - highly variable	
	ranges 1 to 18Å	
	high occurence of between 5 and 7Å	

Table (3.5) Analysis of Crude Oil

3.4 Preparation of Cement Paste Specimens

3.4.1 Introduction

Many tests have been carried out on cement pastes of high W/C ratios but very few details are available in the literature on the methods used to obtain bleed-free pastes. The two most widely used methods - with modifications - are the high speed mixing utilized by Powers and Brownyard[23], and the rotatory method introduced by Spooner[115]. Spooner's method involves casting the pastes in a completely sealed steel mould which was then rotated at 6 rev/min for 12 to 15 hrs. Though this method gave good results as the variation of W/C ratio along the specimen length shows - fig. (3.3); its use requires vast and costly equipment which was not available.

The method used in this investigation is high-speed mixing. The advantages and disadvantages of this method have recently been reviewed by Markestad[116]. He found that the strength-time relationship and the rates of hydration of HCPs were not affected by the high-speed mixing. The mixer used here is the commercially available Moulinex kitchen-type mixer, having a speed of 18,000 rev./min. and a capacity of about 0.001 m^3. The mixer blade was modified in the laboratory making it broader, thicker and stronger. - plate (3.1)

3.4.2 Casting of Cement Pastes

3.4.2.1 Procedure

The required amounts of cement and water were added gradually into the mixer stirring continuously with a glass rod to avoid coagulation, then, mixed for $1\frac{1}{2}$ minutes, rested for $1\frac{1}{2}$ minutes and mixed again for $1\frac{1}{2}$ minutes. This alternate mixing and resting is continued until the desired mixing time is reached. From results of trial mixes, the minimum required mixing times are shown in table (3.6). After mixing, the pastes were poured into a flat broad basin and vibrated for upto 5 minutes, being continuously turned with a trowel, They were then poured into their moulds in two layers each layer being vibrated for about 1 minute. The tops were trowelled flat after about 2 hours and the top plate of the mould tightly screw on. The moulds were then inverted and covered with a polythene sheet for about 24 hours, after which the specimens were demoulded and stored in water at a constant temperature of $16 \pm 1^{o}C$ for 27 days.

W/C Ratios	Mixing times (minutes)	
	OPC	SRPC
0.4	4½	3
0.5	7½	7½
0.6	10½	10½
0.7	13½	15

Table (3.6) Mixing times for cement pastes

3.4.2.2 Effectiveness of the Mixing Technique

The effectiveness of this method of mixing and casting can be judged from the variations of W/C ratio with depth through the specimen. To verify this, test prisms (50 x 50 x 150 mm) were cast at W/C ratios of 0.5 and 0.6 for OPC and SRPC, using two processes: the high-speed mixer and a conventional laboratory Hobart bench mixer - plate (3.2). In the Hobart, the pastes were mixed for 30 and 45 minutes for W/C ratios of 0.5 and 0.6 respectively. 22 hours after casting, the samples were demoulded and with a diamond drill, 32 mm (1¼") diameter cores were taken right through each specimen depth. The cores were then sliced into 10 approximately equal parts with a diamond saw. Each part was weighed in air, in distilled water and then again in air to show whether it had absorbed any water. After igniting to 1,000°C and reweighing, the total water content and the effective W/C ratio were obtained. The variations of W/C ratio with depth for each specimen is illustrated in fig. (3.4).

The maximum variation in the compressive strength of OPC paste was found to be 13.4% and 15.2% for 0.5 and 0.6 W/C ratio respectively for pastes mixed with the Hobart mixer but only 9.5 % and 10% for those mixed with the high speed mixer. Over the middle 50 mm length of the specimens, the variation is only 2.6%.

The drawback of the high speed mixer is that it cannot be used effectively for W/C ratios below 0.40 - this requires a lower speed mixer. For W/C ratios above 0.70, the paste becomes hot and a cooling agent would be necessary to surround the mixing bowl[116].

PLATE (3.1) HIGH SPEED MIXER

PLATE (3.2) HOBART – BENCH MIXER

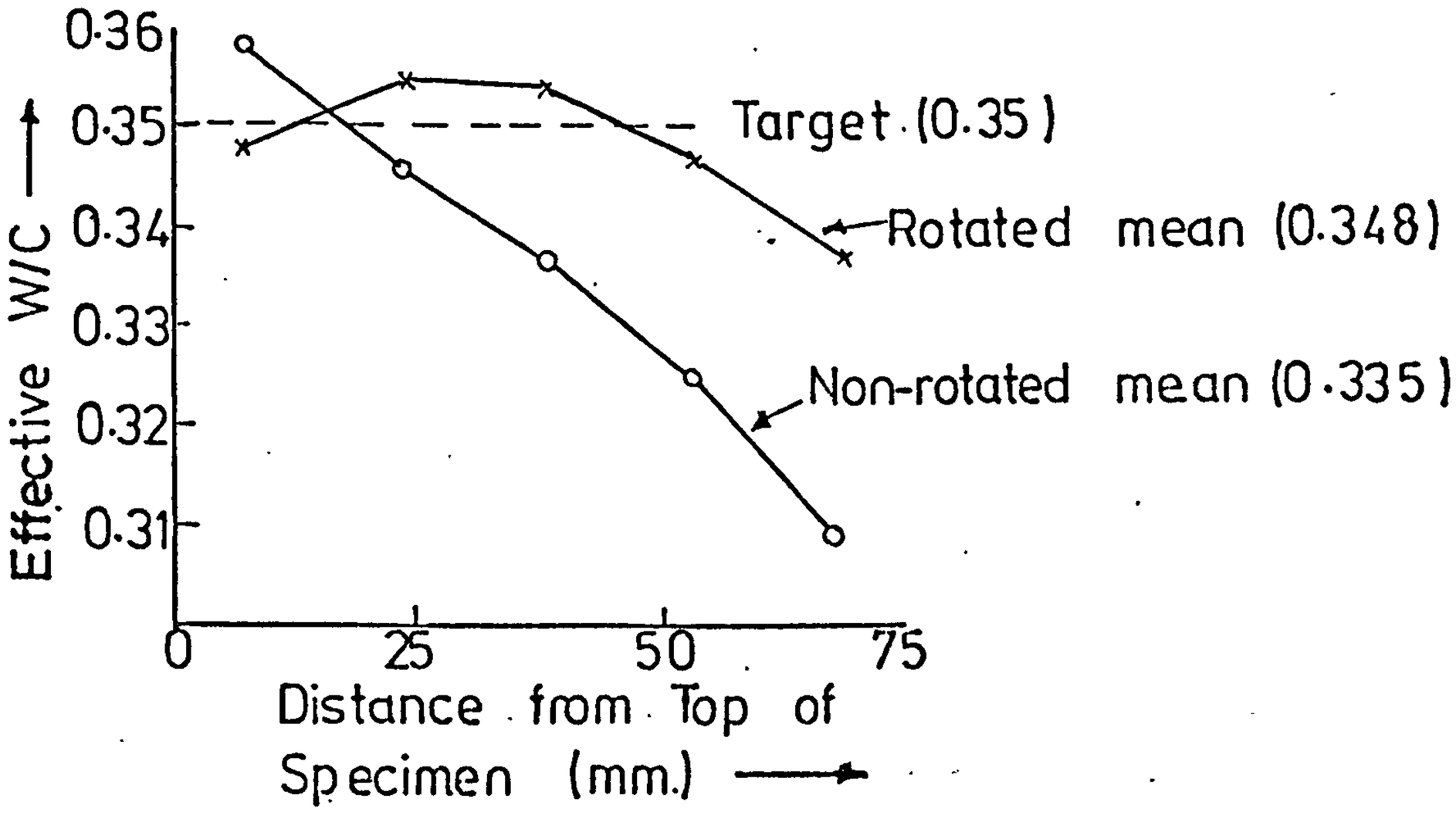

FIG (3.3) VARIATION IN W/C RATIO FOR ROTATED & NON-ROTATED HCP SPECIMENS[115]

HIGH SPEED MIXER ×——×

HOBART MIXER o——o

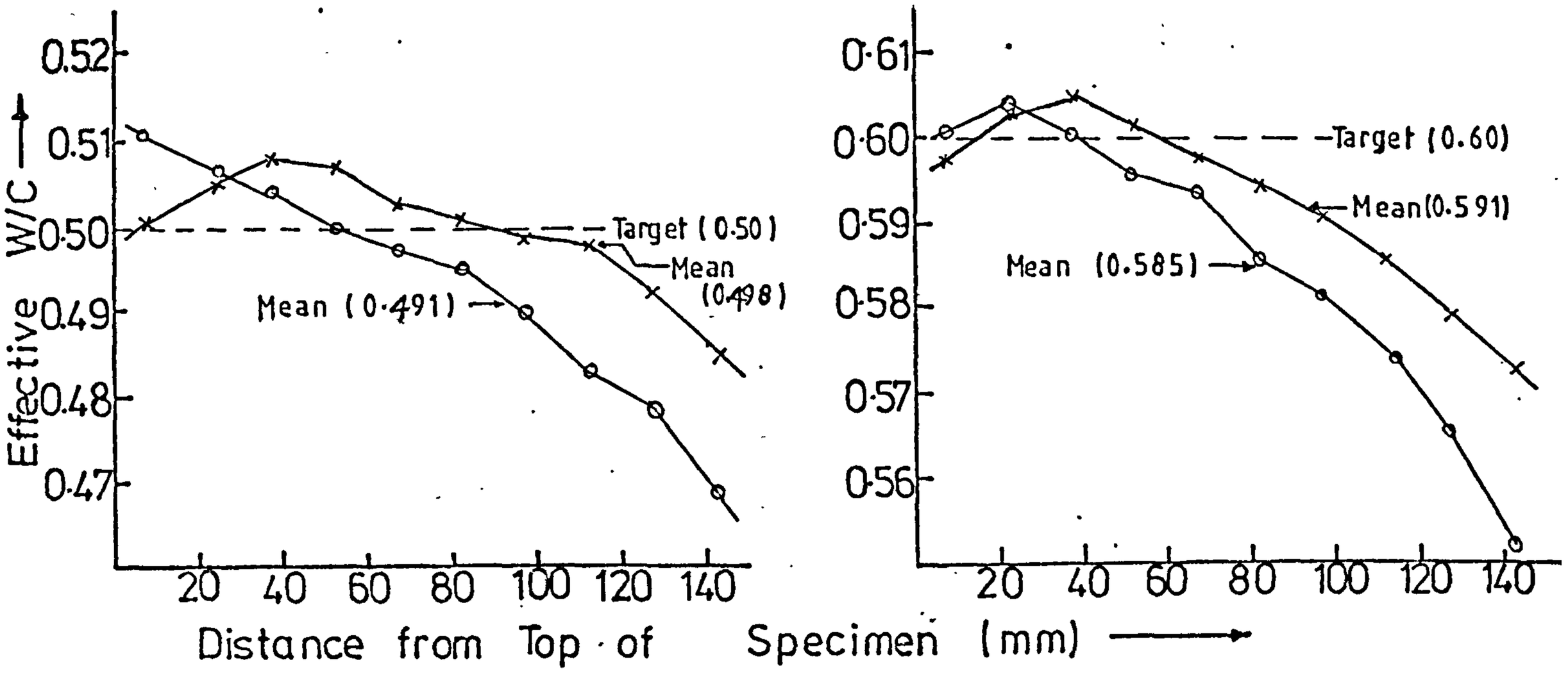

SRPC PASTES

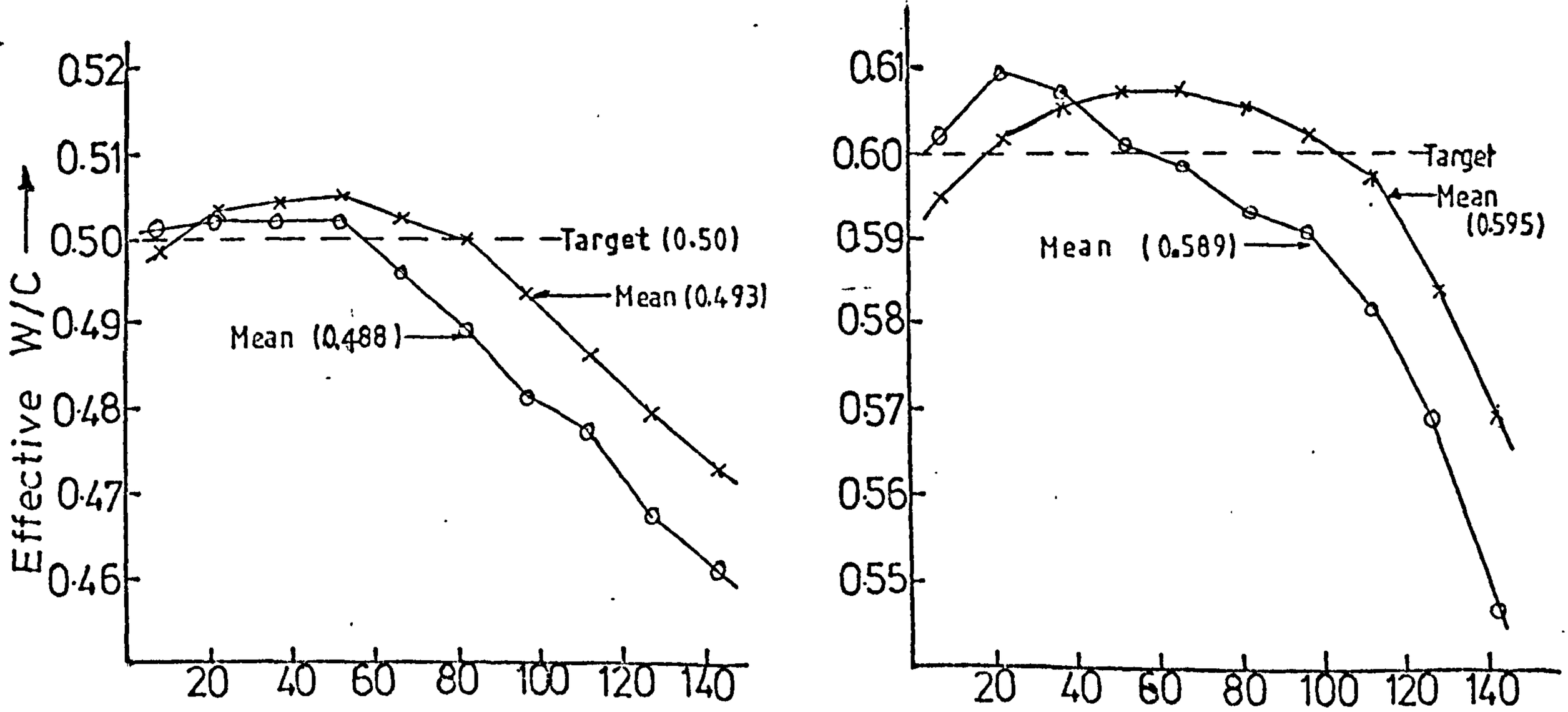

OPC PASTES

FIG(3.4) VARIATIONS IN W/C RATIO FOR HCPS MIXED WITH HIGH-SPEED & HOBART MIXER

3.4.3 Sizes and Shapes of the HCP Specimens

The specimens were made as small as possible in order to get them saturated with oil in a short time. The specimens used for the various investigations were:

1. Compressive strength - 50.8 mm (2") cubes. The crushed specimens were used for porosity and density studies.
2. Permeability tests - 100 mm dia by 25 mm thick discs.
3. Modulus of elasticity - 50 x 50 x 150 mm prisms in completely sealable steel moulds - plate 3.3. This provided a length to width ratio of 3 - as in the concrete specimens - and a gauge length of 50 mm.

3.5 Preparation of Concrete Specimens

3.5.1 Concrete Mixes

W/C ratio is the principal factor governing the mix design for both the permeability test samples and for tests on mechanical properties. Mix design charts of Teychenne et al[117] were used as a guide for obtaining the mix proportions for both trial and final mixes. The mixes were divided into two groups:

1. Permeability - 137 mixes covering various W/C ratios, cement contents, workabilities, admixture concentrations and 4 grading zones of B.S. 882:1965. Actual mix proportions are given in Chapter 5.
2. Mechanical properties - 4 W/C ratios were used with a medium workability of 30 - 60 mm. The mixes are given in table (3.7), and the mixes containing admixtures were designed according to the recommendations of Blakey[112] The mixes given in table (3.7) were used with about 20% of the mixing water removed and 4% by weight of cement content of superplasticising admixture added. The fine aggregate content, passing no.52 B.S. sieve, was increased by 5%. The final mixes are given in table (3.8).

MIX DESIGN.	W/C RATIO	AGGREG. TO CEMENT	CEMENT CONTENT (Kg/m^3)	Proportion by Weight		
				CEMENT	SAND	GRAVEL
M_1	0.4	2.73	575	1	1.20	1.53
M_2	0.5	3.66	460	1	1.65	2.01
M_3	0.6	4.60	383	1	2.21	2.39
M_4	0.7	5.52	329	1	2.76	2.76

Table (3.7) Details of Concrete Mixes for tests on Mechanical Properties - OPC or SRPC

W/C RATIO	AGGREG TO CEMENT	WATER REDUCT. %	EFFECTIVE W/C	CEMENT CONT.	Proportion by Weight		
					CEMENT	SAND	GRAVEL
0.4	2.79	15	0.34	575	1	1.26	1.53
0.5	3.75	17	0.42	460	1	1.73	2.02
0.6	4.71	18	0.49	383	1	2.32	2.39
0.7	5.66	20	0.56	329	1	2.90	2.76

Table (3.8) Details of Concrete mixes, containing 4% Superplasticiser, for tests on Mechanical properties

3.5.2 Casting of Concrete Specimens

The fine and coarse aggregates were generally dried to laboratory room temperature (about 20°C) before use and then knowing the moisture content and absorption, the weight of mixing water was adjusted to bring the aggregates to a saturated surface dry (SSD) condition prior to mixing. Batching was by weight to the nearest 1 gm. Mixing was done in a 1 m^3 horizontal pan mixer with the aggregate and cement mixed alone for 1 minute before the water or water plus admixture was added. The mixing then continued for another $1\frac{1}{2}$ minutes and the slump was taken immediately after mixing.

All the concrete used for the permeability tests was hand mixed, because the quantities were small and it was easier to get the required workability. The procedure was to mix the aggregate and cement thoroughly with a trowel before adding the water or water plus admixture. Part of the mixing water was withheld and after 1 minute of mixing, further water was added (sometimes above the calculated design value) as necessary, in order to obtain the required workability. The total mixing time was approximately 3 minutes and the slump was measured immediately.

The mixed concrete was poured into moulds in 2 layers, each layer being table-vibrated until no more air bubbles emerged but not long enough to cause segregation. The faces were trowelled flat after about 2 hours and covered with polythene sheets. They were normally demoulded after 20 - 24 hours.

3.5.3 Shapes and Sizes of Concrete Specimen

The specimens used for the permeability tests were 150 mm in diameter and 50 mm high - plate (3.4) and for the compressive tests 100 mm or 102 mm (4") cubes; and for the elastic modulus tests 100 x 100 x 300 mm prisms.

3.6 Curing

After demoulding the concrete specimens were stored in water tanks in the laboratory at 20 ± 3°C; and the HCPs in water in the constant temperature room (CTR) at 16 ± 0.5°C for 27 days prior to any tests or further treatments.

Concrete specimens used for the permeability test were dried at a temperature of 55 ± 2°C in a mechanically ventilated oven to a constant weight

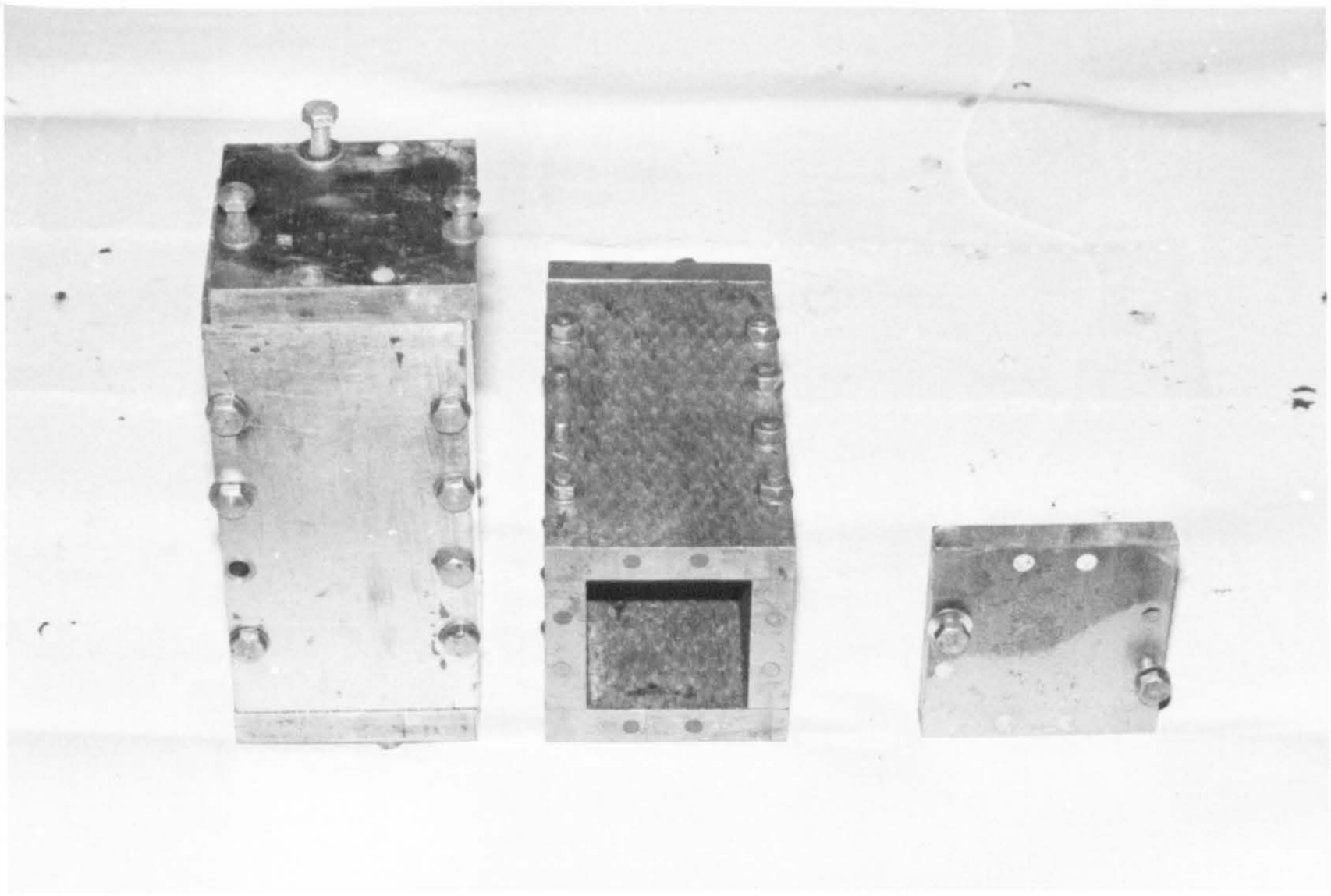

PLATE(3.3) STAINLESS STEEL MOULDS FOR ELASTIC MODULUS OF HCPs — 50 × 50 × 150mm.

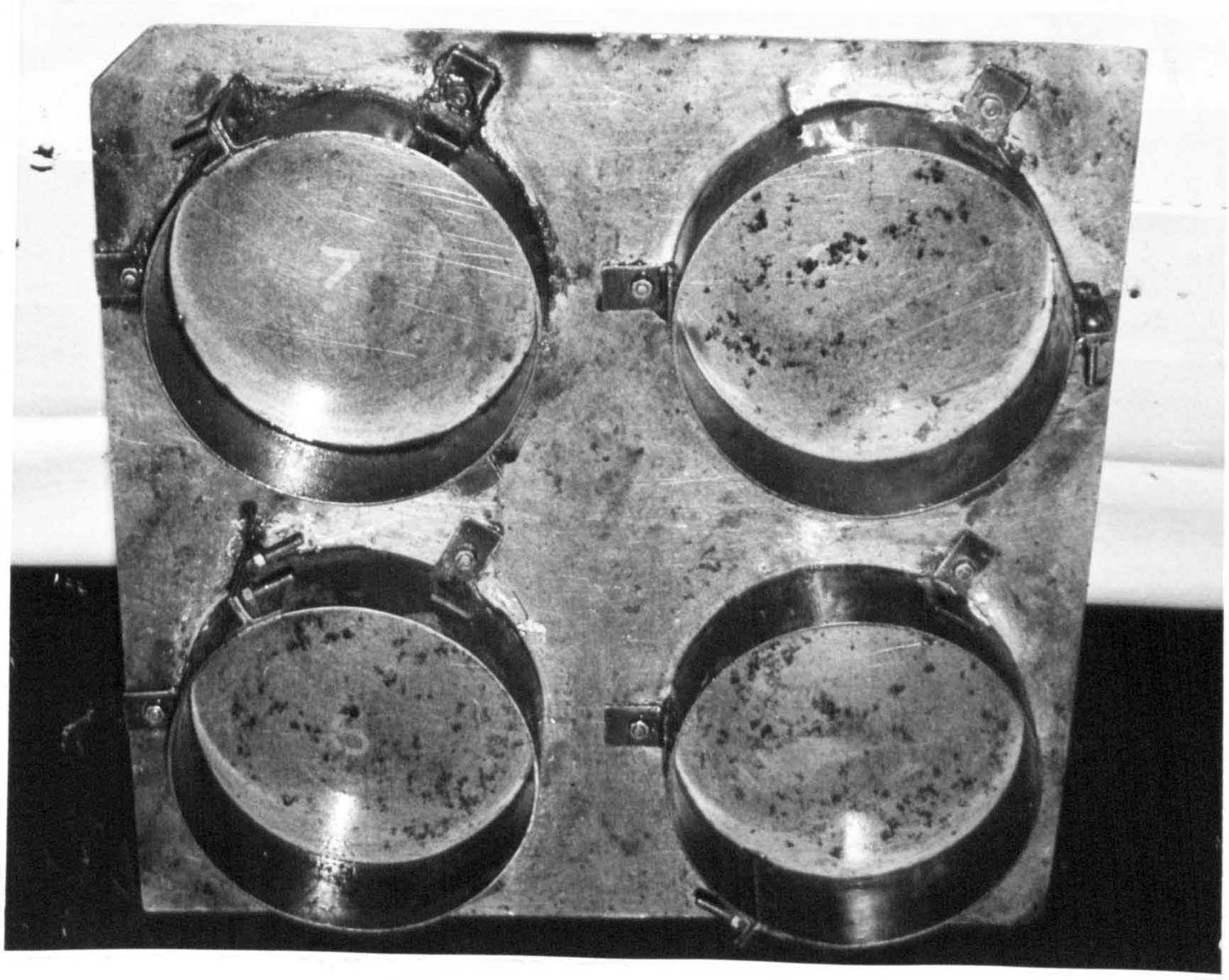

PLATE(3.4) STEEL MOULDS FOR CONCRETE PERMEABILITY SPECIMENS

or until the weight loss was about 1 gm/day. This normally took 12 - 15 days. The samples used for the mechanical property tests were dried at 105 ± 1°C until the weight loss was about 1gm/day. This normally took 18 - 21 days. The oven temperatures were raised or lowered at a rate not greater than 8°C/hour to avoid thermal cracking of the specimens. After drying, the specimens were allowed to cool to room temperature. Some of the samples were then put in a crude oil pressure vessel - plate (3.5) and pressurized for 3 months, while others were completely sealed in polythene bags and kept in the CTR. Oil pressures of about 0.345 N/mm^2 (50 psi) and 0.827 N/mm^2 (120 psi) were used for soaking the permeability specimens and specimens for tests on mechanical properties respectively. After the first 3 months of crude oil soaking, the specimens were stored in a shallow tank of oil at atmospheric pressure prior to testing.

HCPs were similarly treated except that all were oven-dried to 105°C with the samples completely wrapped with aluminium foil to ensure a more uniform temperature in the specimen before any water is allowed to dry out. When the specimens reached the uniform temperature of 105°C - usually in about 30 hours - they were quickly unwrapped inside the oven and left to dry out to a constant weight usually within another 48 hours. This procedure was found to minimize cracking.

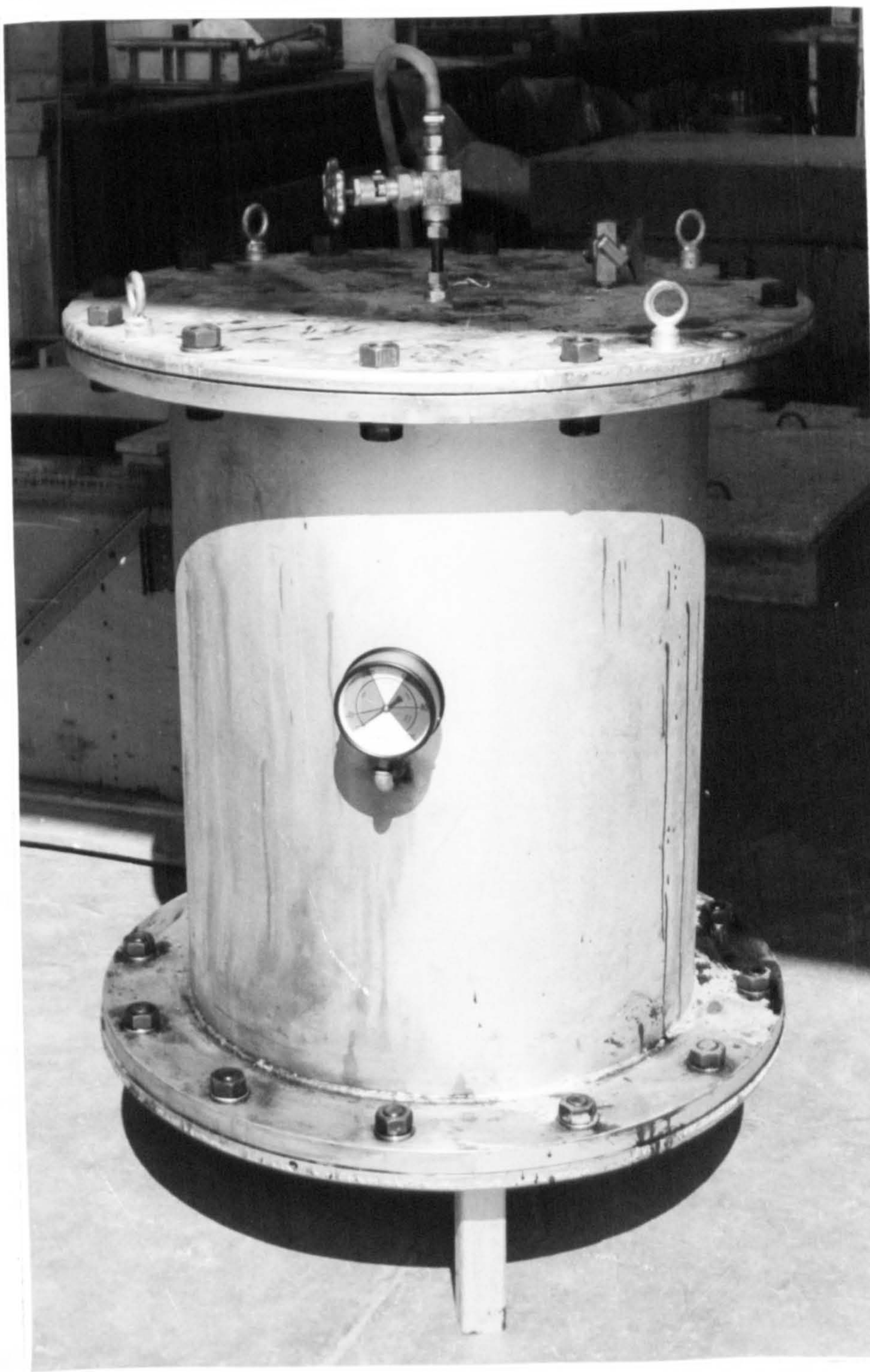

PLATE(3.5) CRUDE OIL PRESSURE VESSEL

CHAPTER 4

PORE STRUCTURE ANALYSIS OF HARDENED CEMENT PASTE (HCP) AND CONCRETE

4.1 Introduction

It is well established that many of the physical and mechanical properties of materials depend on the shapes and sizes of the pores and on the distribution of the volume and surface area of the pores. It is also well known that it is the permeability of HCP and concrete which determines their environmental resistance and that pore size distribution plays a controlling role in permeability.

The characteristics of the pore structure of a material are defined by:

1. Porosity (cc/cc or sometimes in cc/gm) is the fraction of the total volume which is occupied by pores. The pores may be open or closed, open pores may be continuous or 'dead-ended'.

2. Specific surface area (m^2/gm) is the area of the accessible surface contained in unit mass of the solid. In principle, this can be derived from the porosity and pore size distribution.

3. Pore size distribution (cm^3/g) is the fraction of total open pore volume in which the pores are within a stated size range. Actual measurement of pore size distribution is very difficult or even impossible since it is complicated by the shape and the ways in which the pores are interconnected. Usually, to simplify the analysis, idealised pore shape models are assumed.

4. Pore radius. This is likely to vary along any given pore and in the present analysis, it is given by the hydraulic radius, r_h , which is the pore volume divided by the surface area.

Water-vapour adsorption is used in this investigation to study all the above properties of 20 HCPs using Ordinary Portland Cement (OPC) and Sulphate-resisting Portland Cement (SRPC), some containing a superplasticiser admixture - Cormix SP1. 2 OPC pastes had been previously saturated with crude oil.

4.2 Experimental Programme and Technique

4.2.1 Experimental Programme

4.2.1.1 Cement Pastes

The aim of the investigation is to study the pore structure of HCPs as a means of understanding more clearly the crude oil permeability and other physical properties of crude oil saturated HCPs and concrete. The test programme is summarised in table (4.1). In addition to the measurement of pore structure, the density - wet and dry, the chemically combined water content and the degree of hydration were also measured.

All the samples were initially cured in water for 27 days as described in Section 3.6. Samples 1 - 10 and 15 - 20 were D-dried before adsorption ie. they were dried to constant weight at 5×10^{-4} mm Hg water vapour pressure, kept at a temperature of $-79^{\circ}C$ by solid carbon dioxide[37]. Samples Nos. 11 and 12 were oven-dried to study the effect of oven-drying on the pore structure. Samples 13 and 14 were oven-dried then saturated with crude oil (for about 4 months), then oven-dried again. This was done to investigate the effect of crude oil saturation on pore structure.

4.2.1.2 Concrete

The total porosity of the standard concrete samples used for the various test was calculated as described later in section 4.5. The results are related to most other measured properties of the concrete in chapters 5 - 7 of this thesis.

4.2.2 Apparatus for the Measurement of Pore Structure of HCPs

4.2.2.1 D-drying Apparatus

Most of the experiments were done with D-dried[37] pastes in which all water not chemically bound is removed. The apparatus used was similar to that of Copeland and Hayes[37], and is illustrated in fig.(4.1) and plate (4.1). It consists of a vacuum desiccator connected to the side arm of a water glass trap by a 20 mm diameter glass tubing. The trap is immersed in a Dewar-jar filled with dry ice (solid carbon-dioxide) which is at a temperature of $-79^{\circ}C$

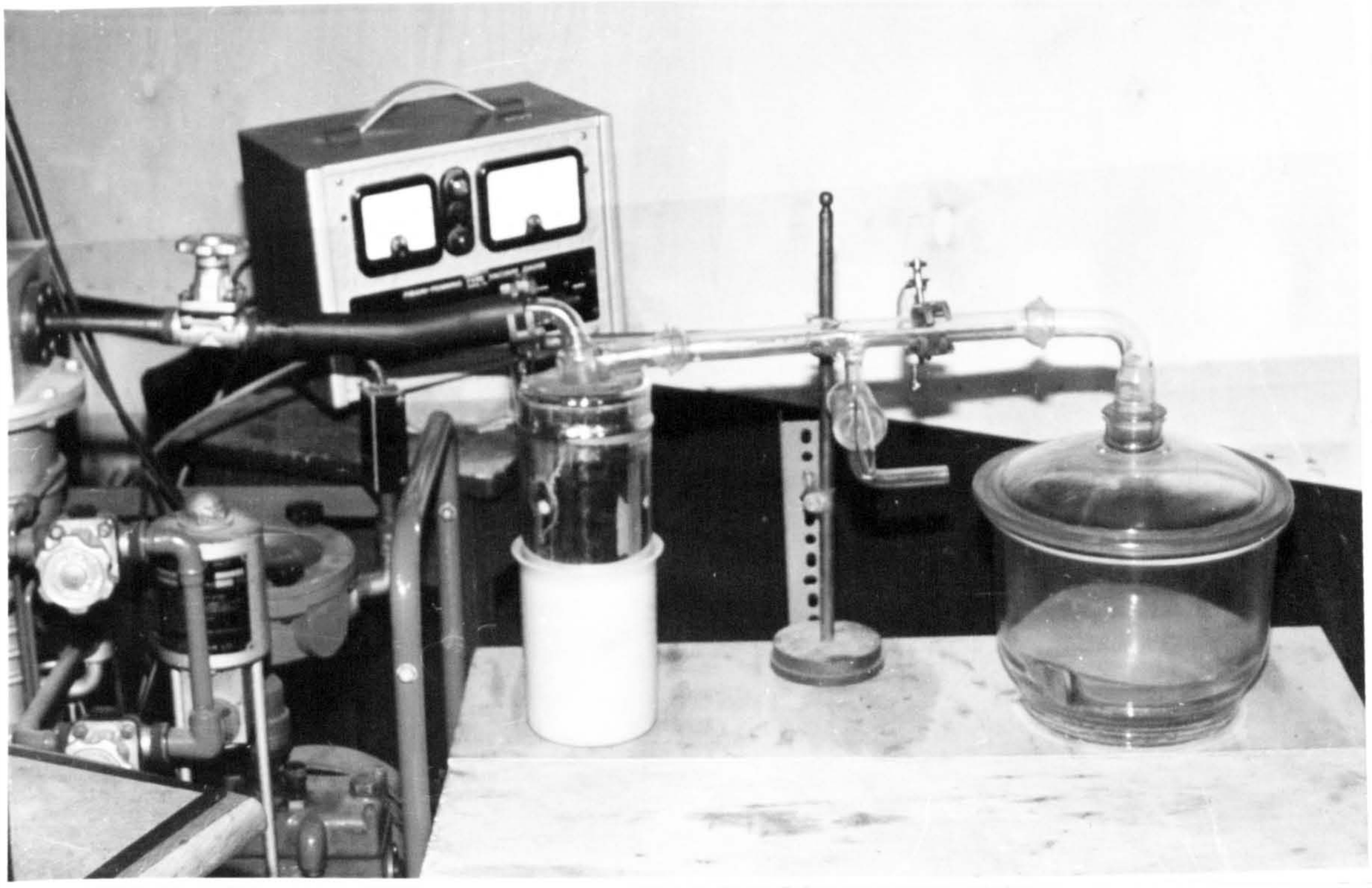

PLATE (4.1) D - DRYING APPARATUS

1. Vacuum Desiccator
2. HCP Samples
3. 30mm glass tubes
4. Air in-let
5. 20mm glass tube to vacuum pump
6. Foam cover
7. Dewar Jar
8. Solid CO_2 + Alcohol
9. Water trap

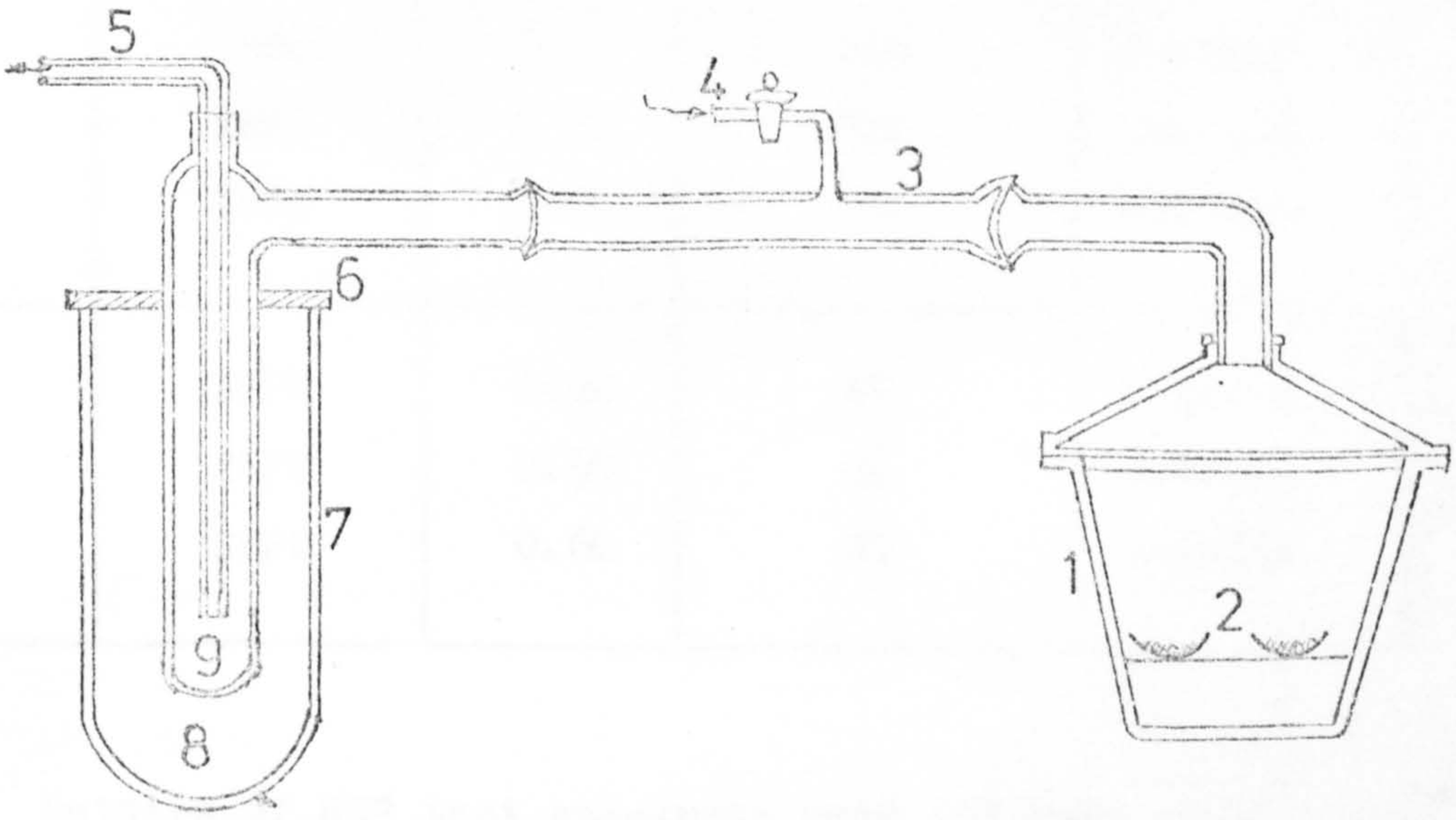

FIG (4.1) D - DRYING APPARATUS

No.	PASTE DESIGNATION	TYPE OF CEMENT	W/C RATIO	ADMIXTURE CONCENTRATION	METHOD OF DRYING
1	OP30	OPC	0.30	Nil	D-dried
2	OP40	OPC	0.40	Nil	D-dried
3	OP50	OPC	0.50	Nil	D-dried
4	OP60	OPC	0.60	Nil	D-dried
5	OP70	OPC	0.70	Nil	D-dried
6	COP4-4	OPC	0.40	4%	D-dried
7	COP5-4	OPC	0.50	4%	D-dried
8	COP6-4	OPC	0.60	4%	D-dried
9	COP4-1	OPC	0.40	1%	D-dried
10	COP4-2	OPC	0.40	2%	D-dried
11	OVP40	OPC	0.40	Nil	Oven-dried
12	OVP60	OPC	0.60	Nil	Oven-dried
13	OSP40	OPC	0.40	Nil	Oven-dried & Oil. Sat.
14	OSP60	OPC	0.60	Nil	
15	SR40	SRPC	0.40	Nil	D-dried
16	SR50	SRPC	0.50	Nil	D-dried
17	SR60	SRPC	0.60	Nil	D-dried
18	CSR4-4	SRPC	0.40	4%	D-dried
19	CSR5-4	SRPC	0.50	4%	D-dried
20	CSR6-4	SRPC	0.60	4%	D-dried

Table (4.1) Details of HCP test specimens used for Pore Structure Measurement

and with methanol alcohol to retard the evaporation of the ice. The trap is connected to a rotary-diffusion vacuum pump capable of holding the vacuum in the system down to below 10^{-5} mm Hg.

4.2.2.2 Adsorption Apparatus

The adsorption apparatus which was a 'net-work' of glass tubings, is illustrated schematically in fig. (4.2) and plate (4.2). It consists of four distinct components: a water-vapour supply system, 2 sets of manometers for pressure reading, 3 glass tubes for the sample compartment and a temperature regulating system.

The water-vapour supply system consists of two glass tubes A and B, connected to a 5 mm diameter glass mercury manometer - C. This manometer is used for checking the saturation vapour pressure of the water in A. It is connected to the sample compartment through 5 mm stop-cocks 10, 13 and 14, and to the 2 manometers through 11 and 12 and the vacuum pump through 4 and 5. The manometer, D, contains mercury while E contains apiezon - B oil recommended for use in high vacuum manometers. This oil is 15.6 times lighter than mercury and pressure differentials are therefore, magnified 15.6 times and is used in detecting very small pressure changes. The manometers are connected to the water-vapour supply system through stoppers 6 and 7.

The sample compartment comprises 3 glass tubes, F, each approximately 700 mm long and 20 mm in diameter. Each tube is closed at the top with a glass-stop head carrying a hook and at the bottom by a 10 mm dia. horizontal tube, G, which carries Parani, H, and Penning, J, vacuum gauge heads. The Parani can read pressures down to 1×10^{-3} mm Hg and the Penning down to 1×10^{-6} mm Hg. The horizontal tube is connected to the vacuum pump by stoppers 1 and 2 and to the manometers and water-vapour supply system. Each sample tube carries a silica spring balance, K, of the McBain- Bakr type[118] hung on to the hook via a long hooked glass rod, X. The springs have sensitivities between 40 - 75 cm/gm and capacities of 0.5 gm. The paste samples were suspended on to the springs with thin walled glass buckets of 0.12 gm maximum weight.

The equipment was contained in a wooden cabinet kept at 30 $\pm$ 0.2°C by means of a tuolene-mercury thermostat, P; fan and heater unit, M; and a temperature control unit, N; which is outside the cabinet. Three thermometers were positioned at points marked T. During the course of the experiment the

1-14	Glass Stop-cocks
A, B	Water vapour Supply unit
C, D	Mercury manometers
E	Oil "
F	Sample compartments
G	Connecting glass tubes
H	Parani vacuum gauge head
J	Penning " " "
K	Silica spring balance
M	Fan & Heater unit
N	Heat control unit
P	Mercury-tuolene thermostat
R	Reference marks
T	Thermometers
X	Glass hooks
S	HCP Samples
W	Wooden Cabinet

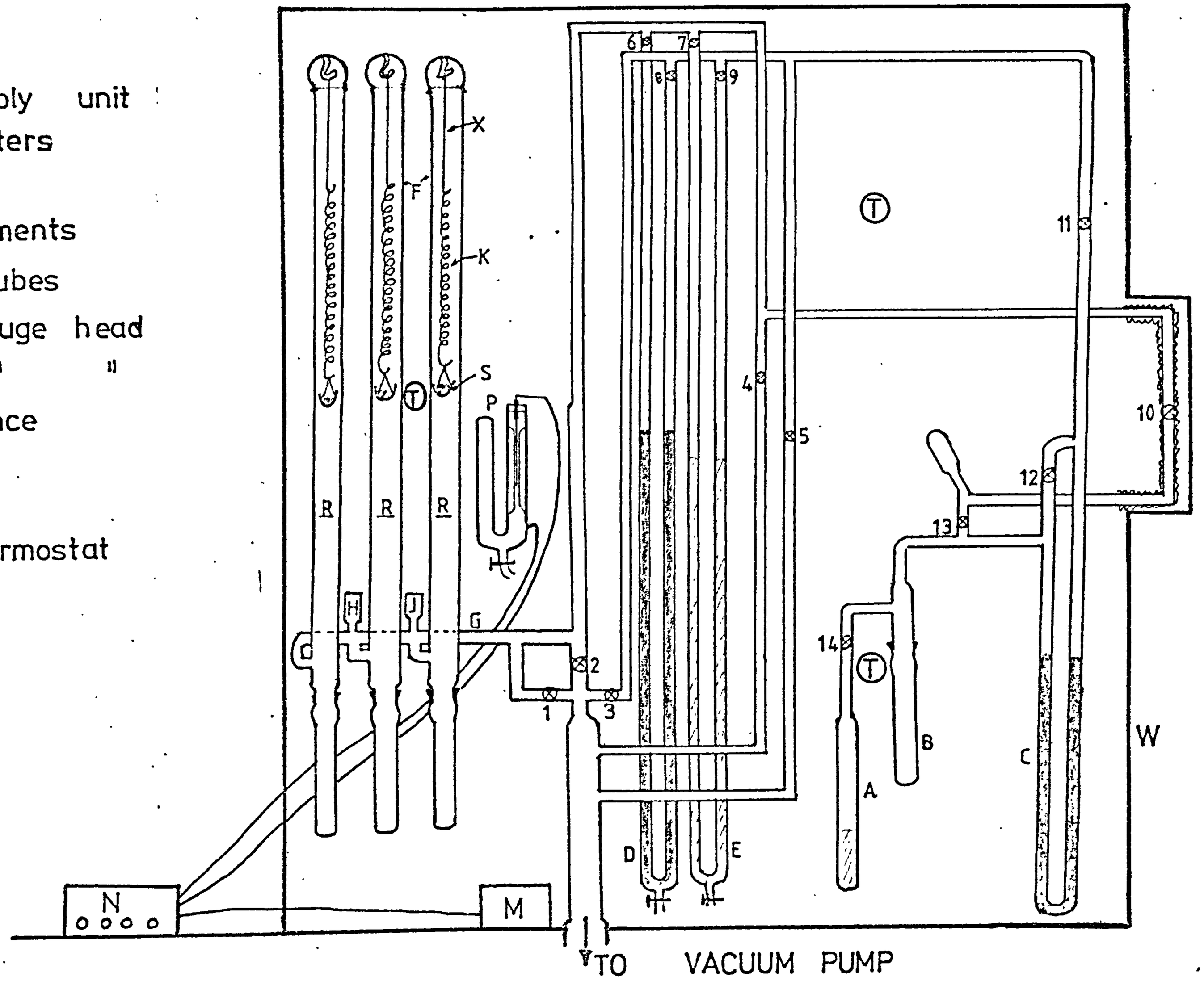

FIG(4.2) WATER-VAPOUR ADSORPTION APPARATUS

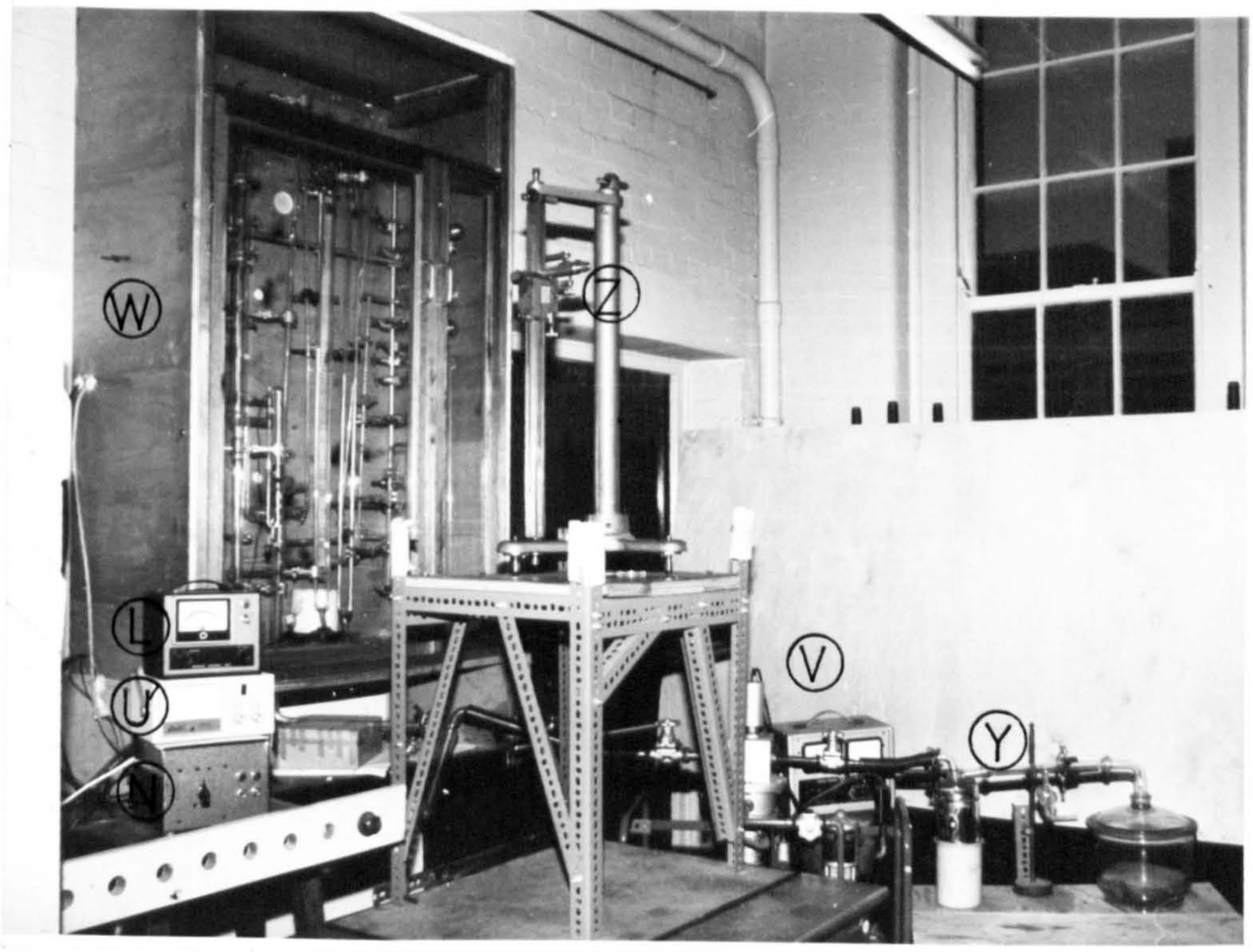

GENERAL SET - UP

W. Wooden cabinet

L. Parani gauge

U. Penning »

N. Heat control unit

V. Vaccum pump

Y. D-drying apparatus

Z. Cathetometer

VIEW OF INSIDE CABINET

PLATE (4.2) WATER VAPOUR ADSORPTION APPARATUS

cabinet was hardly opened. The water-vapour was let into the sample compartment by carefully adjusting the stop-cock 10. The extension of the springs, the thermometer and manometer readings were taken from outside the cabinet by means of a cathetometer - plate (4.2). The cathetometer has an accuracy of 2×10^{-3} cm, hence the silica spring - cathetometer combination easily provides the desired accuracy of 1×10^{-4} gm.

4.2.3 Test Procedure - HCPs

4.2.3.1 General Properties

The measured HCP properties were: density (wet and dry); W_c, the evaporable water content; W_n, the chemically combined water content and the degree of hydration, $M = W_n/W_n^o$ where W_n^o is the chemically bound water of a fully hydrated cement paste.

At the end of the curing period of 28 days, the 50 mm sample cubes were tested for compressive strength and part of the crushed samples were then used for determining the above paste properties. Triplicate samples, each weighing between 25 and 30 gms. were taken from 2 cubes and from a permeability test sample. They were weighed in a saturated surface dry (SSD) state and again while suspended in distilled water so that their volumes could be determined. The samples were then placed in an air circulated oven in which the temperature was controlled at $105^{\circ}C \pm 0.5^{\circ}C$. When the loss in weight is constant, normally within 48 hours, the samples were weighed again and ignited at $1,000^{\circ}C$ for about 2 hours. After cooling to about $60^{\circ}C$ they were weighed again. All weighings were made to the nearest 1 mg.

4.2.3.2 D-drying

Part of the crushed samples from the compressive strength tests were further crushed to pass a B.S. sieve No. 25 and retained on No. 52 sieve. The grinding was performed as quickly as possible to minimize exposure to the atmosphere which could lead to carbonation of the pastes. About 2.5 gms. was placed in flat plastic containers and put in the vacuum desiccator of the drying apparatus described earlier at a pressure of about 3×10^{-6} mm of mercury. After the first 8 days of drying, the samples were weighed daily and were considered to be at or near constant weight when the weight loss was 1 mg/gm of sample/day. At the end of the drying period, part of the sample

was used for an adsorption test while the rest was ignited at 1,000°C for the determination of W_n - the chemically bound water. This value of W_n was only used for comparing with the value obtained from pastes oven-dried to 105°C - Section 4.2.3.1 - before ignition. The difference between these two values of W_n also shows the extent of drying obtained with the D-drying technique.

4.2.3.3 Adsorption

The adsorption apparatus - fig. (4.2) was first used to de-air the water as follows: About 5 cc of distilled water was put in glass B. A was surrounded with liquid nitrogen in a Dewar jar. All stop-cocks, except 3, 5, 11, 12 and 14 (ie. those connecting the water-vapour supply unit to the vacuum pump) were closed. The system was then evacuated for about 2 hrs. All stop-cocks except 14 were then closed. Water in B then evaporated and condensed in A. The reverse process was made with B being surrounded with liquid nitrogen, and the pump ran for 2 hours. The water condensed back into B. The water was finally condensed back into A by the previous process and stopper 14 closed. The water then in A was considered pure and completely air-free. To check this the cabinet was brought to 30°C with the system under the lowest possible vacuum pressure of about 4×10^{-6} mm Hg. All stoppers were then closed and 14 opened. The pressure difference in manometer C should be approximately 31.8 mm Hg - the saturation vapour pressure of water at 30°C. Stop-cock 14 was then closed and the water was ready for use.

About 0.3 gm of the dried sample was weighed out inside the glass bucket to the nearest 1×10^{-5} gm using the calibrated silica-spring and cathetometer. The total weight of the sample and bucket being about 0.45 gm. The sample was then quickly but carefully transfered into the sample compartment (3 samples were tested concurrently). All glass stoppers were then tightly screwed to avoid leaks, each joint being treated with a high vacuum silicone grease. With all stop-cocks open except 14, the whole system was degassed for 48 hours under a vacuum pressure down to below 1×10^{-5} mm Hg. The water-trap at the vacuum pump was surrounded with dry ice thus simulating the D-drying technique. After degassing, stop-cocks 1 to 5 and 10 were closed; 14 opened and the temperature adjusted to 30°C. The adsorption run was carried out by opening stop-cock 10 thus letting water-vapour into the sample compartment. The samples take up the vapour and the spring balance extends. The sucessive differences in reading between a point of contact of the spring and bucket and a reference point, R, gives the extension of the spring within the

period. The difference in levels of the mercury or oil manometers gives the vapour pressure, P, this when divided by the saturation vapour pressure, P_s, and substracted from unity gives the relative vapour pressure, P/P_s. Readings of the spring balance were taken every 24 hours, and continued until the sample was in equilibrium at the particular P/P_s value. The pressure was then changed by letting in more water-vapour and readings taken continuously again. Usually each test was carried out at approximate P/P_s values of 0.05, 0.10, 0.15, 0.20, 0.40, 0.60, 0.80 0.90 and 1.0.

For six samples, corresponding to 2 test runs, desorption runs were carried out - for OPC samples of W/C ratios = 0.3, 0.4 and 0.5 and SRPC pastes with W/C = 0.4, 0.5, and 0.6.

4.3 Analytical Procedure - HCPs

4.3.1 General Properties

The various general properties stated in section 4.2.3.1 were calculated thus:

Vol. of the HCP, $V = W_a - W_w$ (cm^3) (4.1)

Density of the HCP, (SSD), $D_s = W_a/V$ (g/cm^3) (4.2)

Density of the HCP, (105^oC) $D_d = W_d/V$ (g/cm^3) (4.3)

wt. of admixture in sample, $A_w = k \times C$ (g/cm^3)

Wt. of evaporable water in sample,
$W_e = W_a - W_d$ (gm) (4.4)

% volume of W_e or T. porosity (105^oC)
$P = W_e/V \times 100\%$ (4.5)

Wt. of non-evaporable water, $W_n = (W_d - W_i) - A_w \cdot A_i - I_o \cdot C$ (gm)

Wt. of cement in ignition product $C^1 = W_i - A_w \cdot A_i + I_o C$ (gm)

Wt. of original cement in sample $C = C^1/(1 - I_o)$ (gm)

Wt. of W_n/gm of cement $= W_n/C$ (g/g)

Degree of Hydration, $m = W_n/W_n^o \times 100\%$ (4.6)

The following values were determined and used for the various constants

A_i = 0.148 for Cormix SP1 superplasticiser

I_o = 1.4% for OPC pastes

= 1.5% for SRPC pastes

W_n^o = 0.232 g/g for OPC pastes

= 0.230 g/g for SRPC pastes

Numerous values for W_n^o/C were found in the technical literatures viz: 0.23[70], 0.218[55], 0.235[119], 0.215[121], 0.232[120] etc. These values varied because many factors tend to influence W_n^o, such as method of drying, cement composition and, slightly, carbonation. In the present investigation, numerous determinations of W_n were made at 2 W/C ratios and at 28 days, 3 months, 6 months, 12 months and 18 months. The value of W_n^o/C was obtained by plotting W_n/C against 1/t and extrapolating to 1/t = 0 (t = time in days). This gave 0.232 ± 0.005 for OPC and 0.230 ± 0.005 for SRPC.

Equ. (4.5) above assumes that the amount of evaporable water at 105°C measures the porosity of HCP, and this is one of the basic features of Powers' model[23,24]. An alternative is the Feldman's model which rejects this assumption on the basis that some of the evaporable water is interlayer water and functions as part of the solid[39]. Powers model was adopted throughout this thesis but if Feldman's model was used it would affect the results of dry density and porosity quantitatively rather than qualitatively.

4.3.2 Analysis of HCP Pore Structure

4.3.2.1 Introduction

Many adsorption methods are presently used to analyse the pore structure of porous materials. Few of these methods are able to give a complete pore structure distribution which is required in determining permeability. For example the mercury porosimetry method gives only entry pore diameters and measures pores of diameter above 100Å.

For the present investigation, the adsorption isotherms were analysed

by the two methods developed by Brunauer and co-workers - the "MP-method" - for the analysis of micropores[61] ie. pore diameters below 16Å and the "corrected-modelless method"[60] for pore diameters 16 Å and greater. The theories of these two methods and their analytical procedures are briefly discussed below. Reference should be made to the original papers for a full theoretical description which is considered beyond the scope of the present research.

4.3.2.2 "The Corrected-Modelless Method" - Analyses of the Wide-pores

This is based on Kelvin's thermodynamic equation for capillary condensation in a cylindrical capillary[53].

$$S = -\frac{1}{\gamma} \int_{a_h}^{a_s} RT \quad P/P_s \, da \qquad (4.7)$$

where a_h and a_s are the number of molecules adsorbed at the beginning of the hysteresis loop[57] and at saturation respectively; T is the absolute temperature, ^oK; R is the universal gas constant; γ, the surface tension of the liquid condensed in the pore. Brunauer and co-workers divided the hysteresis loop region of the isotherm into a number of intervals of P/P_s, each representing a group of cores - ie. that part of the pore that fills up by capillary condensation. Each interval was then integrated to obtain the core surface of the group:

$$S = K \int_{v_{i-1}}^{v_i} (-\log P/P_s) \, dv \qquad (4.8)$$

where dv is the volume of the adsorbate adsorbed or desorbed from the i-group of cores (cm^3/gm); S_i is in m^2/gm and

$$K = \frac{2.303}{\gamma} \cdot R \cdot T \qquad (4.9)$$

If the relative vapour pressure, P/P_s, intervals are taken sufficiently small, a plot of log x against V will approximate a straight line. Hence equ. (4.8) becomes:

$$\Delta S_i = \frac{K \ (-\log P/P_s)\, i + (-\log P/P_s)\, i-1}{2} (v_i - v_{i-1}) \qquad (4.10)$$

The terms in equ. (4.10) before $(v_i - v_{i-1})$ are constant for each core group hence:

$$\Delta S_i = C_i \cdot \Delta v_i \qquad (4.11)$$

The ratio $\Delta v_i/\Delta S_i$ is the hydraulic radius, r_h, of the core group. The analysis of the core group proceeds thus: the volume desorbed (or adsorbed) between P/P_s = 0.98 and 1.0, Δv_1, multiplied by C_i gives the surface area, ΔS_1, of the first group of cores. The volume desorbed between P/P_s = 0.98 and 0.96, Δv_2, is not just the volume of the 2nd group of cores, because the adsorbed film remaining on the walls of the 1st group is also desorbed. A correction is thus necessary. Brunauer carried out the corrections by means of the t-curve, (t-curves are to be described later - Section 4.3.2.4) and obtained:

$$\Delta v_2 \text{ (corr.)} = \Delta v_2 - t_2 \cdot \Delta S_i \qquad (4.12)$$

where t_2 is called the "thinning correction factor" and it is the difference in value between the highest and lowest values of the "t-curve" at the relative vapour pressure corresponding to the 2nd group of cores. The surface area of this group is given by:

$$\Delta S_2 \text{ (corr.)} = \Delta v_2 \text{ (corr.)} \times C_2 \qquad (4.13)$$

Generally, therefore:

$$\Delta v_i \text{ (corr.)} = \Delta v_i - t_i \int_i^{i-1} \Delta S_i \text{ (corn)} \qquad (4.14)$$

$$\Delta S_i \text{ (corr.)} = \Delta v_i \text{ (corr.)} \times C_i \qquad (4.15)$$

To transform the core properties into pore properties, pore shape models are assumed. The most common are the parallel-plate and the cylindrical pore shapes[38,53]. For the cylindrical pore model:

$$V_{cp} = V_c \frac{(2r_c + t)^2}{(2r_c)^2} \qquad (4.16)$$

$$S_{cp} = S_c \frac{(2r_c + t)}{2r_c} \qquad (4.17)$$

$$r_{cp} = r_c + t/2 \qquad (4.18)$$

where the subscripts cp refer to the cylindrical pore and C to the core, t is the t- curve value. For a parallel-plate pore model ie. the walls of the pore are considered as two parallel plates:

$$V_{pp} = V_c \frac{(r_c + t)}{r_c} \qquad (4.19)$$

$$S_{pp} = S_c \qquad (4.20)$$

$$r_{pp} = r_c \frac{(r_c + t)}{r_c} \qquad (4.21)$$

where the subscript pp refer to the parallel-plate pore model.

In the present investigation, the above analysis was put into a computer programme using fortran, giving core volumes, surfaces and hydraulic radius for cylindrical and for parallel-plate pore shape models. Pore size distributions assuming cylindrical pore shape model were also computed.

4.3.2.3 "MP-method" - Analysis of Micropores

The micropore analysis was done by first converting the adsorption isotherm into a V_l - t plot as proposed by De Boer[62,63]. Here V_l is the amount of water vapour (cc/gm) adsorbed and t, the t-curve value at the particular P/P_s value. The initial portion of the plot should be a straight line passing through the origin, and its slope equal to the total surface area, S_t. If a correct t-curve was used, $S_t = S_{BET}$, where S_{BET} is the total surface area obtained by the BET method of equ. (2.4).

The "MP-method" as proposed by Brunauer[61] was then used to carry out the micropore analysis using an analytical approach proposed by Hagymassy[123] instead of Brunauer's graphical approach. The abscissa of the plot was divided into increments of Δt corresponding to $(P/P_s) = 0.05$ starting from zero. Each increment represents a group of pores. The first group was determined by t values t_i and t_2 corresponding to V_i values of V_1 and V_2. The surface areas for the 1st and ith group of pores, A_1 and A_i are given by:

$$A_1 = S_t - S_1 \qquad (4.22)\ A$$

$$A_i = S_{i+1} - S_i \qquad (4.22)\ B$$

where S_1 = surface area available for further adsorption after the first group of pores was filled; and S_i = the surface area available after the ith group of pores was filled. S_1 and S_i are given by:

$$S_1 = \frac{V_2 - V_1}{t_2 - t_1} \times 10^4 \qquad (4.23)\ A$$

$$S_i = \frac{V_{i+1} - V_i}{t_{i+1} - t_i} \qquad (4.23)\ B$$

The hydraulic radius for the ith group of pores is given by:

$$r_{h,i} = \frac{t_i + t_{i+1}}{2} \qquad (4.24)$$

while the volume of the ith group of pores is given by:

$$V_i = A_i r_{h,i} \qquad (4.25)$$

The analysis is continued until

$$S_{i+1} = S_i$$

4.3.2.4. <u>The 't-curve'</u>

A t-curve is a plot of the statistical thickness of the adsorbate - in this case water-vapour - adsorbed onto the surfaces of a non-porous adsorbent against the relative vapour pressure, P/P_s. This statistical thickness is defined by:

$$t = 10^{-4} V_l / S_{BET} \qquad (4.26)$$

where V_l is the volume of liquid adsorbate in ml. and S_{BET} is the BET surface area in m^2/gm, t is in Ångstroms unit ($1\text{Å} = 10^{-10}$ meter). The choice of a correct reference t-curve for the analyses in the preceeding sections is very important especially in the micropore region. For the adsorption of a particular adsorbate onto a reference non-porous sample the BET-C constant of equ. (2.2), should be of the same order of magnitude as in the sample under investigation. Brunauer and Skalny[64], have pointed out that if a correct

No.	t-curve Nos.	1	2	3	4	5	6
	P/P_s	BET - C CONSTANTS					
		10-200	50-200	30-40	23	18	10-14.5
1	1.00	18.18					
2	0.98	14.16					
3	0.96	13.05					
4	0.94	12.00					
5	0.92	11.25					
6	0.90	10.62					
7	0.85	9.33					
8	0.80	8.34					
9	0.75	7.59					
10	0.70	6.99					
11	0.65	6.38					
12	0.60	5.84					
13	0.55	5.40					
14	0.50		4.94	4.94	4.94	4.94	4.85
15	0.45		4.55	4.55	4.55	4.46	4.36
16	0.40		4.26	4.26	4.26	4.05	3.90
17	0.35		3.95	3.94	3.92	3.69	3.49
18	0.30		3.67	3.63	3.51	3.32	3.09
19	0.25		3.46	3.35	3.19	2.97	2.75
20	0.20		3.23	3.06	2.85	2.64	2.43
21	0.15		2.98	2.75	2.48	2.27	2.06
22	0.10		2.72	2.41	2.09	1.89	1.69
23	0.05		2.30	1.98	1.66	1.46	1.26
24	0.00		0.00	0.00	0.00	0.00	0.00

Table (4.2) 't-Curve' Values used for Pore structure Analysis

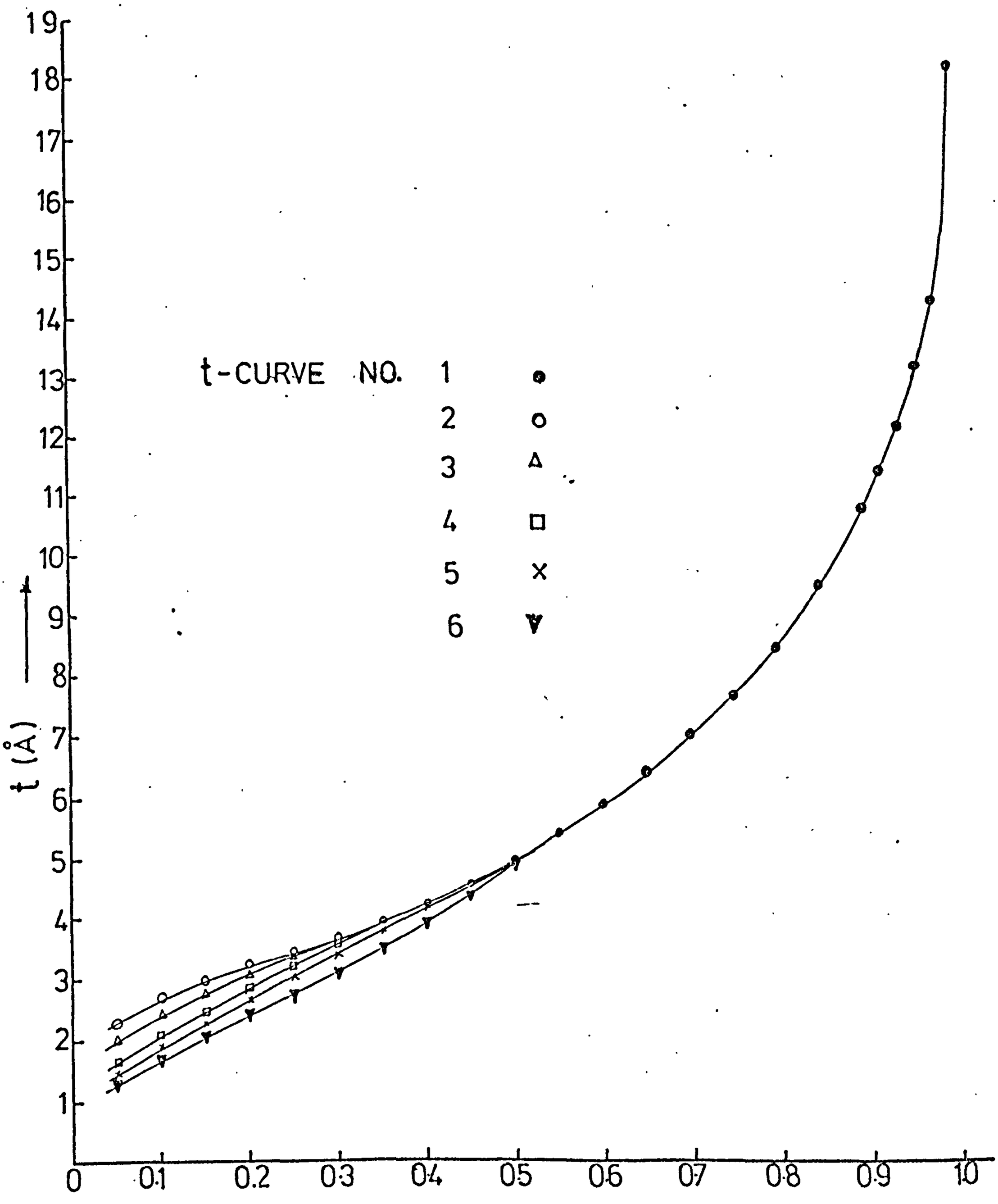

FIG (4.3) PLOTS OF 't-CURVES' FOR WATER-VAPOUR ADSORPTION ANALYSIS

reference t-curve has been used then the De Boer surface area, S_t, should approximately equal S_{BET}.

The t-curves used in the present investigation were published by Hagymassy et al[124] with modifications and interpolations as suggested by Mikhail et al[125]. These are tabulated in table (4.2) and plotted in fig. (4.3).

4.4 Results and Discussions - HCP pore structure

4.4.1 Introduction

The above methods of analysis were used to obtain the pore structure of all the samples tested. The BET theory of equ. (2.2), the De Boer S_t value, and to a large extent the "corrected modelless method" for the analysis of the wide-pores have found favour amongst many chemical scientists[126,127]. Fortunately, this is the range of pore sizes which fall within Powers' range of capillary pores and hence is of the greatest interest in cement paste and concrete research.

The results from experiments and analyses are presented in the following sections, in both tabular and graphical forms. The following points are important in the analysis:

1. The cumulative surface area of all pores, micropores plus wide-pores, must approximately equal the BET surface area - S_{BET}.

2. The cumulative pore volume for the total pore system must approximately equal the total pore volume, V_s - this is the final adsorption of water vapour at saturation pressure (P_s).

3. S_{BET} must approximately equal S_t.

4.4.2 General HCP properties

These properties are shown in table (4.3) for samples used in the adsorption tests. The cube crushing strengths are shown in column 3; variations of compressive strength with such variables as W/C, cement type, and admixture are discussed in chapter 6. In column 6 are shown W_e or total porosity

values ie. weight loss on drying to 105°C. It is a well-known fact that increasing the W/C ratio increases the porosity. The porosity for OP40 is about 0.73 times that of OP60 ; and is of the same order in SRPC pastes. The introduction of a superplasticiser slightly increased the porosity in all cases. The variation of porosity (W_e) with W/C ratio and admixture concentration are illustrated in figs. (4.4) and (4.5) for OPC and SRPC pastes respectively. These pastes contained Cormix SP1 superplasticiser. The corresponding values for pastes containing Melmet L10 showed little or no deviations from these and are, therefore, not presented. For OP50 pastes, for example, the addition of 4% superplasticiser increased porosity from 42.94 to 44.95% ie. 4.7% increase. In practice, the introduction of 4% admixture could lead to as much as 20% water reduction; and using this, OP50 paste reduces to an OP4-4 paste which had a porosity value of 39.72%. Thus the reduction in porosity obtained as a result of reduction in mixing water more than compensates for any porosity introduced by the added superplasticiser.

In columns 4 and 5 are shown the wet and dry densities of the HCPs. The wet density (SSD) of the various pastes with or without admixture are illustrated in fig. (4.6) for OPC and SRPC pastes. It is evident from the density values in the table that OPC pastes possess slightly higher density than SRPC pastes at equal W/C ratio. A general trend also noticed in table (4.2) and fig. (4.6) is that density normally reduces on introduction of the admixture. At low admixture concentrations of 1% the reductions were often negligible.

The combined water content W_n/C, and the degrees of hydration, W_n/W_n^o, of the HCPs used for the adsorption tests were calculated and are shown in columns 6 and 7 of table (4.3). Again the values increased with increasing W/C ratios. They also increased with increasing admixture concentration thus showing that the superplasticiser increases the rate of hydration of the cement pastes. The OPC pastes hydrated more at a given age than the SRPC pastes but at the higher W/C ratio of 0.60 the reverse seemed to be the case.

4.4.3 The Adsorption Isotherms

In the adsorption isotherms, figs. (4.7) to (4.13), the adsorbed volume of water is given in cc/gm of paste reduced to the 1,000°C ignited weight basis because this approximates to the weight of the original

No.	1	2	3	4	5	6	7
	PASTE DESIGN. TABLE (4.1)	COMPR. STR. 28D SSD (N/mm^2)	T. POROSITY (W_e) (%Vol)	WET DENSITY SSD (gm/m^3)	DRY DENSITY AT 105°C	W_n/C (gm/gm)	DEGREE OF HYDRATION W_n/W_n^o (%)
1	OP30	100.7	31.50	2.27	1.94	0.118	50.8
2	OP40	73.1	37.12	2.17	1.78	0.133	57.3
3	OP50	50.1	42.94	2.04	1.66	0.150	64.6
4	OP60	38.6	50.77	1.99	1.49	0.175	75.4
5	OP70	29.3	58.98	1.87	1.38	0.188	81.0
6	COP4-4	64.0	39.72	2.13	1.74	0.145	62.5
7	COP5-4	48.2	44.95	2.02	1.64	0.158	68.1
8	COP6-4	40.7	51.23	1.92	1.50	0.192	82.8
9	COP4-1	74.3	37.70	2.16	1.78	0.151	65.0
10	COP4-2	70.8	38.49	2.15	1.77	0.151	65.0
11	OVP40	70.5+	37.12	2.17	1.79	0.133	57.3
12	OVP60	39.5+	50.77	1.99	1.45	0.175	75.4
13	OSP40	68.3*	37.12	2.17	1.77	0.133	57.3
14	OSP60	36.3*	50.77	1.99	1.45	0.175	75.4
15	SR40	69.0	39.01	2.13	1.77	0.137	59.6
16	SR50	44.2	45.95	2.01	1.61	0.153	66.5
17	SR60	31.2	53.11	1.91	1.47	0.182	79.1
18	CSR4-4	67.0	41.97	2.11	1.74	0.144	62.1
19	CSR5-4	46.9	48.00	1.94	1.56	0.167	72.0
20	CSR6-4	34.1	54.32	1.80	1.41	0.186	80.2

\+ Oven-dried (105°C) compressive strengths

* Oil saturated Compresive Str.

Table (4.3) Properties of HCPs -used for Pore Structure Analysis

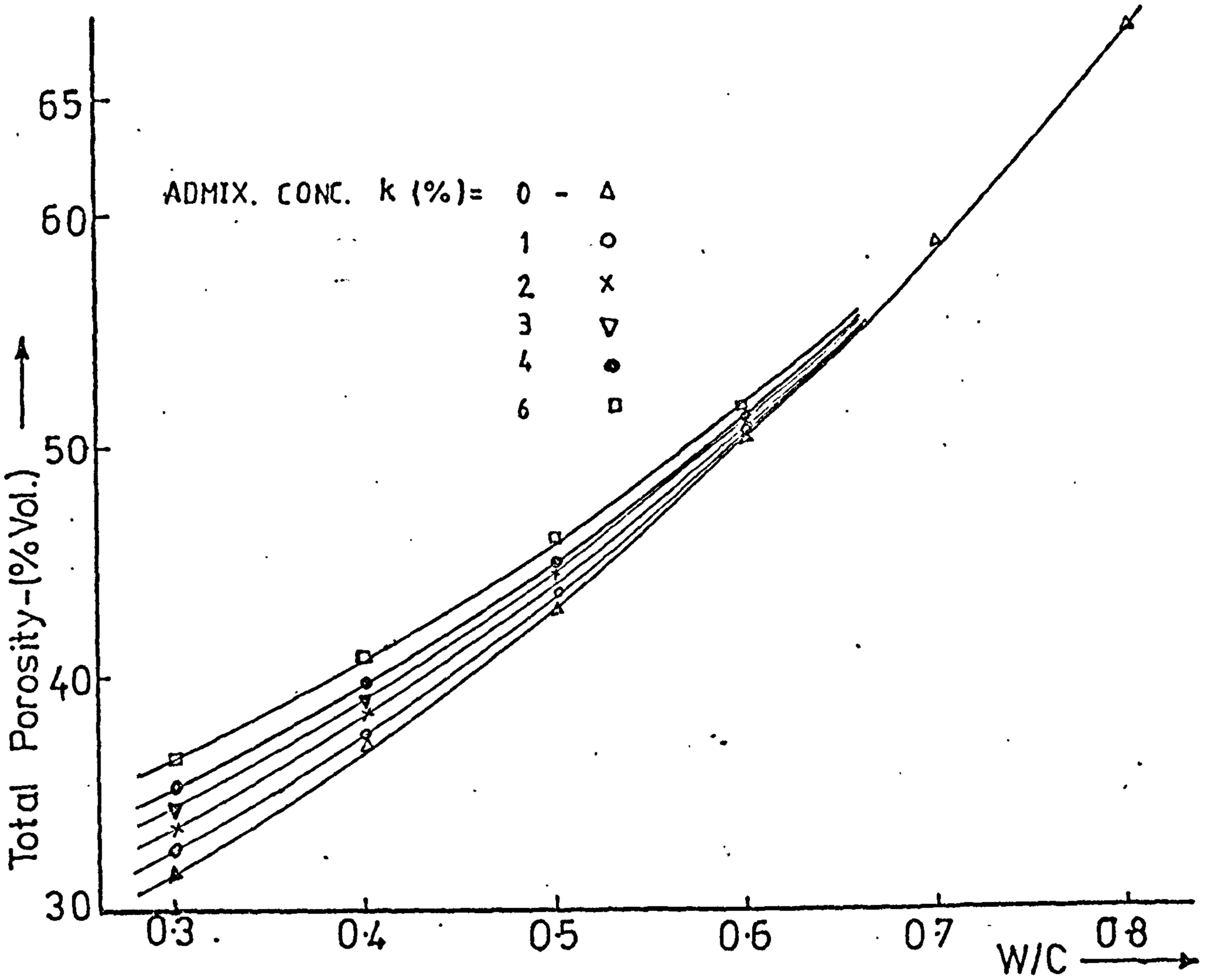

FIG.(4.4) T. POROSITY (We) for OPC PASTES WITH or WITHOUT SUPERPLASTICISER

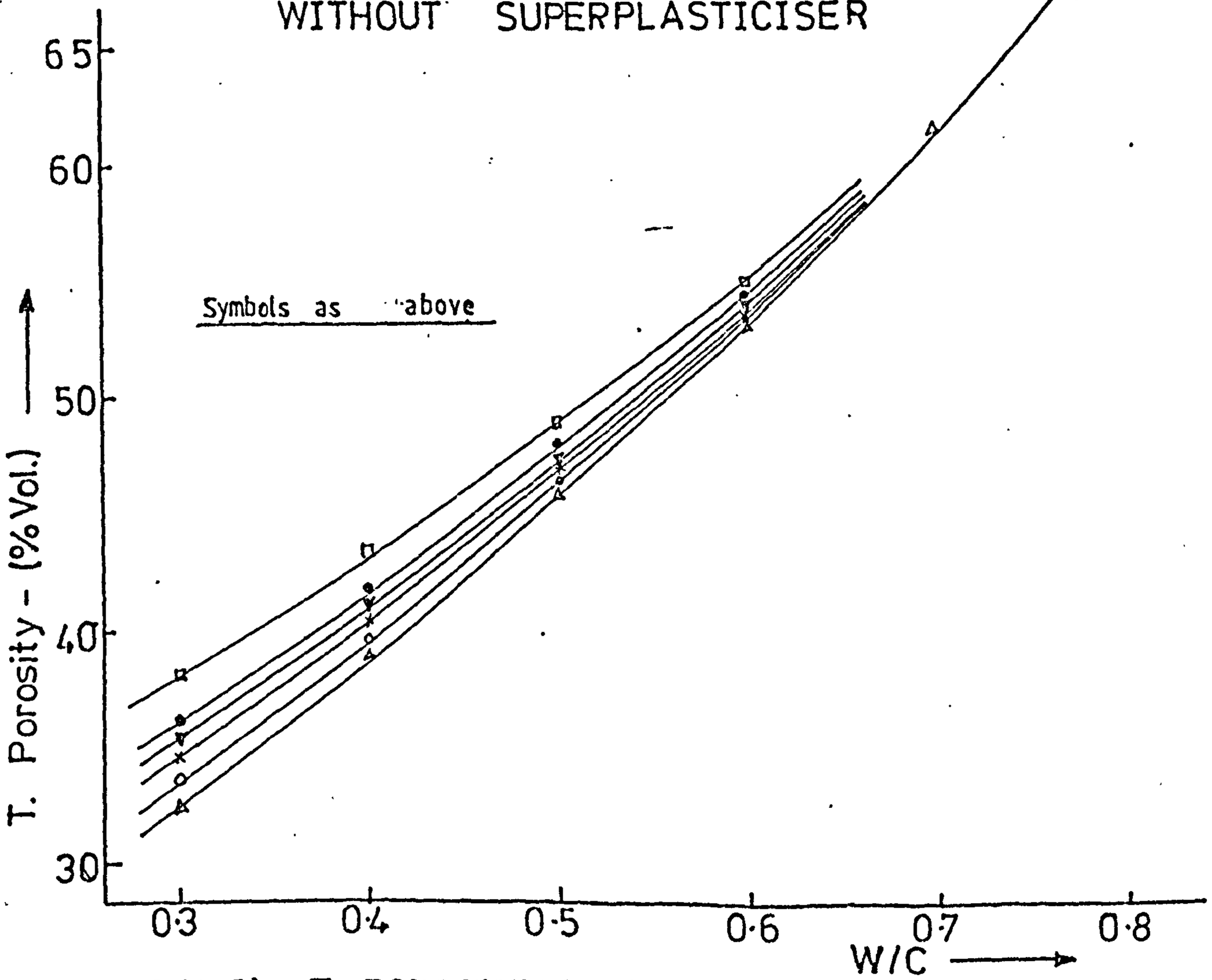

FIG.(4.5) T. POROSITY (We) for SRPC PASTES WITH or WITHOUT SUPERPLASTICISER

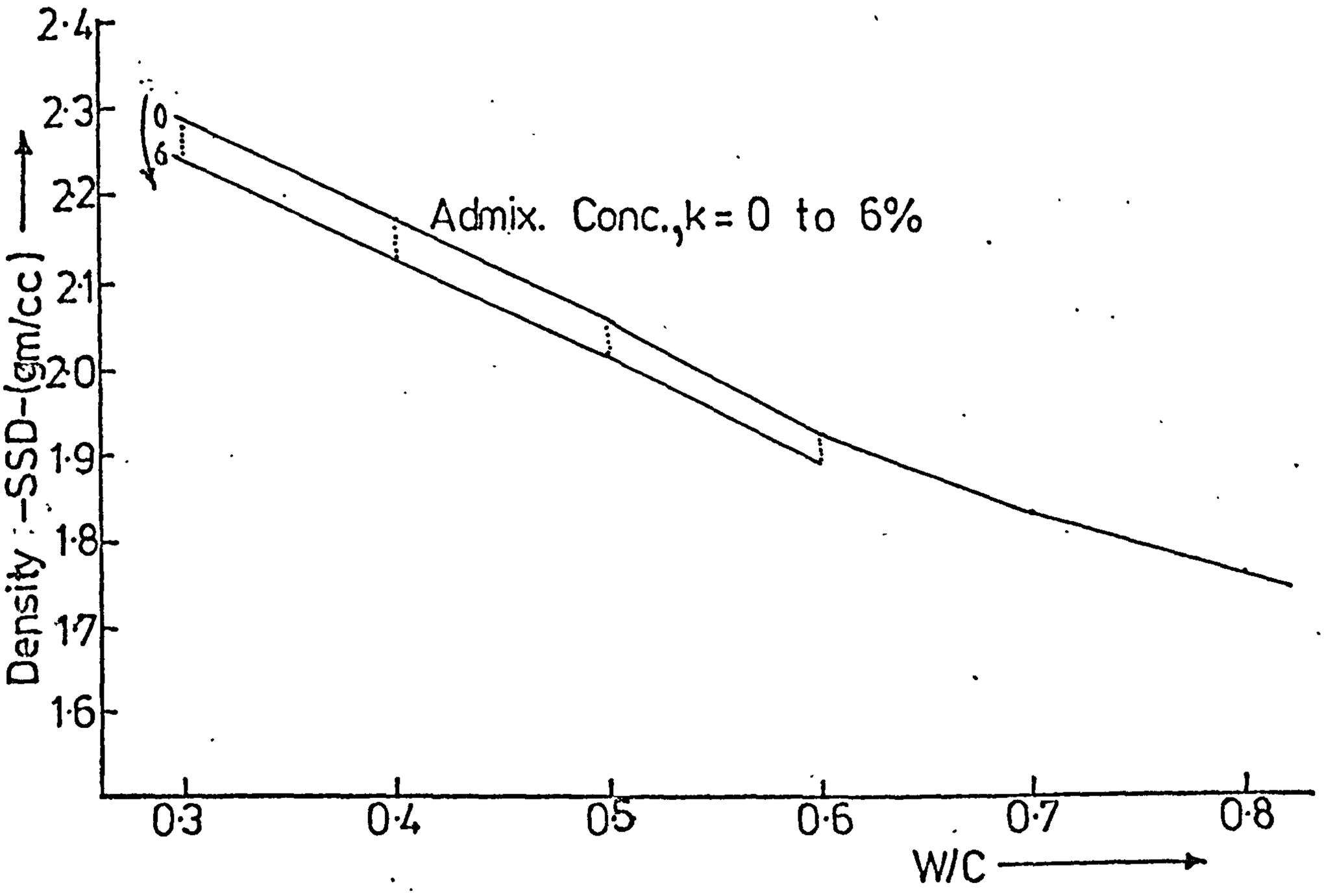

A OPC PASTES

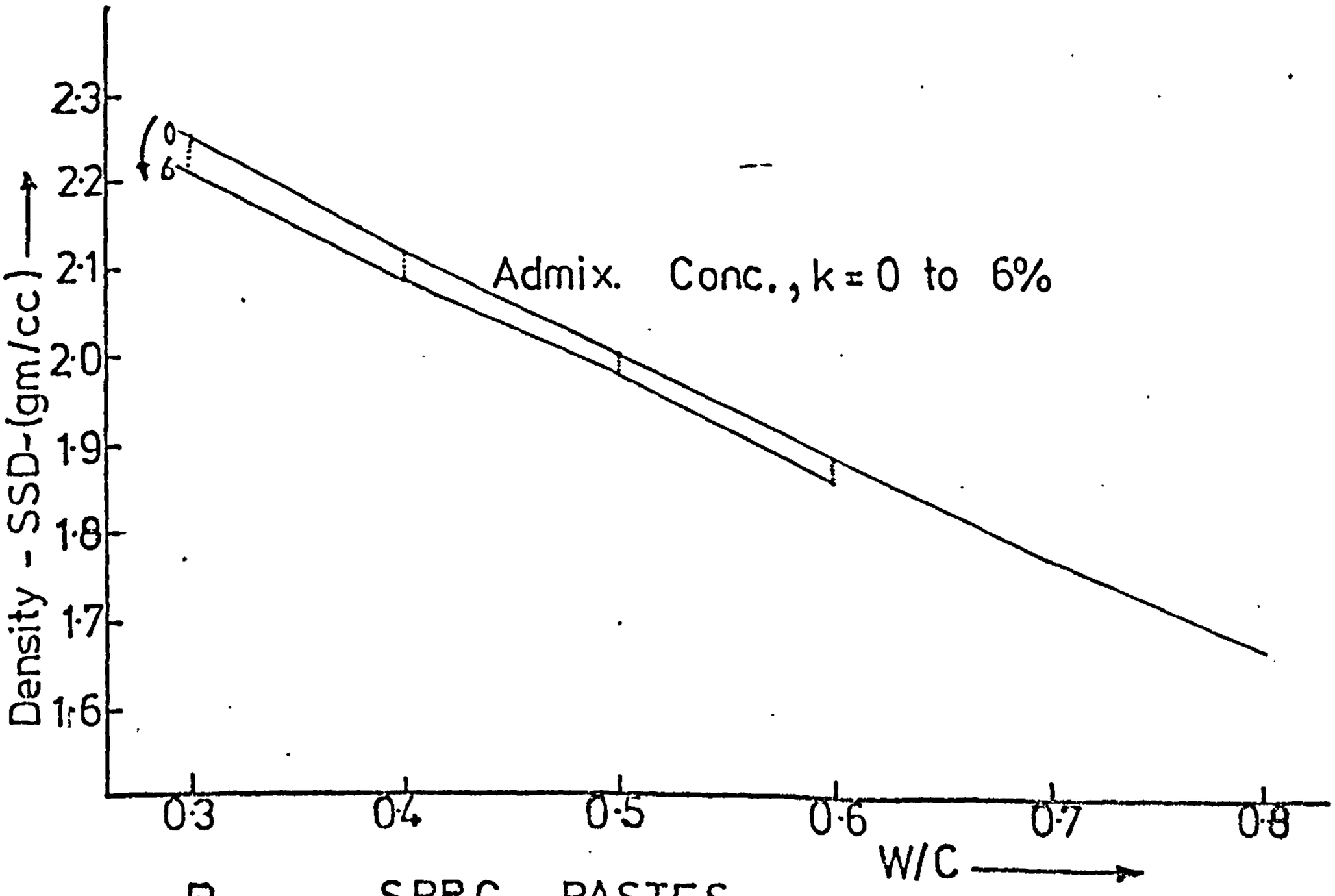

B SPRC PASTES

FIG(4.6) DENSTIES OF HCPS. WITH & WITHOUT SUPERPLASTICISER

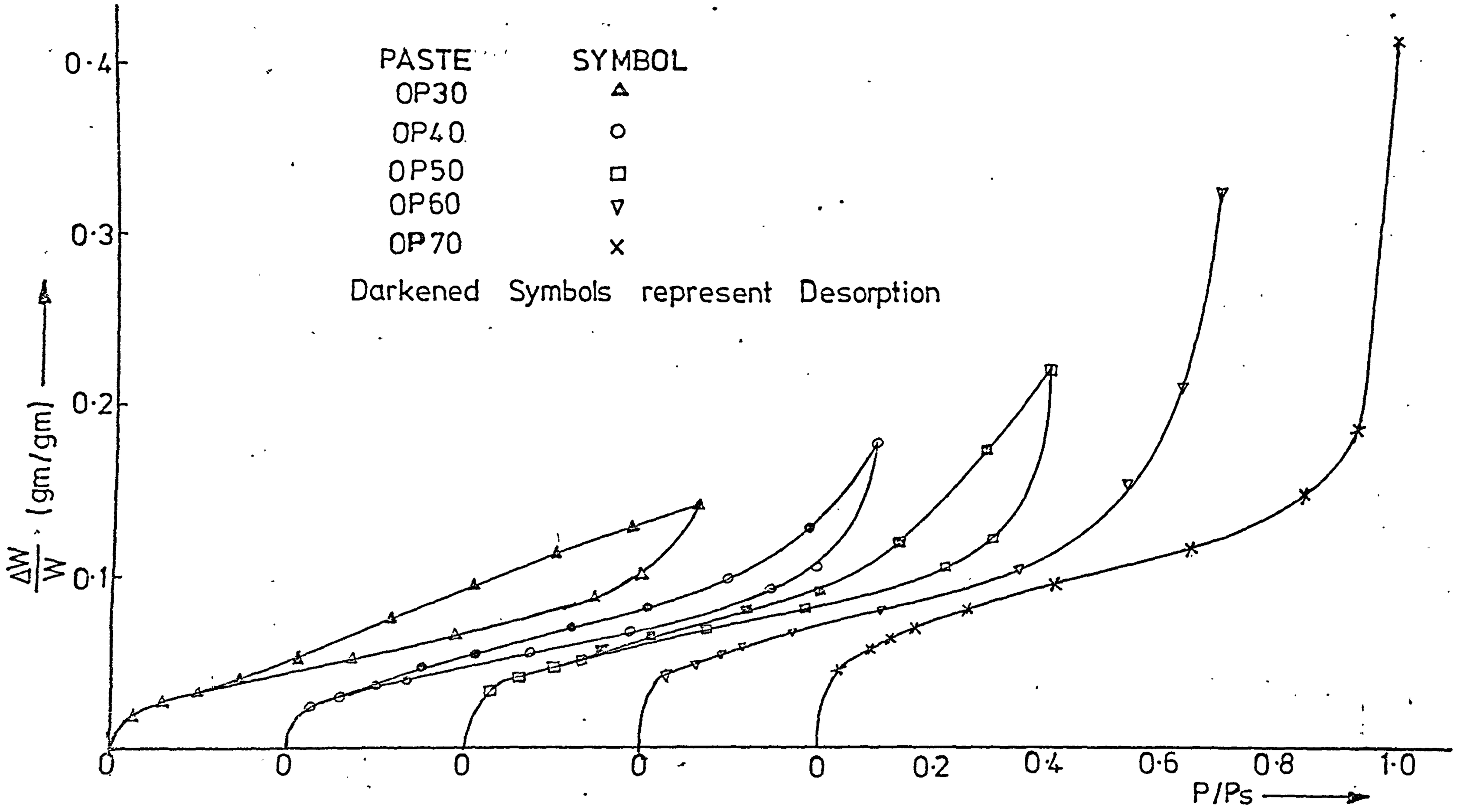

FIG.(4.7) ADSORPTION-DESORTION ISOTHERMS OF WATER VAPOUR ON HCPS. P/Ps IS MOVED TO THE RIGHT BY 0·3P/Ps FOR SUCESSIVE CURVES FOR CLEARER PRESENTATION

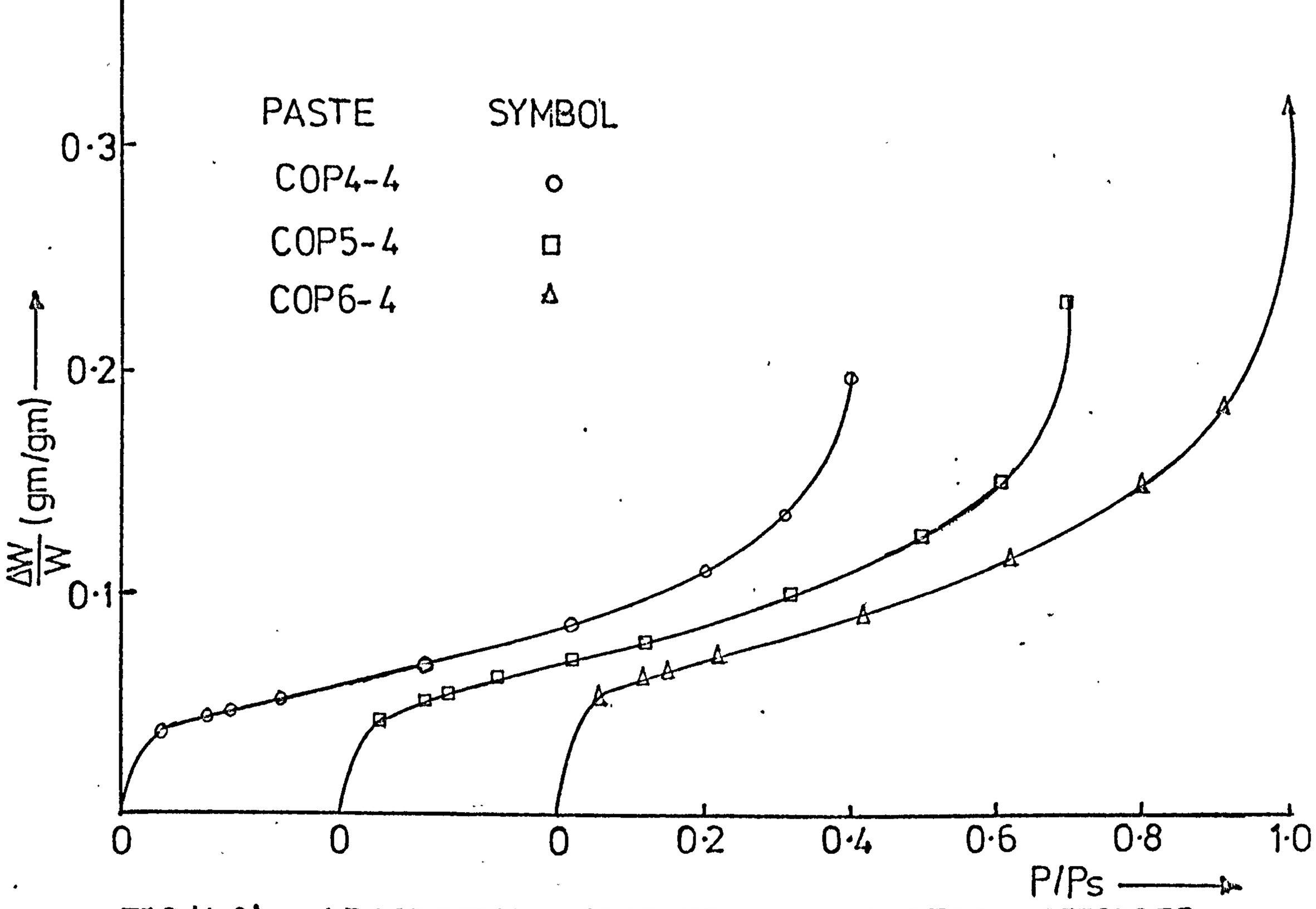

FIG.(4.8) ADSORPTION ISOTHERM ON SUPERPLASTICISED OPC PASTES

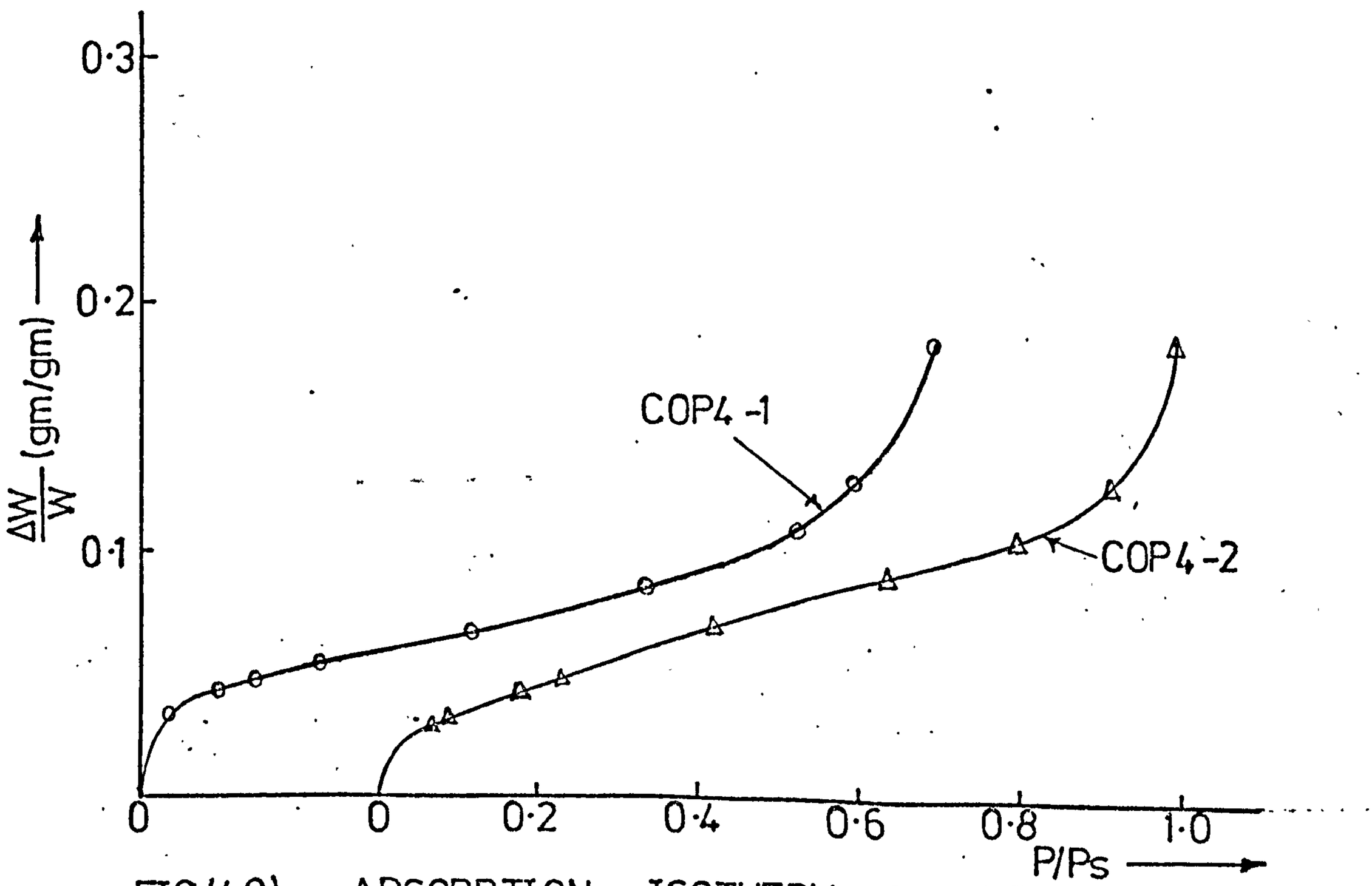

FIG.(4.9) ADSORPTION ISOTHERM ON SUPERPLASTICISED OPC PASTES

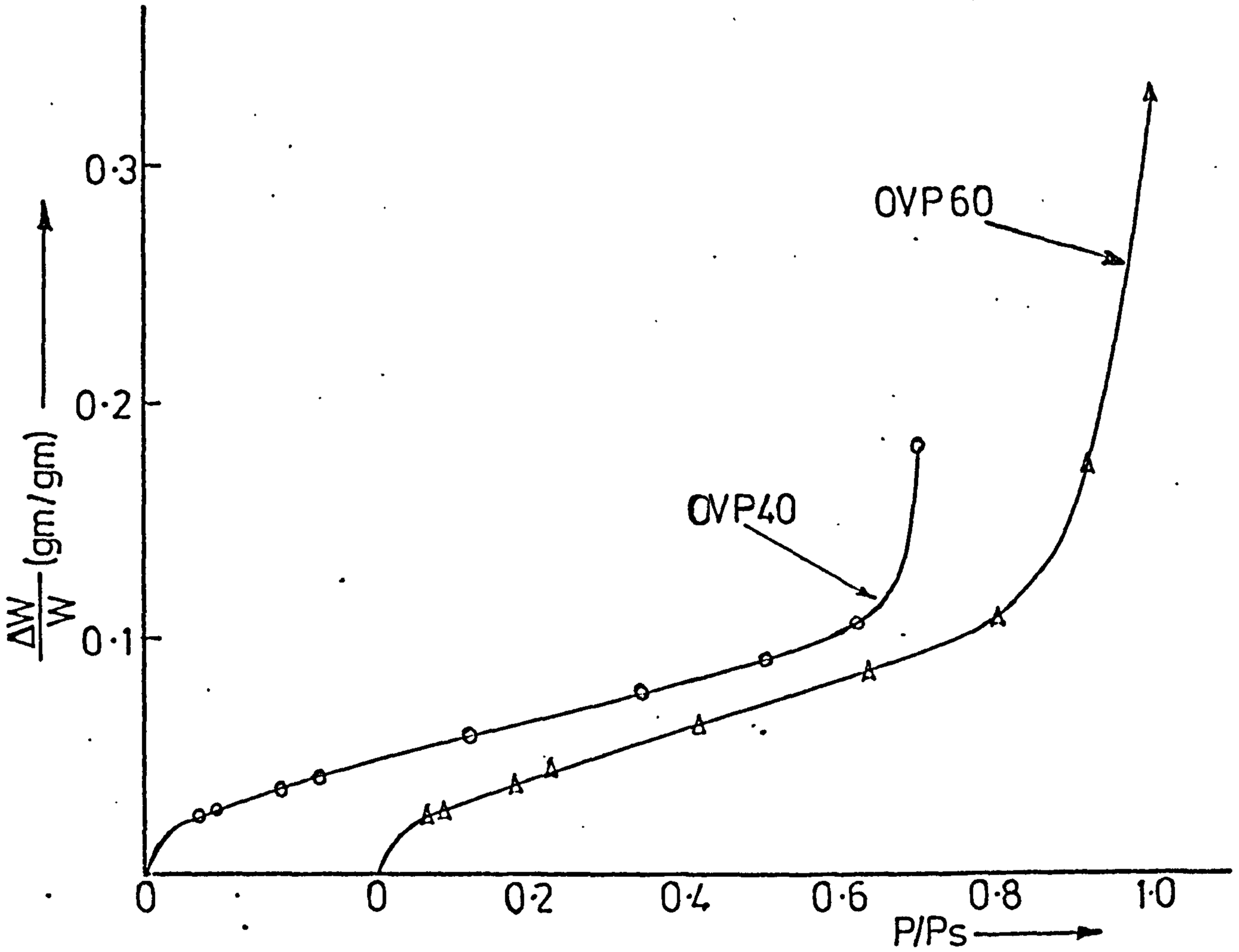

FIG.(4.10) ADSORPTION ISOTHERM ON OVEN-DRIED OPC PASTES

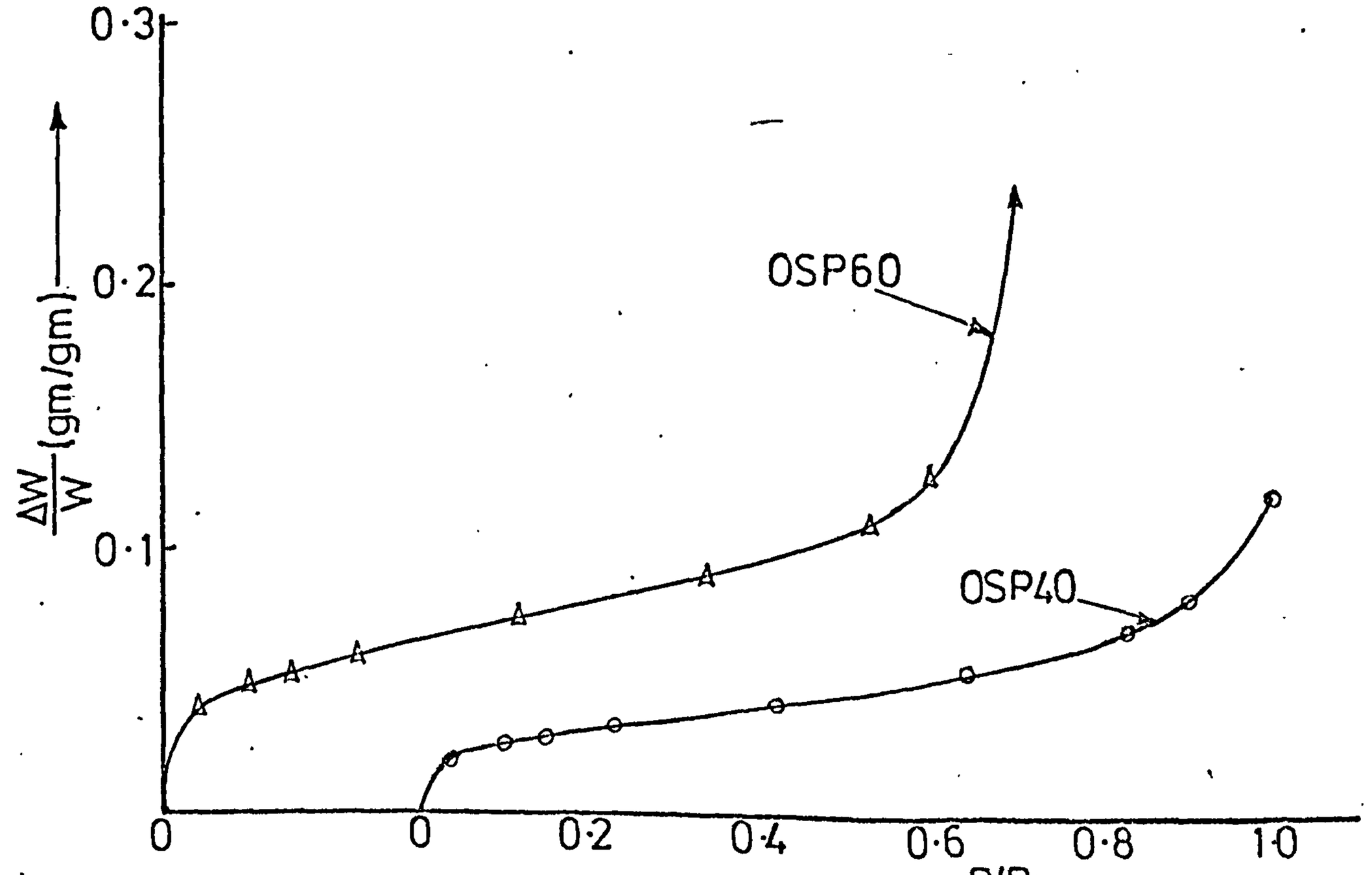

FIG.(4.11) ADSORPTION ISOTHERM ON PREVIOUSLY OIL SAT. OPC PASTES

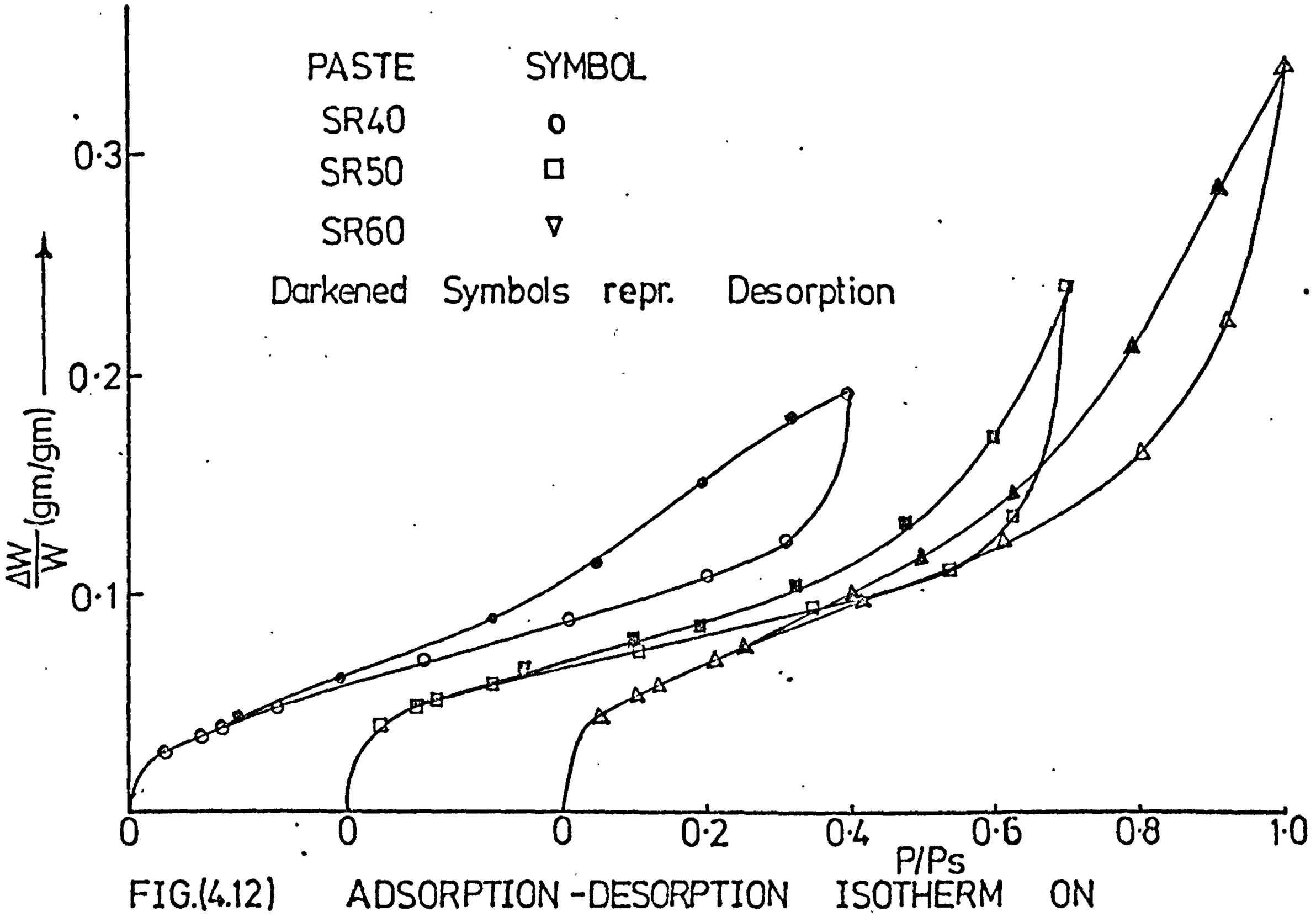

FIG.(4.12) ADSORPTION -DESORPTION ISOTHERM ON SRPC PASTES

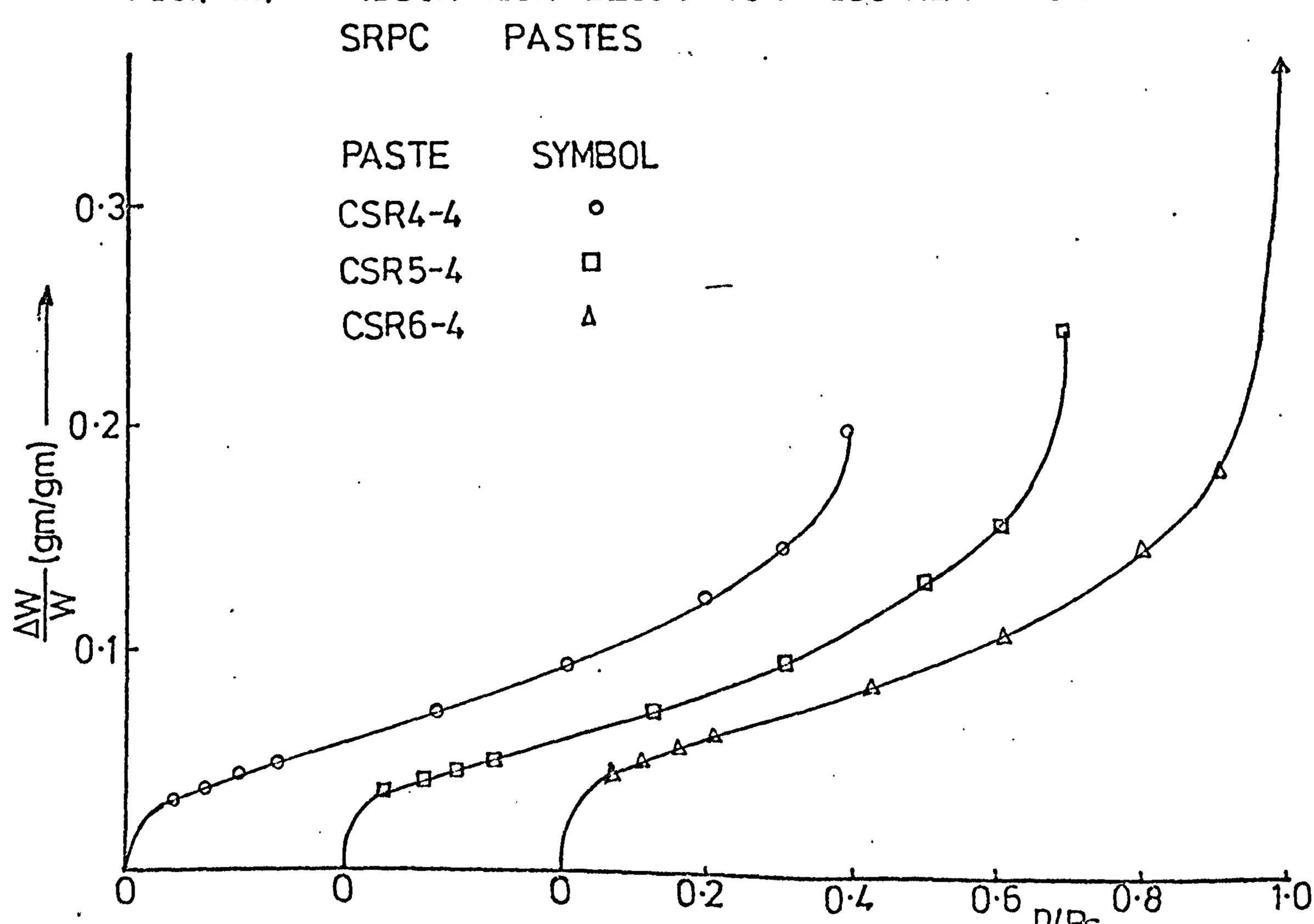

FIG.(4.13) ADSORPTION ISOTHERM ON SUPERPLASTICISED SRPC PASTES

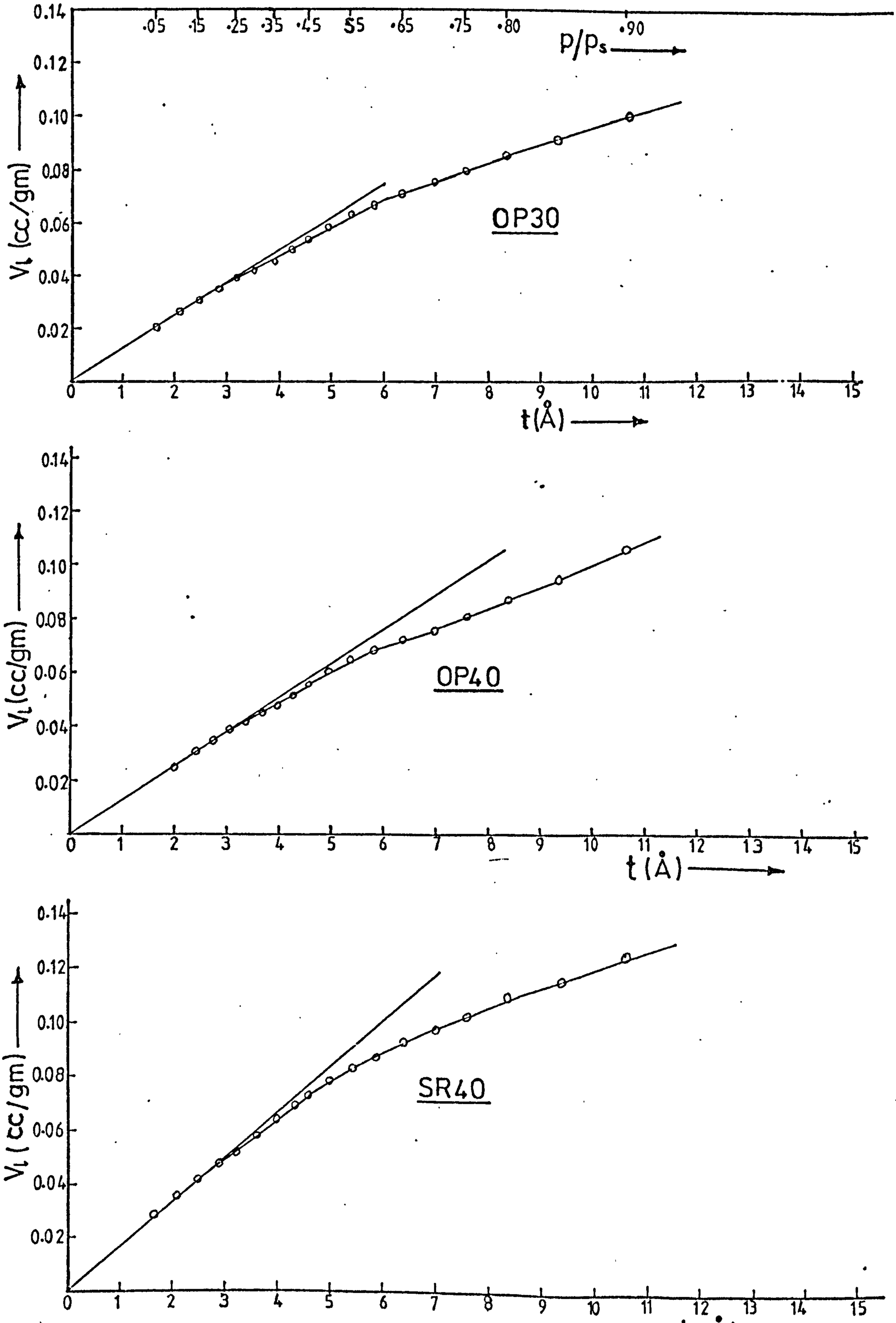

FIG (4.14) $V_l - t$ PLOT FOR OP30, OP40 & SR40

anhydrous cement and gives a common basis for all adsorption values. The absicissa is the relative vapour, P/P_s, and succesive plots were displaced to the right by $0.3P/P_s$ for clearer presentation.

Equilibrium at each P/P_s point was slow and 4 to 8 days was needed. Desorption runs were made on 6 pastes only and near equilibrium required 8 to 12 days, but despite this long period, rather large hysteresis loops were obtained - figs. (4.7) and (4.12). Several theories have been published to explain the existence of this hysteresis loop[27,33,53,57] and is one of the fundamental areas of controversy between Powers' model and the Feldman-Sereda model. The most acceptable explanation is that some of the pores in HCPs are "ink-bottle" shaped ie. have narrow, restricted entrances[27]. The process by which molecules enter such pores is activated diffusion[27], and for molecules to leave such pores, they require the sum of the energy of activation of adsorption plus the heat of adsorption[59]. This means that along the desorption branch much longer time is needed for the molecules to desorp and hence reach equilibrium. Brunauer[27] allowed four and half months and could eliminate hysteresis. In view of this, the adsorption branch is often considered to represent approximate equilibrium and was used here in computing the pore structure characteristics for all HCPs[27,33,59].

All the adsorption isotherms were converted into V_l - t plots as described in section 4.3.2.3. Three typical plots are shown in fig. (4.14) for OP30, OP40 and SR40. These plots serve two main purposes: (a) the slopes at the origin gives the De Boer surface area, S_t. (b) Downward deviation of the plots from the original straight line gives an indication of the existence of micropores[123]. This was the case for all the samples investigated.

4.4.4. Pore Structure Results

Table (4.4) shows the pore structure data for the 20 pastes investigated. S_{BET} values are approximately equal to S_t indicating that the t-curves used, column 17, were probably correct. The small percentage differences in the values in columns 15, 16, also gives some confidence in the analysis.

The measured pore properties will be converted into practical engineering terms as far as possible and compared with published results. Hagymassy et

No.	PASTE	S_{BET} (m^2/gm)	S_t (m^2/gm)	MICROPORES		WIDE PORES				TOTAL PORE SYSTEM				V_s	$\frac{V_s - V_{cp}}{V_s} \times 100\%$	$\frac{S_{BET} - S_{cp}}{S_{BET}} \times 100\%$	t-curve used for analysis
				SS_{mp} (m^2g)	V_{mp} (cc/gm)	S_{pp}	S_{cp}	V_{pp}	V_{cp}	S_{pp}	S_{cp}	V_{pp}	V_{cp}				
	1	2	3	4	5	6	7	8	9	10	11	12	13	14	15	16	17
1	OP30	120	126	65	0.0256	45	56	0.1226	0.1261	110	121	0.1482	0.1517	0.1435	-5.7	-0.8	4
2	OP40	131	130	76	0.0324	43	53	0.1434	0.1458	119	129	0.1758	0.1782	0.1791	0.5	1.6	3
3	OP50	155	163	96	0.0432	43	54	0.1710	0.1734	145	150	0.2142	0.2166	0.2238	3.2	3.2	2
4	OP60	194	197	125	0.0501	63	74	0.2698	0.2733	188	199	0.3199	0.3234	0.3278	1.3	-2.6	2
5	OP70	216	231	148	0.0623	57	68	0.3414	0.3442	205	216	0.4037	0.4065	0.4181	2.8	0.0	2
6	COP4-4	151	157	85	0.0308	50	61	0.1539	0.1569	135	146	0.1847	0.1877	0.1991	5.7	3.3	2
7	COP5-4	168	180	92	0.0395	56	69	0.1783	0.1816	148	161	0.2178	0.2211	0.2309	4.2	4.2	2
8	COP6-4	204	214	119	0.0478	66	80	0.2546	0.2583	185	199	0.3024	0.3061	0.3198	4.3	2.5	2
9	COP4-1	147	161	86	0.0385	45	55	0.1328	0.1354	131	141	0.1713	0.1739	0.1800	3.4	4.1	2
10	COP4-2	161	161	105	0.0501	37	46	0.1265	0.1288	142	152	0.1766	0.1789	0.1824	1.9	5.6	4
11	OVP40	135	138	76	0.0346	41	50	0.1412	0.1435	117	126	0.1758	0.1781	0.1825	2.4	6.7	4
12	OVP60	175	175	102	0.0391	62	73	0.2939	0.2970	164	175	0.3330	0.3361	0.3347	-0.4	0.0	4
13	OS40	91	95	53	0.0268	33	40	0.0946	0.0966	86	93	0.1214	0.1234	0.1210	-2.0	-2.2	2
14	OS60	165	171	118	0.0473	44	54	0.1786	0.1812	162	172	0.2259	0.2285	0.2308	-4.2	1.0	2
15	SR40	163	167	111	0.0555	39	48	0.1365	0.1390	150	159	0.1920	0.1945	0.1925	-1.0	2.5	4
16	SR50	169	179	114	0.0519	42	51	0.1843	0.1865	156	165	0.2338	0.2384	0.2434	2.1	2.4	2
17	SR60	231	228	135	0.0498	81	89	0.2842	0.2890	208	226	0.3340	0.3386	0.3457	2.1	2.2	3
18	CSR4-4	157	170	83	0.0236	59	63	0.1546	0.1583	142	146	0.1756	0.1819	0.1985	8.4	7.0	4
19	CSR5-4	172	173	103	0.0365	61	69	0.1964	0.2001	164	172	0.2329	0.2366	0.2440	3.0	0.0	4
20	CSR6-4	193	203	117	0.0463	73	81	0.3088	0.3131	200	198	0.3551	0.3594	0.3610	0.4	-2.6	3

Table (4.4) Pore Structure Characteristics of HCPs by Water Vapour Adsorption

al[128] obtained the surface area of a cement paste of W/C = 0.4, at 78% hydration to be 156 m^2/gm of dry paste. On an ignited weight basis this comes to 200 m^2/gm. A similar value of 215 m^2/gm was obtained by Winslow and Diamond[36], using the small angle X-ray scattering technique. Since surface area is proportional to the degree of hydration[23], at full hydration, the surface area would be approximately 255 m^2/g. Dividing the S_{BET} surface areas in column 2, table (4.4) by 255 gives degrees of hydration of 47.1, 51.4, 60.8, 76.1 and 84.7% for OP30 to OP70 respectively. Compared with values in column 7 of table (4.3), the highest difference in value is approximately 10%. This difference, though large, is probably due to differences in the chemical compositions of the original cements and also to differences in the severity of drying the HCPs before tests - two factors that considerably influence HCP surface area.

In table (4.4), the pore volumes are given as fractions of the ignited paste mass. In practice, pore volumes are usually expressed as percentages of total volume, as in table (4.3), and can be converted thus: V_B values can be converted to dry paste basis by dividing by $(1 + W_n/C)$; and then multiplying by their respective dry densities in column 5 - table (4.3). For oven-dried pastes OVP40 and OVP60, the alternative values of total porosity are 29.8% and 42.4% respectively. The two sets of values differ by 7.3% and 8.3% respectively.

The following trends were observed from table (4.4).

1. Generally all the pore characteristics - Section 4.1 - increased with an increase in W/C ratio for both the micro - and wide-pores. Exceptions were the SR40, SR50 and SR60 pastes where the micropore volumes decreased with an increase in W/C ratio.

2. The addition of 4%, by weight of cement, of Cormix SP1 super-plasticiser generally reduced the pore characteristics in the micropore region but increased them in the wide-pore region. The S_{BET}, S_t values and the pore surfaces increased for pastes with admixture using OPC but not generally in SRPC pastes; generally, the total pore volumes, V_s and the cumulative pore volume increased for both OPC and SRPC pastes.

3. Reducing the admixture concentration - COP4-1 and COP4-2 - reduces the wide-pore volume and this generally improves engineering properties

of HCPs.

4. SRPC pastes generally had higher pore volumes than corresponding OPC pastes of equal W/C ratio, eg. V_s values were higher by 7.5, 8.7 and 10.1% for SR40, SR50, SR60 respectively. This was similar for superplasticised pastes but SRPC pastes had smaller micropore volumes than had OPC pastes.

5. Oven-drying the HCPs could increase the porosity of the pastes eg. OVP60 was higher than OP60; but wide-pore volume in OVP40 was not higher than fo:· OP40.

6. Oil saturated HCP samples had different pore characteristics from normal, eg. OSP40, OSP60 compared with OVP40, OVP60. The V_s values decreased by 34% and 31% respectively and the S_{BET}, S_t and wide-pore volumes also decreased. There is no clear influence on the micropores.

4.4.5 Hydraulic Radius (r_h) of the Pore System

The hydraulic radius of a pore system is equal to the volume of the pores divided by the surface area. It is a measure of the average width of the pore system. For a cylindrical pore it represents half of the radius, and for a parallel-plate pore it is equal to half of the distance between the plates. In table (4.5) are shown the hydraulic radii of the pore systems of all the pastes, in Ångstrom units ($1\text{Å} = 10^{-10}$ metre). The following trends were observed from table (4.5):

1. The hydraulic radius of the micropores varies randomly, but are of approximately equal magnitude. Hagymassy et al[128] analysed only 3HCPs and concluded that the hydraulic radius of the micropores decreased with increasing W/C ratio, which is not the case here.

2. In the wide pore region, the hydraulic radius usually increases with increasing W/C ratio. The average pore radius of the entire pore system also increases with W/C ratio, but it is the wide pores that are of greater significance to the engineering properties of HCPs[23].

3. Generally, the total pore volumes, V_s of superplasticised pastes were higher than for oridinary pastes but r_h values are the opposite, eg. for

No	1	2	3	4	5
	PASTE DESIGNATION	MICROPORES	WIDE-PORES		ALL PORES
		r_h (Å)	r_h (cp)	r_h (pp)	r_h (V_s/S_{BET})
1	OP30	3.9	22.5	27.2	12.0
2	OP40	4.3	27.5	33.3	13.7
3	OP50	4.5	32.1	39.8	14.4
4	OP60	4.0	36.9	42.8	16.9
5	OP70	4.2	50.6	59.9	19.4
6	COP4-4	3.6	25.7	30.8	13.2
7	COP5-4	4.3	26.3	31.8	13.7
8	COP6-4	4.0	32.3	38.6	15.7
9	COP4-1	4.5	24.6	29.5	12.2
10	COP4-2	4.8	28.0	34.2	11.3
11	OVP40	4.6	28.7	34.4	13.5
12	OVP60	3.8	40.7	47.9	19.1
13	OSP40	5.1	24.2	28.7	13.3
14	OSP60	4.0	33.6	41.2	14.0
15	SR40	5.0	29.0	35.0	11.8
16	SR50	4.3	36.6	43.9	14.6
17	SR60	3.7	32.5	35.1	15.1
18	CSR4-4	3.8	25.1	26.2	12.6
19	CSR5-4	3.5	29.0	32.2	14.2
20	CSR6-4	4.0	38.7	42.3	18.7

Table (4.5) Hydraulic radii (in Å) of the HCP pore Systems

OP40, $r_{h(cp)}$ was 27.5Å and 25.7 Å for COP4-4 - a decrease of 6.5%. Thus the superplasticiser has increased the total porosity of the pastes which was also observed by Dingley[129] for HCPs containing polymers; but it has also broken the pores into smaller pore sizes.

4. Oven-drying the HCPs increases the pore volume and the average pore sizes, e.g. OVP40 and OP40. This pore structure modification or decomposition has been observed by Brunauer et al[130]. Crude oil saturated HCPs have reduced hydraulic radii.

4.4.6 Cumulative Pore Volume and Surface Distributions

The cumulative pore volume and surface area distributions are given in fig. (4.5), I to XX; using the cylindrical pore model. The cumulative pore volumes, V_{cp}, and surface, S_{cp}, were closer using this model, to the V_s and S_{BET} values than using the parallel-plate model. The abscissa is r_h and the ordinate is the percentage of the total volume or surface located in all pores of hydraulic radius, r_h and greater. From the plots, the volumes and surfaces of pores located within a desired pore size range is easily obtained. For example, plot I for OP30 shows that about 44.5% of the total pore volume and 18% of the pore surface are located in pores of radius 20 Å and greater. For OP40, plot II, gives 58.3% and 11% respectively. The pore volume and surface distributions were affected by various factors as follows:

1. Pastes with higher W/C ratios have a greater percentage of both pore volume and surface area within the wide-pore regions, eg. for OPC pastes with W/C = 0.3, 0.4, 0.5, 0.6, 0.7, the percentage of pore volumes located in pores of r_h = 20 Å and greater are 44.5%, 58.3%, 62.3%, 70.4% and 73.5% respectively. Most engineering properties of HCP deteriorate with increases in the W/C ratio and hence the volume of the wide-pores.

2. The addition of a superplasticiser admixture reduces the percentage of pore volume located in the wide-pore regions as admixture concentration increases but at 4%, the values were similar to those of 0%.

3. Oven-dried HCPs have a slightly greater percentage of wide pores; eg. OVP40 and OVP60 have 59.0% and 76.8% respectively of pores volume in pores 20 Å and greater, while OP40 and OP60 have 58.3% and 70.4 % respectively.

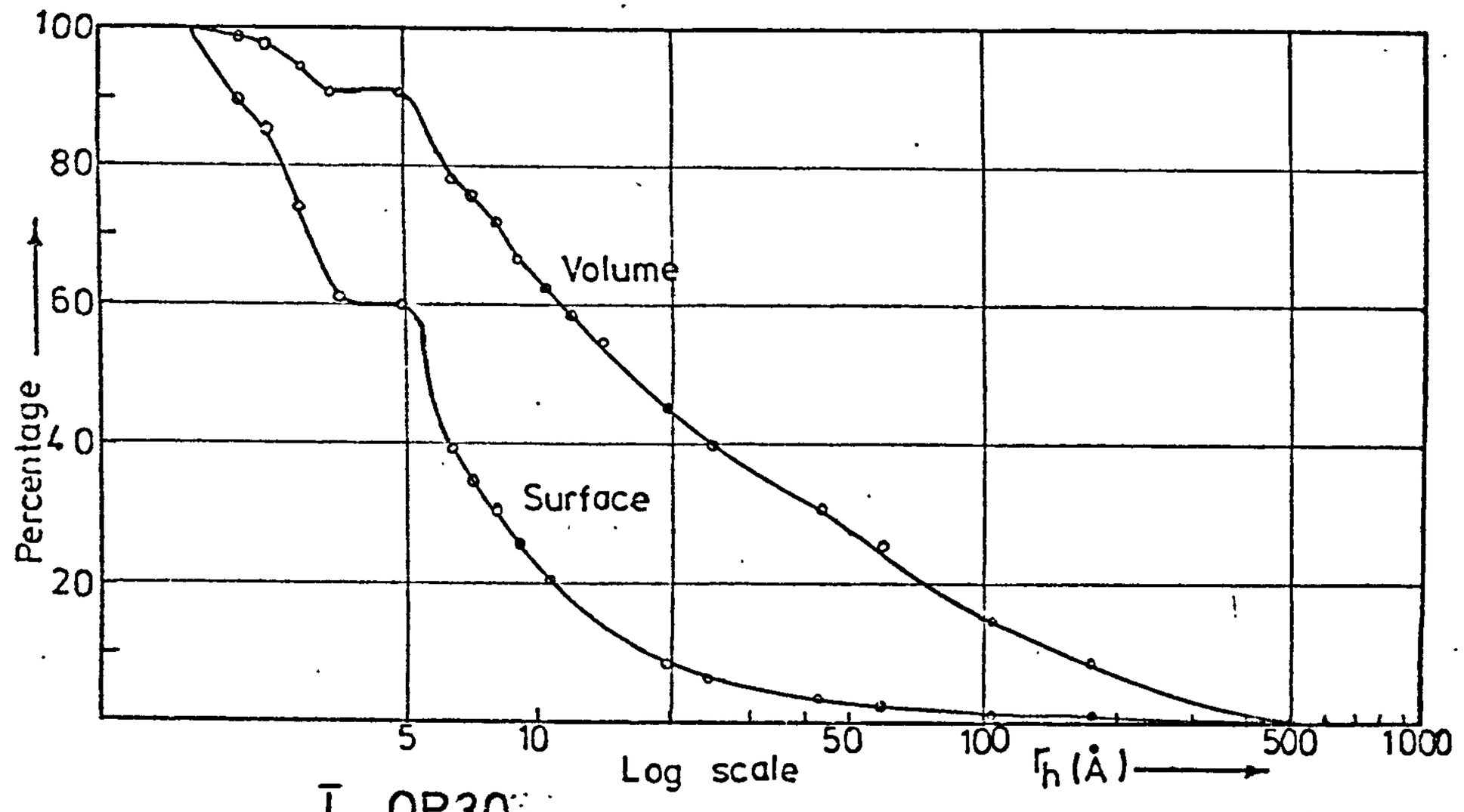

I. OP30

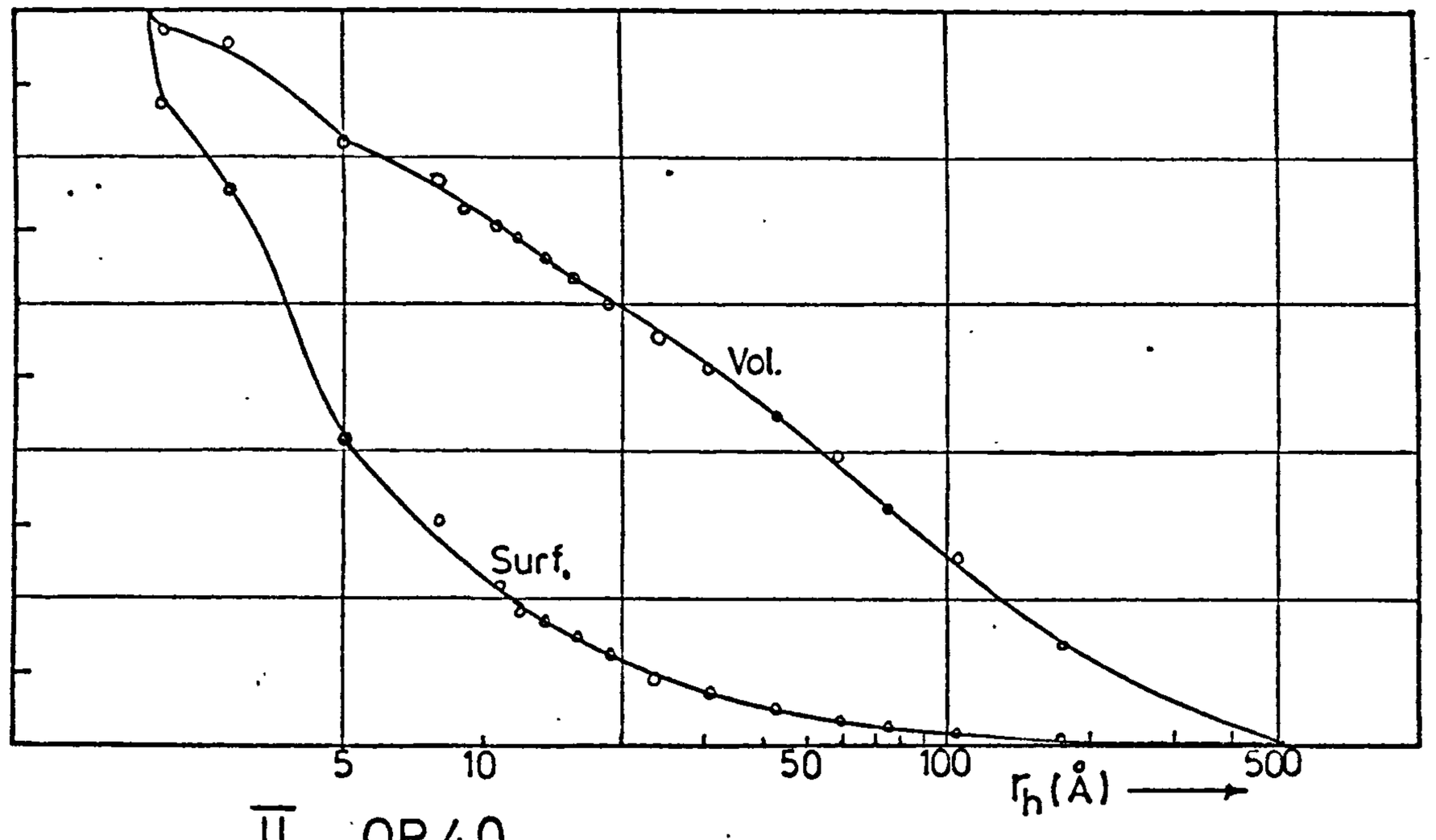

II OP40

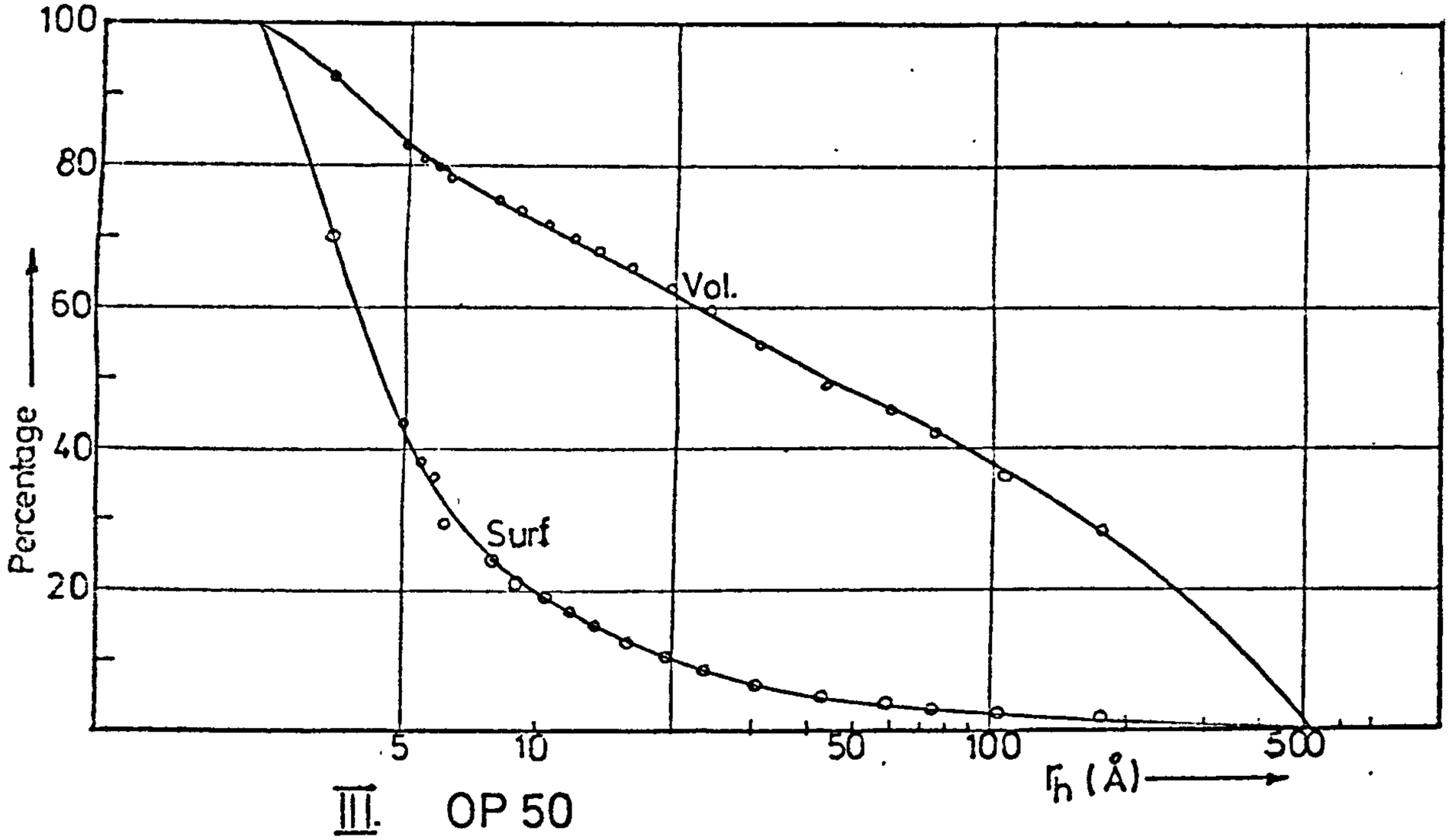

III. OP 50

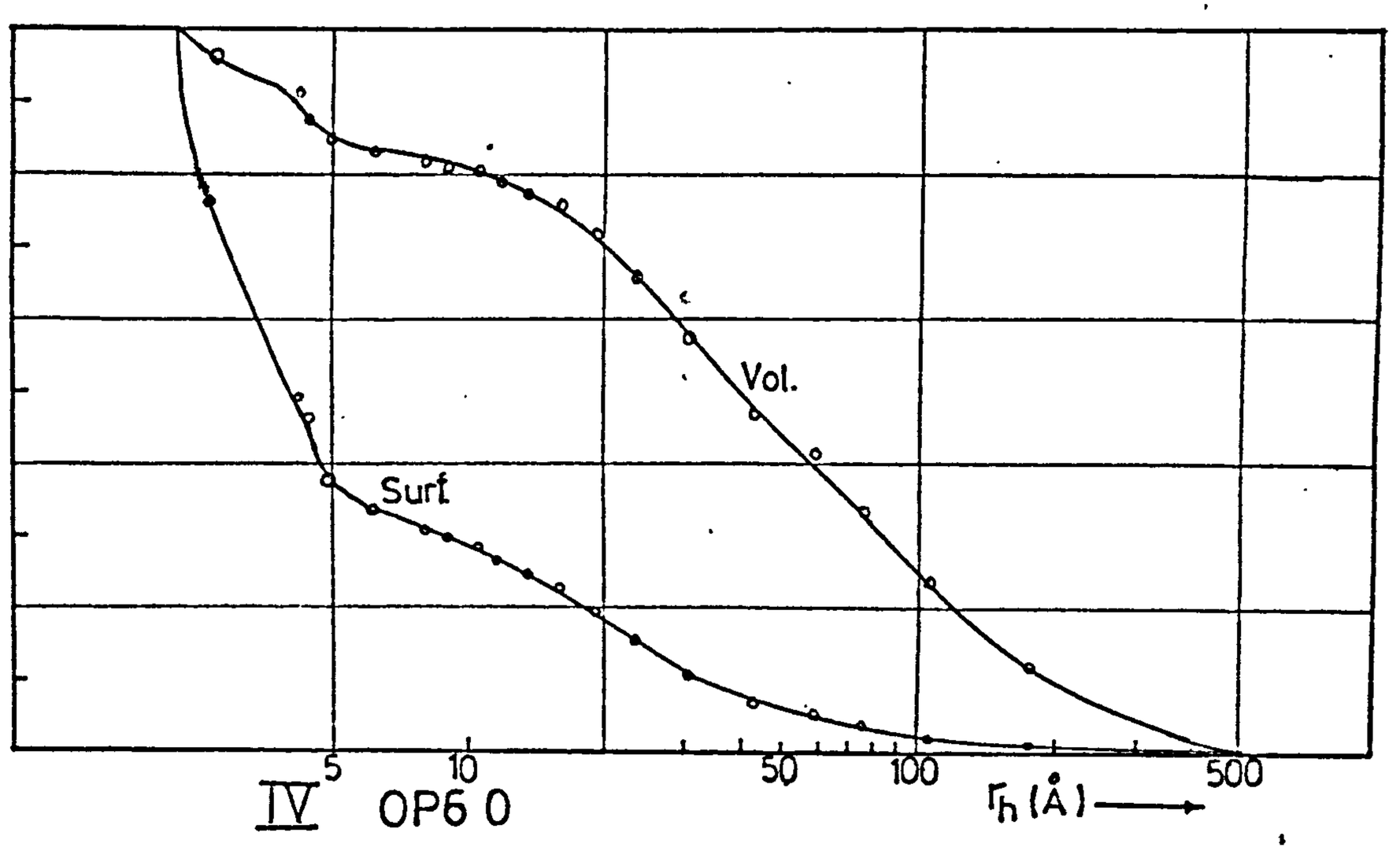

IV OP60

FIG.(4.15) I-IV CUMULATIVE PORE SURFACE & VOLUME DISTRIBUTION CURVES

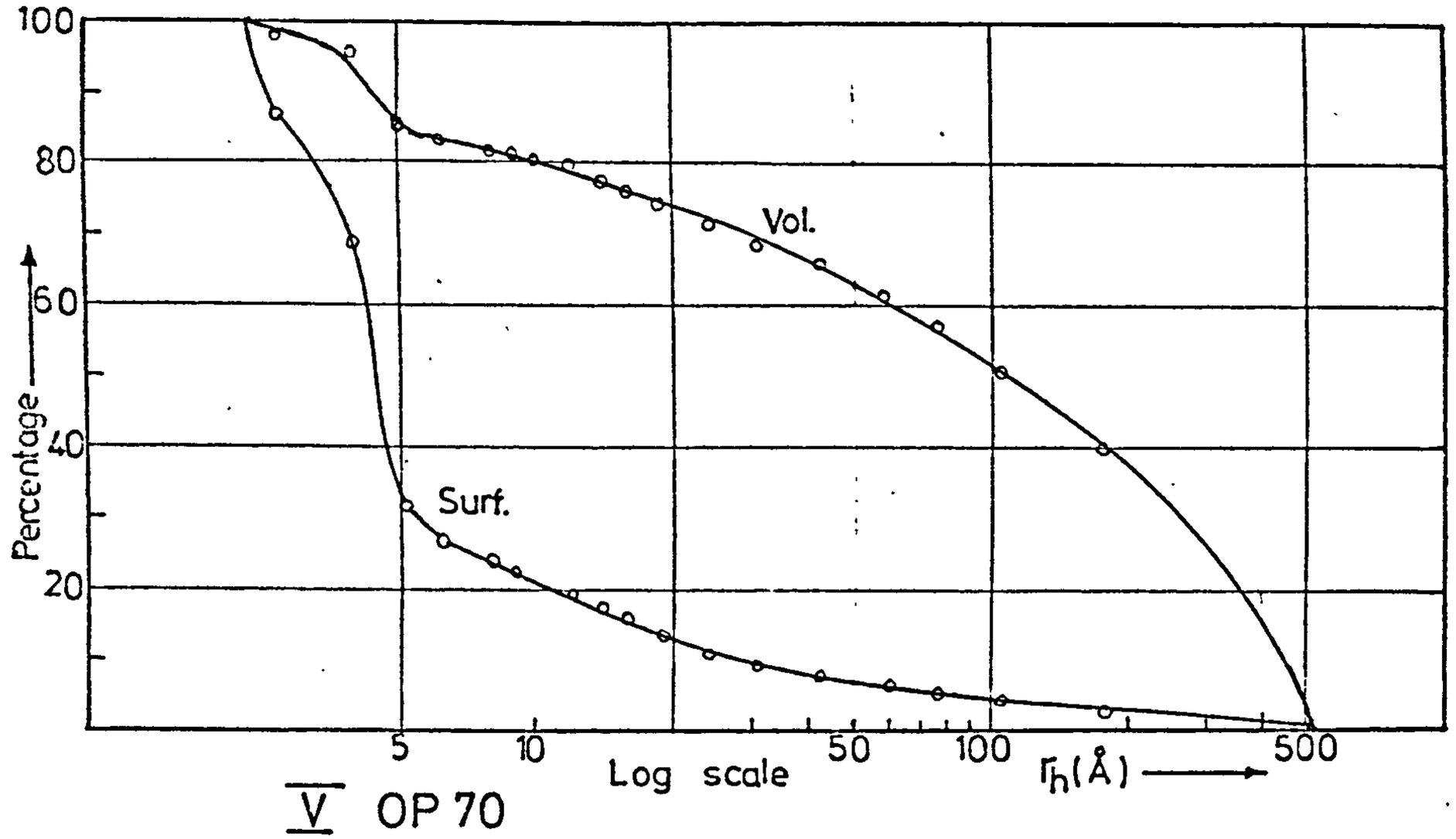

V OP 70

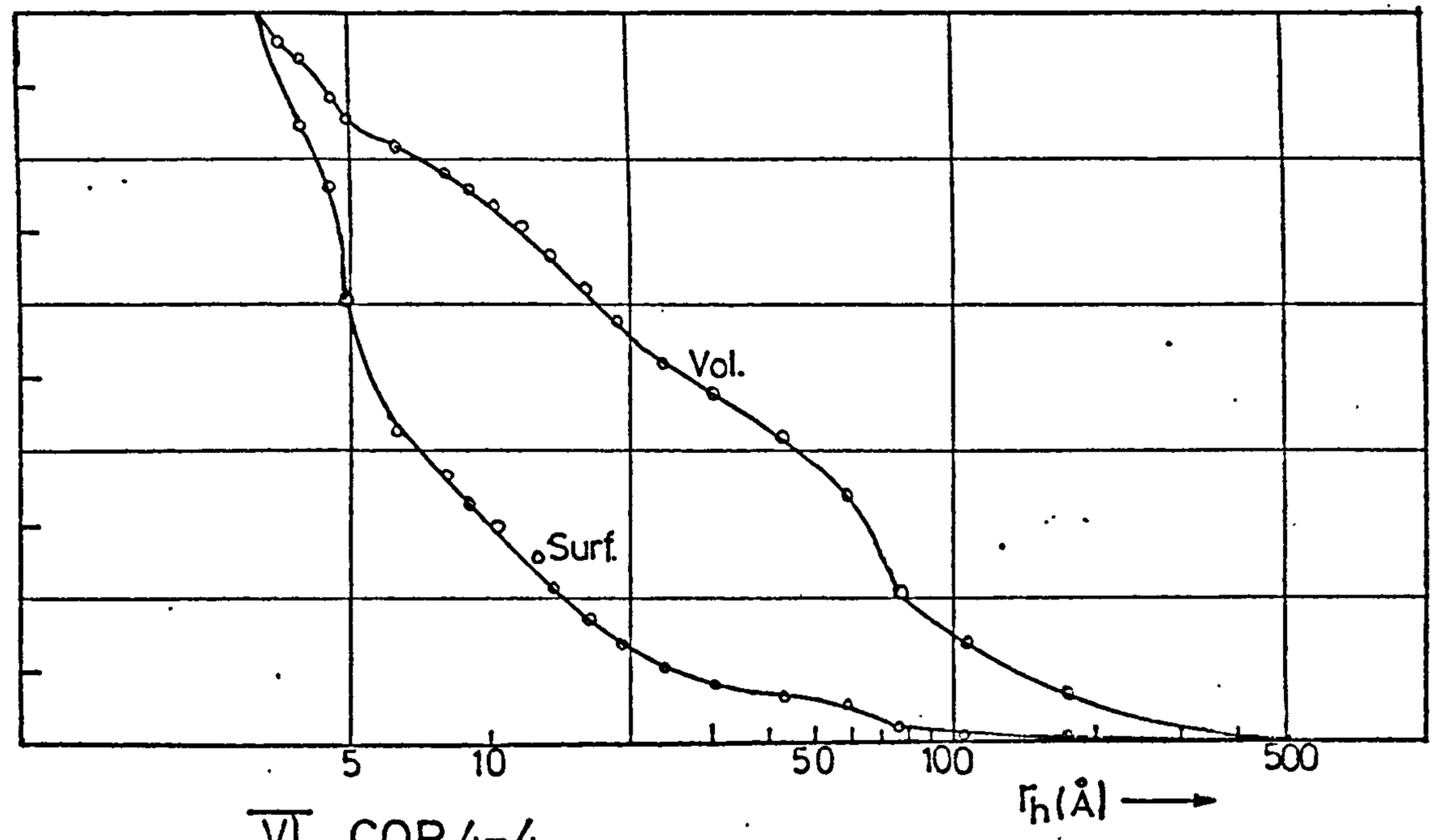

VI COP 4-4

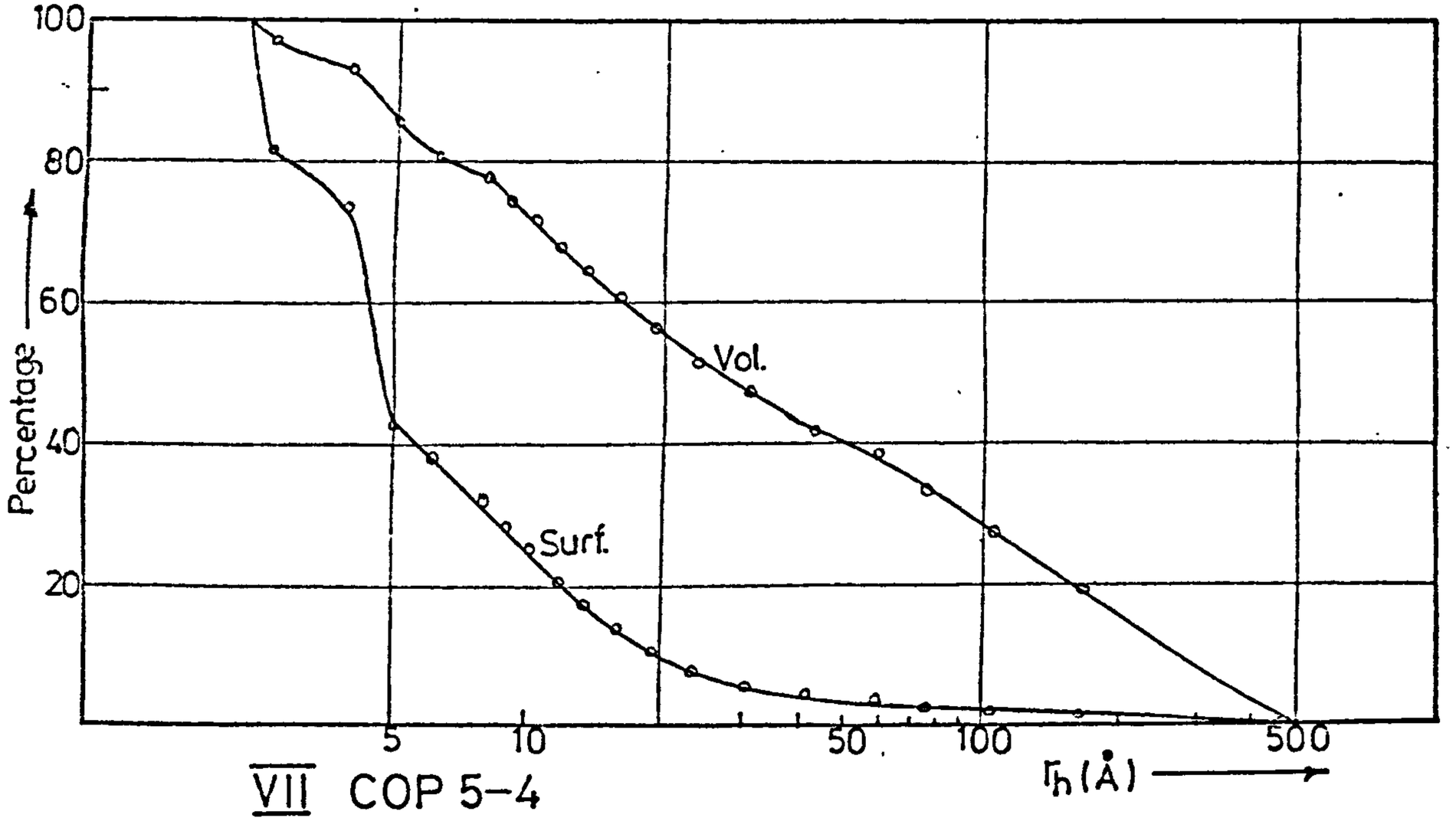

VII COP 5-4

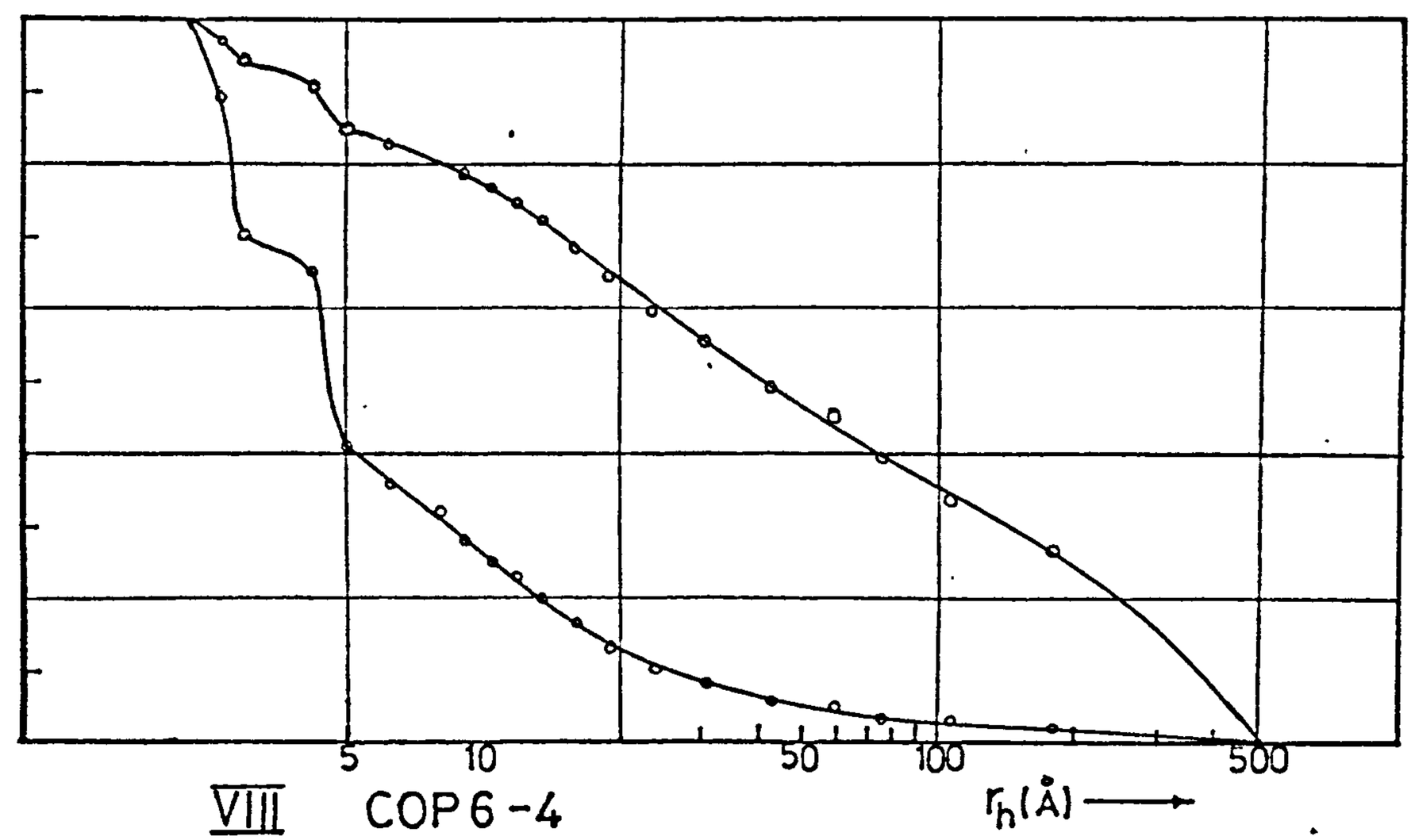

VIII COP 6-4

FIG(4.15) V – VIII CUMULATIVE PORE SURFACE & VOLUME DISTRIBUTION CURVES

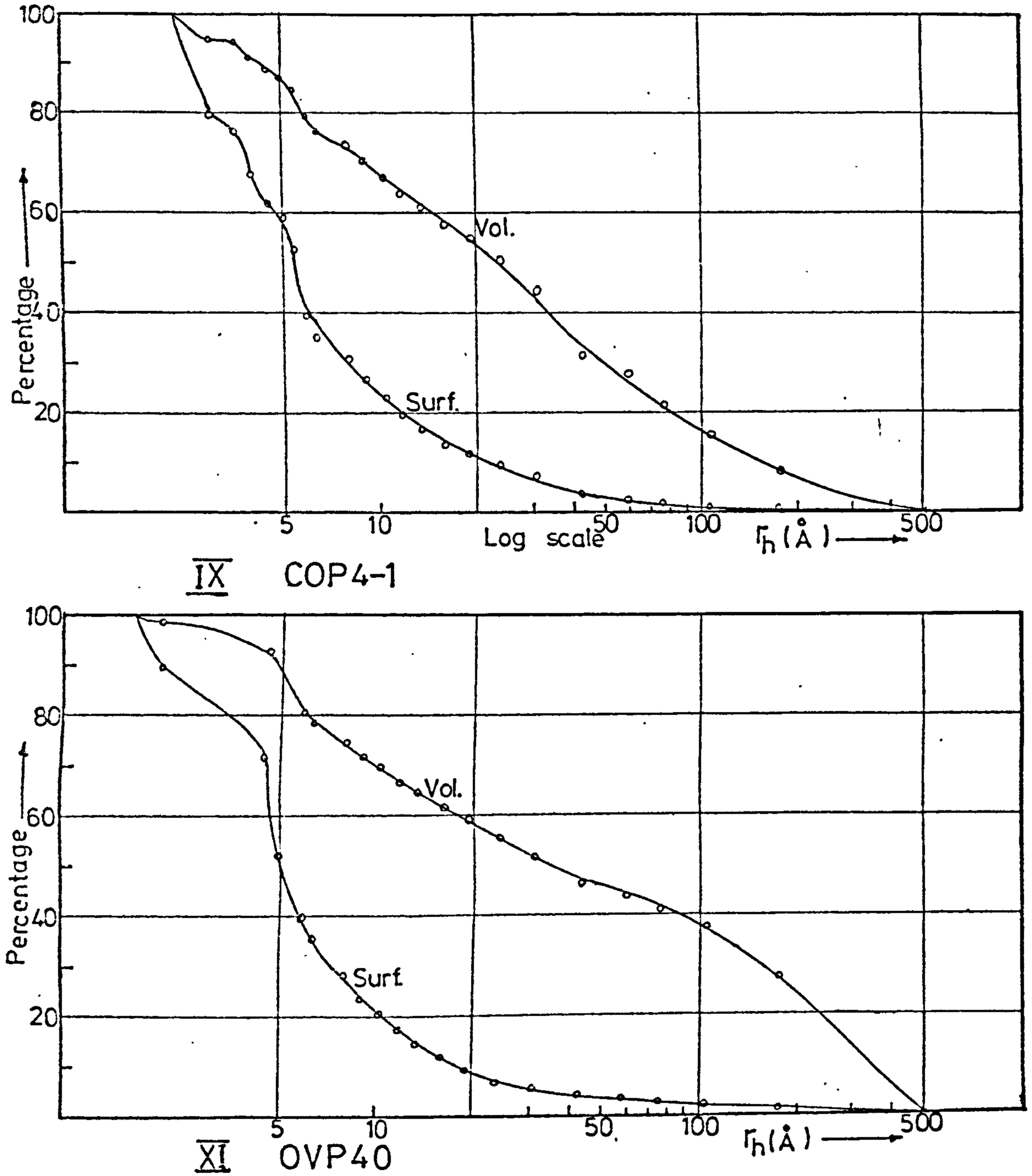

IX COP4-1

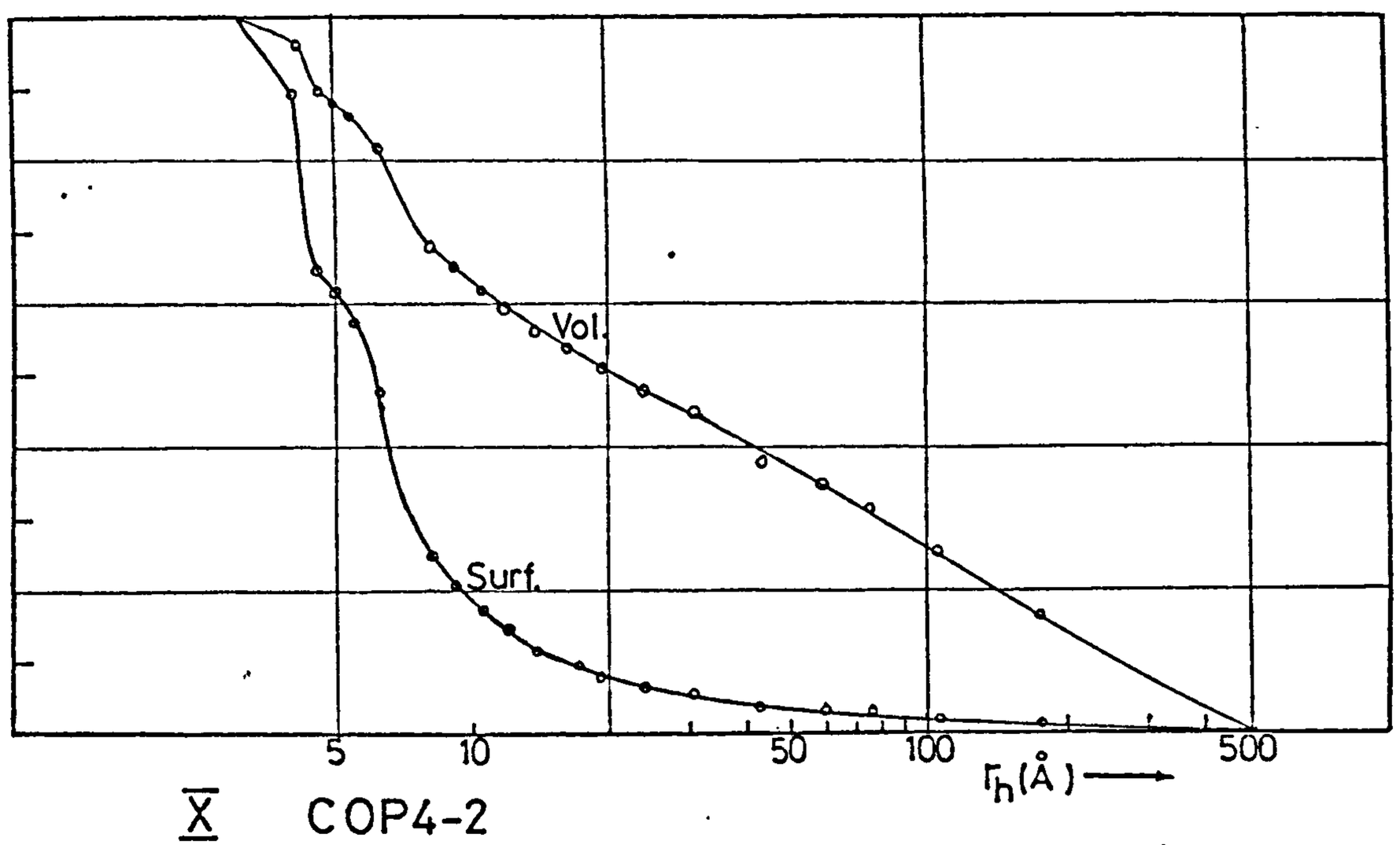

X COP4-2

XI OVP40

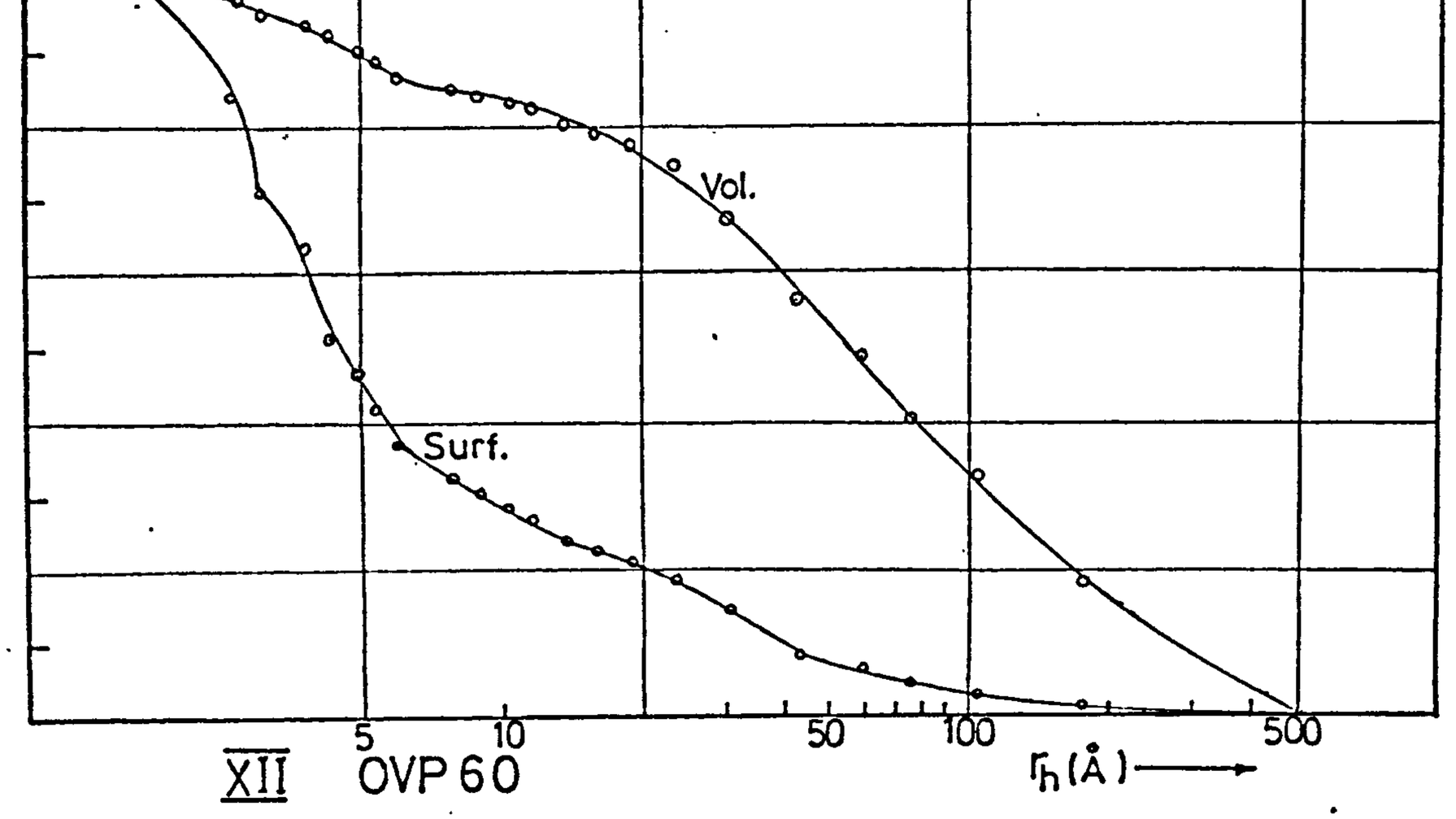

XII OVP 60

FIG (4.15) CUMULATIVE PORE SURFACE & VOLUME DISTRIBUTION CURVES

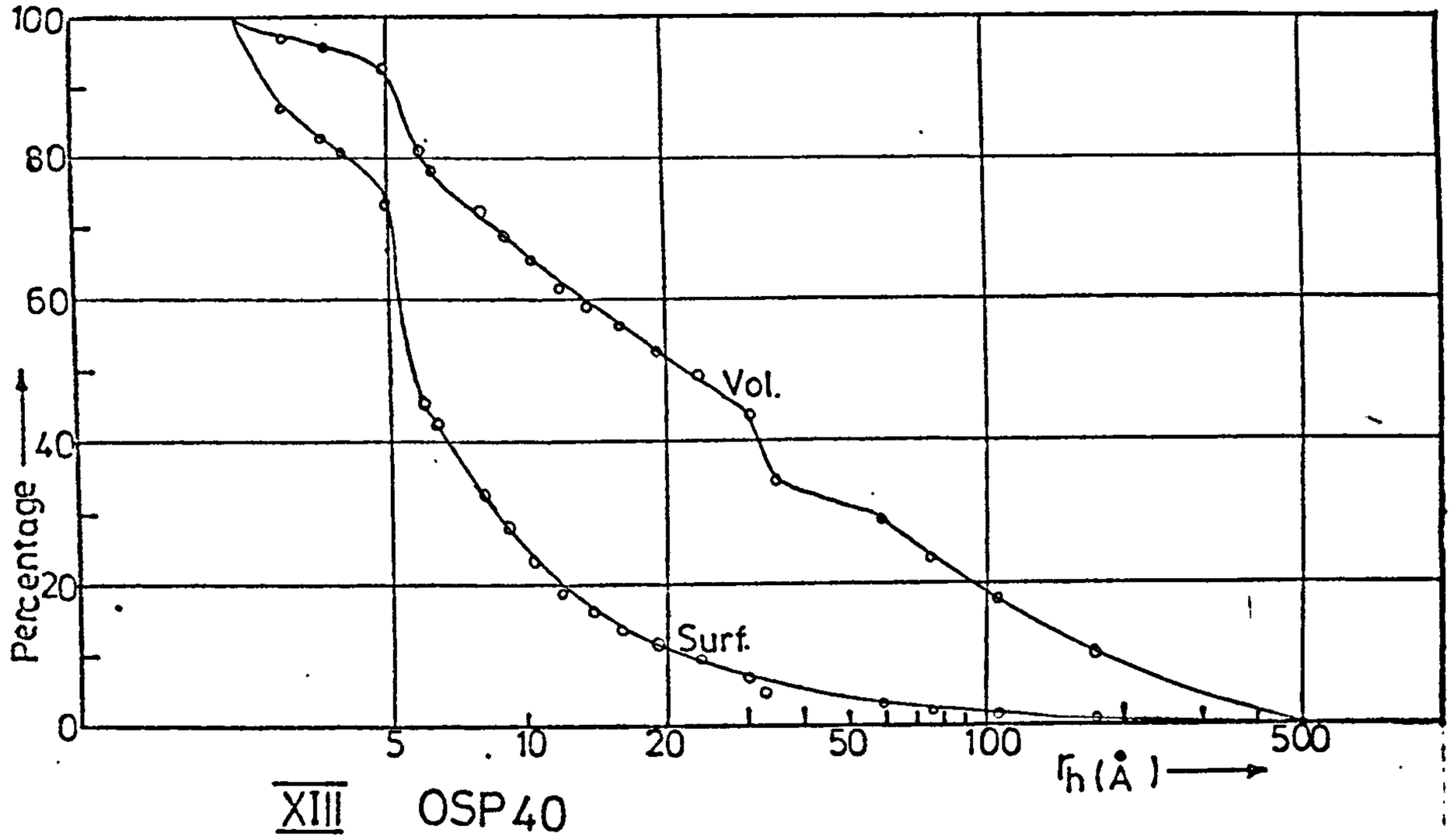

XIII OSP40

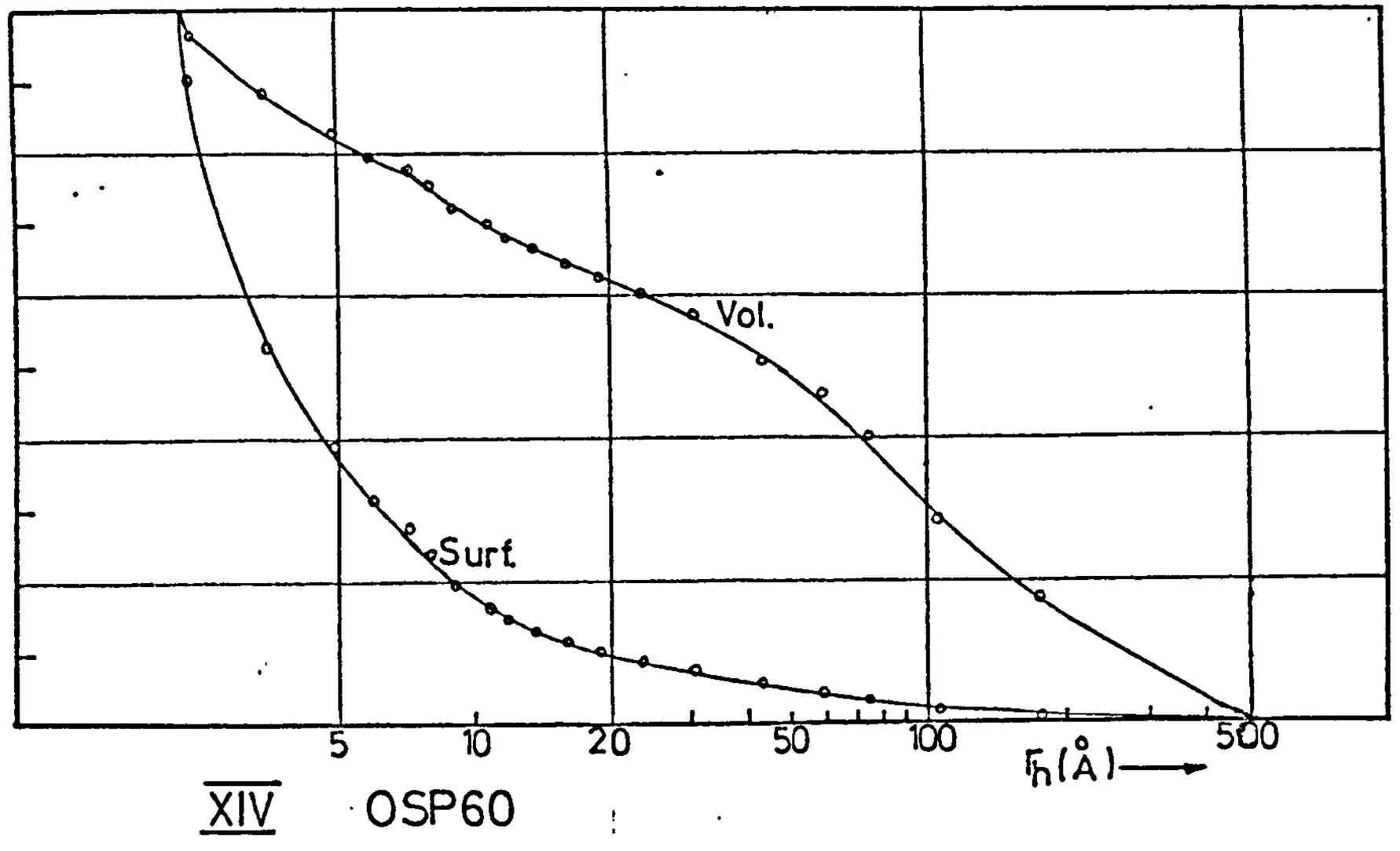

XIV OSP60

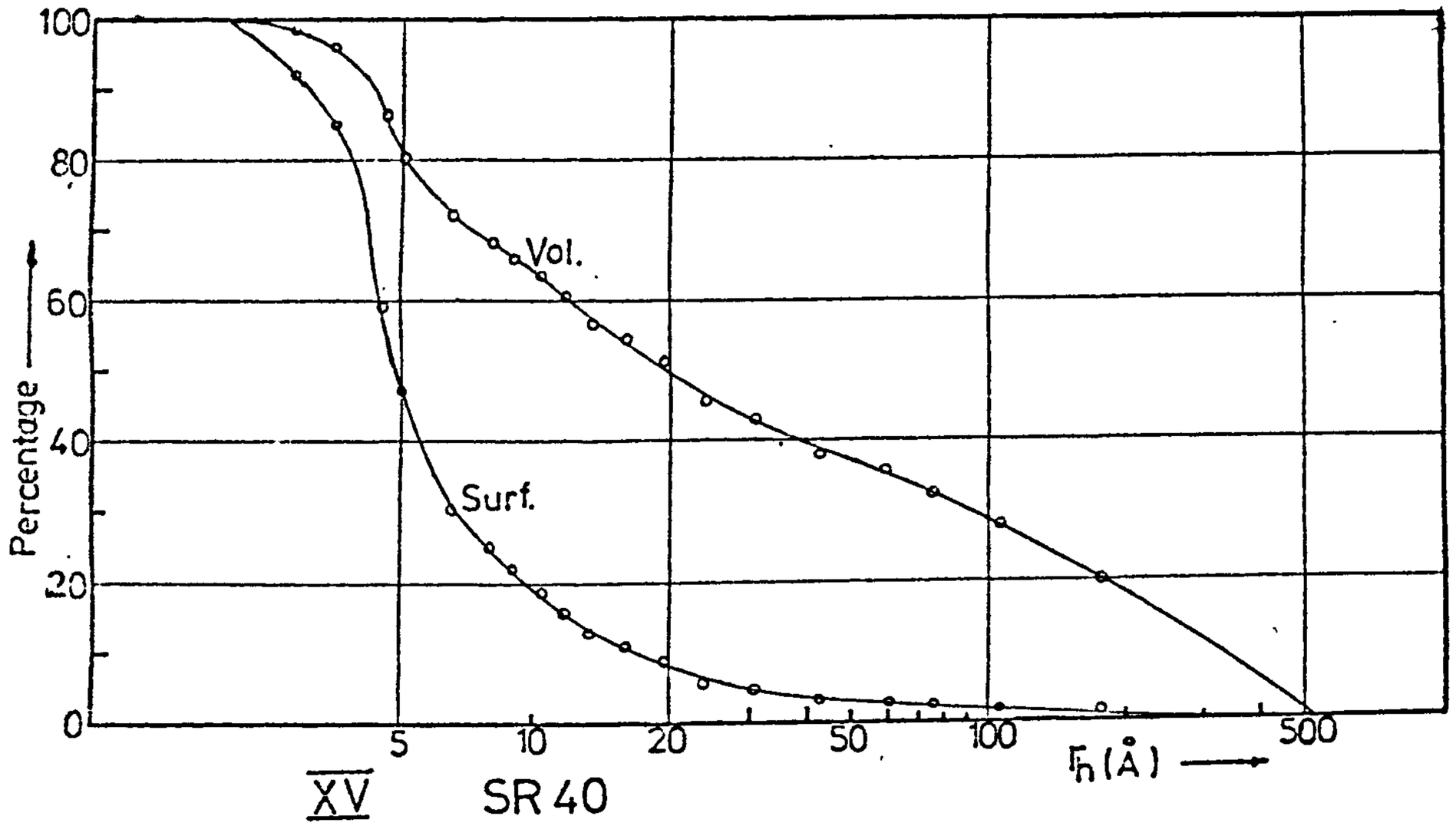

XV SR 40

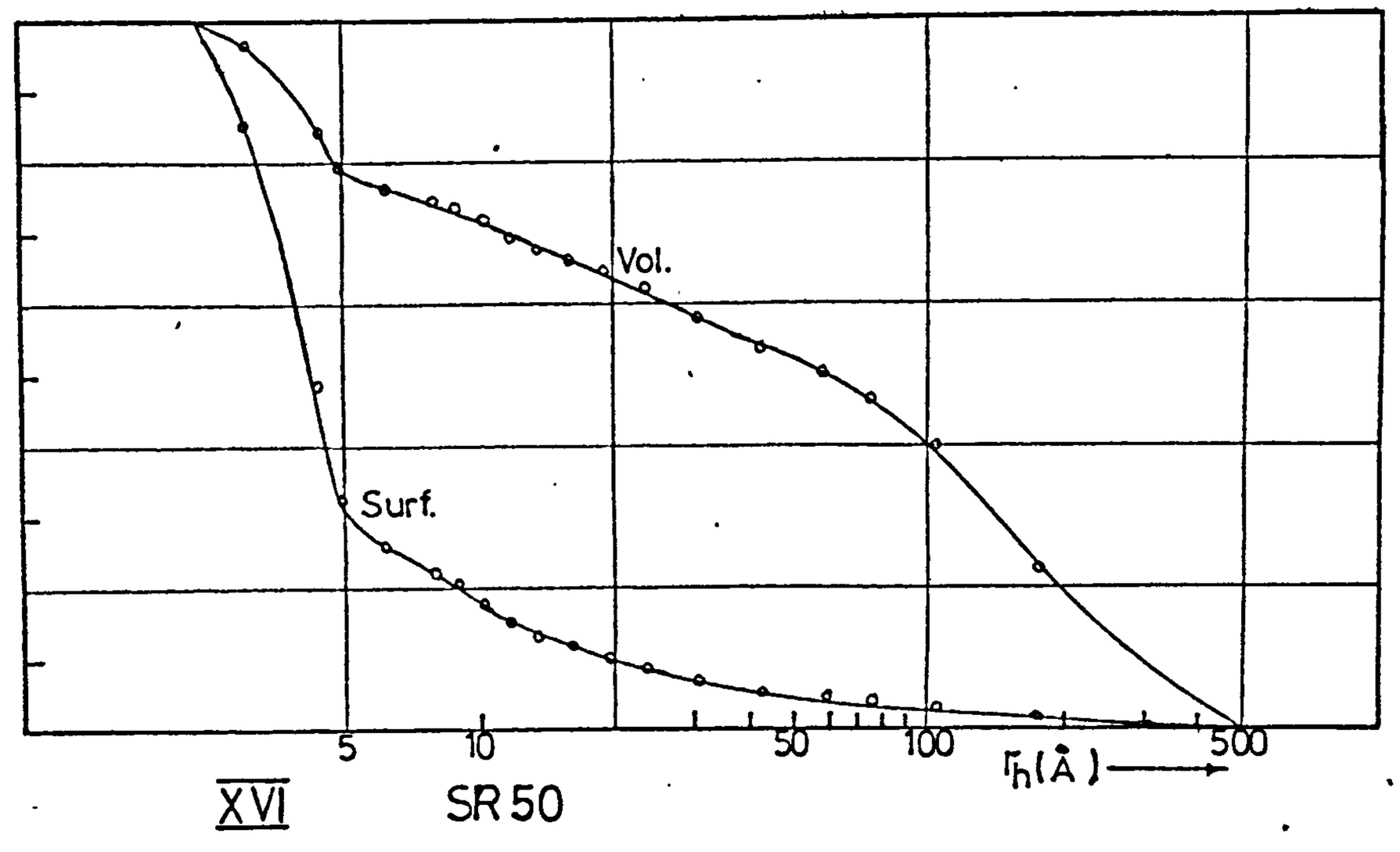

XVI SR 50

FIG (4.15) XIII – XVI CUMULATIVE PORE SURFACE & VOLUME DISTR. CURVES

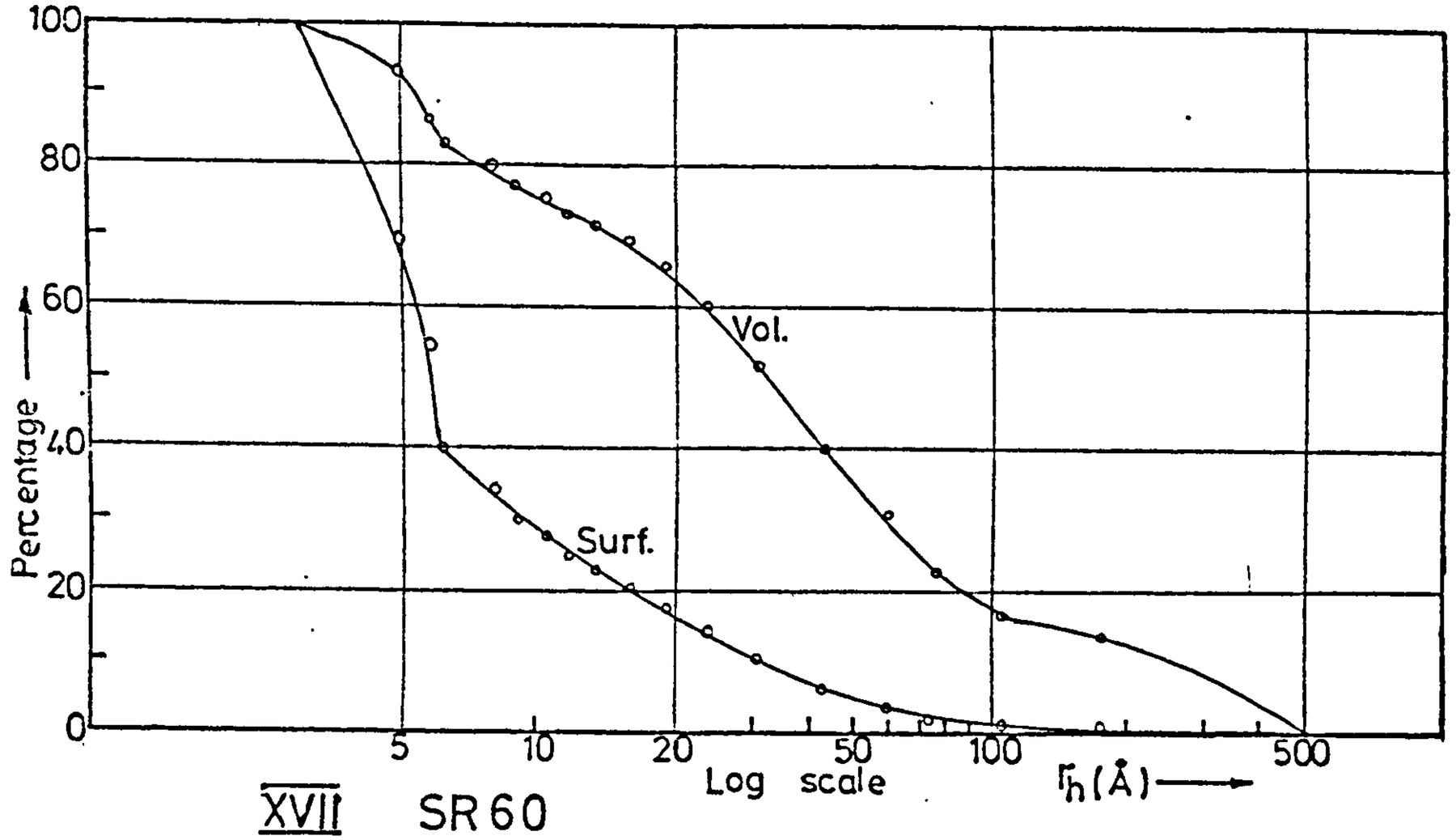

XVII SR 60

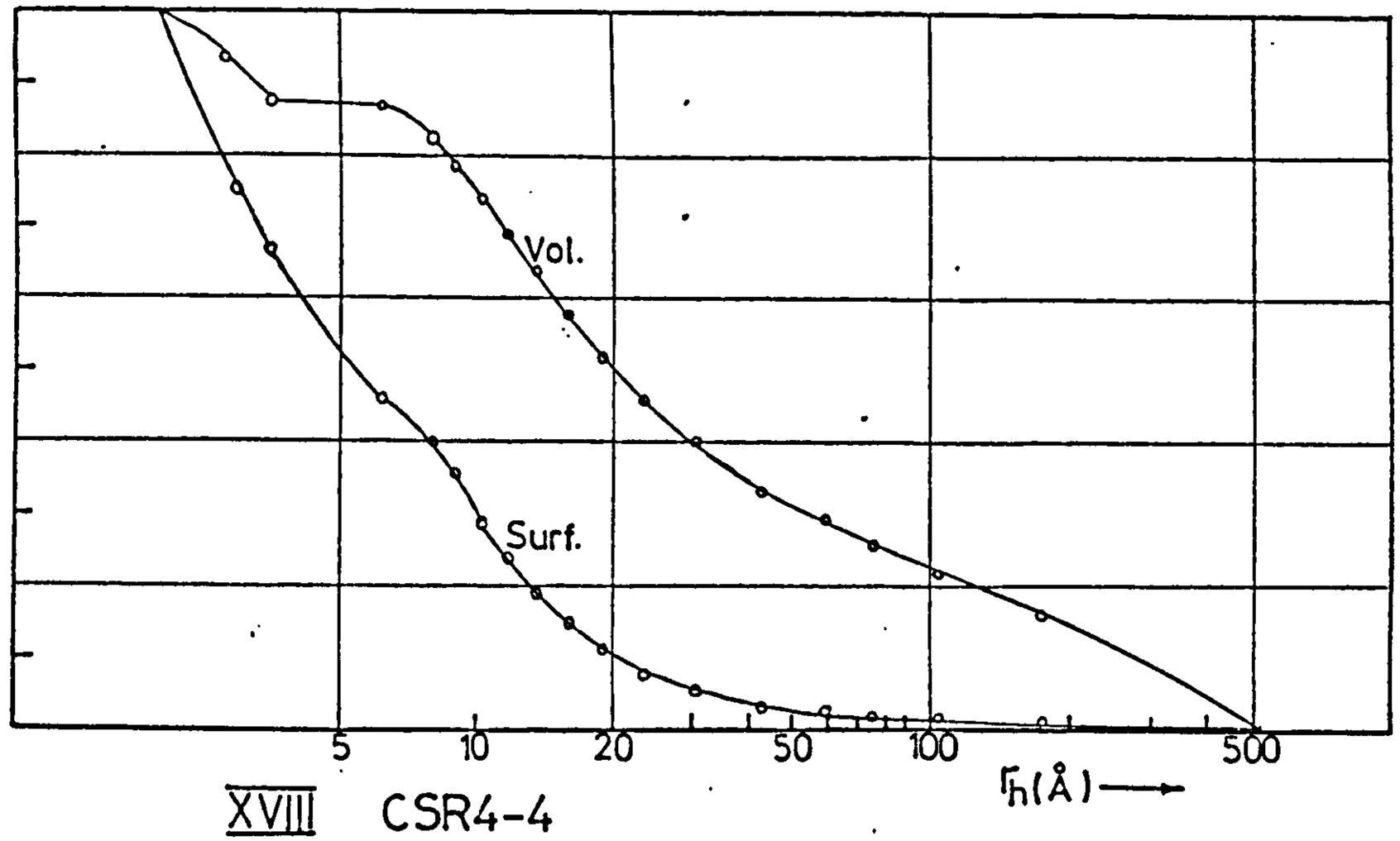

XVIII CSR4-4

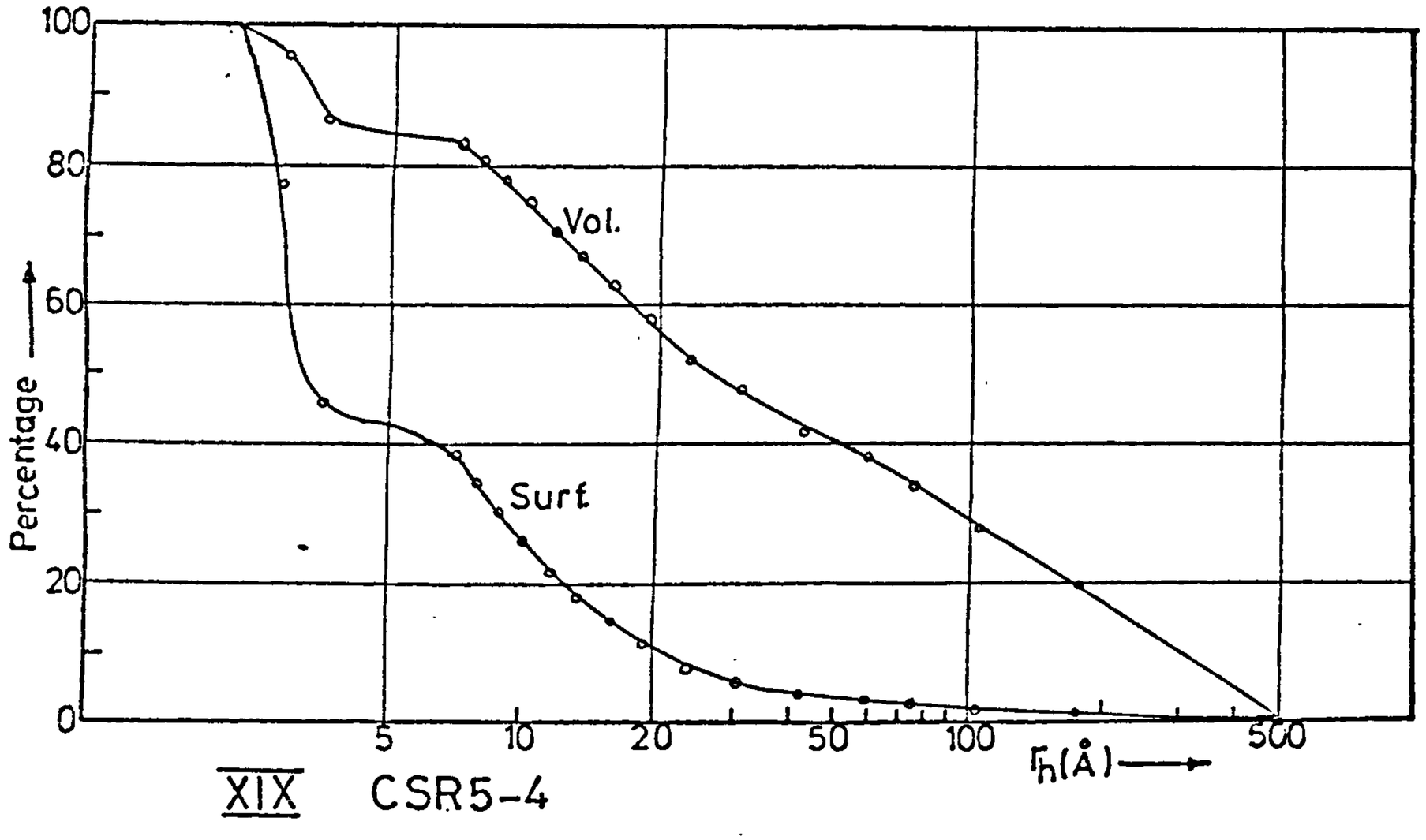

XIX CSR5-4

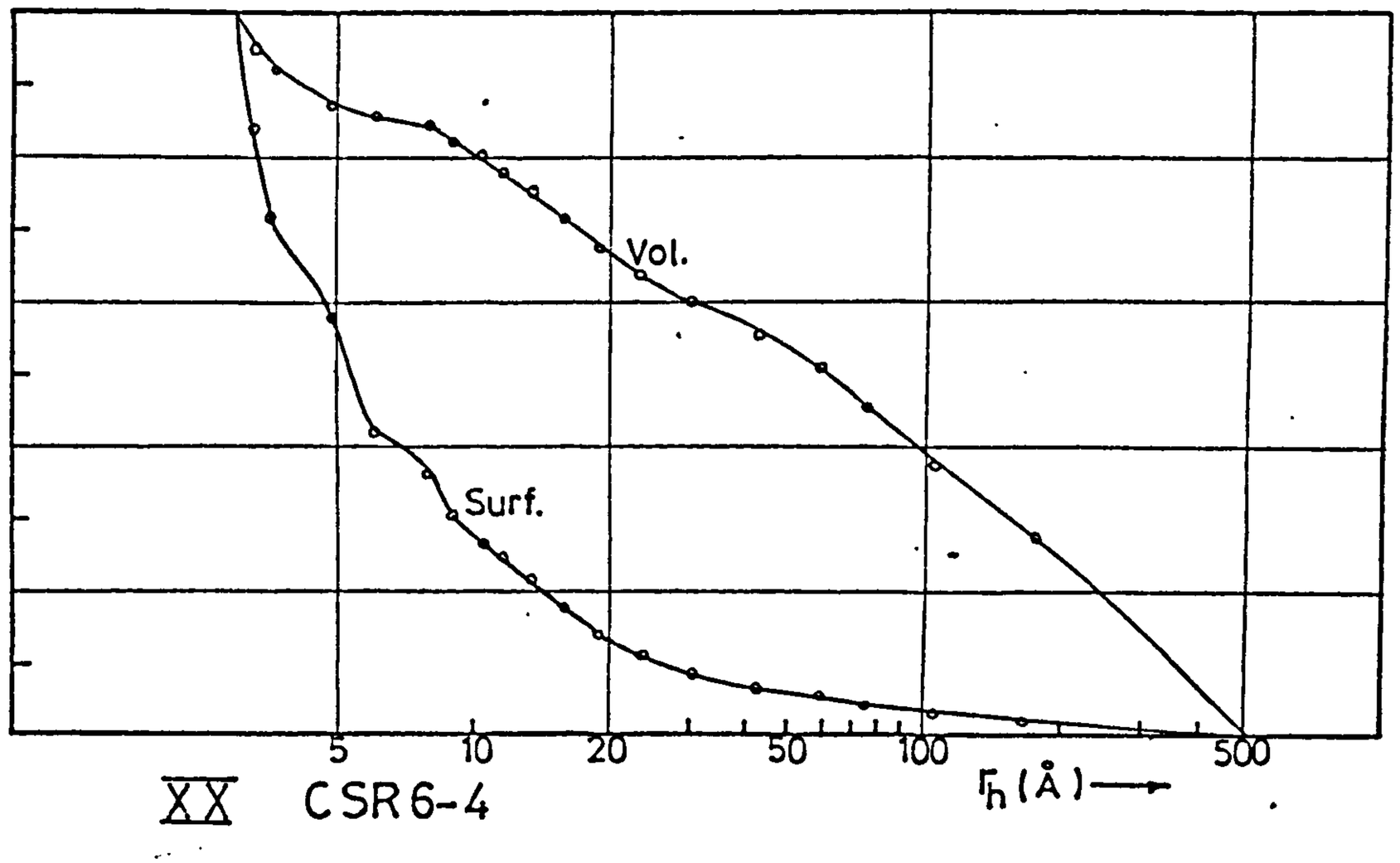

XX CSR6-4

FIG(4.15) XVII—XX CUMULATIVE PORE SURFACE & VOLUME DISTR. CURVES

4.4.7 Pore size Distribution Curves

Cumulative pore volume distribution curves are plots of $V_{(r)}$ against r_h, where $V_{(r)}$ is the volume of all pores having a hydraulic radius r_h and greater. From such curves,plots of $V_{(r)}/\ r_h$ against $\bar{r}_h$ can be obtained, where $V_{(r)}/\ r_h$ is the slope of the cumulative pore volume at $\bar{r}_h$ and $\bar{r}_h$ is the average hydraulic radius. Similiarly, cumulative pore surface curves and pore surface distribution can be obtained. In this thesis, only the pore volume distribution is considered using a wide-pore analysis. Such volume distribution curves are normally referred to as pore size distribution curves.

Pore size distribution curves are presented in figs. (4.16) to 4.22). The ordinate of the plot at any value of $\bar{r}_h$ is the volume per Ångstrom unit of pores with an average hydraulic radius - $\bar{r}_h$. It is thus a measure of the frequency of occurence of pores of different hydraulic radii. The following general observations follow from the figures:

1. Increasing the W/C ratio reduces the frequency of occurence of pores in the small pore size region and produces greater uniformity in pore size distribution. This generally applies to both OPC and SRPC pastes. Eg. from fig. (4.16), OP30 has a peak value of 9.40 at 7.8 Å; OP40 has 6.39 Å; at 9.6 Å; OP50 has 5.85 at 8.5 Å; ; OP60 has 3.95 at 8.50 Å; and OP70, 4.92 at 8.65 Å thus there is a generally decreasing peak value with W/C ratio. The distribution curves, except for OP60, look very similar from about 25 Å onwards.

2. OPC and SRPC pastes with admixtures generally have a larger volume of small size pores than pastes without admixture figs. (4.16) and (4.20) compared with figs. (4.17) and (4.21)respectively. The ordinates of the latter increased at low $\bar{r}_h$.

4.5 Concrete Porosity

The porosity, P_c, of each concrete mix used throughout this thesis was calculated as the sum of the separate porosities of cement paste and aggregate plus air content, and expressed as a percentage volume of the concrete. Equ. (2.5) was rewritten as:

$$P_c = P_p \cdot V_p + P_A (1 - V_p) + A_o \qquad (4.27)$$

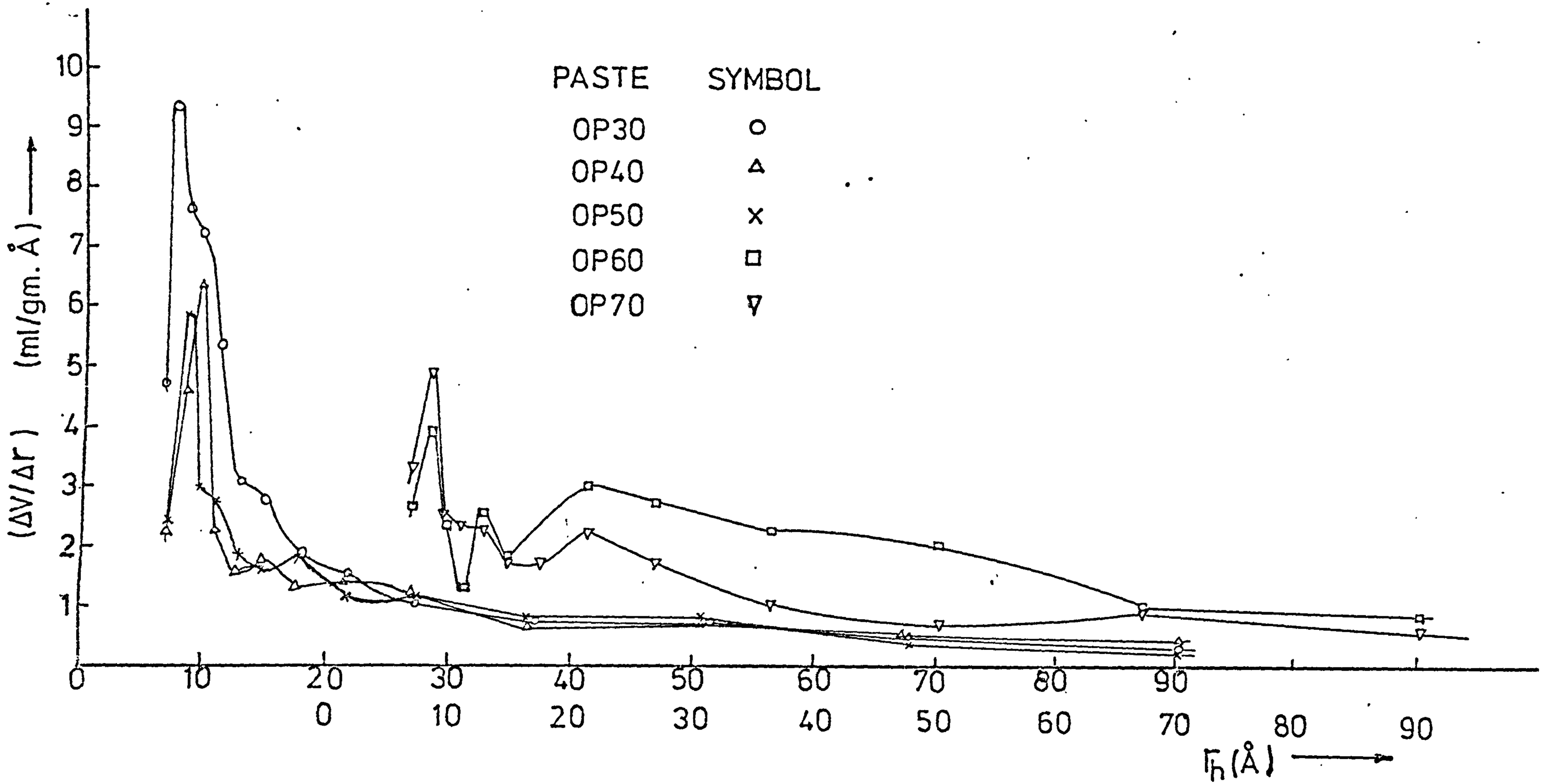

FIG(4.16) PORE SIZE DISTRIBUTION CURVES FOR OPC PASTES

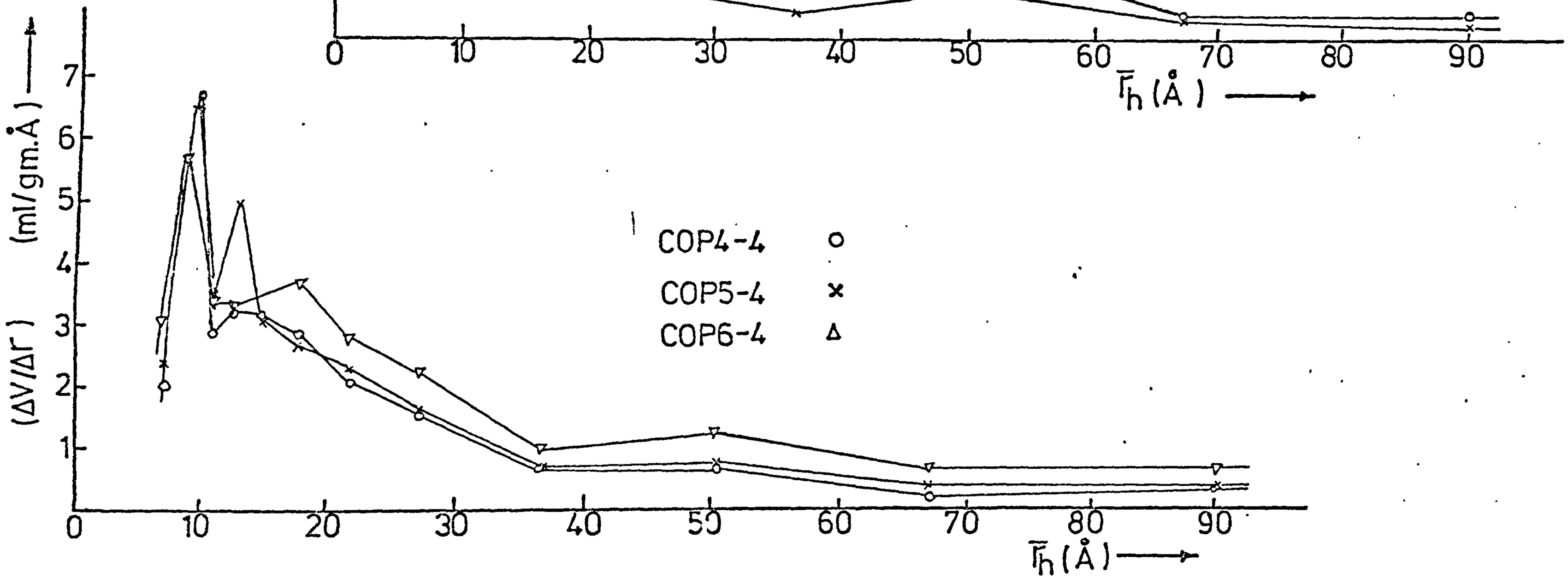

FIG(4.17) PORE SIZE DISTRIBUTION CURVES FOR SUPERPLASTICISED OPC PASTES

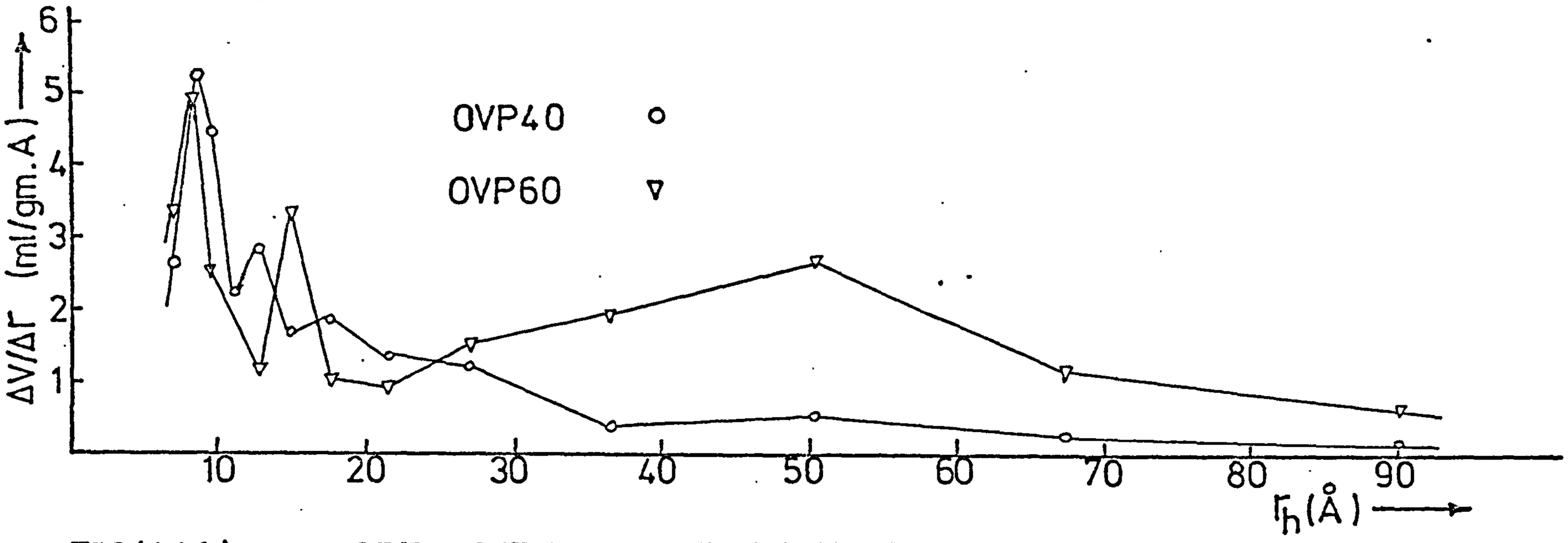

FIG(4.18) PORE SIZE DISTRIBUTION CURVES FOR OVEN-DRIED OPC PASTES

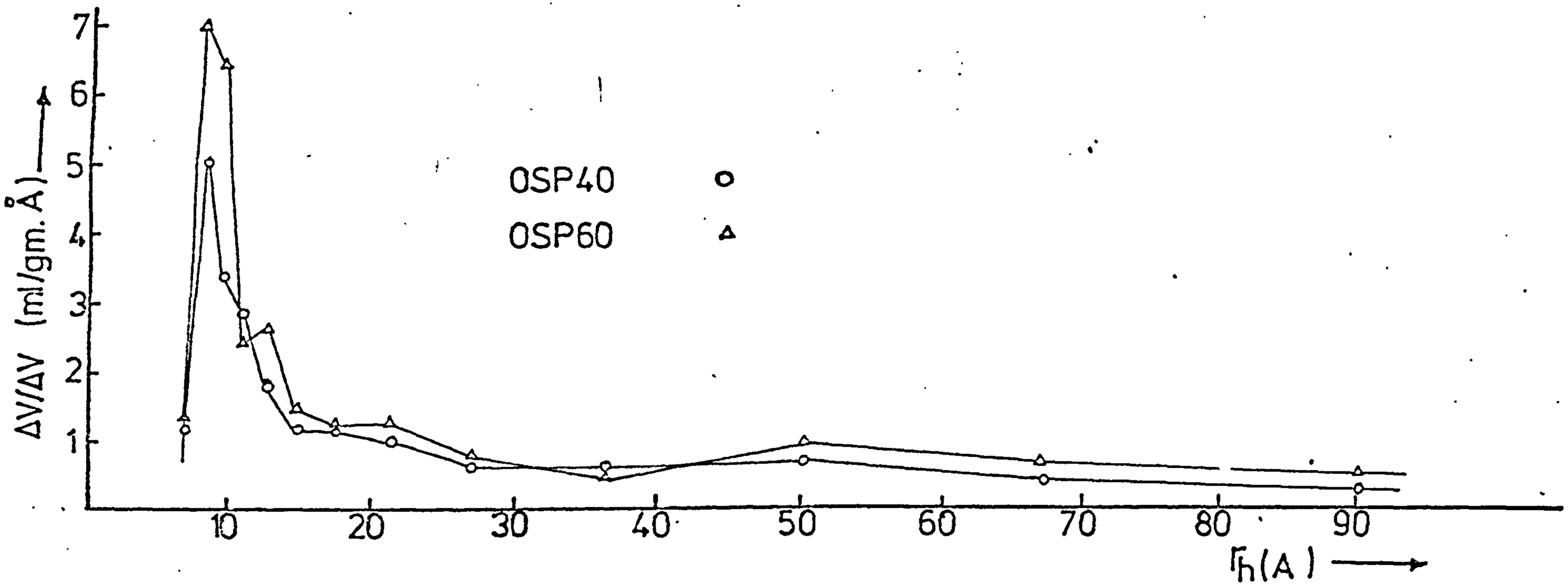

FIG(4.19) PORE SIZE DISTR. CURVES OF PREVIOUSLY OIL SAT. HCPS.

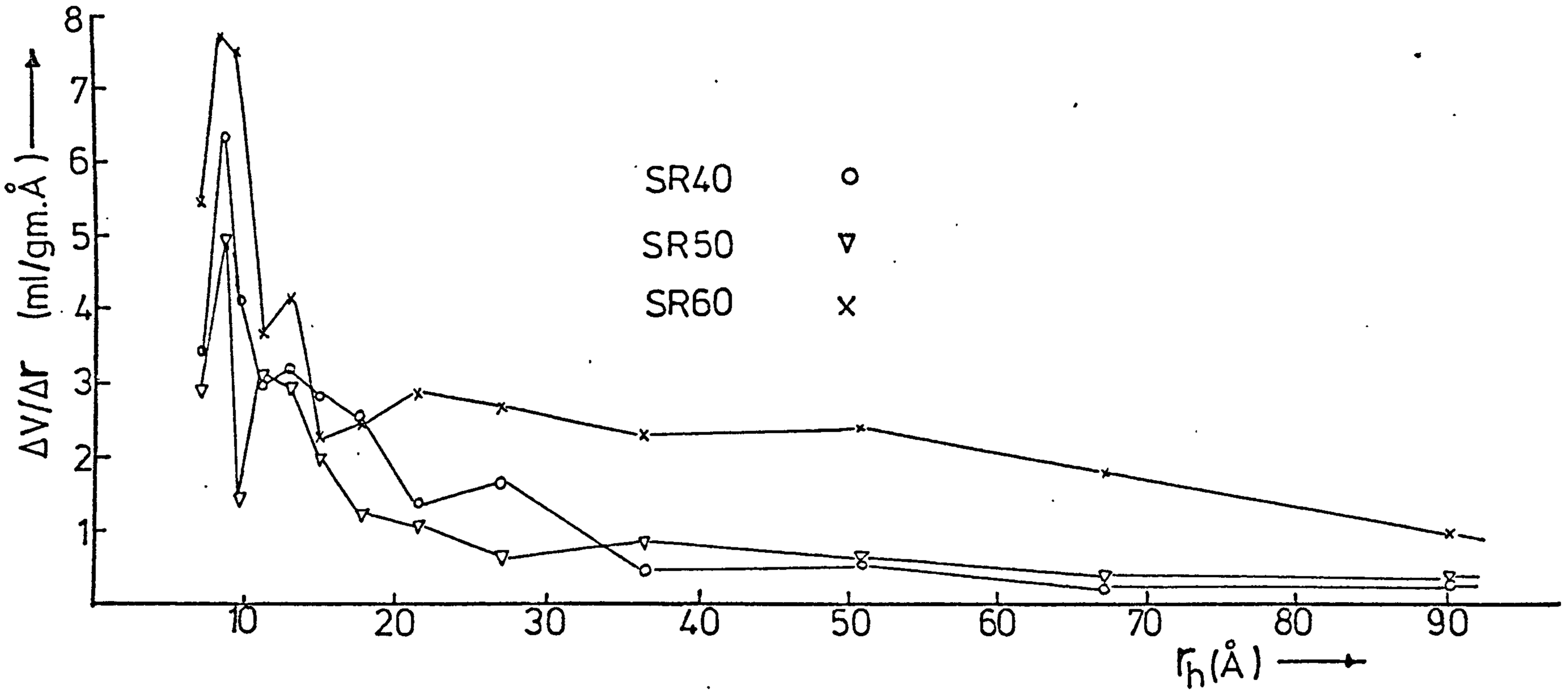

FIG(4.20) PORE SIZE DISTR. CURVES FOR SRPC PASTES

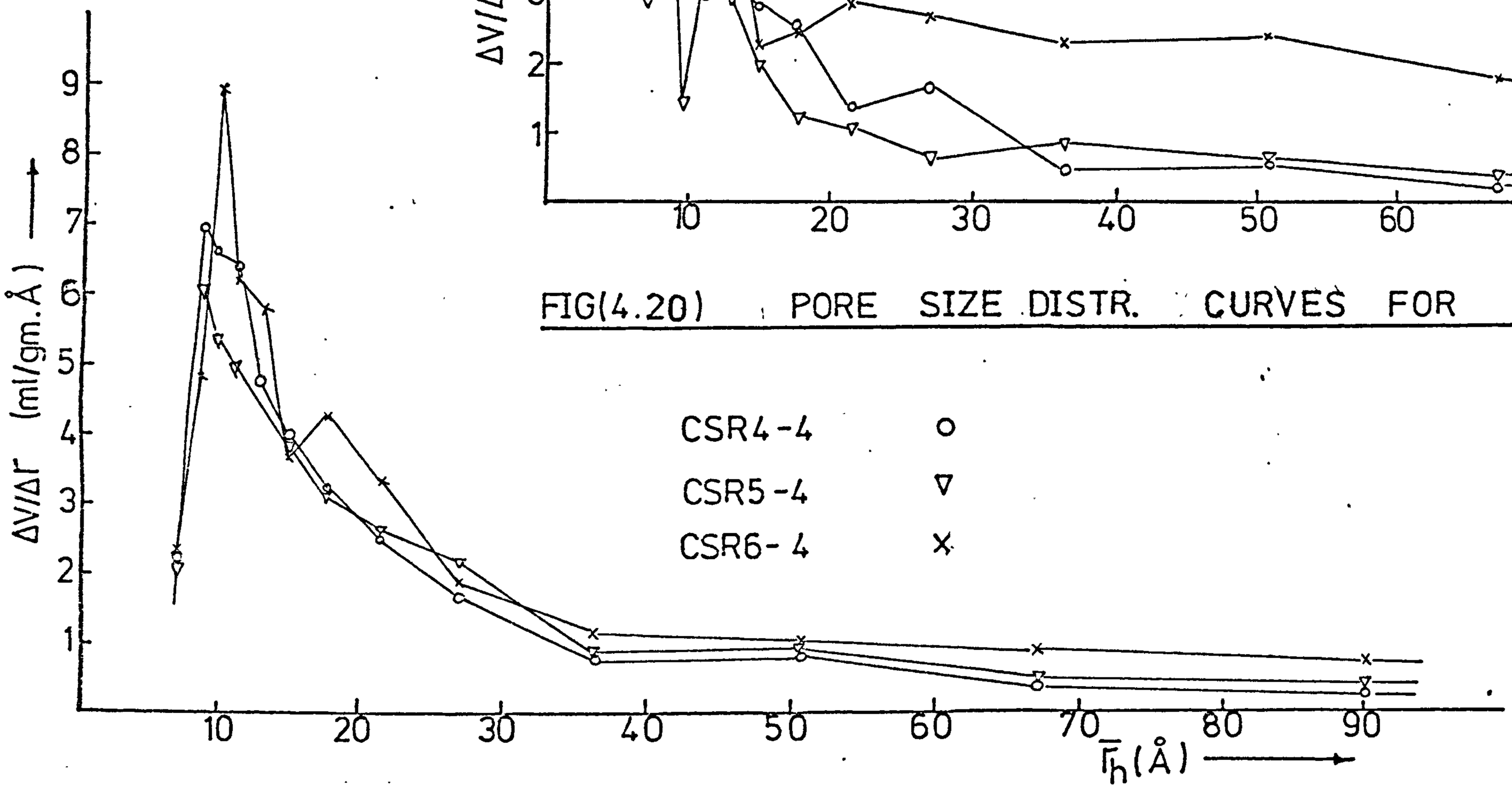

FIG(4.21) PORE SIZE DISTR. CURVES FOR SUPERPLASTICIZED SRPC PASTES

P_p, the HCP porosity was taken from fig. (4.4) and (4.5) for OPC and SRPC respectively. To calculate V_p, the density values given in fig. (4.6) were used. Aggregate porosities, P_A, were determined by the absorption method according to BS 812:1967. These were 1.12% for coarse and 1.42% for fine aggregates. The air content, A_o, was determined by comparing the density of a concrete sample after 20 - 24 hours, d_a, with the density calculated from mix proportions - d, ie. air free concrete. Then, A_o is given by [70]:

$$A_o = 1 - d_a/d \qquad (4.28)$$

Typical calculated values for OPC concrete used for elastic modulus tests - Chapter 6 - are given in table (4.6), with mix proportions given in table (3.7). Other values of concrete porosity are given and treated in various sections of the thesis.

MIX DESIGN. TABLE (3.7)	W/C RATIO	HCP DENSITY (g/CC)	Volume fraction of the Concrete			Total Porosity (% Vol.)
			HCP POROSITY	AGGREGATE POROSITY	AIR CONTENT	
MD40	0.40	2.18	0.1396	0.0075	0.0196	16.67
MD50	0.50	2.05	0.1483	0.0079	0.0170	17.32
MD60	0.60	1.92	0.1603	0.0082	0.0126	18.11
MD70	0.70	1.83	0.1720	0.0084	0.0102	19.06

Table (4.6) Typical Calculation of Concrete Porosity (OPC)

CHAPTER 5

PERMEABILITY OF HARDENED CEMENT PASTES AND CONCRETE TO CRUDE OIL

5.1 Introduction

The permeability of hardened cement pastes (HCPs) and concrete is governed mainly by its W/C ratio, degree of hydration, curing conditions, type and fineness of the cement. The permeability of concrete is a function of the paste permeability, the aggregate permeability, the relative proportions of the two and the effectiveness of compaction of the concrete. The movement of fluids in HCP and concrete takes place in the so-called open pores and depends upon the number and size of the pores connected with the surface.

The investigation studies the oil permeability of HCP and concrete using OPC and SRPC cements with and without admixtures and a Kuwait crude oil. Attempts are made to establish relationships between permeability, pore structure and the applied fluid pressure and also between the mix design parameters and permeability. Adsorption capabilities of the samples were related to HCP and concrete properties.

5.2 Apparatus and testing procedure

The apparatus used for these tests has been fully described[12], and is shown in plate (5.1) and in fig (5.1). The base plates of the permeability cell were modified to hold samples of 150 mm and 100 mm diameter and thicknesses of 15 - 200 mm. The amount of oil flowing into or out of the test specimens can be measured by reading the change in the levels of oil in the 4 mm diameter perspex tubes held against a graduated scale. Ten permeability cells were made and set up in two groups, one of four and the other of six. The oil pressure was held constant with regulating values graduated in psi. which controlled the pressure from a compressed nitrogen bottle of 2,000 psi (13,790 KN/m^2) capacity. Any cell could be disconnected from its group at any time without interfering with the operation of the other units. 7 mm diameter O-rings were used to provide a sealing for oil

1. Inlet valve
2. Outlet valve
3. Bleeding valve
4. Inner sealing O-ring for HCP specimens
5. Outer " " " Concrete "
6. Top flange
7. Bottom flange
8. Eight bolts 12mm dia.
9. Supporting frame
10. Inlet pipe - 5mm internal dia.
11. Outlet pipe
12. Pressure regulating gauges
13. Board fitted with scale in mm.
14. Oil feeding valve
15. Pressure regulating gauges
16. Compressed nitrogen cylinder (2000psi)
17. Oil reservoir

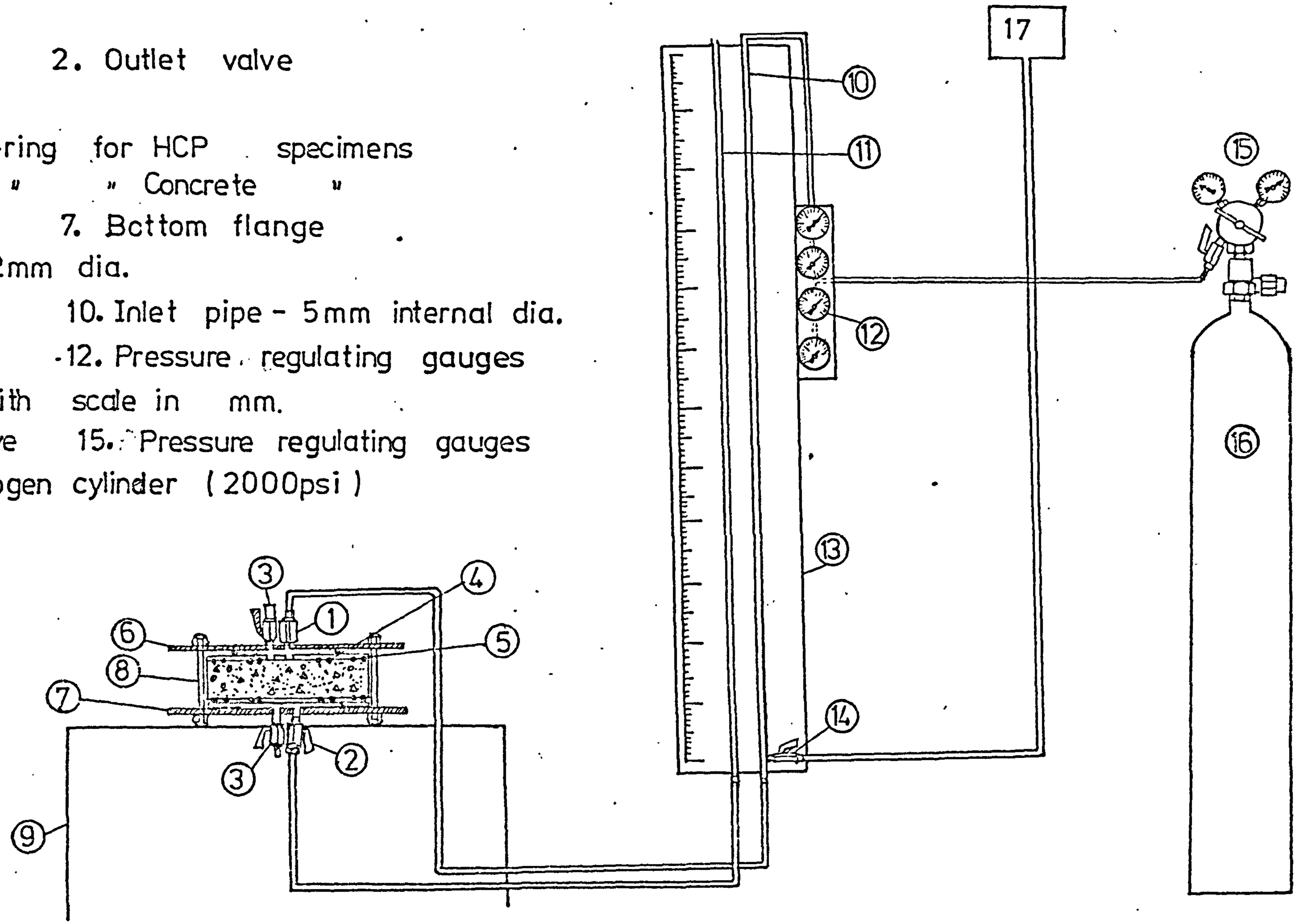

FIG(5.1) SCHEMATIC DRAWING OF THE PERMEABILITY APPARATUS SHOWING A CELL

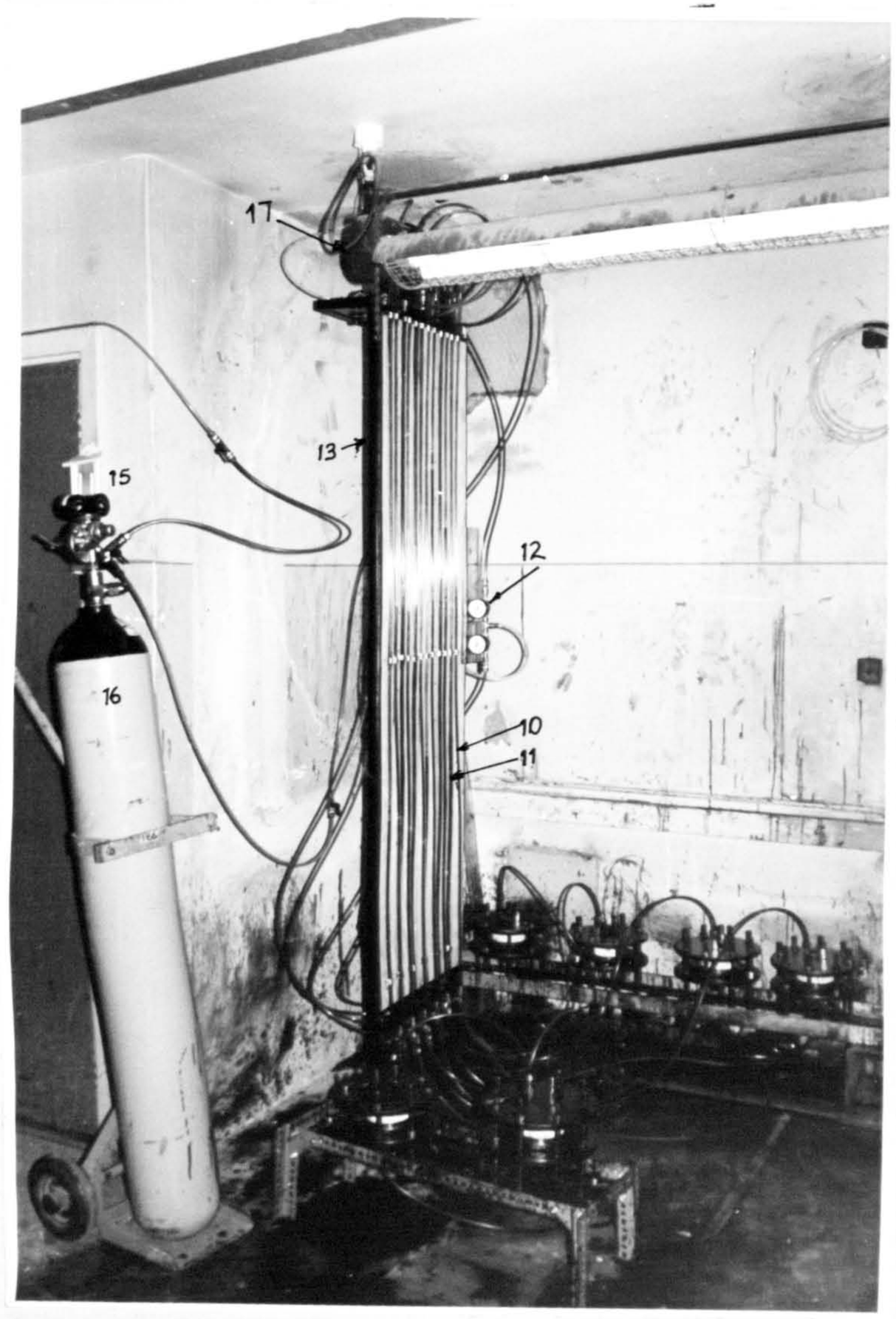

General Set-up

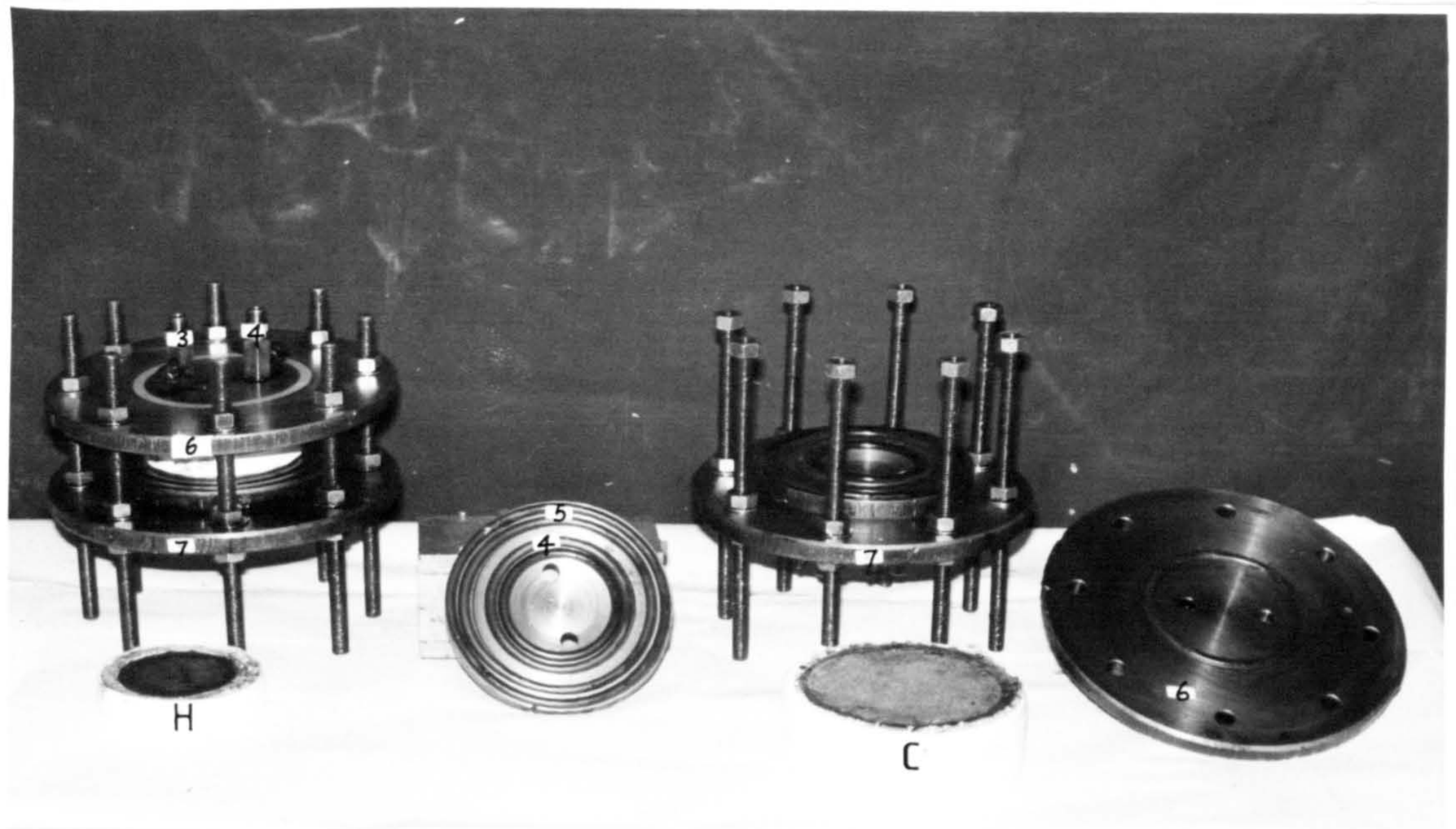

Details of the permeability cell

H. HCP Specimen

C. Concrete "

Other symbols are as in fig(5.1)

PLATE (5.1) PERMEABILITY APPARATUS

pressures upto 1.034 N/mm^2 or about 120 m head of oil.

Before placing the samples in the permeability cell they were given the following treatment. To eliminate any surface effects[90], the concrete specimens were wire-brushed until the rich mortar coating was removed and the aggregate particles became visible. The sides of the specimens were then thoroughly cleaned with dry, fine sand and sealed with two coats of epoxy resin, Febweld No. 2; and the second coat was applied after 8 hours. After partial drying, two rubber membranes of 125 mm diameter were pulled over the sides and tightly held with tough adhesive tape. The specimens were then allowed to dry in the constant temperature room (CTR) for 24 hours before the permeability test proceeded. The HCP specimens were similarly sealed. All samples were tested in the direction of casting, and the tests carried out in the CTR at 16 ± 0.5°C and 50% relative humidity.

The reported results are the average of two samples. Where two samples do not agree to within 90% of each other's value, a third sample was tested and the closest were averaged. All the samples have been fully saturated with oil using the technique described in Section 3.6 before the permeability test began.

5.3 Analytical Technique

The experimental equipment is fully described above. The coefficient of permeability, K, (cm/sec) was calculated using Darcy's fundamental equ. (2.7), section 2.2.2.2. The value of d in equ. (2.7) illustrated below, was 140 mm and 90 mm for concrete and HCPs respectively.

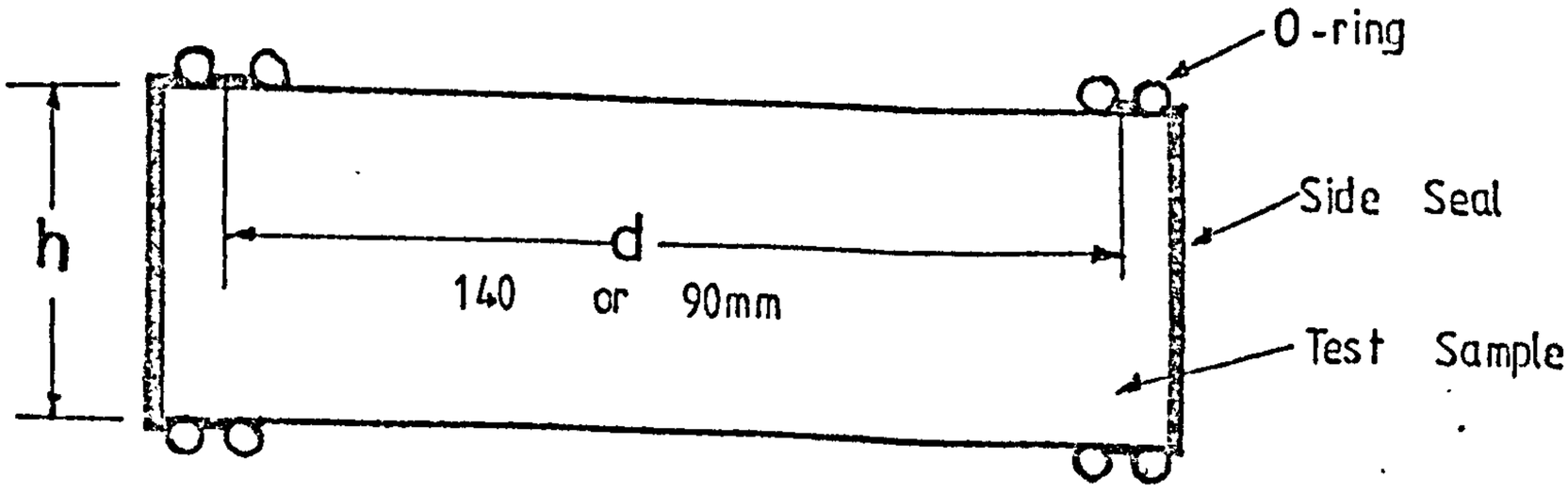

The flow rate decreased continuously with time over about 120 hours. The values of K were calculated at 120 hours. The quantity of oil flowing into the specimens was generally greater than the outflow. The out-flow was

80 - 95% of the inflow in concrete test samples and 90 - 100% in HCP samples. The values of K were calculated using inflow values.

5.4 Permeability of HCPs to Crude Oil

5.4.1 Scope of Study

This is summarised in table (5.1). Cormix SP1 superplasticiser was the admixture used. Most of the specimens were tested at 4 oil pressures: 0.827, 0.690, 0.552 and 0.286 N/mm^2 corresponding to crude oil heads of 96.8, 80.8, 64.8 and 32.9 meters respectively. At each pressure, the test was continued until the flow rate became about constant, normally within 120 hours.

5.4.2 Experimental and other Factors Affecting the Permeability of HCPs

5.4.2.1 Duration of test

The variation of the coefficient of permeability with time throughout the test period is illustrated in figs. (5.2) to fig. (5.7); at a pressure head of 80.8 m of oil (0.690 N/mm^2). The following observations are made from the results:

1. The plots show that the coefficient of permeability, K, and therefore, the rate at which oil flows through the pastes decreased with time during the test period. For OPC pastes, K at 24 hours of flow was between 1.2 - 1.5 times K at 120 hours, depending on the W/C ratio.

2. The reductions were slightly more for OPC pastes than for SRPC pastes. For SRPC pastes K after 24 hours of flow was between 1.2 and 1.4 times the value after 120 hours of flow.

3. The reduction in K with time was greater in pastes containing the admixture - figs. (5.4) to (5.7).

The reduction in the rate of flow could be partly attributed to the clogging of the pore system by waxy deposits from the crude oil. Similar but smaller decrements have been observed for water flow[131].

NO	PASTE DESIGNATION	CEMENT TYPE	W/C RATIO	.ADMIX. CONC. (% CEMENT WT.)
1	OP30	OPC	0.30	Nil
2	OP40	OPC	0.40	Nil
3	OP50	OPC	0.50	Nil
4	OP60	OPC	0.60	Nil
5	OP70	OPC	0.70	Nil
6	COP3-4	OPC	0.30	4%
7	COP4-4	OPC	0.40	4%
8	COP5-4	OPC	0.50	4%
9	COP6-4	OPC	0.60	4%
10	COP4-1	OPC	0.40	1%
11	COP4-2	OPC	0.40	2%
12	COP4-3	OPC	0.40	3%
13	SR34	SRPC	0.34	Nil
14	SR40	SRPC	0.40	Nil
15	SR50	SRPC	0.50	Nil
16	SR60	SRPC	0.60	Nil
17	SR70	SRPC	0.70	Nil
18	CSR3-4	SRPC	0.30	4%
19	CSR4-4	SRPC	0.40	4%
20	CSR5-4	SRPC	0.50	4%
21	SCR6-4	SRPC	0.60	4%
22	CSR4-1	SRPC	0.40	1%
23	CSR4-2	SRPC	0.40	2%
24	CSR4-3	SRPC	0.40	3%

Table (5.1) Details of HCP Samples for Permeability Tests

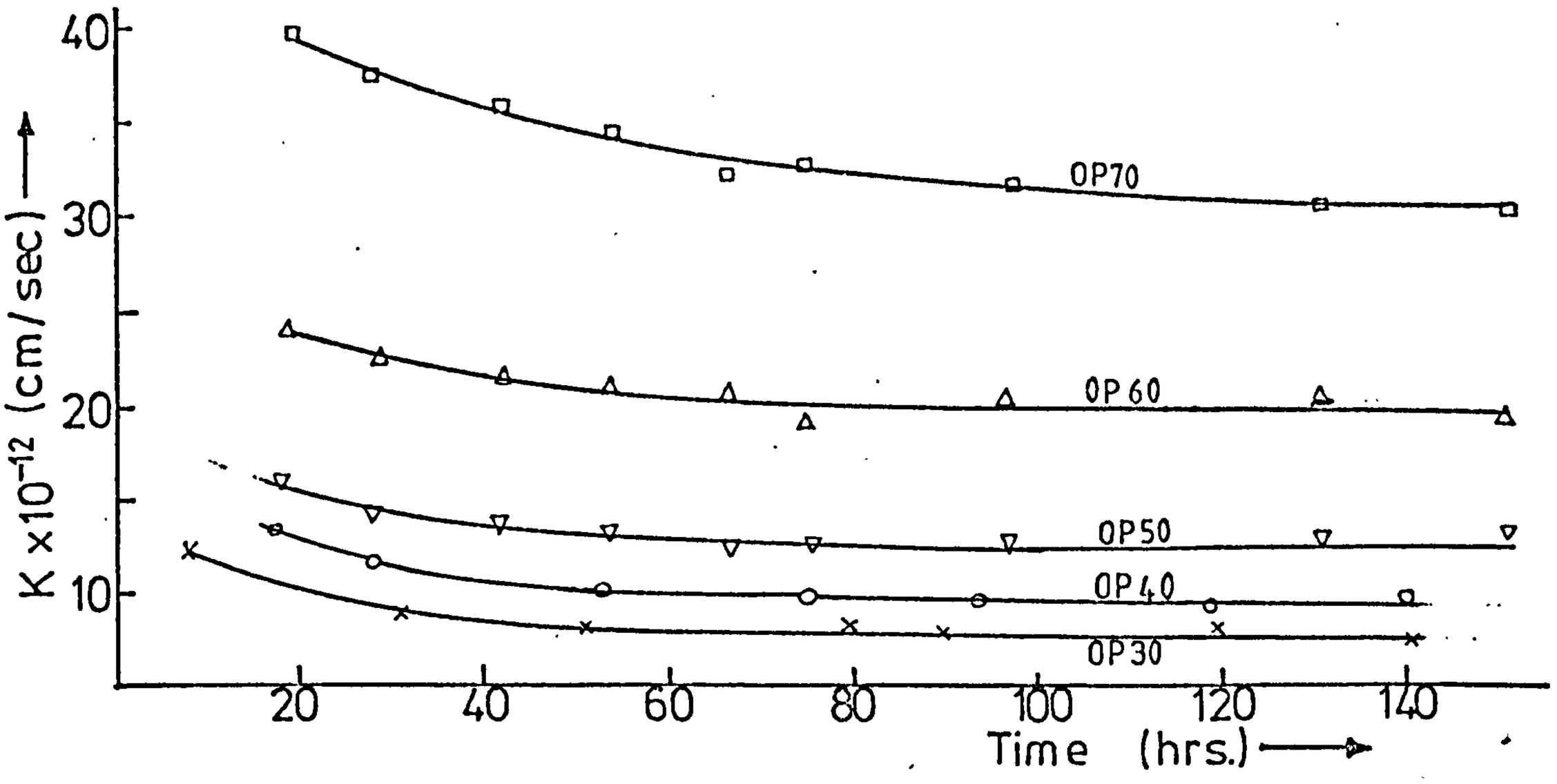

FIG(5.2) COEFT. OF PERM.(K) vs. DURATION OF TEST.
OPC PASTES

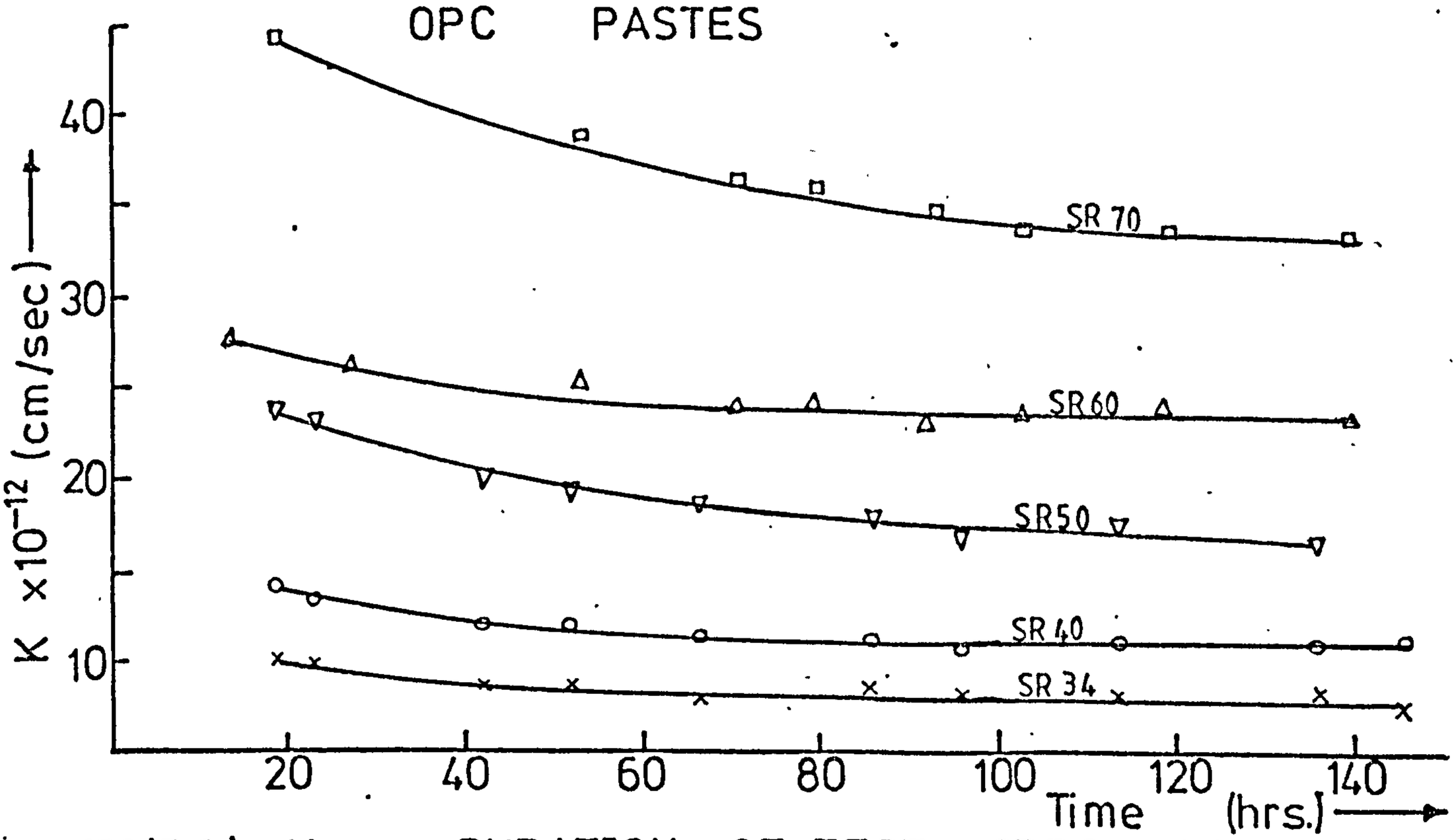

FIG(5.3) K vs. DURATION OF TEST. SRPC PASTES

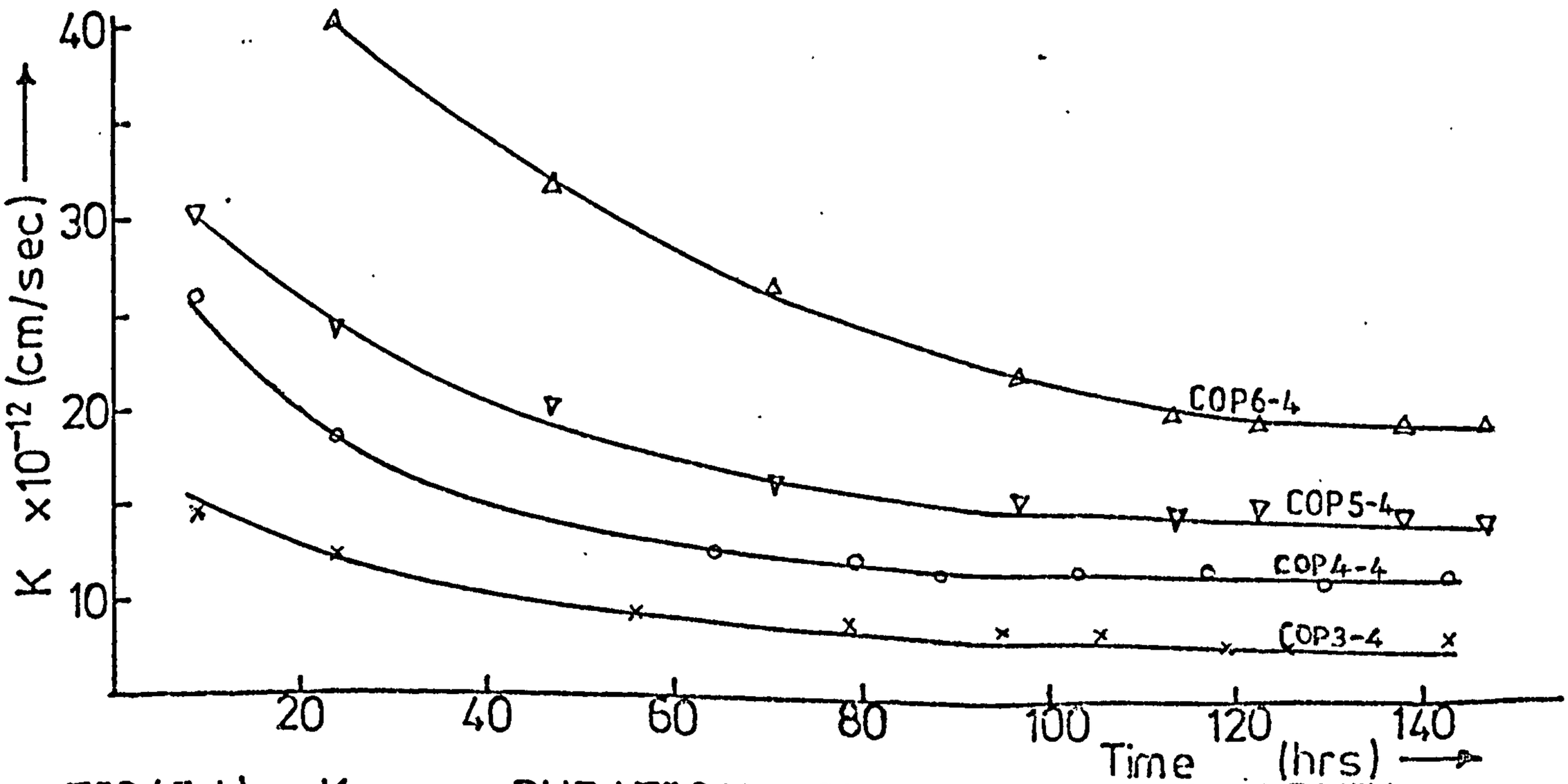

FIG(5.4) K vs. DURATION OF TEST OPC+ADMIX.

5.4.2.2. Applied Hydrostatic Pressure

The variations of K with applied hydrostatic head are illustrated in figs (5.8) and (5.9) for OPC and SRPC pastes respectivcly. Only pastes without admixtures were included in these tests. The following observations were made from the test results:

1. In all cases K increased with an increase in the applied hydrostatic pressure.

2. These increments were independent of W/C ratios; eg. for OPC pastes with W/C = 0.4, increasing the pressure from 32.9 m to 64.8 m, 80.8 m and 96.8 m head of oil, increased K by 1.37; 1.48, and 1.70 respectively times the value after 120 hours of flow at 32.9 m of oil head. For W/C = 0.7 the increases were 1.43, 1.64 and 1.72. For SRPC pastes of W/C = 0.4 and 0.7 the increases were 1.39, 1.55 and 1.63; and 1.17, 1.26 and 1.28 respectively.

The increase in the coefficient of permeability, K, with applied fluid pressure may be an indication that the increased pressure destroys some of the pore partitions and creates more continuous pores, but it may also be that the increased pressure forces oil through smaller pore sizes.

5.4.2.3 W/C Ratio:

Since W/C ratio determines the pore structure of HCPs and it is the pore structure that determines the permeability it is expected that K will vary with W/C ratio. These variations are illustrated in figs. (5.10) - (5.12) for OPC and SRPC pastes, for W/C = 0.3 to 0.7 and applied hydrostatic pressures of 32.9, 64.8, 80.8 and 96.8 m of oil. The following observations are made:

1. For pastes containing no admixtures, the relationship between W/C and K can be represented with an exponential equation of the form:

$$K = K_o \, (exp)^{a\ W/C} \qquad (5.1)$$

where K_o is a theoretical coefficient of permeability at zero W/C, and a is

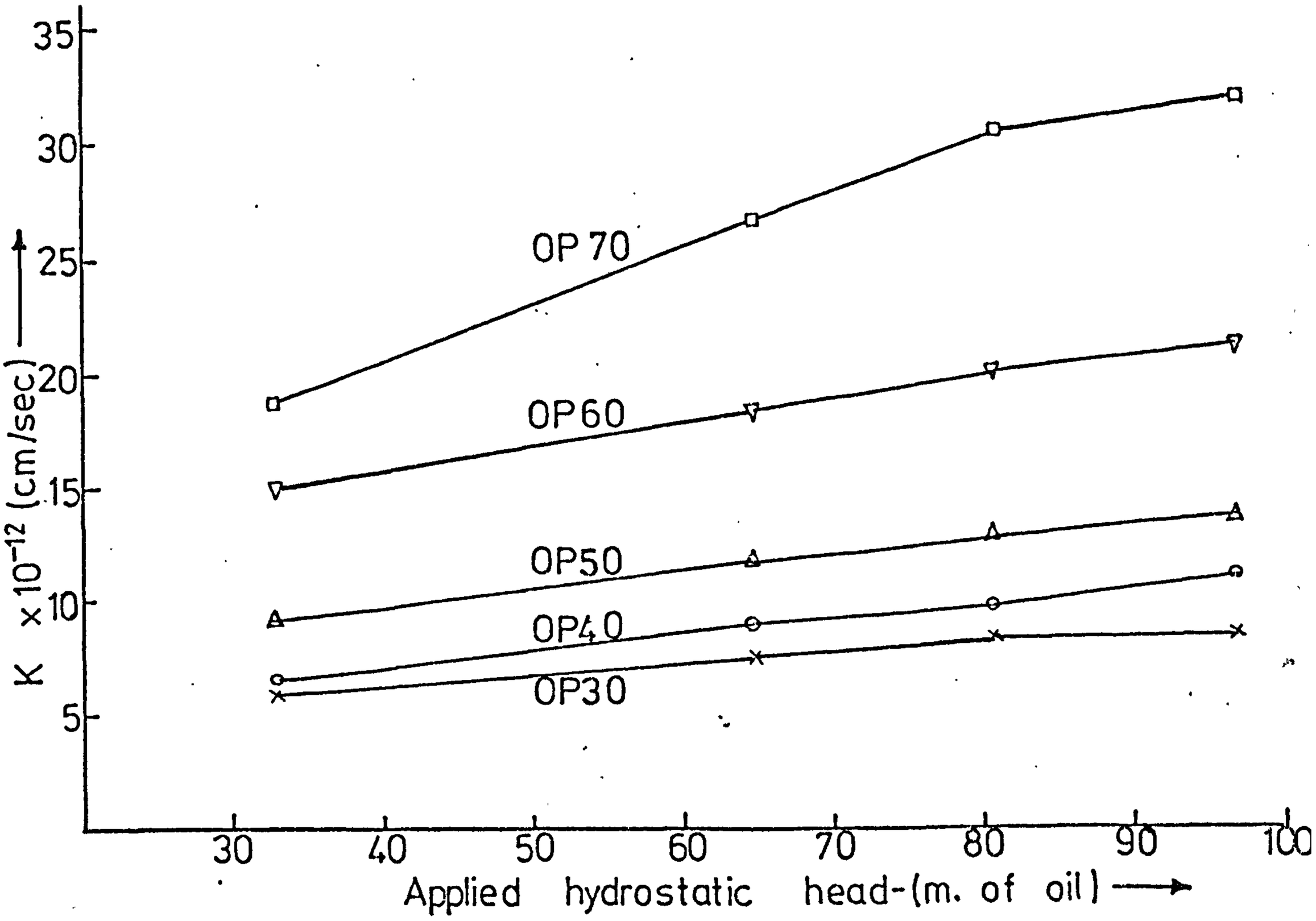

FIG(5.8) VARIATION OF K WITH APPLIED HYDROSTATIC HEAD — OPC PASTES

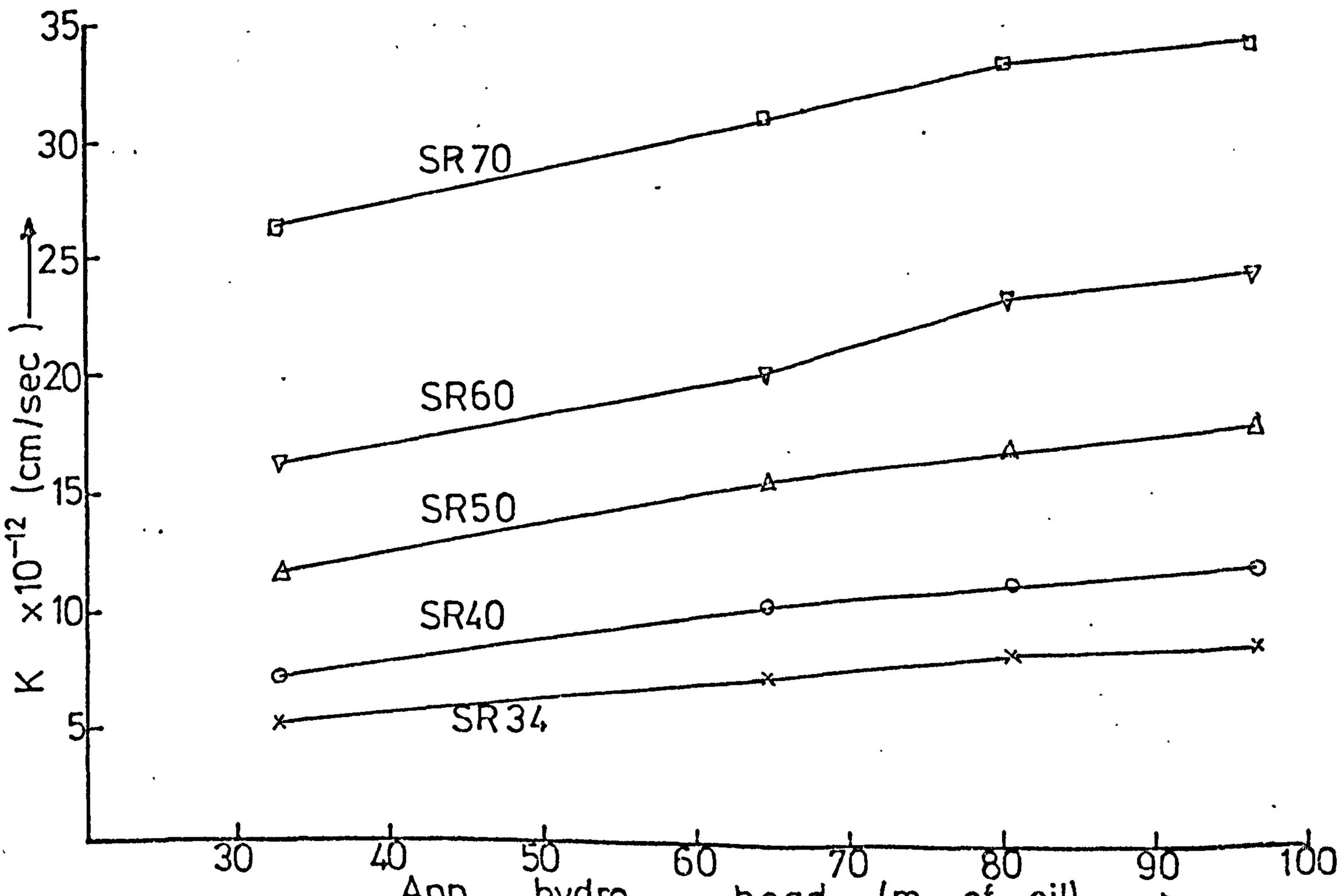

FIG(5.9) VARIATION OF K WITH APP. HYDROSTATIC HEAD — SRPC PASTES

a constant. K_o and a were determined by a regression analysis and are given in table (5.2)

2. At 80.8 m of oil, an increase in the W/C ratio from 0.4 to 0.7 increased K 3.2 times for OPC and 3.0 times for SRPC pastes. These are very low figures compared with upto a hundredfold increase observed with water[69].

3. Fig. (5.12) shows that on addition of 4% by cement weight of Cormix SP1 superplasticiser, the relationship between W/C ratio and K becomes linear. This can be expressed as:

$$K = b(W/C) + C \qquad (5.2)$$

The constants b and c were determined and are given in table (5.3). The change from an exponential function equ. (5.1) to a linear function equ. (5.2) on the addition of an admixture may be due to the re-orientation of the pore system. It was shown in chapter 4, that a larger number of intermediate pores were formed instead of the larger pores, hence resulting in a more uniform pore distribution.

App. Press. (m of Oil)	OPC PASTES			SRPC PASTES		
	$K_o \times 10^{-12}$	a	r*	$K_o \times 10^{-12}$	a	r*
32.9	1.978	3.247	96.9	1.157	4.441	96.6
64.8	2.162	3.570	95.5	2.133	3.810	98.1
80.8	2.127	3.791	94.9	2.553	3.678	99.0
96.8	2.414	3.670	94.9	2.851	3.542	99.2

Table (5.2) Constants of Regression - equ. (5.1) K Vs W/C

* correlation coefficient x 100%

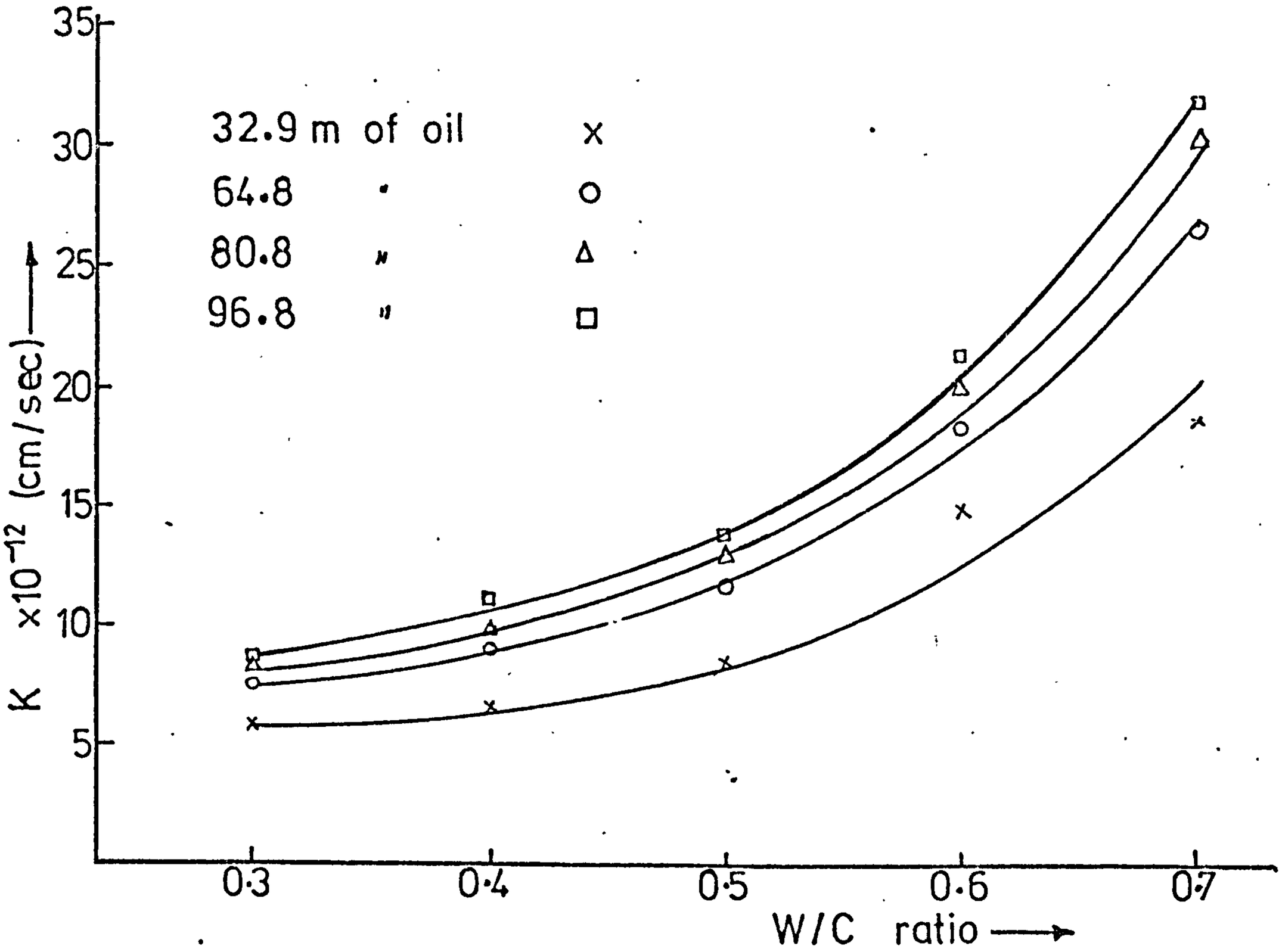

FIG(5.10) VARIATION OF K WITH W/C RATIO
OPC PASTES

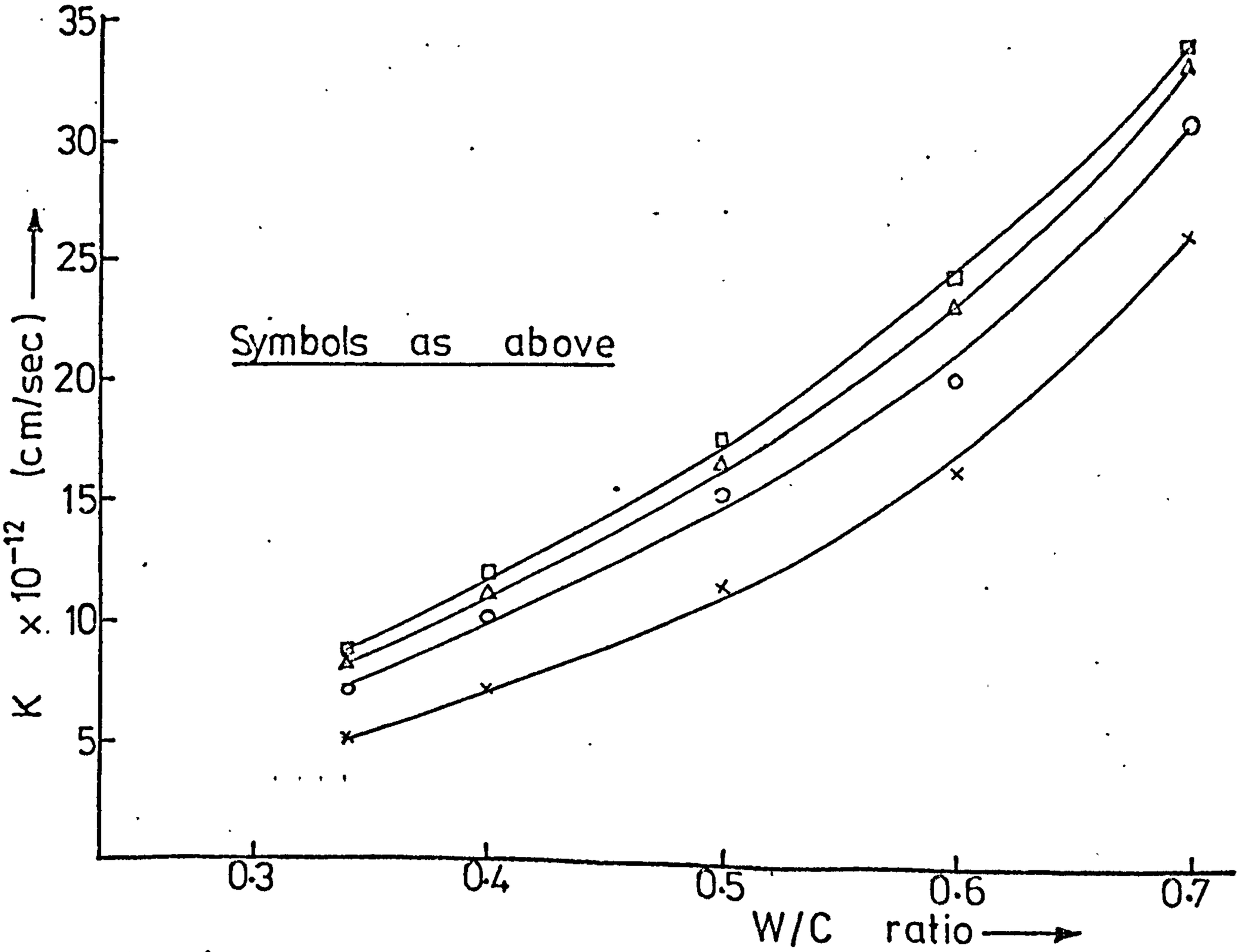

FIG(5.11) VARIATION OF K WITH W/C RATIO
SRPC PASTES

PASTE	b x 10^{-12}	C
OPC	38.38	-3.706
SRPC	50.17	-6.789

Table (5.3) Constants of equ. (5.2)

5.4.2.4 Superplasticising admixture

Cormix SP1 superplasticiser was used for these tests. 4% by weight of the superplasticiser was added to pastes of W/C ratios 0.3, 0.4, 0.5 and 0.6. At a fixed W/C ratio of 0.4; 1, 2 and 3% superplasticiser was added. The HCPs were all tested at one applied hydrostatic pressure, 80.6 m of oil. Test results are shown in table (5.4) and the following observations are made from the results:

1. For pastes containing 4% superplasticiser, a linear relationship was shown to exist between K and W/C ratio - fig. (5.12). It was further noted from section 5.4.2.3 that K at each W/C ratio was higher for pastes with admixture than for those without admixture indicating an increased pore volume, as described in chapter 4, and in table (5.4).

2. For pastes of W/C = 0.4 containing varied concentration of superplasticiser - fig. (5.13), it is observed that for 1% admixture, K decreased by about 11% and 5% for OPC and SRPC pastes respectively compared with pastes of zero admixture. At about 2% concentration, K increased again to the same order as at zero admixture concentration and continued to increase as the admixture content was increased.

The decrease obtained at low admixture concentration does not necessarily indicate a decrease in the total porosity of the HCPs but a redistribution of the pore structure of HCPs giving smaller pores which have a greater frictional resistance.

5.4.2.5 Total Porosity of HCPs

Total porosity values are given by W_e - the evaporable water on drying to 105°C. These values are given in column 2 of table (5.4). The

NO	1	2	3	4	5	6
	PASTE DESIGNATION	AT 4 WEEKS		AT 24 WEEKS		
		T. POROSITY (% Vol.)	COMP. STR. (SSD)	+COMP. STR. (CTR)	+COMP. STR. (oil sat.)	*K x 10^{-12} (cm/sec)
1	OP30	31.50	100.7	102.5	95.1	8.15
2	OP40	37.12	73.1	70.5	68.3	9.79
3	OP50	42.94	50.1	54.2	49.2	13.01
4	OP60	50.77	38.6	39.5	36.3	20.19
5	OP70	58.98	29.9	30.2	28.2	30.75
6	COP3-4	35.33	82.8	86.2	79.7	7.99
7	COP4-4	39.72	64.0	66.6	59.7	11.75
8	COP5-4	44.95	48.2	49.4	45.3	14.73
9	COP6-4	56.23	40.7	40.3	36.4	19.79
10	COP4-1	37.70	74.3	76.9	70.0	8.76
11	COP4-2	38.49	70.8	73.5	67.8	10.75
12	COP4-3	39.08	69.4	68.0	64.1	11.12
13	SR34	35.05	89.5	99.0	88.0	8.01
14	SR40	39.01	69.0	74.8	71.5	11.26
15	SR50	45.95	44.2	49.0	46.8	16.80
16	SR60	53.11	31.2	35.3	30.2	23.21
17	SR70	61.50	20.8	24.1	19.6	33.33
18	CSR3-4	36.32	80.5	69.3	75.3	7.89
19	CSR4-4	41.95	67.0	68.1	64.3	13.91
20	CSR5-4	48.00	46.9	48.4	46.5	18.15
21	CSR6-4	54.32	34.1	37.1	35.4	23.20
22	CSR4-1	39.64	73.8	75.0	70.3	10.78
23	CSR4-2	40.48	70.5	69.5	67.1	11.45
24	CSR4-3	41.20	67.8	69.4	65.0	12.26

Table (5.4) Test Results on Permeability of HCPs

* At 80.6 m of oil, at 120 hours of flow

\+ Dried to 105°C after 28 days and stored sealed in CTR/oil sat. (N/mm^2)

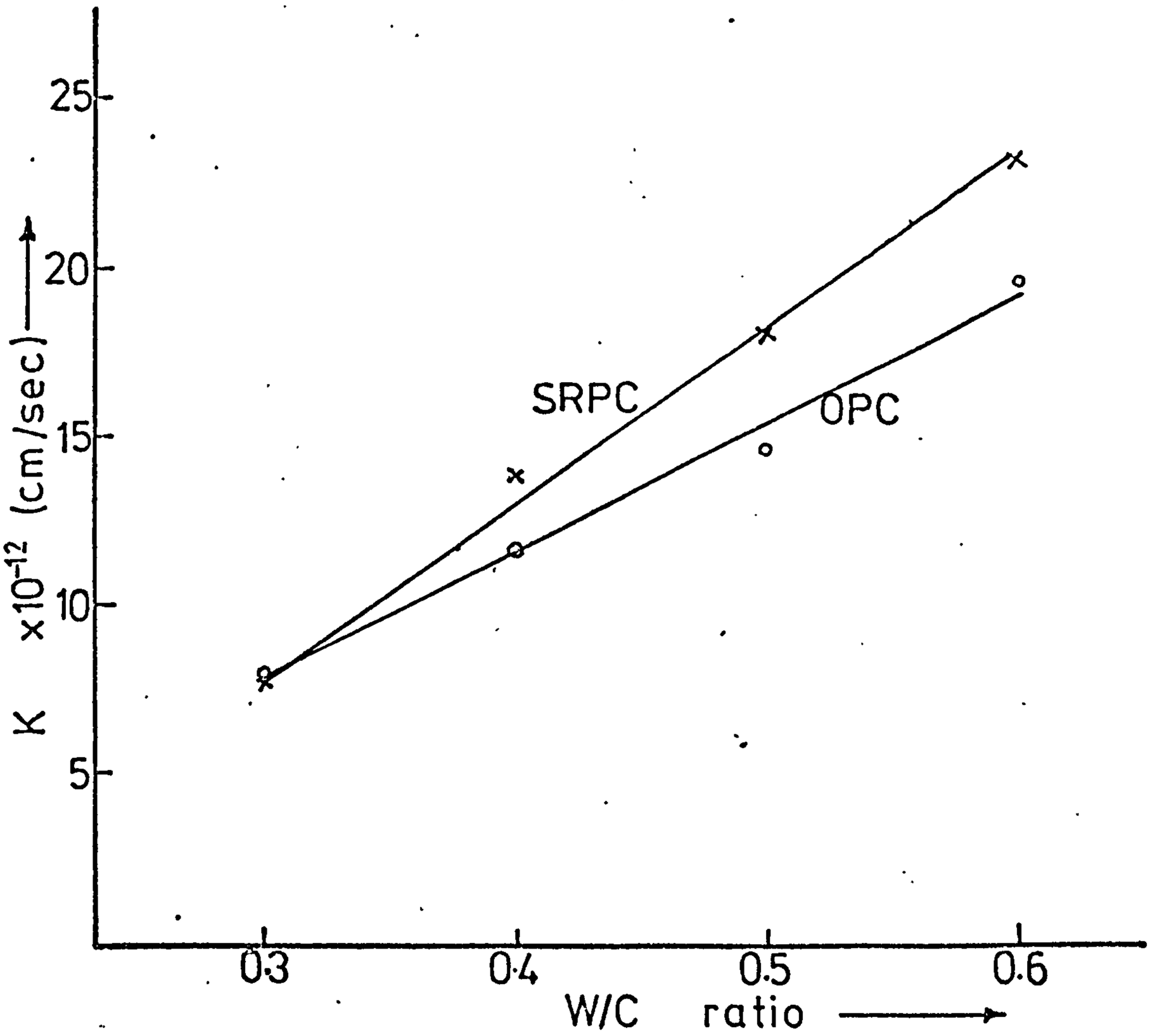

FIG (5.12) VARIATION OF K WITH W/C FOR HCPs CONTAINING 4% ADMIX..

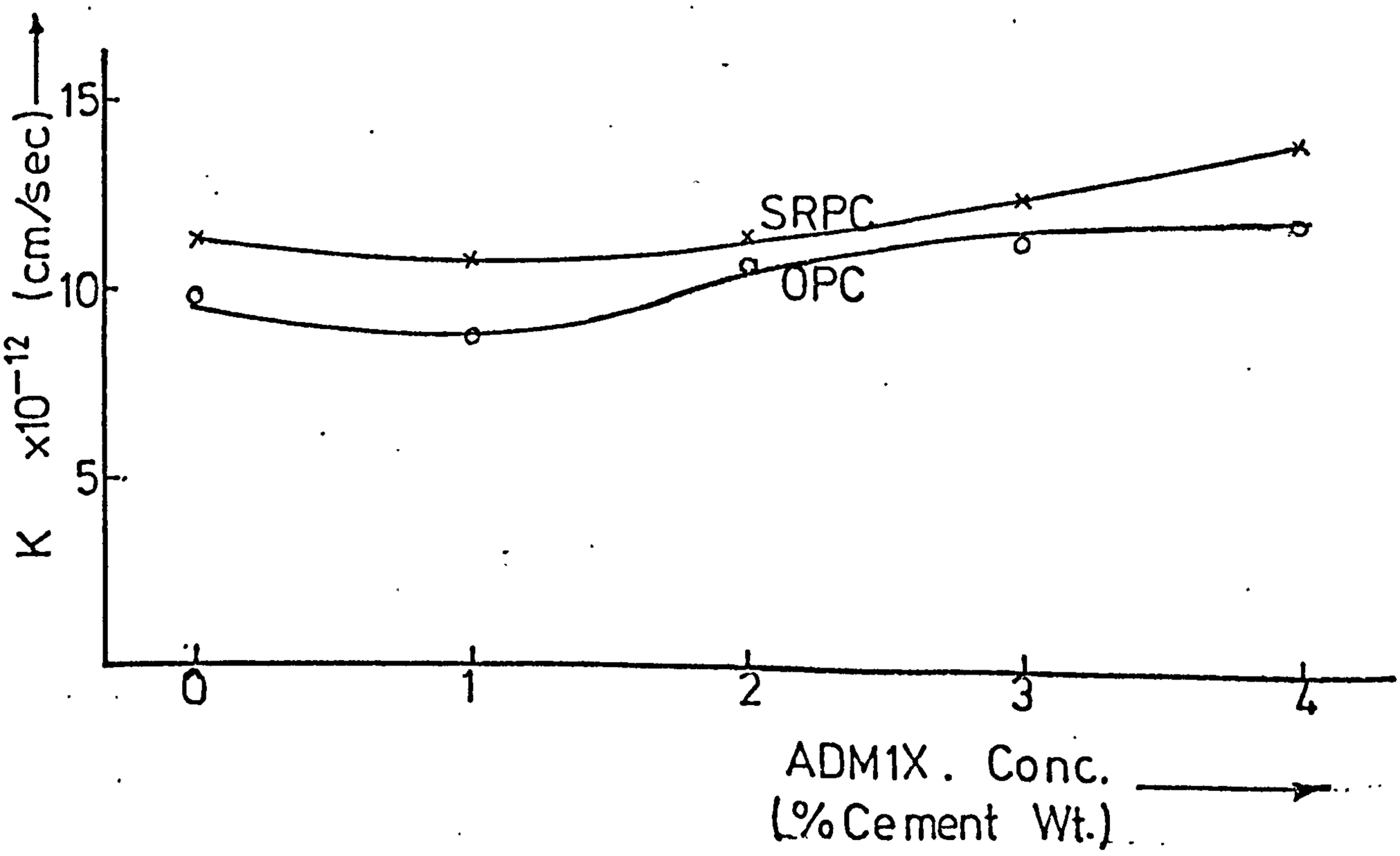

FIG (5.13) VARIATION OF K WITH ADMIXTURE CONC. AT W/C = 0.4

relationship between K and total porosity are illustrated in figs. (5.14) and (5.15) for HCPs with and without superplasticisers. The following observations are made from the results:

1. Fig. (5.14) is similar in shape to figs (5.10) and (5.11) ie. that between K and W/C ratio. This is not surprising since the pore structure of HCP is dependent on the W/C ratio. The relationships take an exponential form as:

$$K = K_o(\exp)^{a.P} \qquad (5.3)$$

where P is the total porosity (% volume), K_o is the coefficient of permeability of a theoretical paste of zero porosity and a, is a constant. Values of K_o and a were determined regressionally and are given in table (5.5).

2. The relationship between K and P for HCPs containing the superplasticiser are linear - figs. (5.15) and (5.16), unlike for pastes without the superplasticiser. It is likely that the redistribution of the HCP pore structure producing a more uniform pore size distribution which is the major cause of this linear relationship. These relationships can be expressed as:

$$K = b_1 (P) + C_1 \qquad (5.4)$$

The constants b_1 and C_1 were determined and are given in table (5.6)

App. Press.	OPC PASTES			SRPC PASTES		
(m. of Oil)	$K_o \times 10^{-12}$	a	r	$K_o \times 10^{-12}$	a	r
32.9	1.444	0.0408	98.5	1.376	0.0444	96.7
64.8	1.531	0.0485	97.8	1.401	0.0504	98.9
80.8	1.489	0.0513	97.3	1.706	0.0486	99.6
96.8	1.691	0.0502	97.3	1.930	0.0468	99.7

Table (5.5) Constants of Regression - Equ. (5.3), K Vs T. Porosity

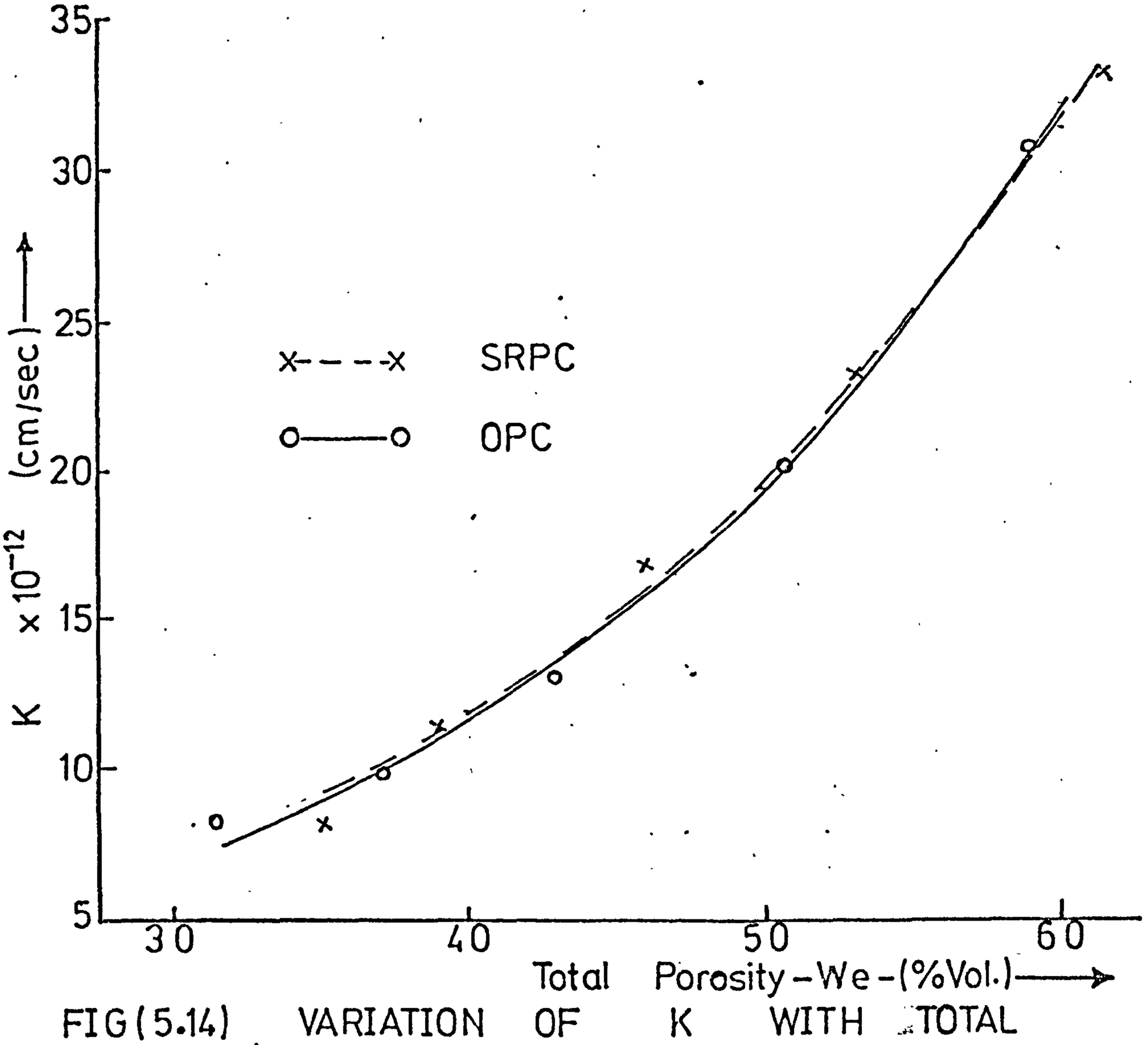

FIG (5.14) VARIATION OF K WITH TOTAL POROSITY. (at 80·8 m of oil)

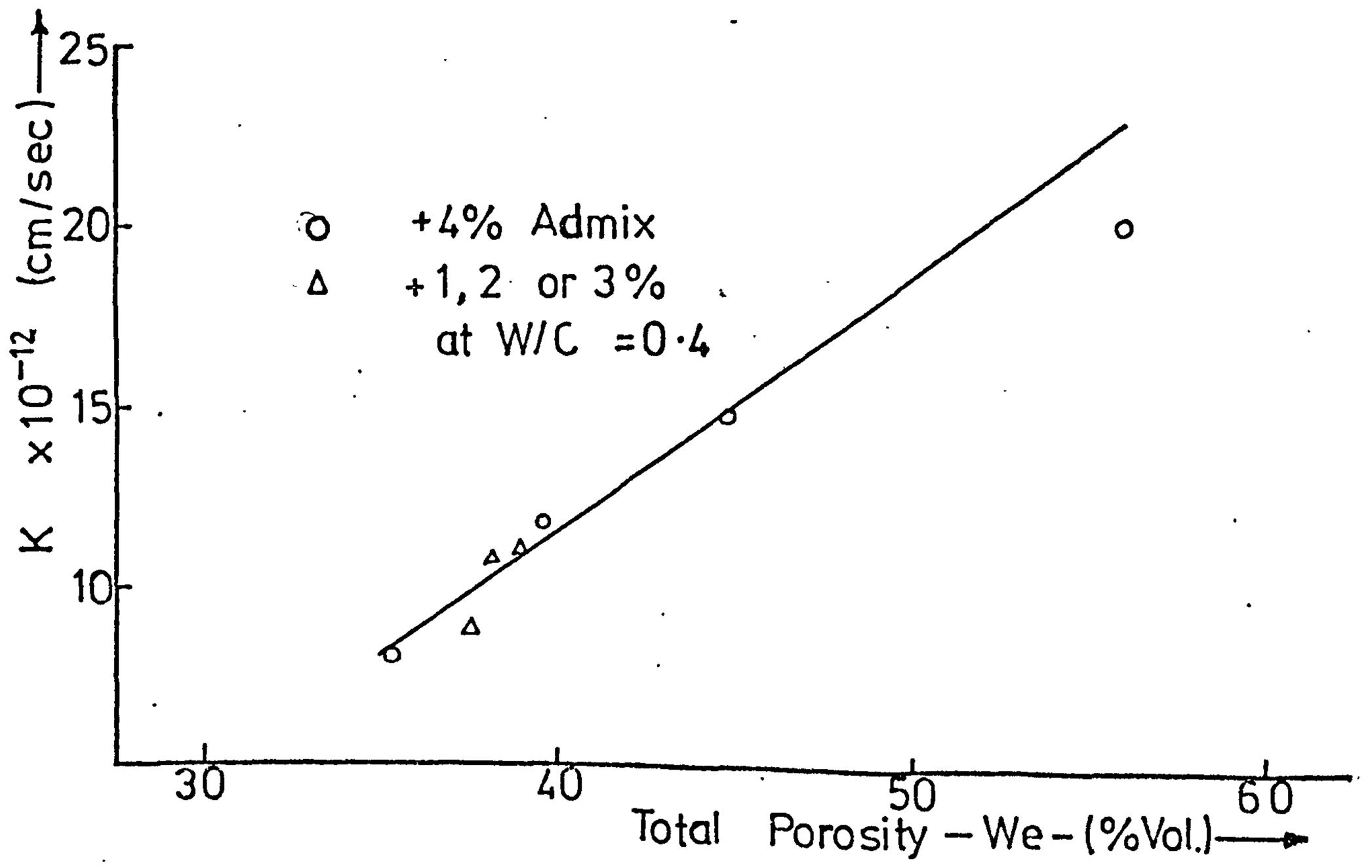

FIG (5.15) VARIATION OF K WITH T. POROSITY OPC + ADMIXTURE

PASTE	$b_1 \times 10^{-12}$	C_1
OPC	0.559	-11.17
SRPC	0.848	-22.62

Table (5.6) Constants of Equ. (5.4)

5.4.2.6 Cement Type

The variations in the values of K for OPC and SRPC pastes for the various testing conditions have been illustrated alongside each other in the preceding figures and in table (5.4). For the purpose of comparing the two types of cements, test results are replotted in fig. (5.17). The following observations are made:

1. In general, SRPC pastes are more permeable than OPC pastes. This is not surprising since from chapter 4; the SRPC pastes showed a more porous texture and the total porosity value in table (5.4) confirms this. At a W/C ratio of 0.70, K for OPC pastes was 30.75×10^{-13} cm/sec but 33.33×10^{-13} cm/sec for SRPC pastes.

2. At lower W/C ratios the differences between the two cements diminished and below 0.40 the two have approximately equal values of K. The value of K for SRPC paste at W/C = 0.34 was in fact lower than for OPC of W/C = 0.30.

5.4.2.7 Variations of K with the Compressive Strength of Crude Oil Saturated HCPs

Since compressive strength is the most commonly determined property of HCP, it would be useful to discover a relationship between it and permeability. Table (5.4) and figs. (5.18) and (5.19) give the compressive strengths (50.8 mm cubes) and the coefficients of permeability (K) for oil saturated HCPs. Three values of compressive strength are given in table (5.4), for the different curing conditions and these results are discussed later in chapter 7. The K values in fig. (5.20) are for 80.6 m head of oil (0.690 N/mm^2), after 120 hours of flow, using different cements and

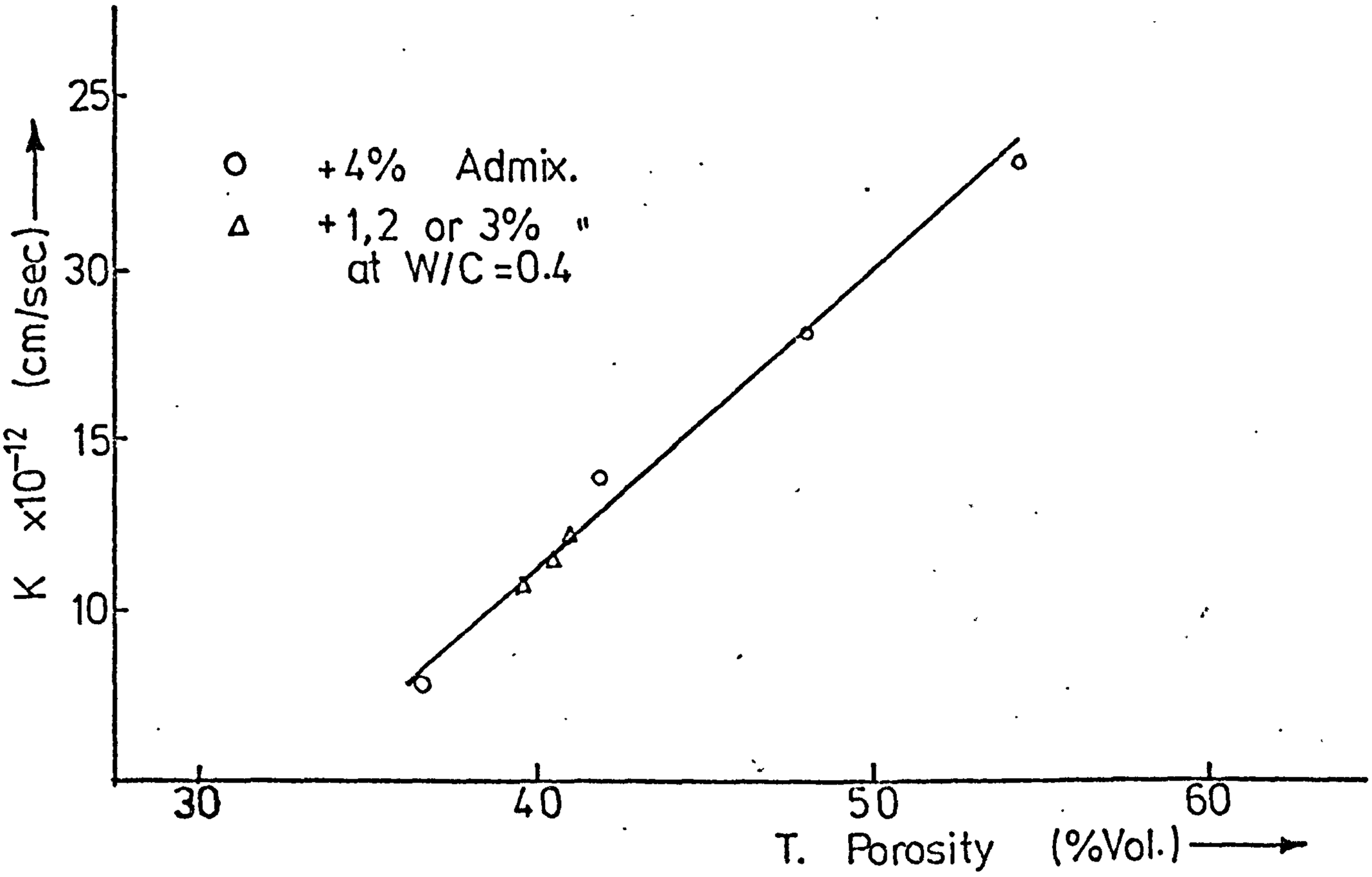

FIG(5.16) VARIATION OF K WITH T. POROSITY SRPC + ADMIX.

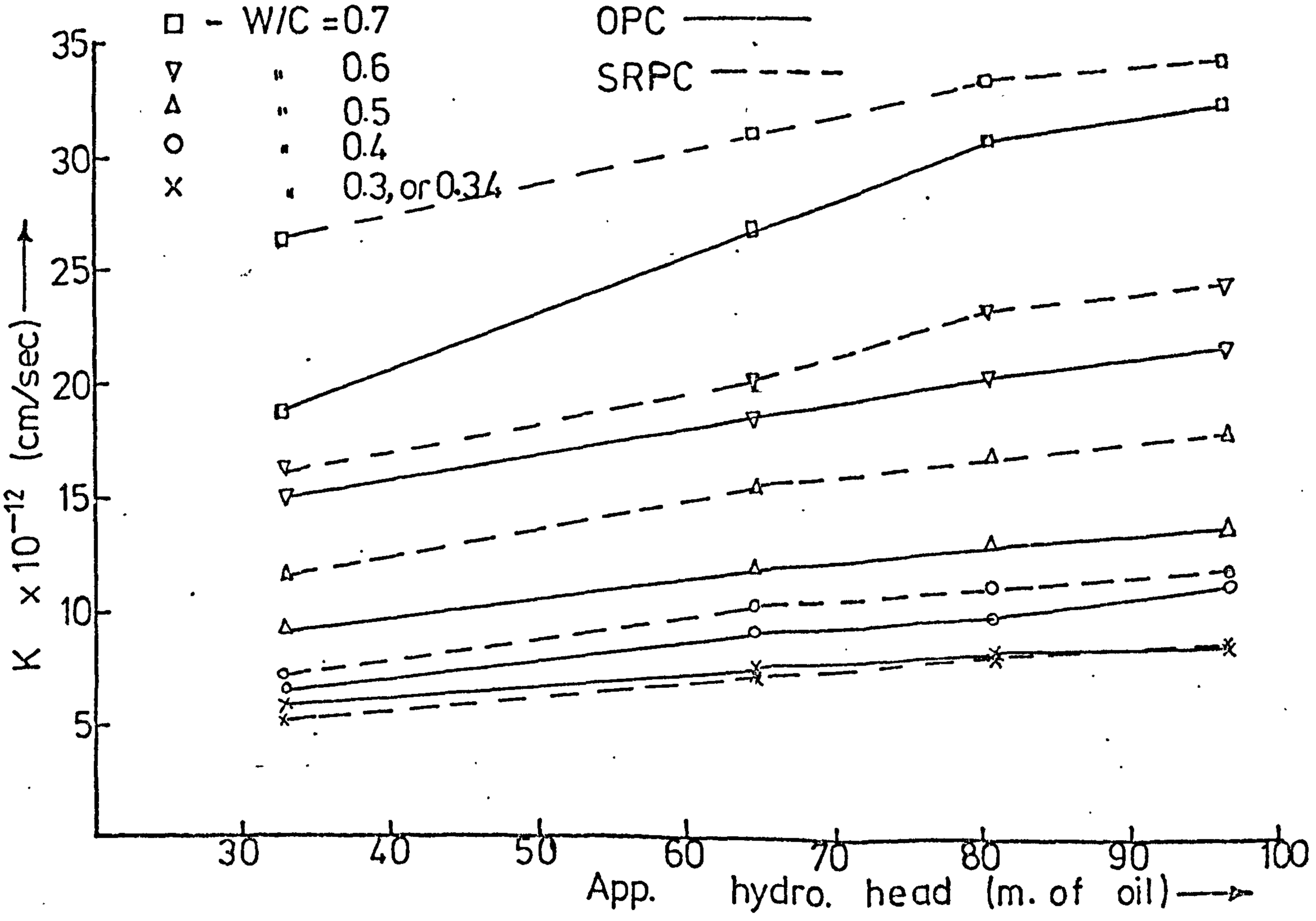

FIG(5.17) EFFECT OF CEMENT TYPE ON K AT VARIOUS APP. HYDRO. HEADS.

incorporating Cormix SP1 superplasticiser. The following observations are made from figs. (5.18) to (5.20) and table (5.4)

1. In general, the higher the compressive strength, the lower the value of K. This trend is as expected[70] since pore structure influences both strength and permeability of HCPs in a similar manner. For example, an increase in compressive strength by 100% results in the decrease of K by between 38 and 52% in OPC, 57 - 43% in SRPC and 53 - 66% in pastes containing superplasticiser.

2. The relationship between compressive strength (S_c) and K can be expressed exponentially in the form:

$$K = K_o (\exp)^{b \cdot S_c} \qquad (5.5)$$

where K_o = coefficient of permeability of a theoretical paste of zero strength, and b is a constant.

Values of K_o and b were obtained by a regression analysis and are given in tables (5.7) and (5.8).

App. Pres. (m. of oil)	OPC PASTES			SRPC PASTES		
	$K_o \times 10^{-12}$	b	r	$K_o \times 10^{-12}$	b	r
32.9	35.09	-0.0235	-89.9	41.29	-0.0269	-91.3
64.8	50.64	-0.0257	-86.9	44.98	-0.0224	-93.9
80.0	61.73	-0.0278	-85.9	48.65	-0.0217	-95.4
96.8	63.37	-0.0267	-86.2	48.57	-0.0282	-95.7

Table (5.7) Constants of Regression - equ. (5.5) K Vs C.Str.

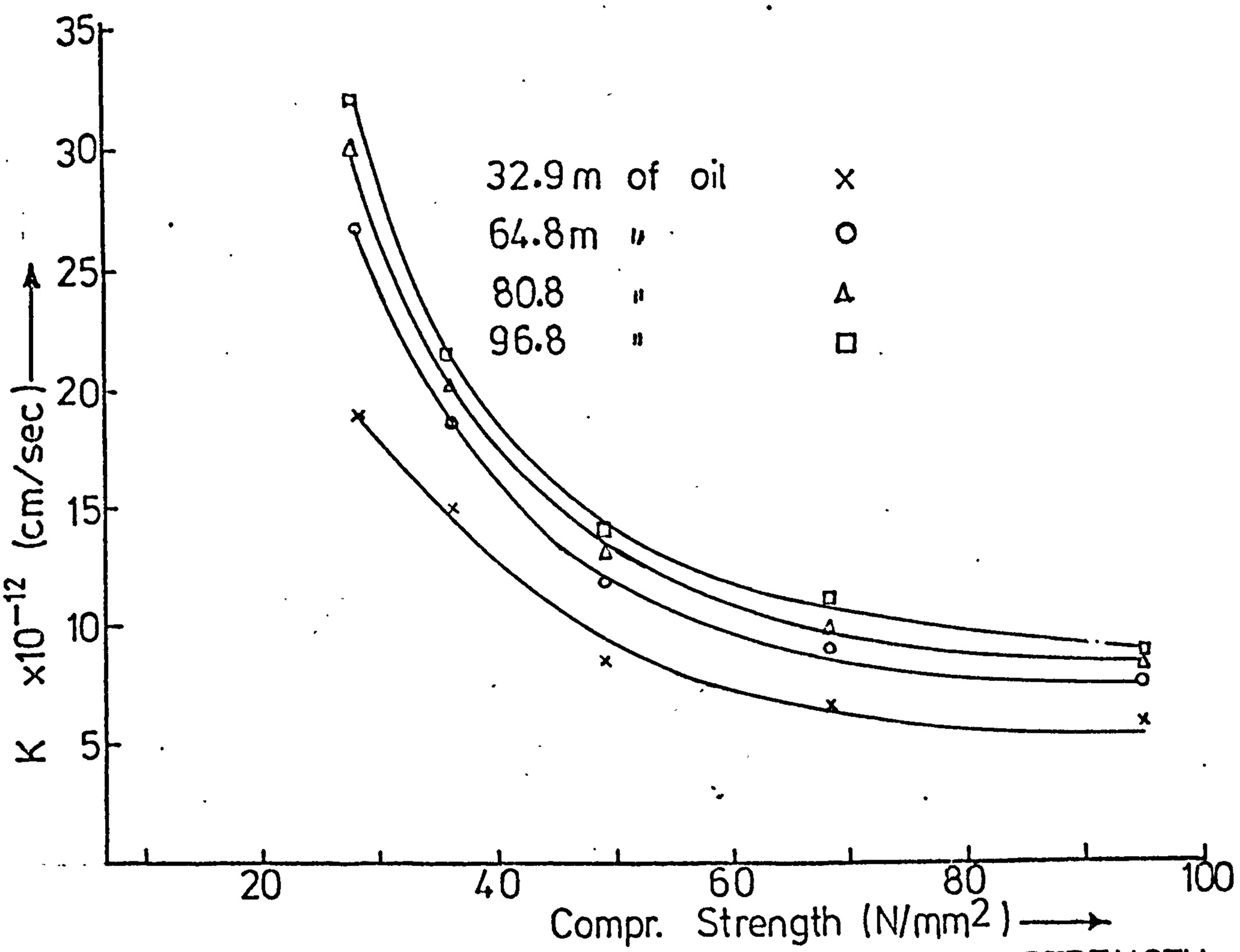

FIG(5.18) VARIATION OF K WITH COMPR. STRENGTH OF OIL SATURATED OPC PASTES

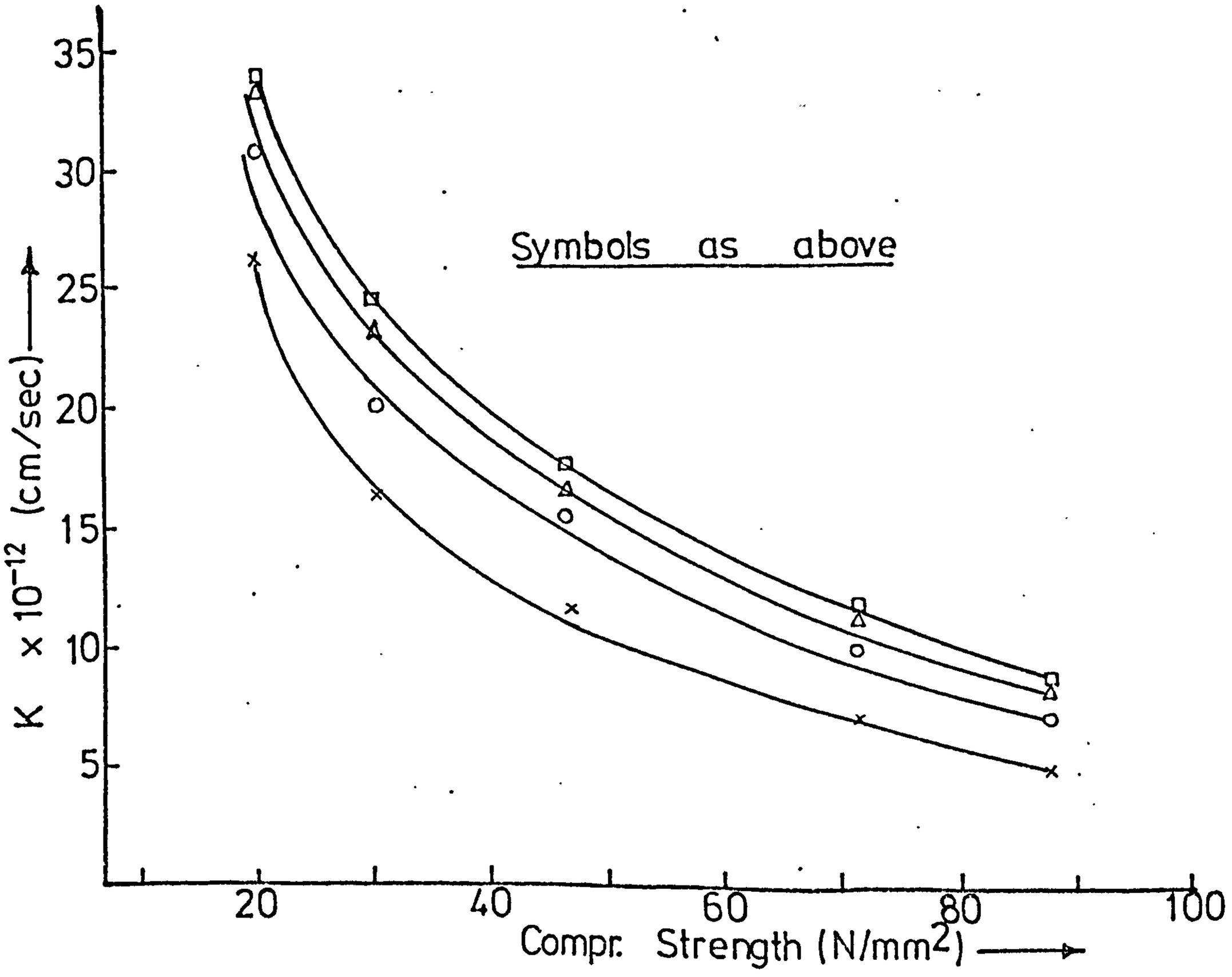

FIG(5.19) VARIATION OF K WITH COMPR. STRENGTH OF OIL SAT. SRPC PASTES

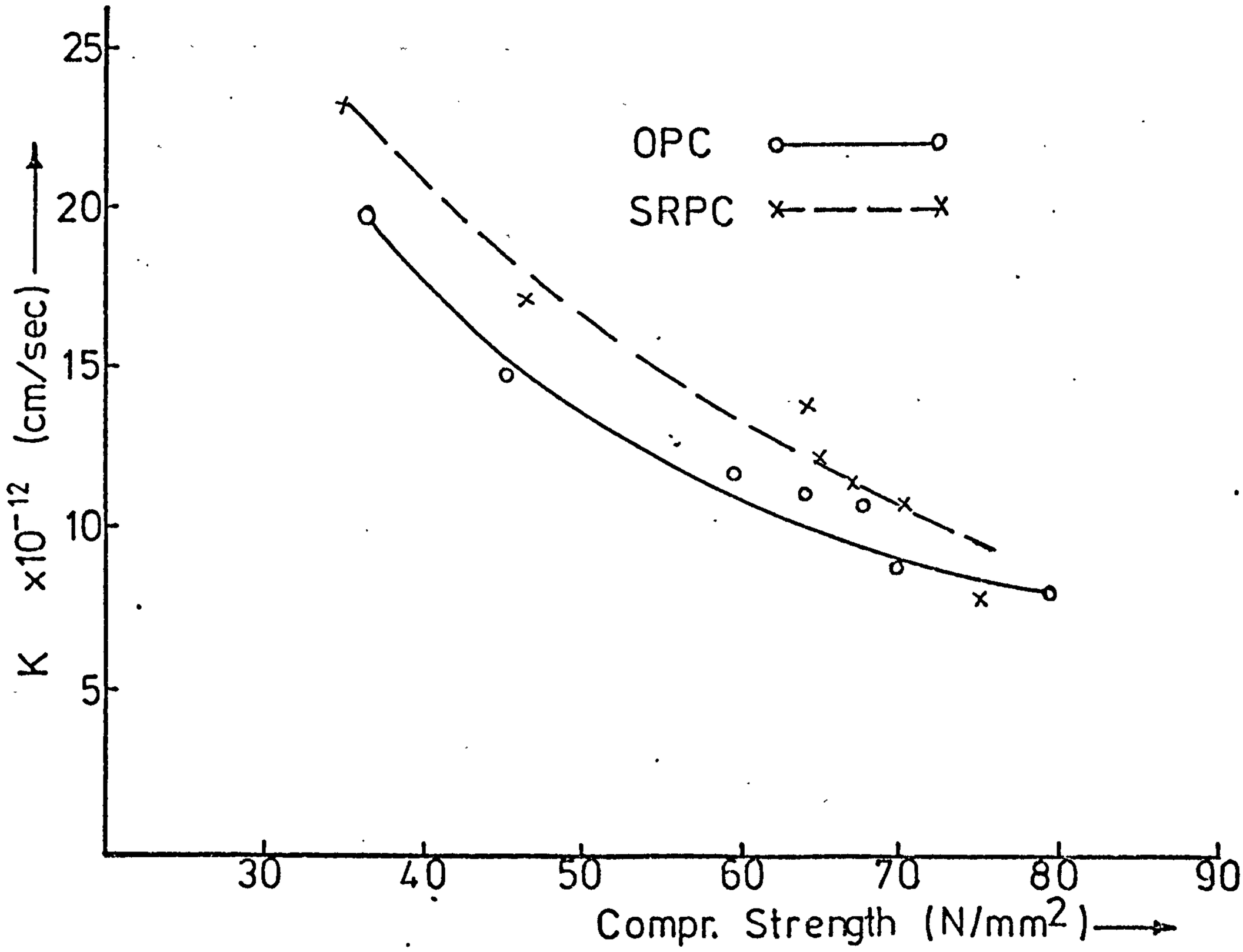

FIG(5.20) VARIATION K WITH COMPR. STRENGTH OF OIL SAT. SUPERPLASTICISED HCPs

App. Pres. (m. of oil)	OPC PASTES			SRPC PASTES		
	$K_o \times 10^{-12}$	b	r	$K_o \times 10^{-12}$	b	r
80.8	40.64	-0.0207	-96.9	51.73	-0.0224	-98.9

Table (5.8) Constants of Regression - equ. (5.5)
HCPs containing admixture

5.5 Permeability of Concrete to Crude Oil

5.5.1 Scope of Study

The concrete mixes chosen were those most often used for liquid structures. Permeability not strength was the design criterion. The mixes covered the following workabilities (slump), aggregate gradings and cement contents: 4 workabilities - very low (0 - 10 mm), low (10 - 30 mm), medium (40 - 70 mm) and high (80 - 150 mm); 4 aggregate gradings designated 1 to 4 and corresponding to zones 1, 2, 3 and 4 respectively in B.S. 882,1965; 3 W/C ratios of approximately 0.4, 0.6 and 0.8. The cement contents varied between 225 to 625 Kg/m^3 - actual contents were calculated from the mix quantities - Section 3.5.2. The mix proportions are given in tables (5.9) and (5.10) for OPC and SRPC concretes respectively.

5.5.2 Mix Design Parameters and Test Results

5.5.2.1 OPC Concrete

The mix proportions and some properties for 41 mixes are shown in table (5.9). Permeability appears to be influenced by cement content, W/C ratio, aggregate content, consistency and aggregate grading but it is difficult to vary one factor without affecting the values of other factors. An attempt to show how the coefficient of permeability (K) varies with these factor is made in the following sections.

Only a few tests (Nos. 1 - 5) were carried out on very low slump concrete (0 - 10 mm). This is because the specimens contained large voids

NO	FRESH CONCRETE						AT 4 WEEKS			AT 24 WEEKS			
	SLUMP (mm)	GRADING ZONE	CEMENT CONTENT (Kg/m^3)	AGGREG. CONTENT (Kg/m^3)	FINE AGGREG. FRAC.	W/C RATIO	DENSITY SSD (Kg/m^3)	TOTAL POROSITY % Vol.	COMPR. STRENGTH (N/mm^2)	COMPR. STRENGTH CTR	COMPR. STRENGTH Oil Sat.	OIL ABSORP. % Dry Wt.	$^{+}Kx10^{-10}$ (cem/sec)
1	2	3	4	5	6	7	8	9	10	11	12	13	14
1		1	293	1924	0.52	0.600	2382	19.25	47.4	49.9	45.6	4.26	19.45
2	VERY	2	296	1934	0.43	0.608	2405	19.37	42.1	44.4	39.9	3.98	19.88
3	LOW	3	293	1927	0.35	0.600	2396	19.26	45.1	47.6	40.7	4.00	19.92
4	0-10	3	220	1992	0.39	0.809	2386	23.67	23.9	25.5	21.7	5.80	37.12
5		4	296	1937	0.30	0.594	2409	19.10	46.0	48.5	44.2	4.03	19.11
6		1	516	1679	0.51	0.407	2403	17.33	65.3	68.0	62.6	3.13	8.49
7		1	340	1850	0.56	0.614	2397	18.34	50.1	52.2	48.8	3.75	13.52
8		1	252	1917	0.61	0.800	2361	19.79	27.6	28.8	26.1	5.18	26.52
9		2	512	1692	0.41	0.416	2415	17.57	72.2	75.2	69.1	2.81	9.05
10		2	339	1843	0.45	0.608	2389	18.54	49.9	50.5	45.4	3.53	15.57
11	LOW	2	252	1919	0.50	0.817	2375	20.03	27.9	28.7	24.8	4.42	27.00
12	10-30	3	521	1710	0.34	0.407	2440	17.48	69.6	72.9	69.6	3.08	8.69
13		3	339	1843	0.37	0.608	2386	18.44	47.2	49.7	46.4	4.01	14.39
14		3	255	1926	0.40	0.809	2382	20.27	27.7	29.4	26.9	5.44	28.64
15		4	514	1696	0.29	0.416	2424	17.43	75.6	77.8	71.2	2.78	8.47
16		4	343	1873	0.31	0.600	2427	18.40	46.4	50.0	45.2	4.15	15.91
17		4	253	1934	0.34	0.817	2395	20.00	28.5	32.0	27.6	4.79	25.47
18		1	573	1565	0.55	0.412	2375	16.94	64.5	66.6	64.8	2.66	5.35
19		1	385	1769	0.59	0.623	2395	18.52	45.6	48.1	43.5	3.36	13.61
20		1	284	1834	0.65	0.865	2364	19.75	24.4	26.3	23.8	4.61	23.34
21		2	578	1578	0.44	0.400	2388	16.59	74.0	76.0	73.2	2.71	5.29
22		2	383	1762	0.48	0.608	2378	18.18	51.1	53.7	47.6	3.20	12.46
23	MEDIUM	2	288	1859	0.52	0.800	2377	19.24	29.9	31.2	27.7	3.76	20.30
24	40-70	3	580	1584	0.36	0.400	2398	16.50	73.3	75.7	72.6	2.50	4.96
25		3	386	1775	0.40	0.600	2393	18.11	58.0	60.4	54.0	3.67	11.47
26		3	287	1854	0.42	0.800	2371	1928	33.0	34.1	31.3	4.43	20.84
27		4	588	1603	0.31	0.391	2413	16.57	74.2	77.0	70.7	2.69	5.68
28		4	388	1792	0.33	0.600	2413	18.26	44.1	47.5	42.3	3.76	14.06
29		4	291	1883	0.36	0.804	2410	19.45	32.6	33.6	29.1	5.02	22.54
30		1	633	1489	0.61	0.400	2376	16.88	72.5	75.5	71.4	2.80	6.02
31		1	419	1691	0.67	0.608	2365	18.47	45.5	48.0	44.1	3.90	13.18
32		1	314	1772	0.72	0.800	2359	19.62	29.8	32.6	29.2	4.29	23.13
33		2	637	1499	0.50	0.400	2391	17.18	71.0	72.8	68.7	2.81	7.55
34		2	418	1686	0.54	0.610	2359	18.54	49.1	51.8	44.6	3.60	15.37
35	HIGH	2	313	1776	0.58	0.792	2338	19.33	28.5	30.3	26.9	4.35	21.12
36	80-150	3	635	1494	0.40	0.394	2388	16.75	78.7	85.2	77.9	2.75	6.05
37		3	419	1691	0.43	0.612	2368	18.71	52.1	55.2	48.5	4.08	16.15
38		3	316	1797	0.46	0.783	2359	19.52	33.1	35.7	31.8	4.69	23.57
39		4	643	1512	0.34	0.400	2417	17.12	73.0	76.3	72.4	3.03	5.97
40		4	424	1713	0.37	0.600	2396	18.60	47.4	50.0	44.9	4.01	14.71
41		4	320	1823	0.40	0.786	2404	19.27	30.0	34.7	30.7	4.44	21.37

Table (5.9) Mix Proportions and Test Results - OPC Concretes

+ At 96.8 m of oil, after 120 hours

NO	FRESH CONCRETE						AT 4 WEEKS			AT 24 WEEKS			
	SLUMP (mm)	GRADING ZONE	CEMENT CONTENT (Kg/m^3)	AGGREG. CONTENT (Kg/m^3)	FINE AGGREG. Frac.	W/C RATIO	DENSITY SSD (Kg/m^3)	TOTAL POROSITY % Vol.	COMPR. STRENGTH (N/mm^2)	COMPR. STRENGTH CTR	COMPR. STRENGTH Oil.Sat.	OIL ABSORP. % Dry Wt.	$^{+}Kx10^{-10}$ (cm/sec)
1	2	3	4	5	6	7	8	9	10	11	12	13	14
1		1	515	1962	0.51	0.416	2421	18.29	69.4	74.6	68.8	3.39	9.90
2		1	337	1851	0.56	0.627	2399	19.99	46.2	49.2	45.1	4.37	16.26
3		1	253	1926	0.61	0.819	2387	22.07	30.4	31.8	28.8	6.01	29.17
4		2	515	1696	0.41	0.408	2422	18.17	74.9	75.8	72.4	3.51	9.75
5		2	339	1846	0.45	0.605	2389	19.65	50.4	53.2	48.6	4.33	16.93
6	LOW	2	252	1923	0.50	0.814	2378	21.86	29.3	31.2	28.0	5.26	29.91
7	10-30	3	518	1705	0.34	0.400	2431	17.98	70.5	71.8	70.5	2.97	8.92
8		3	343	1848	0.37	0.627	2404	20.18	45.5	46.8	43.0	4.20	18.45
9		3	253	1927	0.40	0.819	2388	22.29	29.9	30.6	27.8	6.30	30.72
10		4	512	1696	0.29	0.424	2426	18.36	72.1	76.3	72.0	2.83	9.68
11		4	342	1863	0.31	0.600	2410	19.62	48.0	51.1	47.6	3.64	17.80
12		4	263	1919	0.34	0.780	2386	21.33	31.8	33.8	30.5	5.63	26.65
13		1	578	1580	0.55	0.419	2401	18.53	68.3	74.1	68.9	3.71	10.44
14		1	382	1753	0.59	0.625	2373	20.16	42.3	45.1	42.1	4.70	15.21
15		1	288	1838	0.65	0.812	2371	22.17	28.6	30.0	27.2	5.45	28.29
16		2	580	1585	0.44	0.412	2398	18.34	69.7	74.0	69.6	3.28	10.20
17		2	382	1775	0.48	0.621	2373	19.97	44.7	47.4	43.6	4.33	16.76
18	MEDIUM	2	288	1857	0.52	0.816	2381	22.23	25.7	27.6	25.0	5.88	27.51
19	40-70	3	580	1585	0.36	0.405	2402	18.03	71.9	78.4	72.2	3.06	10.31
20		3	389	1775	0.40	0.600	2400	19.68	41.5	45.0	40.8	3.93	17.48
21		3	292	1863	0.42	0.800	2383	21.72	29.6	32.3	29.4	4.57	28.69
22		4	580	1590	0.31	0.400	2411	18.11	73.7	80.1	74.0	3.48	8.58
23		4	389	1782	0.33	0.589	2398	19.29	47.0	50.2	45.9	3.99	16.64
24		4	292	1860	0.36	0.784	2385	21.75	30.7	33.6	29.3	5.69	28.09
25		2	638	1494	0.50	0.406	2389	18.38	71.5	76.9	72.5	3.09	10.04
26		2	420	1691	0.54	0.621	2374	20.24	44.1	46.6	43.7	4.86	15.64
27	HIGH	2	316	1802	0.58	0.800	2377	22.24	32.7	33.1	32.2	5.55	28.86
28	80-150	3	635	1495	0.40	0.400	2486	17.94	73.6	81.0	73.8	3.23	9.91
29		3	427	1716	0.43	0.600	2398	19.45	46.3	49.6	45.0	4.62	17.49
30		3	317	1814	0.46	0.772	2377	21.39	30.3	31.7	28.1	4.98	28.39

Table (5.10) Mix Proportions and Test Results - SRPC Concrete

+ At 96.8 m of oil, after 120 hours

even after prolonged vibration and trial tests, showed very high permeability. Very low slump concrete especially with coarse aggregate grading (3 and 4), should not be used in liquid retaining structures. Three values of compressive strength (100 mm cubes) are given in tables (5.9) and (5.10) for each mix at different ages and curing conditions. The differences between these strengths are discussed in Chapter 6. The density values were determined by dividing the weight of a water saturated surface dry (SSD) specimen by the weight of water displaced when the same specimen is immersed in water. The values are the average of 6 cubes and 3 permeability test disc specimens. The total porosities were determined as described in Chapter 4. The values of K in column 14 were values at 96.8 m of oil after 120 hours of flow.

5.5.2.2 SRPC Concrete

The mix proportions and some properties for 30 mixes are shown in table (5.10). Because the very low slump OPC mixes contained large voids, these were omitted here. In the high workability region, the very fine and coarse aggregate grading zones (1 and 4) were also omitted due to the poor results from OPC concrete and also because of the high bleeding which occured with SRPC trial specimens in zone 4.

5.5.3 Mix Design Parameters Affecting Concrete Permeability

5.5.3.1 W/C Ratio

The variations of K with W/C ratio are illustrated in figs. (5.21) and (5.22) for OPC and SRPC concretes respectively. The following observations are made from these figures:

1. The relationship between K and W/C ratio is not linear because permeability is not a direct function of concrete porosity, (which is influenced by W/C ratio) but is influenced by other concrete mix parameters.

2. The relationship between K and W/C ratio can be expressed exponentially in the form:

$$K = K_o \, (\exp)^{b(W/C)} \qquad (5.6)$$

By regression analysis, the constants K_o and b were obtained and are given in table (5.11) for OPC and SRPC concretes.

3. For mixes of the same W/C ratio K is slightly affected by workability. This is probably because the more workable the concrete, the easier it is to expel air voids during vibration.

4. To reduce K, the W/C ratio has to be reduced as much as practicable. An increase in W/C ratio from 0.4 to 0.8 increases the permeability by 3.7 and 2.9 times in OPC and SRPC concretes respectively.

CONCRETE	$K_o \times 10^{-10}$	b	r
OPC	2.932	2.607	94.2
SRPC	3.210	2.723	97.9

Table (5.11) Constants of regression - Equ. (5.6) K Vs W/C

5.5.3.2 Cement Content

The relationships between K and cement content are illustrated in figs. (5.23) and (5.24) for OPC and SRPC concretes respectively and it is observed that:

1. K varies non-linearly with cement content. The relationship can be expressed exponentially, and the values at each cement content are considerably influenced by the concrete workability. For example, for OPC concrete with $K = 15 \times 10^{-10}$ cm/sec of low (10 - 30 mm), medium (40 - 70 mm) or high (80 - 150 mm) slump requires cement contents of about 358, 380 and 425 Kg/m^3 respectively. Therefore to obtain a given permeability with a low cement mix requires a good compacting technique.

2. Above a cement content of about 475 Kg/m^3 no significant reduction in permeability is made by further increasing the cement content. For example, increasing the cement content from 250 to 300 Kg/m^3 reduces K by about 6.8 cm/sec, but increasing the cement content from 450 to 500 Kg/m^3 reduces K by

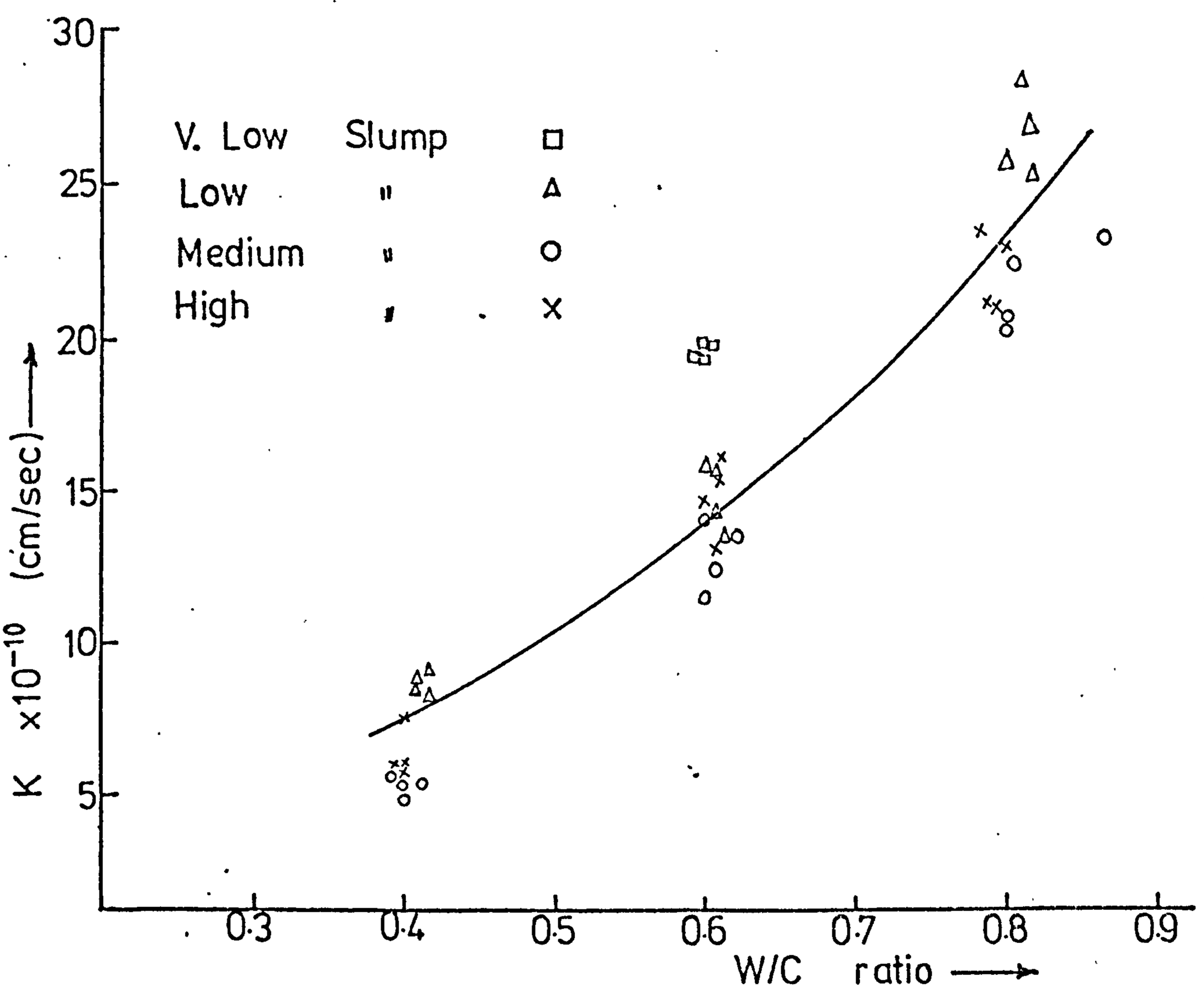

FIG(5.21) VARIATION OF K WITH W/C RATIO
OPC CONCRETE

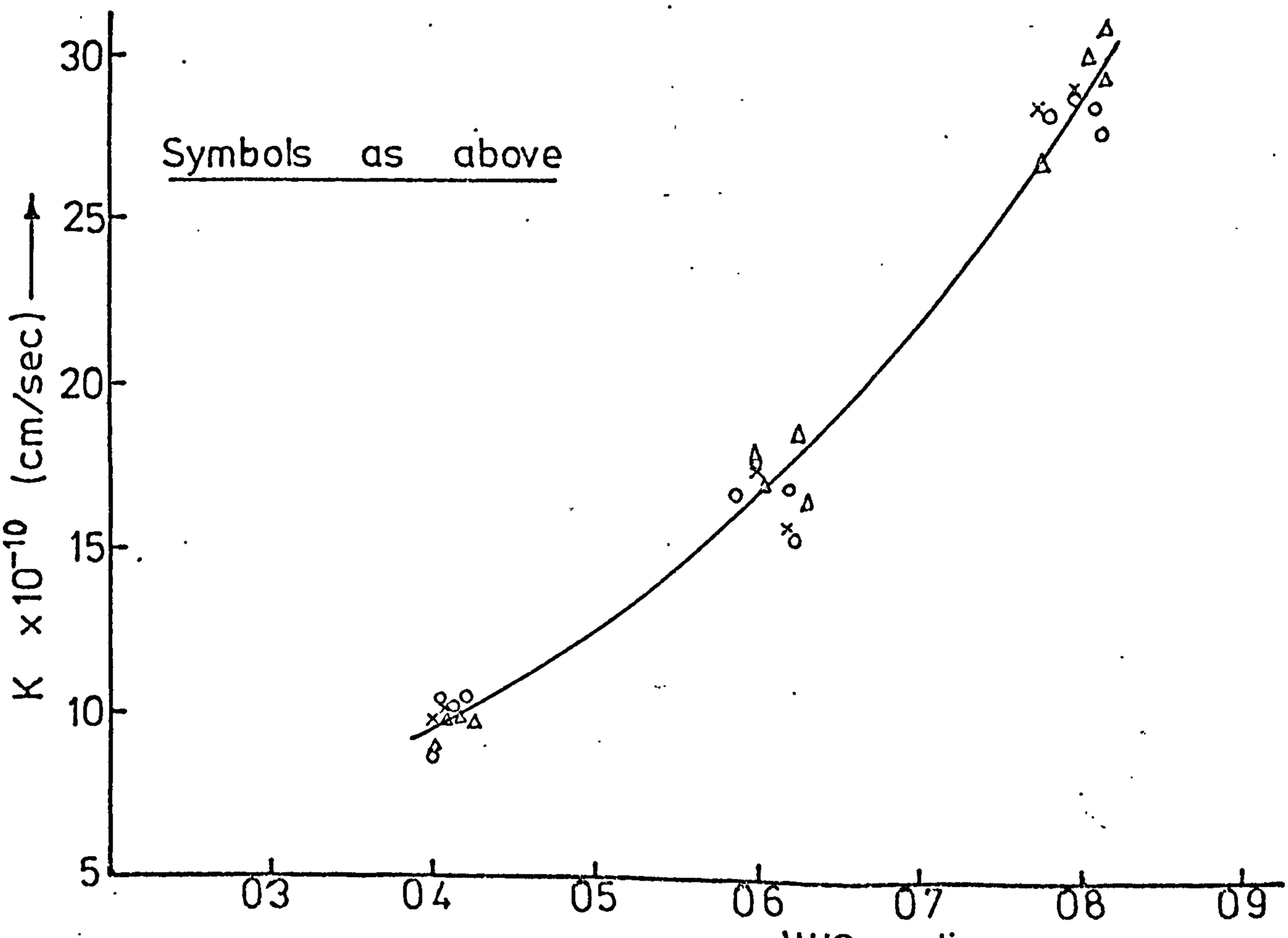

FIG(5.22) VARIATION OF K WITH W/C RATIO
SRPC CONCRETE

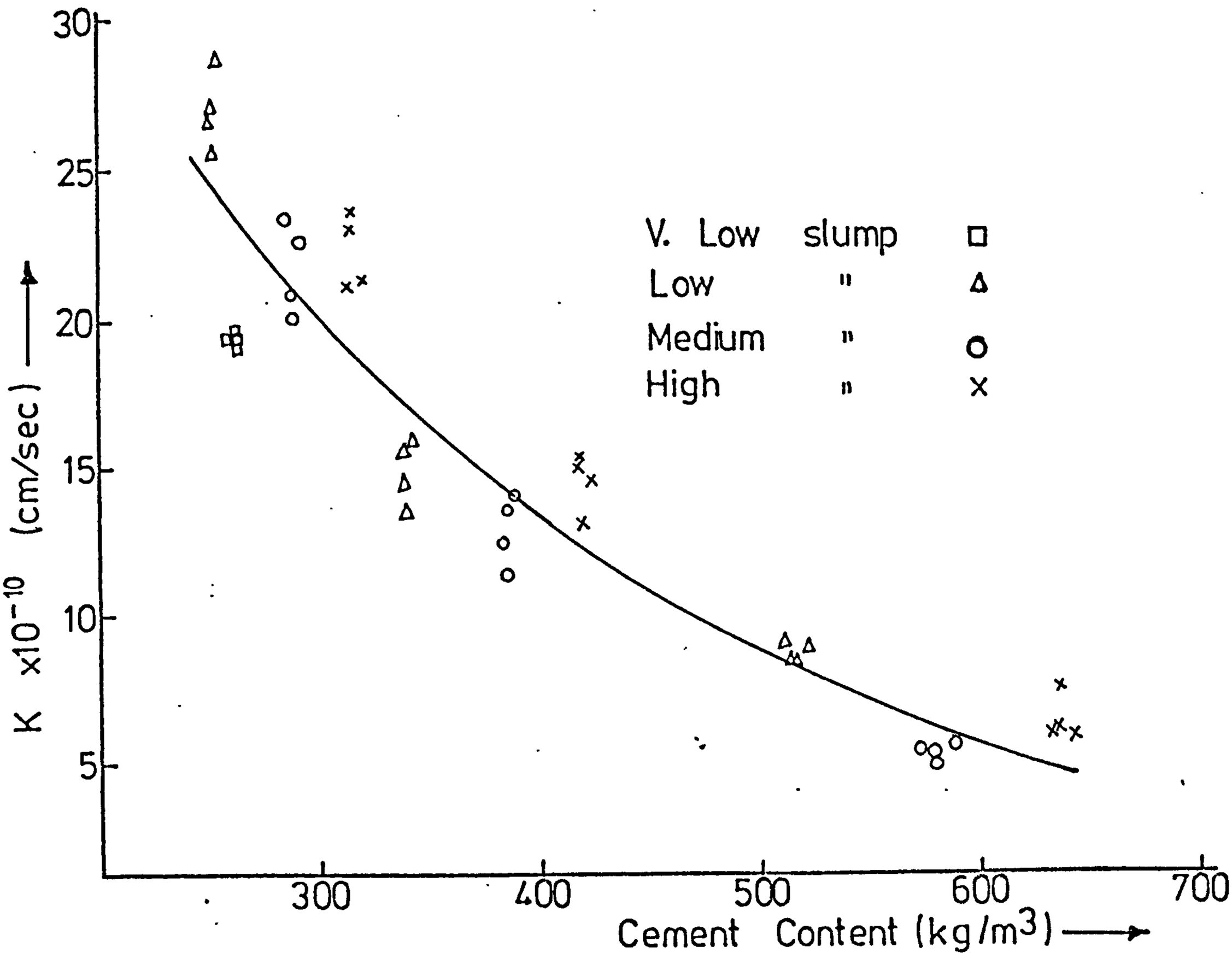

FIG(5.23) VARIATION OF K WITH CEMENT CONTENT OPC CONCRETE

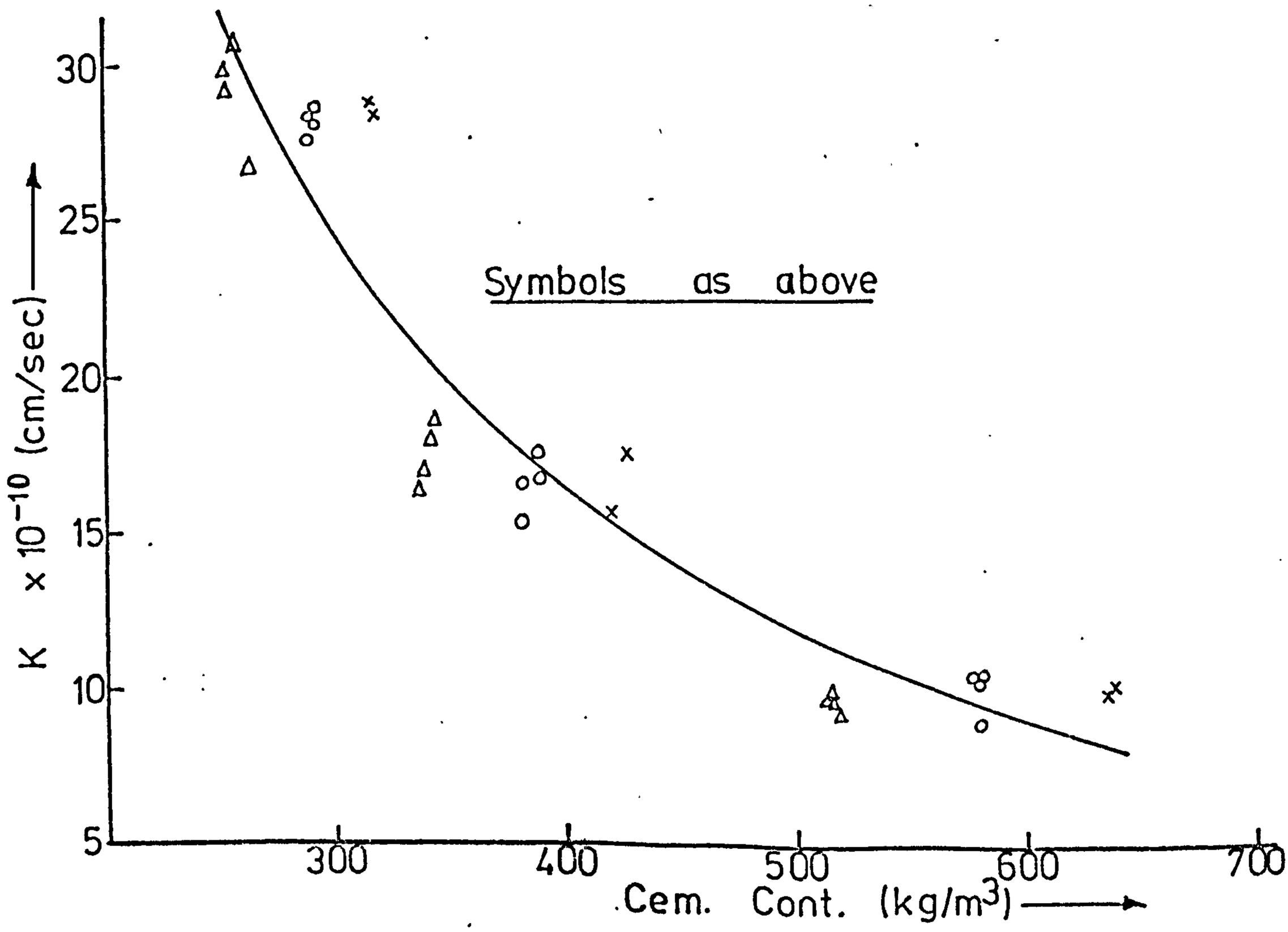

FIG(5.24) VARIATION OF K WITH CEMENT CONTENT SRPC CONCRETE

about 2.1 x 10^{-10} cm/sec.

5.5.3.3 Aggregate Content

The variations of K with aggregate content are illustrated in figs. (5.25) and (5.26) for OPC and SRPC concrete. The following observations are noted:

1. An increase in aggregate content results in an increase in K. This is probably because increasing the aggregate content means decreasing the cement content..

2. The rather large scatter of results in the figures shows that though aggregate content affects K, other factors such as cement content, workability and W/C ratio play very significant role. For example, from fig. (5.25), a concrete mix having K = 22 x 10^{-10} cm/sec can be produced with a medium slump at an aggregate content of about 1857 Kg/m^3 while an aggregate content of about 1782 Kg/m^3 is needed for high slump, but using a higher cement content.

5.5.3.4 Aggregate Grading

The variation in K for OPC concretes as the aggregate grading changes from fine to coarse, zone (1 to 4) is illustrated in fig. (5.27). The workabilities of the different mixes are also indicated. From the figure and test results, the following are noted:

1. No clear conclusions can be drawn from the figure about the affect of aggregate grading on K. Inspection of table (5.9) shows that W/C ratio generally decreased from the fine to the coarse zone and this probably obscured any clear relationship between K and aggregate grading.

2. The medium slump mixes show smaller K values for aggregate grading zones 2 and 3 than for 1 and 4. It appears that for low concrete permeability, very fine and very coarse aggregate gradings should not be used.

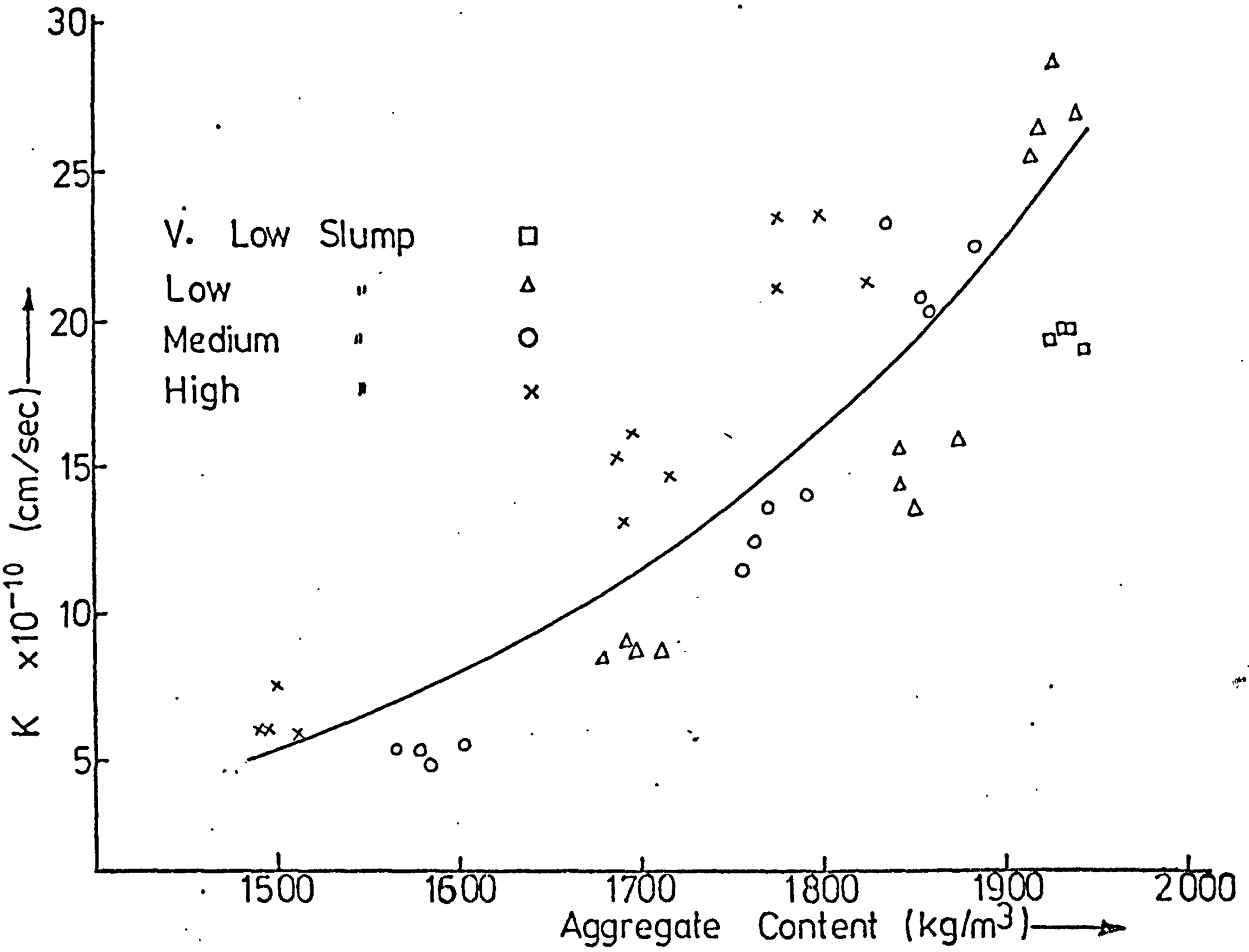

FIG(5.25) VARIATION OF K WITH AGGREGATE CONTENT OPC CONCRETE

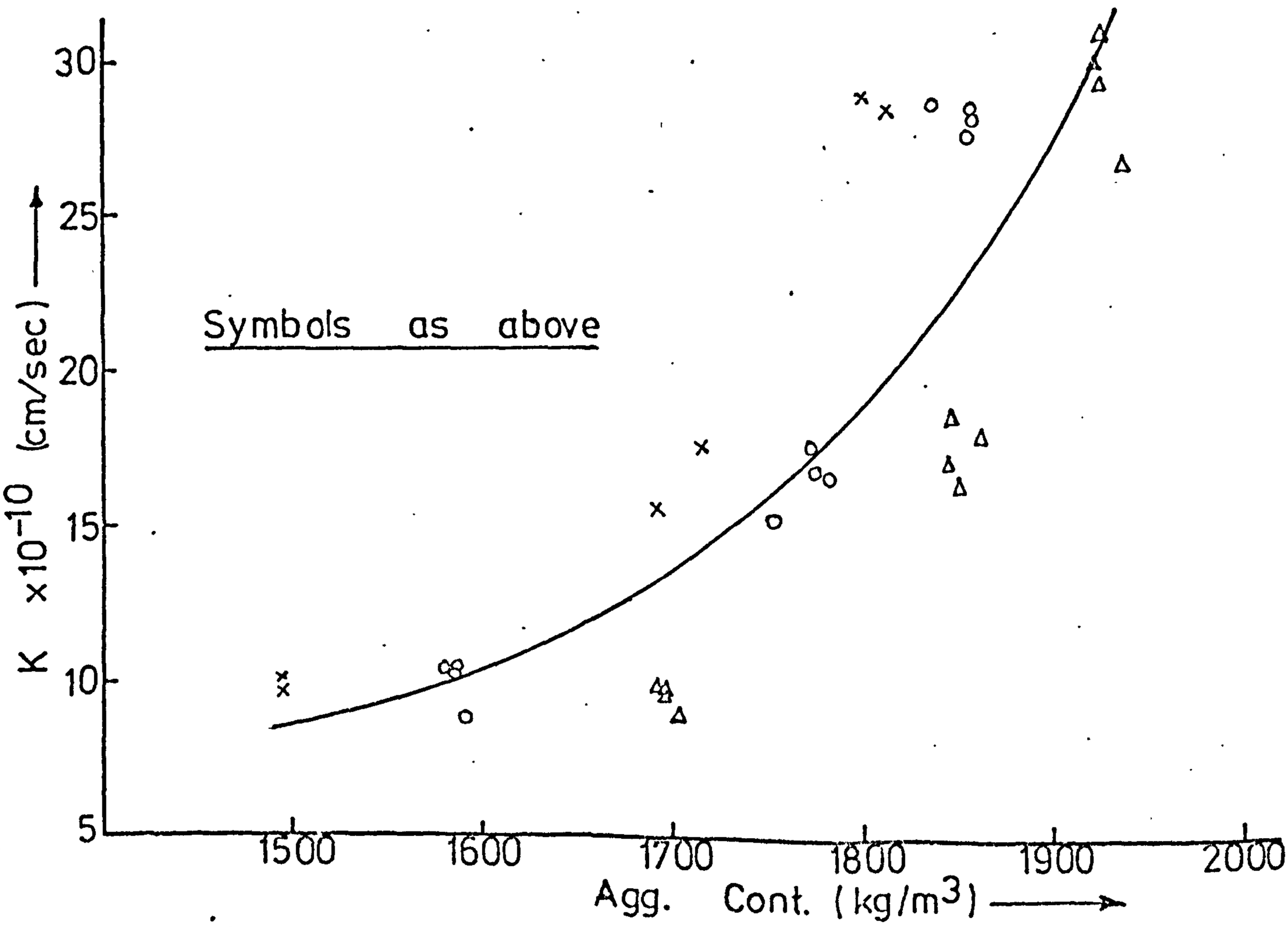

FIG(5.26) VARIATION OF K WITH AGGREGATE CONTENT SRPC CONCRETE

5.5.3.5 Workability

The slump values were obtained immediately after mixing as stated in section 3.5.2. The variations of K with slump are illustrated in fig. (5.28) for OPC concrete. The values for SRPC concrete are not presented because the mixes tended to stiffen very fast leading to misleading slumps especially at W/C ratios of about 0.4. The following observation is made from the figure:

Low slumps, below about 20 mm, gave more permeable concrete and the permeability decreased as the slump increased to the medium ranges - above about 50 mm, and again increased at high slumps - above about 110 mm. The reasons for this appear to be:

1. K decreases with an increase in slump because: (a) concrete of low slump contains air voids due to incomplete compaction, (b) the low slump mixes have a smaller cement content - table (5.9).

2. K increases for high slump concrete because: (a) these mixes tended to bleed and bleeding introduces flow channels in the concrete; (b) at very high slumps above 140 mm segregation often occurs leading to uneven aggregate-cement bond.

Concrete mixes in construction where low permeability is required should have a slump of 60 - 110 mm.

5.5.4 Experimental and other Factors Affecting Concrete Permeability

5.5.4.1 Duration of Test

All the specimens listed in tables (5.9) and (5.10) were tested in the permeability equipment between 5 and 7 days (120 - 168 hours), at each applied fluid pressure. This depended on how quickly a steady or a near steady state of flow was established. Typical results are shown in fig. (5.29) and for OPC concrete. The nos. in the figure are as in table (5.9)

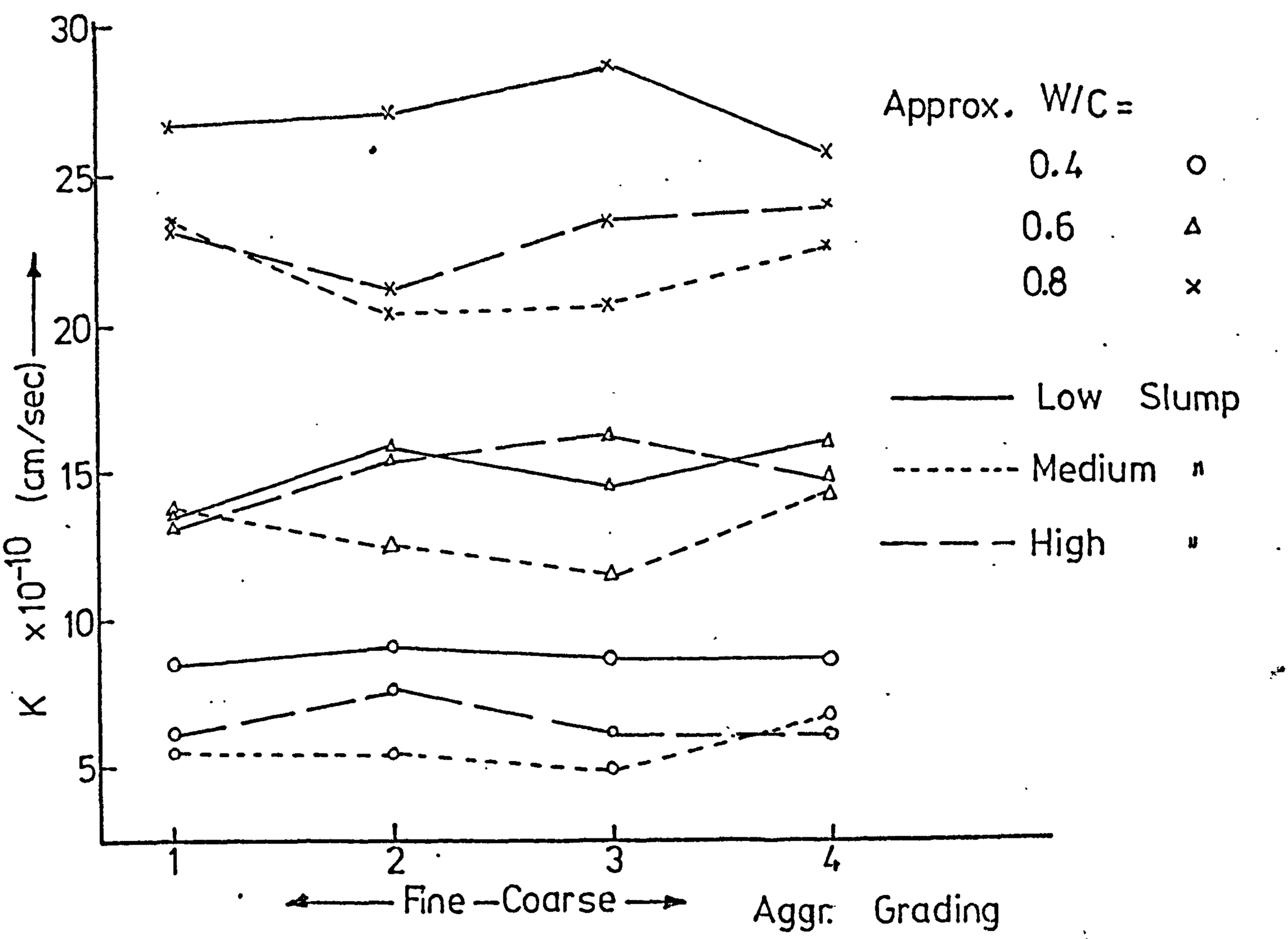

FIG(5.27) EFFECT OF AGGREGATE GRADING ON K. OPC CONCRETE

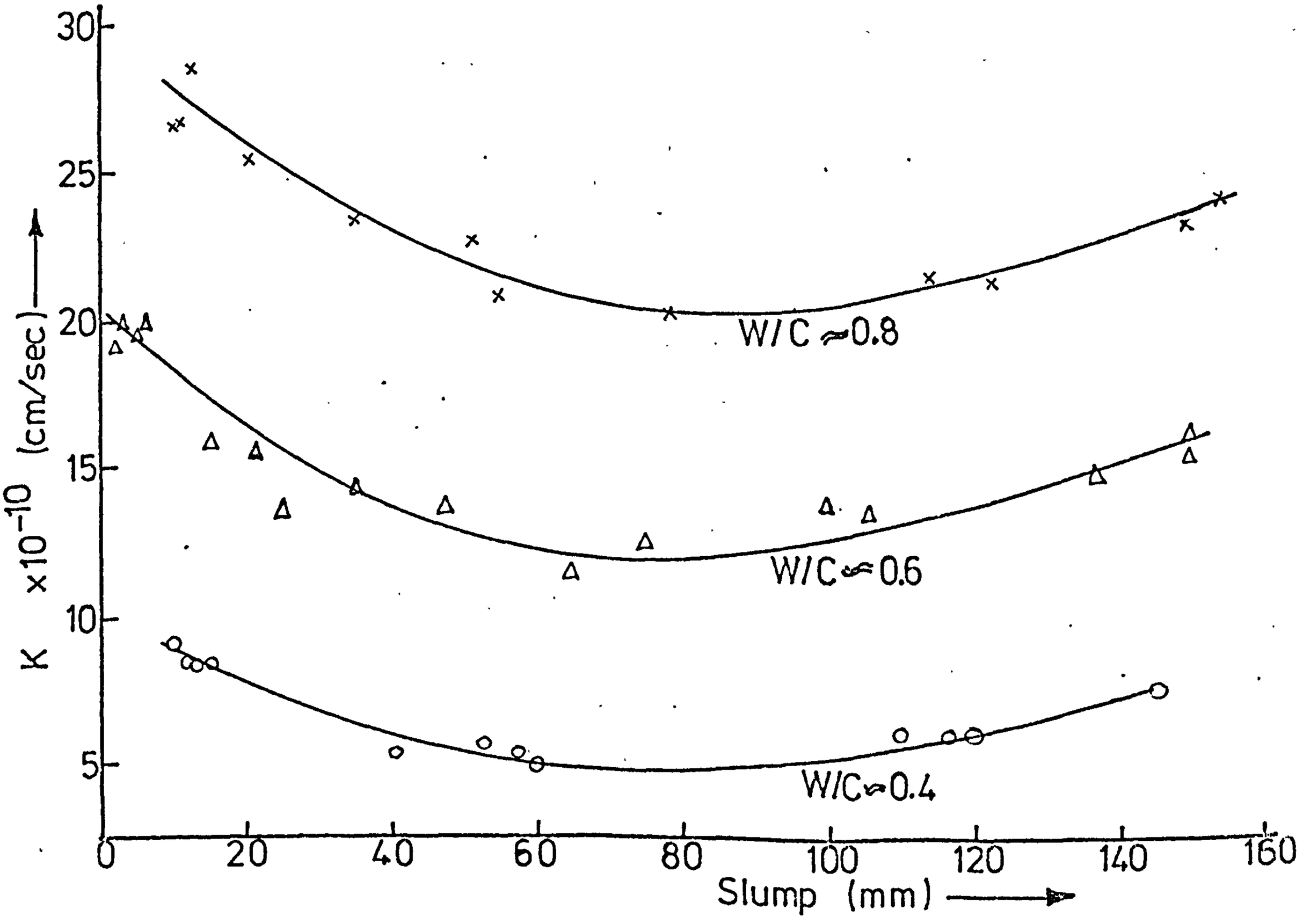

FIG(5.28) VARIATION OF K WITH THE CONCRETE WORKABILITY (SLUMPS) - OPC.

and were so chosen to illustrate the effects of the mix design parameters. The following are observed:

1. In all cases, K decreased with time and this is in keeping with the findings of Matti[12] for unsteady flow. This gradual decrease in K is probably due to the factors given in section 5.4.2.1.

2. The values of K after 6 hours of flow were in all cases very high and varied erratically between 1.65 and 1.27 of its value after 24 hours of flow. This is probably due to the fact that oil will quickly fill any voids or pores close to the surface and any spaces between the sealing epoxy resin and the concrete specimen.

3. Concrete Nos. 21, 22, and 23 of fig. (5.29) illustrate the effect of W/C ratio on the variation of K with time; Nos. 18, 21 and 24 illustrate the effect of aggregate grading while 1, 10, 22 and 34 illustrate the effect of the mix workability. From the similarity of the plots, it can be concluded that these 3 parameters have little significant effect on the variation of K with time.

5.5.4.2 Applied Hydrostatic Pressure

All the concrete specimens in tables (5.9) and (5.10) were tested at 4 different applied hydrostatic pressures of 0.286, 0.552, 0.690 and 0.827 N/mm^2, corresponding to crude oil pressure heads of 32.9, 64.8, 80.8 and 96.8 meters respectively. The testing procedure was as described in section 5.2, and the results are given in figs. (5.30) and (5.31) for OPC and SRPC concretes. As in the preceeding section, typical results only are shown. The following observations are made from the plots:

1. Generally, K increased considerably with an increased applied hydrostatic pressure. The percentage increments were greater in the lower W/C ratio concretes (lower porosity) - nos. 18, 21, 24, and 27 of OPC concrete. Based on K values at 32.9 m of oil for low porosity OPC and SRPC concretes, K increased by between 1.82 and 3.73 and between 2.00 and 2.09

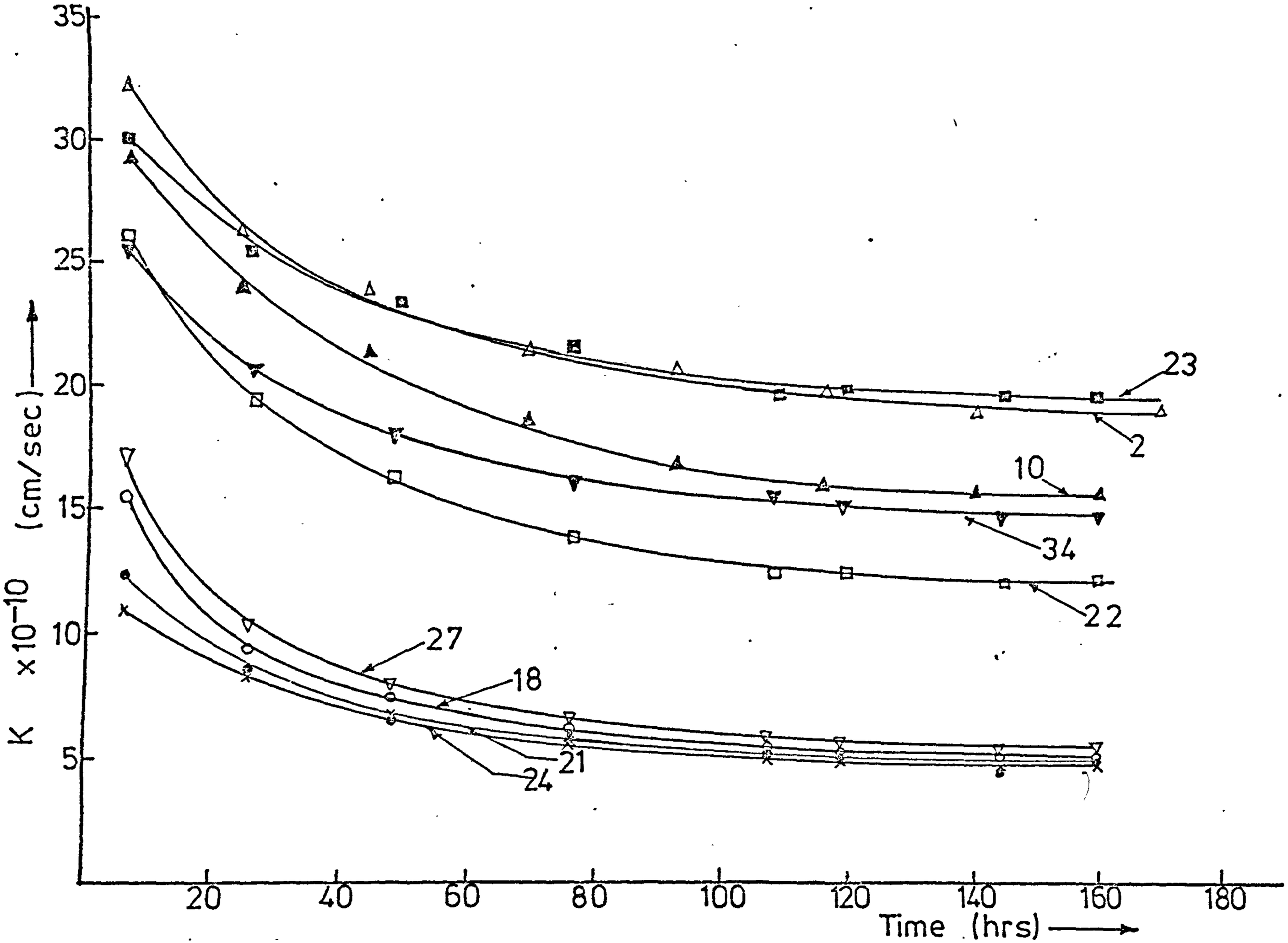

FIG(5.29) VARIATION OF K WITH TIME. OPC CONCRETE

respectively when the pressure increased to 96.8 m of oil. In the higher porosity concretes, the increases were between 1.36 and 2.16, and between 1.39 and 2.32 in OPC and SRPC concretes respectively.

2. No particular functional relationship fitted the variations of K with applied pressure but it was more linear than for HCPs.

5.5.4.3 Total Porosity

The total porosity of the concrete specimens at 28 days is given in column 9 of tables (5.9) and (5.10) for OPC and SRPC concretes respectively. It was calculated by the procedure discussed in chapter 4. The porosity of concrete is influenced principally by its W/C ratio and also by other factors such as aggregate porosity and content, fine/coarse aggregate ratio, cement content and degree of compaction. Figs. (5.32) and (5.33) show the variation of total porosity, P, with the W/C ratio; while figs. (5.34) and (5.35) show the variation of K with total porosity. The following observations are made from the plots:

1. The relationship between P and W/C ratio is non-linear, but can be expressed exponentially as:

$$P = P_o(\exp)^{a_1(W/C)} \qquad (5.7)$$

where P_o is the porosity of a theoretical concrete of zero or negligible W/C ratio and is a constant. By a regression analysis, the values of P_o and a_1 were determined and given in table (5.12).

2. The relationship between K and total porosity can be expressed exponentially in the form:

$$K = K_o(\exp)^{a_2 \cdot P} \qquad (5.8)$$

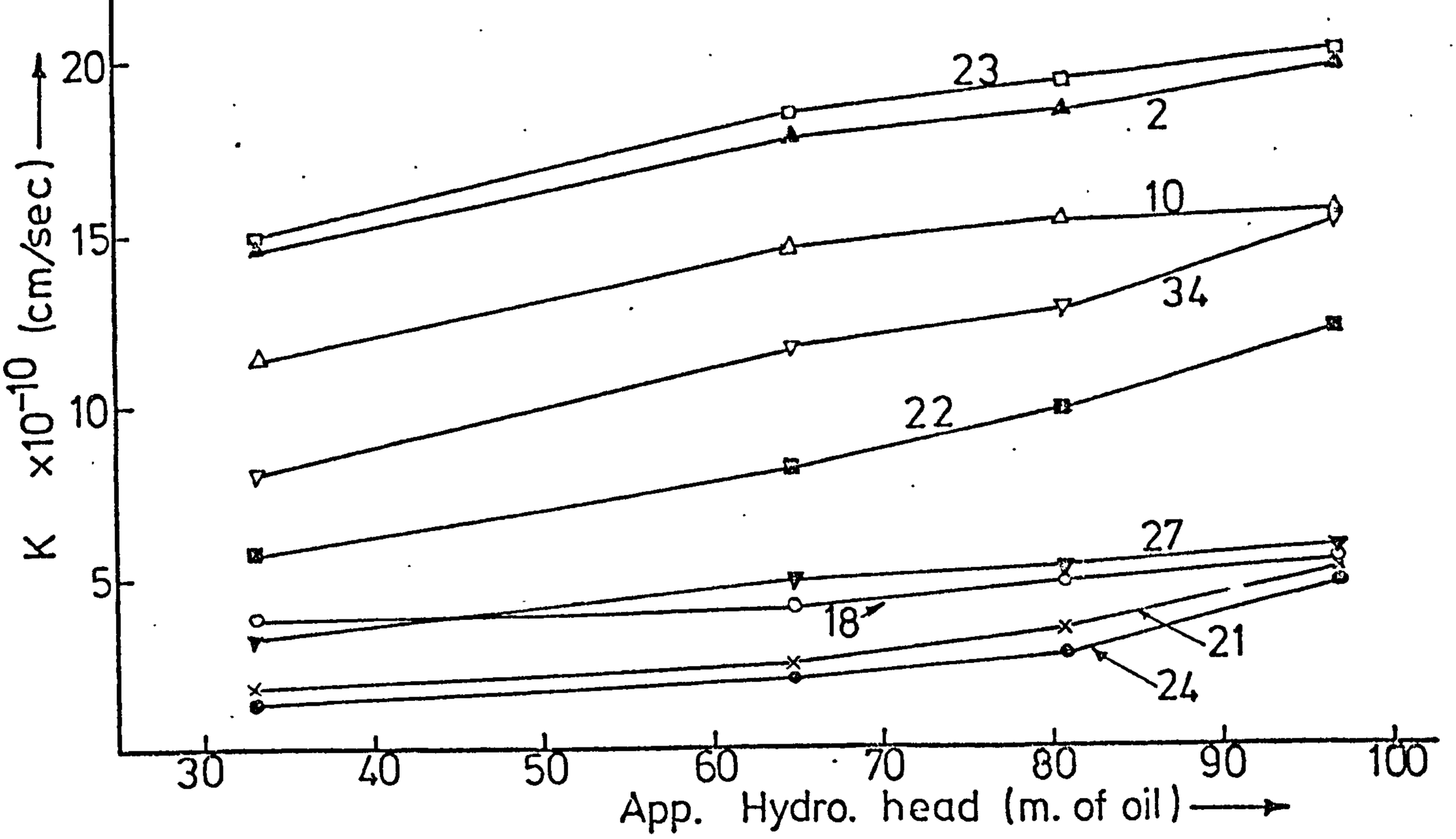

FIG(5.30) VARIATION OF K WITH APPLIED HYDROSTATIC HEAD. OPC CONCRETE

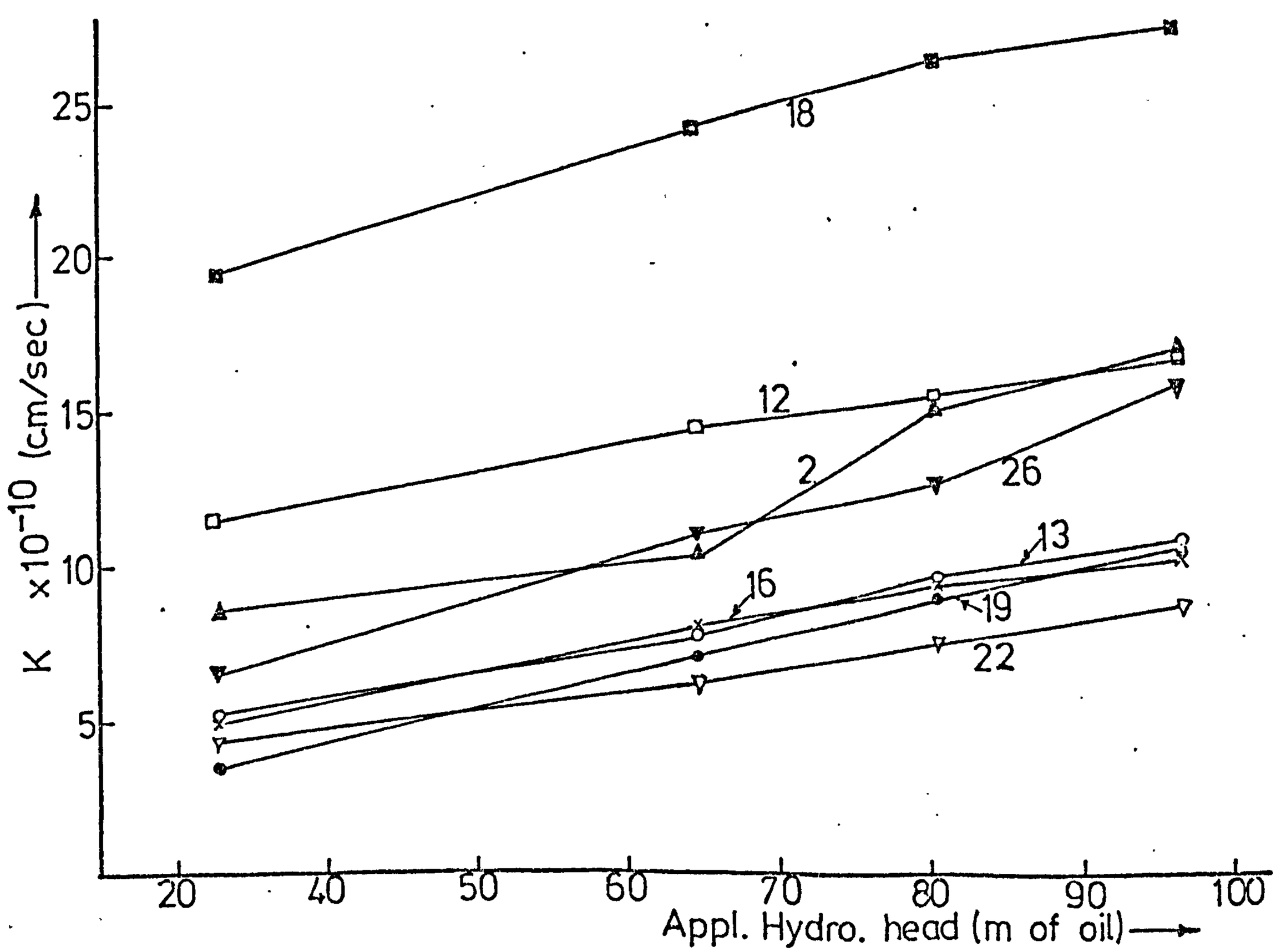

FIG(5.31) VARIATION OF K WITH APP. HYDRO. HEAD. SRPC CONCRETE

where K_o is the coefficient of permeability of a theoretical concrete of zero porosity and a_2 is a constant. By regression analysis K_o and a_2 were determined and are given in table (5.13).

CONCRETE	P_o	a_1	r
OPC	14.95	0.3472	92.5
SRPC	14.93	0.4741	98.8

Table (5.12) Constants of regression - equ. (5.7)
T. Porosity Vs W/C

CONCRETE	$K_o \times 10^{-10}$	a_2	r
OPC	0.00497	0.4298	98.0
SRPC	0.0895	0.2628	97.7

Table (5.13) Constants of regression - equ. (5.8)
K Vs T. Porosity

5.5.4.4 Compressive Strength

It has been established[70,87,92] that the higher the compressive strength of concrete, the lower is its permeability. There are, however, exceptions to this general rule, eg. drying concrete can lead to increased strength[70,71] but permeability generally increases due to cracking inducing by drying shrinkage[12]. Bleeding of concrete can lead to increased strength due to the reduction of the effective W/C ratio but can also lead to increased permeability due to the introduction of bleeding channels.

The oil saturated compressive strengths are given in column 12 of tables (5.9) and (5.10) and plotted anainst K in figs (5.36) and (5.37). These relationships can be expressed exponentially in the form:

$$K = K_o(exp)^{a.fc} \qquad (5.9)$$

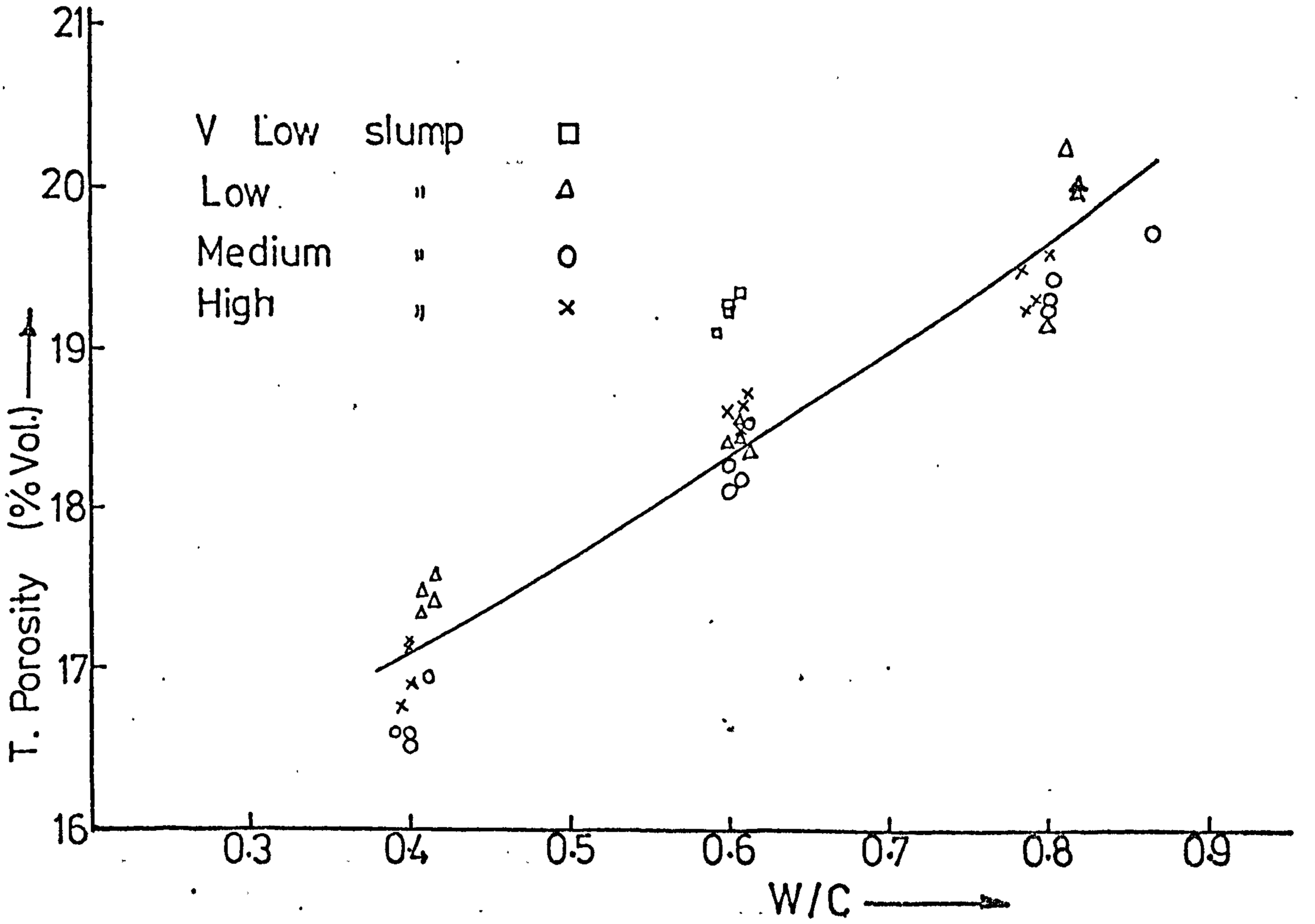

FIG(5.32) VARIATION OF TOTAL POROSITY WITH W/C RATIO. OPC CONCRETE

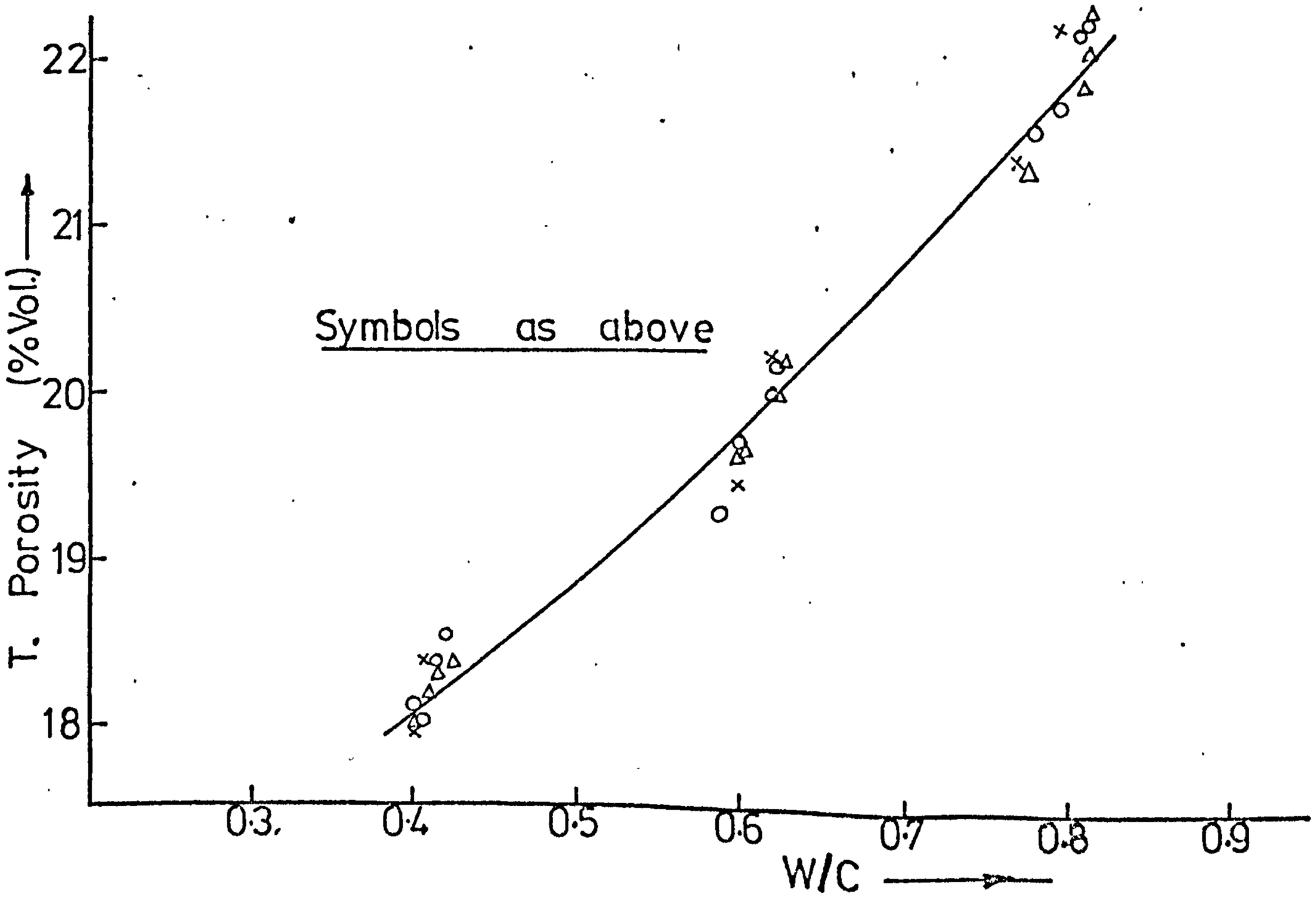

FIG(5.33) VARIATION OF T. POROSITY WITH W/C RATIO. SRPC CONCRETE

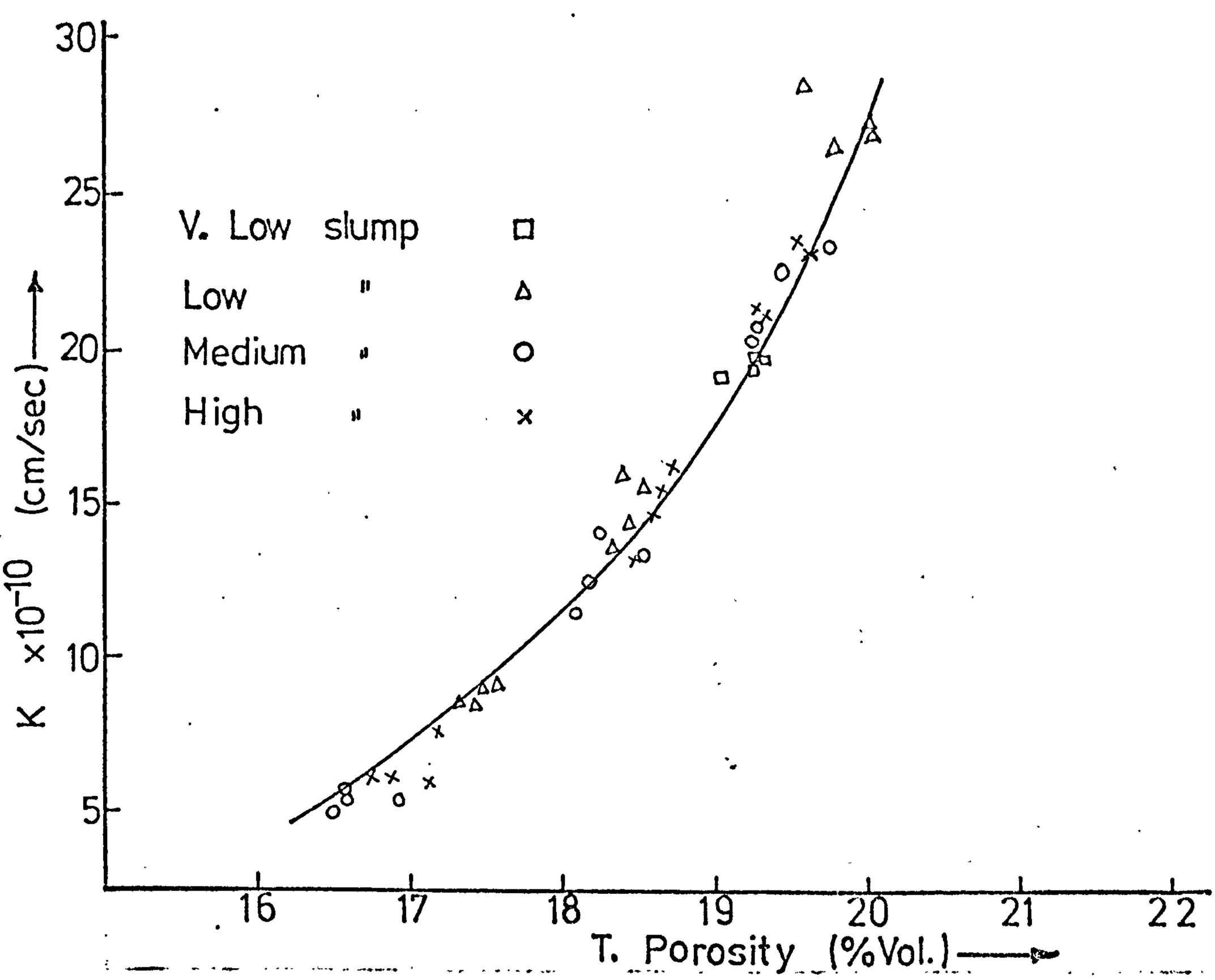

FIG(5.34) VARIATION OF K WITH TOTAL POROSITY OPC CONCRETE

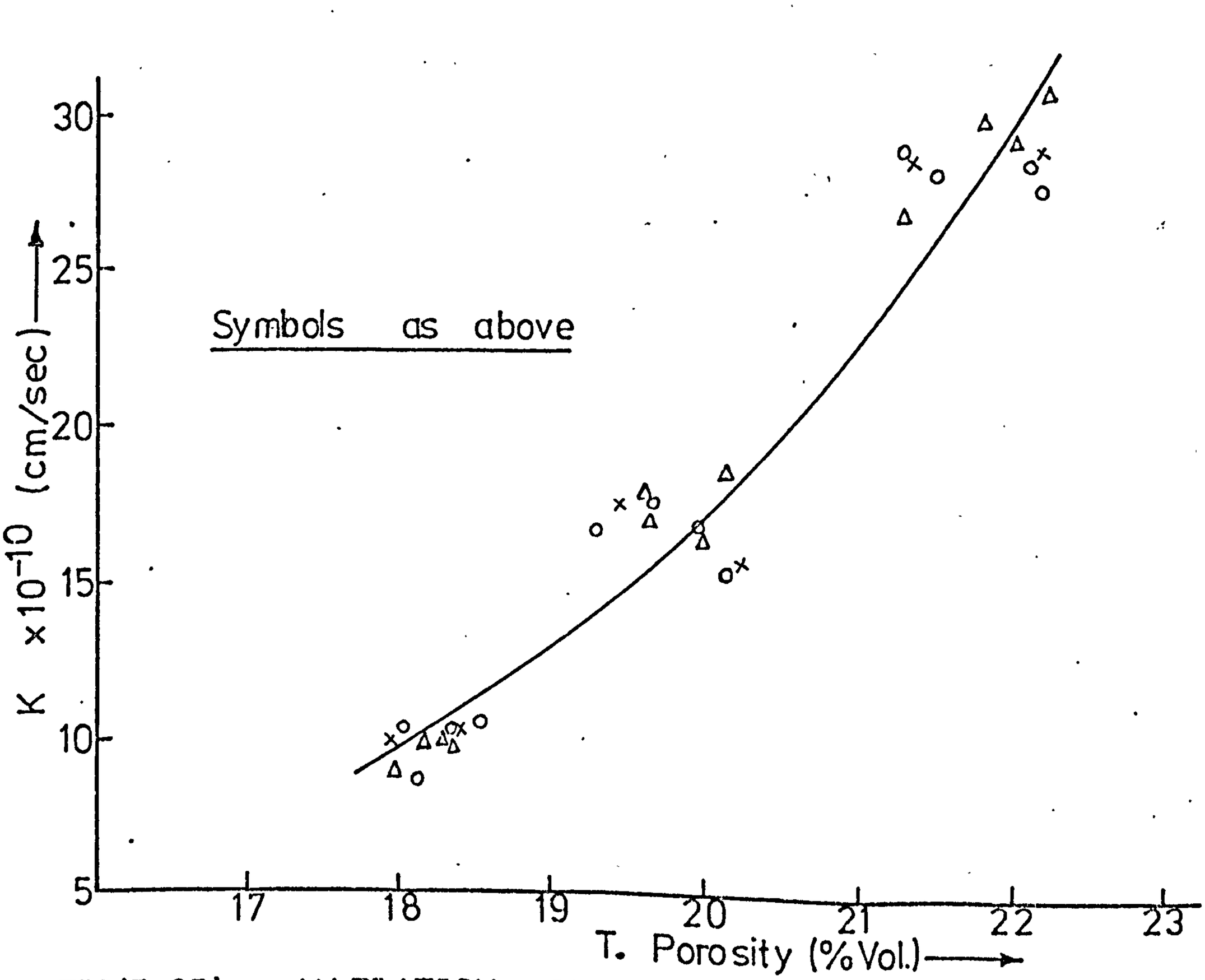

FIG(5.35) VARIATION OF K WITH T. POROSITY SRPC CONCRETE

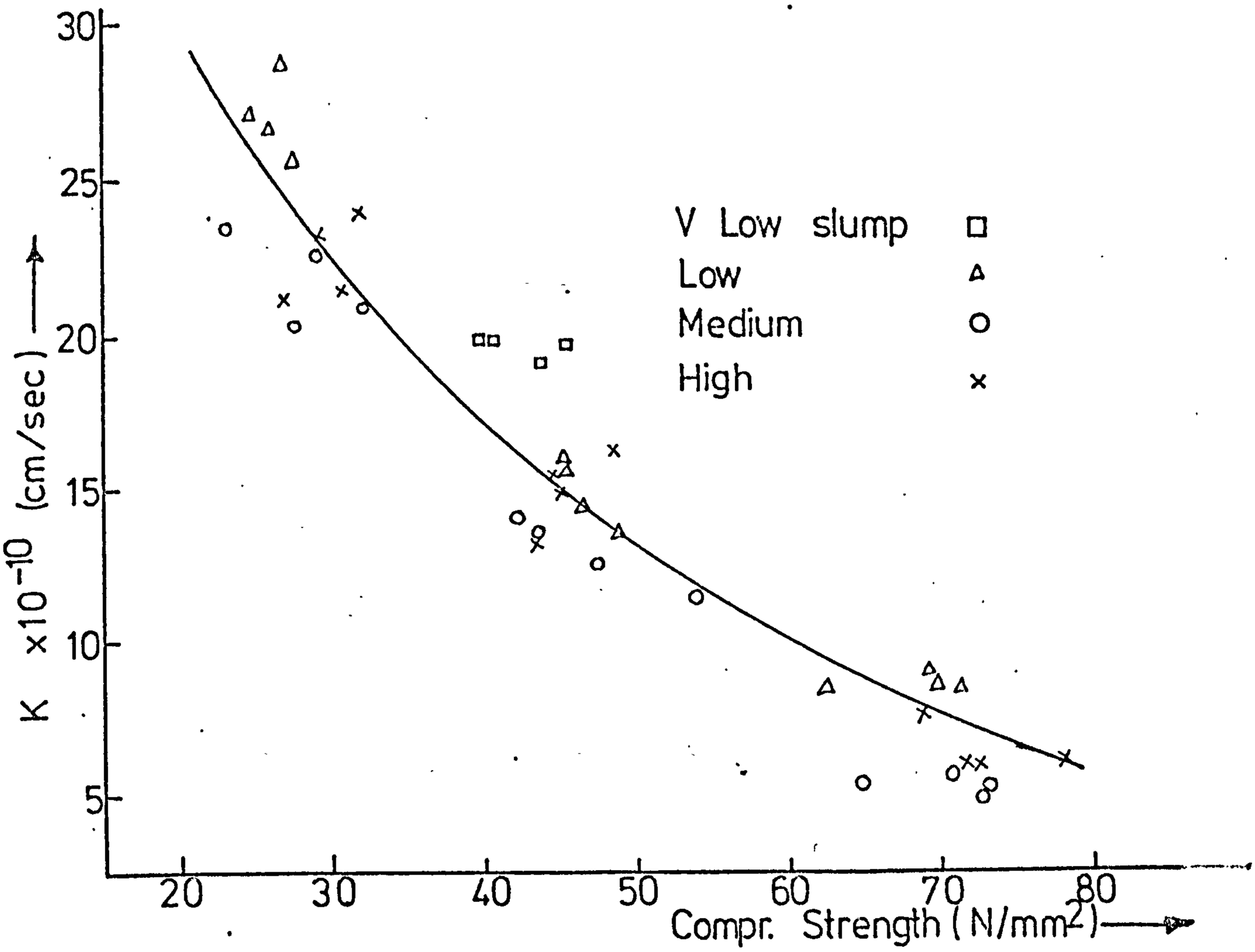

FIG(5.36) VARIATION OF K WITH THE COMPR. STRENGTH OF OIL SATURATED CONCRETE, OPC.

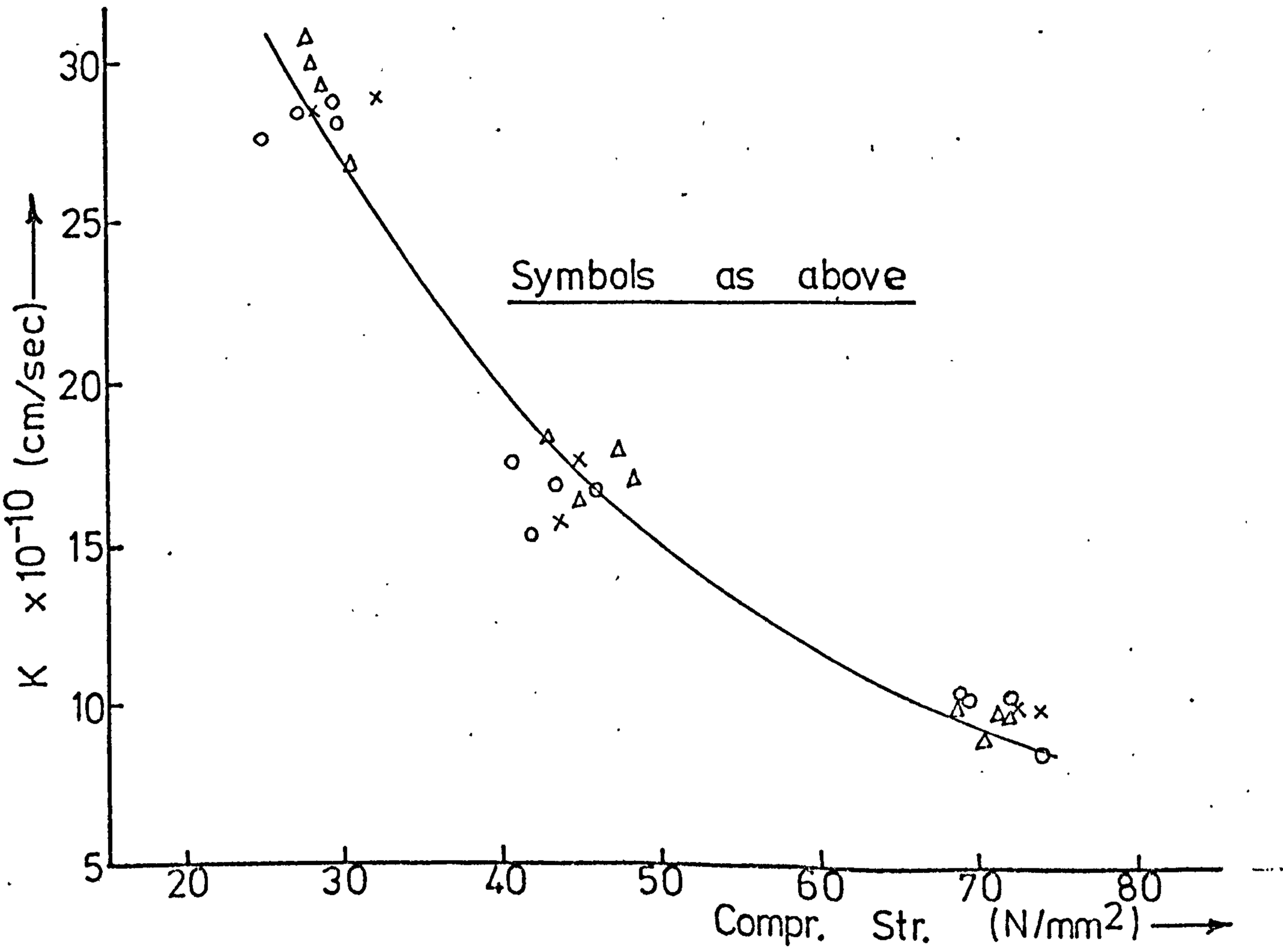

FIG(5.37) VARIATION OF K WITH THE COMPR. STR. OF OIL SAT CONCETE, SRPC.

values of K_o and a are given in table (5.14).

CONCRETE	$K_o \times 10^{-10}$	a	r
OPC	51.51	-0.0274	-95.2
SRPC	59.46	-0.0265	-94.6

Table (5.14) Constants of regression - equ. (5.9)
K Vs Comp. Strength

5.5.5 Optimum Mix design for Reduced Permeability

5.5.5.1 Introduction

The term optimum mix is used here to mean the mix design that will produce concrete of low porosity and permeability. One type of aggregate, and one fine aggregate grading - zone 2 of BS. 882,1965 - were used. One mix design parameter was varied while keeping the rest as constant as practicable. The workability of each mix is given by the slump. The range of variables included in the investigations, their mix proportions and test results are given in table (5.15).

5.5.5.2 W/C ratio

The effect of W/C ratio on water permeability of concrete is widely documented[82-84,90]. In this investigation W/C ratios spanning the reasonable practical ranges were investigated at a cement content of 380 Kg/m^3, and fine aggregate concentration of 0.4 - Nos. 1 to 6 of table (5.15). The variation of K and total porosity with W/C ratio are illustrated in fig. (5.38) A, while fig (5.38) B shows the relationship between K and compressive strength of the mixes with the total porosity. The plots show that to obtain concrete with the lowest possible permeability and porosity, the W/C ratio should be as low as possible; and for W/C ratios less than 0.5, there is negligible reduction in permeability with reduction in W/C ratio.

5.5.5.3 Fine/Coarse Aggregate Ratio

NO	FRESH CONCRETE						AT 4 WEEKS			AT 24 WEEKS			
	MIX PARA-METER	SLUMP (mm)	CEMENT CONTENT (Kg/m^3)	AGGREG. CONTENT (Kg/m^3)	FINE AGGREG. FRAC.	W/C RATIO	DENSITY SSD (Kg/m^3)	TOTAL POROSITY (% Vol.)	COMPR. STRENGTH (N/mm^2)	COMPR. STRENGTH CTR	COMPR. STRENGTH OIL. SAT	OIL ABSORP %Dry Wt.	$^{+}Kx10^{-10}$ (cm/sec)
1	2	3	4	5	6	7	8	9	10	11	12	13	14
1		0	380	1955	0.40	0.40	2442	15.98	75.0	78.0	74.7	2.53	10.03
2		3	380	1902	0.40	0.45	2426	16.89	66.6	68.4	65.5	2.48	10.11
3	W/C	12	380	1865	0.40	0.50	2418	17.26	64.8	60.2	58.9	3.25	12.01
4	RATIO	20	380	1816	0.40	0.55	2397	17.94	58.0	58.8	56.4	3.45	13.35
5		80	380	1765	0.40	0.60	2380	18.18	46.0	49.0	47.6	3.99	18.72
6		152	380	1669	0.40	0.70	2357	19.99	43.1	48.0	40.6	4.39	20.45
7		collapse	380	1765	0.20	0.60	2387	19.27	38.0	40.5	37.5	4.89	16.62
8		170	380	1765	0.30	0.60	2388	18.51	49.6	50.7	44.8	3.80	15.01
9	FINE/	61	380	1765	0.40	0.60	2370	17.99	51.4	54.3	50.9	3.57	11.97
10	TOTAL	48	380	1765	0.50	0.60	2372	18.03	47.8	50.7	47.3	3.24	12.15
11	AGGREG.	25	380	1765	0.60	0.60	2368	18.24	52.7	56.0	49.8	4.29	11.98
12		10	380	1765	0.70	0.60	2375	19.54	47.0	52.5	43.4	4.90	16.95
13		3	380	1765	0.80	0.60	2355	20.14	39.5	42.8	39.6	5.39	18.97
14		0	380	1765	1.00	0.60	2287	21.92	38.8	44.5	42.5	6.40	25.26
15		8	280	2002	0.35	0.60	2428	19.37	42.2	47.0	40.4	4.51	20.88
16		13	330	1890	0.40	0.60	2413	18.65	48.b	50.8	49.0	4.00	20.20
17	CEMENT	58	380	1816	0.42	0.60	2404	18.11	49.5	51.7	50.1	3.84	17.97
18	CONTENT	127	430	1719	0.50	0.60	2407	18.09	49.4	51.0	46.4	3.98	17.45
19	Kg/m^3	168	480	1600	0.55	0.60	2379	18.55	58.9	60.5	55.4	3.70	16.68
20		collapse	530	1527	0.60	0.60	2360	20.33	42.0	46.3	40.8	4.10	22.23
21		collapse	580	1447	0.65	0.60	2355	21.89	38.0	40.1	37.5	5.87	25.26
22	AGGREG. 5	0	380	1765	1.00	0.60	2287	21.92	38.8	45.1	42.5	6.40	25.26
23	SIZE 10	41	380	1765	0.50	0.60	2381	17.90	47.5	53.9	52.5	3.05	12.31
24	20	137	380	1765	0.50	0.60	2387	18.33	35.8	43.3	40.7	4.39	15.18

+ At 96.8 m of oil, after 120 hours of flow

Table (5.15) Mix Proportions and Test Results for Optimum Mixes

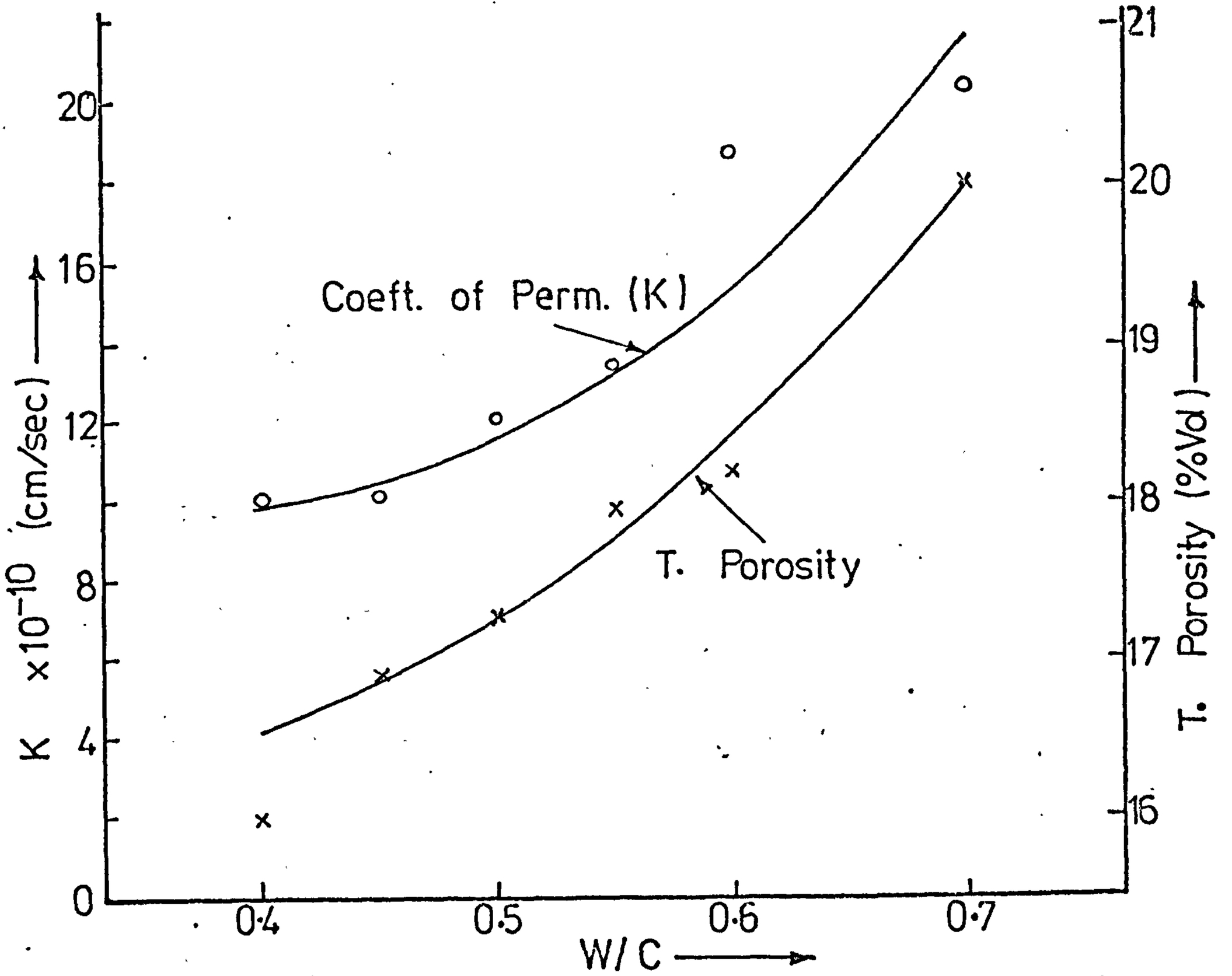

(A) Variations of K and Total Porosity, with W/C ratio.

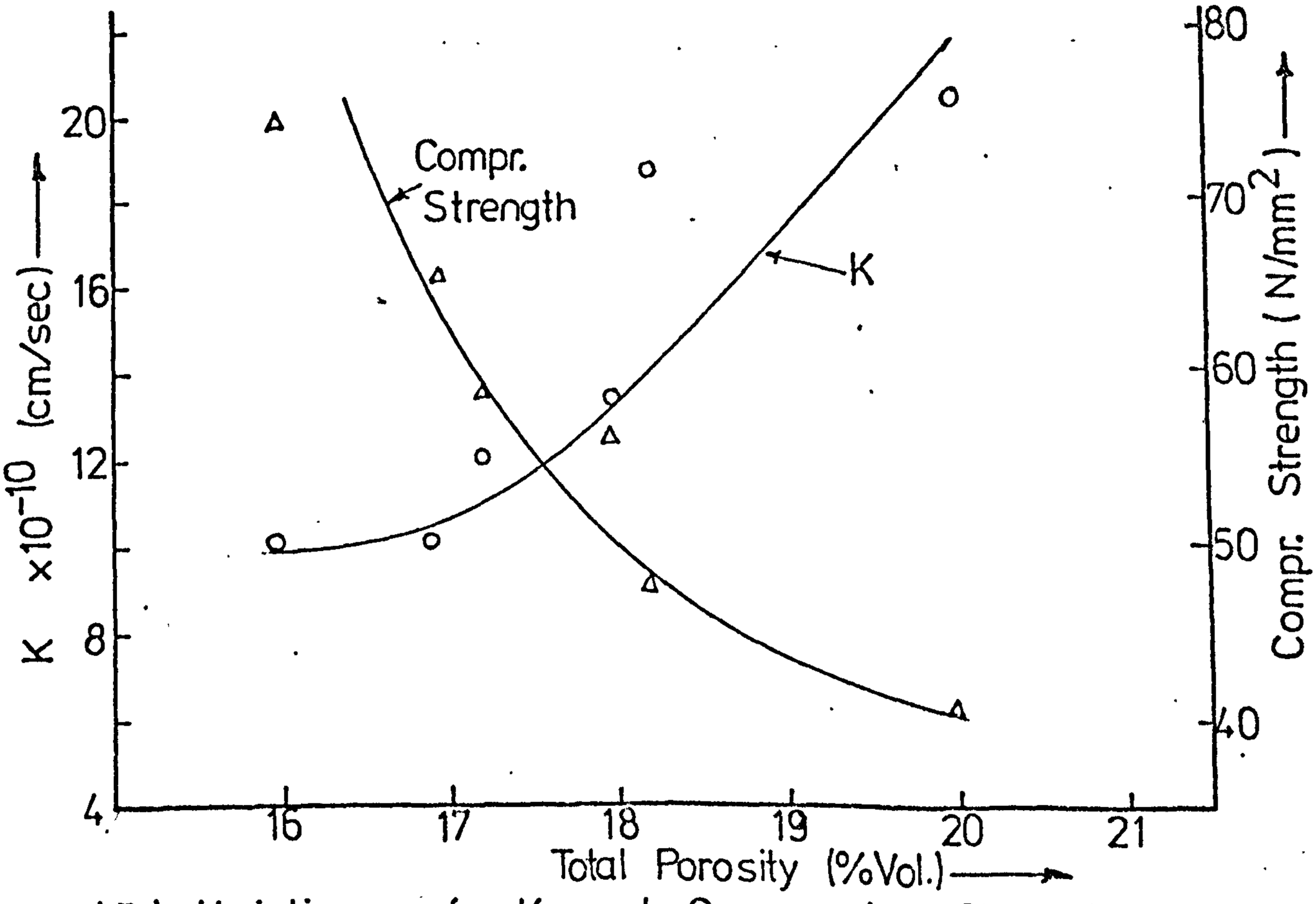

(B) Variations of K and Compressive Strength With Total Porosity

FIG(5.38) OPTIMUM W/C RATIO

The fine aggregate content has a considerable influence on the quality of concrete[132,133]. Earlier work by Hughes[132] has shown that increasing the sand/coarse aggregate ratio can lead to increased concrete porosity. To observe the effect of the fine aggregate concentration on oil permeability, the percentage of fine aggregate to total aggregate was varied from 20% to 100% at a fixed W/C ratio, cement content and aggregate content. The results are shown in table (5.15) Nos. 7 to 14. Fig. (5.39) A, shows the variations of K and total porosity with the percentage of fine aggregate while fig. (5.39) B, shows the variation of compressive strength with the fine aggregate percentage. The following observations are made from the plots:

1. Outside the range of 40 - 60% fine aggregate concentration, both the porosity and permeability increased considerably and the compressive strength fell.

2. Below 40%, the fresh concrete mix tends to be 'uncohesive' and above 60% the mix becomes over-sanded and the sudden rise in porosity is due to the quantity of available cement paste being insufficient to fill the voids in the sand[132].

3. The optimum range of fine aggregate for W/C of 0.6 is therefore between 40 to 55%.

5.5.5.4 Cement Content

Cement is usually the most expensive component of concrete and it is an advantage to use the minimum cement content to achieve the desired concrete quality. Cement contents of between 280 and 580 Kg/m^3 were used to investigate the influence of the cement content on permeability using a constant W/C of 0.60. Fig. (5.40) shows the variations of K, compressive strengths and concrete porosity with cement content. The following observations are made from the plotted test results - tables (5.16), nos. 15 - 21:

1. As the cement content was increased from 280 Kg/m^3 to about 400 Kg/m^3 there was considerable improvement in concrete quality, with the optimum vlaue at about 380 Kg/m^3. The corresponding optimum aggregate - cement (A/C) ratio was between 4.3 and 4.7. A similar decrease in cube and uniaxial compressive strengths at very high cement contents has been noted by Hughes[132] and Hughes and Ash[134].

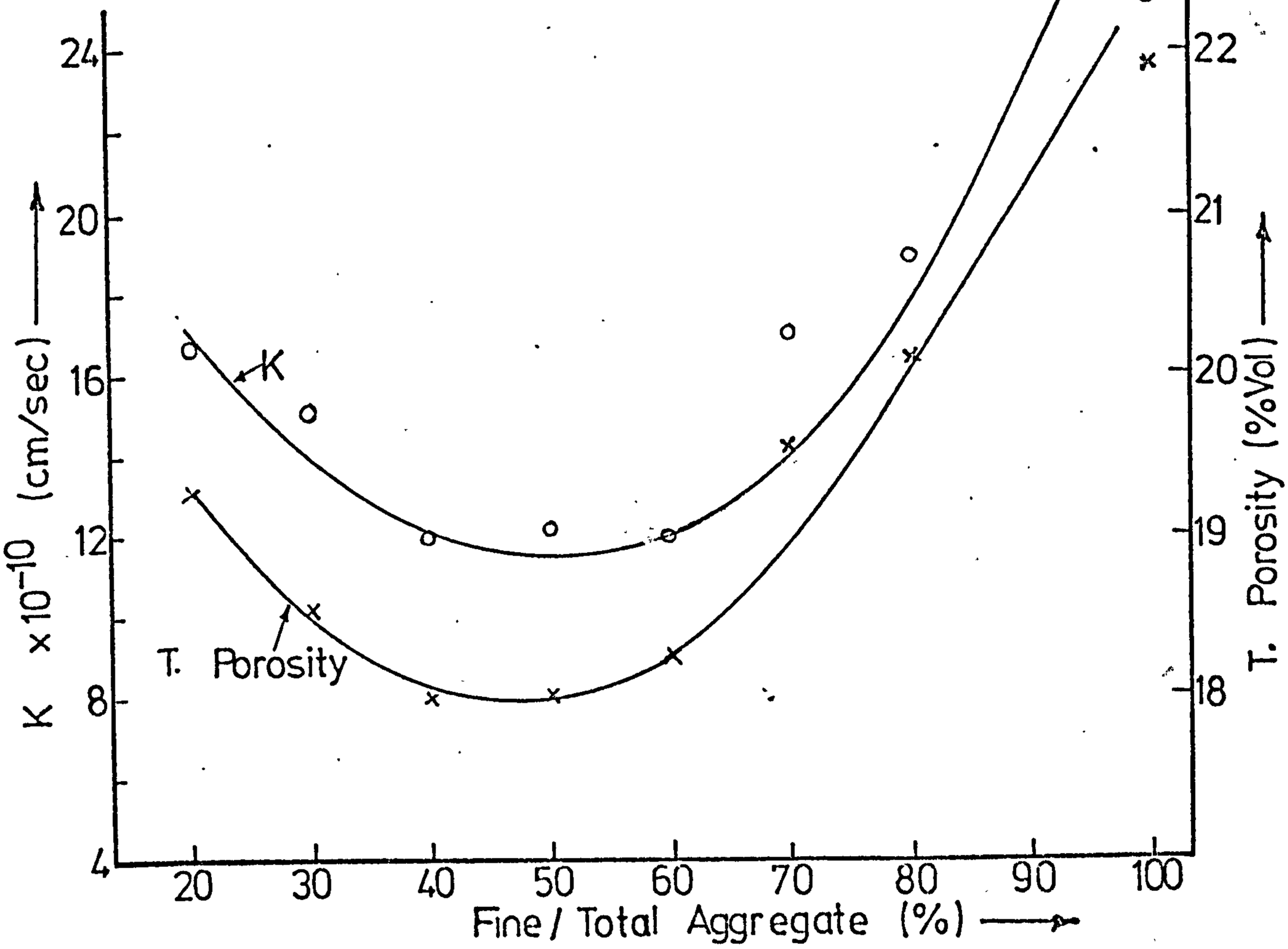

(A) Variations of K and T. Porosity with the Fine Aggregate Concentration

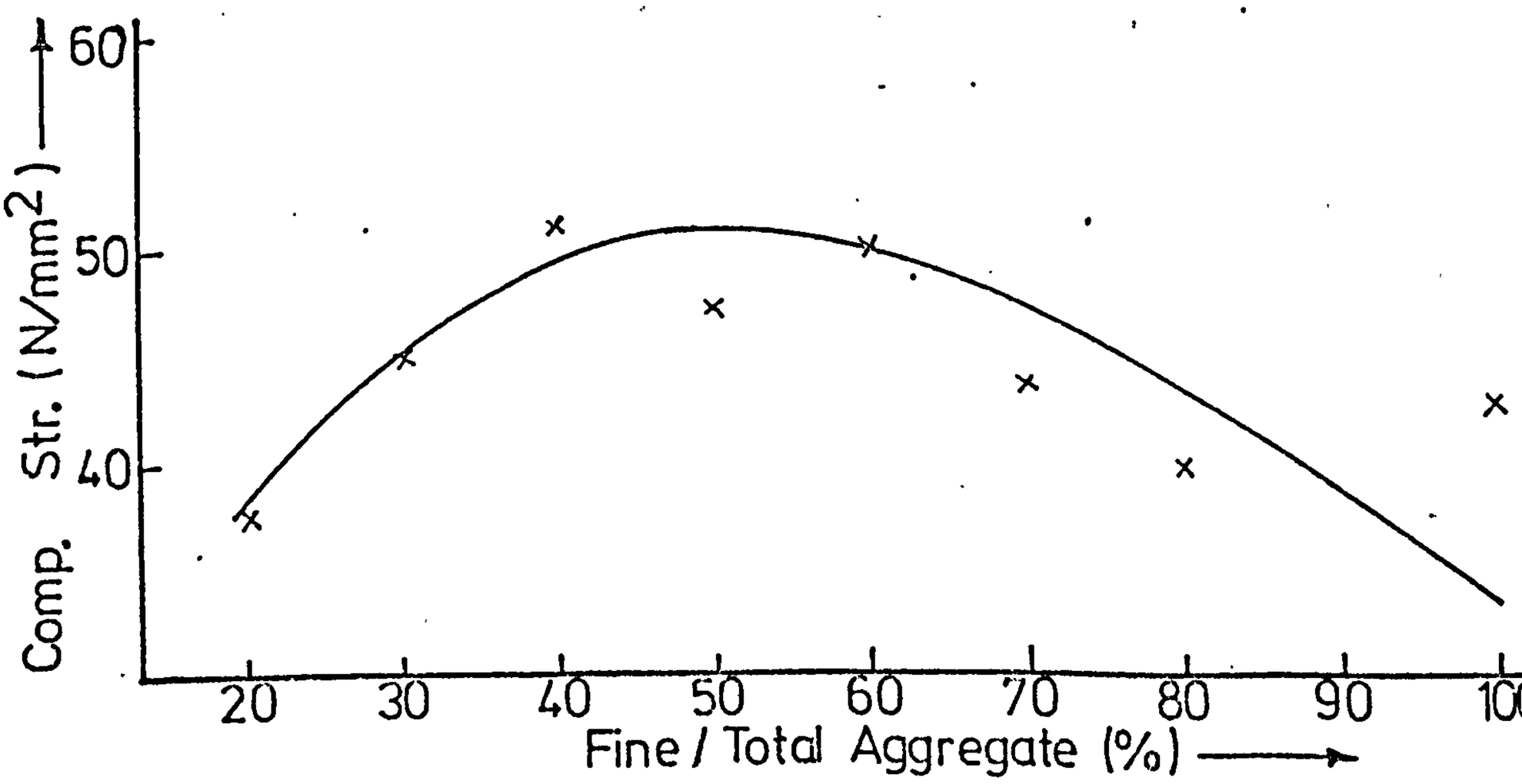

(B) Variation of Compressive Strength with the Fine Aggregate Concentration.

FIG(5.39) OPTIMUM FINE AGGREGATE CONCENTRATION.

2. Using the values of K obtained in Section 5.5.5.2 - fig. (5.39), approximate optimum cement contents can be predicted from fig. (5.23) for various W/C ratios. These predicted values are plotted in fig. (5.41) together with the corresponding calculated A/C ratios at various cement contents. Eg. for W/C = 0.4, optimum cement content is about 575 Kg/m^3 and optimum aggregate - cement ratio is about 2.90.

5.5.5.5 Maximum size of Coarse Aggregate

Three sizes of coarse aggregate were used - 5 mm, 10 mm, and 20 mm. It is unlikely that aggregate size larger than 20 mm will be used in an oil retaining structure. The mix proportions and test results are given in table (5.15), nos. 22 - 24. For the 20 mm size aggregate mix, the coarse aggregate was subdivided into 10 mm and 20 mm and recombined in the ratio of 1:2. The following observations are made from the test results:

1. Using 5 mm maximum size aggregate rather than 10 mm caused the porosity to increase by 22.5%, the permeability by 105% and the strength to fall by 19%. This is mainly due to the larger air voids present in the mix as a result of oversanding.

2. Using the 10 mm maximum size aggregate rather than the 20 mm - the porosity increased by 2.4%, the permeability by 23% while the strength fell by 19%.

The present investigation on maximum aggregate size is however, incomplete and intermediate sizes need be investigated to confirm an optimum size.

5.6 Superplasticised Concrete

5.6.1 Introduction and Scope of Study

Superplasticisers are used to reduce the water content or increase the workability of concrete without changing the W/C ratio. Most of the permeability tests on concrete containing superplasticisers have so far been done by the manufacturers and for water permeability only. Results have shown that permeability reduced by upto 20% for concrete of normal workability[114]

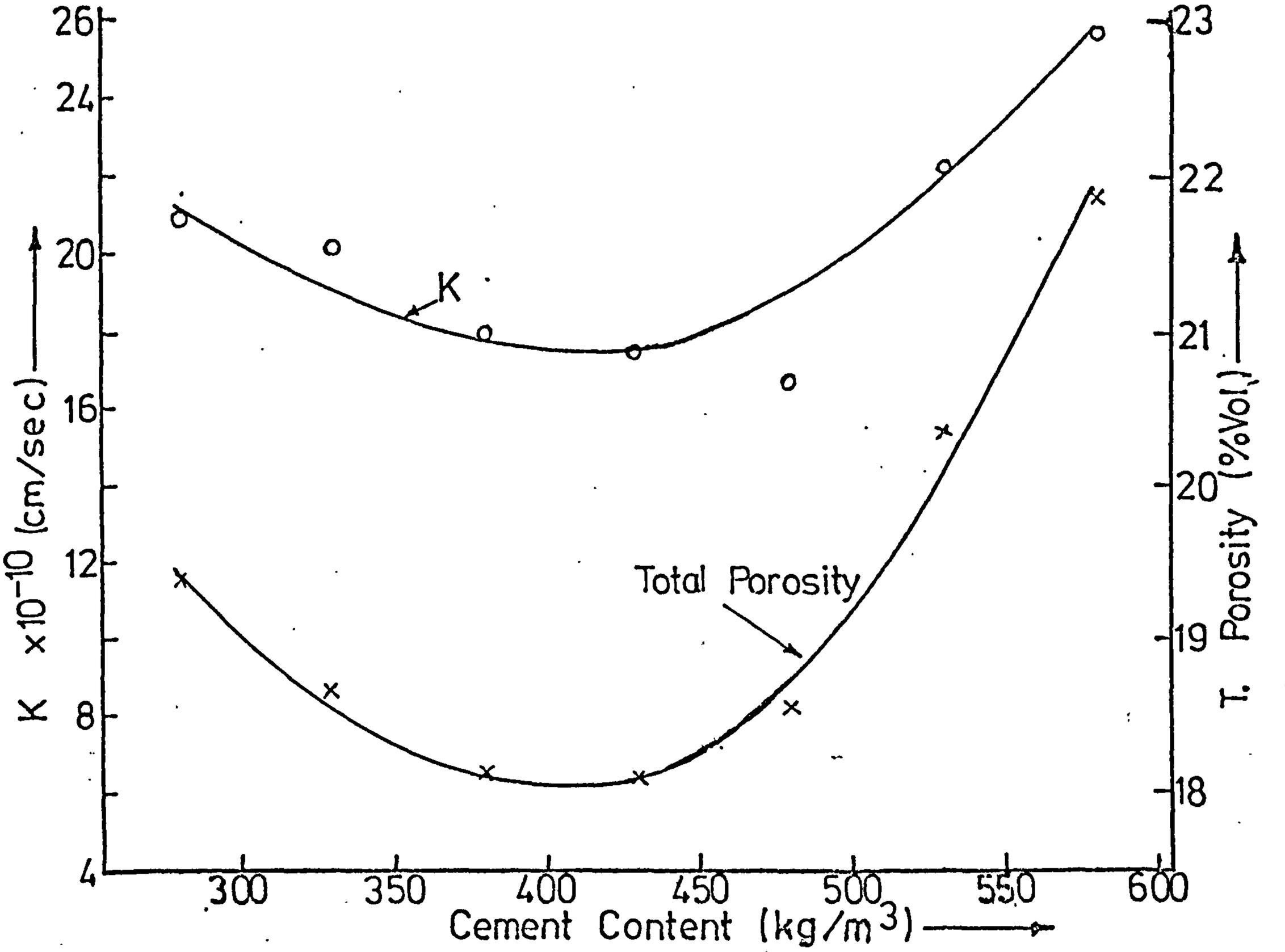

(A) Variations of K and Total Porosity with the Cement Content.

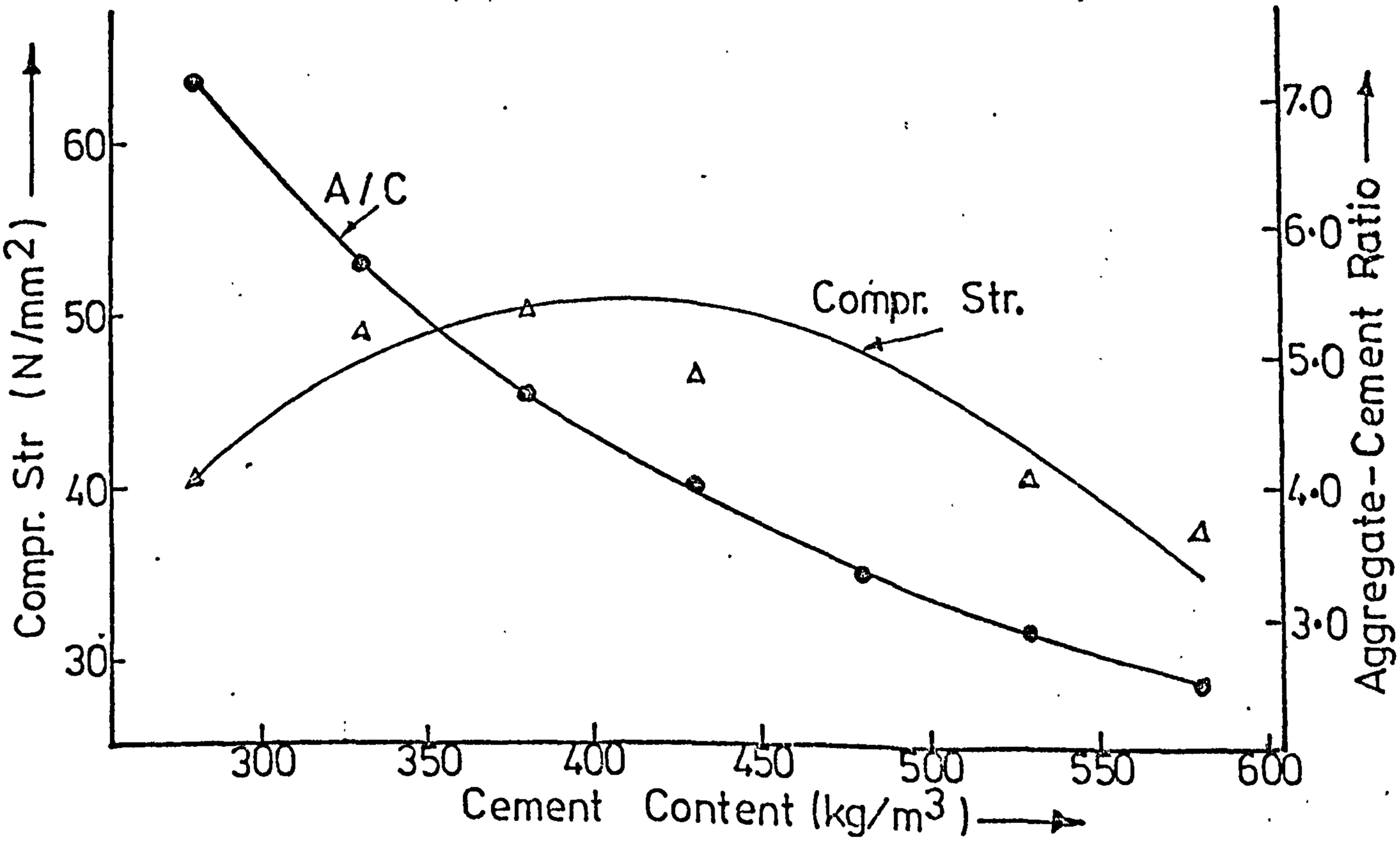

(B) Variations of Compressive Strength and Aggregate-Cement Ratio with Cement Content.

FIG(5.40) OPTIMUM CEMENT CONTENT

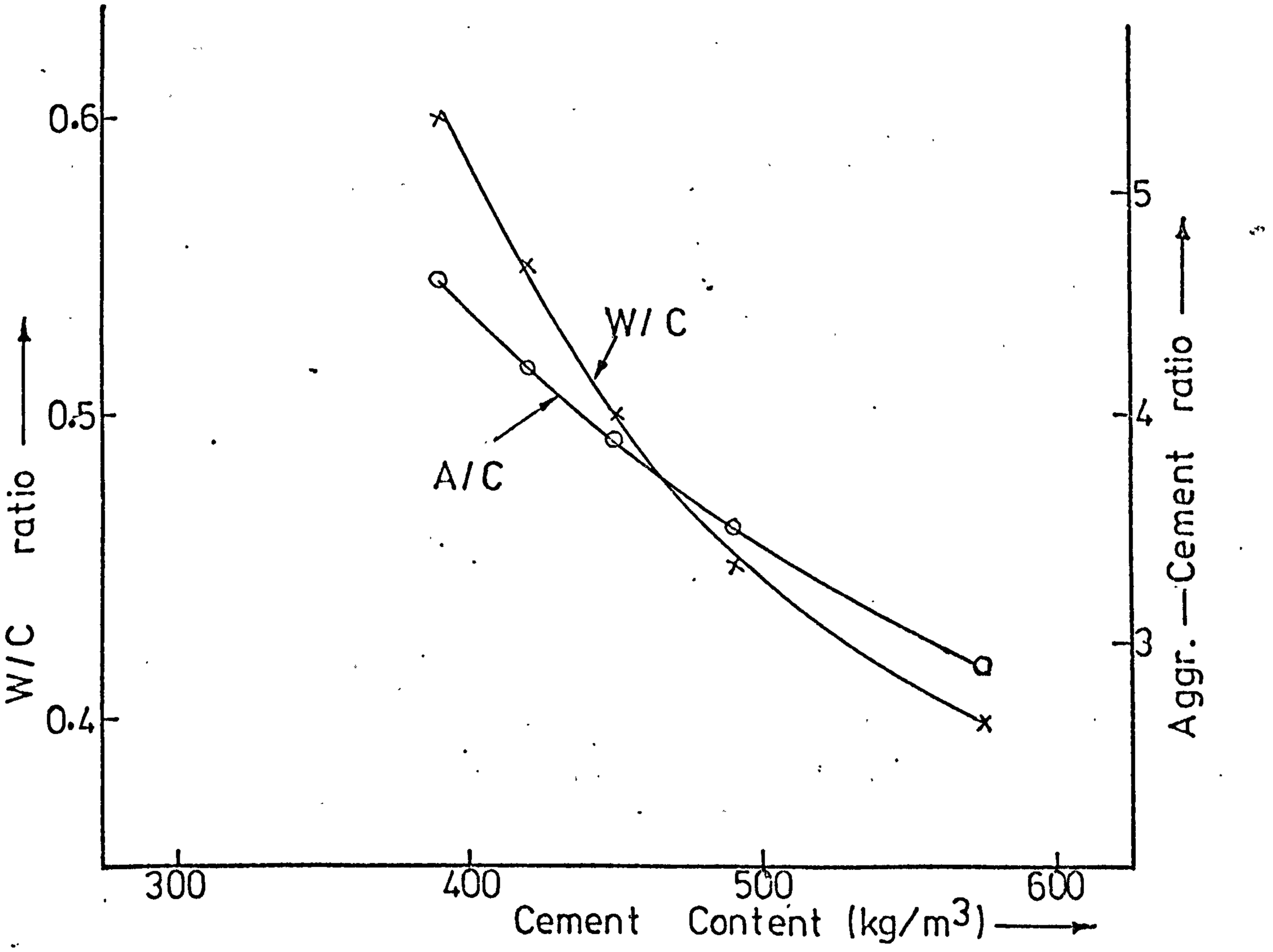

FIG (5.41) OPTIMUM CEMENT CONTENT & AGGR.— CEMENT RATIO AT VARIOUS W/C.

These tests were done to B.S. 1881: part 5, 1970 (ISAT method) with all the disadvantages mentioned earlier.

The present investigation compares the oil permeability of concrete wih with and without superplasticisers using OPC or SRPC, with different W/C ratios and admixture concentrations. Two types of superplasticisers were used - the Cormix SP1 and Melment L10. The mixes were designed as mentioned in section 3.5.1 and are given in table (5.16) The curing and testing procedures were not varied.

5.6.2 Concrete Mixes Containing Cormix SP1 Superplasticiser

The test results are given in table (5.17) and (5.18) for OPC and SRPC concretes respectively. All calculations were done as described in Section 5.3.

5.6.2.1 Variation of Concrete Quality with Admixture Concentration

Fig. (5.42) shows the variation of compressive strength with admixture concentration, while fig. (5.43) shows that between the coefficient of permeability, K, and the admixture concentration - it should be noted that W/C ratio decreases as admixture concentration increases - table (5.16). The relationship between K and compressive strength for oil saturated concrete is shown in fig. (5.44). In the figures, the results for plain concrete are indicated for comparison. The following observations are made from the plots:

1. Compressive strength improved considerably with an increase in admixture concentration, reaching a maximum at about 4% (-20% water content). The largest increased in compressive strength over the control specimen (plain concrete) was 43% in OPC and 28% in SRPC. Average increases were about 21% and 19% in OPC and SRPC concretes respectively.

2. The coefficient of permeability generally decreased continuously as the admxiture content increased. Average decreases were about 30% and 35% in OPC and SRPC concretes respectively. These decreases are higher than should be expected from -24% water reduction alone - figs. (5.21) and (5.22).

3. Plain concrete were generally more permeable than superplasticised

NO	EFFECTIVE W/C RATIO	CEMENT CONTENT (Kg/m^3)	AGGREGATE CONTENT (Kg/cm^3)		MIX DESIGN WATER CONT. (Kg/m^3)	WATER REDUCTION (%)	ADMIX. CONC. (% ccm. wt.)
			FINE	COARSE			
1	0.336	575	725	880	230	16	1
2	0.332					17	2
3	0.324					19	3
4	0.320					20	4
5	0.304					24	6
6.	0.420	460	797	925	230	16	1
7	0.415					17	2
8	0.405					19	3
9	0.400					20	4
10	0.380					24	6
11	0.505	383	889	916	230	16	1
12	0.499					17	2
13	0.487					19	3
14	0.480					20	4
15	0.456					24	6

Table (5.16) Mix Design Parameters for Concrete Containing Superplasticisers

MIX DESIGN.	SLUMP (mm)	AT 4 WEEKS			AT 24 WEEKS		
		DENSITY (SSD) (Kg/m^3)	T. POROSITY (% Vol.)	C. STR. (CTR) (N/mm^2)	C. STR. (OIL SAT). (N/mm^2)	OIL ABSORPTION (% Dry Wt.)	COEFT. OF PERM $Kx10^{-10}$ (cm/sec)
1	28	2440	16.26	87.3	83.8	2.57	6.92
2	58	2438	16.17	90.3	85.9	2.40	5.74
CP4-3	89	2433	16.04	89.1	86.5	2.26	5.70
4	127	2448	16.06	92.6	88.6	2.36	5.35
6	165	2421	16.12	88.1	84.5	2.52	5.50
1	33	2431	17.06	72.3	68.0	2.89	7.36
2	60	2442	16.71	73.4	69.3	2.68	7.29
CP5-3	99	2412	16.67	72.5	70.3	2.65	6.63
4	145	2435	16.64	70.9	69.4	2.83	6.04
6	172	2426	16.78	71.5	68.5	2.69	5.61
1	38	2403	17.50	64.3	60.8	3.30	9.51
2	33	2419	17.53	66.5	63.3	2.85	7.43
CP6-3	122	2421	17.22	67.4	64.5	2.91	8.30
4	137	2428	17.36	68.0	64.4	3.04	7.48
6	collapse	2412	17.28	62.8	58.5	2.88	7.08

Table (5.17) Test Results for OPC Concrete Containing Cormix SP1 superplasticiser

MIX DESIGN.	SLUMP (mm)	AT 4 WEEKS		AT 24 WEEKS			
		DENSITY (SSD) (Kg/m^3)	T. POROSITY (% Vol.)	C. STR. (CTR) (N/mm^2)	C. STR. (OIL SAT.) (N/mm^2)	OIL ABSORPTION (% Dry Wt.)	COEFT. OF PERM $Kx10^{-10}$ (cm/sec)
1	23	2438	17.37	85.0	81.3	2.78	8.00
2	40	2446	17.04	85.7	82.7	2.98	7.21
CS4-3	127	2445	16.95	87.5	83.9	2.74	7.60
4	180	2440	17.01	85.2	82.4	3.10	7.04
6	201	2443	17.21	84.6	82.0	2.99	6.95
1	30	2437	18.22	73.1	69.5	2.96	9.95
2	60	2439	17.73	76.2	71.8	3.15	9.25
CS5-3	102	2441	17.70	74.5	72.1	2.93	8.49
4	150	2418	17.73	70.6	68.1	3.29	7.79
6	collapse	2428	17.81	72.2	68.9	3.20	7.67
1	48	2411	18.39	54.7	49.6	3.62	10.39
2	127	2419	18.46	56.6	51.8	3.29	10.35
CS6-3	152	2409	18.31	60.4	53.3	3.47	10.05
4	165	2419	18.17	64.9	54.9	3.36	8.17
6	collapse	2429	18.23	58.5	56.5	3.31	7.86

Table (5.18) Test Results for SRPC concretes containing Cormix SP1 Superplasticiser

concrete for equal compressive strengths - fig. (5.44). However, for strengths above about 72 N/mm^2, plain OPC concrete appeared less permeable than corresponding superplasticised concrete.

5.6.2.2 Variation of K with Total Pore Volume

Fig. (5.45) shows the variation of K with the calculated total pore volumes. These were calculated as described in chapter 4. For comparative purposes, plain concrete results from fig. (5.34) and (5.35) are shown. The following observations are made:

1. Unlike plain concrete, there is no clearly defined relationship and the results show a large scatter, probably due to variable air contents. At high admixture concentrations compaction by table vibration was difficult and demoulding after about 24 hours was impossible since the concrete had not hardened sufficiently. This made the assessment of the air content less reliable compared with those for plain concrete.

2. At lower porosity (below about 17.4% and 17.9% in OPC and SRPC concrete respectively), the superplasticised concrete was more permeable than plain concrete at equal porosity values; but the reverse was the case at higher porosity values. This agrees with the compressive strength - coefficient of permeability relationship in fig. (5.44).

5.6.2.3 Variation of K with Time

The variation of the coefficient of permeability, K, with time during the test is illustrated in fig. (5.46). As in plain concrete, K decreases continuously with time; but unlike - plain concrete, K continued to decrease after 120 hours. This may be due to the more uniform and reduced pore sizes in the superplasticised concrete - Chapter 4, because these smaller pores are more easily clogged by the crude oil.

5.6.3 Concrete mixes Containing Melment L10 Superplasticiser

The test results are given in tables (5.19) and (5.20) for OPC and SRPC concretes respectively.

5.6.3.1 Variation of Concrete Quality with Admixture Concentration

W/C = 0.6 (CTR) — □

" 0.5 " Δ

" 0.4 " O

Darkened symbols are for oil saturated specimens

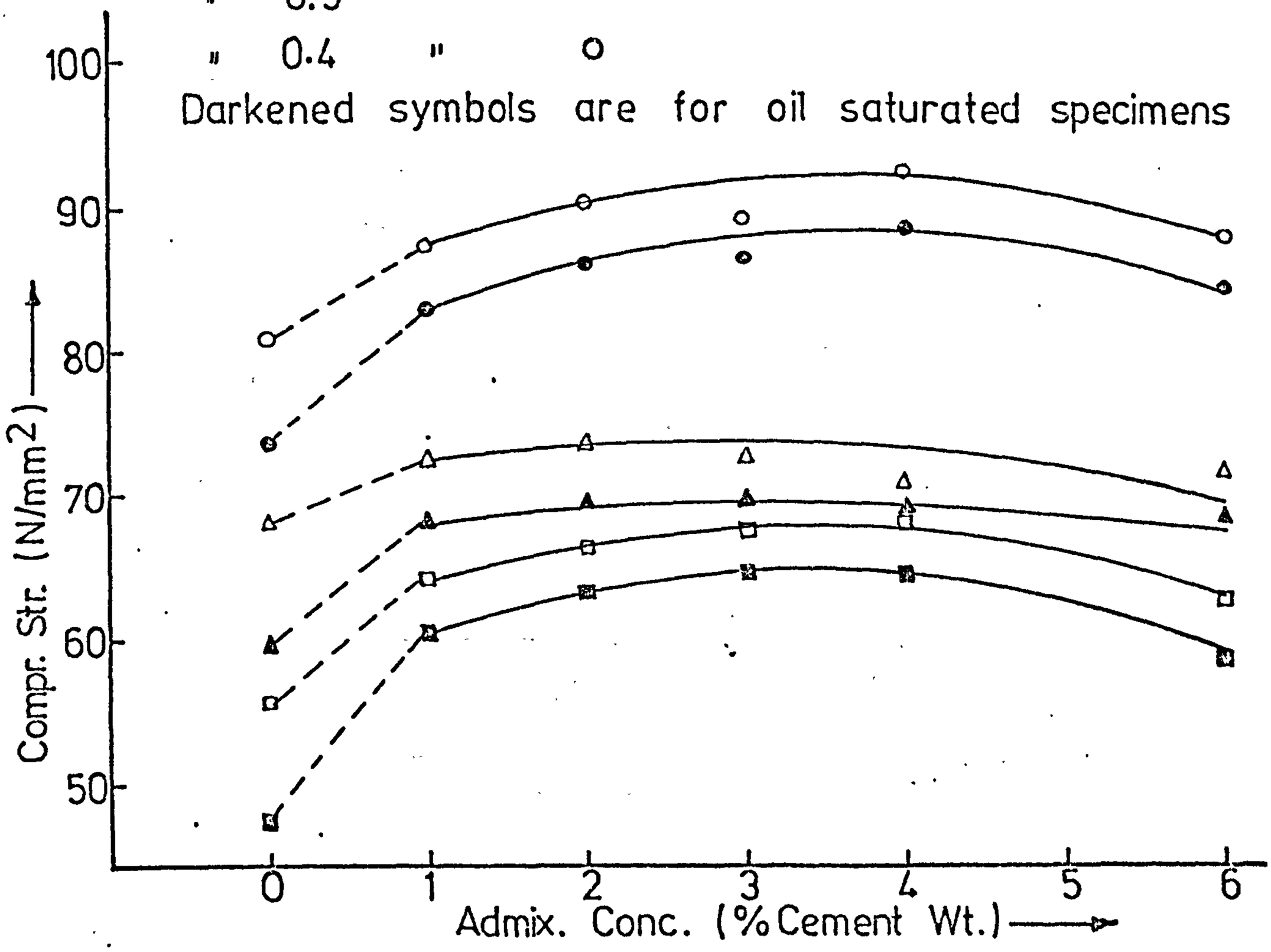

(A) OPC CONCRETE

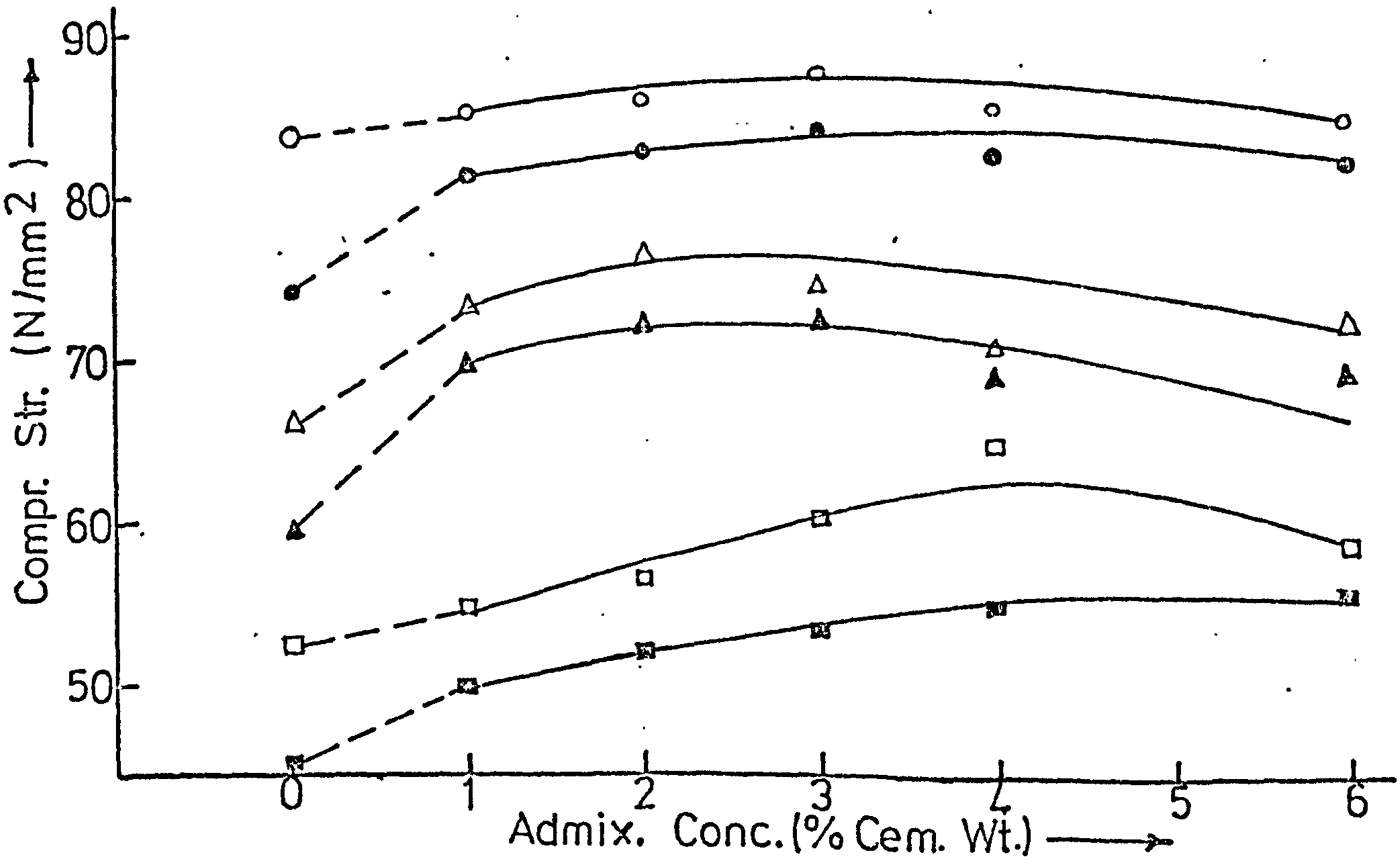

(A) SRPC CONCRETE

FIG (5.42) VARIATION OF COMPR. STRENGTH WITH ADMIX. CONCENTRATION — CORMIX SP 1.

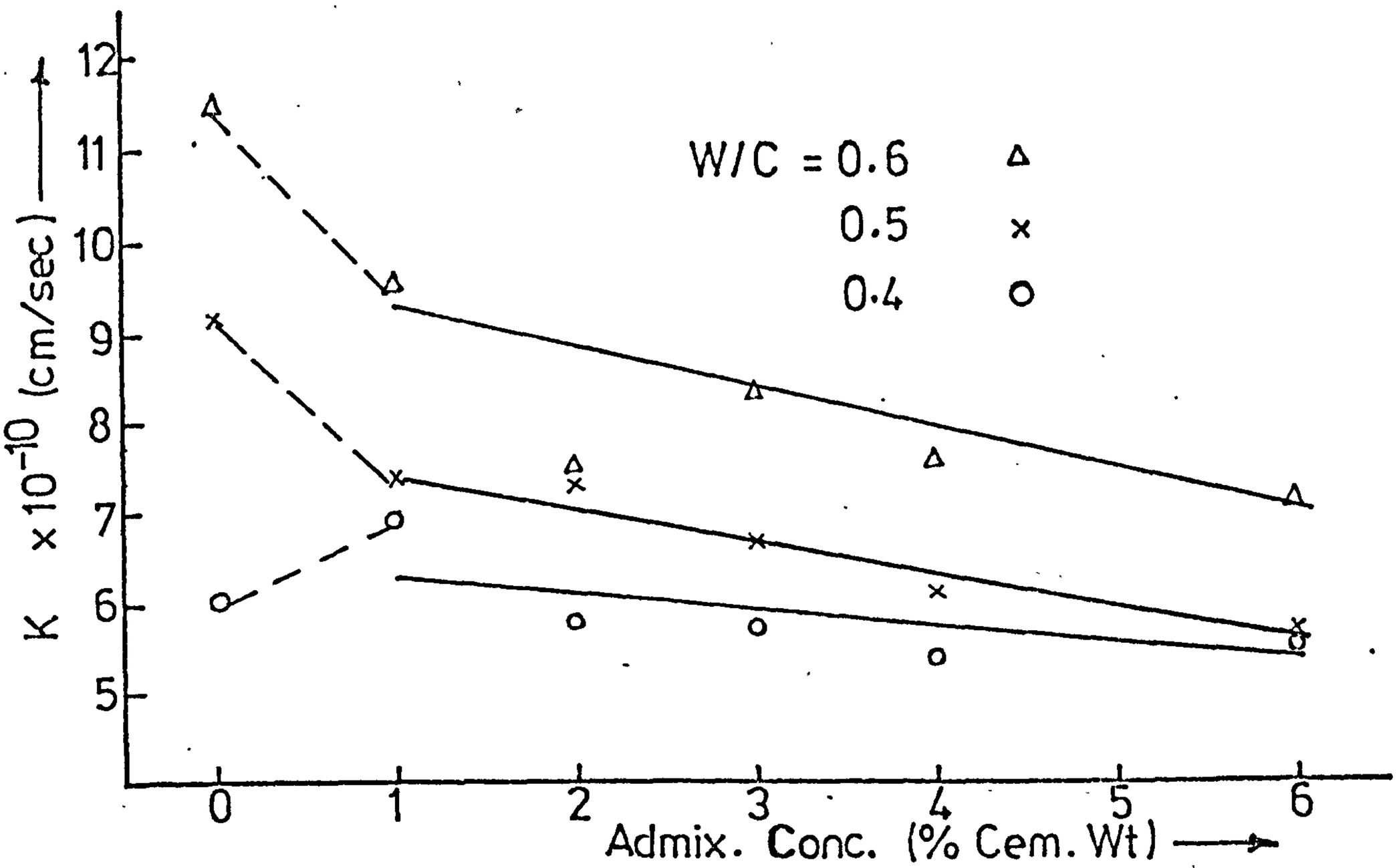

(A) OPC CONCRETE

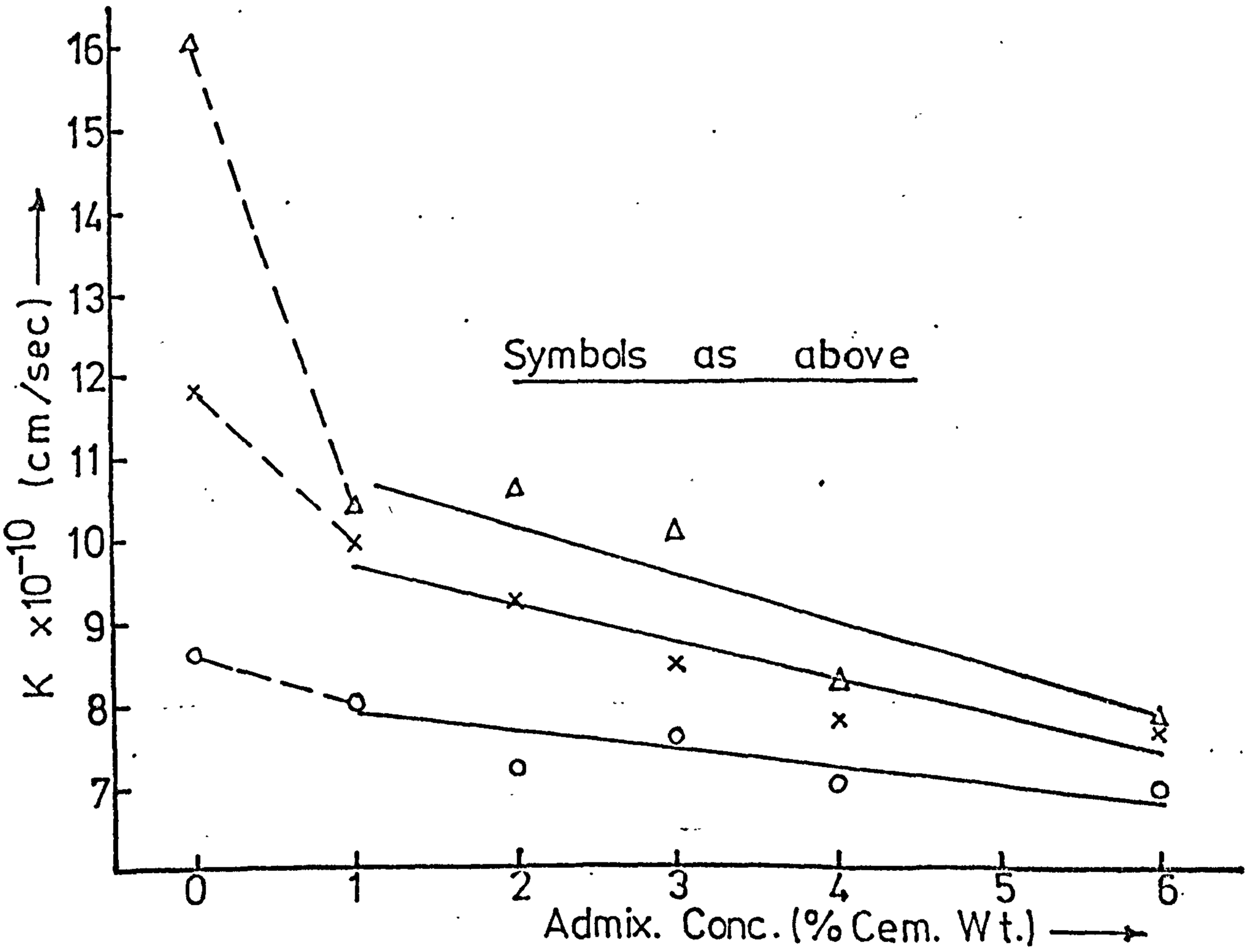

(B) SRPC CONCRETE

FIG(5.43) VARIATION OF K WITH ADMIXTURE CONCENTRATION — CORMIX SP1

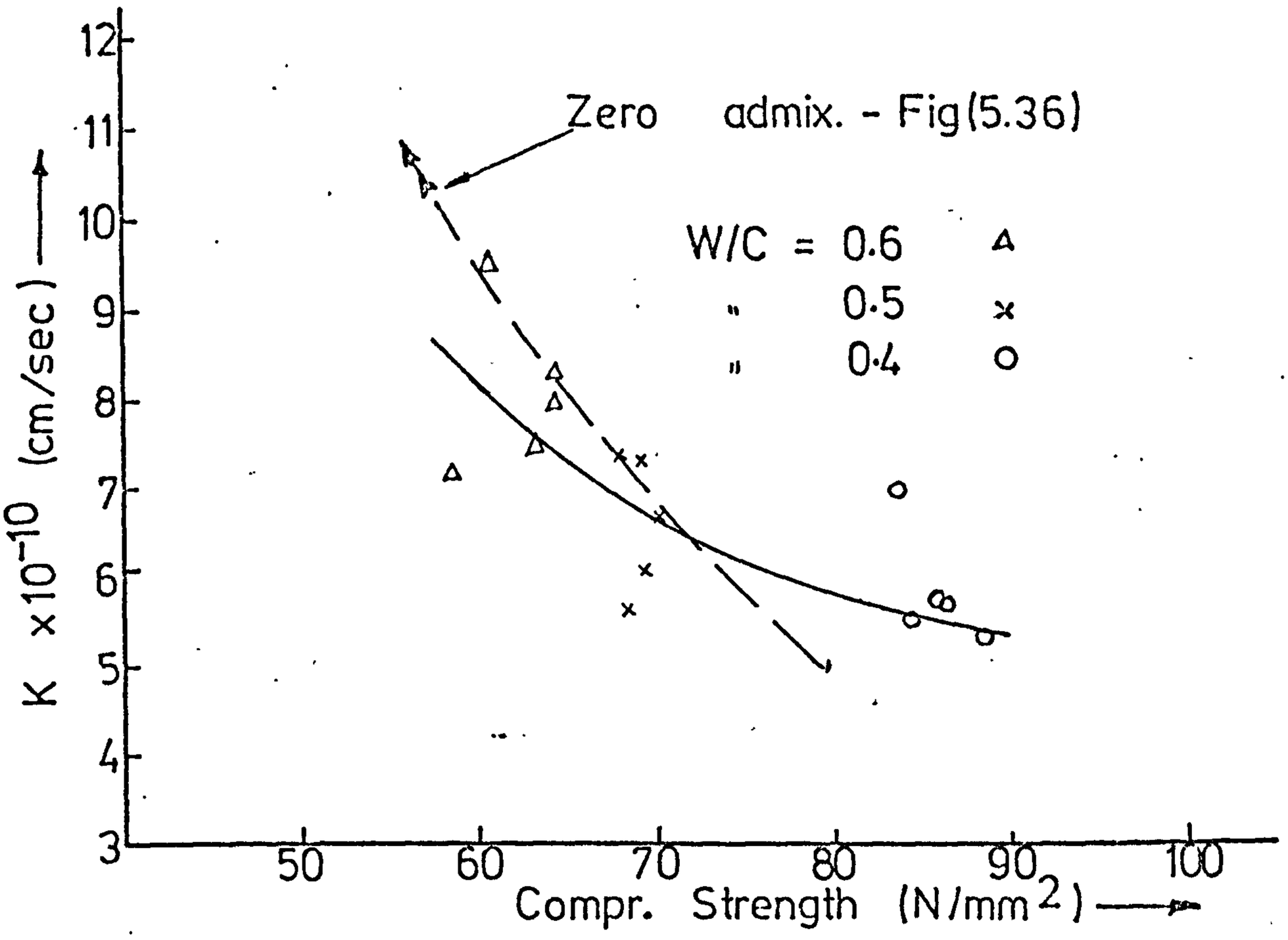

(A) OPC Concrete

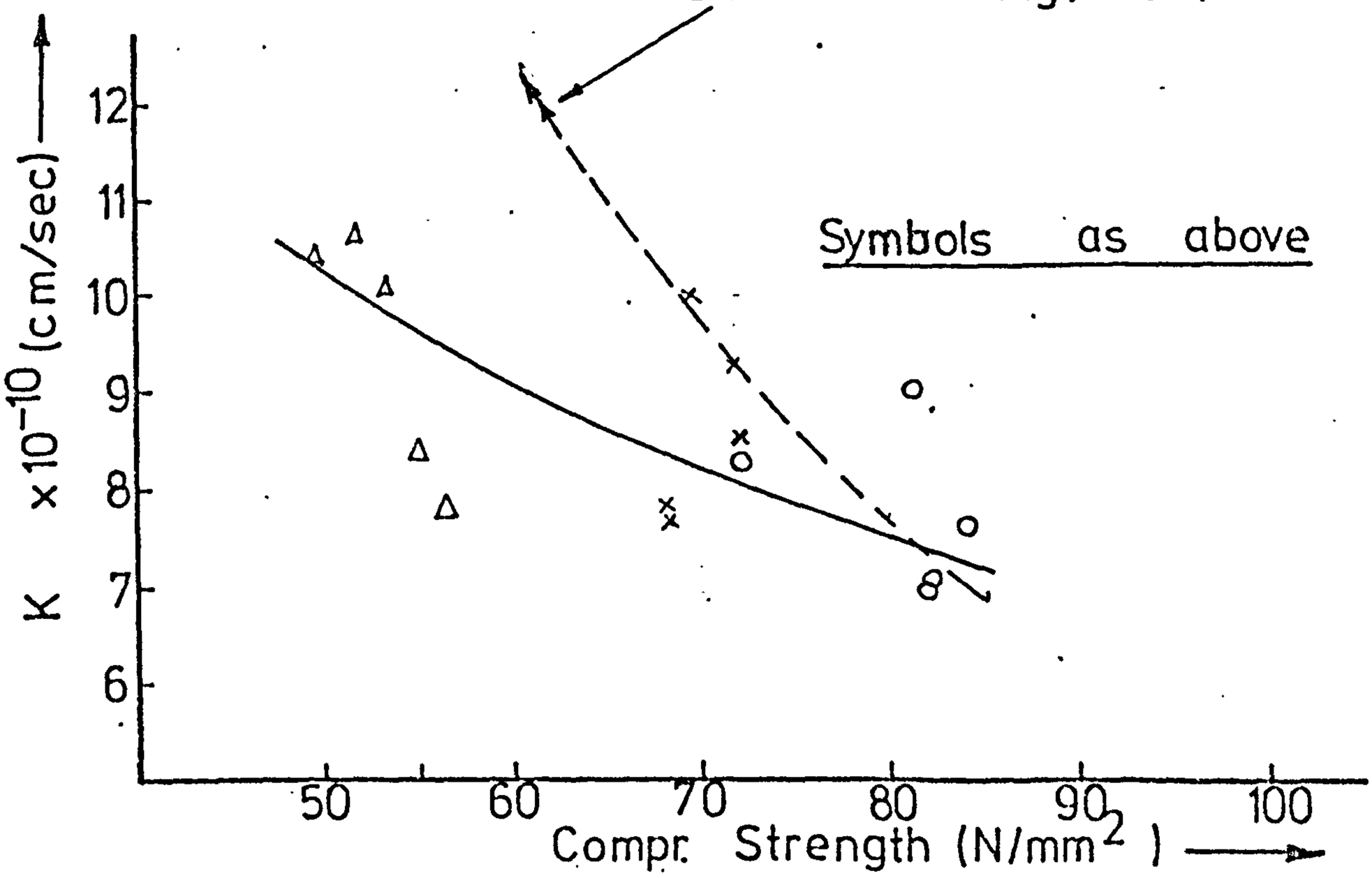

(B) SRPC Concrete

FIG(5.44) VARIATION OF K WITH THE COMPR. STRENGTH OF CONCRETE CONTAINING CORMIX SP1

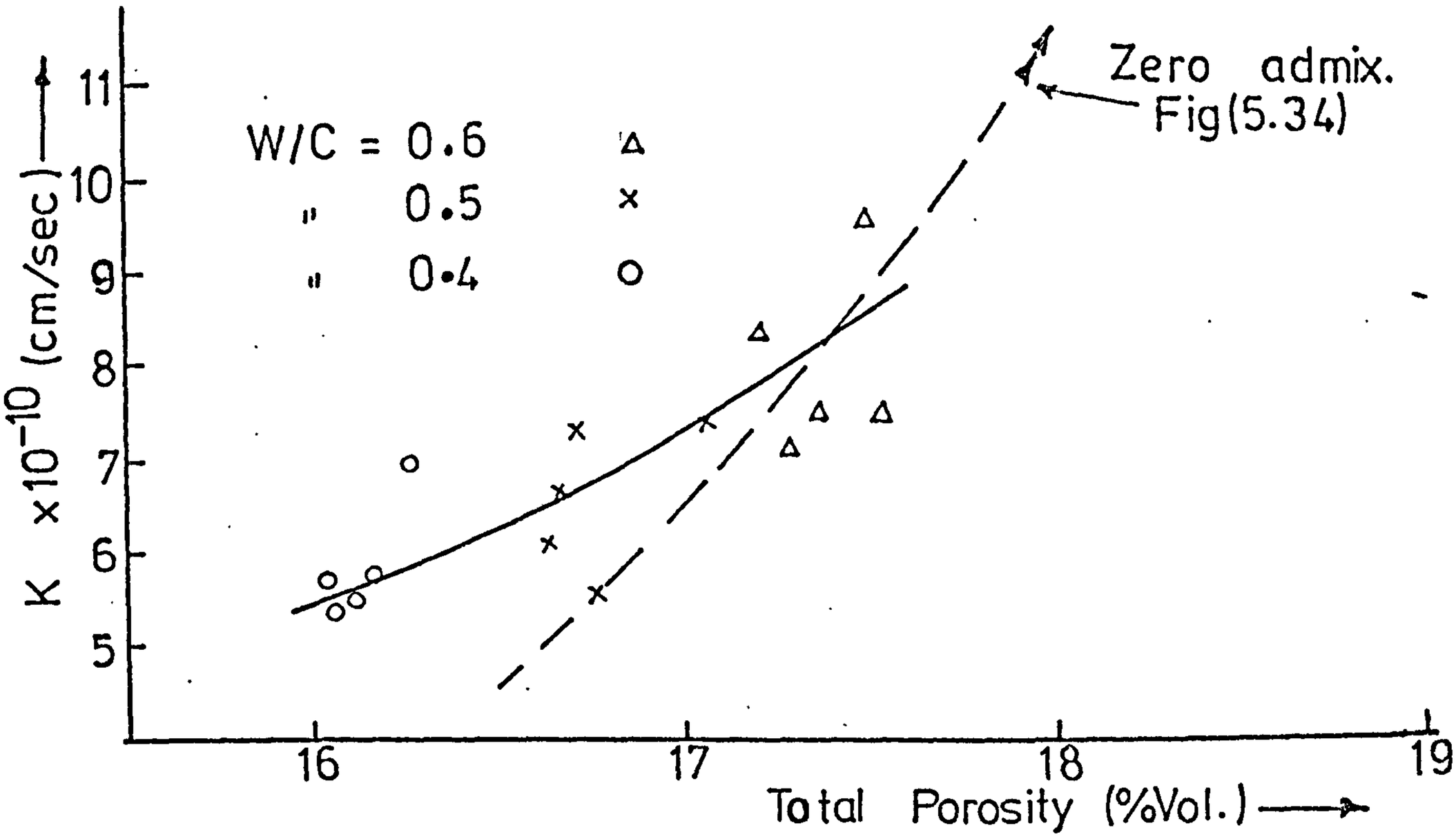

(A) OPC Concrete

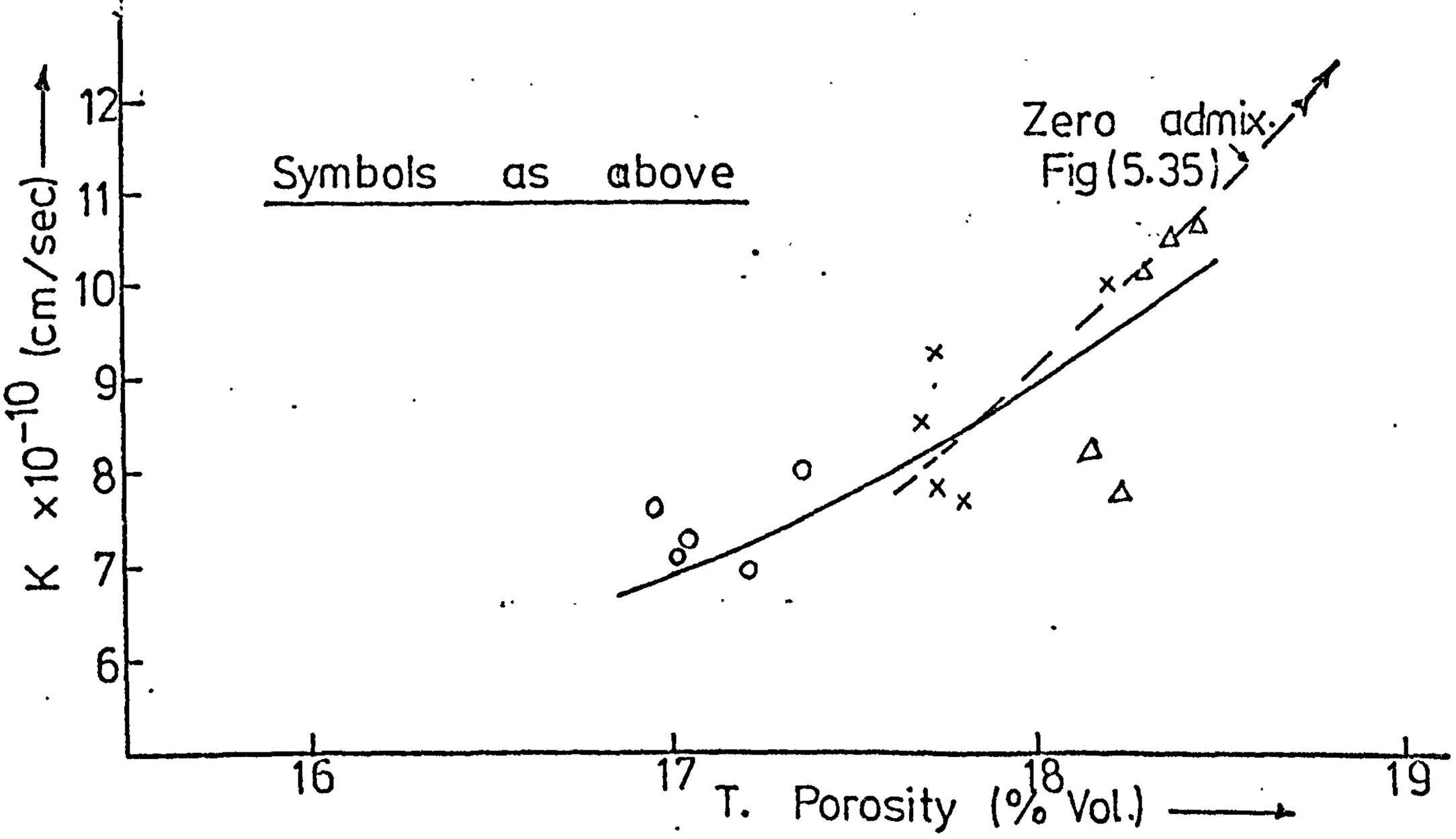

(B) SRPC Concrete

FIG(5.45) VARIATION OF K WITH T. POROSITY OF CONCRETE CONTAINING CORMIX SP1.

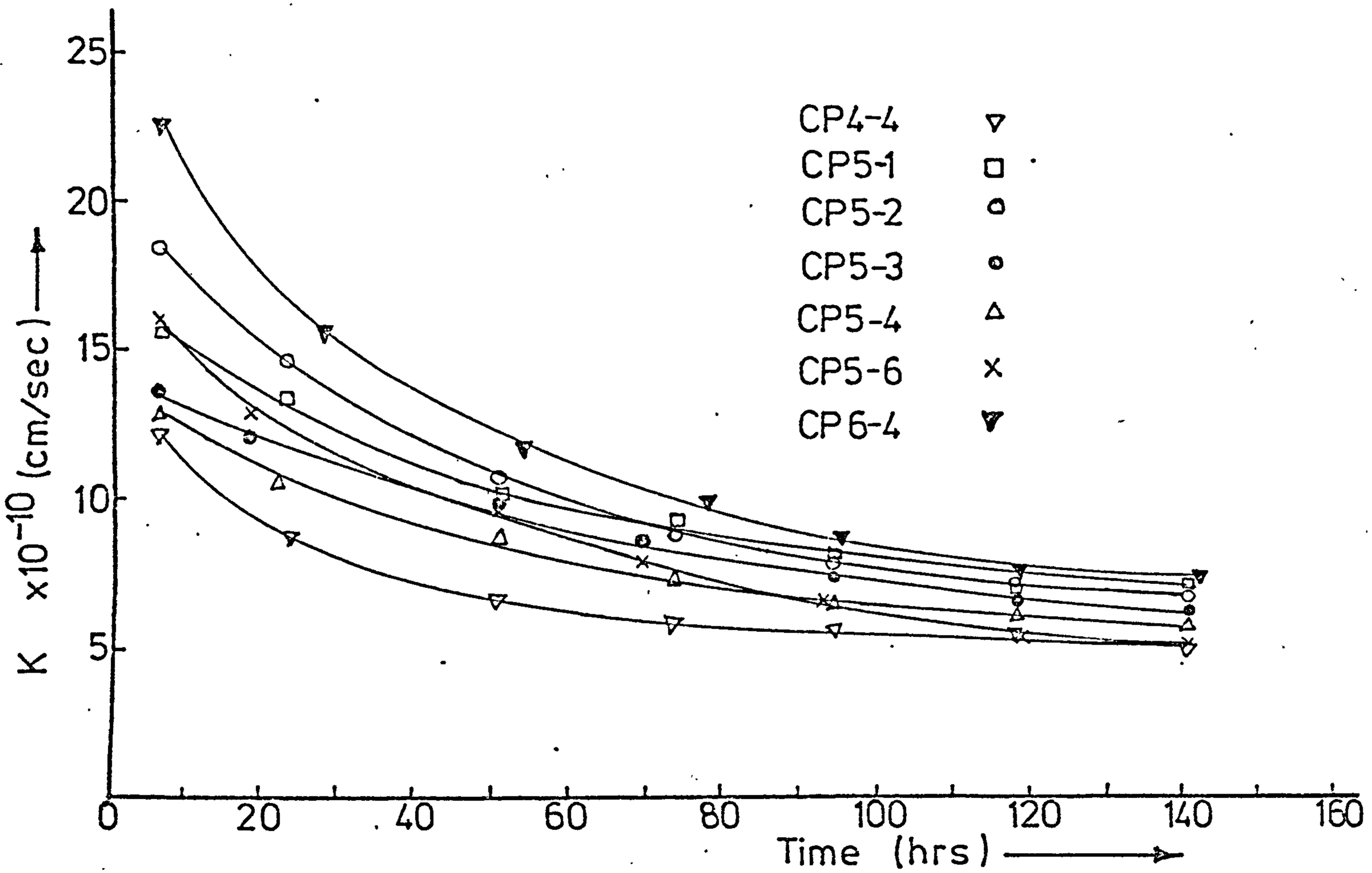

FIG(5·46) K vs DURATION OF TEST FOR CONCRETE CONTAINING CORMIX SP1 SUPERPLASTICISER

MIX DESIGN.	SLUMP (mm)	AT 4 WEEKS		AT 24 WEEKS			
		DENSITY SSD (Kg/m^3)	T. POROSITY (% Vol.)	C. STR.(CTR) (N/mm^2)	C. STR.(OIL SAT.) (N/mm^2)	OIL ABSORPTION (% Dry Wt.)	COEFT. OF PERM $Kx10^{-10}$ (cm/sec)
1	13	2443	16.32	84.2	81.5	2.58	5.84
2	64	2440	16.23	87.8	83.2	2.37	4.91
LP4-3	74	2448	16.09	88.0	83.6	2.52	5.37
4	147	2458	16.01	85.0	83.3	2.29	4.63
6	170	2450	16.02	85.6	84.0	2.68	4.64
1	23	2421	16.95	75.6	72.5	3.08	7.17
2	31	2424	16.77	78.0	74.3	3.12	6.04
LP5-3	104	2428	16.98	80.0	75.3	3.08	6.83
4	160	2437	16.43	78.5	76.0	2.90	5.43
6	collapse	2439	16.52	78.9	76.8	2.95	5.15
1	20	2400	17.59	62.7	57.1	3.25	9.11
2	40	2405	17.72	65.0	60.3	3.12	8.60
LP6-3	119	2417	17.10	64.4	60.8	3.24	7.48
4	170	2422	17.22	63.5	60.3	3.10	6.99
6	collapse	2429	17.00	64.2	59.5	3.06	7.13

Table (5.19) Test results for OPC Concrete containing Melment L10 Superplasticer

MIX DESIGN.	SLUMP (mm)	AT 4 WEEKS		AT 24 WEEKS			
		DENSITY(SSD) (Kg/m^3)	T. POROSITY (% Vol.)	C. STR.(CTR) (N/mm^2)	C. STR.(OIL SAT.) N/mm^2)	OIL ABSORPTION (% Dry Wt.)	COEFT. OF PERM $Kx10^{-10}$ (cm/sec)
1	9	2433	17.38	88.1	84.2	2.94	6.67
2	25	2426	17.13	90.0	86.0	2.99	7.40
LS4-3	99	2438	17.01	91.5	87.6	2.83	7.67
4	152	2432	16.85	91.0	87.2	2.66	6.69
6	163	2423	17.10	90.1	86.1	3.02	6.59
1	33	2432	18.17	75.7	71.5	3.07	9.21
2	99	2422	17.80	77.4	72.5	3.11	8.22
LS5-3	160	2438	17.66	78.0	74.1	3.25	8.45
4	191	2436	17.39	78.2	74.2	3.08	7.82
6	collapse	2430	17.75	78.1	75.8	3.33	6.97
1	28	2408	18.37	66.8	62.1	3.60	10.66
2	23	2411	18.29	68.7	65.4	3.68	9.35
LS6-3	104	2430	18.30	69.0	65.0	3.62	9.85
4	178	2425	18.08	64.6	58.4	3.31	8.69
6	collapse	2422	18.15	64.8	62.0	3.54	8.03

Table (5.20) Test results for SRPC concrete containing Melment L10 Superplasticiser

The concrete qualities experimentally determined are compressive strength and coefficient of permeability, K. Variations of compressive strength and K with admixture concentration are shown in figs. (5.47) and (5.48) respectively. W/C ratio also varied as shown in table (5.16) with admixture concentration. The following observations are made:

1. Compressive strength increased with an increase in admixture concentration, generally reaching a maximum value at about 3% concentration. Maximum increases over values for plain concrete were about 29% and 44% in OPC and SRPC concretes respectively. The SRPC concretes reached strengths considerably higher than those obtained for concretes containing Cormix SP1 but strengths of OPC concretes were of the same order as for Cormix SP1.

2. As in concrete specimens containing Cormix SP1, K decreased continuously with an increase in the admixture concentration. Compared with K for plain concrete, OPC concrete reduced by 38.6, 43.2 and 22.6% for W/C = 0.6, 0.5 and 0.4 respectively. For SRPC concrete, the reductions were 49.8 40.9 and 29.2% respectively. Slightly higher reductions in K values were thus obtained with Melment L10 than with Cormix SP1 superplasticisers.

3. The relationship between K and compressive strength is illustrated in fig (5.49) which is similar to fig. (5.44) but there is less scatter in the results. Comparing the two figures shows that at equal compressive strengths, concrete containing Cormix SP1 superplasticiser have a higher K value than those containing Melment L10 in OPC concrete; for SRPC concretes the reverse is true.

5.6.3.2 Variation of K with total Pore Volume

The total pore volume for concrete with Melment L10 was calculated as for those with Cormix SP1. Paste densities (not shown) were generally slightly less than for Cormix SP1, porosity was slightly more at concentrations of 1 - 2% but slightly less at concentrations of 4 - 6%. The total porosity is related to the coefficient of permeability in fig.(5.50). It is observed that:

1. The shape of the curves is similar to fig. (5.45) but with less scatter in the results. Generally, the Melment L10 produces concrete of lower permeability than Cormix SP1, and K values for the former were between 3 and 19% lower than for thelatter in OPC and SRPC concretes.

2. Equal porosity specimens containing Melment L10 had K values slightly lower than that for corresponding specimens containing Cormix SP1. Based on K values for samples containing Cormix SP1, K values were between 11.2 and 3% lower for OPC concrete and 2% lower in SRPC concretes.

5.7 Oil Absorption Characteristics of HCPs and Concrete

5.7.1 Introduction

The pore volume of HCPs and concrete is sometimes measured by the amount of liquid absorbed at full saturation. Absorption is used to assess the durability of concrete (Section 2.2.1). Absorption is usually measured by drying a specimen to a constant weight (often at 105°C), immersing it in water, and measuring the increase in weight as a percentage of the dry weight. Most good concretes have absorption well below 10%(70).

In the present investigation, all HCPs and concrete specimens were weighed at different ages to determine the water lost on drying, and of oil gained by absorption. The results, expressed as percentages of their dry weights, are presented in tables (5.9), (5.10), (5.15), (5.17) to (5.20), and discussed in the following sections. These absorption results will be related to various other HCP and concrete properties. After 4 months soaking in crude oil, all the HCP samples were regarded as 'fully saturated' because further pressurization or storage in crude oil did not produce any significant increase in weight.

5.7.2 Absorption Characteristics of Hardened Cement Pastes (HCPs)

5.7.2.1 HCPs without Admixture

The absorption characteristics are illustrated in figs. (5.51) to (5.56) and discussed below:

1. The oil absorption increased with W/C ratio - fig. (5.51), with an approximately linear relationship for both OPC and SRPC pastes. The water lost in drying SSD specimen at 105°C and the subsequent oil absorption are higher for SRPC pastes than for OPC in the range of practical W/C ratios. The SRPC absorption values are between 16% to 23% higher.

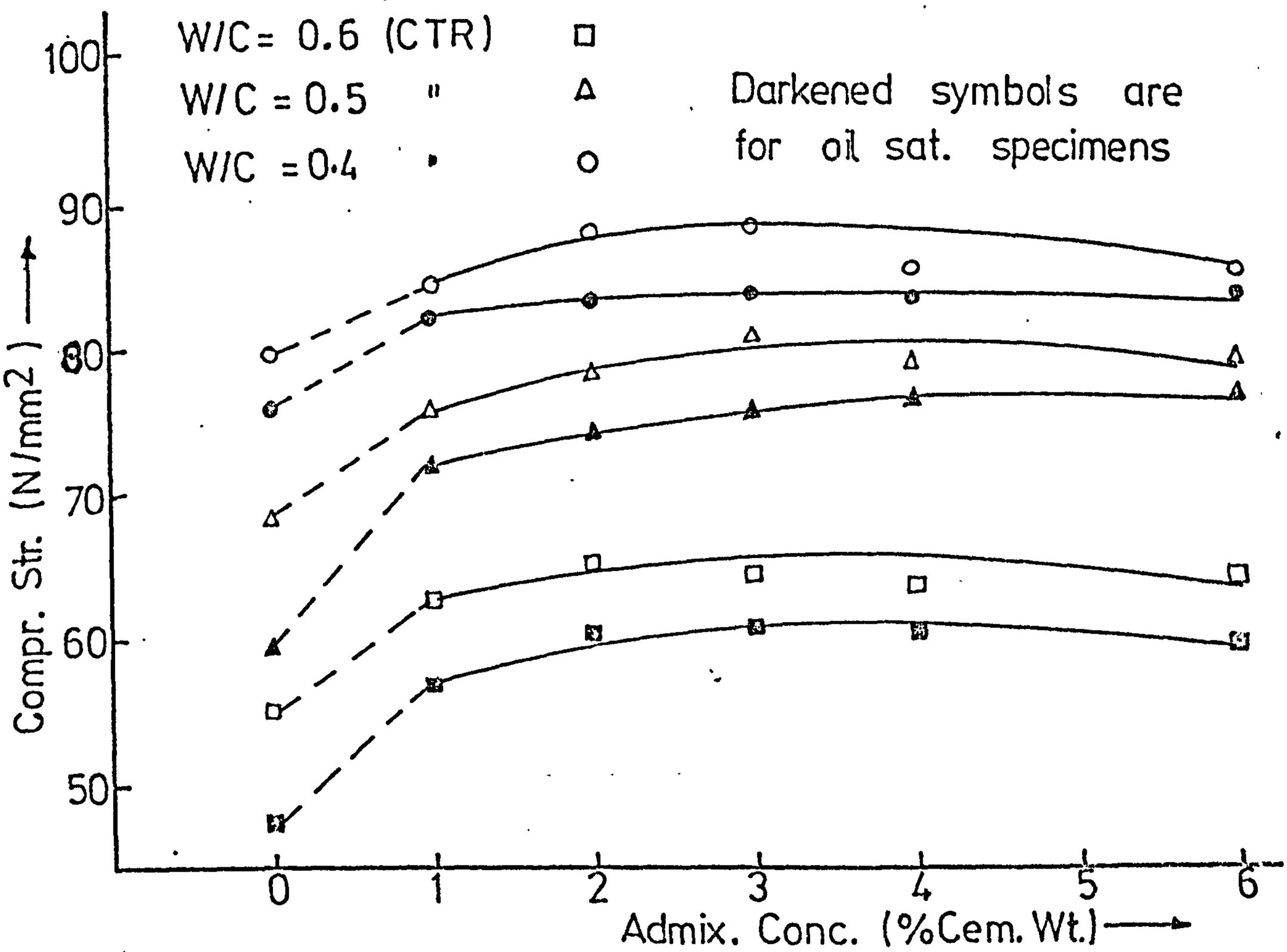

(A) OPC Concrete

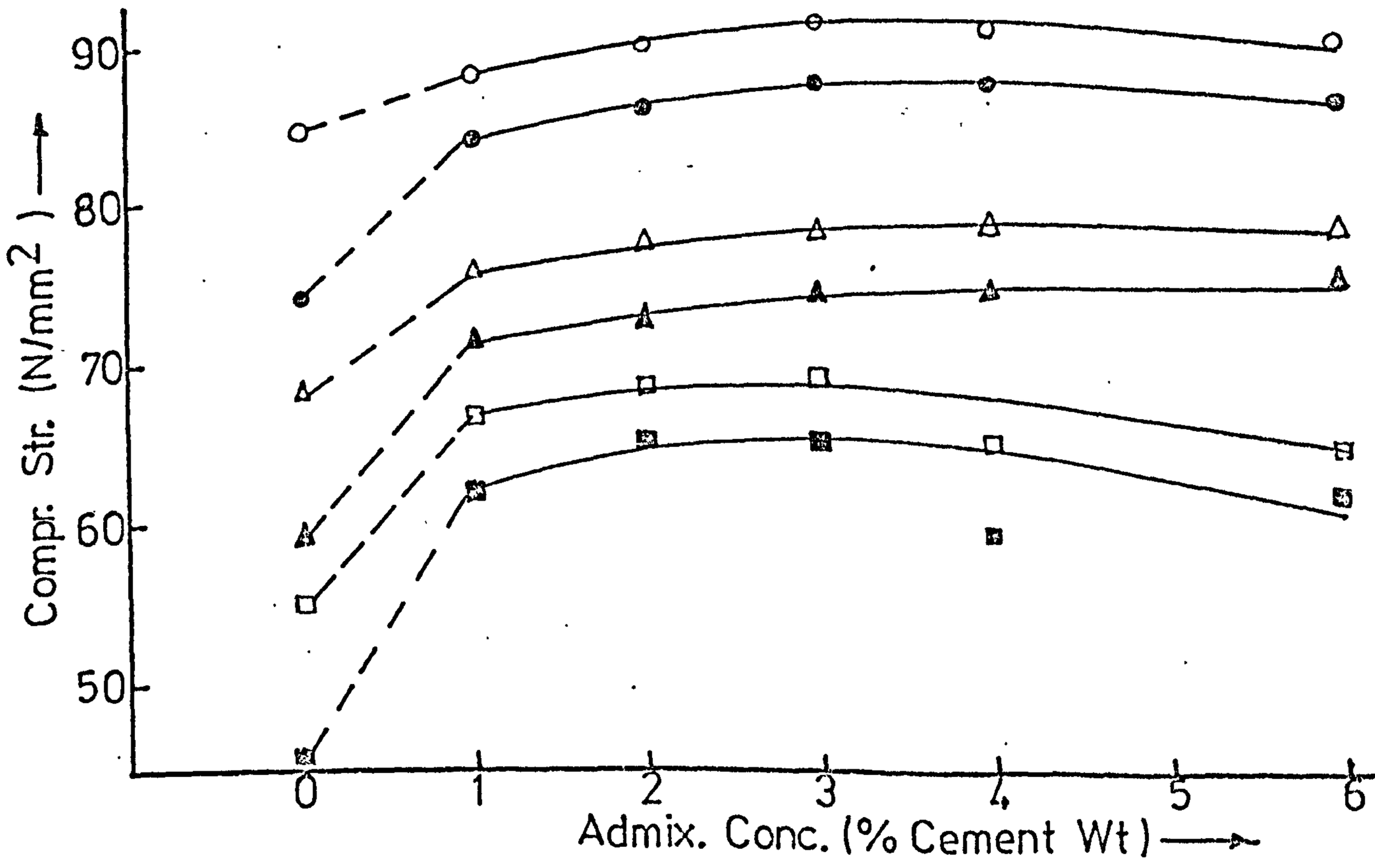

(B) SRPC Concrete

FIG(5.47) VARIATION OF COMPR STRENGTH WITH ADMIX. CONCENTRATION — MELMENT. L10

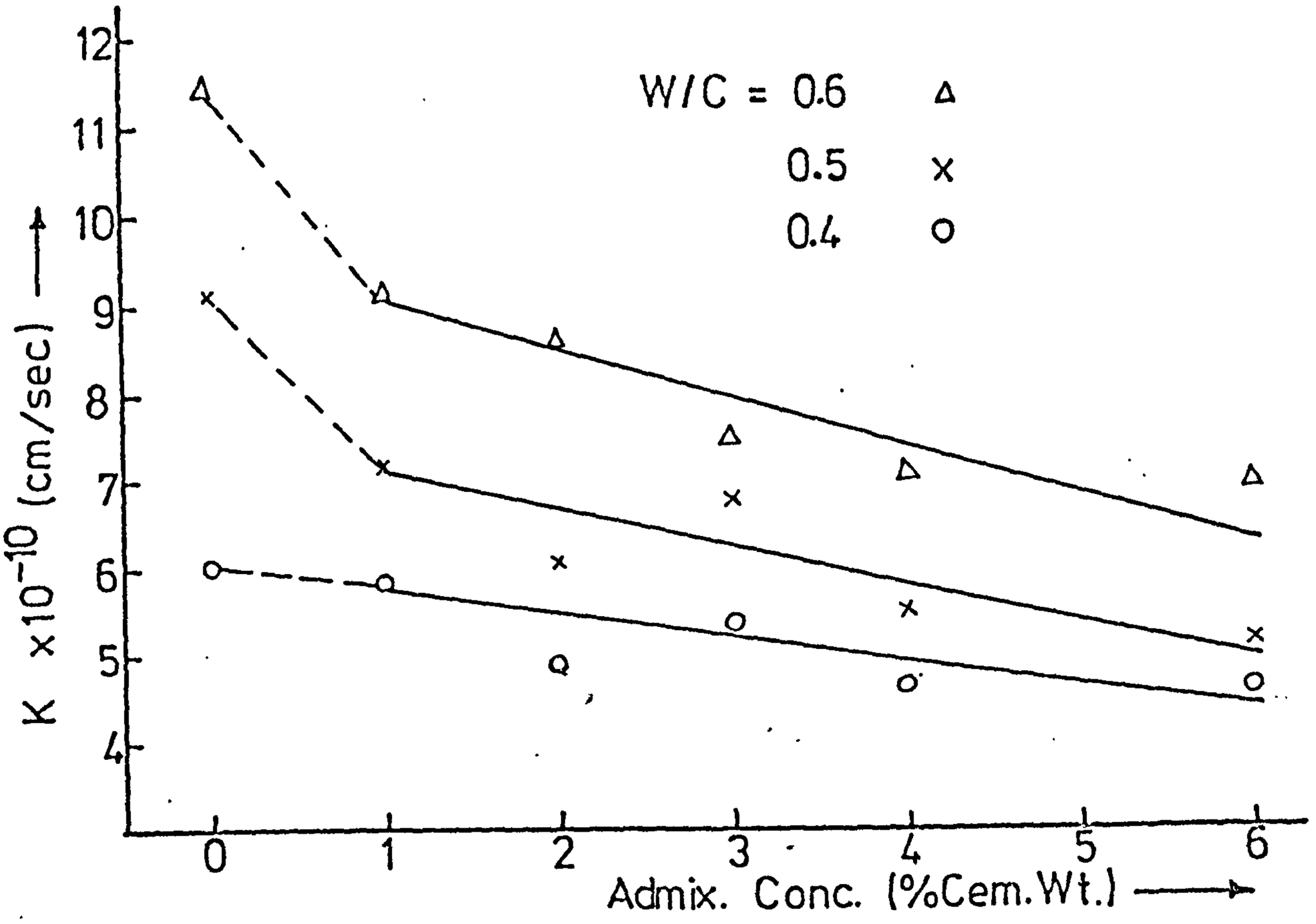

(A) OPC Concrete

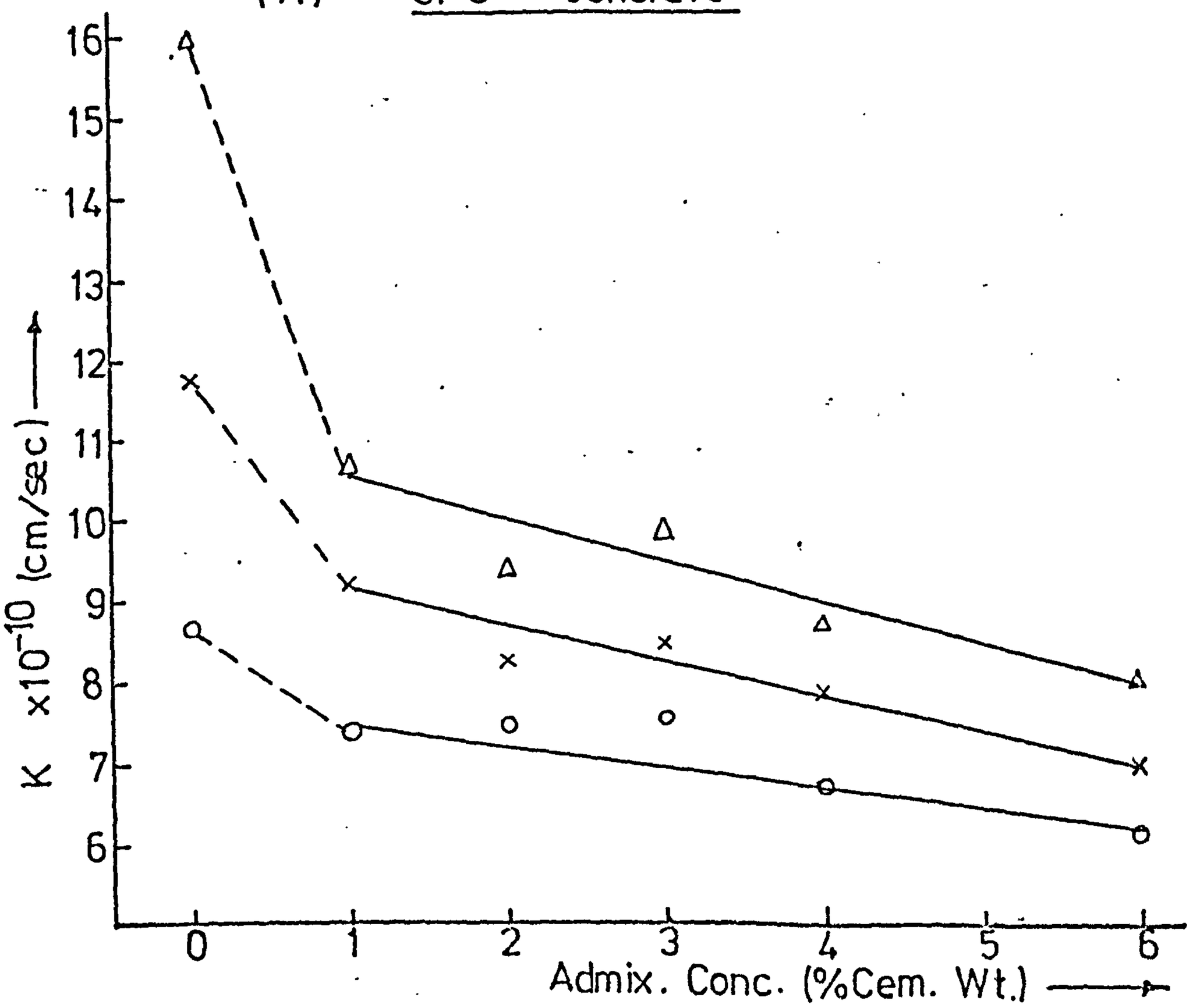

(B) SRPC Concrete

FIG(5.48) VARIATION OF K WITH ADMIXTURE CONC. FOR CONCRETE CONTAINING MELMENT L10.

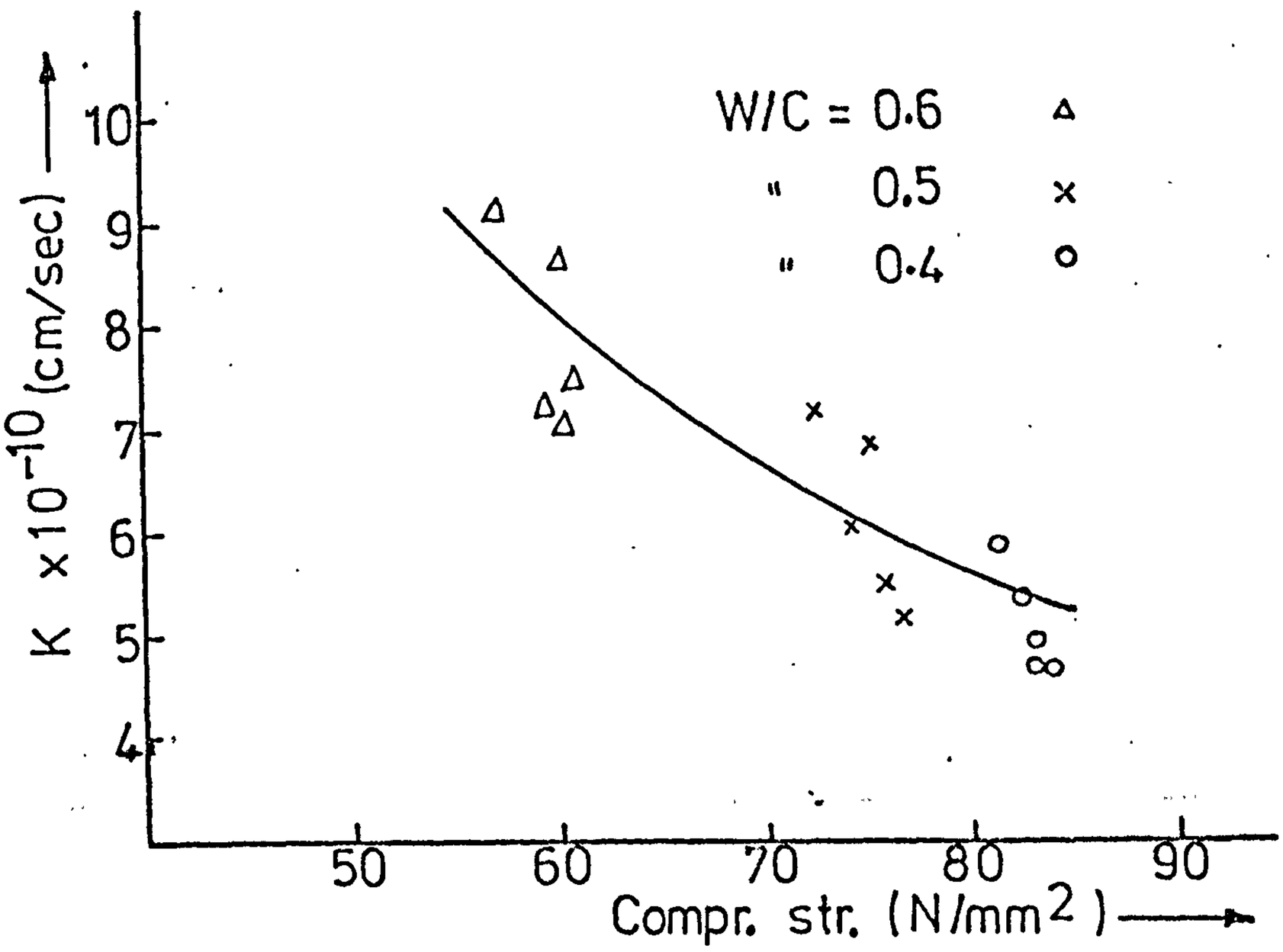

(A) OPC Concrete

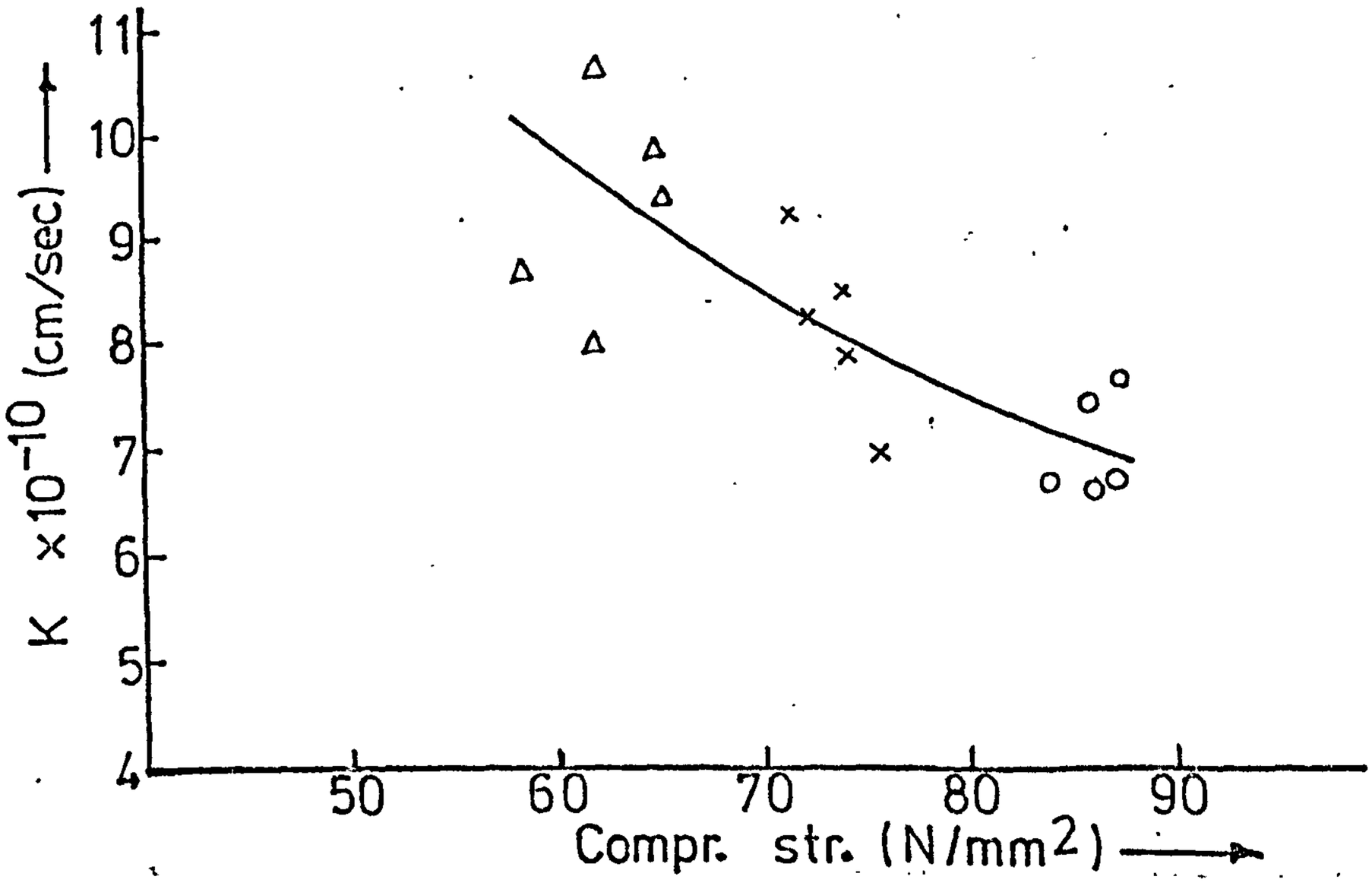

(B) SRPC Concrete

FIG(5.49) VARIATION OF K WITH THE COMPR. STRENGTH OF CONCRETE CONTAINING MELMENT L10.

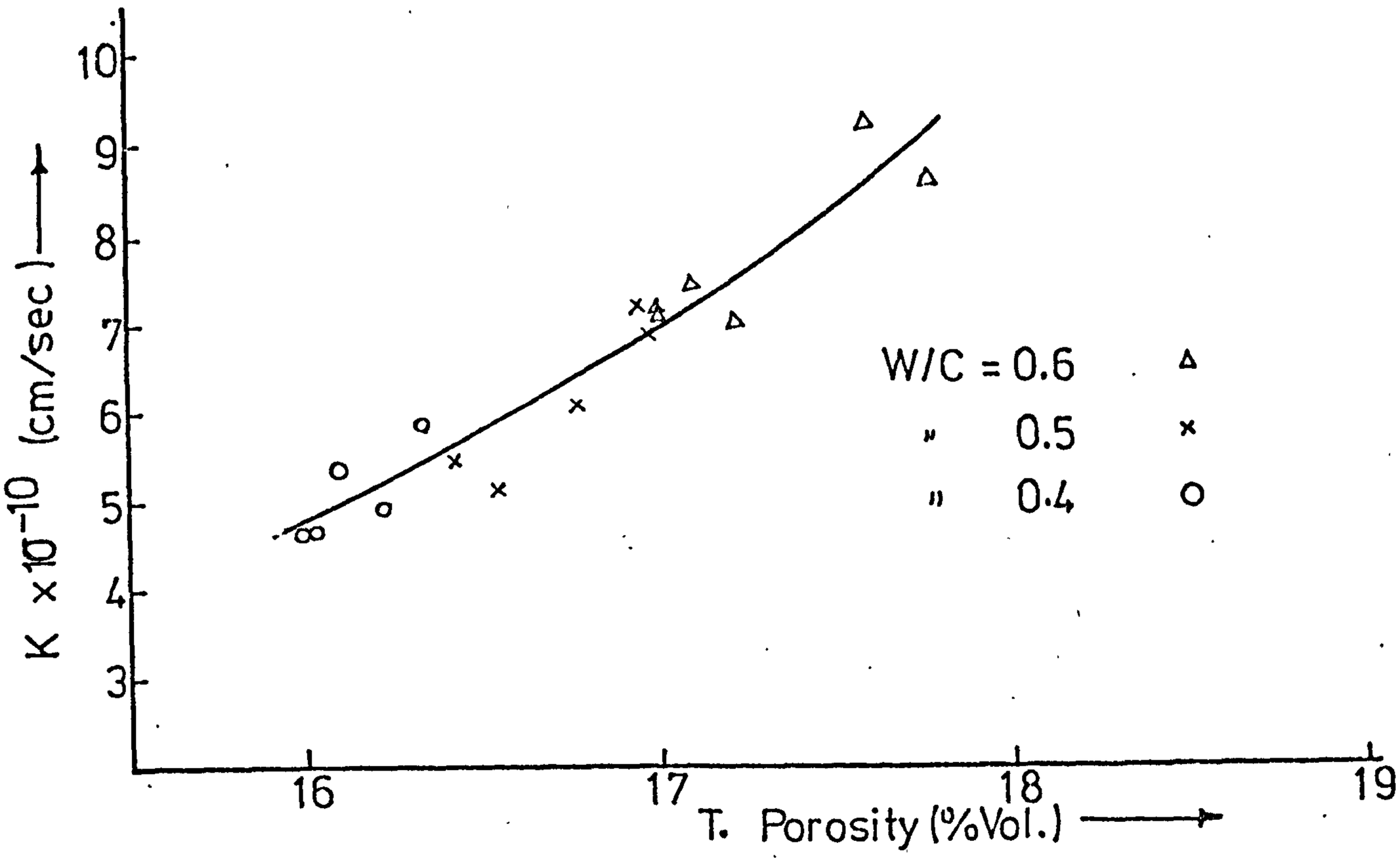

(A) OPC Concrete

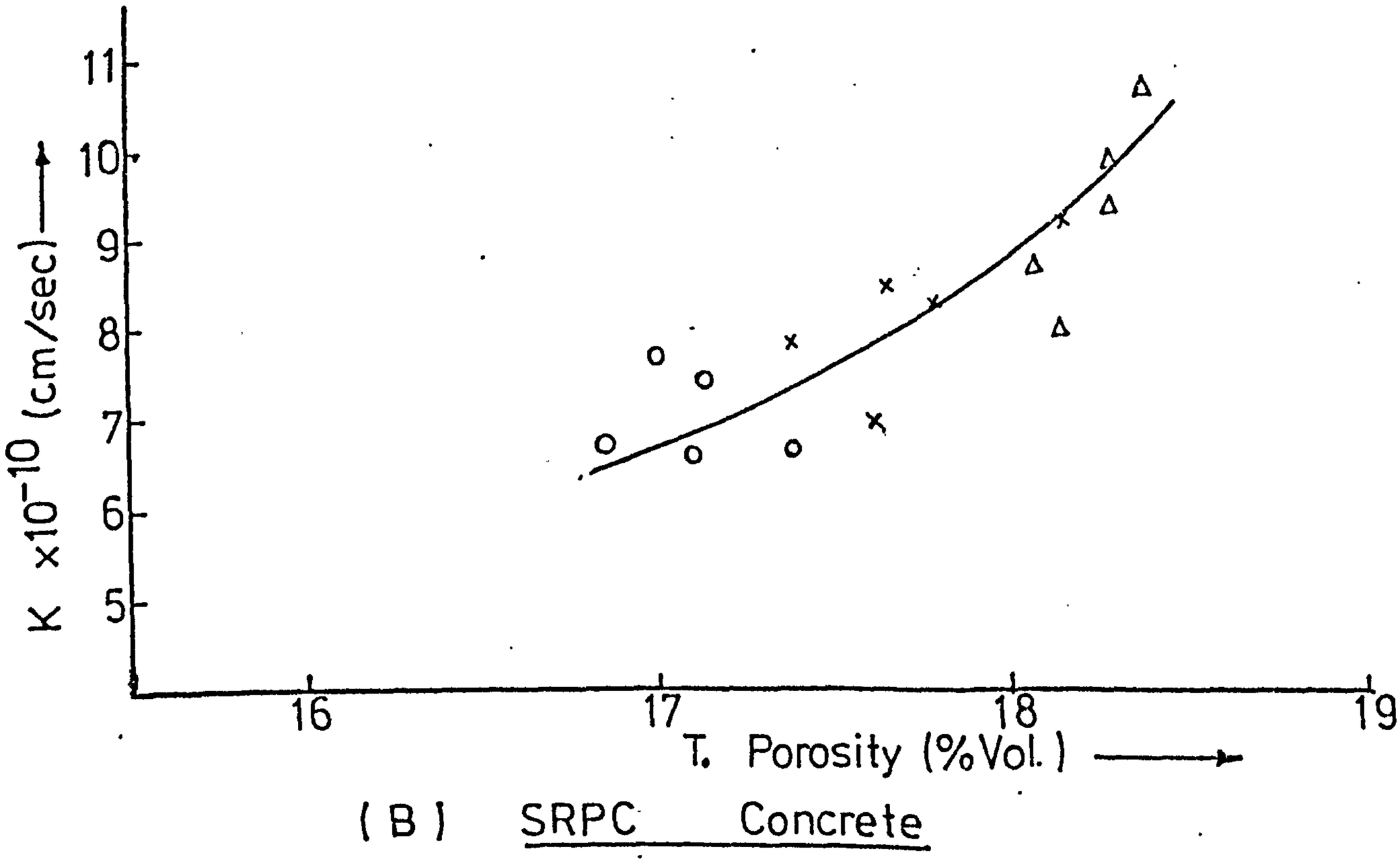

(B) SRPC Concrete

FIG(5.50) VARIATION OF K WITH THE TOTAL POROSITY OF CONCRETE CONTAINING MELMENT L10

2. In fig. (5.52), both the water loss on drying and oil absorption are replotted after dividing by the appropriate specific gravity. In SRPC pastes with W/C ratio from 0.33 to 0.7, between 0.0110 amd 0.0382 cc/gm of the void left by water loss was unfilled by the oil. This represents about 10% of the total void volume for each W/C ratio. For OPC, between 0.4 and 0.7 was unfilled. Matti[12] appeared to obtain 100% replacement of water loss by oil but this would seem to be erroneous because:

a) HCPs have pore sizes as small as 3Å and to fill these pores with oil requires far greater force than the 0.827 N/mm^2 applied.

b) Crude Oil has molecular sizes upto 15Å and it is probable that these larger molecules could clog up the narrow-neck entry pores and thus prevent full saturation.

3. Fig. (5.53) shows the relationship between absorption and total pore volume. It is noticed that absorption is linearly related to porosity, unlike the coefficient of permeability - fig. (5.34). This relationship is given by:

$$A = \gamma P + C \qquad (5.10)$$

where A is the absorption capacity gm/gm x 100% dry weight; γ and C are constants whose values are given in table (5.21).

PASTE	γ	C
OPC	0.786	-15.4
SRPC	0.955	-22.5

Table (5.21) Constants of equ. (5.10)
Absorption Vs T. Porosity

4. Fig. (5.54) shows the relationship between the coefficient of permeability (K) and the oil absorption of HCPs. The graphs show clearly that absorption and permeability are two distinct properties of HCPs. They are related in a similar manner as permeability and porosity - c/f Fig.

(5.14). This is because absorption is more a measure of 'open' pore volume and not the permeable pores which are not only open but interconnected[26]. K can be related exponentially to absorption:

$$K = K_o e^{bA} \qquad (5.11)$$

where K_o = the permeability of a theoretical paste of zero absorption, and b is a constant. The results of a regression analysis are given in table (5.22).

PASTE	$K_o \times 10^{-12}$	b	r
OPC	3.629	0.0718	95.5
SRPC	5.100	0.0530	99.3

Table (5.22) Constants of regression - equ. (5.11)
K Vs Absorption - HCPs

5.7.2.2 HCPs containing Superplasticisers

These absorption values were obtained from samples used for permeability and cube strength tests. Only Cormix SP1 superplasticiser was used as follows: 4% admixture by wt. of cement content in pastes of W/C = 0.3, 0.4,0.5 and 0.6; 1%, 2%, 3% and 4% admixture in pastes of W/C = 0.4. The results are illustrated in figs. (5.55) and (5.56). The following observations are made from these plots:

1. In fig. (5.55) the water loss on drying at 105°C and the oil absorbed for the various W/C ratios are illustrated for pastes with and without admixtures. Both increased almost linearly with W/C ratio. Absorption values for superplasticised pastes were from 2 - 17% higher than ordinary pastes. For SRPC pastes, absorption appears to be higher for ordinary pastes at the higher W/C ratios of 0.5 and 0.6 but this needs to be checked.

2. In fig. (5.56), the oil absorbed and the water loss on drying at 105°C are shown for HCPs of W/C = 0.4 but with increasing admixture concentrations. It is clear from the plots that absorption is not very sensitive to admixture concentration.

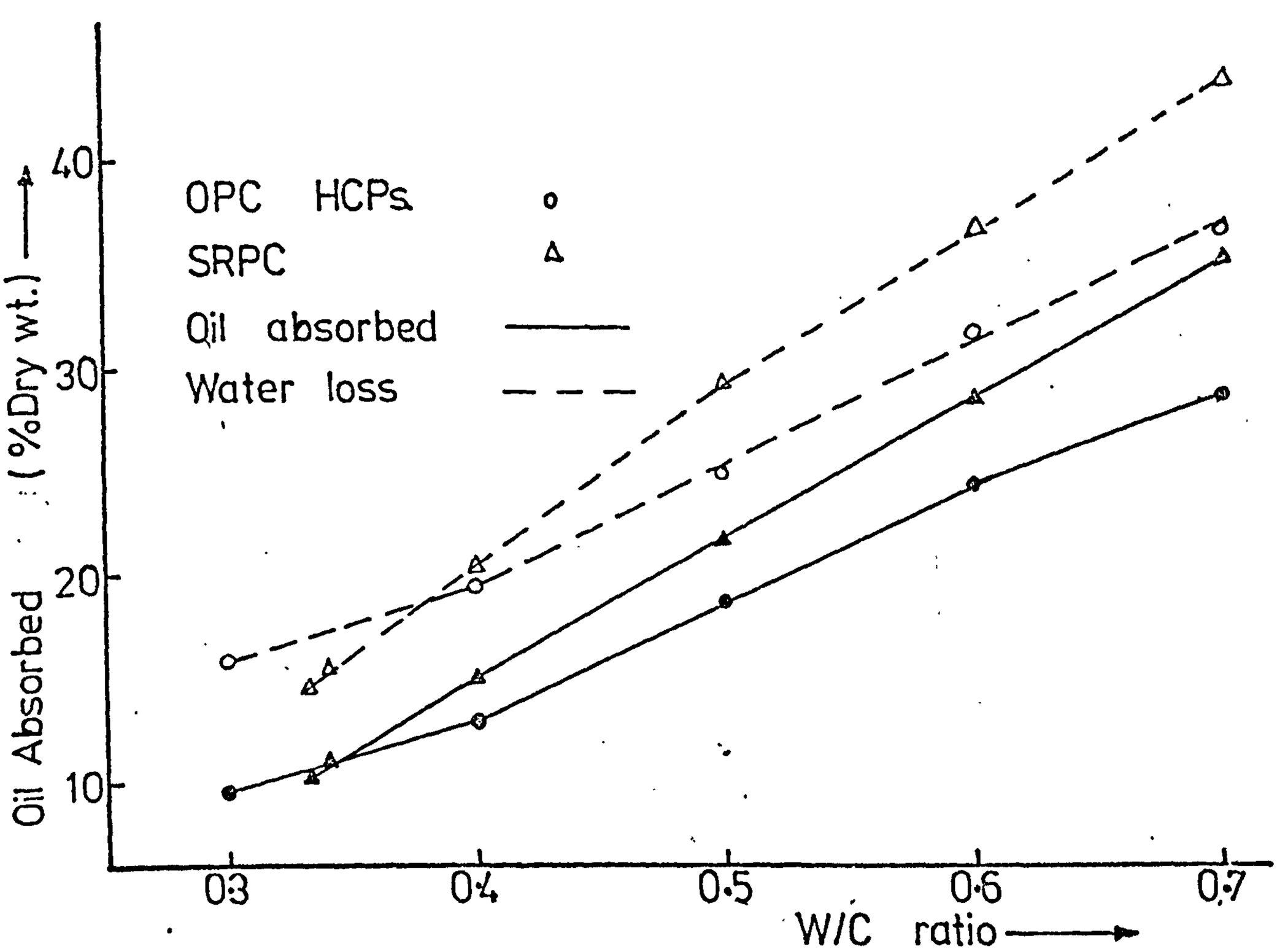

FIG(5.51) WEIGHT OF OIL ABSORBED & WATER LOST ON DRYING TO 105°C

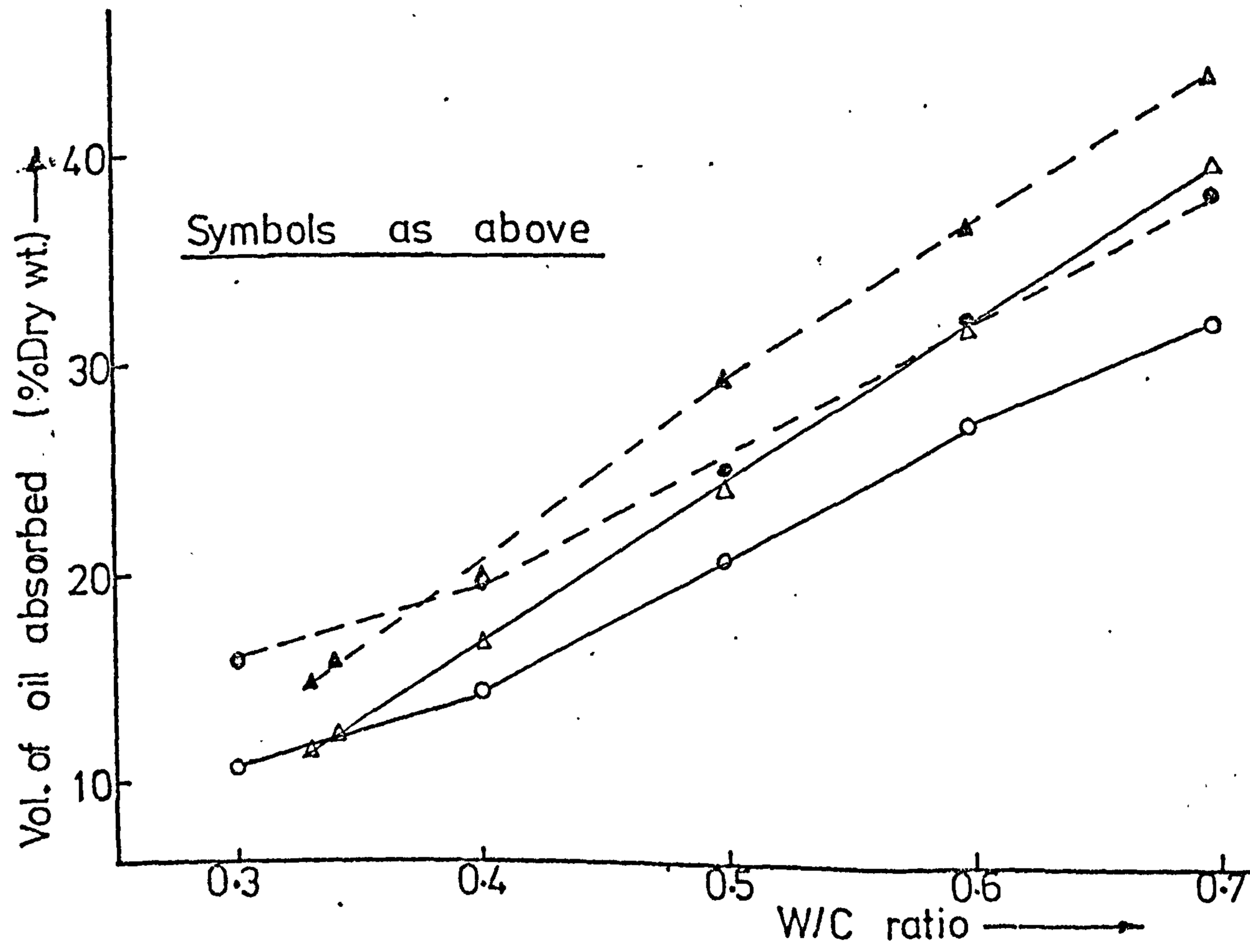

FIG(5.52) VOLUME OF OIL ABSORBED & WATER LOST ON DRYING TO 105°C

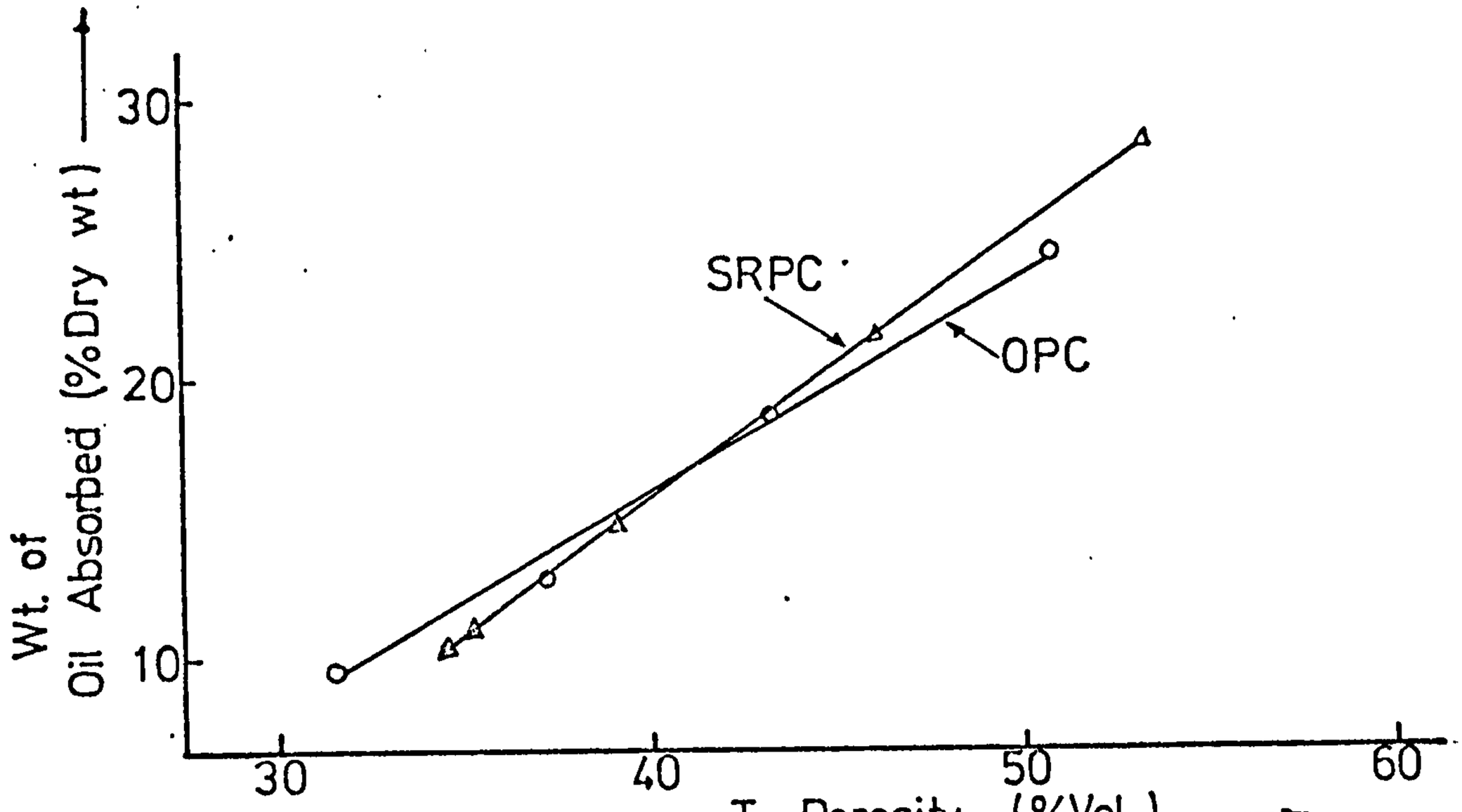

FIG(5.53) VARIATION OF OIL ABSORPTION WITH THE HCP POROSITY

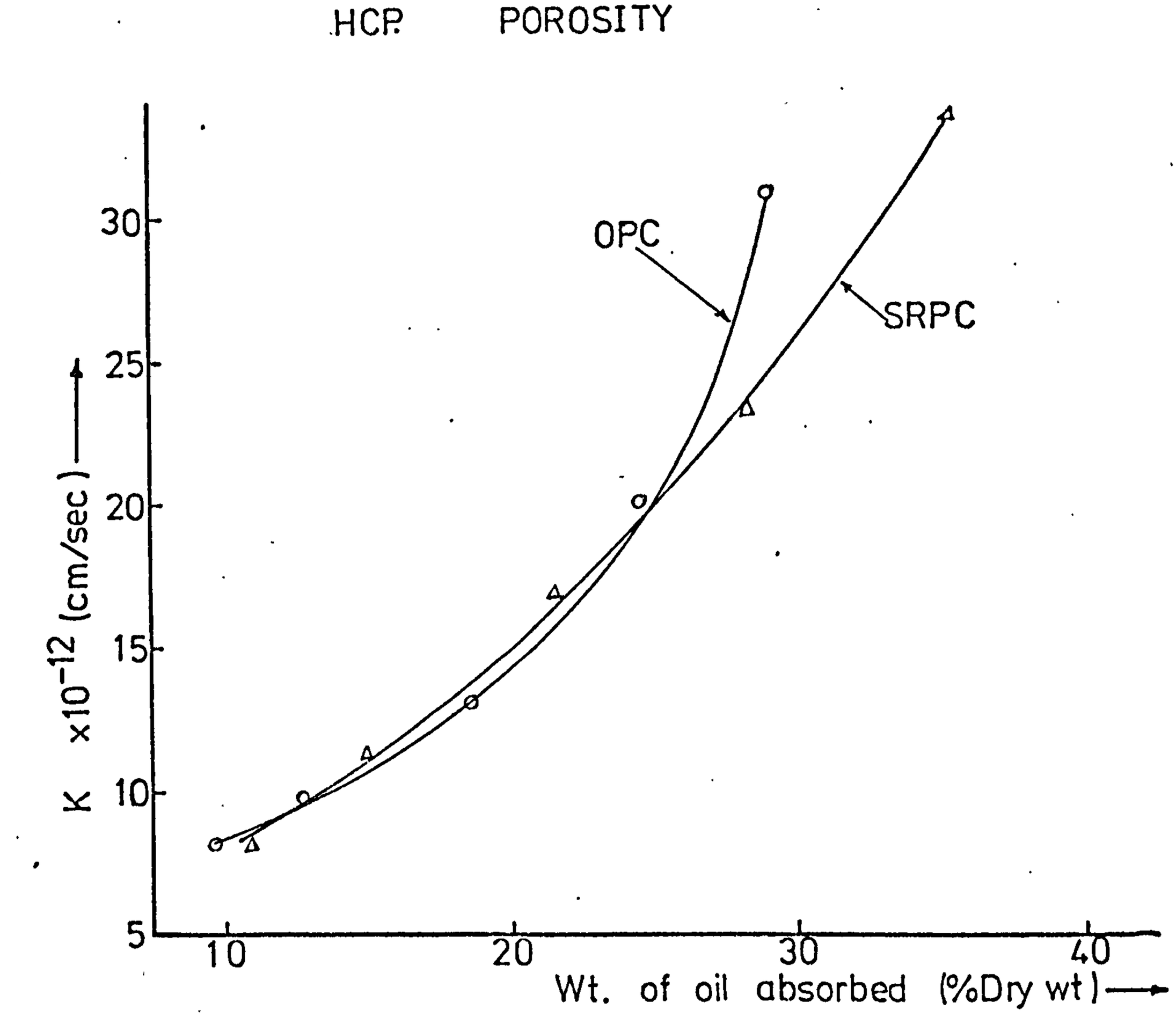

FIG(5.54) RELATIONSHIP BETWEEN OIL ABSORPTION & K OF HCPs.

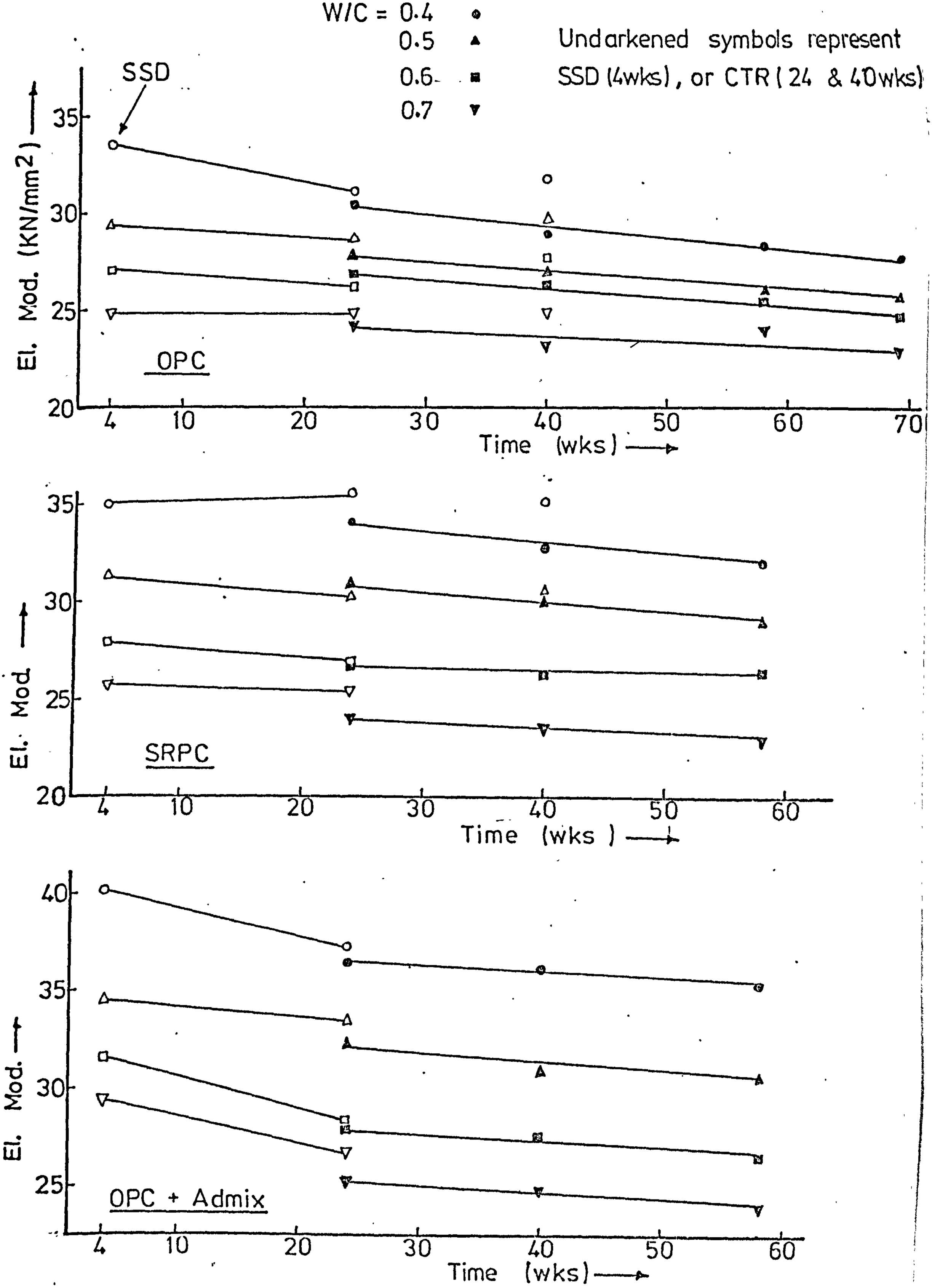

FIG(6.14) VARIATION OF THE ELASTIC MODULUS OF CONCRETE WITH PERIOD OF STORAGE IN OIL.

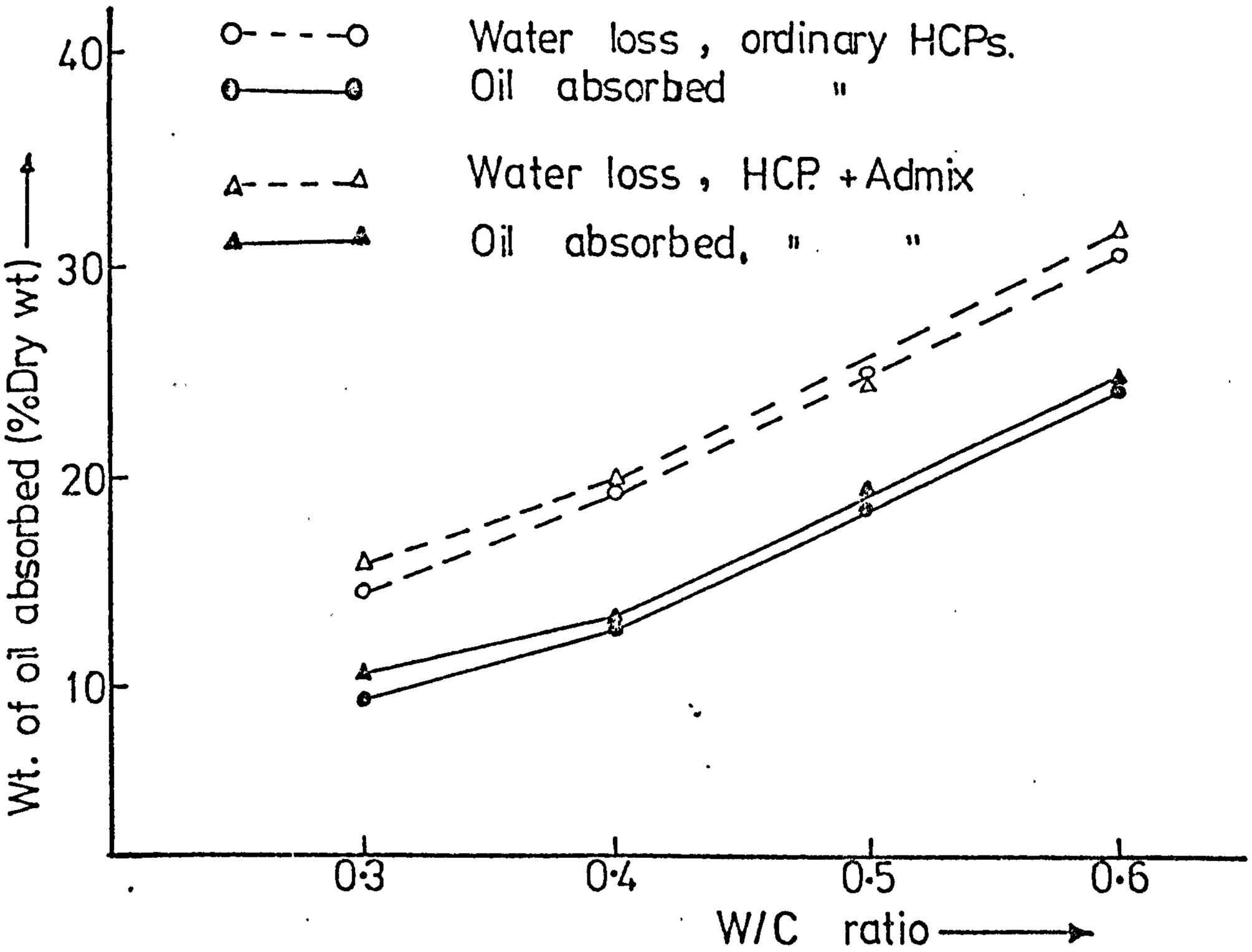

(A) OPC Paste

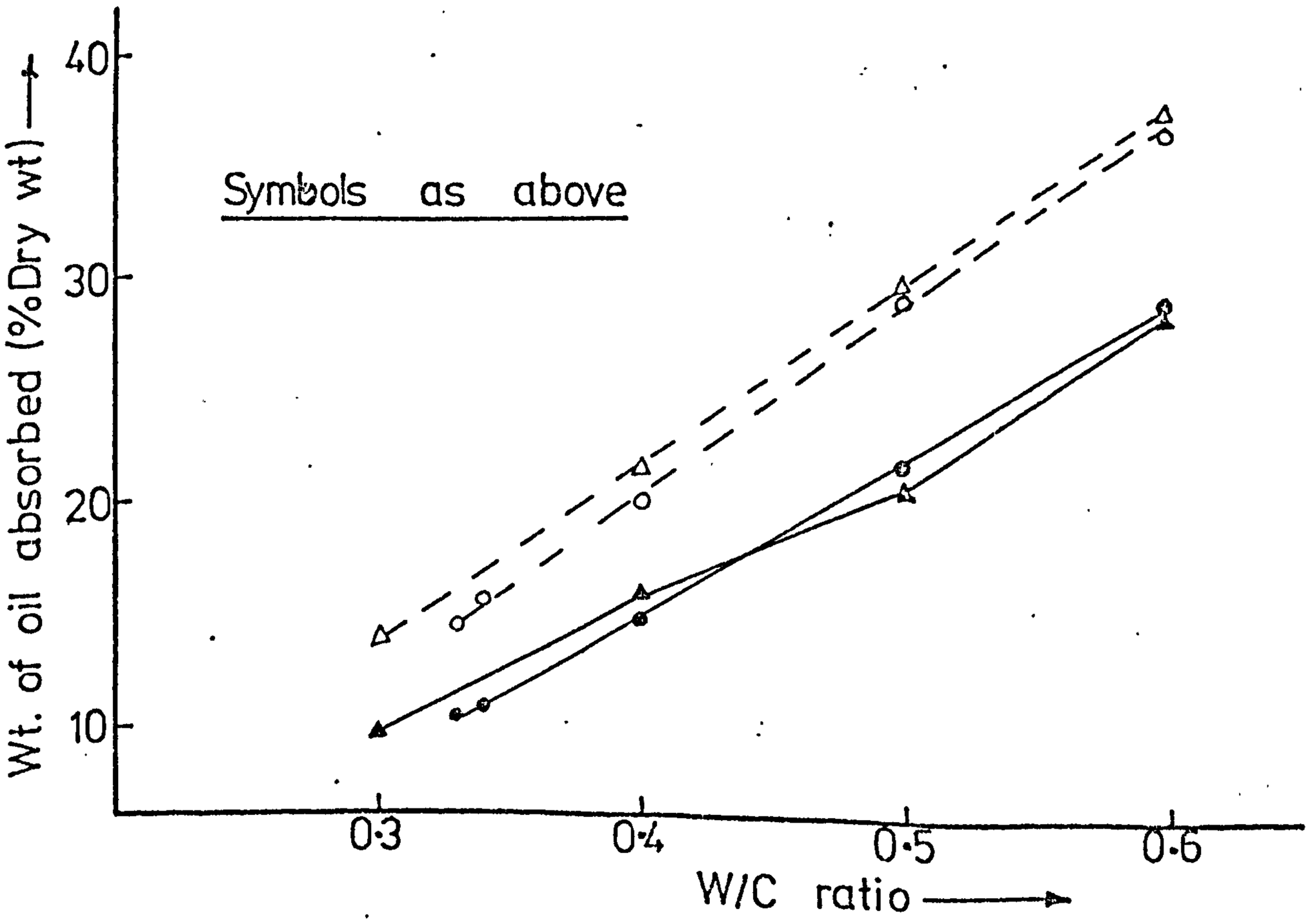

(B) SRPC Paste

FIG(5.55) OIL ABSORBED BY HCPs. CONTAINING SUPERPLASTICISER.

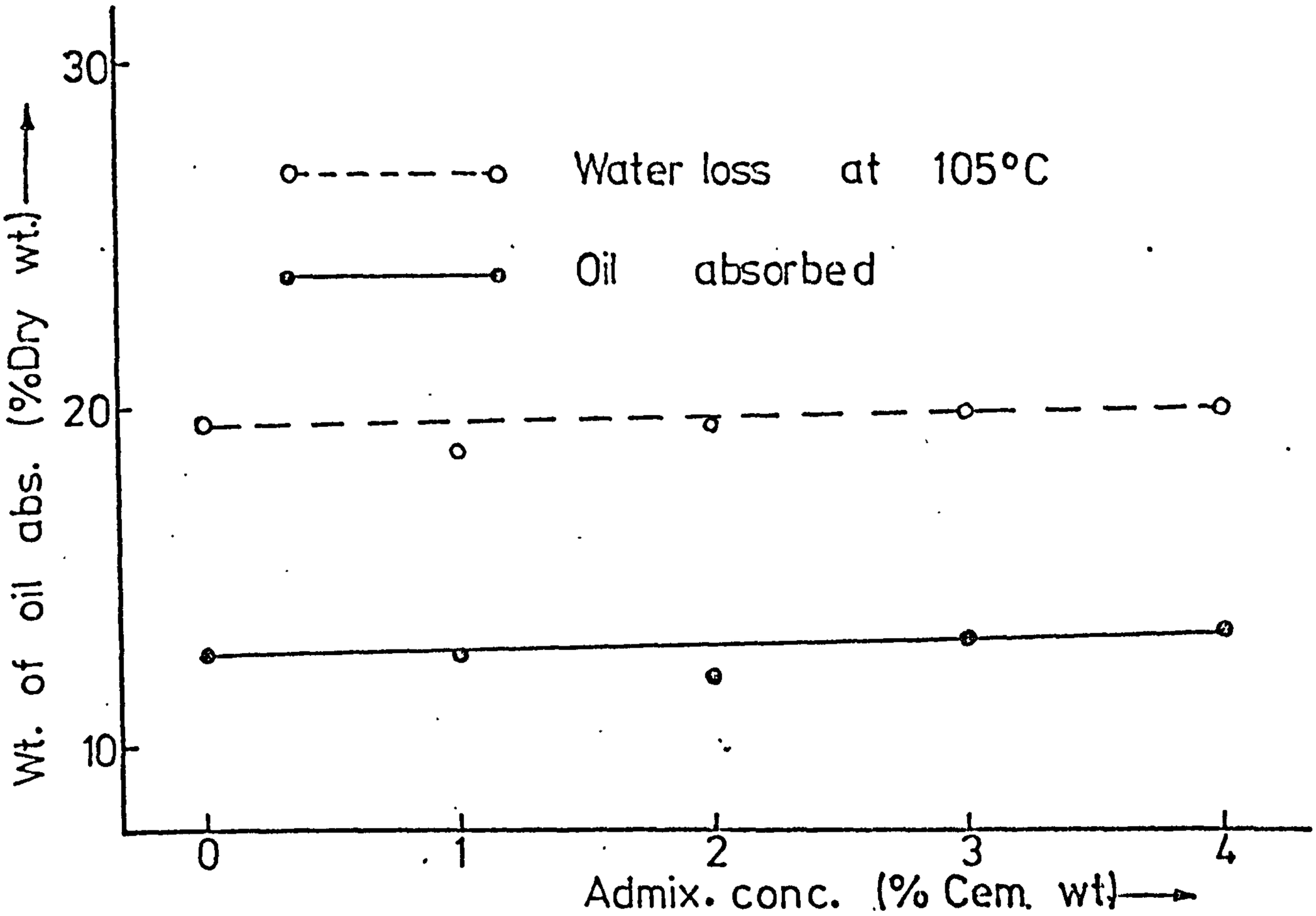

(A) OPC Paste

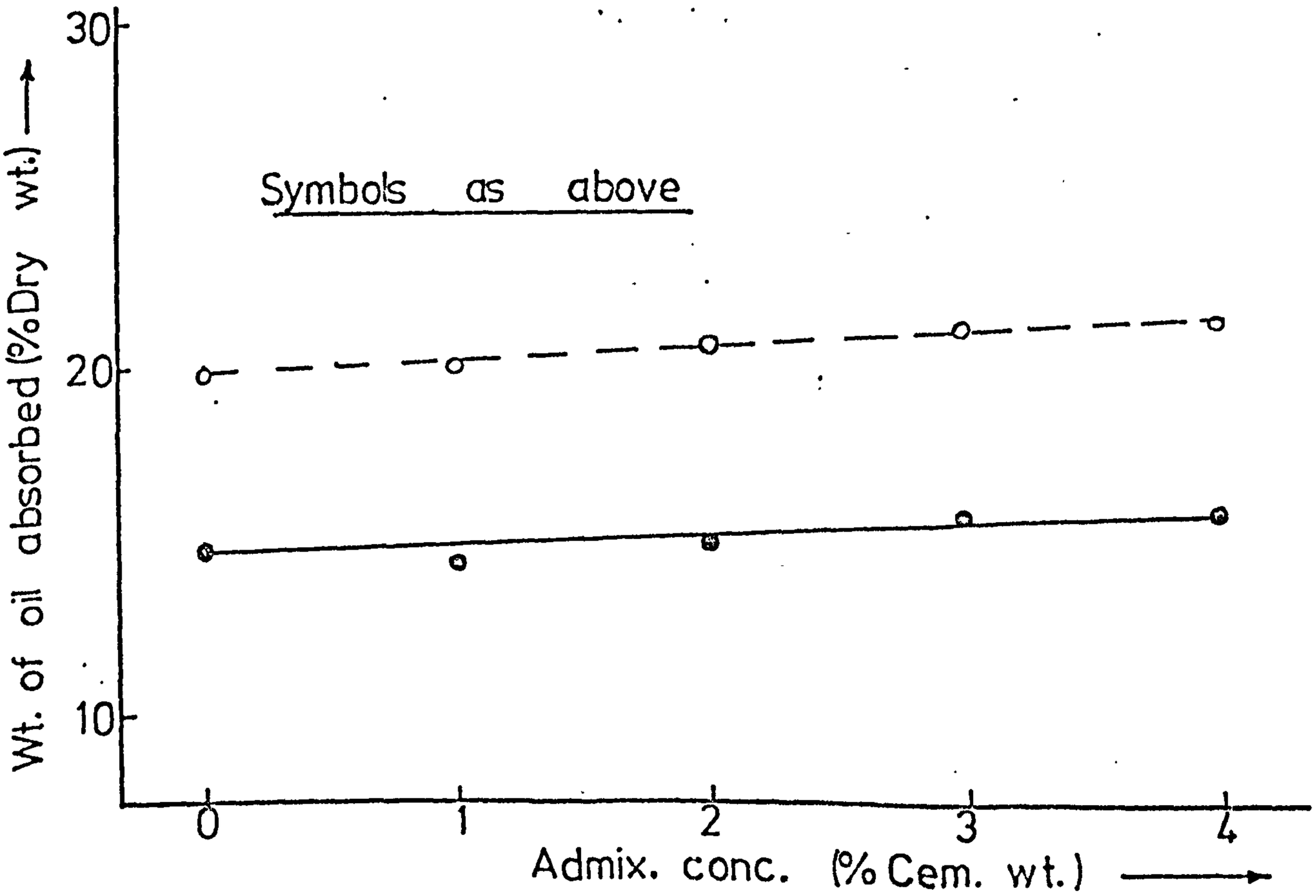

(B) SRPC Paste

FIG(5.56) VARIATION OF OIL ABSORPTION WITH ADMIX. CONCENTRATION.

5.7.3 Absorption Characteristics of Plain Concrete

The absorption characteristics of OPC and SRPC concrete containing no admixture are illustrated in figs. (5.57) to (5.65).

5.7.3.1 Variation of Absorption with total porosity

The total porosity and oil absorption are given in tables (5.9) and (5.15) for OPC and table (5.10) for SRPC concretes. The relationship between total porosity and absorption are illustrated in figs. (5.59) and (5.58) for OPC and SRPC concretes.

The results had a large scatter. Generally, the higher the total porosity the higher the absorption; and the relationship between the two can be expressed exponentially as:

$$A = A_o(\exp)^{bP} \qquad (5.12)$$

where A_o = absorption of concrete of zero porosity and b a constant. A_o and b were determined by a regression analysis and given in table (5.23).

CONCRETE	A_o	b	r
OPC	0.1661	0.1685	89.6
SRPC	0.2497	0.1416	93.4

Table (5.23) Constants of regression - Equ. (5.12) Absorption Vs T. Porosity

5.7.3.2 Variation of Absorption with Compressive Strength

Figs. (5.59) and (5.60) illustrate the relationship between compressive strength and oil absorption of OPC and SRPC concretes respectively. It is observed that:

1. There is a large scatter in the results and regression lines of an exponential form could be drawn:

$$A = A_o(\exp)^{bf_c} \qquad (5.13)$$

Values of A_o and b were obtained and are given in table (5.24).

2. Concrete of higher strength had lower absorption. For equal strengths, SRPC concretes had a higher absorption than OPC concrete - being higher by between 7 to 17%.

CONCRETE	A_o	b	r
OPC	6.614	-0.0119	-85.7
SRPC	7.801	-0.0128	-89.6

Table (5.24) Constants of regression - equ. (5.13)
Absorption Vs Compr. Strength

5.7.3.3 Oil Absorption of Concretes dried to 105°C

Fig. (5.61) shows the relationship between the quantity of oil absorbed and W/C ratios for specimens dried to 105°C, after 4 months of oil storage. These results were obtained from specimens used latter for tests on static modulus of elasticity - tables (3.7) and (3.8). The following is observed:

1. SRPC concretes absorbed more oil than OPC concretes and the superplasticised OPC concretes absorbed less than plain OPC concretes.

2. The volumes of crude oil absorbed per gm. of concrete are plotted in fig. (5.62) and compared with the amount of water lost on drying to 105°C. It is clear that, as for HCPs, less than 100% of voids were filled by oil, probably for the same reasons.

5.7.3.4 Variation of Oil Absorption with time

Fig. (5.63) shows the variations in the quantity of oil absorbed by the concrete with the length of time stored in oil. It is observed that:

1. Most of the absorption occured within the first 4 months of

storage and pressurisation. This agrees with Faiyadh's results[13] for oil absorbed, depth of penetration and area of oil penetration over a six month period. He recorded only a very gradual increase after the first 80 to 100 days.

2. The greatest increases recorded, after 4 months, were 7.8% over the absorption at 4 months for OPC concrete, W/C = 0.5; 16% for SRPC concrete, W/C = 0.5 and 2.2% for OPC superplasticised concrete, W/C = 0.4.

5.7.3.4 Relationship between the Coefficient of Permeability and Absorption

The quantity of oil absorbed by the various concrete specimens was related to their coefficients of permeability as shown in figs. (5.64) and (5.65) for OPC and SRPC concretes. There was a large scatter of results, making it difficult to clearly define a relationship. This will be examined further in Chapter 7.

5.7.4 Absorption Characteristics for Superplasticised Concrete

These results are obtained from the same specimens used for the permeability tests. The results are plotted in figs. (5.66) and (5.67) for concretes containing Cormix SP1 and Melment L10 superplasticisers.

5.7.4.1 Variation of Absorption with Admixture Concentration

The oil absorbed by specimens with the two types of admixture and cements, and different admixture concentrations are shown in fig. (5.66). The following is observed:

1. Oil absorption appears not to be very sensitive to admixture concentration. The numerical difference between the highest and lowest absorption values at any particular W/C ratio was only 0.7% in OPC + Cormix SP1, 0.42% in OPC + L10, 0.26% in SRPC + Cormix and 0.33% in SRPC + L10.

2. Absorption values for concretes without admixture are also shown in fig. (5.67). These values were taken or interpolated from tables (5.9) and (5.10) and some of the values are, therefore, approximate. It is evident that OPC concrete containing no admixture has similar absorption to superplasticised

OPC concrete, the largest difference being 0.5%. SRPC concrete containing no admixtures has greater absorption than superplasticised SRPC concrete, the percentage reduction was between 15.6% and 27%.

5.7.4.2 Variation of Absorption with Total Porosity

The relationship between absorption and the calculated total porosity is illustrated in fig. (5.67). Although the results are scattered, the following is noted:

1. Absorption increases with increasing total porosity and the relationship is linear. It is difficult to compare the absorption for concrete with and without admixtures but of equal porosity because of the scatter of results but there appears to be little difference.

2. At equal porosity, SRPC concretes absorbed more oil than OPC concretes. This is probably because of the larger pore sizes found in SRPC pastes - table (4.5).

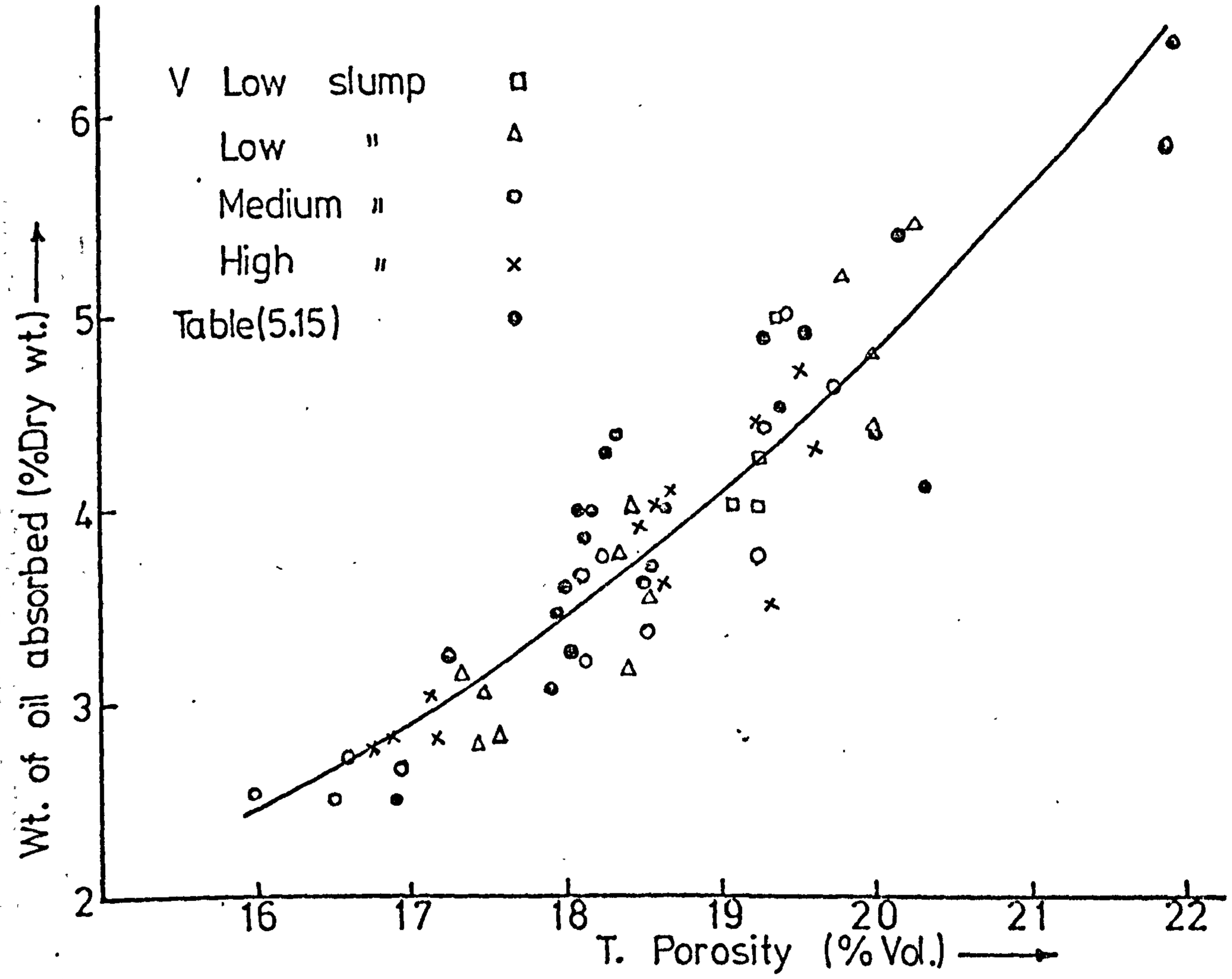

FIG(5.57) VARIATION OF OIL ABSORPTION WITH THE TOTAL POROSITY OF OPC CONCRETE

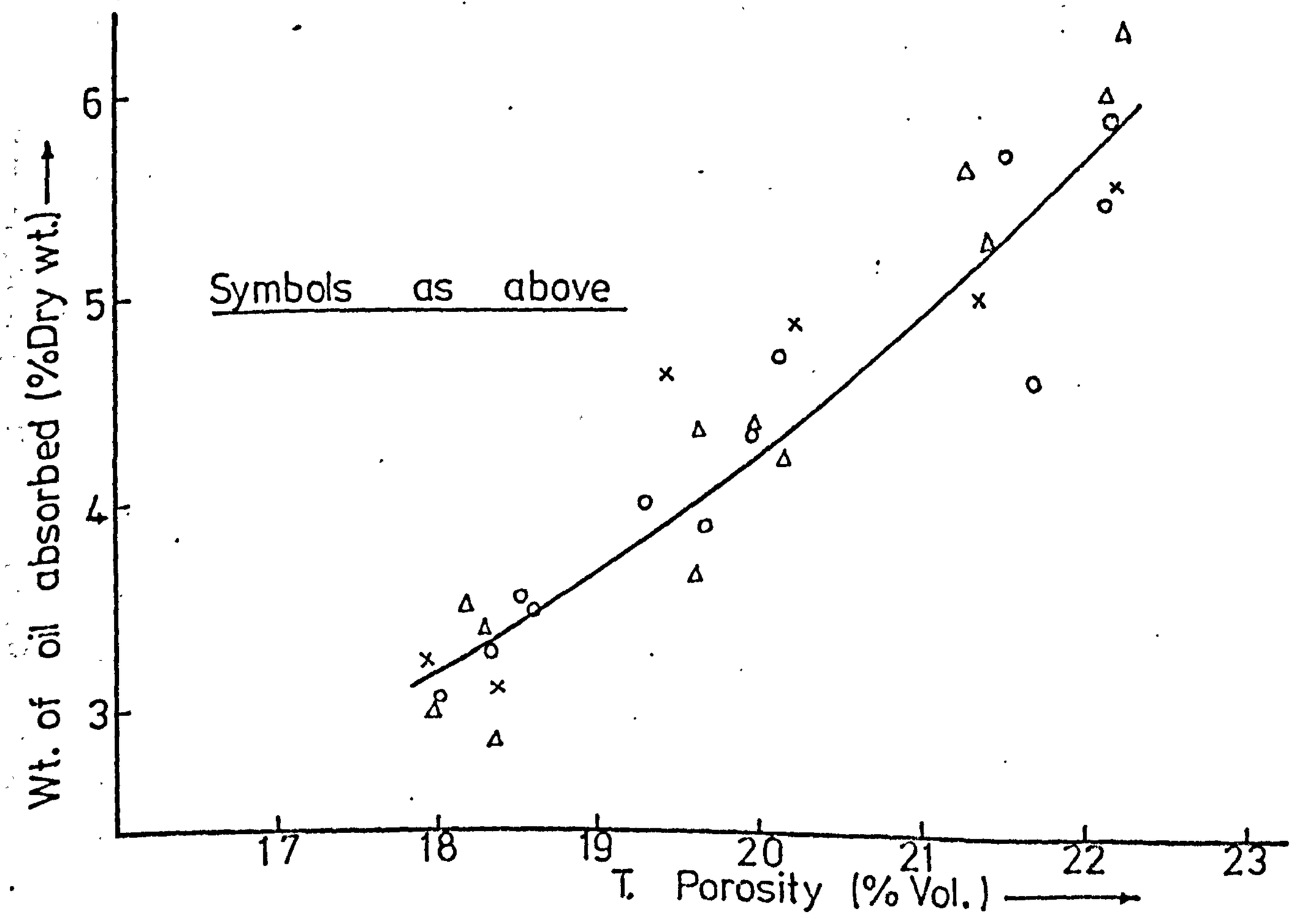

FIG(5.58) VARIATION OF OIL ABSORPTION WITH THE TOTAL POROSITY OF SRPC CONCRETE

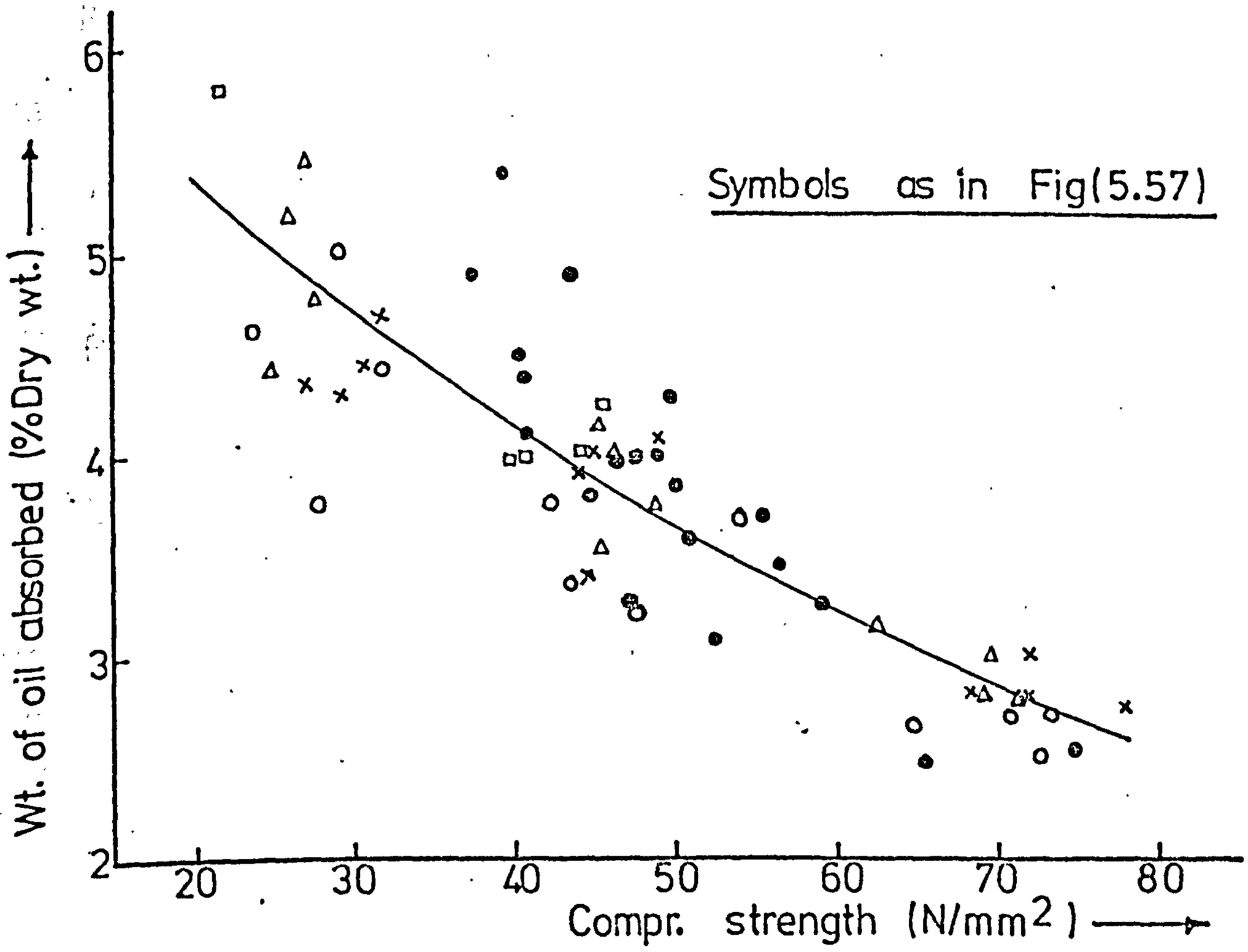

Symbols as in Fig(5.57)

FIG(5.59) RELATIONSHIP BETWEEN OIL ABSORPTION & THE COMPR. STRENGTH OF OIL SAT. CONCRETE, OPC.

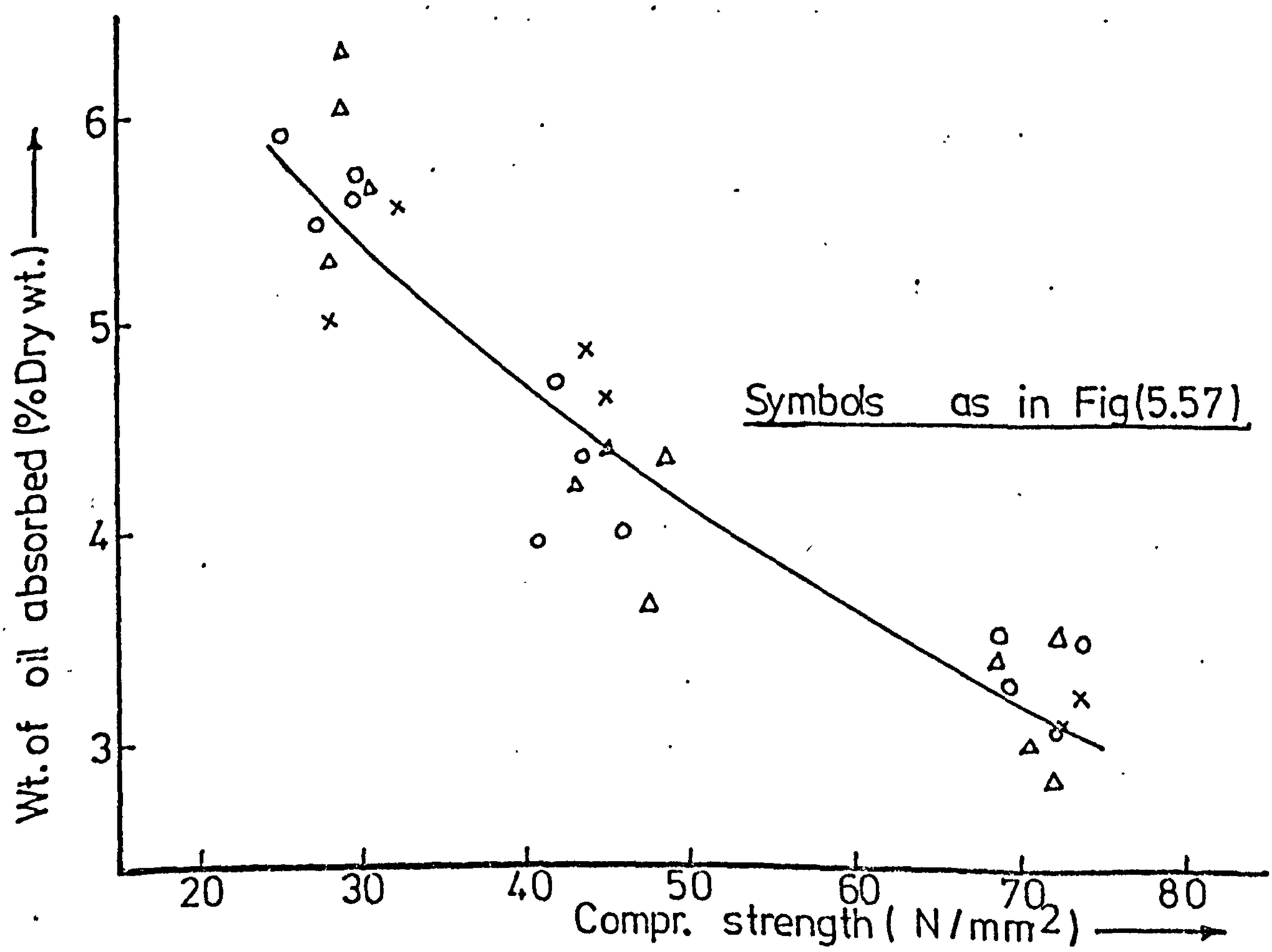

Symbols as in Fig(5.57)

FIG(5.60) RELATIONSHIP BETWEEN OIL ABSORPTION & THE COMPR. STRENGTH OF OIL SAT. CONCRETE, SRPC.

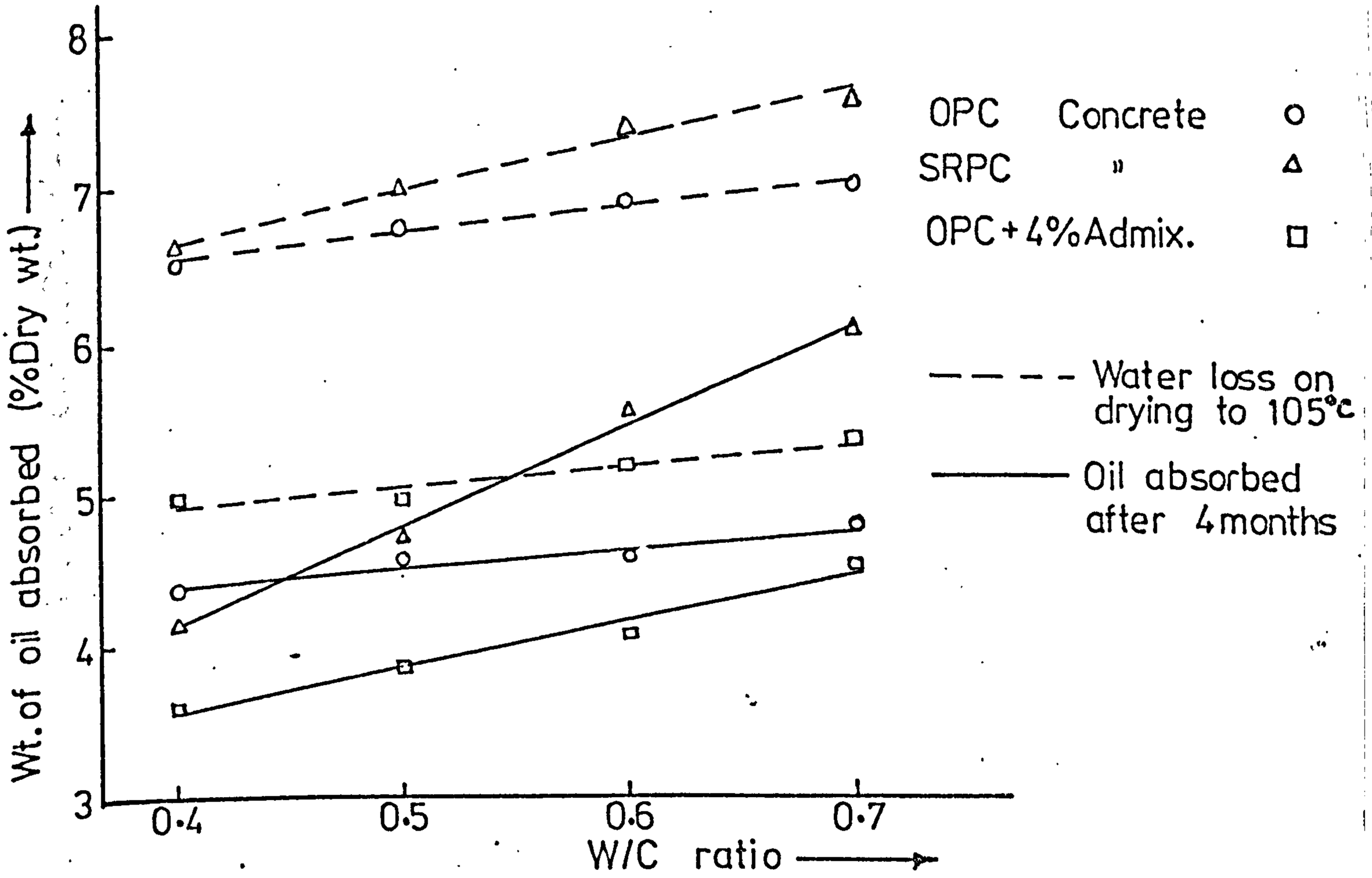

FIG(5.61) OIL ABSORBED & WATER LOST BY CONCRETE DRIED TO 105°C

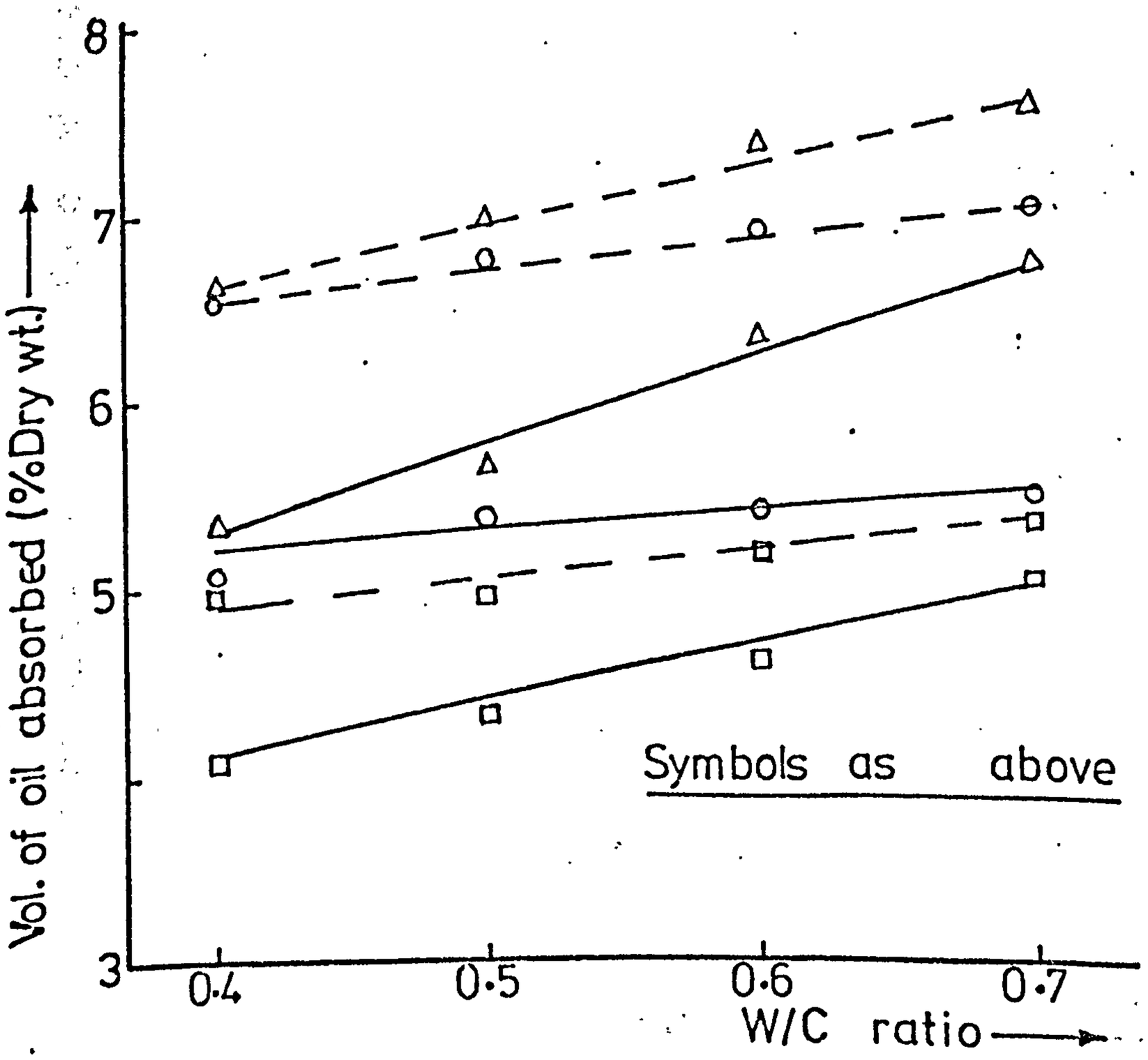

FIG(5.62) VOLUME OF OIL ABSORBED & WATER LOST BY CONCRETE DRIED TO 105°C

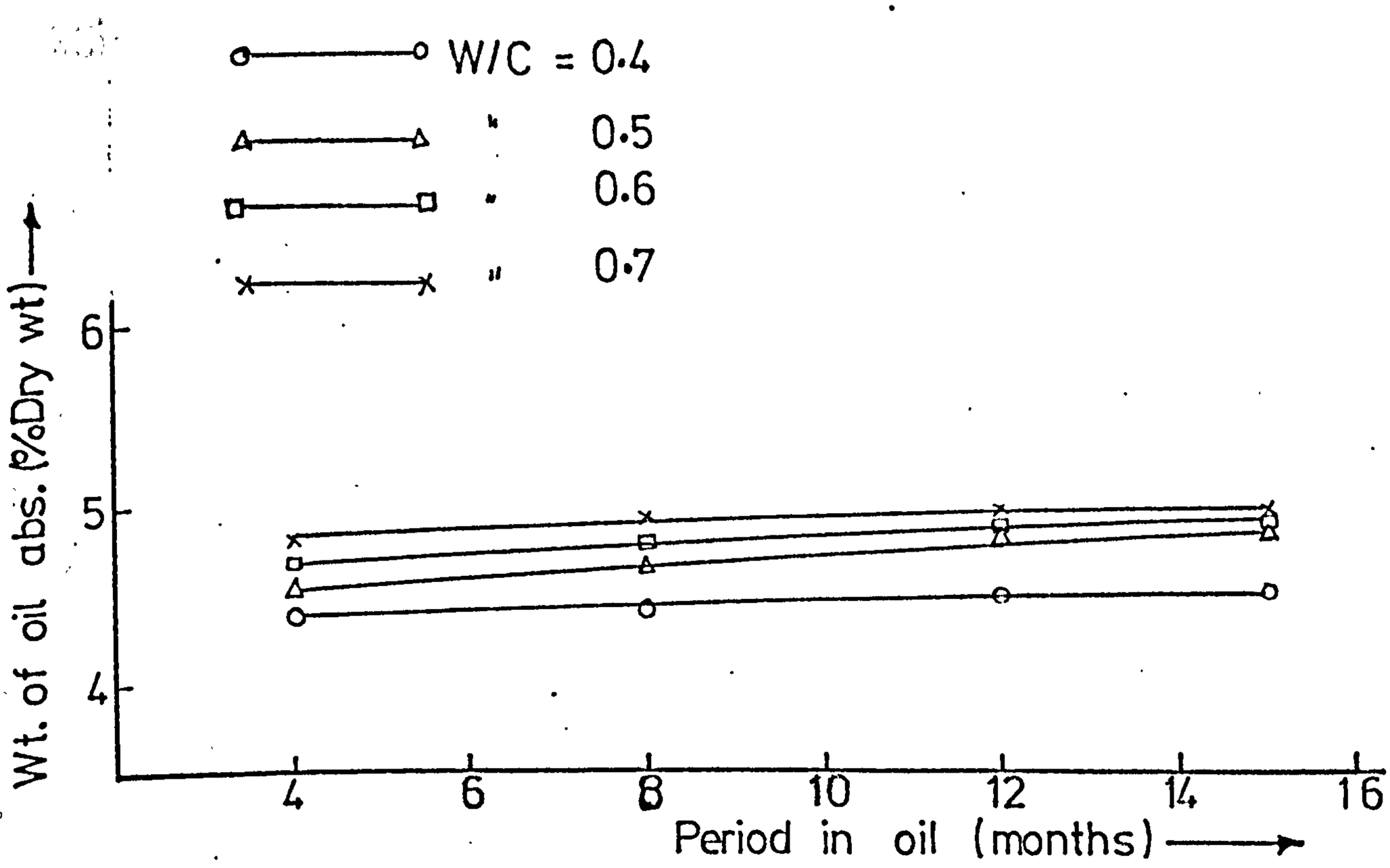

(A) OPC Concrete

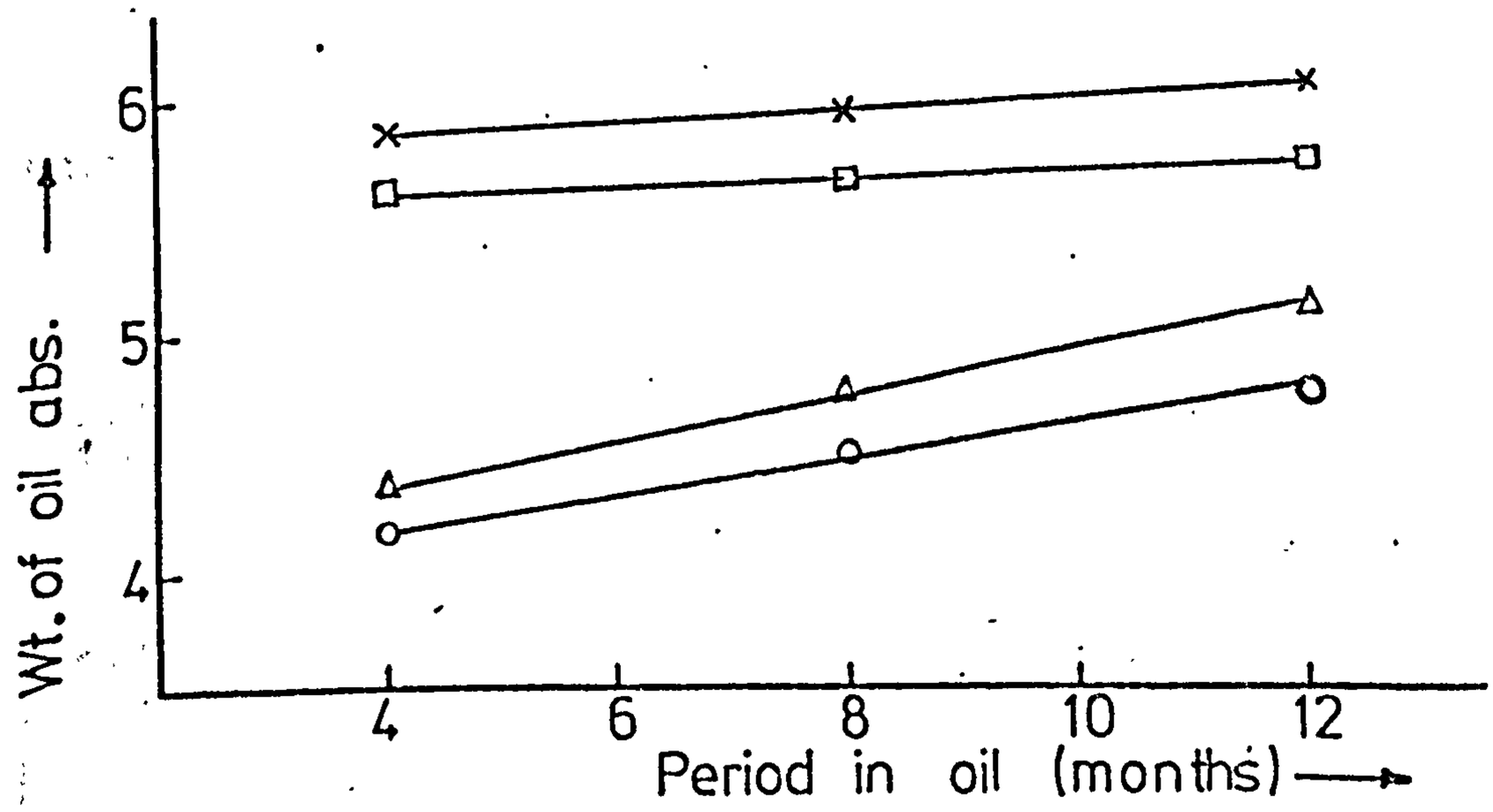

(B) SRPC Concrete

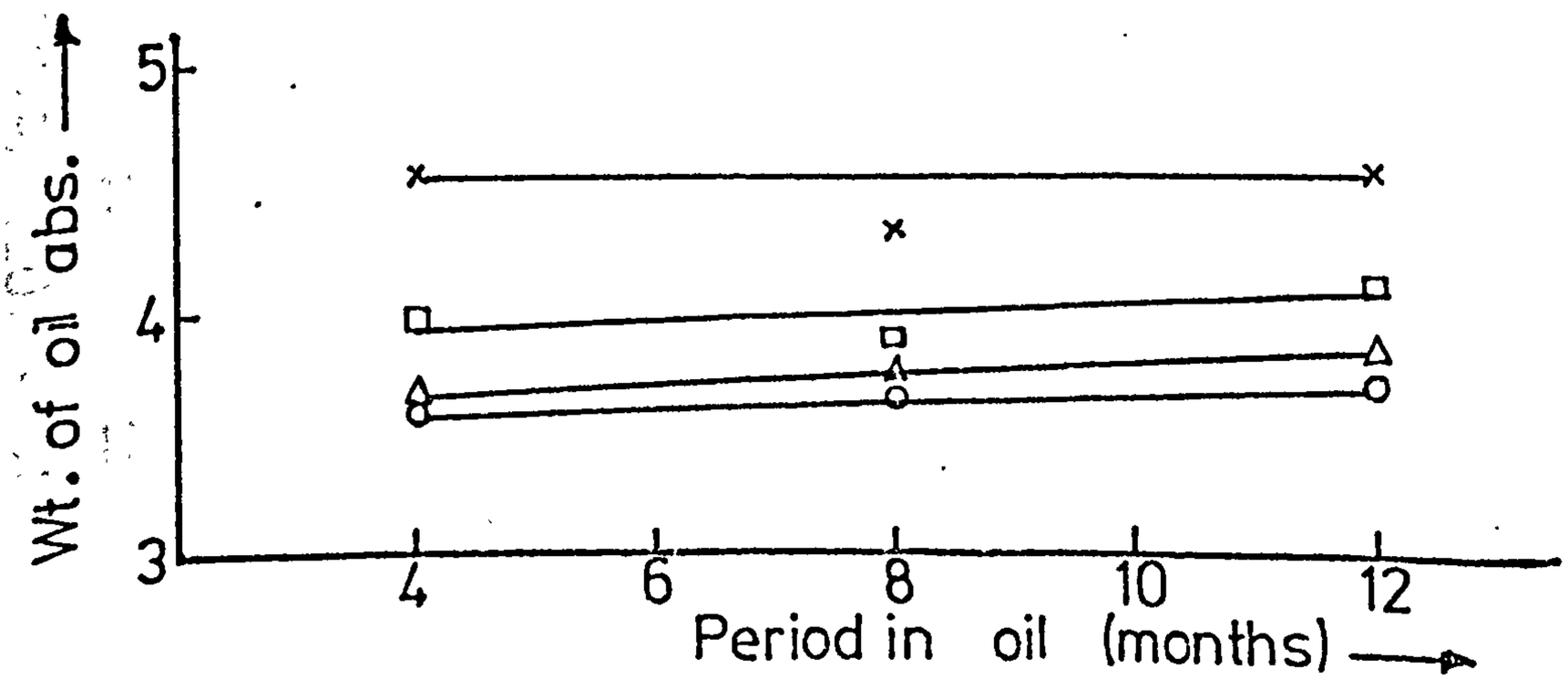

(C) OPC + Admix.

FIG(5.63) VARIATION OF OIL ABSORPTION WITH PERIOD OF STORAGE IN THE OIL.

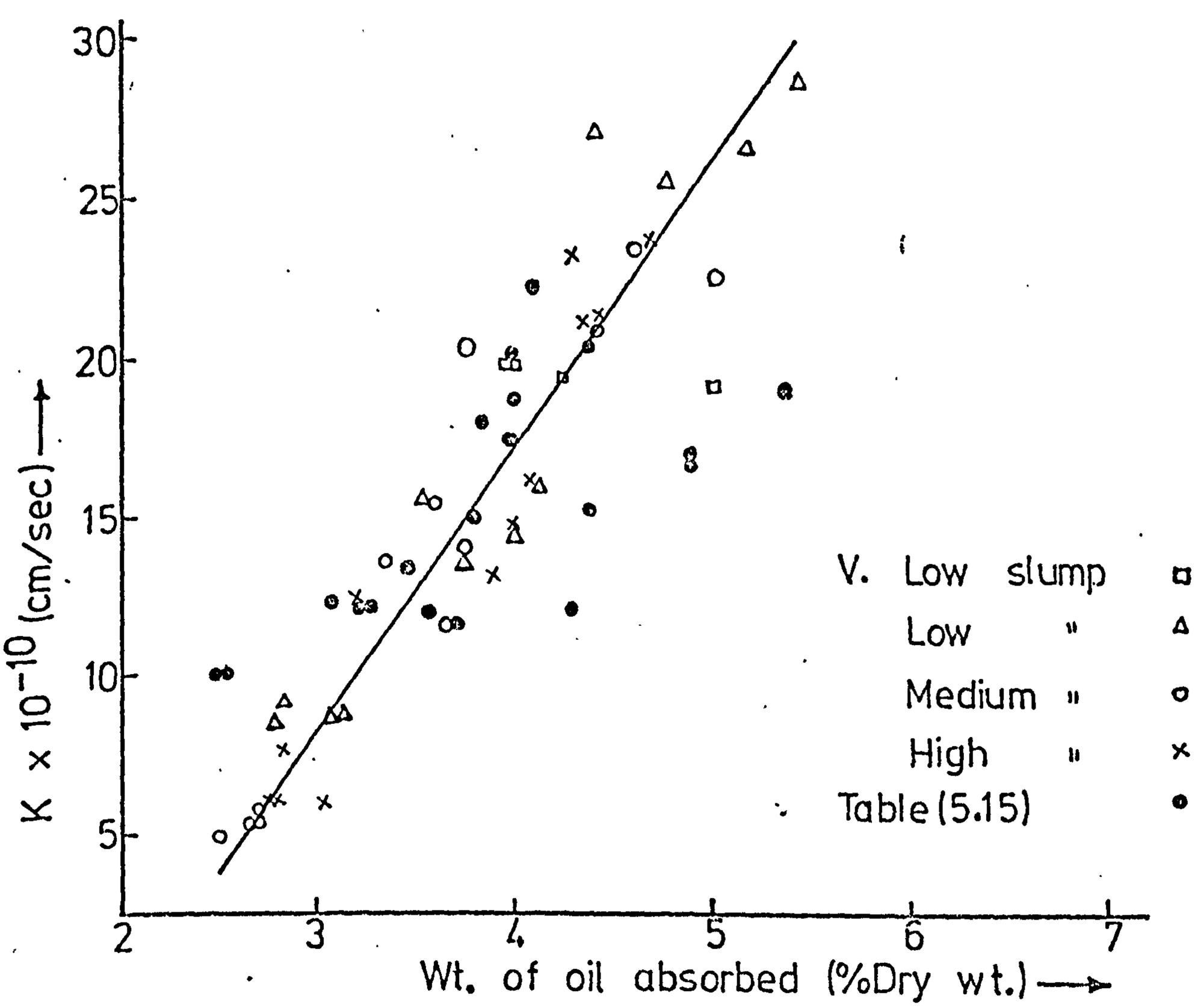

FIG(5.64) RELATIONSHIP BETWEEN K & OIL ABSORPTION — OPC CONCRETE

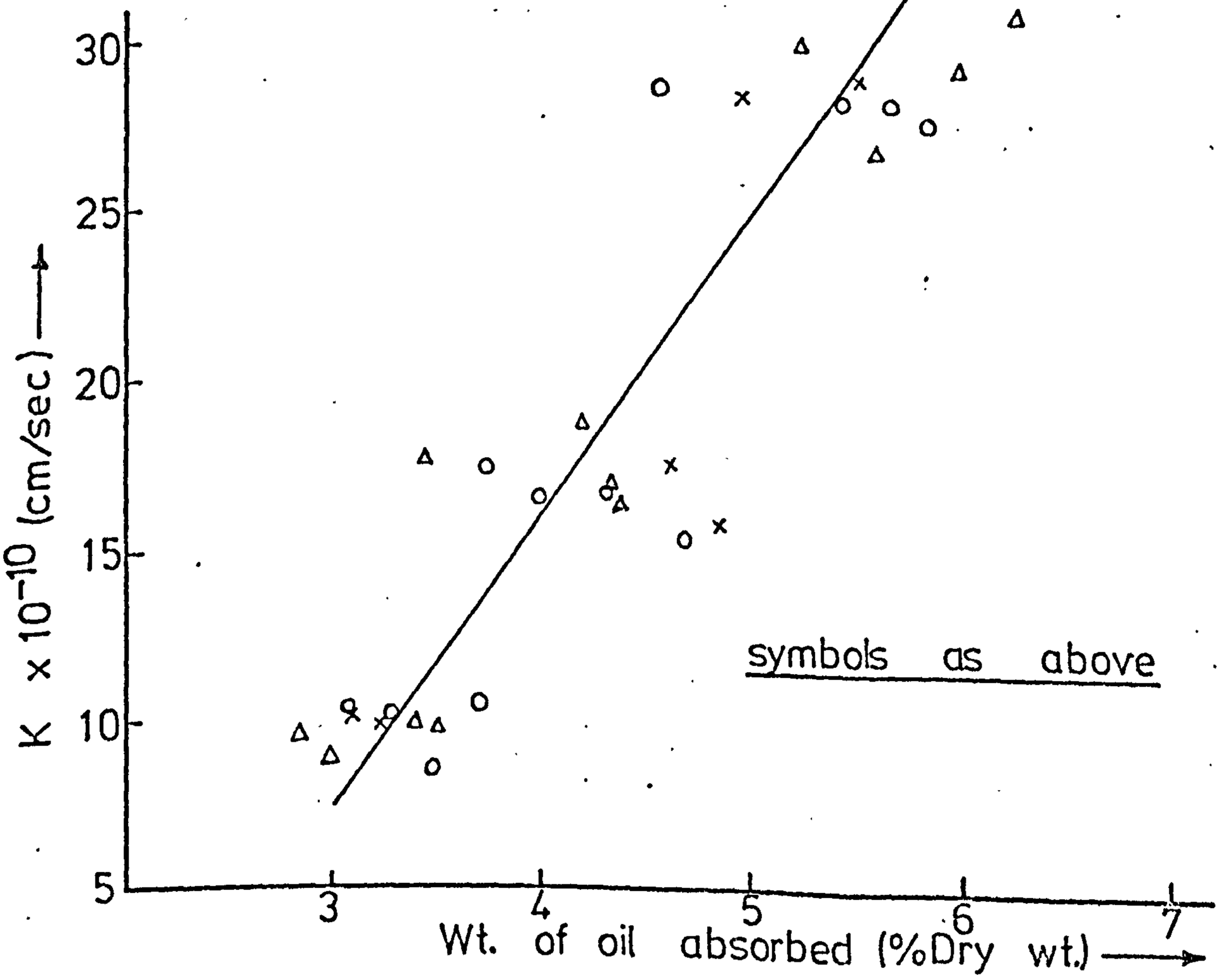

FIG(5.65) RELATIONSHIP BETWEEN K & OIL ABSORPTION — SRPC CONCRETE

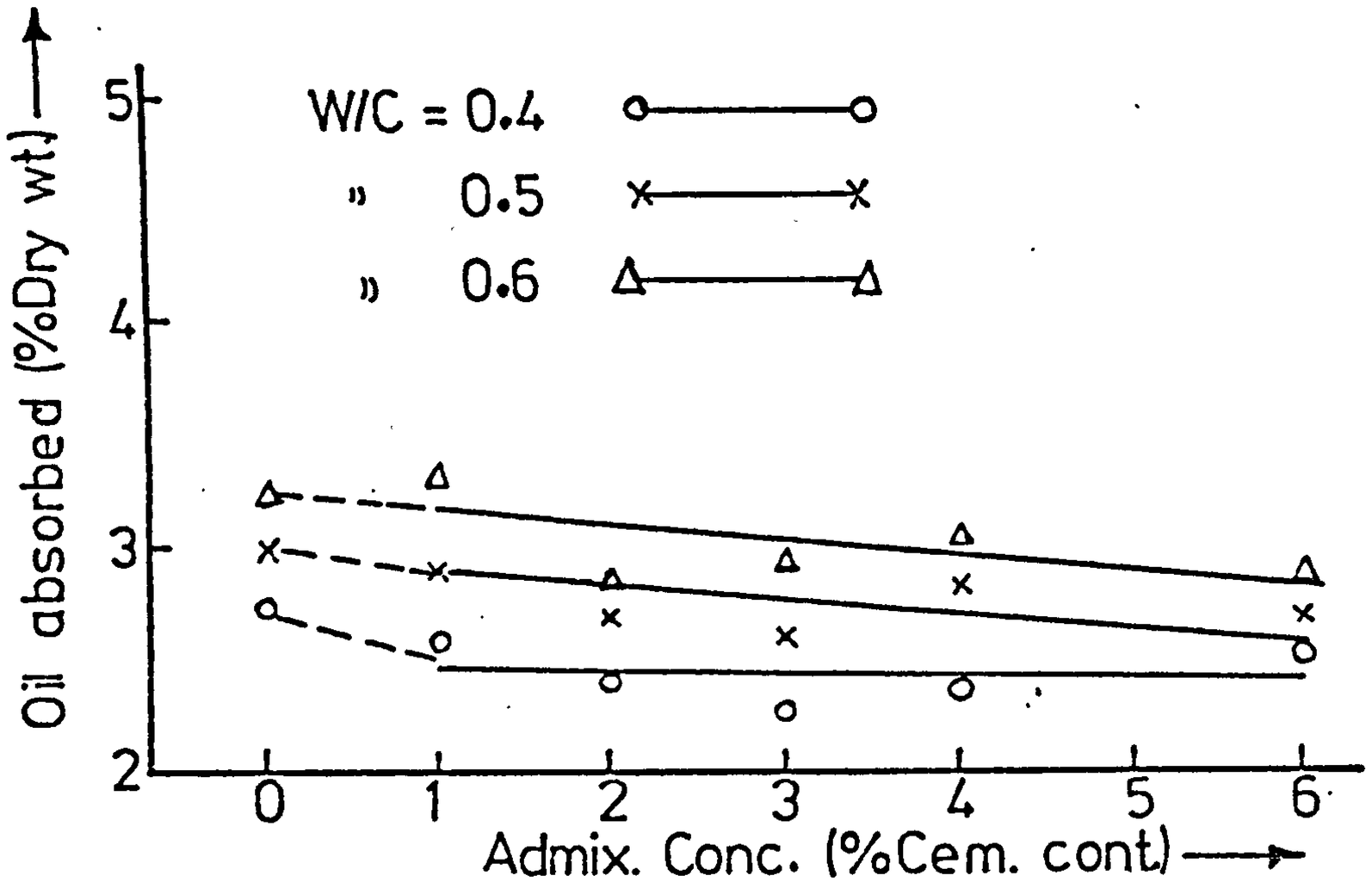

(A) OPC + Cormix SP1

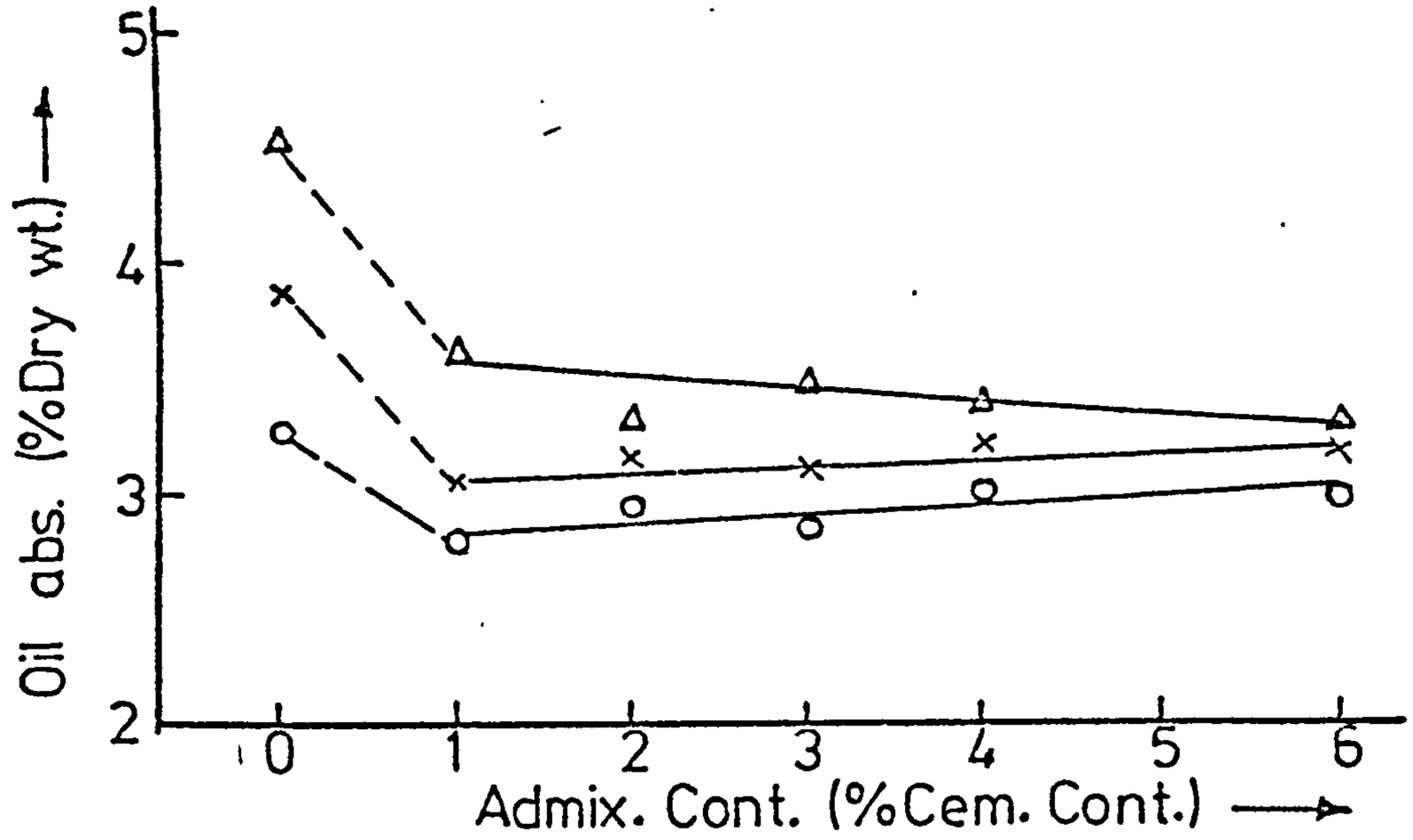

(B) SRPC + Cormix SP1

(C) OPC + Melment L10

(D) SRPC + Melment L10

FIG(5.66) VARIATION OF OIL ABSORPTION WITH ADMIXTURE CONCENTRATION

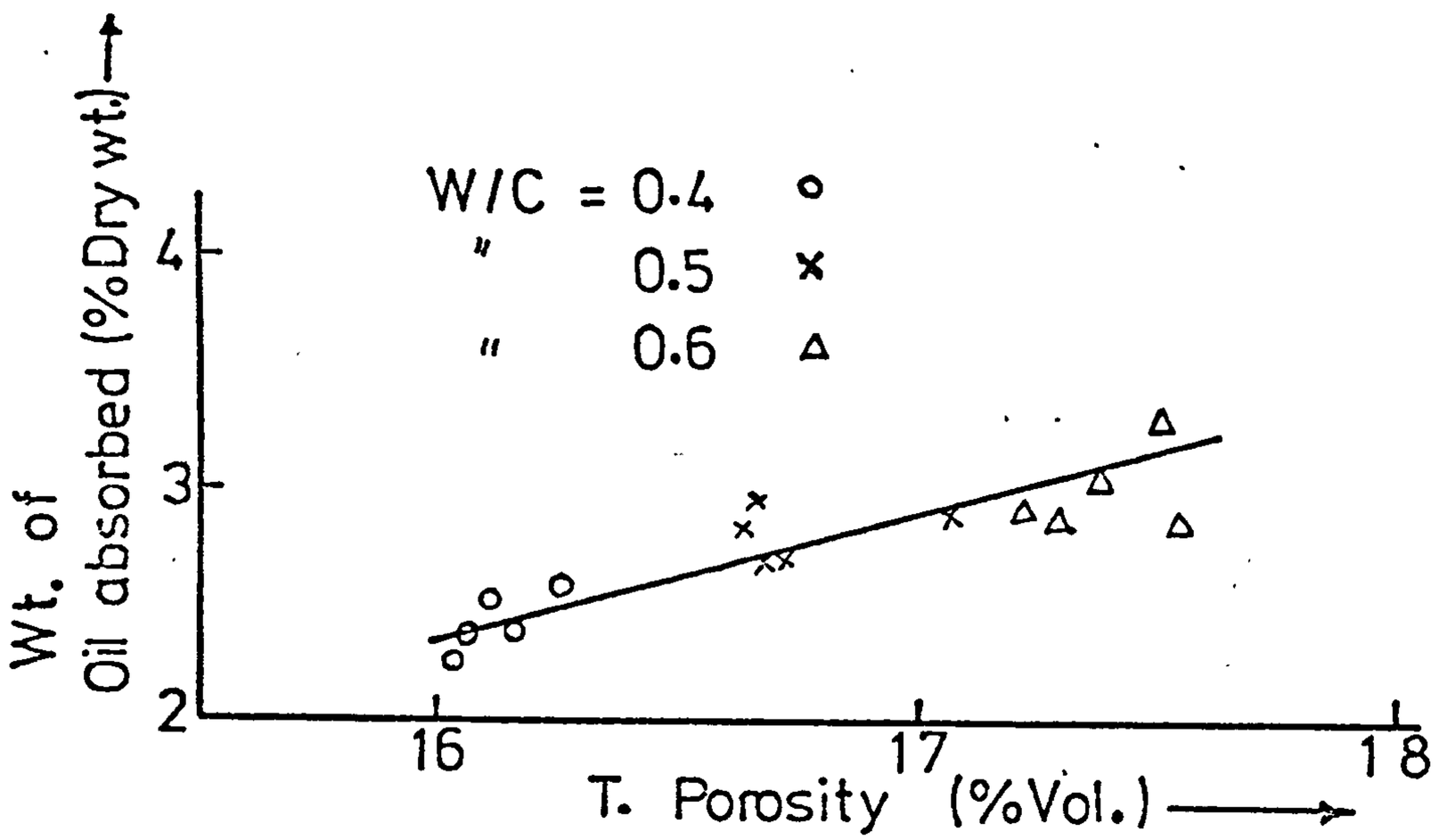

(A) OPC + Cormix SP1

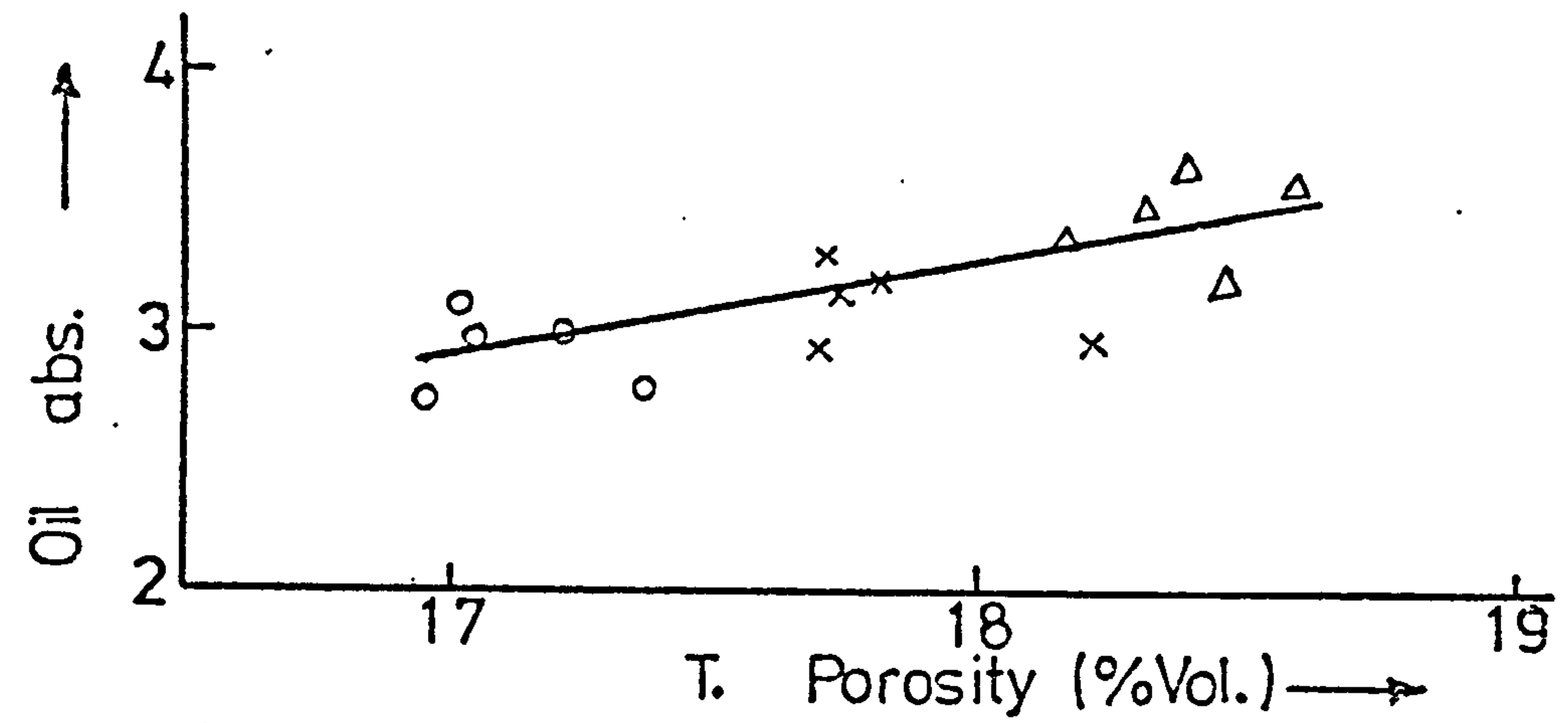

(B) SRPC + Cormix SP1

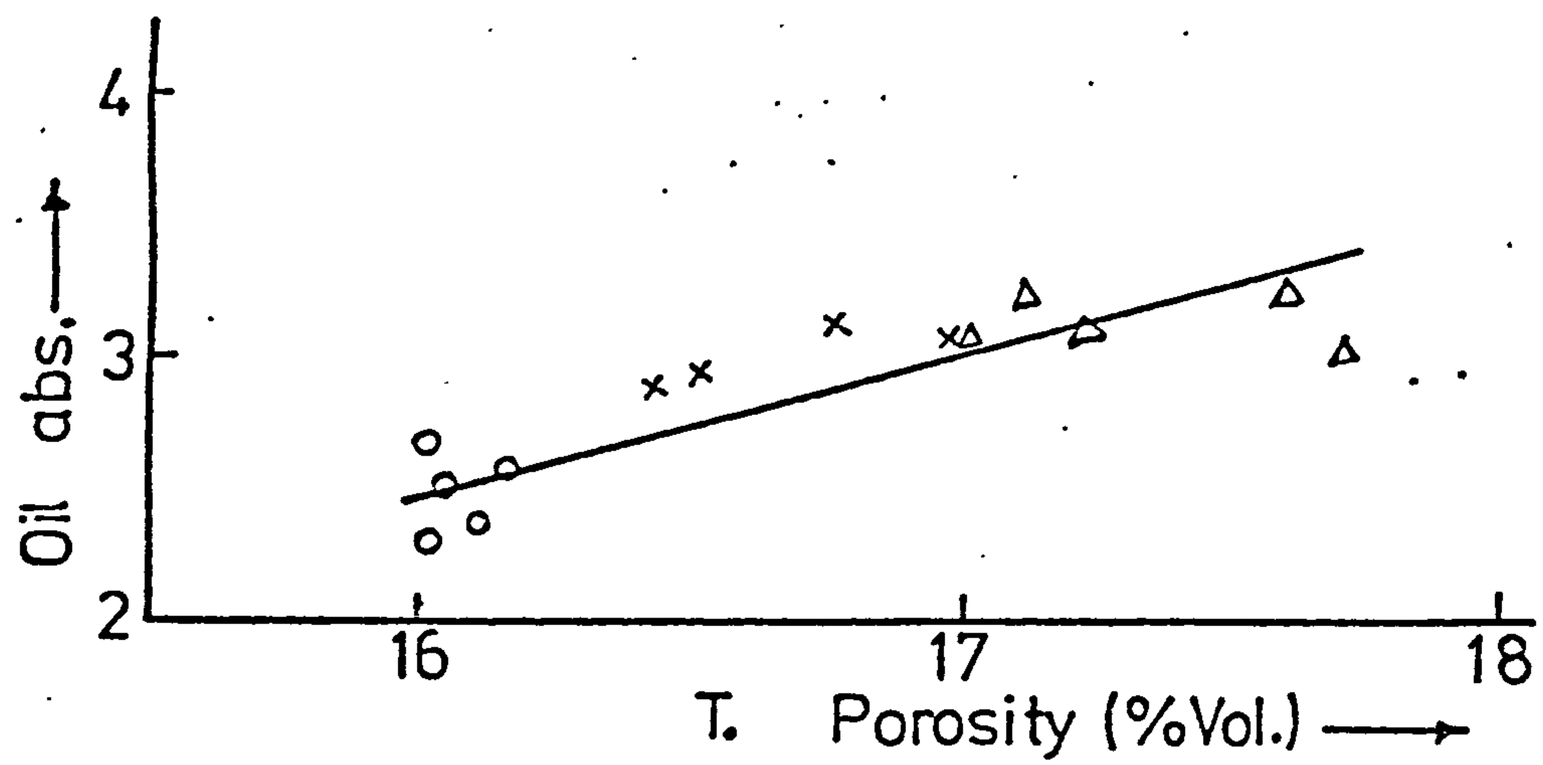

(C) OPC + Melment L10

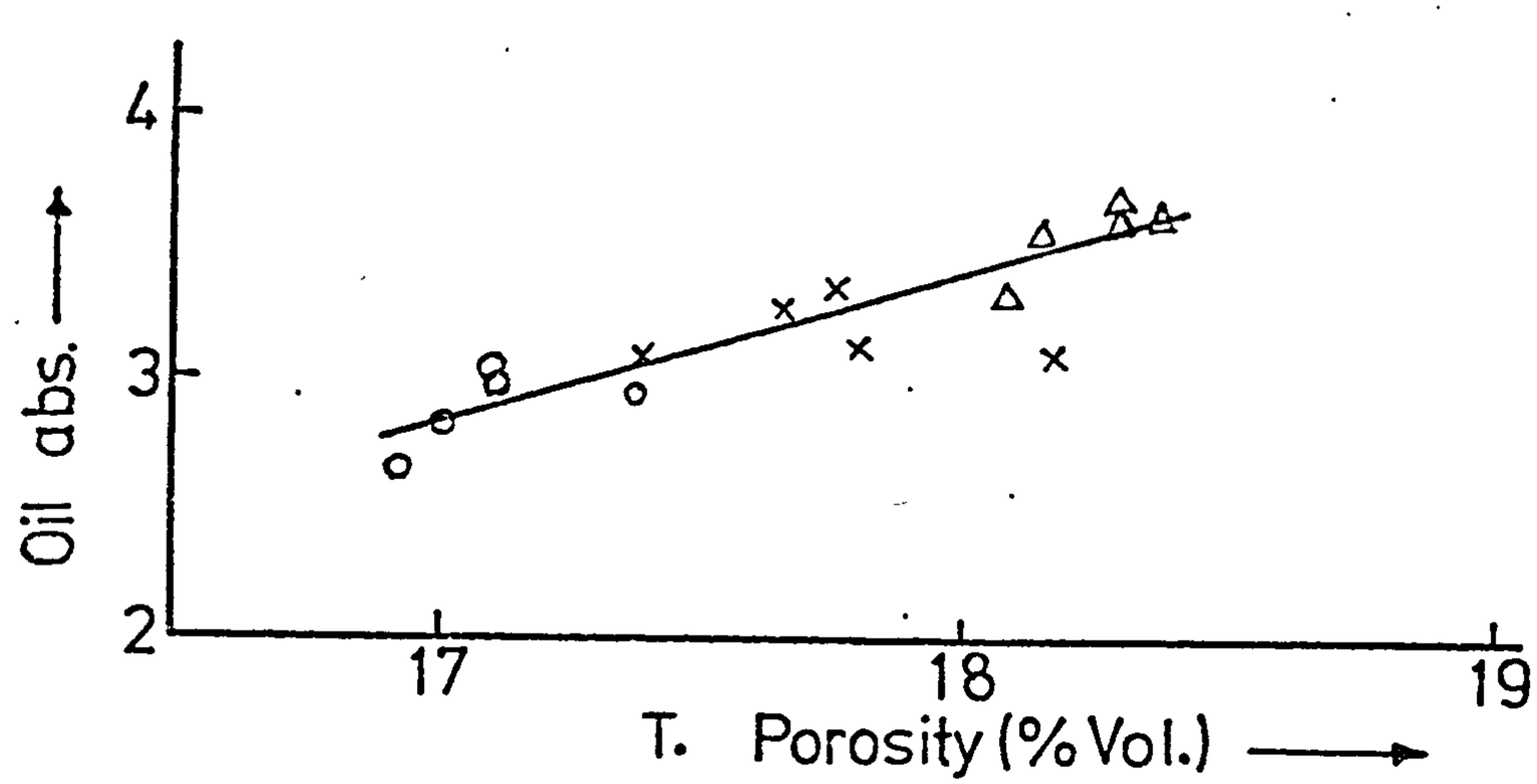

(D) SRPC + Melment L10

FIG(5.67) VARIATION OF OIL ABSORPTION WITH TOTAL POROSITY OF SUPERPLASTICISED CONCRETE

CHAPTER 6

SOME MECHANICAL PROPERTIES OF OIL SATURATED CEMENT PASTES AND CONCRETE

6.1 Introduction

Deflections, loss of prestress and bond in reinforced and prestressed concrete are influenced by Young's modulus and Poisson's ratio of the concrete. In this chapter, compressive strength (cube) and static modulus of elasticity of hardened cement pastes (HCPs) and concrete,were investigated at various ages and under various curing conditions. Poisson's ratio and volume expansion of concrete were also studied. The results show the changes that occur in these properties as a result of crude oil saturation using HCPs and concrete of various W/C ratios, cement types and admixture concentration. Oil saturation of the specimens was produced according to the procedure described in Section 3.6.

6.2 Experimental Programme and Procedure

6.2.1 Cement Pastes

The HCP specimens were cast and cured as described in chapter 3. The compressive strength samples were 50.8 mm (2") cubes and were tested at a loading rate of 15N/mm^2 per min. 2 cubes were crushed at each test and the average value taken.

The elastic modulus samples were 50 x 50 x 150 mm prisms. Two demec discs, 50 mm apart, were fixed at the centre of two opposite sides on each sample and strain readings were taken using a Demec gauge sensitive to to 1.98 x 10^{-5} mm/mm. To obtain a flat surface on the specimens and produce uniform contact between the upper plate of the testing machine and the upper surface of the specimen, a thin layer of plastic padding was placed on the specimen's top suface and covered with a sheet of thin aluminium foil. The plastic padding was then allowed to harden under a load of 1KN (0.4 N/mm^2) in the testing machine. A tangent elastic modulus was obtained from the stress-strain curve at 10 N/mm^2. Tests were carried out for upto 52 weeks (12 months) for compressive strengths and 39 weeks (8 months) for elastic modulus.

6.2.2 Concrete

The compressive strength tests were made on 100 mm or 101.6 mm (4") cubes according to BS 1881[135]. At each test, 3 cubes were crushed.

The elastic modulus tests were carried out according to BS. 1881: part 5[81]. Two specimens (100 x 100 x 300 mm) were tested at each age. Strains were measured with a Demec gauge on a 100 mm gauge length at the centre of two opposite sides of each prism. The gauge sensitivity was 1.65×10^{-5} mm/mm. A tangent elastic modulus was determined from the stress-strain curve at 10 N/mm^2. Poisson's ratio was determined from the modulus test using two additional Demec discs at 50 mm apart fixed in the lateral direction at the centre of the specimens. Test results are reported for upto 69 weeks (16 months).

6.3 Test Results for Hardened Cement Pastes (HCPs)

6.3.1 Compressive Strength of HCPs

6.3.1.1 Effect of Crude Oil Saturation on Compressive Strength at Various W/C Ratios

The variation of compressive strength with W/C ratio is illustrated in fig. (6.1), for the 3 storage conditions. These results were from the paste specimens used for the permeability tests given in table (5.4). It is observed that:

1. The compressive strength of crude oil saturated HCPs was generally lower than water saturated, surface dry samples (SSD) or those samples which had been dried and stored in a constant temperature room (CTR). The greatest decrease in value over the SSD samples was about 6.7%, but average decreases were between 4% and 5%. The strength variations of individual cubes from the mean values was small. The largest variations being about ± 2.5%.

2. The CTR pastes had higher strengths than either SSD or oil saturated pastes. The greatest increase over the SSD pastes was 15.9%, but the average increase was between 5% and 6% for OPC pastes, and about 11%

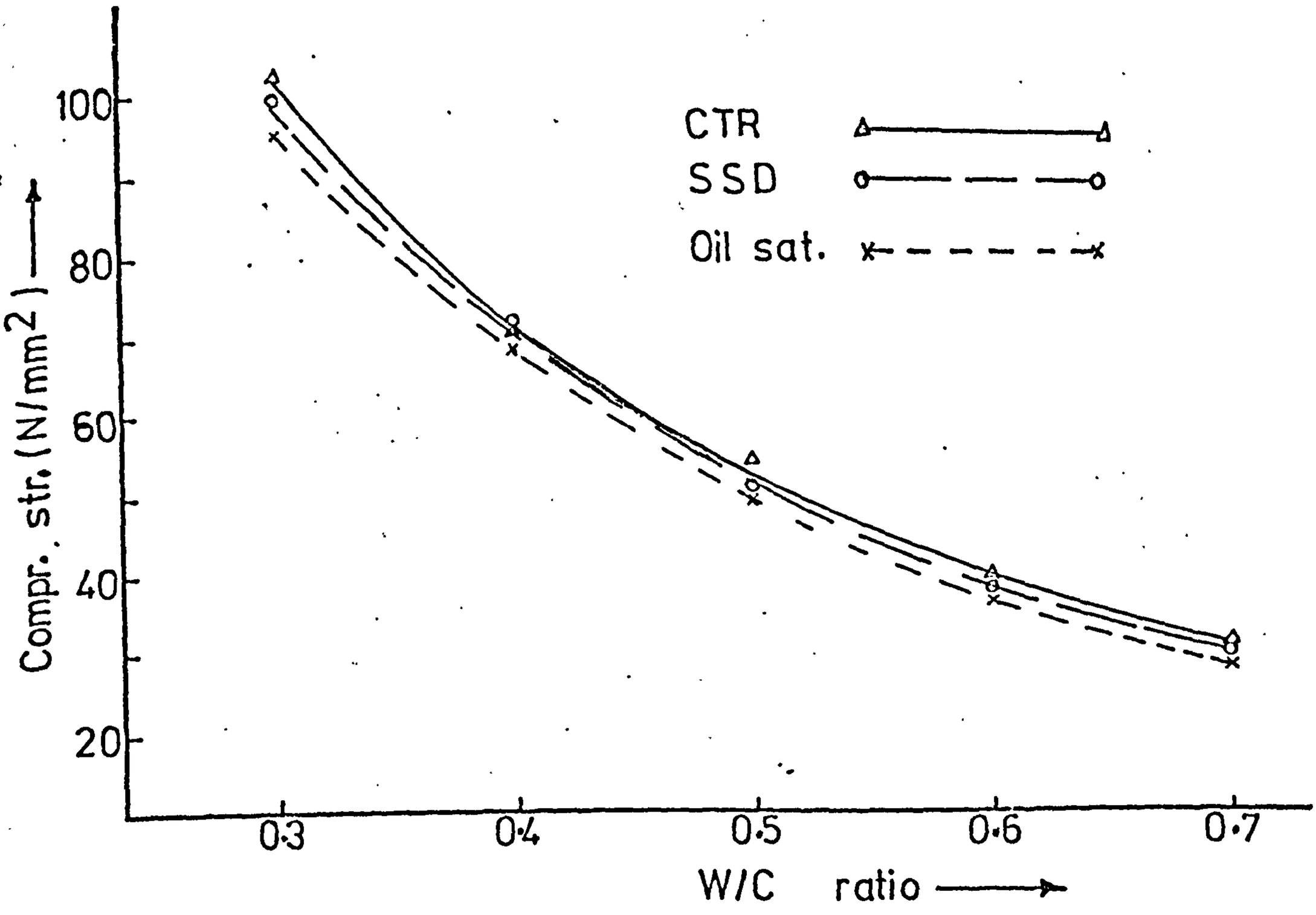

(A) OPC Paste

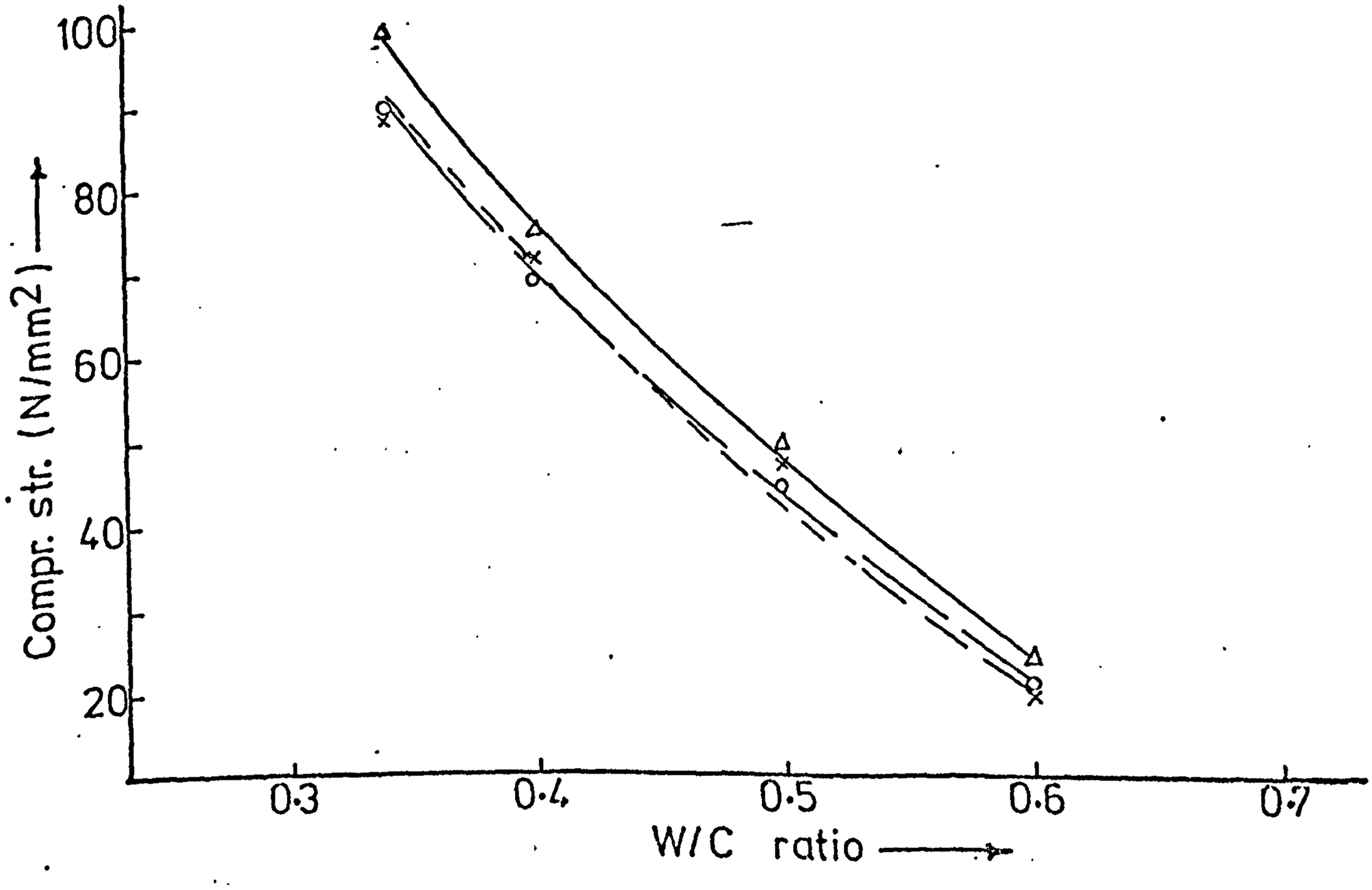

(B) SRPC Paste

FIG(6.1) VARIATION OF COMPR. STRENGTH WITH W/C RATIO & STORAGE CONDITIONS.

in SRPC pastes. The CTR pastes had strengths significantly higher than the oil saturated. The largest decrease due to oil saturation, over corresponding CTR pastes was 10.4% and 18.6% in OPC and SRPC pastes but the average decrease was about 8.5% for both pastes.

3. The relationship between compressive strength and W/C ratio, for any of test condition , can be expressed exponentially in the form:

$$S = S_o \text{ (exp) } b \text{ (W/C)} \qquad (6.1)$$

values of S_o and b were obtained for the pastes at SSD conditions and given in table (6.1).

PASTE	S_o	b	r^+
OPC	261.9	-3.203	-97.3
SRPC	363.9	-4.145	-97.4
OPC & Admix.	173.7	-2.489	-98.4
SRPC & Admix.	189.1	-2.762	-99.6

r^+ = correlation coefficient x 100%

Table (6.1) Constants of Regression - equ. (6.1)
Compr. Str. Vs W/C

6.3.1.2 Effect of Oil Saturation on the Cube Strength of HCPs at various ages and W/C Ratios

At 1, 2, 4, 13, 26 and 52 weeks, two cubes of HCPs which had been continuously cured in water at a constant temperature of $16^o \pm 0.5^oC$, were tested in the SSD condition and 4 were oven-dried to 105^oC. Two of these were saturated with crude oil (for 4 months) as described in Section 3.6 while the other two were sealed and stored at a constant temperature, also for 4 months. It is assumed that drying to 105^oC removes all evaporable water and therefore, hydration of the pastes stops[130]. Any change in strength is therefore due to crude oil saturation of the HCPs. The test results are given in table (6.2) and plotted in fig. (6.2).

It was observed that the strength of oil saturated cubes was lower

W/C RATIO	1 WEEK			2 WEEKS			4 WEEKS			13 WEEKS			26 WEEKS			52 WEEKS		
	SSD N/mm^2	CTR* N/mm^2	OIL SAT* N/mm^2	SSD N/mm^2	CTR N/mm^2	OIL SAT. N/mm^2	SSD N/mm^2	CTR N/mm^2	OIL SAT. N/mm^2	SSD N/mm^2	CTR N/mm^2	OIL SAT. N/mm^2	SSD N/mm^2	CTR N/mm^2	OIL SAT. N/mm^2	SSD N/mm^2	CTR N/mm^2	OIL SAT. N/mm^2
0.30	87.5	90.0	84.6	94.4	95.4	90.7	99.7	102.5	95.1	124.3	123.9	119.9	139.2	140.7	135.5	144.0	148.8	141.1
0.35	69.9	71.9	68.0	76.0	78.5	73.8	87.2	86.5	84.9	100.8	102.0	96.8	104.8	108.1	99.8	114.0	116.4	110.2
0.40	61.1	62.5	58.8	63.6	65.7	65.2	72.1	70.5	68.3	83.2	87.5	81.0	86.2	90.4	84.0	90.4	93.8	88.0
0.50	42.2	45.8	40.1	48.4	51.6	46.6	51.1	54.2	49.2	62.4	64.4	58.6	68.0	72.2	70.5	75.3	77.4	72.3
0.60	32.8	35.9	31.0	38.4	39.0	38.4	38.6	39.5	36.3	47.4	46.8	44.0	47.6	50.8	44.7	53.7	54.6	51.0
0.70	18.4	20.5	16.5	24.8	27.0	21.8	30.2	31.2	28.2	34.0	34.9	31.2	36.8	37.5	34.0	38.5	41.8	36.2

* CTR and Oil Saturated pastes were tested 4 months from the periods given above

Table (6.2) Compressive Strength of OPC Cement Pastes at Various Ages, W/C Ratios and Storage Conditions

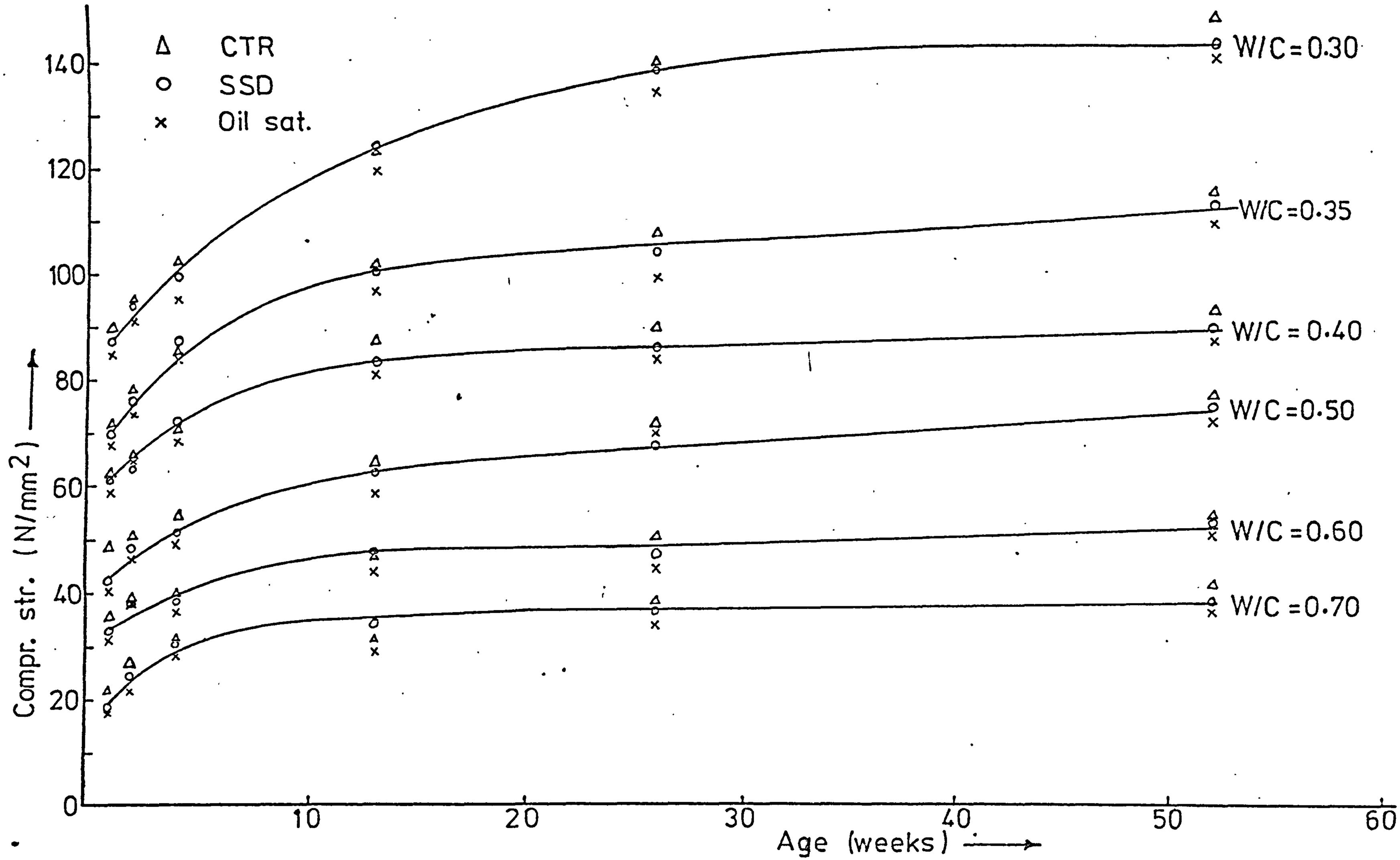

FIG(6.2) EFFECT OF STORAGE CONDITIONS ON THE COMPR. STRENGTH OF OPC PASTES AT VARIOUS AGES & W/C.

at all ages and W/C ratios than those tested in either SSD condition or dried condition (CTR). There was some indications that older pastes have lower percentage strength reductions. This tendency is thought to be as a result of reduced pore volume and will be examined further in chapter 7.

6.3.1.3 Effect of Crude Oil Saturation on the Strength of Superplasticised HCPs

The variations of compressive strength with W/C ratio for HCPs containing 4% of the cement content weight of Cormix SP1 superplasticiser are illustrated in fig. (6.3). The effect of varying the admixture concentration at a constant W/C ratio of 0.4 is illustrated in fig. (6.4). These HCPs were used latter for permeability tests and the strengths are given in table (5.4). As for plain HCPs, the scatter of individual paste strength was small with a maximum scatter of about ± 3.0%. It is observed that:

1. The strength of HCPs containing 4% admixture was generally lower than those without admixture at equal W/C ratios. At low admixture concentrations of 1% and 2%, the HCP strengths were slightly higher than for plain pastes.

2. The reductions in strength for the oil saturated cubes were generally of the same order of magnitude as was observed in ordinary HCPs. The largest decrease in strength over SSD paste was 10.6% but the average decrease was about 6% and 4% in OPC and SRPC pastes respectively.

6.3.2 Static Modulus of Elasticity of HCPs

6.3.2.1 Stress-strain Curves

Typical stress-strain curves are shown in fig. (6.5) for OPC and SRPC pastes, and in fig. (6.6) for pastes containing various concentrations of Superplasticiser. The following is observed:

1. The curves were generally non-linear and as expected the non-linearity increased with an increase in W/C ratio. The non-linearity was also affected by the curing process of the samples. Pastes continuously cured in water exhibited greater linearity hence stiffness than the oil saturated samples. The non-linearity slightly increased with prolonged storage in

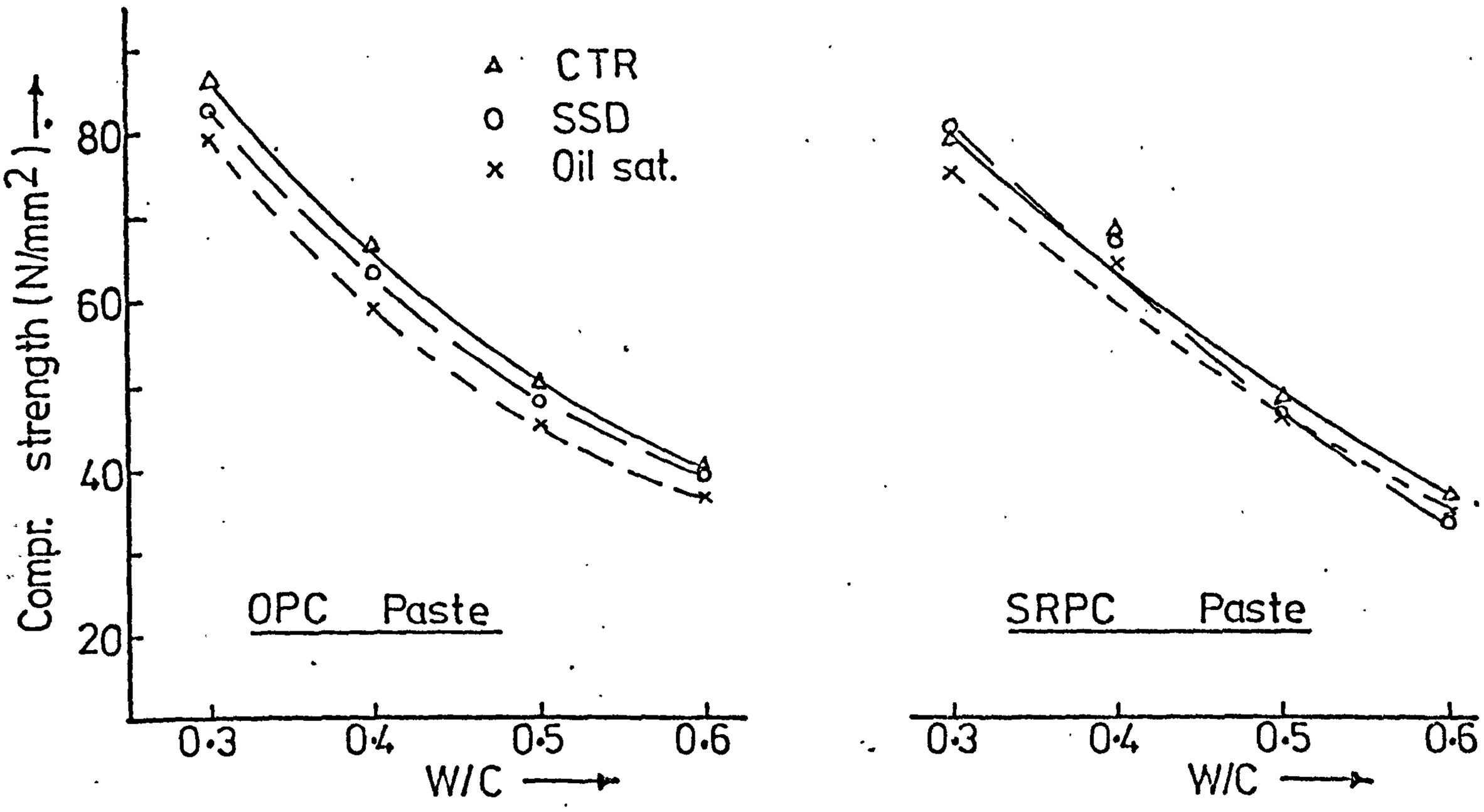

FIG(6.3) EFFECT OF STORAGE CONDITIONS ON THE COMPR. STRENGTH OF SUPERPLASTICISED HCPs AT VARIOUS W/C.

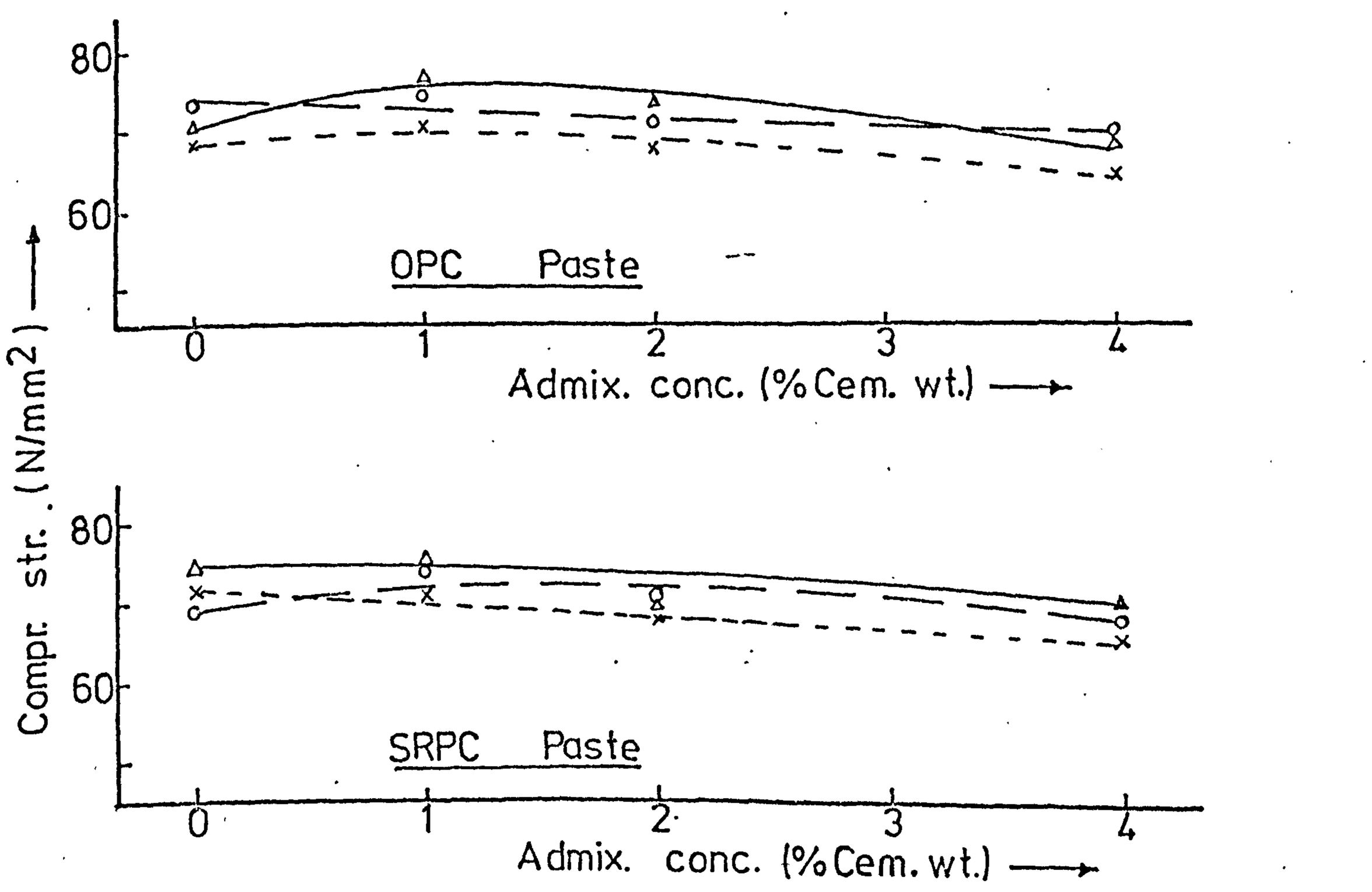

FIG(6.4) COMPR. STRENGTH OF OPC PASTES (W/C=0·4) AT VARIOUS ADMIX. CONC. & STORAGE CONDITIONS

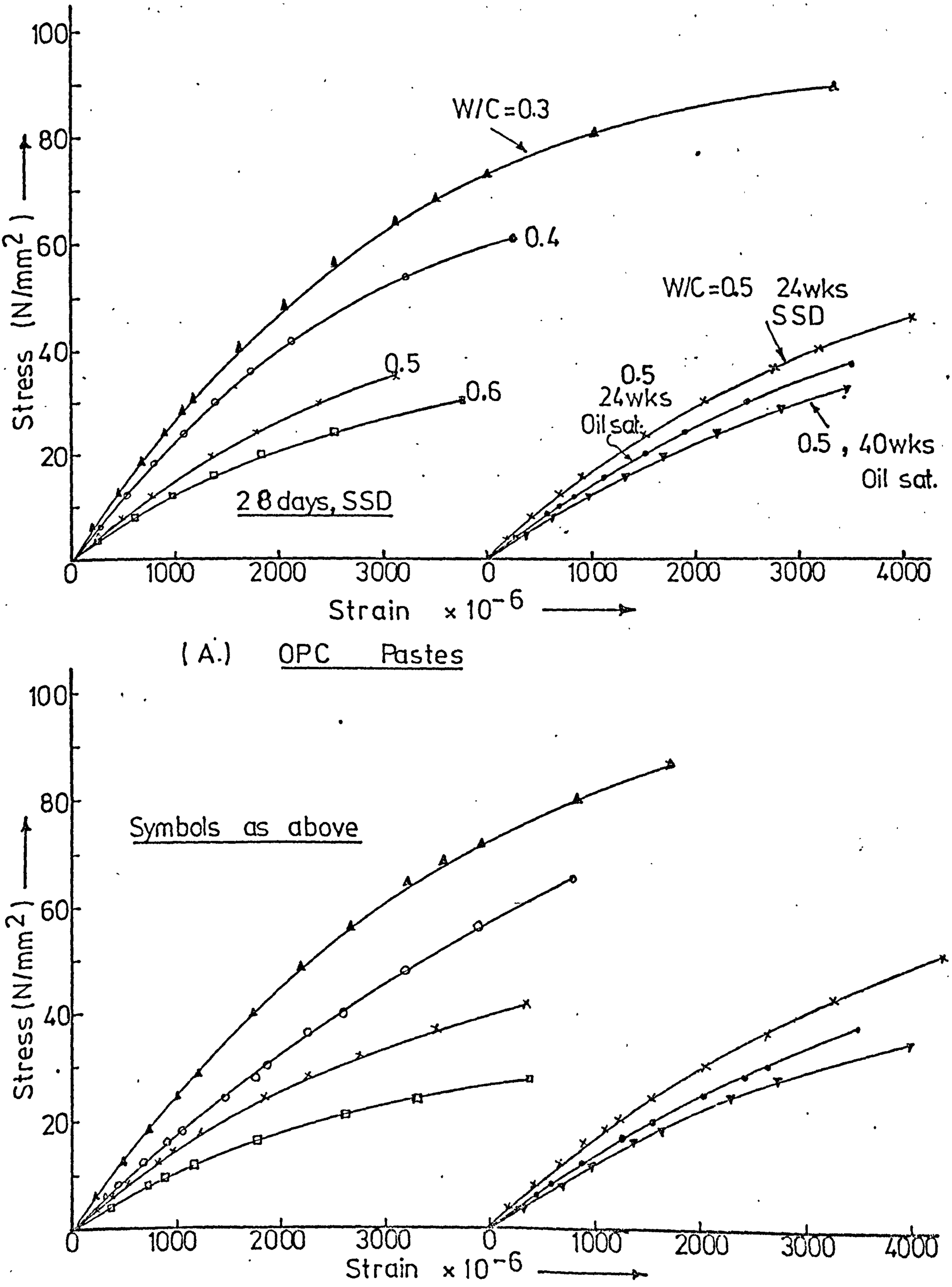

(A.) OPC Pastes

(B) SRPC Pastes

FIG(6.5) EFFECT OF STORAGE CONDITIONS & W/C ON THE STRESS—STRAIN RELATIONSHIP — HCPS.

crude oil.

2. The failure of the specimens generally, was instant and violent, and particularly so for pastes of low W/C ratio and for CTR dried specimens. The failure of the crude oil saturated specimens was almost similar to the dried ones.

Tables (6.3) and (6.4) give the modulus of elasticity and failure stress for all the HCPs tested. Results for pastes containing superplasticiser are shown in tables (6.6) and (6.7).

6.3.2.2 Effect of Crude Oil Saturation on the Elastic Modulus and Prism Strength of Plain HCPs

The variation of elastic modulus with W/C ratio is illustrated in fig. (6.7) and for failure stress in fig. (6.8). Two samples were tested to failure at each test. Variations of each individual sample from the mean values was small and of the order of ± 2%. The following is observed.

1. Generally, elastic modulus decreased with an increase in the W/C ratio following an exponential relationship of the form:

$$E = E_o (exp)^{b\,(W/C)} \qquad (6.2)$$

The constants E_o and b were obtained by regression analysis and are given in table (6.5).

2. For each W/C ratio, the storage condition considerably affected the values of the elastic modulus. HCPs continuously cured in water (SSD) have a higher elastic modulus, than those stored in oil. The dried specimens (CTR) had the lowest elastic modulus, eg. after 24 weeks, the SSD samples were between 5 to 14% higher than the modulus of the specimens at 4 weeks; but CTR samples were between 11 and 22% less and the oil saturated samples were between 4 and 13% less.

3. The elastic modulus decrease slightly during storage in crude oil. For OPC pastes, the elastic modulus of oil saturated specimens was between 2 and 7% less at the 40th week than at the 24th week. For SRPC pastes, the decrease was between 0 and 9%.

AGE	4 WEEKS	24 WEEKS			40 WEEKS	
W/C	SSD (KN/mm^2)	SSD (KN/mm^2)	CTR	OIL SAT.	SSD	OIL SAT.
0.30	26.8 (90.8)	28.6 (101.5)	20.9 (94.0)	25.3 (76.4)	30.1 (120.4)	24.8 (76.1)
0.40	21.7 (61.0)	22.8 (69.0)	18.2 (56.0)	20.3 (52.4)	24.2 (74.3)	19.5 (51.3)
0.50	16.6 (36.2)	18.8 (46.7)	14.5 (41.2)	16.0 (37.6)	20.0 (49.6)	15.2 (34.2)
0.60	13.4 (30.2)	14.8 (34.9)	12.0 (32.0)	12.8 (31.2)	16.2 (37.6)	11.6 (30.8)

Values in brackets represent failure stresses - N/mm^2

Table (6.3) Elastic Modulii and Failure stresses for OPC pastes

AGE	4 WEEKS	24 WEEKS			40 WEEKS	
W/C	SSD (KN/mm^2)	SSD (KN/mm^2)	CTR	OIL SAT.	SSD	OIL SAT.
0.33	26.3 (86.4)	28.9 (100.0)	21.6 (92.0)	24.9 (76.8)	31.1 113.2	24.9 (76.3)
0.40	21.5 (62.8)	23.9 (71.5)	18.1 (66.0)	18.6 (52.8)	26.0 (83.7)	17.9 (52.9)
0.50	15.8 (41.6)	18.1 (53.2)	14.0 (44.2)	14.9 (37.2)	18.2 (56.0)	13.6 (36.4)
0.60	11.5 (29.6)	13.4 (33.9)	10.9 (31.0)	11.4 (30.0)	15.4 (36.4)	10.7 (29.9)

Values in brackets represent failure stresses - N/mm^2

Table (6.4) Elastic Modulii and Failure Stresses for SRPC pastes

CEMENT	AGE AND CURING		E_o	b	r
OPC	28 D	SSD	54.12	-2.331	-99.5
	24 Weeks	SSD	54.60	-2.159	-99.5
	24 Weeks	CTR	36.94	-1.852	-99.8
	24 Weeks	Oil Sat.	43.21	-2.054	-99.2
	40 Weeks	SSD	55.73	-2.065	-99.4
	40 Weeks	Oil Sat.	38.77	-2.110	-98.2
SRPC	28D	SSD	72.12	-3.044	-99.6
	24 Weeks	SSD	72.90	-2.800	-99.6
	24 Weeks	CTR	49.86	-2.538	-99.5
	24 Weeks	Oil Sat.	48.03	-2.369	-99.7
	40 Weeks	SSD	76.72	-2.733	-98.8
	40 Weeks	Oil Sat.	45.74	-2.441	-99.5

r = correlation coefficient x 100%

Table (6.5) Constants of Regression - equ. (6.2)

El. Mod. Vs W/C

4. Plots of the variation of failure stress with W/C ratio are given in fig. (6.8). The following observations are made:

(a) The plots are similar in form to those obtained for the elastic modulus.

(b) The failure stress depends upon the curing procedure of the pastes, eg. specimens continuously cured in water (SSD) increased with age- being between 12 and 29% higher after 24 weeks than after 4 weeks. CTR samples were between 3 and 14% higher while oil saturated pastes were between 3 and 16% less.

(c) The failure stress decreases slightly over a longer period during storage in oil. After 40 weeks, the failure stresses for OPC pastes were between 0.4% and 9% less than after 24 weeks. Reductions in SRPC pastes on prolonged storage were negligible - after 40 weeks the failure stresses were only between 0.5% and 4% less than after 24 weeks.

6.3.2.3 Effect of Crude Oil Saturation on the Elastic Modulus of Superplasticised HCPs

In this series of tests 1, 2 and 4% by weight of cemert content, of Cormix SP1 superplasticiser was added to the pastes at a constant W/C ratio of 0.4. The pastes were cured as described in section 3.6. The test results are shown in tables (6.6) and (6.7) for OPC and SRPC pastes respectively. Typical stress-strain curves are illustrated in fig. (6.6). The variations of elastic modulus with admixture concentration are illustrated in fig. (6.9), for different ages and storage conditions. The following observations are made:

1. Pastes containing 1% and 2% admixture have higher elastic modulus than ordinary pastes but there is very little difference at higher admixture concentrations of 4%. The highest increases were for SSD samples and were between 11 and 37% higher in OPC pastes, and 4 to 15% in SRPC pastes.

2. The elastic modulus was also affected by the curing procedure of the HCPs, eg. after 24 weeks CTR pastes were between 15 and 28% less than the value at 4 weeks of SSD pastes and oil saturated pastes were between 5% and 14% less. Prolonged storage in crude oil produced almost similar

AGE	4 WEEKS	AT 24 WEEKS			AT 40 WEEKS		
PASTE DESIGN.	SSD (KN/mm^2)	SSD	CTR	OIL SAT.	SSD	CTR	OIL SAT.
COP4-1	26.2 (64.4)	30.0 (73.5)	18.8 (72.0)	22.4 (65.6)	32.1 (78.0)	19.8 (61.2)	21.6 (64.0)
COP4-2	24.2 (69.6)	28.0 (74.9)	20.4 (70.8)	22.3 (71.2)	33.1 (80.2)	20.7 (74.4)	22.0 (68.6)
COP4-4	20.8 (68.0)	22.5 (70.3)	16.7 (51.6)	19.7 60.2)	25.5 (72.8)	18.3 (54.4)	18.5 (60.0)

Values in brackets represent failure stresses - N/mm^2

Table (6.6) Elastic Modulii and Failure Stresses for OPC Pastes, W/C = 0.4 + 1, 2, & 4% Superplasticiser

AGE	4 WEEKS	AT 24 WEEKS			AT 40 WEEKS		
PASTE DESIGN.	SSD (KN/mm^2)	SSD	CTR	OIL.SAT.	SSD	CTR	OIL SAT.
CSR4-1	23.4 (57.2)	26.0 (71.4)	18.0 (69.8)	20.0 (61.2)	29.9 (80.0)	20.1 (69.2)	19.4 (60.8)
CSR4-2	21.1 (66.0)	23.3 (75.2)	17.1 (66.6)	21.1 (64.8)	29.7 (79.6)	18.2 (70.4)	20.0 (63.2)
CSR4-4	18.2 (56.4)	20.9 (63.8)	17.5 (49.6)	19.2 (48.0)	23.6 (65.0)	17.6 (55.6)	18.7 (47.8)

Values in brackets represent failure stresses - N/mm^2

Table (6.7) Elastic Modulii and Failure Stresses for SRPC Pastes, W/C = 0.4 + 1, 2, and 4% Superplasticiser

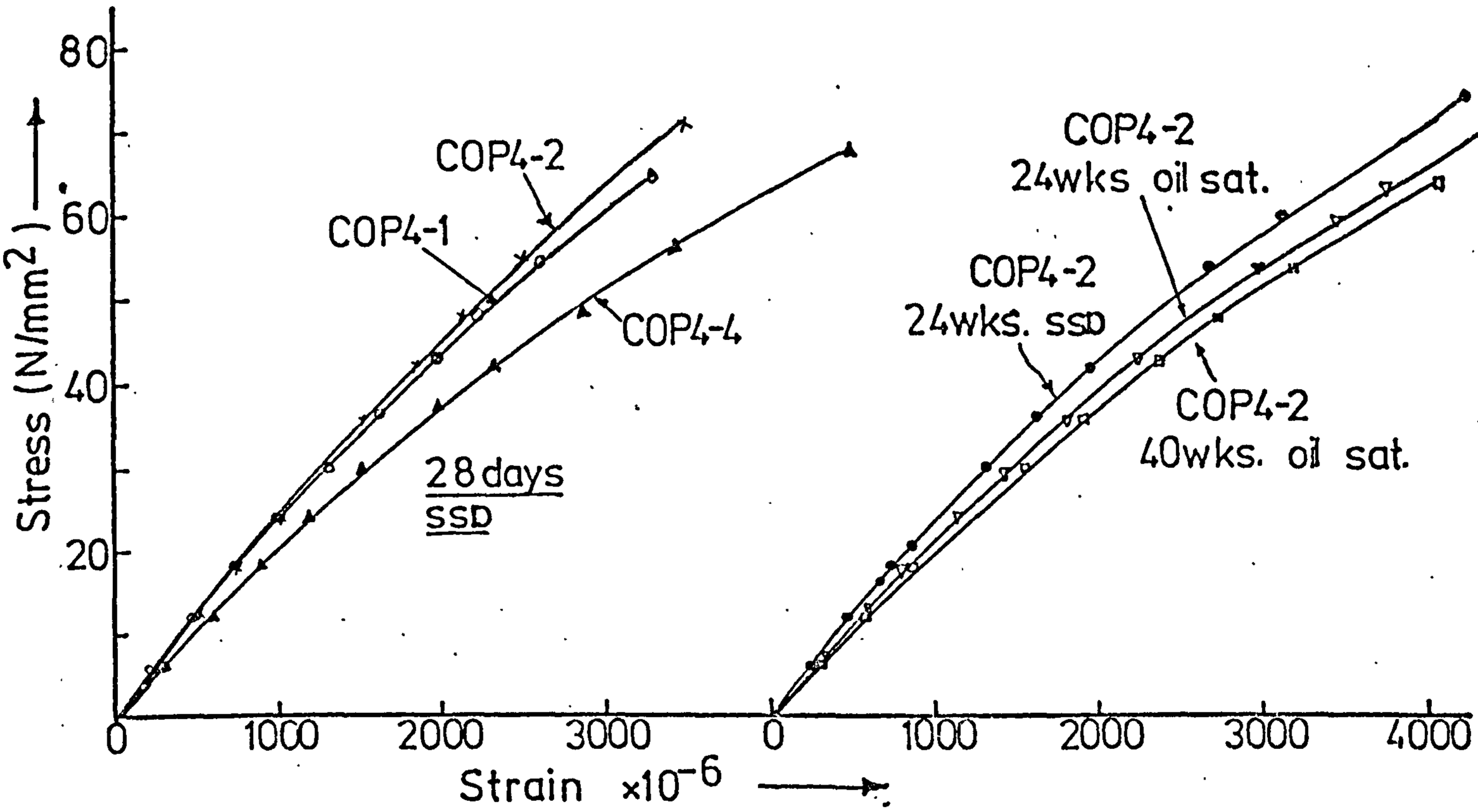

(A) OPC Pastes

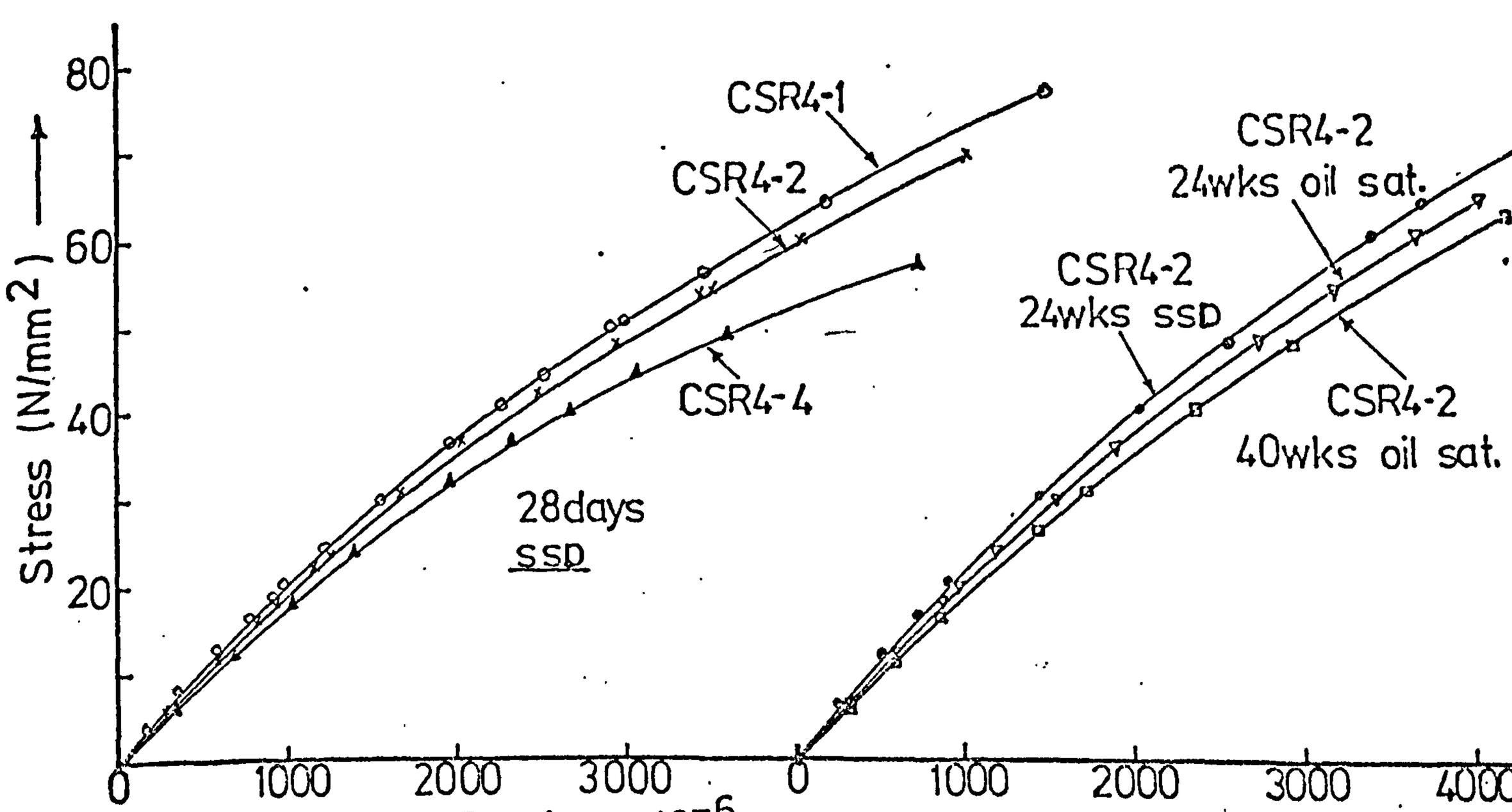

(B) SRPC Pastes

FIG(6.6) EFFECT OF STORAGE CONDITIONS ON THE STRESS-STRAIN RELATIONSHIP FOR SUPERPLASTICISED HCPs.

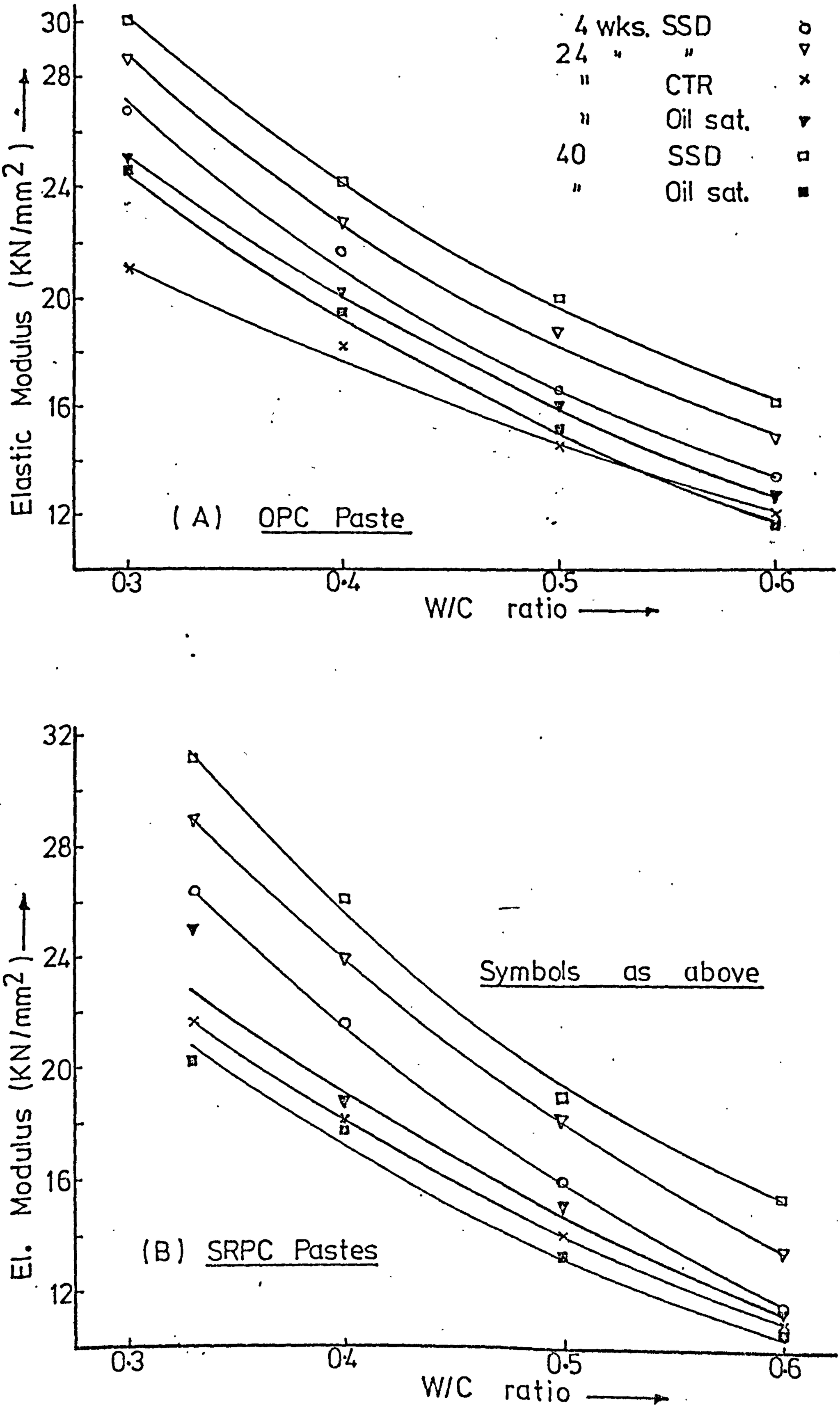

FIG(6.7) EFFECT OF STORAGE CONDITIONS & W/C ON THE ELASTIC MODULUS OF HCPs.

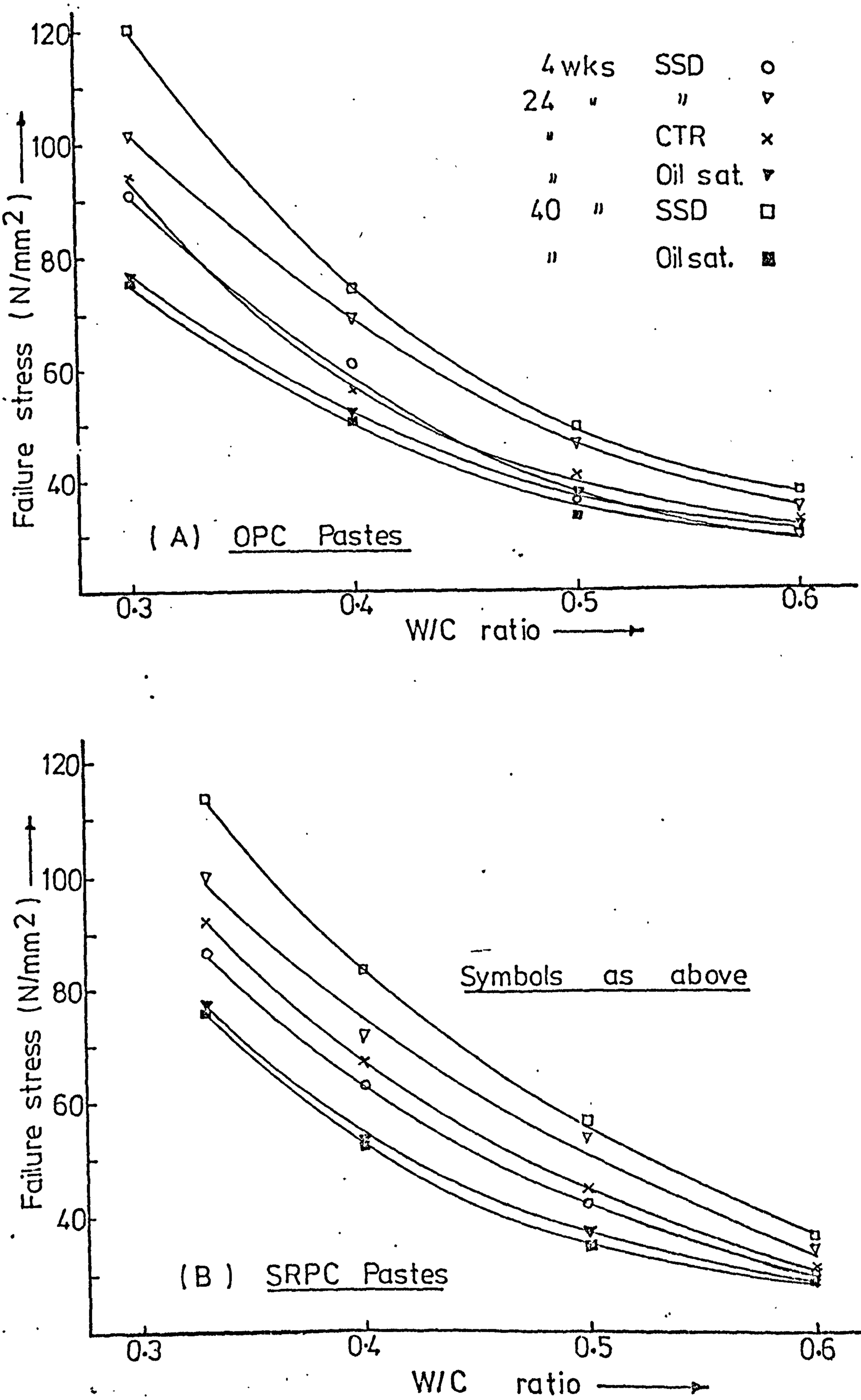

FIG(6.8) EFFECT OF STORAGE CONDITIONS & W/C. ON PRISM FAILURE STRESS, HCPs.

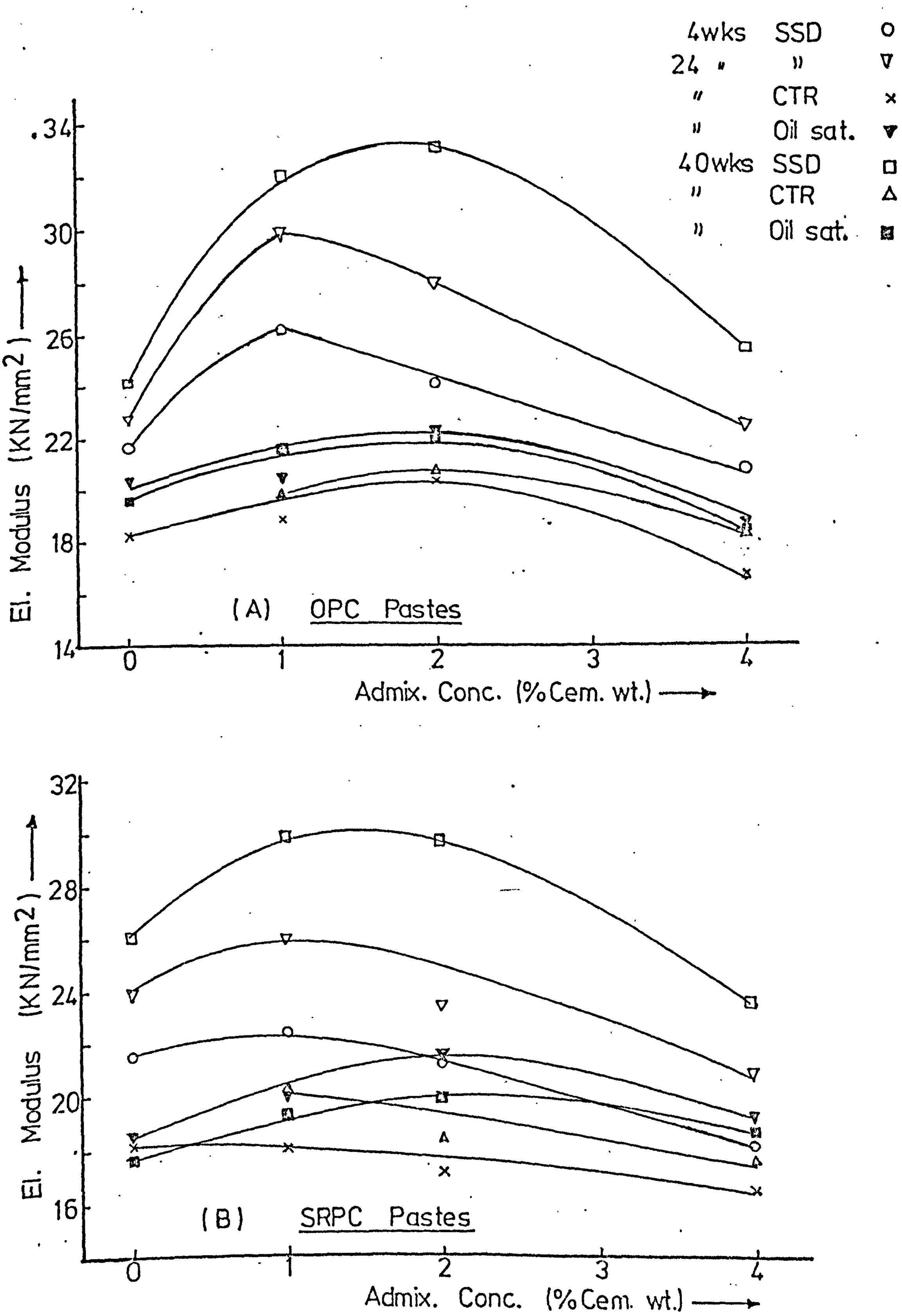

FIG(6.9) EFFECT OF STORAGE CONDITIONS & ADMIX. CONC. ON THE ELASTIC MODULUS OF HCPs.

changes in modulus and failure stresses in superplasticised pastes as in ordinary pastes.

3. At every age the value of oil saturated superplasticised pastes were generally higher than for ordinary pastes at the same W/C ratio (0.4), eg., after 24 weeks superplasticised OPC pastes were about 13.3% higher for concentrations of 1% and 2% but 3% less for concentration of 4% than for ordinary paste of W/C = 0.4

6.4 Test Results for Concrete Mixes

6.4.1 Compressive Strength

6.4.1.1 Effect of Crude Oil Saturation on the Compressive Strength of Concrete

In tables (5.9) and (5.10), 3 values of compressive strength were given, for each OPC and SRPC concrete mix at 3 different storage conditions. The values were the mean of the three cubes results. Variation of individual sample strength from the mean value was small with a maximum difference from the mean of about ± 5% and the average difference about ± 2.5%. The values are plotted in fig. (6.10) against the corresponding W/C ratios. The experimental points were omitted for clarity. The following observations are made:

1. The relationship between strength and W/C ratio, for each curing procedure, can be expressed in the exponential form:

$$f_c = f_o \, (\exp) \, b(W/C) \qquad (6.3)$$

The constants f_o and b are given in table (6.8).

2. The compressive strength of crude oil saturated cubes were lower than those of the reference CTR samples. For OPC concrete, the smallest and largest strength reductions were 2.7% and 16.5%. Average reductions were of the order of 9%. For SRPC concrete, the reductions were 1.8% and 11.3%, with an average of about 8%. For both concrete, the actual numerical reduction was almost similar and independent of W/C. For OPC concrete, the maximum reduction within the 4 months period in oil was about

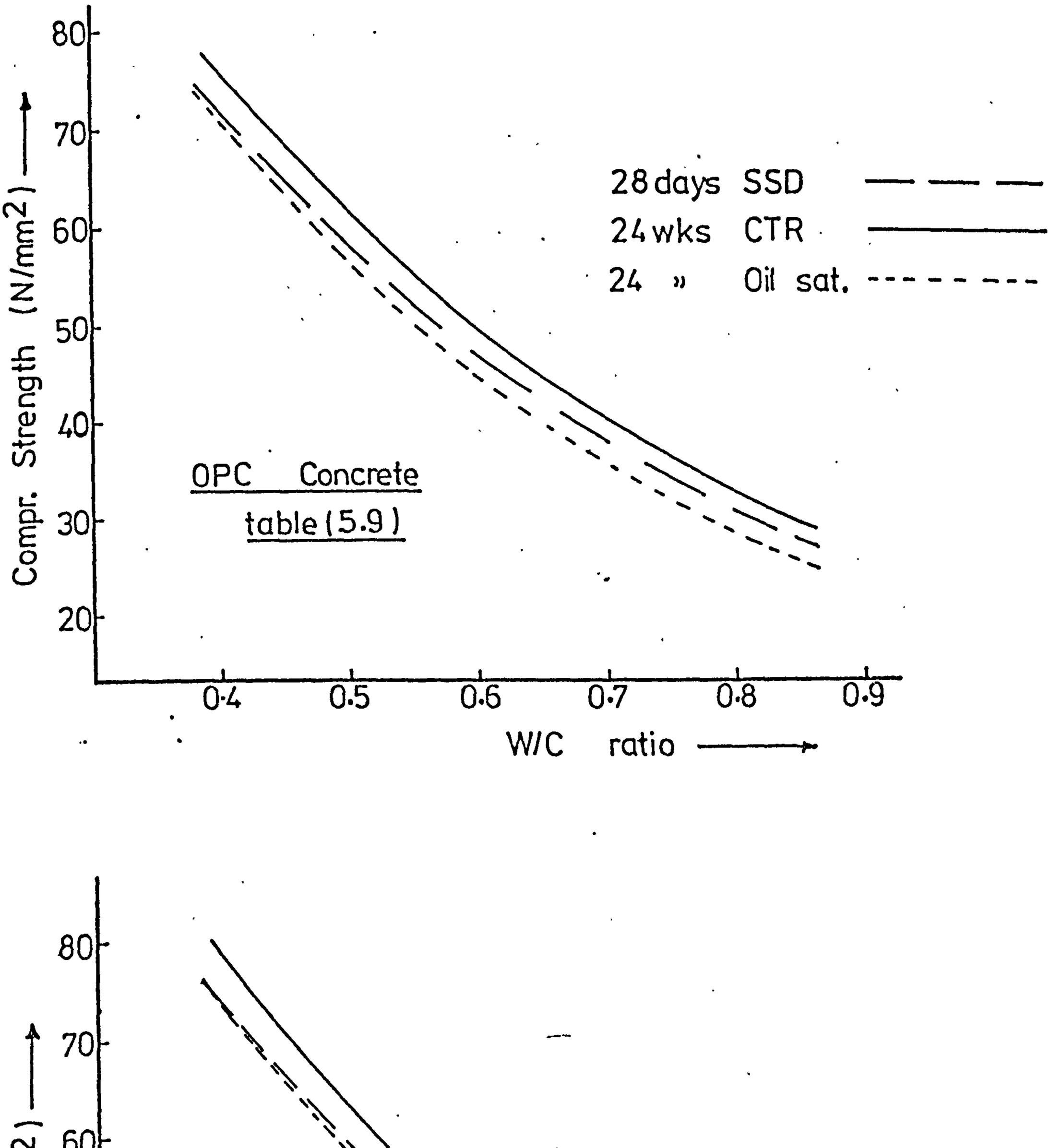

FIG(6.10) EFFECT OF STORAGE CONDITIONS & W/C. ON THE CUBE STRENGTH OF CONCRETE.

7.2 N/mm^2 with an average value of about 5 N/mm^2. The average reduction in SRPC concrete was about 4 N/mm^2.

3. The strength of crude oil saturated samples was generally lower than the SSD cubes ie. the value at 28 days. The average reduction for OPC concrete was about 4%. The reductions were very small for high strength concretes, and for high strength SRPC concretes, the reductions were negligible.

CONCRETE	STORAGE	f_o	b	r
OPC	SSD	173.2	-2.159	-97.7
	CTR	175.5	-2.091	-97.6
	Oil Sat.	174.9	-2.248	-97.8
SRPC	SSD	177.4	-2.222	-98.6
	CTR	192.0	-2.248	-98.6
	Oil Sat.	185.0	-2.327	-98.6

Table (6.8) Constants of Regression - Equ. (6.3)
Strength Vs. W/C

6.4.1.2 Effect of Prolonged Storage in Crude Oil on the Compressive Strength of Concrete

The specimens used here have mix parameters as shown in table (3.8) and (3.9). They were cured as described in Section 3.6. The test results are shown in table (6.9) and illustrated in fig. (6.11). The following observations are made:

1. The strength of the Concrete increased on drying. After 24 weeks, the strength of the reference CTR cubes were between 8 to 12% higher than at 28 days SSD. The strength of the dried specimens fell during storage and after 40 weeks had reduced by between 2 and 3.8% of their values after 24 weeks.

2. The compressive strength of concrete decreased continuously during storage in crude oil. After 24 weeks, the reduction in strength over

CEMENT TYPE	W/C RATIO	4 WEEKS	AT 24 WEEKS		AT 40 WEEKS		AT 58 WEEKS
		SSD_2 (N/mm^2)	CTR^+ (N/mm^2)	(N/mm^2)	CTR^+	OIL SAT.	OIL SAT.
OPC Table (3.8)	0.40	81.0	88.8	83.3	86.7	80.5	79.8
	0.50	65.7	69.8	65.8	68.1	63.1	62.8
	0.60	50.0	55.0	53.5		49.3	48.1
	0.70	43.4	48.3	45.3		42.0	40.3
SRPC Table (3.8)	0.40	79.5	85.6	82.3	84.5	79.0	77.3
	0.50	62.9	70.5	66.5	67.8	61.7	60.8
	0.60	42.4	46.4	44.1		41.8	40.1
	0.70	31.8	35.7	33.8		31.0	29.5
OPC + 4% Cormix Table (3.9)	0.40	84.5	93.0	88.5	89.8	84.3	83.7
	0.50	75.6	83.0	76.5	79.9	71.8	70.0
	0.60	58.7	65.1	60.3	64.0	57.6	56.0
	0.70	46.5	51.9	47.7	50.3	45.7	44.1

$^+$ Dried to 105°C and stored, sealed in CTR

Table (6.9) Compressive Strength of Concrete Cube Specimens

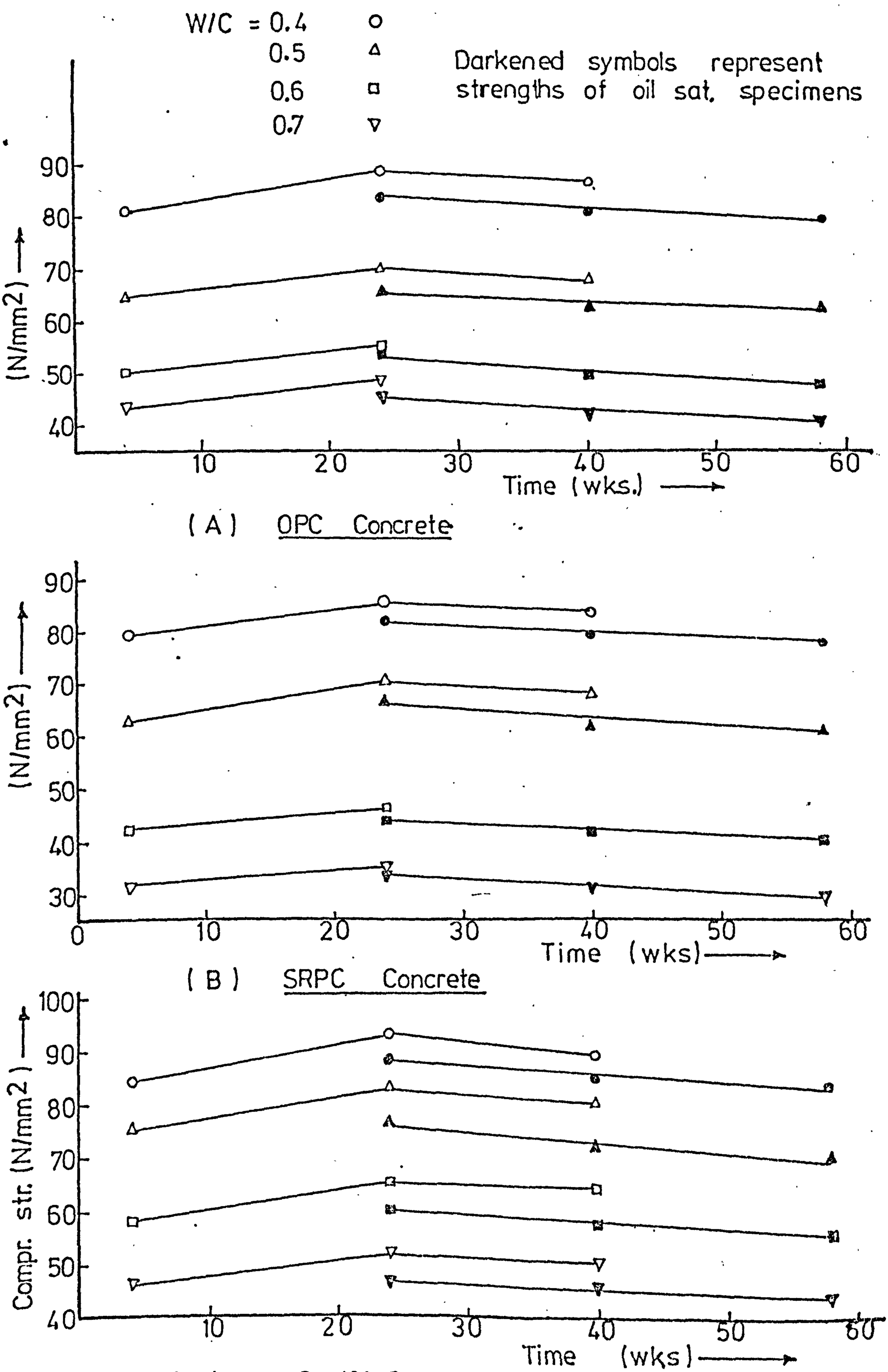

FIG (6.11) VARIATION OF COMPR. STRENGTH WITH STORAGE IN CRUDE OIL.

CTR samples was between 6 and 10%. After 58 weeks, the strength had reduced by between 10 and 17.4%. Compared with the 28 days SSD strength, the reductions were only between 1.5% and 7.3%.

6.4.2. Elastic Modulus of Concrete

6.4.2.1 Stress-strain Curves

The static modulus of elasticity was determined from stress-strain curves for prisms tested to failure. Typical curves are given in fig. (6.12) for concrete of 0.4 W/C ratio. The following observations are made:

1. For most specimens with the same W/C ratio, the stress-strain relationship was identical at low loadings irrespective of curing condition For OPC concrete, fig (6.12), the relationships were identical for the three storage conditions to about 10 N/mm^2 ie. 15% of the failure stresses. After this point, the curves branched out.

2. At high loads, the curves for oil saturated specimens branched off more sharply. In fig. (6.12), for OPC concrete, the curve for oil saturated specimens branched off at about 35% of the failure stress. The points at which the curves branched off varied in the various test specimens between 7.5 and 25 N/mm^2 depending on the W/C ratio. These represent between 20% and 45% of the failure stresses.

3. Table (6.10) shows the values of the failure stress. The values decreased as a result of crude oil saturation. For OPC concrete, crude oil saturation leads to between 2.2% and 6.2% reduction in the failure stress after 4 months in oil (24 weeks). After 15 months (69 weeks), the reductions were between 6 and 15% of the CTR values at 24 weeks.

6.5.2.2 Effect of Oil Saturation on Elastic Modulus of Concrete

Table (6.11) gives the values of the elastic modulus of OPC and SRPC concretes at various storage conditions. Two samples were crushed at each test and the mean value taken. The maximum deviation of any individual specimen from the mean was about ± 6%, the average deviations was ± 3%. The variation of elastic modulus with W/C ratio is illustrated in fig. (6.13) for SSD, CTR and samples stored in oil for 4 months. The following

CEMENT TYPE	W/C RATIO	4 WEEKS	24 WEEKS		40 WEEKS		58 WEEKS	69 WEEKS
		SSD (N/mm^2)	CTR+	OIL SAT.	CTR+	OIL SAT.	OIL SAT. (N/mm^2)	OIL SAT.
OPC	0.40	65.6	68.0	64.9	67.7	64.7	63.8	63.0
	0.50	46.9	49.9	48.7	47.3	45.5	45.0	44.2
	0.60	40.0	43.1	41.5	36.0	38.5	38.0	35.8
	0.70	27.0	33.8	31.7	32.7	31.1	30.3	29.5
SRPC	0.40	66.6	73.4	69.5	68.8	66.6	65.4	
	0.50	44.0	55.8	53.4	49.1	52.8	51.3	
	0.60	28.8	34.5	33.5		32.5	31.1	
	0.70	22.6	28.4	29.4		25.4	24.3	
OPC	0.40	69.5	75.4	72.3		70.9	70.3	
+	0.50	48.5	59.6	63.8		57.8	56.5	
4%	0.60	36.5	41.0	40.1		40.1	28.0	
Cormix	0.70	29.8	35.8	32.0		32.2	31.5	

+ Dried to 105°C and stored sealed in CTR

Table (6.10) Failure Stresses (N/mm^2) for Concrete

CEMENT TYPE	W/C RATIO	4 WEEKS	24 WEEKS		40 WEEKS		58 WEEKS	69 WEEKS
		SSD (KN/mm^2)	CTR+ (KN/mm^2)	OIL SAT.	CTR+	OIL SAT.	OIL SAT.	OIL SAT. (KN/mm^2)
OPC	0.40	33.4	31.2	30.6	31.8	29.0	28.4	27.8
	0.50	29.4	28.6	27.8	29.7	27.0	26.9	25.8
	0.60	27.0	26.1	26.7	27.8	26.2	25.6	25.0
	0.70	24.9	24.9	24.2	24.9	23.2	24.0	23.4
SRPC	0.40	35.1	35.6	34.1	35.2	32.8	32.0	
	0.50	31.3	30.3	31.0	30.6	30.0	29.1	
	0.60	27.9	27.0	26.8		26.3	26.6	
	0.70	25.8	25.5	24.0		23.7	22.9	
OPC + 4% Cormix	0.40	40.1	38.3	36.4		35.9	35.3	
	0.50	34.5	33.4	32.3		30.7	30.6	
	0.60	31.6	28.4	28.0		27.6	27.0	
	0.70	29.5	26.8	25.2		24.8	24.0	

+ Dried to 105°C and stored sealed in CTR

Table (6.11) Static Modulus of Elasticity of Concrete (KN/mm^2)

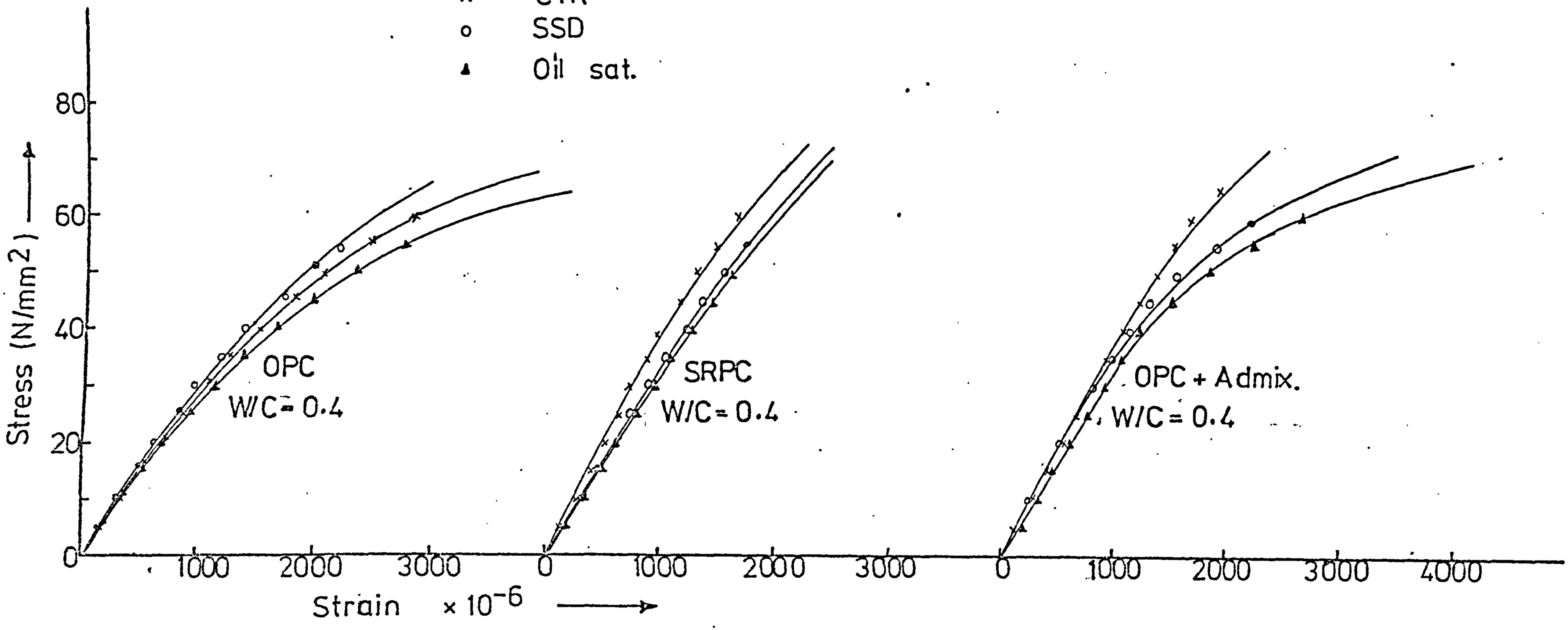

FIG(6.12) TYPICAL STRESS-STRAIN CURVE SHOWING THE EFFECT OF STORAGE CONDITION ON PLAIN & SUPERPLASTICISED CONCRETE (AT 24 WKS)

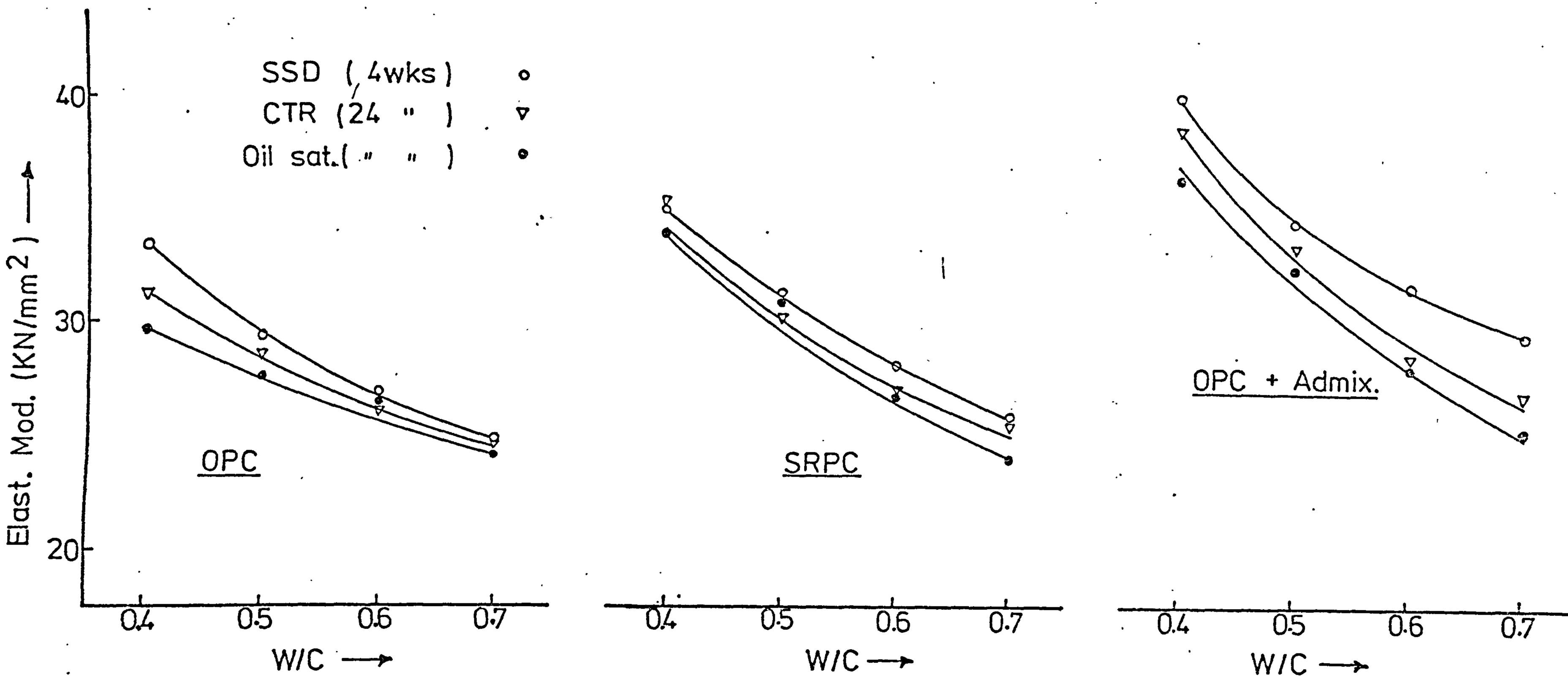

FIG(6.13) EFFECT OF STORAGE CONDITIONS & W/C RATIO ON THE ELASTIC MODULUS OF CONCRETE.

observations are made:

1. Wet concrete (SSD) possesses a higher elastic modulus than dried concrete (CTR) which had a higher modulus than oil saturated concrete. This is a striking difference between concrete and HCPs where oil saturated HCPs had a modulus higher than the dried samples. The elastic modulus of oil saturated concrete was between 1.5% and 11% less than for SSD samples after 4 months of oil soaking.

2. Generally, the elastic modulus of SRPC concrete was greater than for OPC concrete. For SSD specimens, SRPC concrete were greater by between 3.3 and 5.1%. This difference was less at higher W/C ratios. Reduction in the modulus due to oil saturation was slightly less in SRPC concrete than in OPC concrete.

3. A significant increase in the elastic modulus was obtained by the use of the superplasticiser. The elastic modulus rose by between 17 and 20% in SSD samples over corresponding SSD samples in concrete without the admixture. The reduction in the modulus due to crude oil saturation was of the same percentage magnitude as for plain concrete.

6.4.2.3. Effect of Prolonged Storage of Concrete in Crude Oil on the Elastic Modulus

The elastic modulus of oil saturated concrete decreased slightly but continuously with storage in crude oil, fig. (6.14). It was further observed that:

1. The elastic modulus of oil sat. OPC concrete fell by a maximum value of 5.6 KN/mm^2 after 58 weeks of oil storage ie. at the 69 week. Relative to the 24 weeks values ie. after the initial pressurisation, the modulus fell by between 0% and 4.6% in a further 45 weeks storage ie. at 69 weeks.

2. After 12 months of crude oil storage, the modulus of SRPC concrete was reduced by a maximum value of 3.1 KN/mm^2. Compared with the 24 weeks value, the modulus of SRPC concrete fell by between 1 and 6% over a further storage of 34 weeks ie. at 58 weeks.

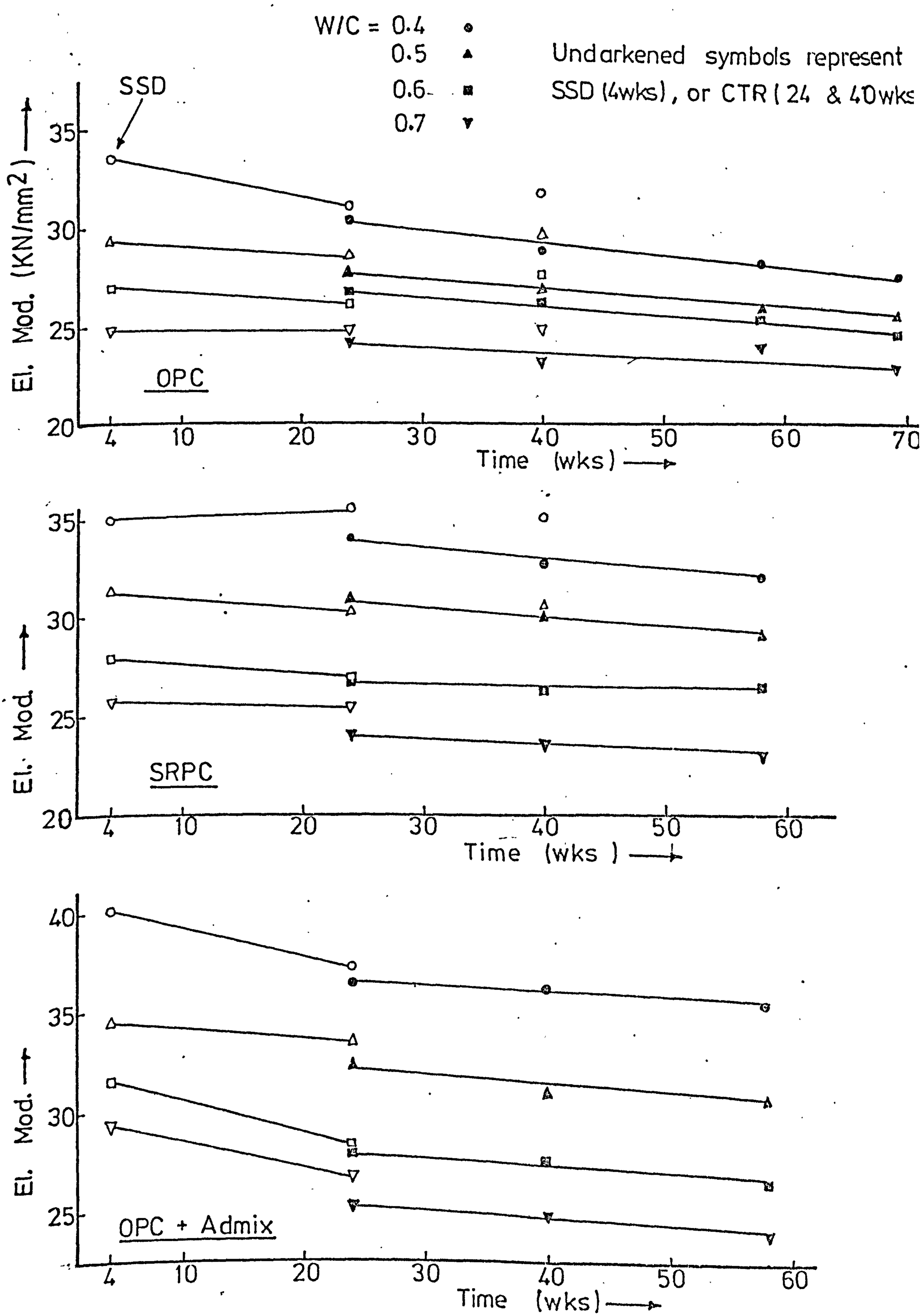

FIG(6.14) VARIATION OF THE ELASTIC MODULUS OF CONCRETE WITH PERIOD OF STORAGE IN OIL

6.4.3 Volumetric Changes under Compressive Load

It is known[136] that when concrete is subjected to increasing compressive load, the volume decreases until at a certain stress, σ_c, the critical stress, the volume and Poisson's ratio start to increase. It is also known that Poisson's ratio is lower in higher strength concrete[70].

In the present investigation, volumetric strain was claculated from the strain relationship[136]:

$$\frac{\Delta V}{V} = E_L - 2E_T \qquad (6.7)$$

and Poisson's ratio $= \dfrac{E_T}{E_L}$ (6.8)

where E_L is the longitudinal and E_T the lateral strain.

6.4.3.1 Volumetric Strain

Fig. (6.15) illustrates the changes in volumetric strain with stress. The stress is expressed as a percentage of the failure stress. The following observations are made:

1. The dried concrete specimens (CTR), generally increased in volume more than the SSD or oil saturated specimens. For concrete of W/C = 0.4, the dilation of the SSD prisms was less than for oil saturated prisms but the reverse is true for W/C = 0.6. Generally, volumetric expansion at high loads was highest in oil saturated specimens.

2. The critical stress, σ_c, denoting the points at which the curves deviated from linearity, was highest for SSD prisms and least for oil saturated prisms. For example, for OPC of W/C = 0.4, σ_c = 60% for SSD, 55% for CTR and 53.3% for oil saturated concrete.

6.4.3.2 Poisson's Ratio

Changes in Poisson's ratio with stress are illustrated in fig. (6.16). The following observations are made:

1. Poisson's ratio is between 0.10 and 0.20 at low loads. In SRPC concrete of W/C = 0.6, Poisson's ratio was very low (<0.10) for both SSD and CTR specimens. The values are considered to be in error.

2. The Poisson's ratio of oil saturated specimens were generally higher than those for SSD and CTR specimens of the same W/C ratio and at the same stress level. CTR specimens generally had the smallest values. The increase in Poisson's ratio at high loads was slightly greater for oil saturated prisms.

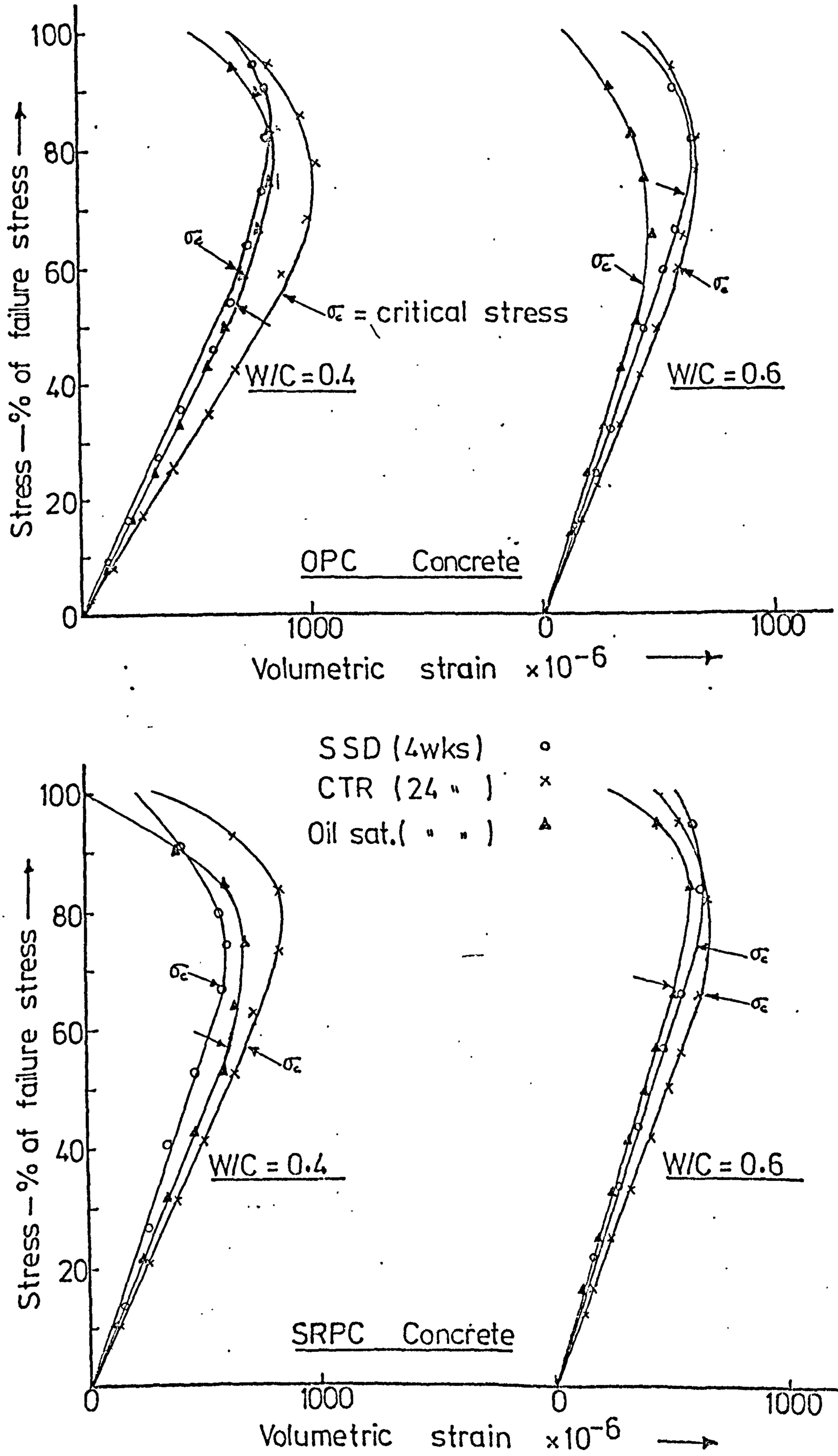

FIG (6.15) TYPICAL PLOTS OF VOLUMETRIC CHANGES UNDER COMPRESSIVE LOAD (AT 24 WKS.)

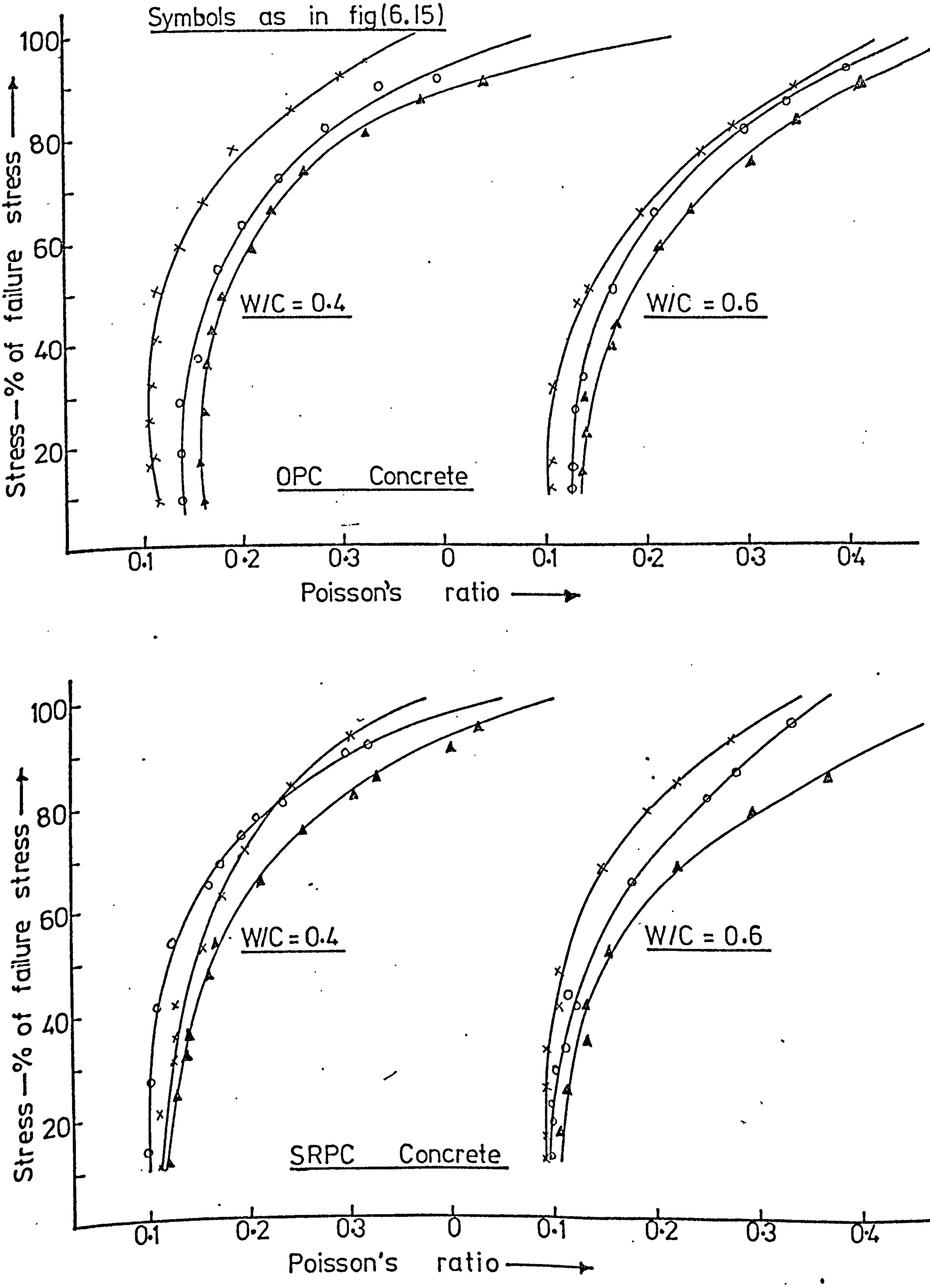

FIG(6.16) TYPICAL PLOTS OF POISSON'S RATIO CHANGES OF CONCRETE UNDER COMPRESSIVE LOAD (AT 24WKS)

CHAPTER 7

DISCUSSION OF RESULTS

7.1 Introduction

In chapters 4 to 6, a brief discussion of the experimental results has already been made while presenting the test results. The present chapter attempts to:

1. Discuss in greater detail the pore structure of HCPs, particularly the wide-pore volume, which affects engineering properties.

2. Obtain some theoretical correlation between the measured pore structure and permeability, strength and the elastic modulus of HCP and concrete.

3. Assess concrete permeability and deterioration in crude oil and describe the performance of crude oil saturated concrete.

7.2 Pore Structure of HCPs

Powers[23] has shown that many of the basic engineering properties of HCP are influenced largely by the volume and distribution of the wide pores - the capillary pores. The pore structure and its variation with various mix parameters was described in chapter 4.

7.2.1 Variation with W/C Ratio

Generally, all pore properties are greatly affected by changes in W/C ratio. The wide-pore volume increased non-linearly with an increase in W/C ratio - fig. (7.1) for pastes with or without admixture. At $W/C \leq 0.5$, OPC and SRPC pastes had nearly equal wide-pore volumes but for $W/C > 0.5$, OPC paste had a significantly lower wide-pore volume.

The hydraulic radius of OPC pastes varies linearly with W/C ratio upto 0.60. Above this it increased more rapidly - fig. (7.2). The variation obtained for SRPC pastes were more erratic than for corresponding OPC pastes. The average hydraulic radius of the entire pore system was lower in SRPC than

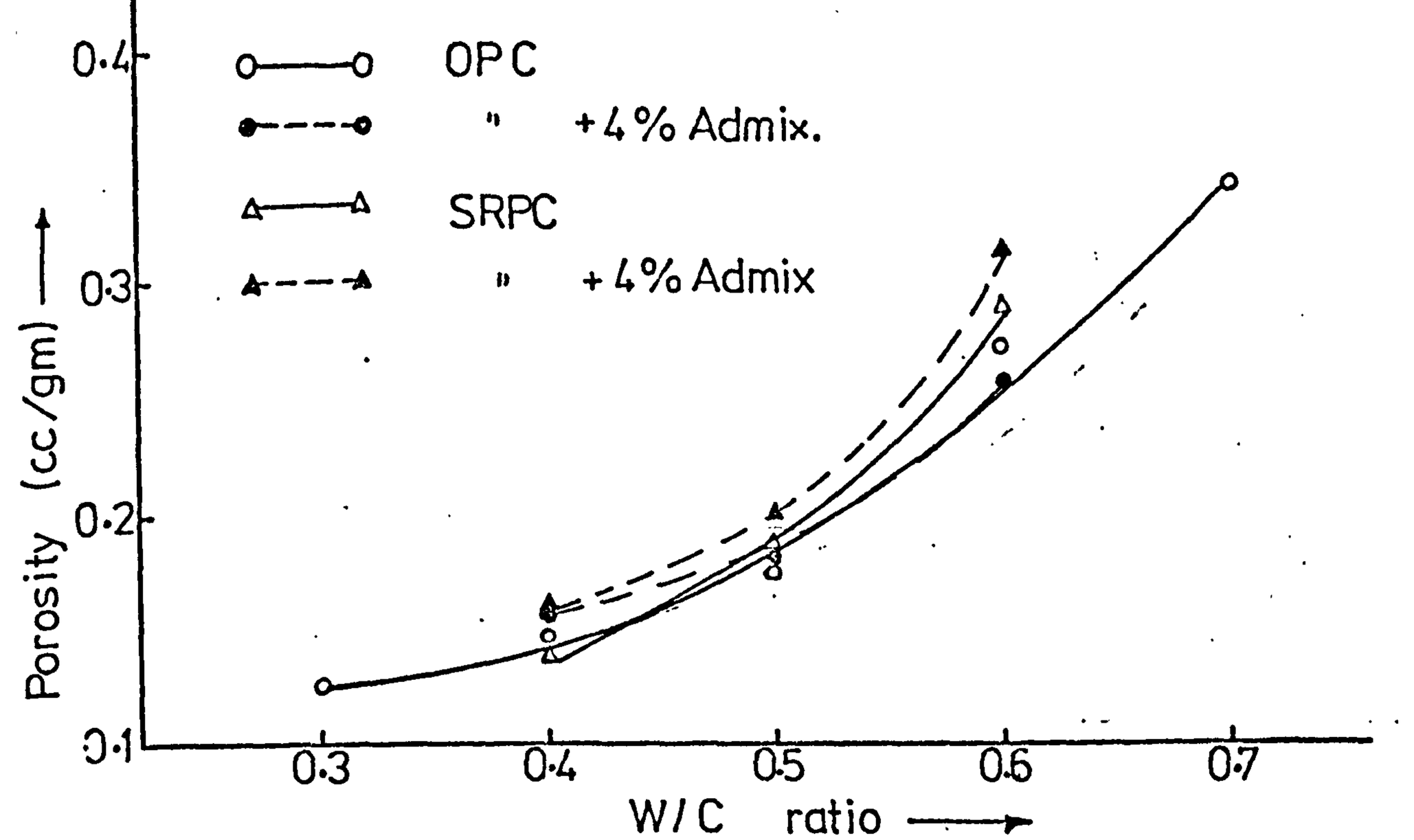

FIG(7.1) VARIATION OF WIDE-PORE VOLUME WITH W/C.

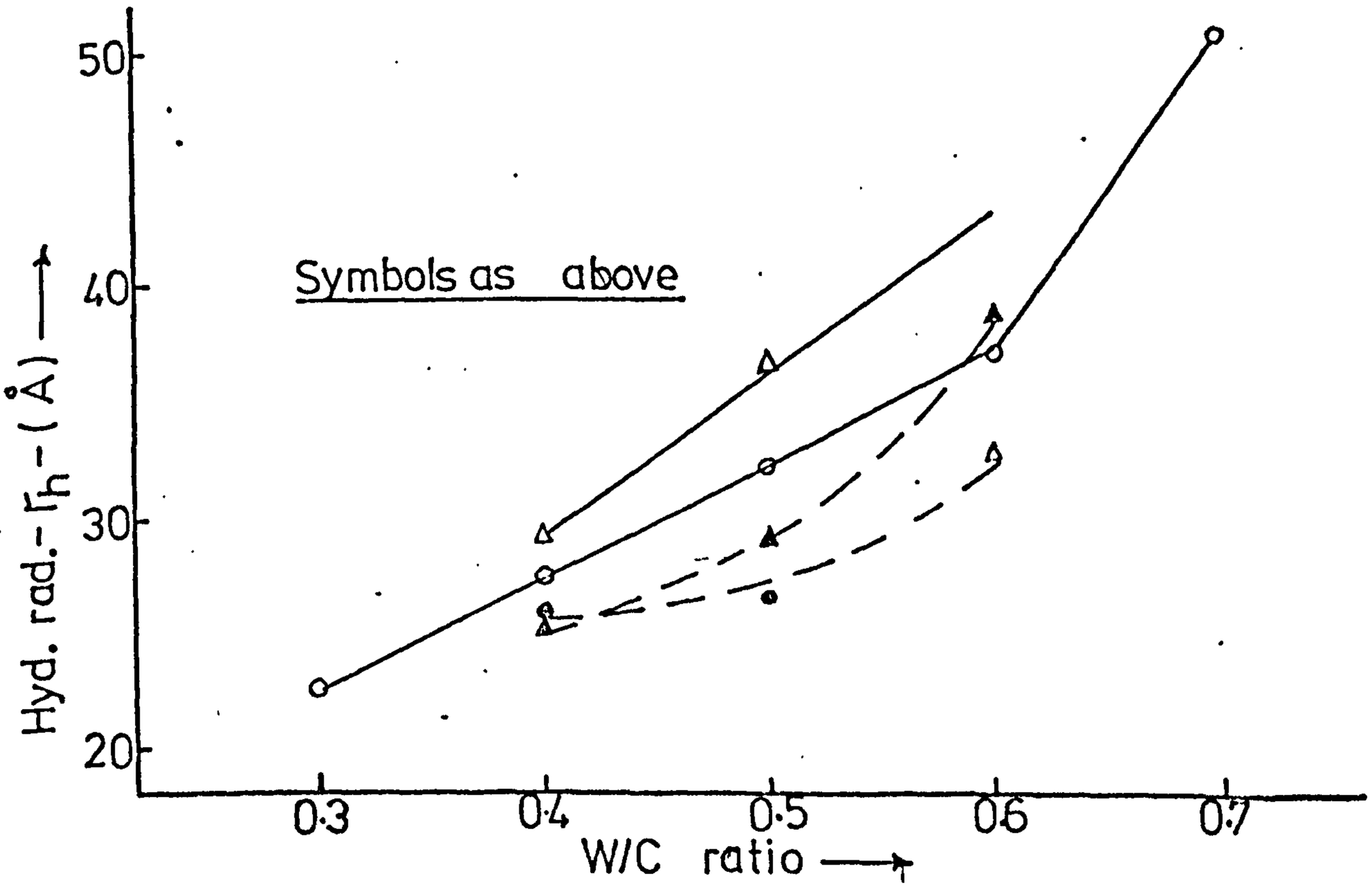

FIG(7.2) VARIATION OF WIDE-PORE r_h WITH W/C.

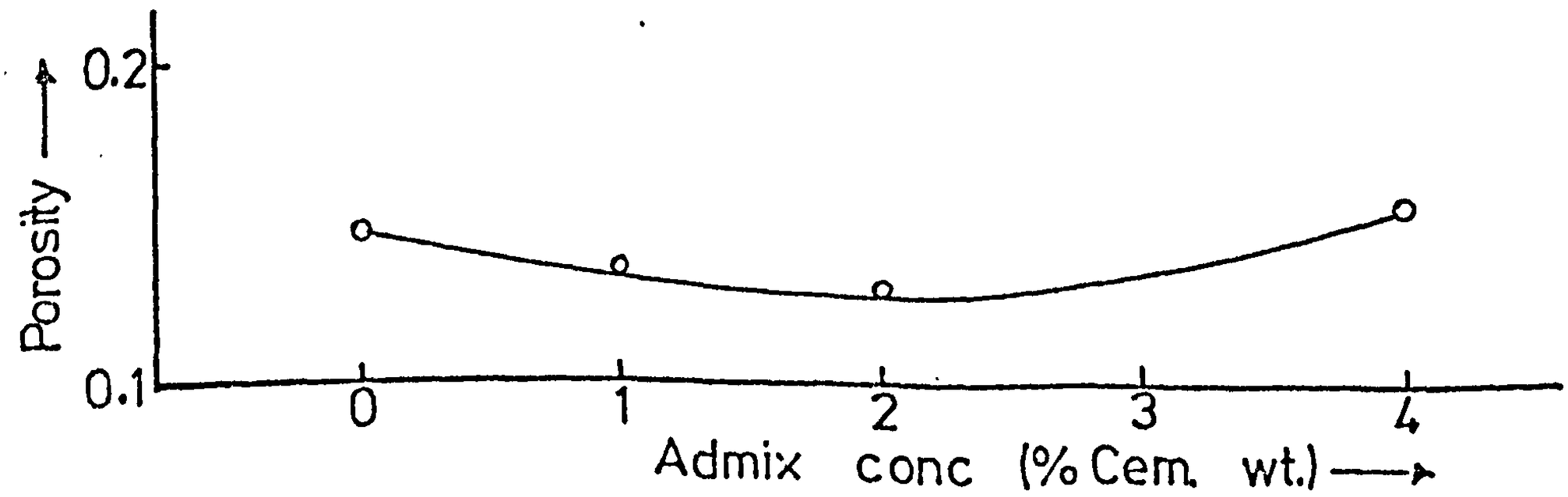

FIG(7.3) VARIATION OF WIDE-PORE VOLUME WITH ADMIX. CONCENTRATION

in OPC pastes - table (4.5)

7.2.2 Effect of Superplasticising Admixture on Pore Structure

The superplasticiser modified the pore structure of the HCPs, particularly in the wide-pore region.

The variation of the wide-pore volume with admixture concentration is illustrated in fig. (7.3) for OPC pastes of W/C = 0.4. Low admixture dosage reduces the wide-pore volume. The highest reduction of 11.7% over that without admixture was obtained at 2% dosage. Above 2% concentration the wide-pore volume increased and at 4% concentration its value was 7.6% higher than with no admixture. The addition of 4% superplasticiser to pastes of W/C = 0.4, 0.5 and 0.6 generally increased the wide-pore volumes for both OPC and SRPC pastes - fig. (7.1). For OPC pastes, the increases over that for zero admixture was 7.6%, 4.7% and-5.5% and for SRPC pastes the increases were 13.9%, 6.8% and 8.3%.

The average hydraulic radius of the wide-pores also reduced with low admixture concentrations - table (4.5). The variation of the hydraulic radius with W/C ratio for pastes containing 4% admixture is illustrated in fig. (7.2). Non-linear variations were obtained and the hydraulic radius of pastes with admixture were generally lower than for those without admixture.

The superplasticiser affects pore structure of HCPs in two differing ways. Firstly, it increases the total pore volume of the HCPs ie. a sort of "added porosity" like adding more water to a fresh paste. This increases the total pore volume, V_s - table (4.4) or W_e, table (4.3). It also reduces the density - table (4.3) and figs. (4.4) and (4.5). Similar effects have been found by other investigators. Dingley[129] using polymer latex found it increased the porosity indicated by drying losses - W_e. Mikhail et al[137] found reduced density and increased porosity in HCPs containing an air-entraining admixture, using nitrogen adsorption on D-dried HCPs.

Secondly, pastes with the superplasticising admixture have higher degrees of hydration - table (4.4). This increased hydration, increases the number of smaller pores[54,138] by reducing the wide-pore volumes and the average hydraulic radii of the pore system. However, the smaller pores could also result from the deflocculating action of the superplasticisers on the

cement resulting in cement particles which are closer to one another. Similar reductions were obtained by collepardi and Massidda[139] on HCPs containing a synthetic polymer. They obtained reductions of upto 28% in the "capillary" porosity (pores 1.0 to 0.01 microns) using mercury porosimeter. However, Ciach and Swenson[140] investigated lignosulphonate based plasticisers in HCP and found that this admixture and most other types of water-reducing admixtures do not affect the final paste structure and its mechanical properties at advanced ages of hydration.

In practice, superplasticisers are used to increase concrete workability or to reduce the W/C ratio. The latter is the case where improvement in concrete impermeability or strength is sought. In table (5.16) it was shown that the use of 1, 2, 3, 4 and 6% superplasticiser led to reductions of 16, 17, 19, 20, and 24% in the mixing water required. The use of 2% admixture with a 17% water reduction in OPC concrete gave medium slumps (50 - 80 mm) in almost all cases. The effective W/C ratio was reduced and interpolations from fig. (7.1) would give reductions in wide-pore volumes of 10.4, 14.1 and 35.1% for original W/C ratios of 0.4, 0.5 and 0.6 respectively. The use of 2% admixture concentration reduces the wide-pore volume by upto 11.7%. Hence expected total reductions in wide-pore volume are 20.8, 24.1 and 42.7% over their original values with no admixtures. Similarly, the average hydraulic radius of the wide-pores are expected to reduce from 27.5, 32.1 and 36.9 Å - table (4.5) - to 24.0, 28.0 and 32.2 Å ie. reductions of 9.1, 12.8 and 12.7% over the values with no admixture. These large reductions in wide-pore parameters with the use of superplasticiser is expected to lead to considerable improvement in concrete strength and impermeability.

7.2.3 Likely Effects of Crude Oil Saturation on Pore Structure

The effect of crude oil saturation on the pore properties of HCP can be observed by comparing the pore structure of oven-dried HCPs - OVP40 and OVP60 - with that oven-dried, then oil saturated and oven-dried again - OSP40 and OSP60 - table (4.5). The wide-pore volume decreased by 33% and 39% for OSP40 and OSP60 respectively and the hydraulic radii reduced by 4.5 Å and 7.1 Å ie. 18.6% and 17.4%. These effects may be due to the clogging up of some of the pores of the HCPs by the larger (wax-like) molecules of the crude oil. It was stated in chapter 3 that analysis of the crude oil revealed molecular sizes ranging in size from as low as 1 Å to as large as 18 Å

diameter. The larger molecules cannot possibly pass through the narrow entry pores but may instead block up the pores. Also the deposited crude oil. waxy molecules do not seem to evaporate on drying to 105°C but instead may form deposits that narrow down the pore sizes.

This would affect the engineering properties of crude oil saturated HCPs and concrete. The narrowing of the pore system would decrease permeability, and the absorption of the larger crude oil molecules would affect some engineering properties of HCPs[141,142]. This will be examined further in this chapter.

7.2.4 Comparison with Published Works

7.2.4.1 Capillary Porosity

Capillary porosity, P_c, is most often derived from the formula due to Copeland and Hayes[143] which is a modification of the original ideas of Powers[23,122]. Copeland and Hayes made an allowance for the partial decomposition of the pastes during drying by substracting from the drying loss a fraction of the combined water content, W_n. Taking the specific volume of cement as 0.319 and average value of V_m/W_n of 0.321[143], then their formula reduces to:

$$P_c = \frac{W/C - 1.51\ (W_n/C)}{0.319 + W/C} \qquad (7.1)$$

W_n/C values used in equ. (7.1) were taken from the work of Taplin[119] after finding a good comparison at 28 days with values obtained in this investigation - table (4.3). However, it is possible that some errors in P_c may arise due to the W_n/C values used because the chemical composition of the cement used by Taplin may differ from that used here. Values of P_c obtained using this formula are tabulated in table (7.1). The variation of P_c with W/C ratio are illustrated in fig. (7.4) for various ages.

Converting the wide-pore volume (cc/gm) into equivalent porosity values in cc/cc of paste by the process described in section 4.4.4 gives 0.2188, 0.2308, 0.2513, 0.3466 and 0.4001 for W/C ratios of 0.3 to 0.7 respectively. Comparing these values with P_c values at 28 days - table (7.1) - shows that P_c values are greater by —10.5%, 11.2%, 18.1%, 5.3% and 4.1%. Hence except for the large difference at W/C = 0.5, the wide-pore volumes are

W_c / P_c	1 WEEK	2 WEEKS	4 WEEKS	13 WEEKS	24 WEEKS	26 WEEKS	40 WEEKS	52.WEEKS
0.30	.214	.202	.198	.161	.149	.132	.120	.106
0.35	.248	.238	.225	.193	.184	.168	.156	.141
0.40	.288	.270	.260	.228	.219	.209	.198	.187
0.50	.353	.334	.308	.290	.285	.277	.272	.270
0.60	.410	.388	.366	.346	.344	.340	.339	.337
0.70	.459	.437	.417	.398	.397	.396	.394	.393

Table (7.1) Capillary Porosity (P_c) at various ages - equ. (7.1)

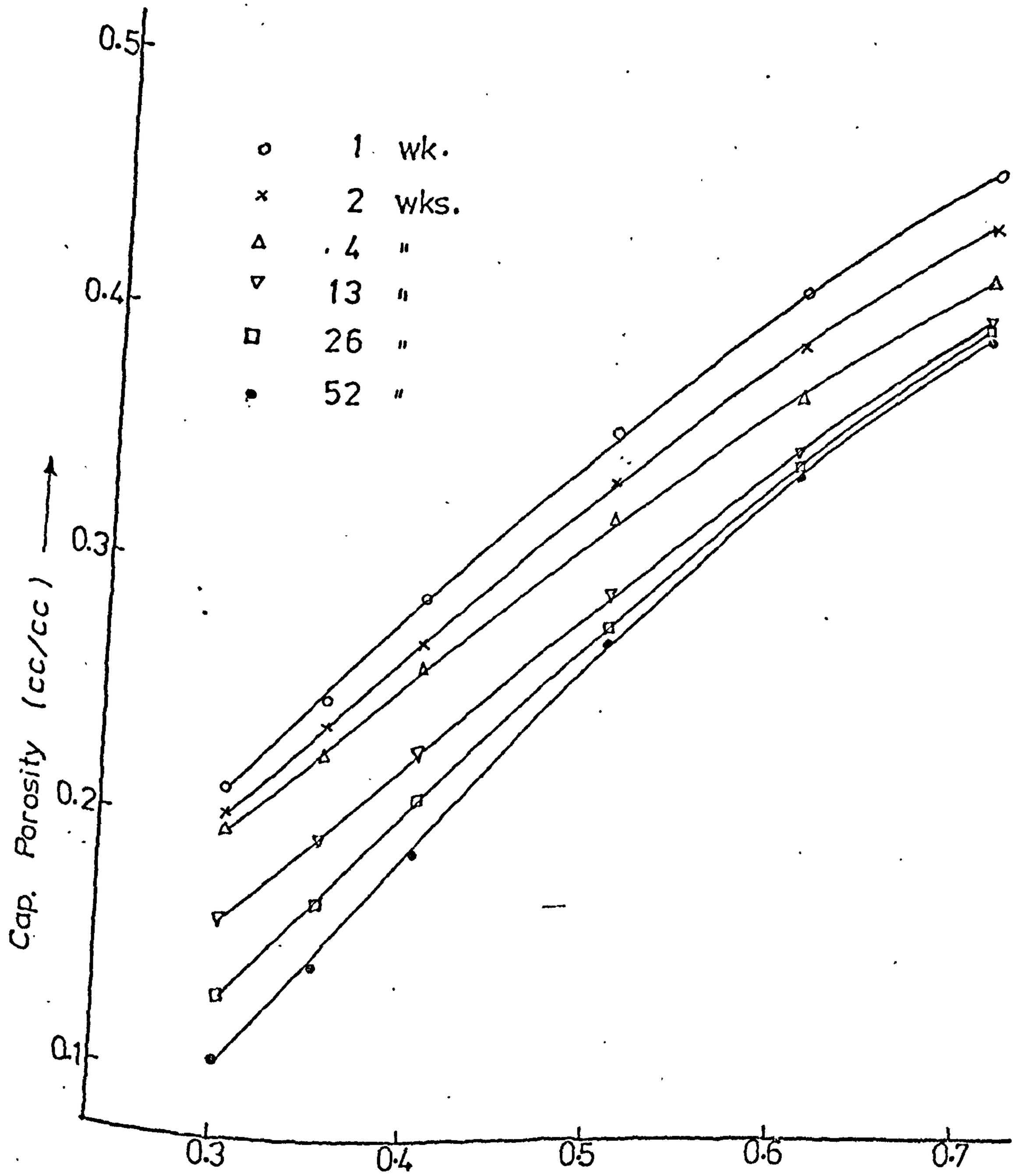

FIG(7.4) VARIATION OF CAPILLARY POROSITY, Pc, WITH W/C RATIO & AGE. OPC PASTES.

of the same order of magnitude as the capillary porosities.

7.2.4.2 Porosity obtained with other Techniques

The two most widely used methods of porosity measurements at present are the mercury porosimetry and the capillary condensation (water vapour or nitrogen adsorption). For the same paste, results from the two methods differ in two ways:

1. Mercury porosimetry shows much less pore space particularly in pores 100 Å diameter and less, than capillary condensation.

2. Mercury porosimetry gives pore size distributions much larger than capillary condensation.

Available results are most often difficult to compare exactly since degrees of hydration of the HCPs differ considerably. It has also been pointed out earlier that nitrogen adsorption gives smaller pore structure parameters - section 2.1.4.3. However, recent research show that nitrogen adsorption on HCPs gives inconsistent results[47] and hence more recent investigations are made using either the water vapour adsorption, mercury porosimetry or the more recently helium flow pyconometry. Table (7.2) compares available results from these three methods. It should be noted that some of these results were taken from graphs in published works and are, therefore approximate.

The table shows clearly that porosities differ for the same HCP depending on the methods of testing, the pore size range measured and the drying procedure prior to testing. These three conditions should therefore, be clearly defined when the porosity of HCP is given. Porosity values obtained with the mercury porosimeter are close to the wide-pore volumes; and it is, therefore, probable that only wide-pores can be measured accurately by the mercury porosimeter. The porosity measured by the Helium flow pyconometer is generally higher but the pore size range is not defined and is likely to have included micropores, $r_h < 3$ Å and pores larger than can be measured with water-vapour adsorption (510 Å hydraulic radius). The values are, therefore, only comparable to the total porosity, V_s - table (4.5).

7.3. Permeability of HCP and Concrete

NO	SAMPLE W/C RATIO	AGE (Days)	POROSITY (cc/cc)	PORE DIA. RANGE (μm)	METHOD OF TESTING	METHOD OF DRYING	REF.
1	0.25	90D	0.123	>.0012*	H.F.P.	11% R.H.	144
2	0.28	28D	0.112	.006 - 2.5	M.P.	Oven+	56
3	0.30	28D	0.219	.002 - .20	W.V.	D-dried	T
4	0.30	33D	0.240	.002 - .20	W.V.	D-dried	145
5	0.35	90D	0.200	>.0012*	H.F.P.	11% R.H.	144
6	0.40	28D	0.231	.002 - .20	W.V.	D-dried	T
7	0.40	28D	0.237	.008 - .38	M.P.	Oven	54
8	0.40	90D	0.220	>.0012*	H.F.P.	11%R.H.	144
9	0.46	28D	0.246	.006 - 6.0	M.P.	Oven	56
10	0.50	28D	0.251	.002 - .20	W.V.	D-dried	T
11	0.50	90D	0.360	>.0012*	H.F.P.	11% R.H.	144
12	0.60	28D	0.345	.0025 - 5.3	M.P.	Oven	56
13	0.60	28D	0.285	.008 - .38	M.P.	Oven	54
14	0.60	28D	0.347	.002 - .20	W.V.	D-dried	T
15	0.70	28D	0.400	.002 - .20	W.V.	D-dried	T

H.F.P. - Helium flow pyconometry

M.P. - Mercury Porosimetry

W.V. - Water Vapour Adsorption

T - Work from this Thesis

R.H. - Relative Humidity

\+ - Oven dried to $105^{o}C$

* - Actual values are unknown. These values are estimated from water vapour distribution at 11% P/P_s

Table (7.2) Comparison of HCP Porosity Values of Different Workers and Techniques

7.3.1 Permeability of HCP

7.3.1.1 Permeability and Pore Structure

The permeability of HCP is governed by its internal pore structure which is defined by the effective pore volume, pore size distribution and shape and the interconnectivity of the pores. Assumptions are normally made to simplify theoretical calculations. Here a cylindrical pore shape model is used, the effective pore volume is taken as the wide-pore volume and a tortuosity factor - T is introduced to account for the unknown orientation of the pores.

The most widely used theory connecting permeability and the internal structure of a porous material is the Kozeny equation - equ. (2.17):

$$K = \frac{CP^3}{TS^2}$$

$$= \frac{C}{T} \cdot P \cdot R^2 \qquad (7.2)$$

where C = constant

T = tortuosity factor defining the actual flow path

P = effective porosity = the wide-pore volume

R = average pore radius = the hydraulic radius of the wide-pores

Fig. (7.5) shows a linear relationship between the coefficient of permeability (K) and the square of the hydraulic radius - r_h^2. Line 2 and 3 are for HCPs without and with admixtures respectively. Line 1 is the relationship between K and r_h^2 for all the HCPs. The considerable scatter of results for line 1 is due to the change in the pore structure due to admixture and indicates that hydraulic radius alone is not a true indicator of permeability.

Fig. (7.6) shows a linear relationship between K and the wide-pore volume. The scatter of results is less than obtained in fig. (7.5) indicating that wide-pore volume alone is a more reasonable indicator of permeability.

A correlated regression analysis gives:

$$K = T.. P^{\beta} \cdot r_h^{\gamma} \qquad (7.3)$$

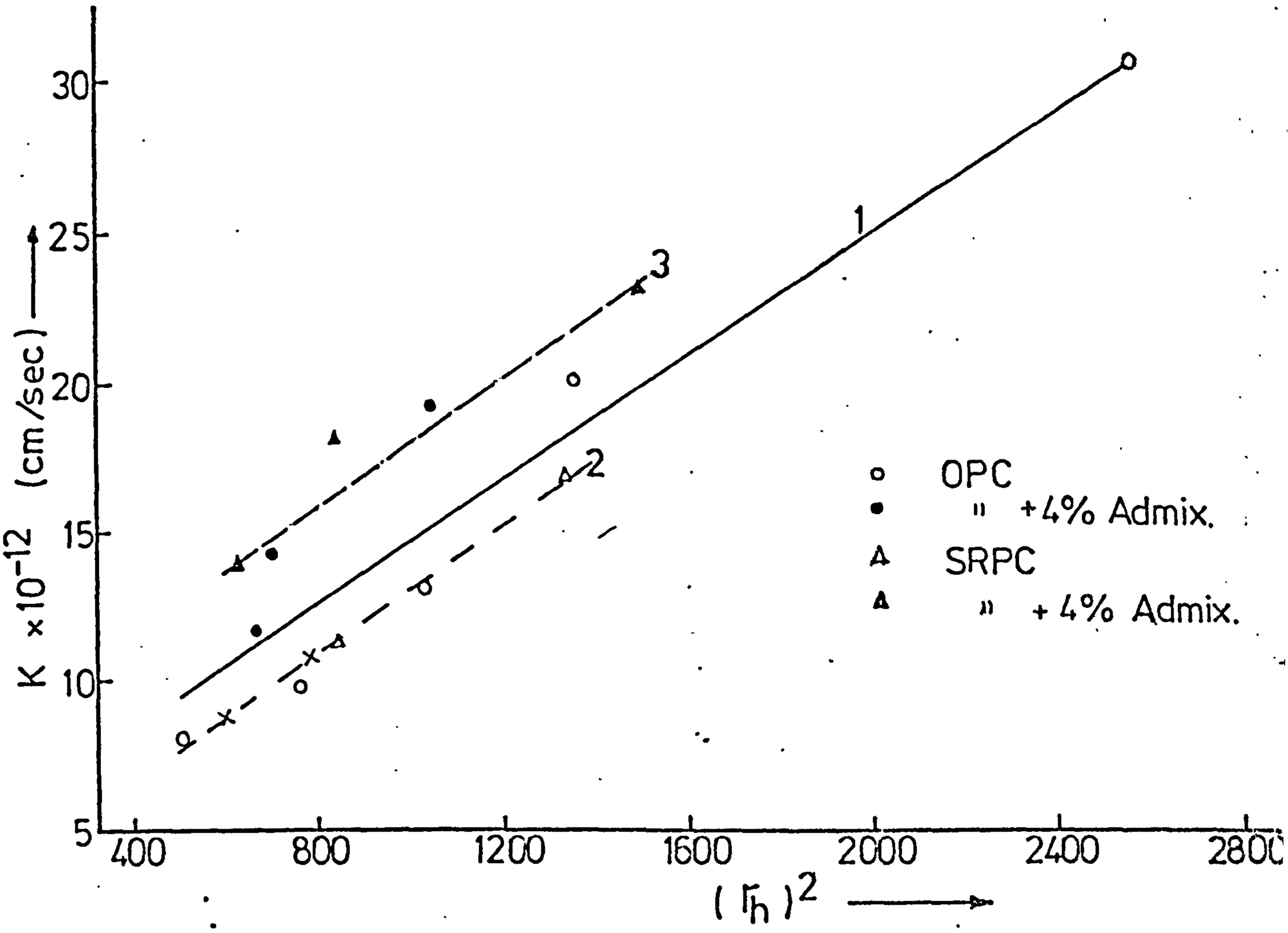

FIG(7.5) VARIATION OF K WITH THE SQUARE OF THE HYDRAULIC RADIUS

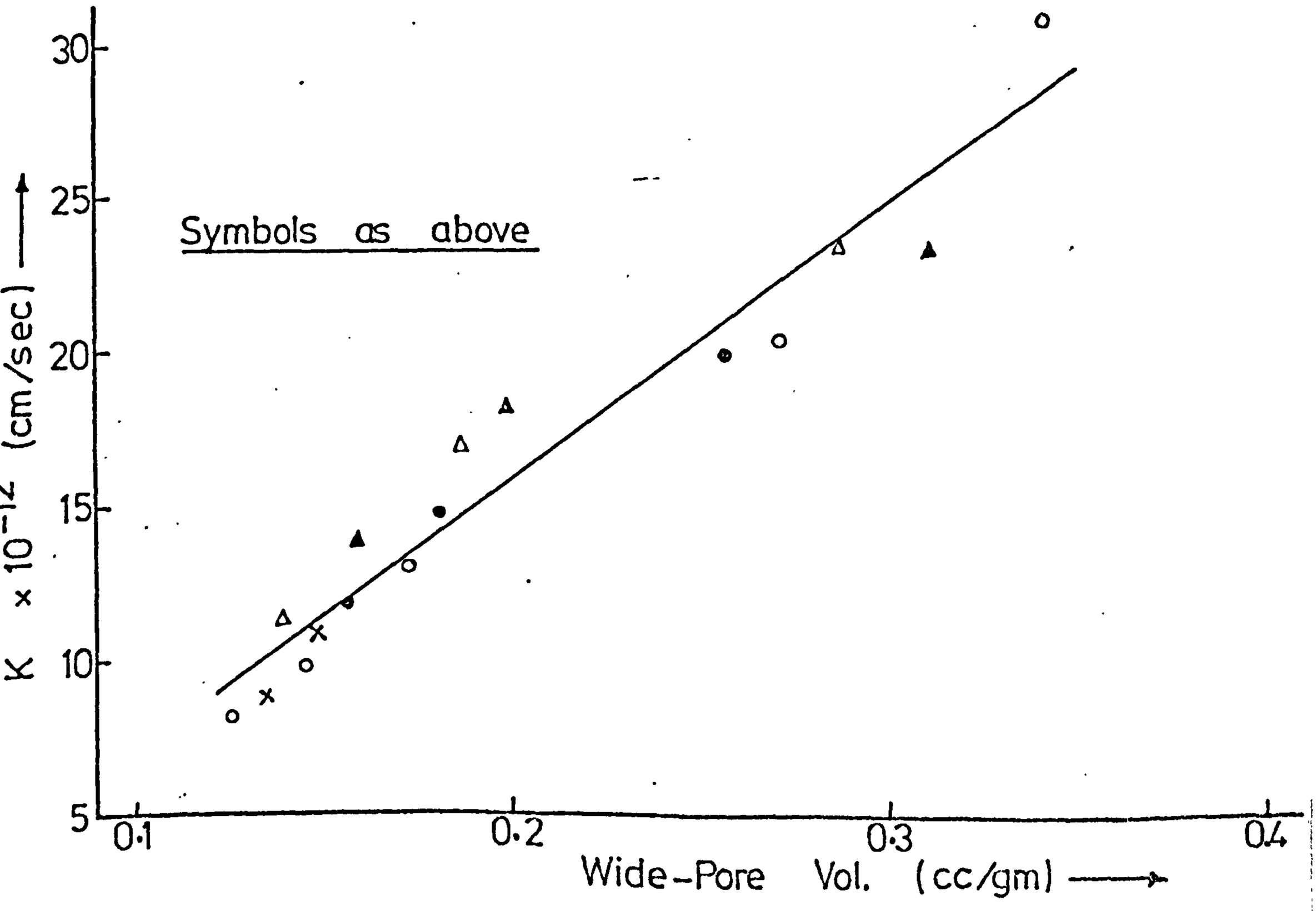

FIG(7.6) VARIATION OF K WITH WIDE-PORE VOLUME

with the values of T, β, and γ given in table (7.3). Equ. (7.3) has the limitation that it cannot be used at all applied hydrostatic pressures (A). It was shown in section 5.4.2.2, that K increases almost linearly with A, and this was attributed to the fact that the increased pressure breaks down pore partitions thus introducing more flow-paths. If a further assumption is made, ie. that increased pressure decreases the flow-path ie. reduces the tortuosity then

$$K = T \cdot A^{\theta} \cdot P^{\beta} \cdot r_h^{\gamma} \qquad (7.4)$$

Values of T, θ, β and γ are given in table (7.4). Equation (7.4) can therefore be used to predict K when Porosity (P) and pore radius (r_h) are known, for any applied hydrostatic pressures. Further experimentation is needed to obtain values of P and r_h by other pore measurement techniques eg. mercury porosimeter, and hence predict K when these parameters are known.

PASTE	T	β	γ	STD. ERROR
OPC	18.75	0.940	0.378	1.01
SRPC	47.96	0.765	0.055	1.23

Table (7.3) Constants of Regression - Equ. (7.3)

PASTE	T	θ	β	γ	STD. ERROR
OPC	2.47	0.450	0.938	0.382	0.82
SRPC	8.41	0.400	0.816	0.067	0.98

Table (7.4) Constants of Regression - equ. (7.4)

7.3.1.2 Water and Oil Permeabilities of HCPs

To understand more clearly the permeability of HCP to crude oil, it is important to compare the oil permeability with that for other liquids. Water permeability is the only readily available result and Fig. (7.7) compares the water and oil permeabilities of HCPs at equal W/C ratios and equal capillary porosities - P_c.

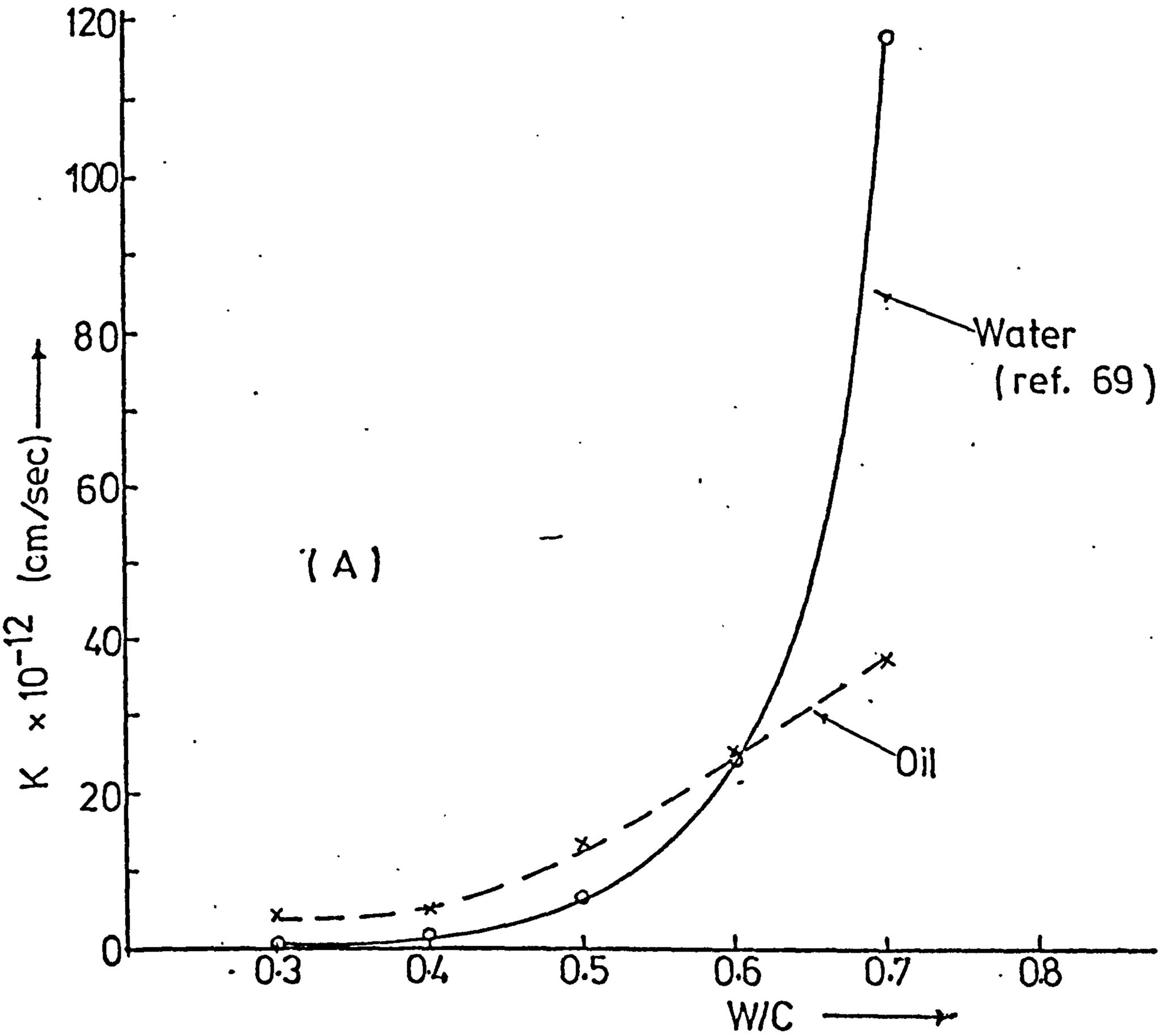

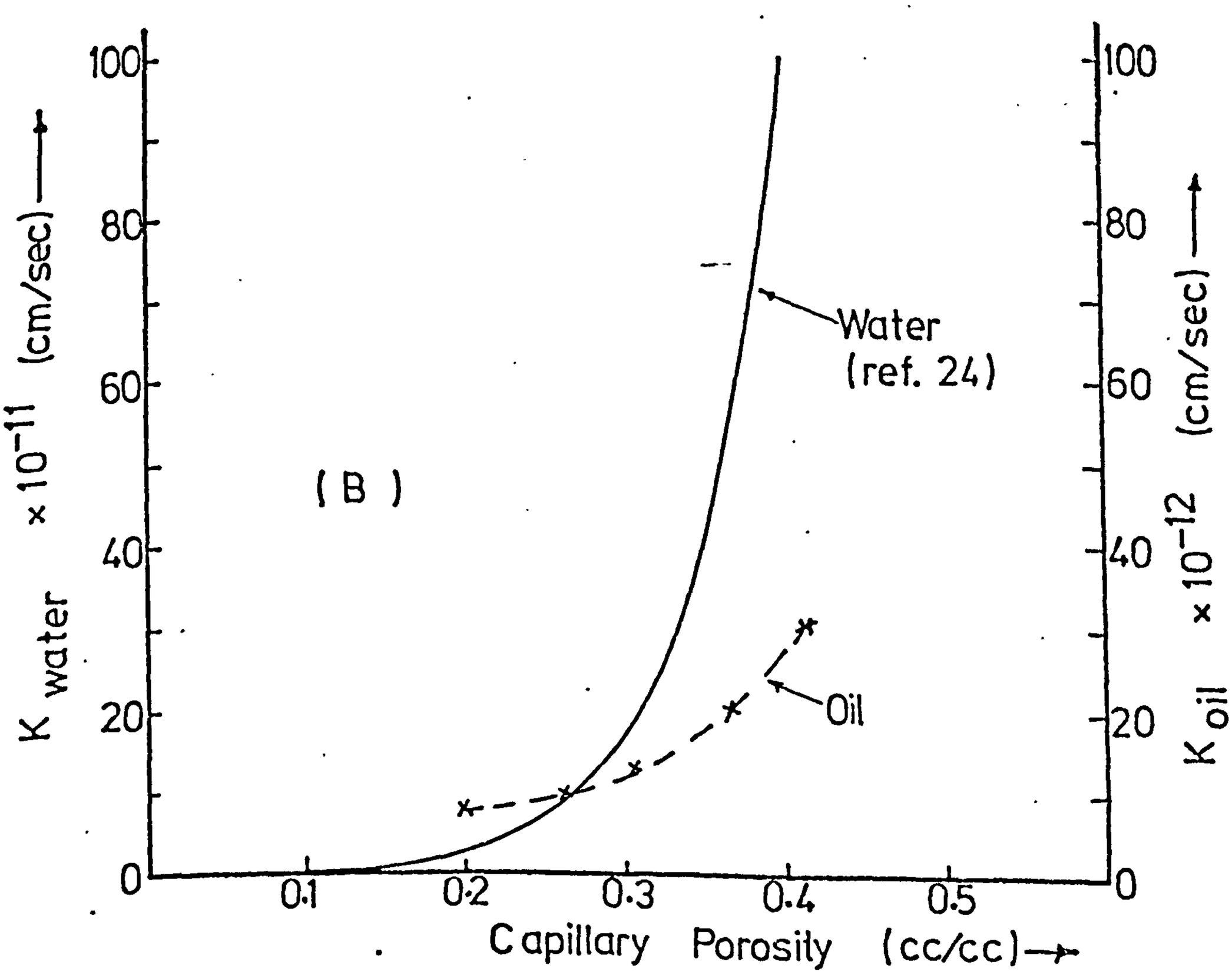

FIG(7.7) COMPARISON OF WATER & OIL PERMEABILITIES OF HCPs.

In Fig. (7.7)A the HCP used for water permeability measurement is 93% hydrated while that for oil is between 50 and 81% hydrated - table (4.3). If the HCPs for oil tests had been equally hydrated as for the water tests, K for oil may have been reduced about 1.5 times[69]. Also the HCPs used for the oil test were oven-dried to 105°C and Powers[69] had noted that drying HCPs at 79% relative humidity could increase K by upto 70 times, and therefore drying to 105°C may have increased K even more. Matti[12] noted that drying concrete to 105°C increased the rate of crude oil penetration in a concrete test specimen by 4 - 20 times depending on the applied hydrostatic head. In fig. (7.7)A, K for oil is approximately equal to K for water at W/C = 0.6, but taking the above factors into consideration, K for oil will be upto 100 times less than K for water. A more independent basis for comparing the two permeabilities is the capillary porosity - (P_c) - fig. (7.7)B. For example, at P_c = 26.7%, K for water is 10 times K for oil, but the HCP used for the oil test was dried thus increasing K.

It is therefore, obvious from the above considerations that HCP is much less permeable to crude oil than to water. In pastes of equal W/C ratio or equal capillary porosity, K for water is expected to be upto 100 times more than K for oil. The reason for this large difference is primarily because of the larger molecular sizes of crude oil (upto 18 Å) compared with water (3.2 Å). The flow of oil in HCP also differs from that of water. In water K is independent of the applied hydrostatic head when steady state is reached, unlike oil - section 5.4.2.1. Also, K reaches a constant value after about 24 hours of flow in water unlike oil where an absolute constant value was not reached.

7.3.2 Permeability of Concrete to Crude Oil

7.3.2.1 Prediction of Concrete Permeability

An accurate measurement of concrete permeability is often very time consumming and a quicker, indirect method is desirable. The methods considered in this work are: A) compressive strength, B) Absorption capacity, C) W/C ratio, D) Calculated total porosity. The accuracy of each method is discussed in relation to a 95% confindence limit.

If K^1 is a regression estimate of K corresponding to a value x_o of the variable, x, such as compressive strength, absorption, W/C or total porosity,

then the confidence intervals are given by:

$$K^1 \pm \text{S.E.}\ (K^1) \times t_{\alpha} \qquad (7.5)$$

where S.E.(K^1) denotes the standard error of estimate of K obtained from the regression analysis, t is called the 't-multiplier' at α degrees of freedom obtainable from statistical tables, and α is the number of data points minus two. Values of t used here are from the book by Davies and Goldsmith[146].

I Prediction from Compressive Strength

The relationship between K and the compressive strengths of all the specimens tested is illustrated in fig. (7.8) for OPC and SRPC concretes with and without admixture. The 95% confidence interval is also shown. The relationship can be expressed exponentially in a form similar to equ. (5.9). Generalised values of the constants K_o and b are given in table (7.5).

All the test results fall within the 95% confidence intervals in both concretes and with a large error of estimate of K. For example, for a grade 50 concrete, the coefficient of permeability lies within $13.34 \pm 4.99 \times 10^{-10}$ cm/sec in OPC concrete and $15.01 \pm 5.11 \times 10^{-10}$ cm/sec in SRPC concrete ie. an error of ± 36% in the estimated value of K is possible. This large error indicates that compressive strength alone is not a reliable means of determining the concrete permeability

II Prediction from Absorption

The relationships between K and the quantity of crude oil absorbed after 4 months soaking are illustrated in fig. (7.9) for OPC and SRPC concretes with and without admixtures. These relationships can be expressed as a power function of the form:

$$K = K_a A^{\gamma} \qquad (7.6)$$

values of K_a and γ were obtained by regression analysis and are given in table (7.6).

All but 5 of the 91 test results in OPC and 1 out of the 60 in SRPC concrete fall in the 95% confidence interval but a large error in K is

obtained if estimated from absorption. For example, an OPC concrete with an absorption value of 3.7% has a K value of 13.34×10^{-10} cm/sec (as the grade 50 concrete), and error of estimate of K of $\pm 5.8 \times 10^{-10}$ cm/sec. Percentage error of estimate in the two concretes is about $\pm$ 42%. This large error indicates that absorption alone is also not a complete means of expressing concrete permeability. The probable reasons for this have been discussed in section 2.2.4.

III Prediction from W/C Ratio

Fig. (7.10) shows the relationship between K and W/C ratio for all the samples tested. For the superplasticised concretes, the effective W/C ratios (table 5.17) was used. K is seen to vary exponentially with W/C ratio and the relationship is of the form:

$$K = K_o (exp)^{b(W/C)} \qquad (7.7)$$

values of K_o and b are given in table (7.7).

All but 6 of the 71 results for OPC and all the 60 for SRPC fall in the 95% confidence interval. The error of estimate of K for the grade 50 concrete (as described in the preceeding sections) is $\pm$ 3.99 in OPC and $\pm$ 3.50×10^{-10} cm/sec in SRPC concretes. These represent errors of estimate $\pm$ 29.9% and 23.3% in OPC and SRPC concretes respectively. Thus, the error of estimate of K is less from W/C ratio than from either compressive strength or oil absorption.

IV Prediciton from Total Porosity

The relationship between K and the calculated total porosity of concretes is illustrated in fig. (7.11) for OPC and SRPC concretes with and without admixture. K is seen to vary exponentially with total porosity and the relationship is of the form:

$$K = K_o (exp)^{bP} \qquad (7.8)$$

Values of K_o and b are given in table (7.8).

All but 2 of the K values fall in the 95% confidence interval for

OPC and 3 out of 60 for SRPC concretes. Errors of estimate of K from porosity are $\pm$ 3.35 x 10^{-10} cm/sec for OPC and $\pm$ 3.52 x 10^{-10} cm/sec for SRPC concrete. For a grade 50 concrete, K = 13.34 x 10^{-10} cm/sec with OPC; the error = $\pm$ 25% for OPC and $\pm$ 24% for SRPC concretes. Therefore, the best estimate of K is obtained from the calculated total porosity.

CONCRETE	K_o x 10^{-10}	b	r
OPC	52.66	-0.0275	-92.5
SRPC	61.91	-0.0283	-90.6

Table (7.5) Constants of Regression: Equ. (7.5) K Vs Compr. Strength

CONCRETE	K_o x 10^{-10}	γ	r
OPC	1.153	1.893	89.5
SRPC	1.028	1.904	92.9

Table (7.6) Constants of Regression: Equ. (7.6) K Vs absorption

CONCRETE	K_o x 10^{-10}	b	r
OPC	2.222	2.964	95.1
SRPC	2.585	2.997	96.5

Table (7.7) Constants of Regression: Equ. (7.7) K Vs W/C

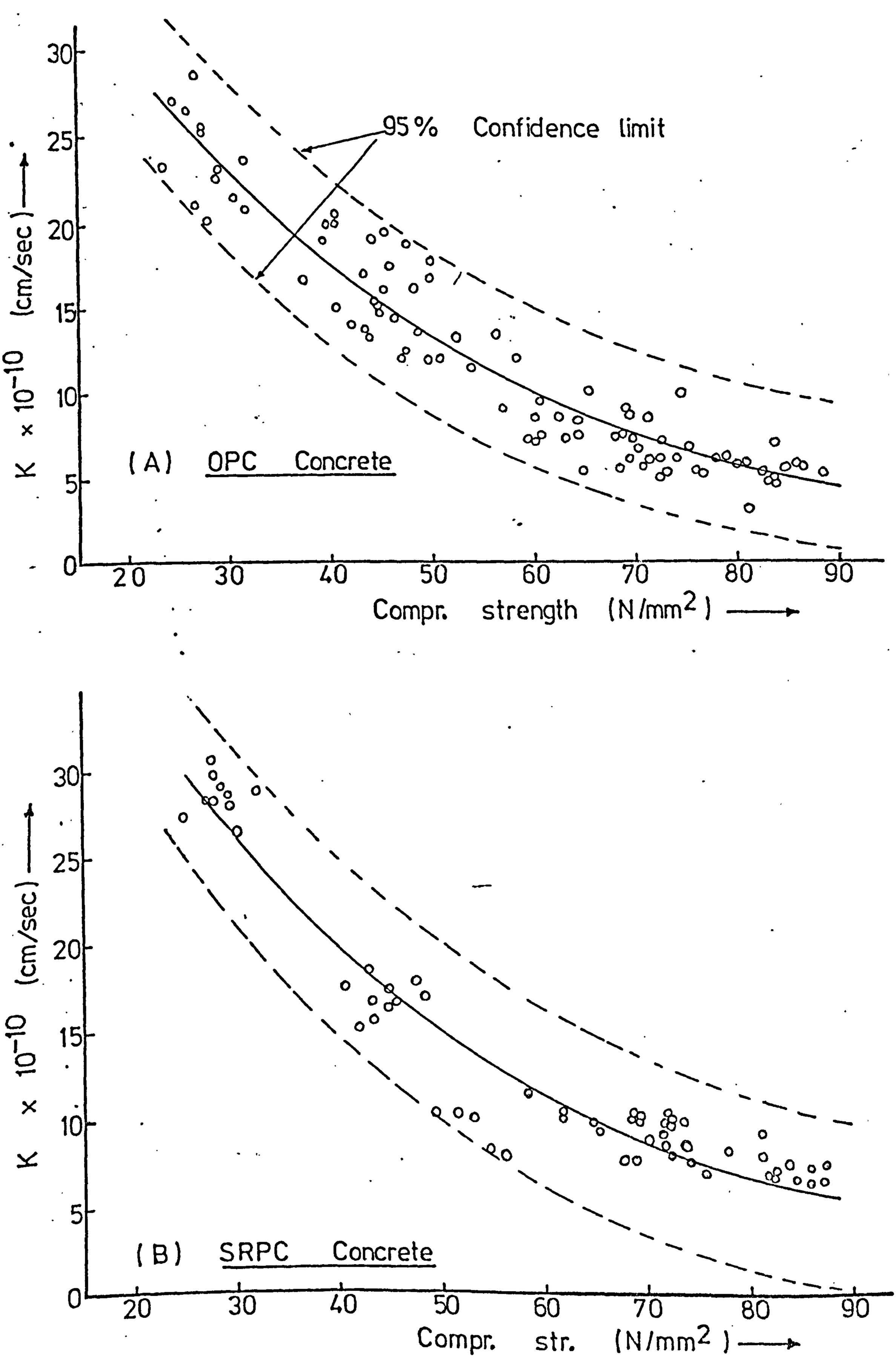

FIG(7.8) PREDICTION OF K FROM THE COMPR. STRENGTH OF CONCRETE

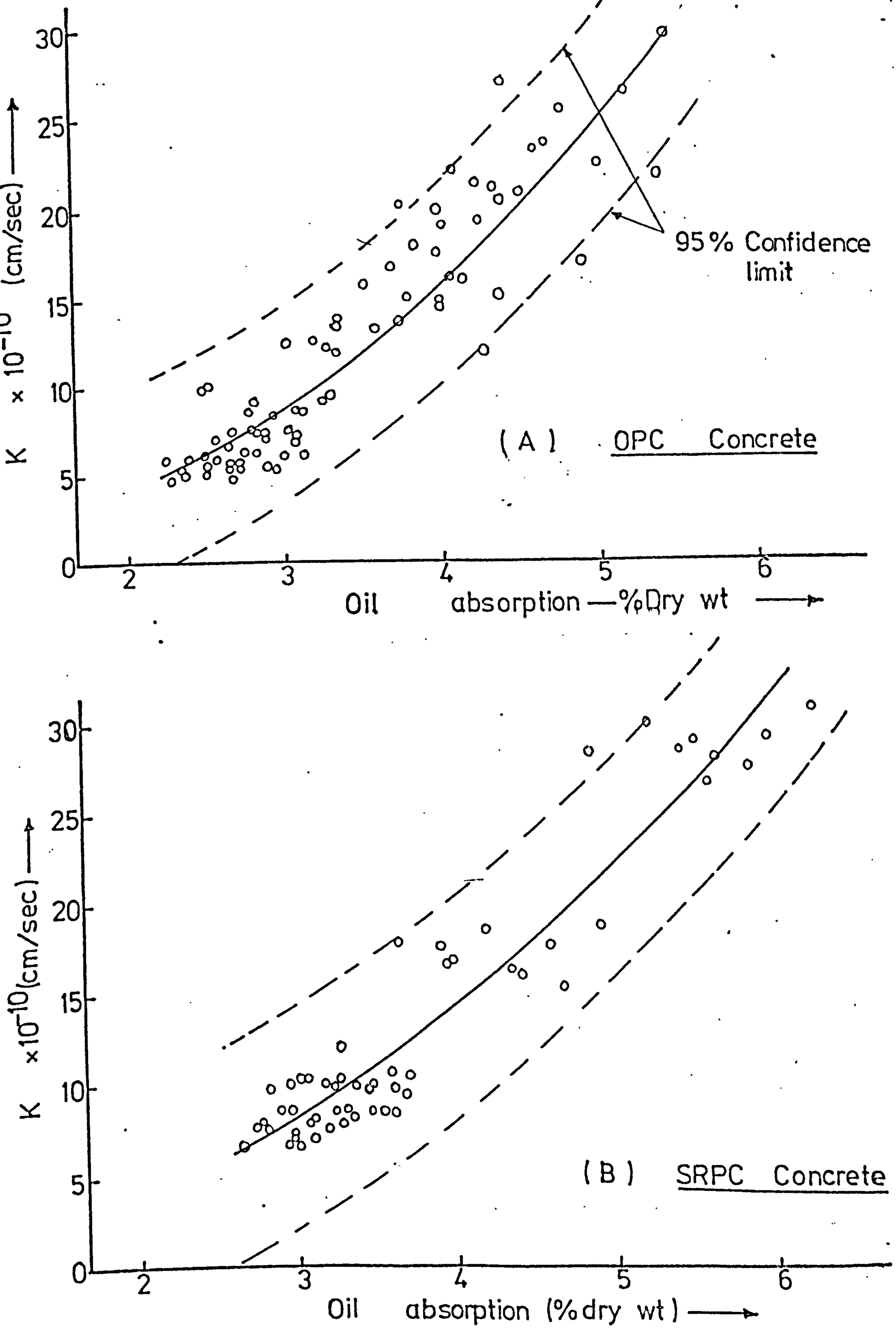

FIG (7.9) PREDICTION OF K FROM OIL ABSORPTION OF CONCRETE

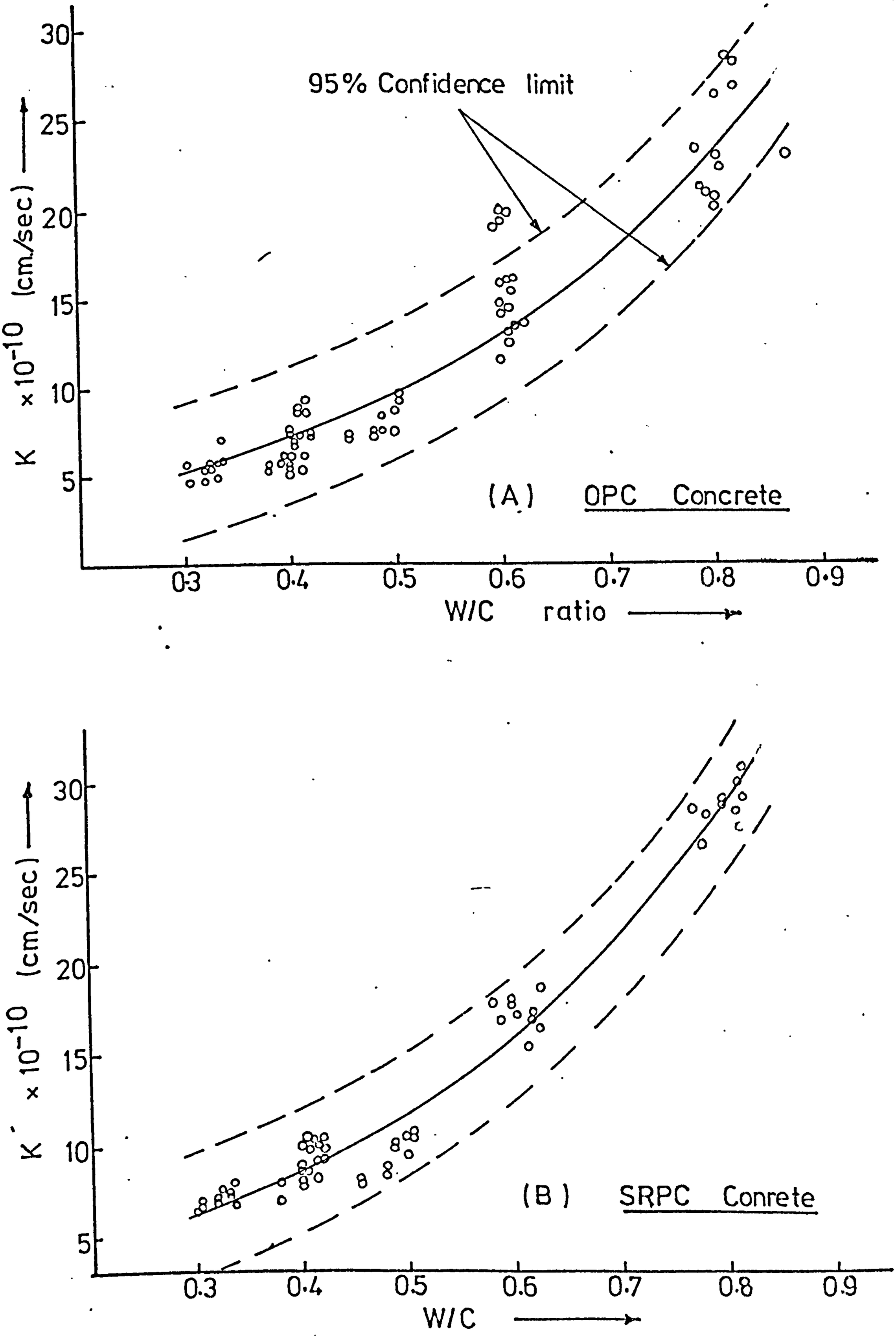

FIG(7.10) PREDICTION OF K FROM THE CONCRETE MIX W/C RATIO

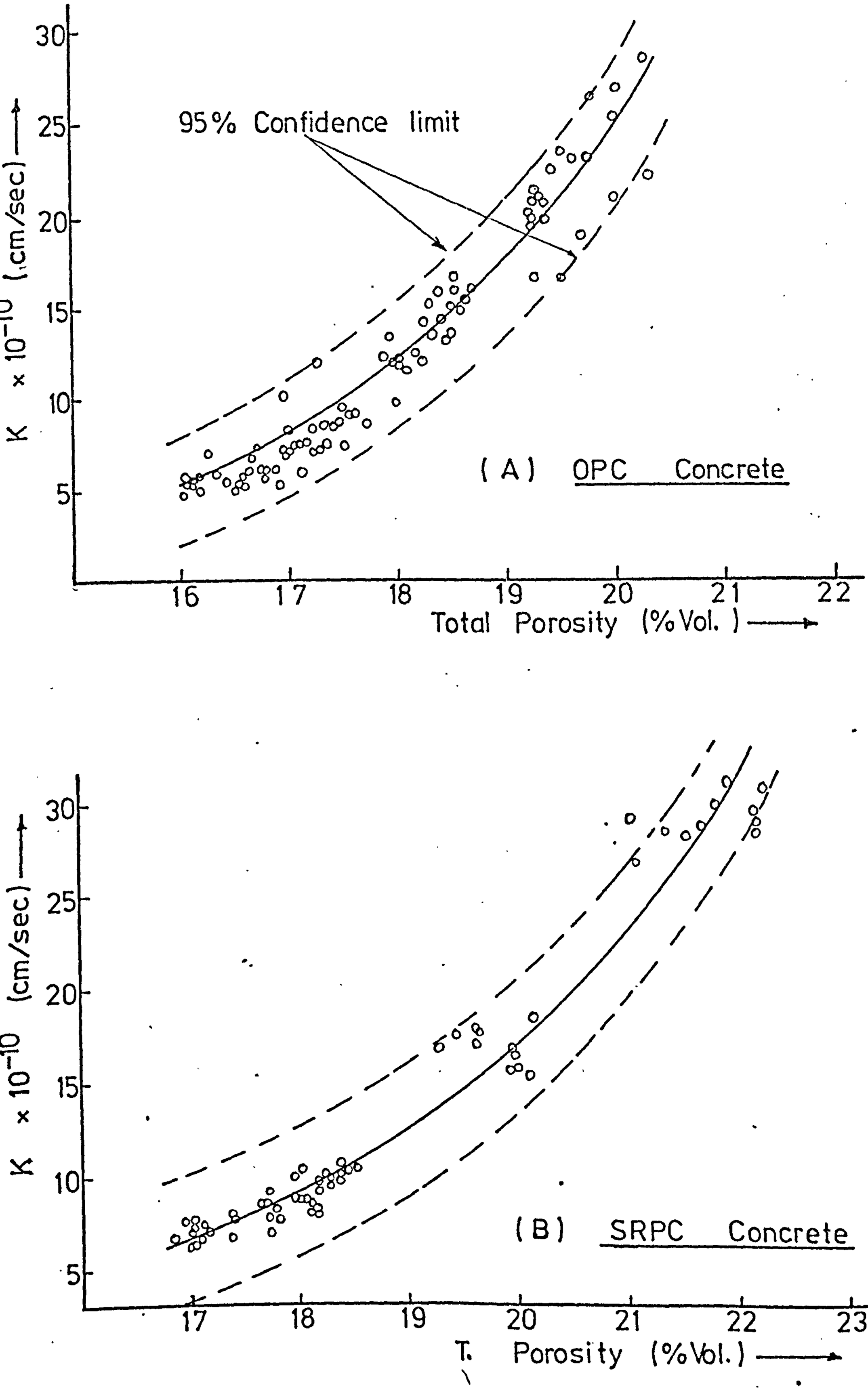

FIG (7.11) PREDICTION OF K FROM THE CONCRETE TOTAL POROSITY

CONCRETE	$K_o \times 10^{-10}$	b	r
OPC	0.0151	0.3702	94.2
SRPC	0.0396	0.3027	97.5

Table (7.8) Constants of Regression: equ. (7.8) K Vs Total Porosity

7.3.2.2 Results of Oil Permeability of Concrete by Other Investigators

Matti[12] made an extensive study of the permeability of concrete to crude oil in an unsteady state of flow (ie. no outflow). He obtained an empirical relationship between rate of flow and depth (D) of oil penetration with time for a concrete test specimen, from which he estimated K, as:

$$K = \alpha t^{\beta}$$

where $\alpha = A^2B/h$

and $\beta = -0.4285$

A and B are empirical constants with B = 1/3.4. To obtain A, he found that:

$$D = At^{B}$$

The K value as in the present work, varied linearly with the applied hydrostatic pressure and time, but unlike the present work was also a function of D - the depth of oil penetration. For example, after 120 hours of oil penetration, typical K values were between 0.009 and 1.515×10^{-10} cm/sec for W/C = 0.4 and oil pressure of 65.54 meters, and for D between 0.101 and 1.225 mm. For W/C 0.6, K was between 0.232 and 3.415×10^{-10} cm/sec.

To verify this empirical relationships for the estimation of K using the rate and depth of oil penetration at a given time, Matti carried out a steady state flow test on concrete specimens of W/C = 0.6. Using either Darcy's law or empirical formulae, he obtained K values of between 1.168 and 1.515×10^{-11} cm/sec for applied hydrostatic pressures of 113.5 m and 65.5 m of oil head. These K values are about 10 times less than for similar samples in the present tests. This difference may be due to differing test conditions and techniques and the sample casting and curing.

Maxson and Achenbach[147] carried out tests on the properties of concrete in contact with pressurised hydrocarbons and sea-water. Permeability tests were made with air, water, pentane and crude oil on concrete cores 38 mm dia. by 76 mm long. They failed to obtain any results from crude oil tests and although no details were given in their paper, they concluded that the permeability of concrete to light hydrocarbons is very low and this is unlikely to be a problem in submerged concrete storage tanks.

Apart from these two investiations no other work could be found in the technical literature on the permeability of oil to concrete.

7.3.2.3 Water and Oil Permeability of Concrete

Most test to-date on concrete permeability have been carried out with water as the fluid[83-92]. In these investigations both the test apparatus and the test technique differed greatly producing large differences in the calculated coefficient of permeability (K). Many of the investigators concluded that their apparatus was only useful for comparative tests. A range of typical coefficients of permeability to water found for concrete is given in table (7.9).

It is obvious from the table that the K values differ considerably by as much as a factor of 20. The K values obtained for oil in the present tests varied between 3.0×10^{-10} and 30.0×10^{-10} cm/sec in OPC and 6.0 and 33.0×10^{-10} cm/sec in SRPC concretes. These values are less than the values obtained for water. Considering the fact that the specimens used in the oil tests were dried, which could result in upto 9 - 20 times increase in permeability[12], the permeability to oil for concrete is at least 20 times less than for water. K values obtained in the present tests and the ones in table (7.8) can be compared with a recommended arbitrary limit of 15×10^{-10} cm/sec set by the United States Bureau of Reclamation[70], for the construction of concrete storage and retaining structures for water.

W/C	AGE (days)	CONCRETE DETAIL	K (cm/sec)	Ref.
0.5	28	38 m Max. Aggregate	0.06×10^{-10}	90
0.6	28	38 m Max. Aggregate	1.10×10^{-10}	90
0.7	28	38 m Max. Aggregate	4.10×10^{-10}	90
0.68	7	1:1.65:5.84	3.63×10^{-8}	148
0.76	7	1:3.36:4.11	2.51×10^{-7}	148
0.60	7	Cem. Cont. = 283 Kg/m^3	4.2×10^{-9}	77

Table (7.9) Typical K values for Water

7.4 Compressive Strength and Elastic Modulus of Crude Oil Saturated HCPs and Concrete

Test results presented in chapter 6 have shown that the strength and elastic modulus of HCP and concrete saturated with crude oil were below those tested in a water saturated condition (SSD) and were considerably below those dried sealed and stored in the constant temperature room (CTR). The effect of oil saturation and sample porosity on the strength and modulus of HCP and concrete are discussed in this section.

7.4.1 Compressive Strength and Elastic Modulus of HCPs

7.4.1.1 Compressive Strength of HCPs

The compressive strength of OPC pastes at various curing conditions are shown in table (6.2) and the calculated capillary porosities, P_c in table (7.1) and fig. (7.4). Two mathematical expressions are widely used to describe the strengths of HCPs and concrete in terms of their porosities. These are the inverse exponential functions of porosity and the Power functio of the 'gel-space' ratio, X, proposed by Powers and Brownyard. Both were discussed in detail in Section 2.3.3. These two methods are used here to compare test results obtained at various curing and storage conditions and also with other published results. All test samples were 2" or 50 mm cubes.

The exponential expression for HCP strength is:

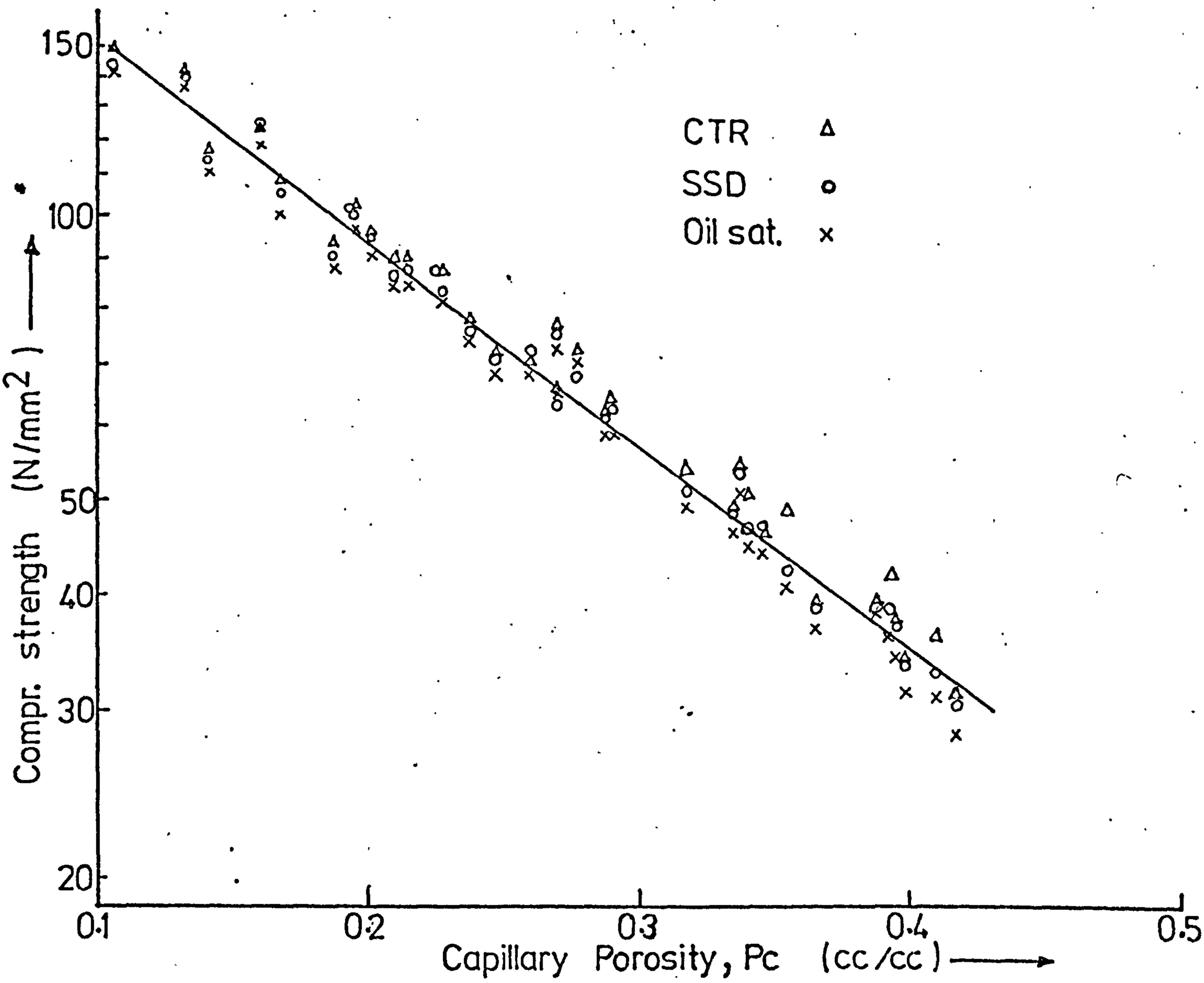

FIG (7.12) STRENGTH/CAP. POROSITY RELATIONSHIP FOR ALL STORAGE CONDITIONS

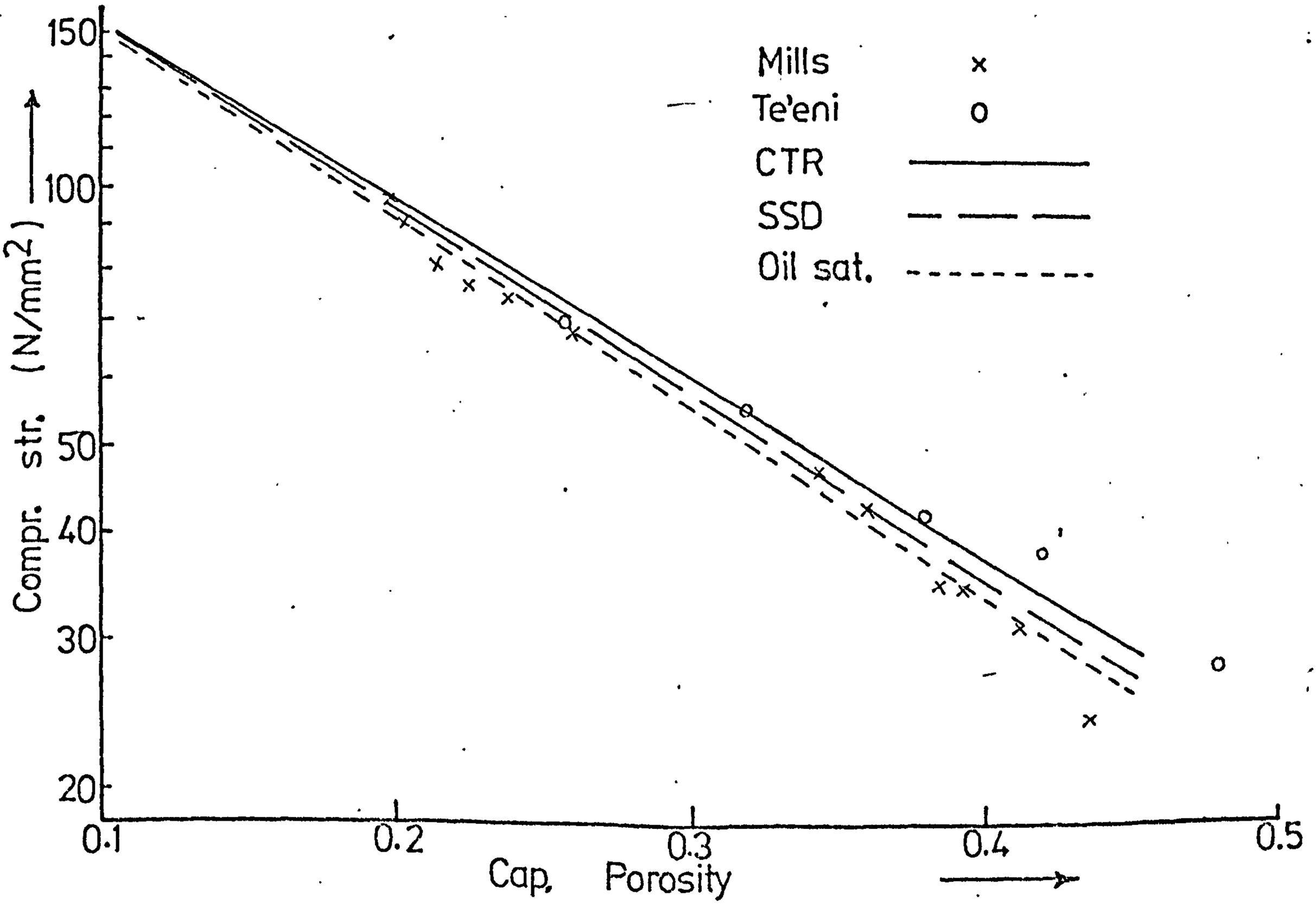

FIG (7.13) STRENGTH / CAP. POROSITY RELATIONSHIP

$$S = S_o (exp)^{-bP} \qquad (7.9)$$

Fig. (7.12) shows a semi-logarithmic plot for compressive strength against porosity for HCPs in the SSD, CTR and Oil Saturated conditions. The results fit closely to a straight line with slope (b) = 4.91. The results are replotted in fig. (7.13) with the individual experimental results omitted but including the results (SSD) from Te'eni[100] and Mills[101]. Mills results were taken from a graph in his paper and therefore may not be very accurate and the capillary porosity of his paste was calculated by the present author as described in section 7.2.4.1

The slope, b, of the different plots describes the variation in strength with porosity - the lower the slope, the less sensitive is the strength of the paste to the porosity. The respective slopes are: CTR 4.78, SSD 4.89, Oil Sat. 4.98, Te'eni 3.87, Mills 4.94, and thus Te'eni's pastes are stronger at any given porosity than either those of Mills or this investigation. This may be due to the different testing apparatus or errors in his calculated capillary porosity, since Mills' pastes are of similar strengths to the SSD ones in the present work. A more important observation is that the slope of the oil saturated HCP is greater than for either SSD or CTR pastes. This means that the strength of oil saturated pastes is more sensitive to the porosity, in other words oil in the HCP pores reduces the strength more than when water is in the pores.

Powers and Brownyard[23] related the strength of HCPs to the gel-space ratio (x) - section 2.3.3 - as:

$$X = \frac{2.06 U_c \, a}{U_c a + W/C} \qquad (7.10)$$

All symbols have their former meaning. For cement of specific volume, $U_c = 0.319$ cm^3/gm and $W_n^o/C = 0.232$, then:

$$X = \frac{2.832 \; W_n/C}{1.375 W_n/C + W/C} \qquad (7.11)$$

Powers found that the strength of HCP followed the relationship:

$$S = S_o X^n \qquad (7.12)$$

where n is a constant which he found to be approximately equal to 3[24]

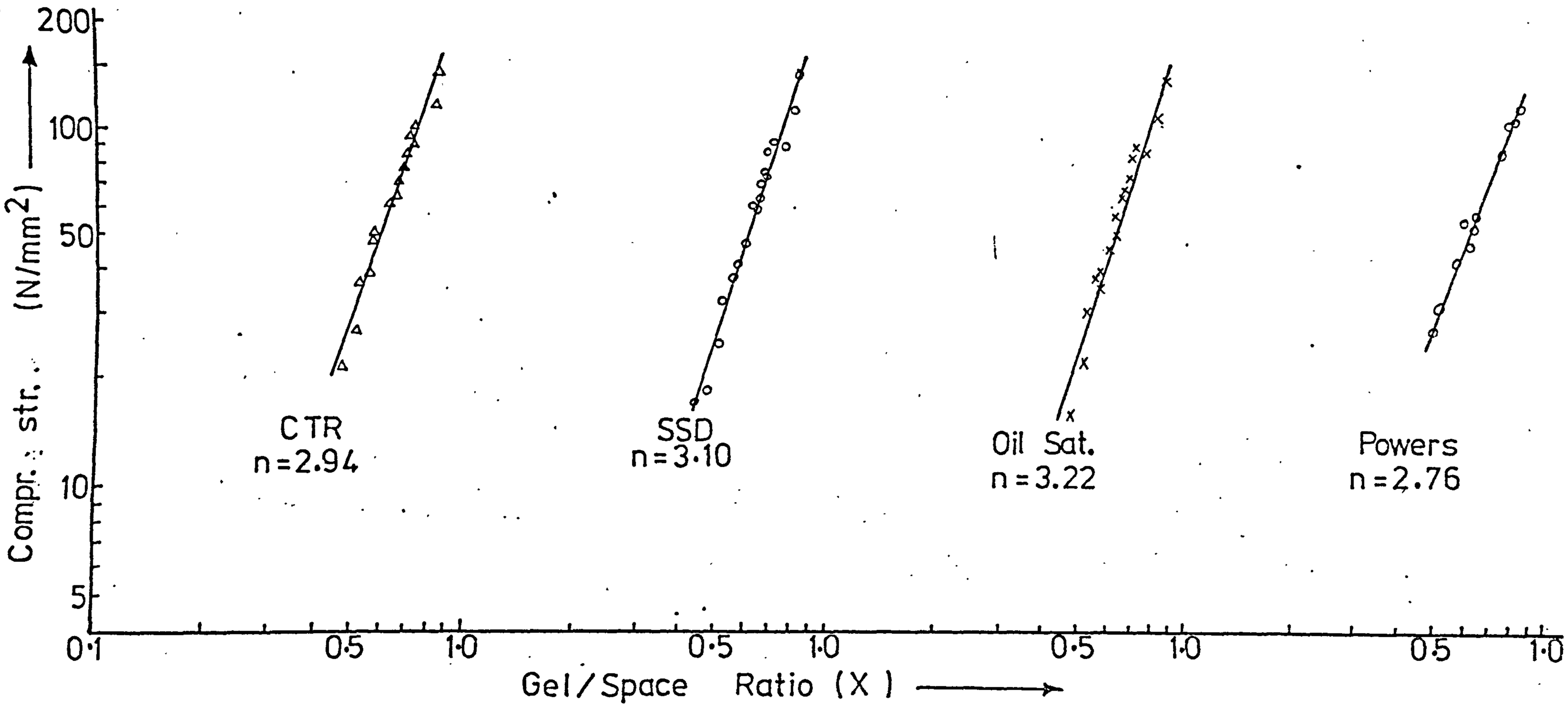

FIG(7.14) COMPR. STRENGTH VS. GEL-SPACE RATIO FOR HCPs.

A plot of log S against log X would give a straight line of slope n. Values of X were calculated and are plotted against strength in fig. (7.14), with Powers' results[24]. The following values were obtained: for SSD samples; n = 2.94, CTR; n = 2.65, Oil Saturated; n = 3.18, Powers; n = 2.86. Powers pastes are stronger which maybe an error due to obtaining strength values from Powers' graph. The value of n for oil saturated pastes confirms the earlier conclusion that oil saturation reduces the strength of HCP.

The reduction in strength of HCP due to crude oil saturation is further investigated in fig. (7.15) which is a plot of the percentage decreases in strength for samples stored in crude oil over the reference CTR strength - table (6.2), against the capillary porosity. A negative percentage obtained in one case was omitted as it is thought to be in error. Though considerable scatter of results was obtained, it is evident that higher strength reductions were obtained in pastes of higher capillary porosity. The highest strength reduction was about 19.5% in the 1 week old paste of W/C = 0.7 although this may have been due to cracking of the HCP during drying. Mean reductions are of the order of $7.4 \pm 4\%$.

The strength of HCP is known to increase on drying[101] resulting in the lower slope value, b and the lower power value n for CTR pastes in figs. (7.13) and (7.14) respectively. The absorption of any liquid into HCP and concrete pores is known to result in the dilation of the cement gel thereby decreasing the cohesive forces between the cement particles and reducing the strength. This phenomenum has been termed the wetting-weakening effect[149]. In the present investigation, the strengths of oil saturated HCPs were below those in the water saturated condition (SSD) and chemical, microstructural and physical phenomena might explain this strength reduction.

Chemically, petroleum oil is known to have little effect on concrete provided it is free from any impurities and is of mineral origin, containing no fatty oils or greasy materials[150]. Crude oil is, however, a mixture of such substances. From the crude oil analysis (chapter 3), the sulphate content was only about 2% which is too small to have a serious effect in such a short time.

From the microstructural view-point, it has been suggested that in a brittle material like HCP and concrete it is possible to relate the strength to the surface energy[141,142]. On saturation with fluids, the

surface energy decreases and hence reduces strength, and the amount of reduction can be related to the molecular size of the fluid adsorbed. It was shown in chapter 4 that the pore structure of HCP changed after oil saturation resulting in a decreased surface area after redrying and, according to Power's explanation of strength - section 2.3.2, the strength is determined primarily by Van der Waals forces, so that if the surface area decreases then the strength decreases[36]. On oil saturation further surface area is lost, even after redrying - table (4.4), which leads to further reduction of the physical forces of attraction between the gel particles and hence to a reduction of strength below that due to water. Cook and Haque[141] have shown that benzene and paraffin with molecular sizes about 2 and 3 times greater than water, do not reduce the strength of concrete, but ethyl alcohol with molecular size only 50% greater than water, reduced the strength by as much as water would. Crude oil has molecular sizes 3 times lower and upto 6 times higher than water.

Physically, the testing machine and the contact surface between the machine plattens and the HCP surfaces could contribute to the strength reduction. Oil saturated HCP cubes were thoroughly cleaned before the test, but if any oil seeped out, it could reduce the friction between the machine plattens and the test cubes. This would lead to an apparent reduced strength[70].

7.4.1.2 Elastic Modulus of HCPs

The elastic modulus of HCP and concrete is usually related to its porosity using Powers cube law or the equation due to Hansen - section 2.3.4. The results obtained for OPC pastes are studied here using Powers' and Brownyards equation[23]:

$$E = E_o(1 - P)^n \qquad (7.13)$$

where n is a constant, and E_o the modulus of a theoretical paste of zero porosity. Fig. (7.16) is a semi-logarithmic plot of E against $(1 - P_c)$, where P_c = capillary porosity, for the three storage conditions together with the results by Mills and Ono[151]. It is assumed for this study that after drying the HCPs to 105°C, no further hydration takes place when sealed and stored (CTR) or when oil saturated and hence the porosity is constant and of value equal to that before drying ie. at 28 days. By a regression

analysis values of n were obtained as: SSD; 2.66, CTR: 2.62, Oil Saturated: 2.67 at 24 weeks and 2.65 at 40 weeks, Mills and Ono: 2.62. Thus equ. (7.13) would give the modulus of the cement pastes irrespective of the curing and storage conditions with the power factor n approximately equal to 2.65.

Fig. (7.16) also shows that the elastic modulus of water saturated (SSD) samples is higher than for corresponding dried (CTR) or oil saturated samples. The elastic modulus was lowest for the dried samples. Several theories have been put forward to explain the decrease in elastic modulus on drying on the following assumptions[152]:

a) Water held in the capillary pores has a structural load-bearing role.

b) Microcracking occurs on drying which reduces the modulus

c) Dehydration of calcium silicate hydrate (C-S-H) in the paste at high humidities reduces the modulus.

In the present investigation, microcracking is assumed not to have occured to any significant extent since the compressive strengths - section 7.4.1.1 - were not reduced on drying. C-S-H is known to dehydrate on drying and to rehydrate on re-saturation with water[18,38] but the rehydration is not expected to occur during oil saturation and cannot therefore account for the increased modulus of oil saturated specimens over dried ones. It is therefore likely that when liquid - water or oil - is in the HCP pores it assists in carrying the load and the resultant pore pressure in the compressed capillaries is not sufficient to split the paste.

The elastic modulus of HCP and concrete is generally considered to be related to its compressive strength. Fig. (7.17) shows the elastic modulus plotted against the corresponding compressive strengths for samples at ages of 4 and 24 weeks stored in water or oil or dried. The considerable scatter of results obscures any precise relationship, but generally, as expected, the modulus increases with increasing strength; and for equal strengths SSD samples possess the highest modulus and the dried samples the least. The scatter of results may be due to:

a) Drying HCP increases the strength but reduces the modulus.

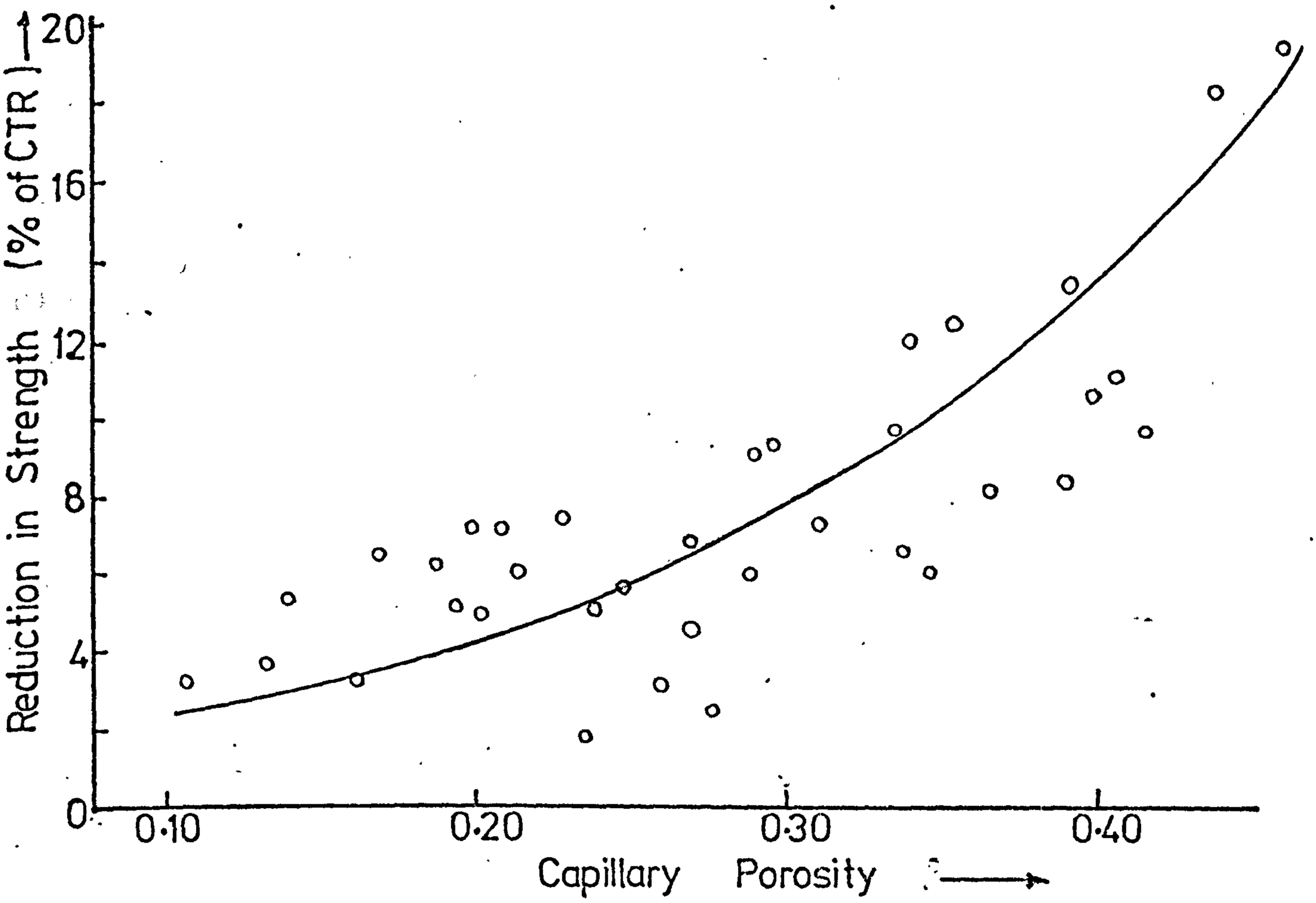

FIG(7.15) PERCENTAGE REDUCTION IN STRENGTH DUE TO OIL SATURATION VS. Pc.

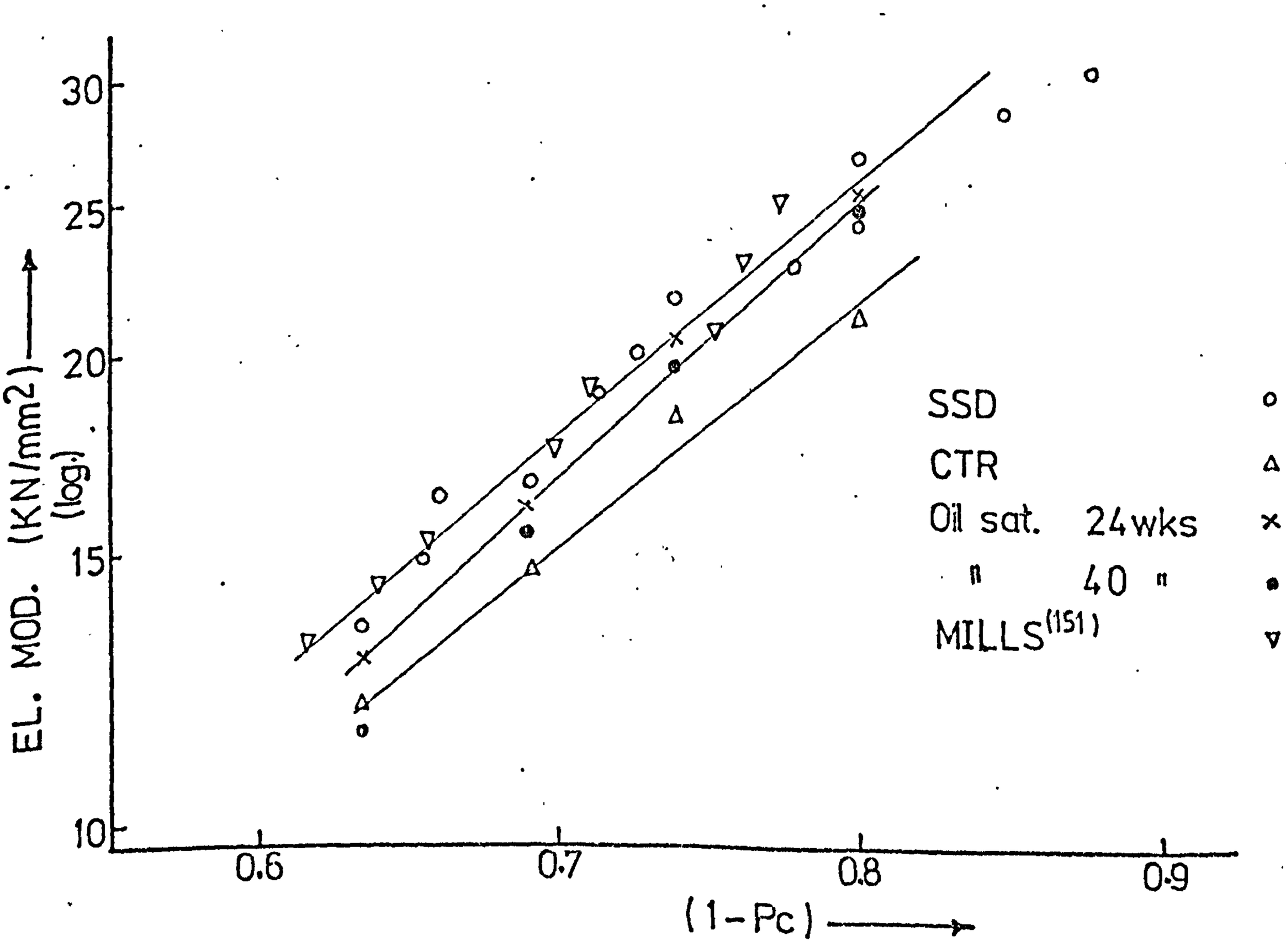

FIG(7.16) ELASTIC MODULUS OF HCP VS. (1-Pc)

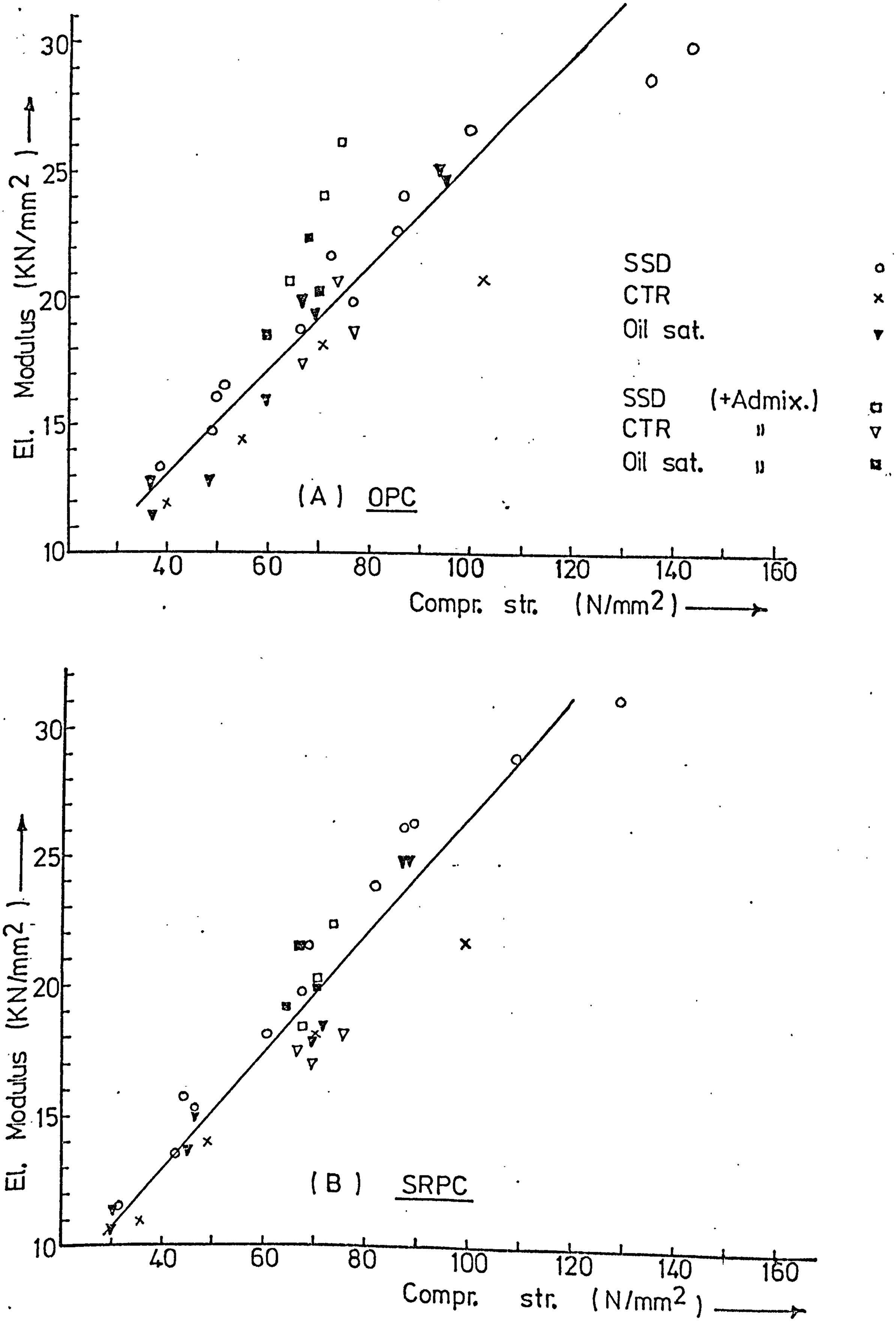

FIG(7.17) VARIATION OF THE ELASTIC MODULUS WITH THE COMPRESSIVE STRENGTH OF HCPs

This also accounts for the modulus of dried specimens being less than for SSD specimens at equal strengths.

b) The rate of gain of strength with age during water-curing is higher than the rate of gain in elastic modulus.

7.4.2 Compressive Strength and Elastic Modulus of Concrete

7.4.2.1 Compressive Strength of Crude Oil Saturated Concrete

Porosity is an important factor affecting the strength of HCP and concrete. Pores reduce the strength by acting as stress concentrators and by reducing the effective load-bearing section of the concrete[14]. The exponential relationship is used here to relate the strength of crude oil saturated concrete cubes to the total porosity. The values are given in tables (5.9) and (5.10) for OPC and SRPC concretes and tables (5.17) to (5.20) for superplasticised concretes. The relationship is illustrated in fig. (7.18) and can be expressed as:

$$f_o = f_o(\exp)^{-bP} \qquad (7.14)$$

The values of f_o and b are obtained by regression analysis and are given in table (7.10).

It was shown in chapter 6 that the strength of the oil saturated samples was below the SSD or CTR samples. Fig. (7.19) shows the percentage reduction in the strength of crude oil saturated specimens over the reference CTR concretes after 24 weeks, against the calculated total porosity. Considerable scatter of results was obtained for both concretes, but it is clear that a greater percentage reduction in strength was obtained in concrete of higher porosity. An important observation stated in section 6.4.11 is that the actual numerical reductions was about similar in all specimens and was independent of the W/C ratio.

The reduction in cube strengths found in crude oil saturated specimens can be partially explained by the reasons given in section 7.4.1.1 for HCPs, but for concrete some additional factors need be considered viz:
a) Concrete took longer to reach maximum saturation in oil than the 4

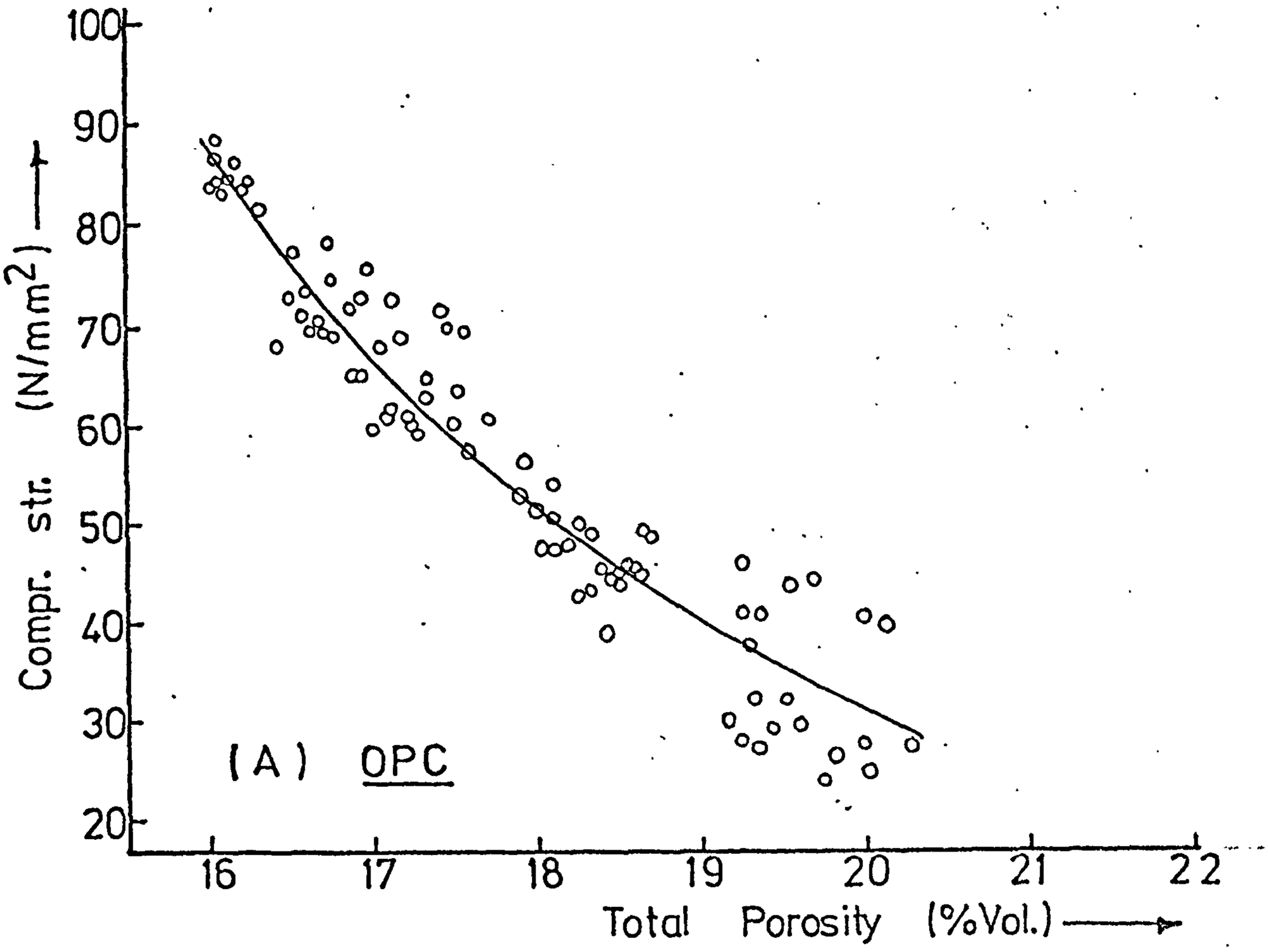

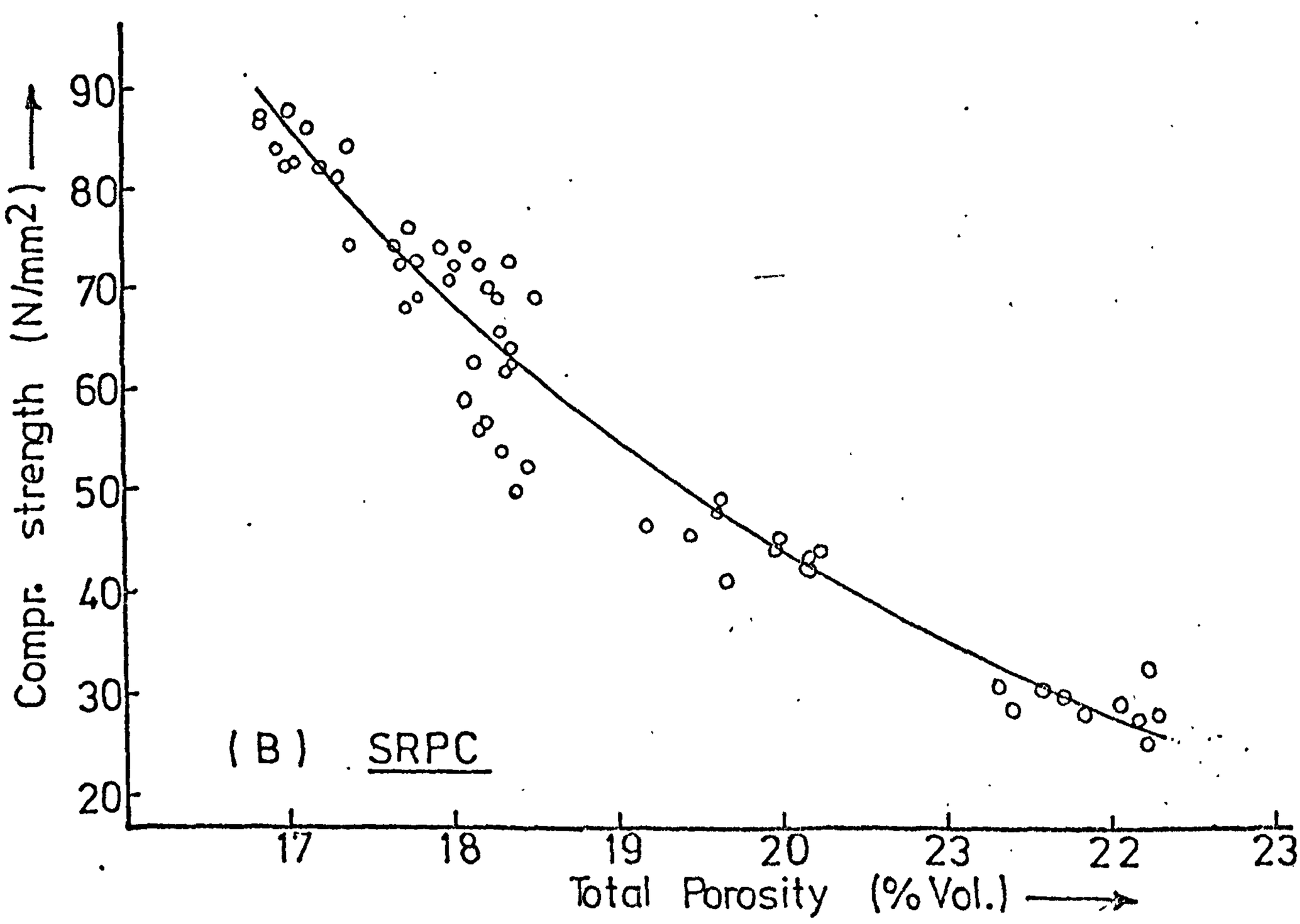

FIG(7.18) RELATIONSHIP BETWEEN COMPR. STRENGTH & THE TOTAL POROSITY OF CONCRETE

months required by HCP - section 5.7.3.4. b) The cube strength of concrete changed significantly from its value at 24 weeks. c) The overall strength of concrete is influenced by the coarse aggregate component of the mix - its size, smoothness, type and quantity. Since very fine cracks exist at the interface between coarse aggregate and cement paste in concrete even before the application of any external load[153,154], these cracks will fill with water or oil and affect the mechanical bond between aggregate and cement paste. For oil saturated concrete the extent of the reduction will be higher than for water saturated concrete partly due to the reasons already discussed and also due to the chemical nature, smaller molecular size range and viscosity of the crude oil.

The numerical reduction in strength due to crude oil saturation was apparently independent of W/C ratio. This is probably due to the fact that at low W/C ratio the paste-aggregate bond contributes considerably to the overall strength of the concrete but at higher W/C ratio its contribution is negligible[70]. In these mixes the coarse aggregate content is lower at lower W/C ratio than at higher W/C ratio and a higher reduction in paste-aggregate bond is expected in concrete of higher W/C ratio.

Test results were given in table (6.9) and fig. (6.11) on the variation of compressive strength with prolonged storage in crude oil. The strength is seen to decrease continuously with time and although the average rate of strength reduction is small it increases with increasing W/C ratio.

Table (7.11) shows the numerical and percentage strength reduction of the concrete specimens averaged over a monthly period, and it can be seen that the rate of strength loss decreases with time. High reductions were obtained before maximum saturation ie. after 4 month. The continued reduction of strength with time is due to the continued absorption of oil into the pores and microcracks of the concrete resulting in the continued reduction of the cement paste-aggregate bond and hence the compressive strength. Absorption of oil reached an almost constant rate after the 8th month of oil soaking - fig. (5.63) and consequently the reduction of strength of concrete was found to be very small after that time.

CEMENT TYPE	W/C RATIO	24TH WEEK		40TH WEEK		58TH WEEK	
		+Reduction N/mm^2	+% Reduction	*Reduction N/mm^2	*% Reduction	**Reduction N/mm^2	**% Reduction
OPC	0.40	1.38	6.2	0.70	3.4	0.18	0.9
	0.50	1.00	5.7	0.68	4.1	0.08	0.5
	0.60	0.38	2.7	1.05	7.9	0.30	2.4
	0.70	0.75	6.6	0.83	7.3	0.43	4.0
SRPC	0.40	0.83	3.9	0.83	4.0	0.43	2.2
	0.50	1.00	5.7	1.20	7.2	0.23	1.5
	0.60	0.58	5.0	0.58	5.2	0.43	4.1
	0.70	0.48	5.3	0.70	8.3	0.38	4.8
OPC	0.40	1.23	4.8	1.05	4.7	0.15	0.7
+	0.50	1.63	7.8	1.18	6.1	0.45	2.5
4%	0.60	1.20	7.4	0.68	4.5	0.40	2.8
Admix	0.70	1.05	8.1	0.50	4.2	0.40	3.5

\+ Reduction and % reduction over CTR

* Reduction and % reduction over 24th week oil sat.

** Reduction and % reduction over 40th week oil sat.

Table (7.11) Reduction in Compressive Strength (Per month) due to Crude Oil Saturation

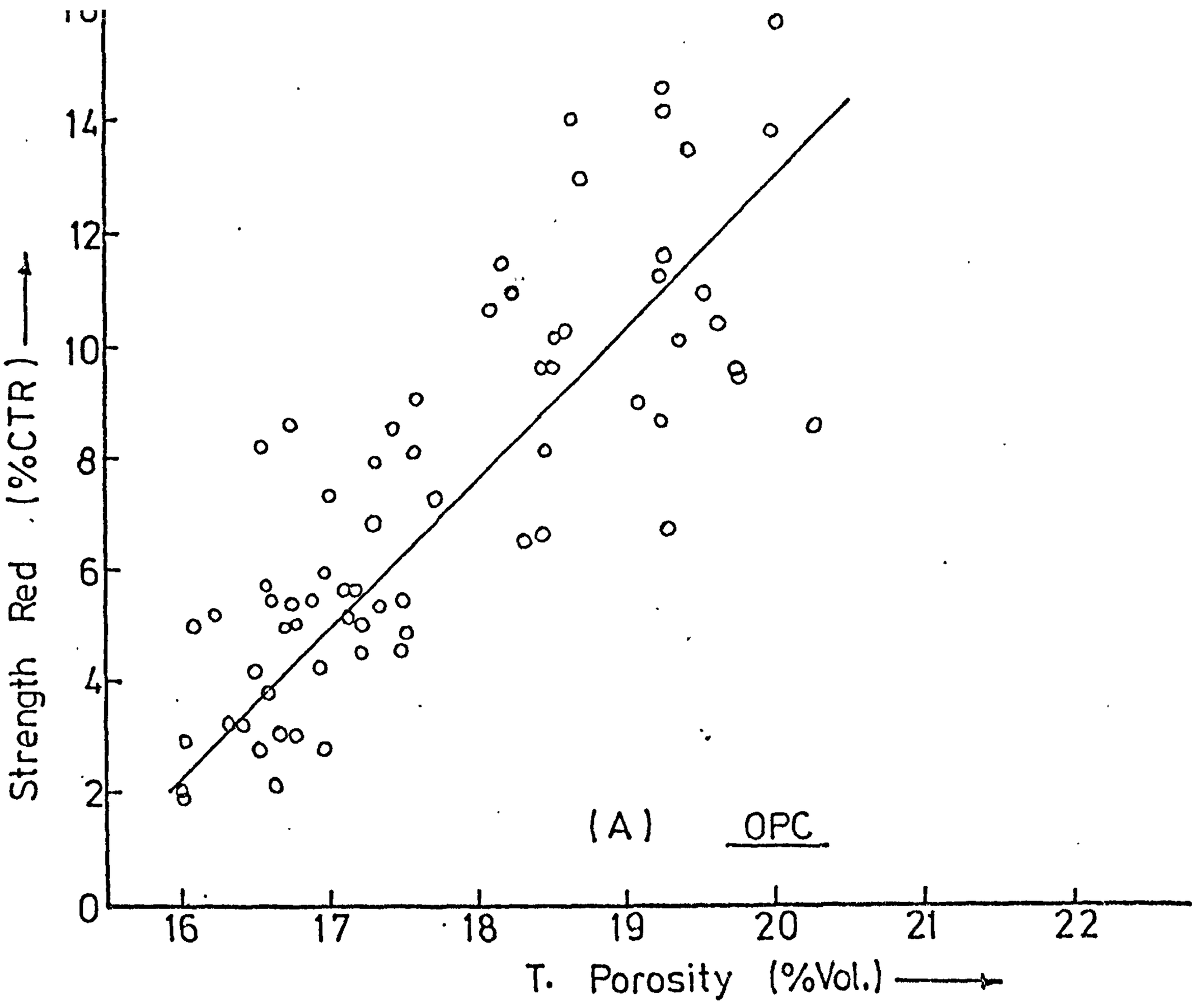

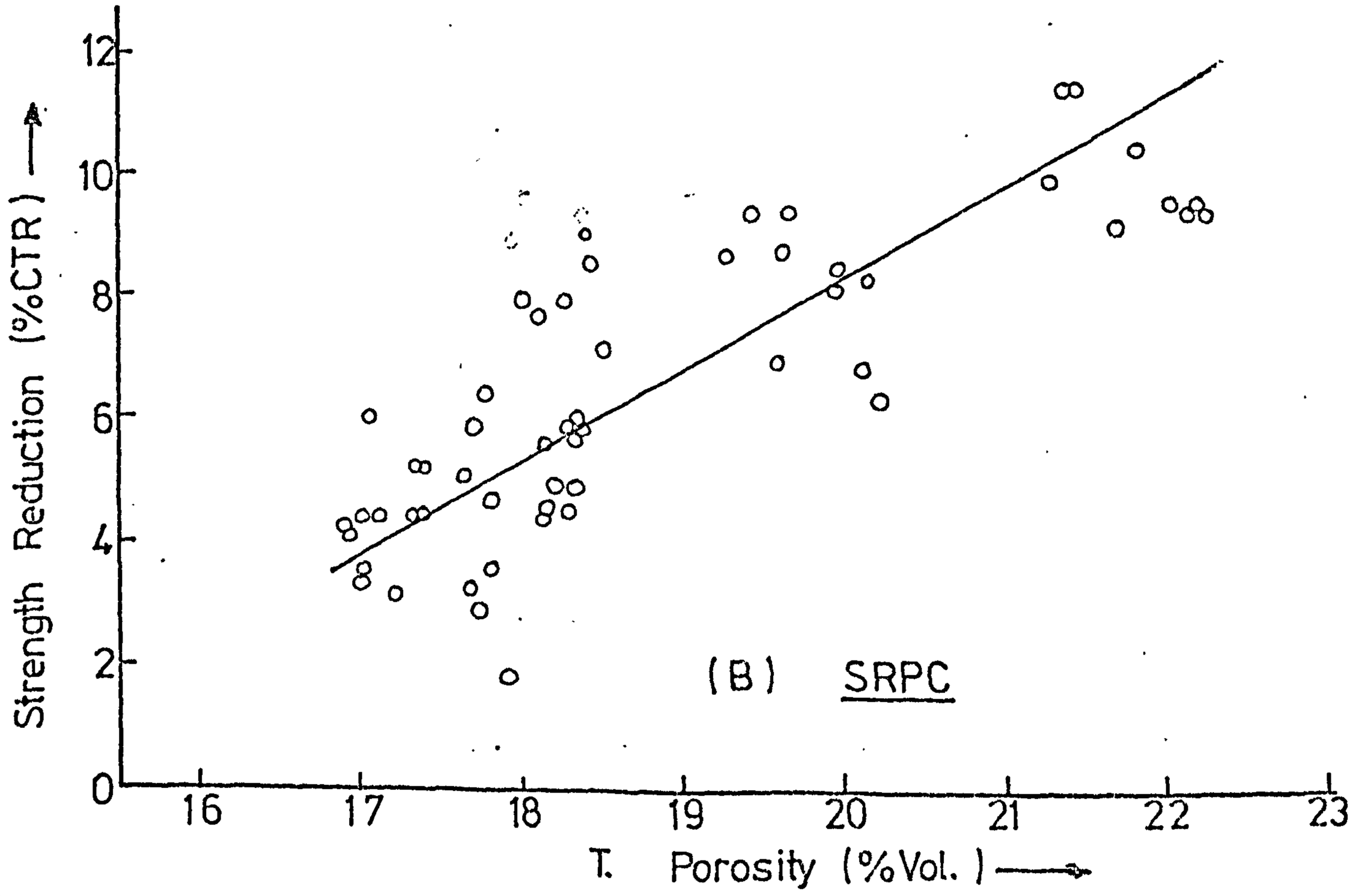

FIG (7.19) REDUCTION - IN STRENGTH OF CONCRETE DUE TO OIL SATURATION VS. TOTAL POROSITY

CONCRETE	$f_o \times 10^3$	b	r
OPC	6.47	0.2685	-96.8
SRPC	4.01	0.2262	-95.1

Table (7.10) Constants of Regression - Equ. (7.14) Compr. Strength Vs T. Porosity

7.4.2.2 Elastic Modulus of Crude Oil Saturated Concrete

I General Behaviour of the Concrete Prisms Under Compressive Load

The general behaviour of the concrete prisms under compressive laod can be studied from the stress-strain relationships presented in chapter 6 - for the various test conditions. Test results for the elastic modulus of concrete are also given in table (6.12).

The relationships show that at low loads the behaviour of the crude oil saturated concrete is similar to either the dried (CTR) or the wet (SSD) concrete. As load increases, crude oil saturated concrete tends to be more flexible and weaker. The greater flexibility is shown by the lower modulus, the greater increase in Poisson's ratio and the higher volumetric expansion. The peak stresses was lower in the oil saturated specimens by between 6.2 and 11.8% for OPC concrete, 8.1 and 14.4% for SRPC and 5.2 and 12% for OPC concrete containing admixture, after 1 year of crude oil storage.

This behaviour of crude oil saturated concrete is similar to that observed by Shah and Chandra[136], and Darwin and Slate[155] for concrete in which the paste-aggregate bond was reduced by coating the coarse aggregate. They observed that concrete containing the coated aggregate behaves like concrete containing uncoated aggregate at low loads, but is more flexible at loads approaching the ultimate value. It appears that apart from weakening the cement paste component of concrete - section 7.4.1.1, crude oil saturation also weakens the aggregate-cement paste bond and further study is necessary in this area. The rate at which the elastic modulus reduces with prolonged storage in crude oil decreases continuously with time ie. as the concrete becomes more saturated with oil; and after 1 year in oil the reduction was

negligible - Table (6.11). Generally, the rate of reduction in the modulus was erratic and unlike strength was apparently unrelated to the mix W/C ratio and hence the porosity of the concrete.

II Relationship Between Elastic Modulus and Compressive Strength of Concrete

Generally the factors which influence strength also influence the modulus of elasticity in a similar manner, though to a lesser degree. The elastic modulus is therefore, generally considered to be directly related to the compressive strength and this is followed in most codes of practice. The experimental relationships between elastic modulus and compressive strength are illustrated in fig. (7.20). The relationships are not linear and this agrees with previous work[70] eg. CP110: 1972[156] relates the tangent modulus, E_c (KN/mm^2), to the concrete cube strength, f_c, (N/mm^2) by the expression:

$$E_c = 4.5\sqrt{f_c} \qquad (7.15)$$

for concrete of density 2,300 Kg/m^2 and greater. It is claimed that the modulus so determined falls within $\pm$ 7 KN/mm^2 of its real value when determined according to BS 1881: Part 5: 1970[81]. Using the compressive strengths given in table (6.9), the elastic modulus obtained from the experimental results are compared with the predicted values, using equ. (7.15) in table (7.12). For the SSD samples the results fall within -0.4 and +7.1 KN/mm^2, for CTR: +1.4 and +11.2, and for Oil Saturated: +2.2 and 12.0 KN/mm^2. These rather large deviations from the expected values show that the modulus is not just a simple function of the strength.

A better relationship between cube strength and the modulus for the experimental results is:

$$E = \beta (f_c)^{\alpha} \qquad (7.16)$$

The constants β and α are obtained by regression analysis and are given in table (7.13), together with the standard deviations.

28D (SSD)		24 WEEKS CTR		24 WEEKS Oil. Sat.		58 WEEKS Oil Sat.	
CODE	THESIS	CODE	THESIS	CODE	THESIS	CODE	THESIS
40.5	33.4	42.4	31.2	40.4	30.6	40.2	28.4
36.5	29.4	37.6	28.6	35.7	27.8	35.7	26.9
31.8	27.0	33.4	26.1	31.6	26.7	31.2	25.6
29.6	24.9	31.3	24.9	29.2	24.2	28.6	24.0
40.1	35.1	41.6	35.6	40.0	34.1	39.6	32.0
35.7	31.3	37.8	30.3	35.3	31.0	35.1	29.1
29.3	27.9	30.7	27.0	29.1	26.8	28.5	26.6
25.4	25.8	26.9	25.5	25.1	24.0	24.4	22.9
41.4	40.1	43.4	38.3	41.3	36.4	41.2	35.3
39.1	34.5	41.0	33.4	38.1	32.3	37.6	30.6
34.5	31.6	36.3	28.4	34.2	28.0	33.7	27.0
30.7	29.5	32.4	26.8	30.4	25.2	29.9	24.0

Table (7.12) Comparison of the Experimentally obtained Elastic Modulus with that predicted from CP10

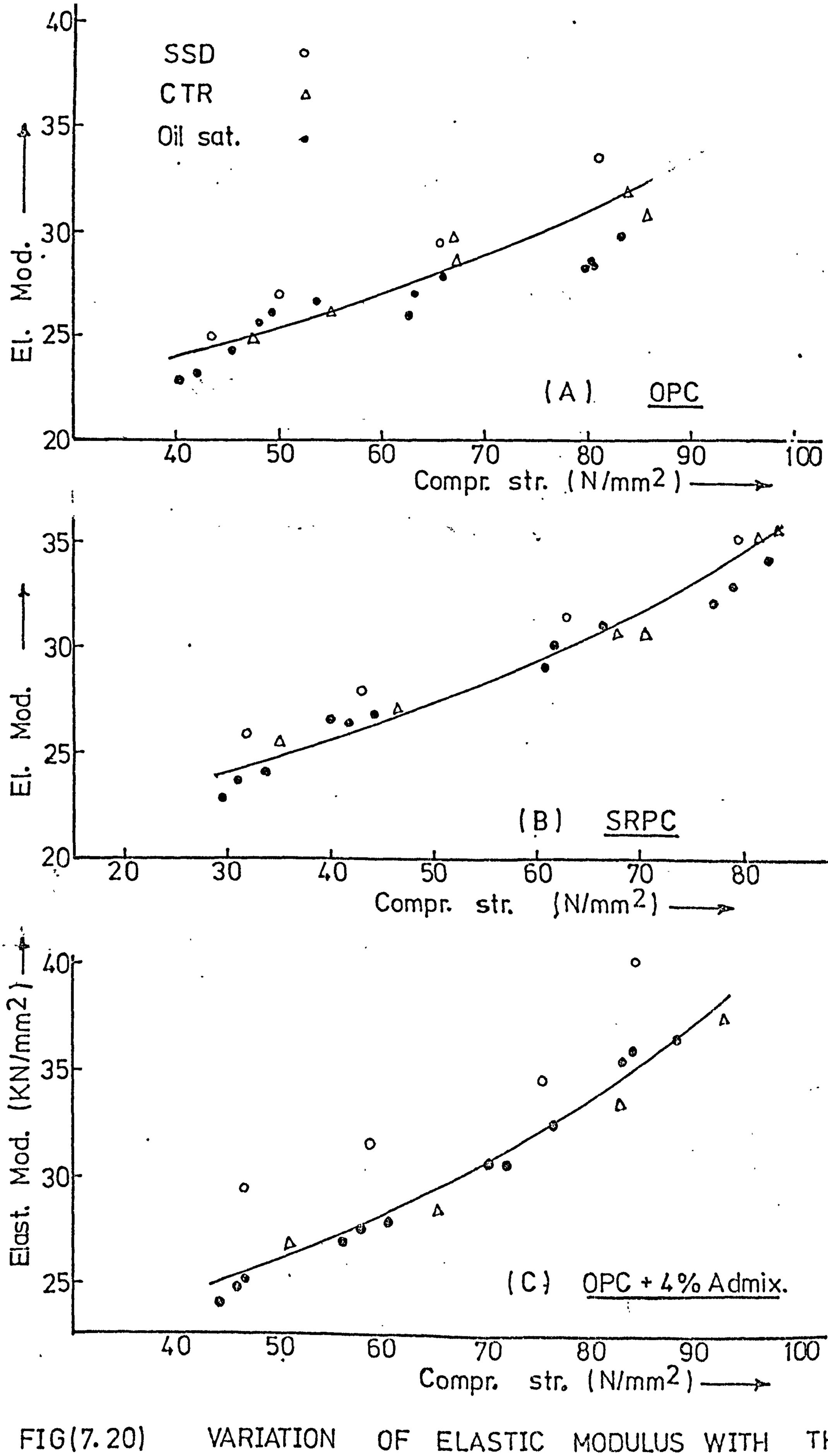

FIG(7.20) VARIATION OF ELASTIC MODULUS WITH THE COMPR. STRENGTH OF CONCRETE

CONCRETE			STANDARD DEVIATION	r
OPC	6.81	0.339	2.37	89.1
SRPC	6.99	0.352	3.78	97.4
OPC + Admix.	2.74	0.578	4.30	92.0

Table (7.13) Constants of Regression Equ. (7.16)
El. Modulus Vs Compr. Strength

7.4.4 Concrete Corrosion in Crude Oil

The deterioration of concrete in contact with various organic and inorganic fluids has been studied and the effects are listed in section 2.3.5.

The first two effects are visual and chemical changes. Visual deterioration is often described with reference to the number and size of external cracks and the extent of warping in the specimen[157]. None of these phenomena is noticeable in crude oil saturated concrete after storage of upto 1 year. No chemical changes were investigated but previous research had not established any chemical changes in either oil[11] or concrete[150] after direct contact with each other.

Changes in the strength of HCP and concrete - compressive or tensile - have been observed both in the present investigations and previous ones [11,13]. The extent of cube strength reduction and its variation with time has been considered in chapter 6 of this thesis. Matti[11] also found that the cube strength of partially dried concrete ($20^{o}C$ air-dry) decreased by about 8% after being in contact with crude oil for about 26 weeks and this reduction depends on the quantity of oil.absorbed. Faiyadh[13] found about 9% strength reduction over a similar length of time, for concrete dried to $55^{o}C$ before soaking. None of the specimens used in the above tests was 'fully' saturated but Faiyadh's investigations are continuing at the present time. Increased saturation was obtained here by drying to $55^{o}C$ for the permeability test samples and to $105^{o}C$ for the samples used for the mechanical property tests and also by storage over a longer period. Percentage reductions in strength are plotted in fig. (7.19) and discussed in section

7.4.2.1. The rate of strength reduction diminished as saturation increased and by the 12th month was very small. Both Matti and Faiyadh found an increase in the splitting tensile strength of about 5%, and a 3% reduction in the flexural strength. Thus there is evidence that concrete deteriorated in crude oil.

A reduction in the static elastic modulus has been recorded in chapter 6 and discussed in section 7.4.1.2 and 7.4.2.2. Matti[13] investigated changes in the dynamic modulus and resonant frequency of oil soaked concrete. He observed an increase in the dynamic modulus of upto 10% for an air-dry concrete specimen after 540 days of oil soaking. This was 8 - 10% less than the increase found for similar specimens kept in water. Neville[158] has pointed out that the measurement of resonant frequency is a good indicator of deterioration in concrete because a decrease is due to the opening of cracks or removal of concrete binder materials. Matti's results would therefore, appear to show that there is no deterioration in oil soaked concrete but this is not borne out by the other tests. It may be that Matti's tests did not detect the structural changes like microcracking but the changes which do occur become apparent only during the application of loads, indicated by changes in static modulus, volumetric expansion and Poisson's ratio.

CHAPTER 8

CONCLUSIONS

8.1 Conclusions

Within the limitations of this study, the following conclusions are drawn.

8.1.1 Pore Structure of HCP and Concrete

1. The porosity of OPC pastes after 28 days water curing, measured by water-vapour adsorption on D-dried pastes, was between 0.1435 and 0.4181 cc/gm of paste for W/C ratios from 0.3 to 0.7. SRPC porosity was from 0.1925 to 0.3457 cc/gm for W/C ratios from 0.4 to 0.6. The porosity as measured from drying losses at 105°C, was from 0.3150 to 0.5898 cc/cc of paste for OPC, and from 0.3901 to 0.5311 for SRPC; for the same W/C ratios.

2. The wide-pore volumes, corresponding to Powers' capillary pores occupy between 77.5 and 90% of the pore volume in OPC and between 72 and 83% in SRPC pastes for W/C from 0.3 to 0.7 and 0.4 to 0.6 respectively.

3. The addition of 4% by weight of cement content, of Cormix SP1 superplasticiser increased the wide-pore volume slightly by 5 to 8% in OPC and 8 to 14% in SRPC pastes for W/C ratios of 0.4 to 0.6.

4. The addition of 1% and 2% of the superplasticiser reduced the wide-pore volume by 7% and 12% respectively for OPC pastes of W/C = 0.4.

5. The average hydraulic radius of the entire pore system lies between 12 Å and 19.4 Å for all pastes. Wide-pores in OPC pastes have an average hydraulic radius of between 22.5 Å and 50.6 Å for W/C between 0.3 and 0.7; SRPC pastes have between 29 Å and 45 Å for W/C between 0.4 and 0.6. Superplasticiser admixture reduced the hydraulic radius of the wide-pores.

6. Crude oil saturation of HCP, cloggs up some of the pores thus reducing the measured porosity and surface area.

7. The porosity of Concrete can reasonably be calculated from equ.

(4.27), ie. by summing the separate porosities of the cement paste and aggregate, and air content. The porosities were between 16.0 and 23.4% in OPC concrete for effective W/C ratios between 0.31 and 0.87 and between 16.8 and 22.3% in SRPC concrete for effective W/C ratios between 0.31 and 0.82. SRPC concrete were generally more porous than OPC concrete.

8.1.2 Permeability of HCPs and Concrete

8.1.2.1 Permeability of HCPs

1. The coefficient of permeability, K, decreases with time. For OPC, K after 24 hours was between 1.2 and 1.5 times that after 120 hours of flow. K reached an almost constant value after about 120 hours.

2. K increases almost linearly with applied hydrostatic pressure, with greater increases for pastes of high W/C ratio.

3. K increases exponentially with W/C ratio and can also be related exponentially to the porosity and compressive strength. Increasing the W/C ratio from 0.4 to 0.7 increases K 3 times. For pastes containing superplasticiser K increases linearly with W/C ratio and the paste porosity.

4. Generally, SRPC pastes were more permeable than OPC pastes, but were the same at low W/C ratios of about 0.4.

5. K can be related reasonably accurately to the HCP wide-pore volume, P, and hydraulic radius, r_h, at any applied oil pressure A in the form:

$$K = T \cdot A^{\theta} P^{\beta} r_h^{\gamma}$$

where θ, β and γ are empirical constants and T the tortuosity factor.

8.1.2.2 Permeability of Concrete

1. K increases exponentially with increasing W/C ratio or total porosity. Increasing W/C ratio from 0.4 to 0.8 increases K about 3.7 times in OPC and 2.9 times in SRPC concrete.

2. K decreases with increasing cement content upto 425 Kg/m^3 of cement, after which no significant change in K occurs on further increasing the cement content. For W/C = 0.6, the optimum cement content was 380 Kg/m^3 and the aggregate/cement ratio was between 4.3 and 4.7. Optimum values, for reduced K, at other W/C ratios were obtained.

3. K is influenced by the fine to coarse aggregate ratio. For W/C = 0.6, the optimum fine to total aggregate percentage, for reduced K, was between 40 to 55%. Optimum values for other W/C ratios were obtained.

4. Aggregate grading corresponding to zones 2 and 3 of BS.882,1965 produced concrete of lower K than zones 1 and 4.

5. Concrete workability influences K. Low and high slump concrete were more permeable than medium slumps. Optimum ranges were between 60 to 110 mm slump.

6. K decreased continuously with time. The decrease was very high within the first 24 hours but became almost constant after 120 hours. In superplasticised concrete K continued to decrease significantly after 120 hours.

7. K increased almost linearly with applied oil pressure. Increasing the pressure from 32.9 m to 96.8 m of oil increased K by between 1.82 and 3.73 times depending on the concrete porosity.

8. K decreased in superplasticised concrete (with reduced W/C ratio) by average values of about 30% and 35% in OPC and SRPC concrete respectively using Cormix SP1. For concrete containing Melment L10, the decreases were between 22.6 and 43% in OPC, and 29 and 50% in SRPC concretes.

9. K can be predicted most accurately from the original W/C ratio and the calculated total porosity of concrete. Large errors of upto ± 35% and ± 42% were obtained in trying to estimate K from the compressive strength and oil absorption respectively. Lower errors of ± 30% and ± 23% were obtained for OPC and SRPC concretes using W/C ratio, and about ± 24.5% from calculated total porosity. These results are for a grade 50 concrete.

8.1.2.3 Oil Absorption

1. Generally SRPC pastes absorbed more oil than OPC pastes by between 16 to 23% at equal W/C ratios. Pastes containing 1 and 2% superplasticiser absorbed slightly less oil than ordinary pastes.

2. SRPC concrete generally absorbed more oil than OPC concrete, eg., at equal compressive strengths SRPC absorbed more by between 7 to 17%.

3. Most of the absorption occured within the first 4 months of storage. HCPs were saturated at 4 months. In concrete further oil absorption was slight or negligible after about 8 months.

4. Superplasticised concrete absorbed slightly less than ordinary concrete of the same total porosity.

8.1.3 Mechanical Properties

8.1.3.1 HCPs

1. The compressive strength of oil saturated pastes were about 4 to 5% less than for pastes tested in the water saturated surface dry state (SSD) and about 15% less than dried samples (CTR). HCPs of lower porosity have smaller percentage strength reductions. No significant reductions occured after the first 4 months.

2. The compressive strength of HCPs containing 1 and 2% superplasticiser are higher than for ordinary pastes of the same W/C ratio, but were lower at a higher concentration of 4%.

3. The compressive strength and elastic modulus of HCPs can be related exponentially to W/C ratio and the paste porosity.

4. The elastic modulus of oil saturated HCPs at 24 weeks is 4 to 13% less than that for SSD samples at 28 days and the decreases on prolonged storage in crude oil were slight or negligible . Failure stresses of oil saturated prisms were lower by 3 to 14% and further decrease was negligible on prolonged storage.

5. HCPs with W/C = 0.4 containing 1% and 2% superplasticiser had an elastic modulus higher by 11 to 37% for OPC and 4 to 15% for SRPC pastes

without admixture and of equal W/C.

8.1.3.2 Concrete

1. The compressive strength of oil saturated concrete reduced, after 24 weeks, by about 9% for OPC and 8.5% for SRPC concrete over samples of the same age but dried to 55°C (CTR); and were about 4% less than SSD samples. Percentage reduction in strength was higher in concrete of higher porosity.

2. Average rates of strength reduction due to storage in crude oil were small. For OPC, the strength reduced by between 0.6 to 0.8 N/mm^2 per month or 0.84 to 1.38% per month; 0.8 to 1.45% in SRPC and 0.83 to 1.31% in superplasticised concrete.

3. At low loads, the behaviour of SSD, CTR and oil saturated concrete prisms (100 x 100 x 300 mm) were similar, but at higher loads crude oil concrete became more flexible with higher Poisson's ratio, volumetric expansion and longitudinal strain; and weaker with lower failure loads.

4. Crude oil saturation decreased the elastic modulus. The decrease being more for OPC than SRPC concrete. For example, after 12 months in oil, OPC concrete decreased by a maximum value of 5.0 KN/mm^2, SRPC by 3.1 KN/mm^2 and superplasticised concrete by 5.5 KN/mm^2.

5. SRPC concretes had a higher elastic modulus than OPC - between 3.3 and 5.1% higher. The modulus increased by 17 to 20% for superplasticised concrete.

6. The rate of reduction of elastic modulus due to storage in crude oil were small and reduced with time. The average rates of monthly reduction were between 0.4 to 1.1% for OPC, 0.4 to 0.9% for SRPC, and 0.9 and 1.2% in superplasticised OPC concrete.

7. The elastic modulus, E, of the concrete can be related to its compressive strength, f_c by the formula:

$$E = \beta (f_c)^{\alpha}$$

where β and α are empirical constants.

8.2 Limitations of the Present Work

The limitations of the present investigation are considered to be as follows:

8.2.1 Materials

1. Only Kuwait crude oil has been used and at a constant temperature.

2. Only one type of aggregate - natural river, of 10 mm maximum size - has been used.

3. Only superplasticising admixtures were considered.

8.2.2 Pore Structure Studies

1. Only Power's model has been assumed and used in the analysis and the inadequacies of this model are discussed in sections 2.1.4.3 and 2.3.3.

2. Porosity tests on HCPs were done on small crushed samples. Tests on larger uncrushed samples are still required.

3. Carbonation of the pastes during the preparation of the tests was not investigated.

8.2.3 Permeability Studies

1. Tests were carried out at one temperature only ie. $16 \pm 0.5^{\circ}C$, and a relative humidity of $50 \pm 2\%$.

2. Tests were only made on small concrete specimens.

3. Tests were only done in the direction of casting of the specimens.

8.2.4 Mechanical Properties

1. Attempts were made to prevent oil accumulating in-between the testing machine platens and the specimen ends during tests, but could not

be prevented completely.

2. To accelerate the oil saturation, samples were first dried to 105°C which may have an adverse effect on the HCP and concrete properties.

8.3 Recommendations for Future Work

Areas in which further work is needed for a fuller understanding of the effects of crude oil saturation on the structure and properties of HCPs and concrete are:

1. Microscopic examination of the pore structure of HCPs with and without admixture and saturated with oil.

2. The study of the permeability and mechanical properties of oil soaked concrete made with different aggregates.

3. Further study of the permeability of concrete containing other types of admixtures especially air-entraining admixtures and polymers.

4. Study of the flow of crude oil into cracks in concrete.

5. Study of aggregate - cement paste bond in oil saturated concrete.

6. Study of creep characteristics of oil saturated concrete.

7. Study of the structural behaviour of reinforced and prestressed oil soaked concrete members.

8. Comparative study of the mechanical properties of concrete dried and oil saturated, and those dried and water resaturated.

REFERENCES

1. Hampe, E. "Recent Developments in the Construction of Liquid Tanks". F.I.P. notes 67, March - April 1977, pp 11 - 16

2. P.C.A. "Concrete Tanks for Fuel Oil Storage". 1920, abstracted in Concrete and Constructional Engineering, Vol. 17, 1922, pp. 32 - 35.

3. Macpherson, A. R. "Precast Concrete Oil Tanks". Tacoma Builders Supply Co., Concrete Products, June 1952 pp. 182 - 183.

4. Gerwick, B. and Hognestad. "Concrete Oil Storage Tank placed on North Sea floors". A.S.C.E. Civil Engineering Journ., Aug. 1973, pp. 81.

5. Richardson, C. "North Sea Oil Structures". Proc. Symp. University of Birmingham, on 'concrete - can it hold water' Sept. 1974, pp. 47 - 54.

6. Marion, H. and Mahfouz, G. "Design and Construction of the Ekofish Artificial Island". Proc. I.C.E., Vol. 56 part 1, Nov. 1974, pp. 497 - 511, pp. 635.

7. Meissner, H. and Pearson, J. Discussion of the paper, "Tests of Gasoline Resistance Coatings". A.C.I. Proc., Vol. 15, No. 6, 1944, pp. 292.

8. Biczok, I. "Concrete Corrosion and Concrete Protection", Publishing house of the Hungarian Academy of Science, Budapest, 1964, pp. 324 - 329.

9. Lea, F. "The Chemistry of Cement and Concrete". Edward Arnold (Publishers) Ltd., 1970, pp. 659 - 665.

10. Hansen, T. C. "Creep of Oil-Saturated Concrete". Proc. Int. Conference on Mechanical Behaviour of Materials, Kyoto, August 1971, pp. 257 - 261.

11. Matti, A. M. "The Properties of Oil Soaked Concrete". M. Eng. thesis, University of Sheffield, 1974.

12. Matti, A. M. "Some Properties and Permeability of Concrete in Direct Contact with Crude-oil". Ph.D. thesis, University of Sheffield, 1976.

13. Faiyadh, F. "Further Investigations into the Properties of Oil Soaked Concrete". M. Eng. thesis, University of Sheffield 1976.

14. Popovics, S. "Effect of Porosity on the Strength of Concrete". J. of Materials, JMLSA, Vol. 4, No. 2, June 1969, pp 356 - 371.

15. Lawerence, C. "Porosity/Strength Relationships for Portland Cement Pastes". IUPAC/RILEM Int. Symp. on Pore structure and Properties of Materials. Vol. 2, Prague, 1973, pp. D167 - 176.

16. Roy, D. and Gouda, G. "Opitimiztion of Strength in Cement Pastes". Cem. and Conc. Res., Vol. 5, 1975. pp. 153 - 162.

17. Powers, T. C. "Fundamental Aspects of the Shrinkage of Concrete". 3rd Int. Congress of the Precast Industry, Stockholm, 1960.

18. Feldman, R. "Sorption and Length Change Scanning Isotherms of Methanol and Water on Hydrated Portland Cement Pastes". Proc. 5th Int. Symp. on the Chemistry of Cement, Tokyo, Part 3, Vol. 3, 1968, pp 36 - 44, 53 - 66.

19. Helmuth, R and Turk, D. "The Reversible and Irreversible Drying Shrinkage of Hardened Portland Cement Paste and Tricalcium Silicate Pastes". Bulletin 215, Port. Cem. Assoc., 1967.

20. Helmuth, R. and Turk, D. "Elastic Modulii of Hardened Portland Cem. and Tricalcium Silicate Pastes: Effect of Porosity".

Highway Res. Bd. Special Rept. 90, 1966, pp. 135 - 144.

21. Fagerlund, G. "Elastic Modulus of Concrete". IUPAC/RILEM Int. Symp. on Pore Structures and Properties of materials, Vol. II, Prague, 1973, pp. D129 - D149.

22. Parrott and Illston, J. "Load-Induced Strains in Hardened Cement Paste" Journ. of the Engrn. Mechancis div., A.M.S.C.E., Vol. 101 Feb. 1975, pp. 13 - 24.

23. Powers, T. and Brownyard. "Studies on the Physical Properties of Hardened Cement Pastes". Proc. A.C.I., Vol. 43, 1947, pp. 101, 249, 469, 549, 845, and 933.

24. Powers, T. "Structure and Physical Properties of Hardened Cement Pastes". Journ. Amer. Ceramics Soc., Vol. 41, No. 1, Jan. 1958, pp. 1 - 6.

25. Powers, T. "Freezing effects in Concrete". Durability of Concrete, SP-47, A.C.I., 1975, pp. 1 - 11

26. Powers, T., Copeland, L. and Mann, H. "Capillary Continuity or Discontinuity in Cement Pastes". Portl. Cement Assoc., Res. and Dev. lab., Vol. 1, No. 2, May 1959, pp. 38 - 48.

27. Older, L, Hagymassy, J., Boder, E. Yuden Freud and Brunauer, S. "Hardened Portland Cement Pastes of Low Porosity: IV. Surface Area and Pore Structure". Cem. and Conc. Res., Vol. 2, 1972 pp. 577 - 589.

28. Yudenfreud, et al. "Hardened Portland Cement Pastes of Low Porosity: 1. Material and Experimental Methods". Cem. and Cond. Res., Vol. 2, No. 3, 1972, pp. 313 - 330, 331 - 366.

29. Manning, D. and Hope, B. "The Effect of Porosity on the Compressive Strength and Elastic Modulus of Polymer Impregnated Concrete". Cem. and Conc. Res., Vol. 1, 1971, pp. 631 - - 644.

30. A.C.I. Committee 22. "Guide for Admixtures". Proc. A.C.I., Vol. 68, No. 9, Sept. 1971, pp. 646 - 676.

31. Ishai, O. "The Dependent Deformational Behaviour of Cement Pastes, Mortar and Concrete". Proc. Int. Conf. on the Structure of Concrete. C. & C.A., London, 1965, pp. 345 - 363.

32. Brunauer, S., Emmett, P. and Teller, E. "Adsorption of Gases in Multi-molecular Layers". J. Amer. Chem. Soc., Vol. 10, No. 2, 1938, pp. 309 - 319.

33. Mikhail, et al, "Pore Structure and Surface Areas of Hardened Portland Cement Pastes by Nitrogen Adsorption". Canadian J. of Chemistry, Vol. 42, 1964, pp. 426 - 438.

34. Brunauer, S. "Tobermorite gel - the Heart of Concrete". American Scientist, Vol. 50, No. 1, March 1962, pp. 210 - 229.

35. Powers, T. "Mechanics of Shrinkage and Reversible Creep of Hardened Cement Paste". Proc. Int. Conf. on the Structure of Concrete. C. and C.A.,London, 1965. pp. 315 - 344.

36. Winslow, D. and Diamond, S. "Specific Surface Area of Hardened Portland Portland Cement Paste as Determined by Small-angle X-ray Scattering". Journ. of Amer. Cer. Society, Vol. 57, No. 5, May 1974, pp. 193 - 197.

37. Copeland, L. and Hayes, J. "The Determination of Non- evaporable Water in Hardened Cement Paste". A.S.T.M. Bul., No. 194, Dec. 1953, pp. 70 - 74.

38. Mikhail, R., Turk, D. and Brunauer, S. "Dimensions of Average Pore, the Number of Pores and Surface Area of Hardened Portland Cement Pastes". Cem. and Conc. Res., Vol. 5, 1975. pp. 433 - 442.

39. Feldman, R. and Sereda, P. "Model for Hydrated Portland Cement Paste as Deduced from Sorption-length Change and Mechanical

Properties". Materials and Structures, Vol. 1, No. 6 1968, pp. 509 - 520.

40. Feldman, R. "Assessment of Experimental Evidence for Models of Hydrated Portland Cement". Highway Res. Rec., No. 370, 1971, pp. 8 - 24.

41. Feldman, R. and Ramanchandran, V. "Differentiation of Interlayer and Adsorbed Water in Hydrated Portland Cement by Thermal Analysis". Cem. and Concrete Res., Vol. 1, No. 6, 1971, pp. 607 - 620.

42. Feldman, R. "Helium Flow and Density Measurement of Hydrated Tricalcium Silicate - Water System". Cem. and Cons. Res., Vol. 2, No. 1, 1972, pp. 123 - 136.

43. Feldman, R. "Mechanism of Creep of Hydrated Portland Cement Paste". Cem. and Cons. Res., Vol. 2, No. 5 1972, pp. 521 - 540.

44. Soreda, P. and Ramachandran, V. "Prediction Gap Between Science and Technology of Cements: II. Physical and Mechancial Behaviour of Hydrated Cements.", J. Amer. Cer. Soc,. Vol. 58, No. 5 - 6, 1975, pp. 249 - 253.

45. Feldman, R. "Density and Porosity Studies of Hydrated Portland Cements". Cement Technology, Vol. 3, 1972, pp5 - 14.

46. Hope, B. and Brown, N. "A Model for the Creep of Concrete". Cement and Conc. Res., Vol. 5, No. 5, 1975; pp. 577 - 586.

47. Brunauer, S. et al, "The New Model for Hardened Cement Paste". Highway Res. Rec., No. 328, 1970, pp. 89 - 101, 105 - 107.

48. Brunauer, S. "Discussion of Helium Flow Results". Cem. and Conc. Res., Vol. 2, No. 4, 1972, pp. 489 - 492.
No. 6, 1972, pp. 749 - 753.

49. Feldman, R. "Reply to Discussions by Brunauer". Cem. and Cons.

Res., Vol. 2, No. 4, 1972, pp. 493 - 498.

50. Illston, J. "Aspects of the Behaviour of the Cement Paste Phase of Composite Materials with reference to Practical Problems of Concrete Technology". Proc. Int. Conf. on Hydraulic Cement pastes, University of Sheffield, 1976, pp. 232 - 247.

51. Ritter, H and Drake, L. Ind. Engineering Chemical Analysis, Vol. 17, 1945, pp 782.

52. Wheeler, A. Advanced Catalysis, Vol. 3, 1951, pp. 249.

53. De-Boer, J. "The Shape of Capillaries". Proc. Symp. on the Structure and Properties of Porous Materials, Univ. of Bristol, 1958, pp. 68 - 94.

54. Winslow, D. and Diamond, S. "A Mercury Porosimetry Study of the Evolution of Porosity in Portland Cements". J. of Materials, JMLSA, Vol. 5, No. 3, 1970, pp. 564 - 585.

55. Diamond, S. "Pore Structure of Hardened Cement Pastes as Influenced by Hydration Temperature". IUPAC/RILEM Int. Symp. on Pore Structure and Properties of Materials, Vol. 1, Prague, 1973, pp. B73 - 88.

56. Diamond, S. "A Critical Comparison of Mercury Porosimeter and Capillary Condensation Pore Size Distribution of Portland Cement Pastes". Cem. and Conc. Res., Vol. 1, 1971, pp. 531 - 545.

57. Gregg and Sing, K. "Adsorption, Surface Area and Porosity". London Academic Press, 1967.

58. Fagerlund, G. "Determination of Specific Surface by BET Method". Materials and Structures, Vol. 6, No. 33, 1973, pp. 239 - 245.

59. Mikhail, R. and Oweimreen, G. "Surface Area and Pore Structure of

Compressed Low-porosity Cement Pastes". Cem. and Conc. Res., Vol. 3, 1973, pp. 561 - 573.

60. Brunauer, S. et al, "Pore Structure Analysis Without a Pore Shape Model". Journ. Colloid and Interface Sci., Vol. 24, 1967 pp. 451 - 463.

61. Mikhail, R. et al, "Investigations of a Complete Pore Structure Analysis: 1.Analysis of micropores." J. Colloid and Interface Sci., Vol. 26, 1968, pp. 45 - 53.

62. De Boer, J. et al "Studies on the Pore System of Catalysts". Journ. of Catalysis, Vol. 3, 1964, pp. 32 - 37, 38 - 44, 44 - 49, 268 - 273.

63. De Boer, J. et al "Studies on the Pore System of Catalysts". Journ. of Catalysis, Vol. 4, 1965, pp. 319 - 323, 643 - 648, 649 - 653.

64. Brunauer, S. and Skalny, J. "Complete Pore Structure Analysis". IUPAC/RILEM Int. Symp. on Pore Structure and Properties of Materials, Vol V, Prague, 1973, pp. C3 - C27.

65. Feldman, R. "The Flow of Helium into the Interlayer Spaces of Hydrated Portland Cement Pastes". Cem. and Conc. Res. Vol. 1, 1971, pp. 285 - 300.

66. Haynes, J. "Determination of Pore Properties of Constructional and other Materials - General Introduction and Classification of methods". Materials and Structures, Vol 6, No. 33, 1973, pp. 169 - 174, pp. 175 - 179.

67. Fagerlund, G. "Strength and Porosity of Concrete". IUPAC/RILEM Int. Symp. on Pore Structure and Properties of Materials, Vol. V, Prague, 1973, pp. D51 - 73.

68. Valenta, O. "Main Properties of the Pore System of Non-metallic Structural Materials, their Significance and Experimental Determination". IUPAC/RILEM Int. Symp. on Pore

Structure and Properties of Materials, Vol. V, Prague, 1973, pp. E78 - 101.

69. Powers, T. et al "Permeability of Portland Cement Paste". J. Amer. Conc. Inst., Vol. 51, Nov. 1955, pp. 564 - 585.

70. Neville, A. M. "Properties of Concrete". Pitman Publishing Co., 1975, pp. 10 - 58, 59 - 102, 309 - 381, 382- 454

71. Powers, T. et al "Flow of Water in Hardened Portland Cement Paste". Highway Res. Bd., Spec. Rept., No. 40, 1959, pp. 308 - 323.

72. Muskat, M. "The Flow of Homogeneous Fluids through Porous Media." Mcgraw - Hill. 1937.

73. Scheidegger, A. "The Physics of Flow through Porous Media". University of Toronto press, 1957.

74. Scheidegger, A. Producers Monthly, Vol. 17, No. 10, 1953, pp. 17.

75. Carman, P. "In Symposium on New Methods of Particle Size Distribution in Subsieve Range". ASTM Publication, 1941, pp.24.

76. Powers, T. "The Properties of Fresh Concrete". John Wiley and Sons, Inc., New York, 1968, pp 605.

77. Murata, J. "Studies on the Permeability of Concrete". Rilem Bulletin (Paris), New Series, No. 29, Dec. 1965, pp. 47 - 54.

78. Barrer, M. R. "Diffusion in and through Solids". Cambridge Univ. Press, 1941, pp. 1 - 54.

79. Hughes, P. B. et al. "The Diffusion of Water in Concrete at Temperatures between 50°C and 95°C". Brit. J. of App. Physics, Vol. 17, 1966, pp. 1545.

80. Nurse, R. W. "Assessment of Concrete Durability". Proc. Symp. on Concrete Quality, London, 1967, Published C. and C.A., 1966, pp. 71 - 77, 78 - 88.

81. B.S.I. "Methods of Testing Hardened Concrete for Other than Strength". B.S. 1881, part 5, 1970. Clauses 6, 7.

82. Loughborough, M. "Permeability of Concrete to Air". Onatario Hydro. Res. Quarterly., Vol. 18, No. 1, 1966, pp.14 - 16.

83. Muratta, J. "Proposal of a Method of Testing Permeability of Concrete and its Applications". RILEM/CIB Symp. on Moisture problems in buildings, Helsinki, Vol. 1, Sect. II, 1965. pp. 11.

84. Van Der Meulen, G. and Van Dijk, J. "A Permeability Testing Apparatus for Concrete". Mag. of Concrete Res., Vol. 21, No. 67, 1969, pp. 121 - 123.

85. Levitt, M. "Non-Destructive Testing of Concrete by the Initial Surface Absorption Method". Symp. on Non-destructive Testing of Conc. and Timber, London, 1969, I.C.E., 1970 pp. 23 - 26.

86. Levitt, M. "Durability of Precast Products". The Consulting Engineer (Supplement), April-May, 1971, pp. 25 - 29.

87. Figg, J. W. "Methods of Measuring the Air and Water Permeability of Concrete". Mag. of Conc. Res., Vol. 5, No. 85, 1973, pp. 213 - 219.

88. Valenta, O. "Kinetics of Water Penetration into Concrete as an Important Factor of its Deterioration and of Reinforcement Corrosion". RILEM Int. Symp. on Durability of Concrete, Part 1, 1966, pp. A177 - A199.

89. Tyler, I. and Erlin, B. "A Proposed Simple Method of Determining the Permeability of Concrete". Journ. Portland Cem. Assoc., Res., and Dev. Lab., Vol. 3, Part 3, 1961,

pp. 2 - 7.

90. Ruettgers, A. et al "An Investigation of the Permeability of Mass Concrete with Particular Reference to Boulder Dam". Proc. A.C.I., Vol, 31, 1935, pp. 382 - 416.

91. Vallerga, B. and Hicks, R. "Water Permeability of Asphalt Concrete Specimens Using Back-pressure Saturation". J. of Materials, JMLSA, Vol. 3, No. 1, 1968, pp. 78 - 86.

92. Pihlajavaara, S and Paroll, H. "On the Correlation between Permeability Properties and Strength of Concrete". Cem. and Conc. Res., Vol, 5 1975, pp. 321 - 328.

93. Taylor, M. "General Behaviour Theory for Cement Pastes, Mortars and Concrete". J. A.C.I., Vol. 68, No. 10, 1971, pp. 756 - 762.

94. Powers, T. C. "The Physical Structure and Engineering Properties of Concrete". Portl. Cement Assoc., Res. Dept., Bull. 90 Chicago, 1958.

95. Williamson, R. "Portland Cement: Pseudomorphs of Original Cement Grains Observed in Hardened Pastes". Science, Vol. 164, 1969, pp. 549 - 551.

96. Philleo, R. "The Origin of Strength of Concrete". Highway Res. Bd., Spec. Rept. 90, 1966, pp. 175 - 185.

97. Griffith, A. "The Phenomena of Rapture and Flow in Solids". Phylosophical transactions, Royal Soc. of London, Vol. 221, 1921, pp. 163 - 198.

98. Lawrence, C.D. "The Properties of Cement Paste Compacted Under High Pressure". Cem. and Conc. Assoc. Res. Rept. No. 19 London, June 1969.

99. Kaplan, M. "The Effects of Incomplete Consolidation on Compressive and Flexural Strength, Ultrasonic Pulse Velocity, and

Dynamic Modulus of Elasticity of Concrete". J. A.C.I., Proc. 50, No. 9, 1960, pp. 853 - 867.

100. Te'eni, M. "Cemented Granular Systems", Ph.D. thesis, University of Southampton, 1970.

101. Mills, R. H. "Factors Influencing Cessation of Hydration in Water Cured Cement Pastes". Highway Res. Bd. Spec. Rept. 90, 1966, pp. 406 - 424.

102. Sereda, P. and Soroka, I. "Interrelation of Hardness, Modulus of Elasticity and Porosity in Various Gypsum Systems". J. Amer. Cer. Soc., Vol. 51, No. 6, 1968, pp. 337 - 340.

103. Hansen, T. "Influence of Aggregate and Voids on Modulus of Elastiicty of Concrete, Cement Mortar and Cement Paste". J. A.C.I., Vol. 62, 1965, pp. 193 - 195.

104. Lawrence, P. et al "The Application of the Mackenzie Model to the Mechanical Properties of Cements". Cem. and Conc. Res., Vol. 1, No. 1, 1971, pp. 75 - 99.

105. Ryshkewitch, E. "Compressive Strength of Porous Alumina and Zirconia". J. Amer. Ceramic Soc., Vol. 36, 1953, pp. 65 - 68.

106. Biczok, I. Ref. 8, pp. 136 - 143.

107. Prudil, S. "Model of Concrete Behaviour in Aggressive Environments". Cem. and Conc. Res., Vol. 7, 1977, pp. 77 - 84.

108. Blue Circle Cement, Hope Works, Hope, Sheffield. Private communication.

109. Ref. 70 pp. 177

110. Joint Working Party; Cement Admixture Assoc. and C. & C.A. "Superplasticising Admixtures in Concrete". C. & C.A.,

Slough, 1976.

111. "The Concrete That Fills", Concrete, J. of Concrete Society, Vol. 10, No. 12, Dec. 1976, pp. 14 - 15.

112. Blakey, H. "Superplasticisers". C. &. C.A., Training Leaflet TDH5418, Slough, 1975.

113. Hoeshst Chemicals "Melment Data Sheet Compendum". (Available from Hoechst Chemicals, Hoeschst House, Salisbury Rd., Hounslow, TW4 6JH)

114. Crosfield Chemicals. "Cormix Superplasticiser One". (Available from Joseph Crosfield and Sons, Ltd., Warrington, WA5 1AB)

115. Spooner, D. C. "The Stress-strain Relationship for Hardened Cement Pastes in Compression". Mag. of Conc. Res., Vol 24, No. 79, June 1972, pp. 85 - 92.

116. Markestad, S. "Gukild - Carlsen Method for Making Stabilised Pastes of Cements". Materials and Structures, Vol. 9 No. 50, 1976, pp. 115 - 117.

117. Teychenne, D., Franklin, R. and Erntroy, H. "Design of Normal Concrete Mixes". Department of the Environment, B.R.E., HMSO, London, 1975.

118. McBain, J. and Bakr, A. "A New Sorption Balance". J. Amer. Chemical Soc., 48, 1926, pp. 690 - 695.

119. Taplin, J. "A Method For Following the Hydration Reaction in Portland Cement Paste". J. Applied Science, Vol. 10, 1959, pp. 329 - 345.

120. Soroka, I and Relis, M. "Variation in Density of Portland Cement Hydration Products". Cement and Conc. Res., Vol. 7, 1977, pp. 673 - 680.

121. Frigone, G. and Marra, S. Relationship Between Particle Size Distribution and Compressive Strength in Portland Cement". Cem. and Conc. Res., Vol. 6, 1976, pp. 113 - 128.

122. Powers, T. "The Non-evaporable Water Content of Hardened Portland Cement Paste: Its Significance for Concrete Research and Its Determiantion". A.S.T.M. Bulletin, No. 158, 1949, pp. 68 - 76.

123. Hagymassy, J. "Pore Structure Analysis By Water Vapour Adsorption". Ph.D. Thesis, Clarkson College of Technology, 1970.

124. Hagymassy, J. et al. "Pore Structure Analysis By Water Vapour Adsorption: 1. t-curve for Water Vapour". J. Colloid and Interface Sci. Vol. 29, No. 3, 1969, pp. 485 - 491.

125. Mikhail, R. et al. "Surface Properties of Cement Hydration Products 1. Pore Structure of Calcium Silicate Hydrates Prepared in a Suspension Form". J. Applied Chem., Vol. 19, 1969, pp. 324 - 328.

126. Dubinin, M. "On the Specific Surface Area of Micropore Containing Adsorbents". IUPAC/RILEM Int. Symp. on Pore Structure and Properties of Materials, Vol V, Prague, 1973, pp. C27.

127. Brunauer, S. and Mikhail, R. "Some Remarks on Pore Structure Analysis". J. Colloid and Interface Sci., Vol. 52, No.3 1975.

128. Hagymassy, J. et al. "Pore Structure Analysis By Water Vapour Adsorption: III. Analysis of Hydrated Calcium Silicate and Portland Cements". J. Colloid and Interface Sci., Vol. 38, No. 1, 1972, pp. 20 - 34.

129. Dingley, R. "The Structure and Properties of Hydraulic Cement Pastes Modified by Polymer Latex". Ph.D. thesis, Univ. of Southampton, 1974.

130. Brunauer, S. et al. "The Stoichiometry of the Hydration of - Dicalcium Silicate and Tricalcium Silicate at Room Temperature". J. Amer. Chem. Soc., Vol. 80, 1958, pp. 761 - 767.

131. Kirillov, A. P. "The Mechanism of Water Seepage through Concrete". Hydrotechnical Construction, No. 5, May 1968, pp. 411 - 415.

132. Hughes, B. "Particle Interference and Workability of Concrete". A.C.I. Journ. Proc., Vol. 63, March 1966, pp. 369 - 372.

133. Hughes, B. and Bahramian, B. "Some Factors Affecting the Compressive Strength of Concrete". Mag. of Concrete Res., No. 60, 1967, pp. 165 - 172.

134. Hughes, B. and Ash, J. "The Effect of Mix Proportions and Aggregate Dust Upon the Compressive Strength of Concrete". Mag. of Conc. Res., Vol. 20, No. 63, 1968, pp. 77 - 84.

135. B.S.I. "Methods of Testing Concrete for Strength", B.S. 1881; part 4, 1970.

136. Shah, S. and Chandra, S. "Critical Stress, Volume Change and Microcracking of concrete". Journ. A.C.I., 1968, pp. 770 - 781.

137. Mikhail, R. et al, "Air Entrainment in Portland Blast Furnace Slag Cement Pastes: Effect on Strength and Pore Structure". Cem. and Conc. Res., Vol. 7, No. 5, 1977, pp. 515 - 522.

138. Powers, T. C. in "Chemistry of Cement". Chapter 10, H.F. Taylor Editor, Academic press, New York, 1964, pp. 391.

139. Collepardi, M. and Massida, L. "The Influence of Water-Rducing Admixtures on the Cement Paste and Concrete Properties". Proc. Int. Conf. on Hydraulic Cement Pastes", Univ. of Sheffield. 1976, pp. 256 - 267.

140. Ciach, T. and Swenson, E. "Morphology and Microstructure of hydrating Portland Cement and its Constituents, III. Changes in the Hydration of a Mixture of C_3S, C_3A and Gypsum with and without Triethanolamine and Calcium Lignosulphate present". Cem. & Cons. Res., Vol.1, 1971, pp. 257 - 271.

141. Cook, D. and Haque, M. "The Effect of Sorption on the Tensile Creep and Strength Reduction of Desiccated Concrete". Cem. and Conc. Res., Vol. 4, 1974, pp. 367 - 379.

142. Cook, D. and Haque, M. "Strength Reduction and Length changes in Concrete and Mortar on Water and Methanol Sorption". Cem. and Conc. Res., Vol. 4, 1974, pp. 735 - 744.

143. Copeland, L. and Hayes, J. "Porosity of Hardened Portland Cement Pastes". Journ. of Am. Conc. Inst. Vol. 52, 1956, pp. 633 - 640.

144. Feldman, R. and Beaudoin, J. "Microstructure and Strength of Hydrated Cement". Cem. and Conc. Res., Vol. 6, No. 3, 1976, pp. 389 - 400.

145. Older, A. et al, "Pore Structure Analysis by Water Vapour Adsorption". IV Analysis of Hydrated Portland Cement Pastes of Low Porosity". J. of Colloid & Interface Sci., Vol. 38, No. 1, 1972, pp. 265 - 276.

146. Davies, O. and Goldsmith, P. "Statistical Methods in Research and Production". Published for I.C.I. by Oliver and Boyd, Edinburgh, 1972, pp. 237 - 286, pp. 438.

147. Maxson, O. and Achenbach, G. "Properties of Concrete in Direct Contact with Pressurised Hydrocarbons and Sea-water". J. of Petroleum Technology, April, 1977, pp. 360 - 362.

148. Kocataskin, F. "Permeability of Concrete". Habilitation, Istanbul, 1954, pp. 50 - 56.

149. Pihlajavaara, S. "Effect of Moisture Conditions on Strength, Shrinkage and Creep of Mature Concrete". Cem & Conc. Res. Vol. 4, No. 5, 1974, pp. 761 - 771.

150. Lacraix, R. "Special Problems in Connection with Under-water Oil Storage Tanks of Prestressed Concrete", FIP Symposium on Concrete Sea Structures, TBILISI Sept., 1972, pp. 94.

151. Mills, R. and Ono, K. "Estimation of Elastic Modulus of Concrete from Hydration Parameters". Proc. Int. Conf. On Mechanical Behaviour of Materials, Vol. IV, Kyoto, 1971, pp. 143 - 152.

152. Parrot, L. J. "The Effect of Moisture Content Upon the Elasticity of Hardened Cement Pastes". Mag. of Conc. Res., No. 82, Vol. 25, 1973, pp. 17 - 20.

153. Hsu, T. et al "Microcracking of Plain Concrete and the Shape of the Stress-strain Curve." J. A.C.I., Vol. 60, 1963, pp. 209,-224.

154. Jones, R. and Kaplan, M. "The Effect of Coarse Aggregate on the Mode of Failure of Concrete in Compression and Flexure". Mag. of Concrete Res., Vol. 9, No. 26, 1957, pp. 89 - 94.

155. Darwin, D. and Slate, F. "Effect of Paste-Aggregate Bond Strength on Behaviour of Concrete". J. of Materials, JMLSA, Vol. 5, No. 1, 1970, pp. 86 - 98.

156. B.S.I. "CP 110: Code of Practice for the Structural Use of Concrete, Part 1, Design, Materials and Workmanship". 1972.

157. Kuenning, W. "Resistance of Portland Cement Mortar to Chemical Attack - a Progress Report". Highway Res. Rec., No. 113, 1965, pp. 43 - 87.

158. Neville, A. "Behaviour of Concrete in Saturated and Weak Solutions of Magnesium sulphate and calcium chloride". J. of Materials, JMLSA, Vol. 4, 1969, pp. 781 - 816.